

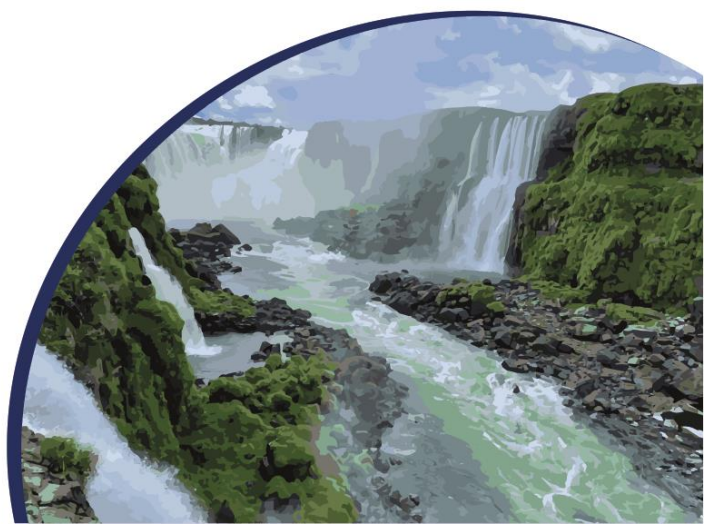
Abstracts



55th Brazilian Congress of Pharmacology and Experimental Therapeutics

Rafain Palace Hotel &
Convention Center
Foz do Iguaçu, PR, Brazil

September
25-28
2023



Summary

01. Cellular and Molecular Pharmacology	3
02. Neuropharmacology	17
03. Psychopharmacology	61
04. Inflammation and Immunopharmacology	88
05. Pain and Nociception Pharmacology	142
06. Cardiovascular and Renal Pharmacology	163
07. Endocrine, Reproductive and Urinary Pharmacology	200
08. Respiratory and Gastrointestinal Pharmacology	209
09. Natural Products and Toxinology	230
10. Cancer Pharmacology	275
11. Clinical Pharmacology, Pharmacokinetics, Pharmacogenomics and Toxicology	289
12. Drug Discovery and Development	314
13. Pharmacology Education and Technology	337
14. Pharmacology: Other	339
Authors Index	354

01. Cellular and Molecular Pharmacology

01.001 **CDR1as Overexpression in MPP+ Injured SH-SY5Y Dopaminergic Cells.** Ferrari SSAR, Silva LDS, Duarte CDM, Gomes GMO, Schlemmer F, Xavier ME, Titze-de-Almeida SS, Titze-de-Almeida R UnB, Brasília, Brasil

Introduction: Circular RNAs (circRNAs) are molecules generated through backsplicing of single-stranded RNAs. These molecules have critical roles in neuron biology, such as regulating gene expression, immune responses, and central nervous system development. Recent research has highlighted the association between dysregulated circRNAs and numerous disorders, including cancer, cardiovascular diseases, and neurodegenerative conditions like Parkinson's and Alzheimer's. One notable circRNA is cerebellar degeneration-related protein 1 antisense RNA (CDR1as), which is abundantly expressed in the mammalian brain. CDR1as functions as a reservoir for an important regulatory microRNA, miR-7. This microRNA has been implicated in underlying mechanisms of Parkinson's disease, including the regulation of alpha-synuclein, dopaminergic cell death, and neuroinflammation. Our study aimed to investigate whether the expression of CDR1as is altered in SH-SY5Y dopaminergic cells damaged by MPP+. **Methods:** cells were cultured in DMEM media supplemented with GlutaMAX, fetal bovine serum (FBS), and antibiotic/antimycotic solution and exposed to MPP+ for 24 hours. Cell viability was assessed using colorimetric MTT assay, while CDR1as expression was determined by RT-qPCR. MPP+ exposure caused a significant dose-dependent reduction in cell viability at concentrations of 0.5mM, 1mM, and 2mM ($P < 0.05$). For RT-qPCR, RNA was purified using a commercial kit (RNeasy Plus Mini kit, Qiagen) and reverse transcribed with random primers (SuperScript First-Strand Synthesis System for RT-PCR, Invitrogen). The qPCR reaction was executed via SYBR Green method (Fast SYBR Green Master Mix, Applied Biosystems) with previously published primers for CDR1as, GPBP1, and beta-actin. **Results:** SH-SY5Y cells exposed to 1mM MPP+ for 24 hours showed a 2.05-fold increase in CDR1as expression compared to controls ($P = 0.0071$; Student's t-test). **Conclusion:** MPP+ induced dopaminergic damage results in CDR1as overexpression, suggesting CDR1as may be implicated in dopaminergic cell death mechanisms associated with Parkinson's disease. **Financial Support:** Fundação de Apoio à Pesquisa do Distrito Federal - FAP-DF; Conselho Nacional de Desenvolvimento Científico e Tecnológico (CNPq); Coordenação de Aperfeiçoamento de Pessoal de Nível Superior (CAPES); Ministério da Educação (MEC) - TED MEC n.9249. **Affiliation:** Research Center for Major Themes at UnB – Division of Parkinson's Disease. Centro de Pesquisa em Grandes Temas da Universidade de Brasília - UnB/FAV, Campus Darcy Ribeiro, Instituto Central de Ciências, ASS-128. **References:** Kristensen LS. *Nat. Rev. Genet.*, v. 20, p. 675, 2019. Kleaveland B. *Cell*, v. 174, p. 350, 2018. Titze-de-Almeida R. *Curr. Gene Ther.*, v. 18, p.143, 2018. Mehta SL., *Prog. Neurobiol.*, 186, 101746, 2020.

01.002 Does the P2Y12 Receptor Adjust the Daytime Pinealocytes Melatonin Levels?

Santos UJ, Correa JC, Nekrasius LB, Markus RP, Sousa KS, Silva ZF. IB-USP, Dept of Physiology, São Paulo, SP, Brazil

Introduction: The rat pineal gland is a neuroendocrine organ that synthesizes and releases melatonin, the darkness hormone, in response to the environmental photoperiod. The pineal gland's main innervation that regulates melatonin synthesis is sympathetic fibers from the superior cervical ganglion that release noradrenaline and ATP. ATP acts as a co-transmitter of noradrenaline, potentiating the beta1-adrenergic melatonin synthesis through P2Y1 receptors (Mortani-Barbosa et al., Eur. J. Pharmacol. 401: 59, 2000; Sousa et al., Neuroscience, 499: 12, 2022). ATP is metabolized into ADP, AMP, and adenosine by the ectoenzymes which are present in the pinealocytes and peaks at night (Nikodijevic and Klein, Endocrinology 125: 2150, 1989; Ornelas, 2013). However, *in vitro* stimulation of ADP-induced P2Y1 receptors during the day inhibits melatonin production suggesting different receptor stimulation. According to the pharmacological characterization of P2Y receptors, P2Y1, P2Y11, P2Y12, and P2Y13 receptors are activated by the adenine nucleotides and couple via Gq proteins to stimulate phospholipase C and mobilization of calcium from intracellular stores (P2Y1 and P2Y11), via Gs proteins followed by increased adenylate cyclase activity (P2Y11) or via Gi proteins and inhibition of adenylate cyclase activity or control of ion channel activity (P2Y12, P2Y13) (Abbracchio et al., Pharmacol. Rev. 58: 281, 2006). The present study aimed to investigate the profile expression of ADP-induced P2Y receptors in the rat pineal. **Methods:** Wistar rats (1-to-2-month-old male or female housed under a 12: 12h LD cycle, lights on at 06h00 (ZT0) were killed by decapitation in the light phase (ZT9). Pinealocytes were prepared by trypsinization (0.25%, 37°C, 15 min) followed by mechanical dispersion in the presence of trypsin inhibitor (0.3%) in a solution containing (mmol/l): NaCl 120, KCl 5, KH₂PO₄ 1.2, MgSO₄ 1.2, NaHCO₃ 25, glucose 13 and 0.1% w/v bovine serum albumin. After centrifugation (5 min, 1000 g), the cells were resuspended in DMEM supplemented with 10% v/v fetal bovine serum, 100 U/ml penicillin/streptomycin, and plated (2x10⁵) on an 8-well chamber slide coated with 25 ug/ml poly-D-lysine (37°C, 95% O₂/5% CO₂, 18h). For immunohistochemistry, the cells were fixed in 4% paraformaldehyde (10 min) and permeabilized if necessary for intracellular staining (0.5% Triton X-100 in PBS Blocking buffer: 5% FBS in PBS. The rabbit polyclonal primary antibodies (Alomone) Anti-P2Y1 (1: 100; APR-021), anti-P2Y11 (1: 100; APR-015), anti-P2Y12 (1: 100; APR-020) and anti-P2Y13 (1: 100; APR-017) were incubated overnight. In the negative controls, the primary antibody was omitted. Alexa Fluor 488 (1: 200, 1h, room temp. in the dark, Invitrogen) was used as a secondary antibody. The slides were coverslip with mount medium with DAPI. Immunostaining was analyzed on a confocal microscope Leica TCS SP 8 X, with oil x63 **Objective: Results:** Pinealocytes showed specific immunostaining for P2Y1, P2Y11, and P2Y12, whereas in control preparations in the absence of the antibodies, the immunostaining was abolished. No specific immunostaining was observed for P2Y13 receptors in pinealocytes. **Conclusion:** As a major ATP degradation product, ADP could be a tool to mediate melatonin synthesis. A Gi-coupled ADP-induced P2Y12 receptor in the rat pineal gland points to a fundamentally new mechanism and a functional role in adjusting the pineal melatonin levels during the daytime. Support: FAPESP: 2019/03348-4; CNPq: 480097/2013-5.

01.003 Crosstalk between Endothelial Purinergic P2Y₂/P2X₇ Receptors Increases Leukocyte Adhesion favoring Mesenteric Inflammation during Schistosomiasis. Oliveira NF¹, Mainieri NS¹, Tamura AS², Coutinho-Silva R², Savio LEB², Silva CLM¹ ¹ICB-UFRJ, Brazil; ²CBBF-UFRJ, Rio de Janeiro Brazil

Introduction: The endothelial damage caused by chronic intravascular schistosomiasis promotes inflammation and ATP release, which modulates host immune responses through purinergic P2 receptors. Our previous data showed reduced levels of the endothelial P2X₇R in the infected group compared to the control (Oliveira SDS., Purinergic. Signal., v.9 p.81, 2013). Since P2Y₂R and P2X₇R signaling favors inflammation, our aim was to investigate the role of endothelial P2Y₂R/P2X₇R co-activation to schistosomal mesenteric inflammation in mice. **Methods:** Primary cultures of mesenteric endothelial cells (EC) were obtained from control (uninfected) and *Schistosoma mansoni*-infected mice (50-70 days p.i.; CEUA UFRJ 124/22) and used for Western blotting (WB), ELISA and leukocyte adhesion assays. Confluent EC were stimulated with UTP (1–300 μM) for 5h and/or with ATP 500 μM (30 min) in the presence or absence of antagonists or inhibitors (30 min pretreatment). Then, EC were co-incubated with isolated mononuclear cells (MC) (30 min), and then washed. Four fields/well were imaged to count the number of adherent MC (400X). Data were expressed as mean and SEM. **Results:** UTP (1–300 μM) increased MC adhesion to EC in a concentration-dependent manner in control and infected groups, but the maximal effect was higher in the infected (12.4 ± 0.6 cells/field) than in the control group (6.5 ± 0.3 cells/field, P < 0.001, Student's t test, n= 5-6). Similar data were observed with 500 μM ATP (P < 0.01). Both the P2Y₂R selective antagonist (ARC-118925 10 μM) or P2X₇R antagonist (A740003 50 nM) blocked the respective agonist's effect. In both groups, phospholipase C inhibitor (U73122 1 μM), intracellular Ca²⁺ chelator (BAPTA-AM 3 μM), Src inhibitor (SU6656 5 μM) and VCAM-1 or ICAM-1 antibodies (1: 50) impaired the UTP (100 μM) effect, corroborating the role of canonical and non-canonical P2Y₂R signaling to leukocyte adhesion (P < 0.01). Of note, in the infected group U73122, BAPTA or VCAM-1 antibody not only blocked the UTP effect, but also decreased the basal MC adhesion (*i.e.* in the absence of agonist) suggesting that these EC have an enhanced Ca²⁺-dependent VCAM-1-mediated pro-adhesive phenotype (P < 0.001). However, WB data showed similar levels of P2Y₂R expression. Regarding the putative receptors' crosstalk, in the infected group, the P2Y₂R and P2X₇R co-activation (100 μM UTP + 500 μM ATP) stimulated higher MC adhesion and IL-1β release than each agonist alone (P < 0.01). While in the infected group caspase inhibitor (z-VAD-FMK 20 μM) and NF-κB inhibitor (PDTC 3 μM) reduced the effect of ATP, UTP or both agonists, in the control group both inhibitors did not diminish MC adhesion. Moreover, the EC treatment with IL-1β (3 pg/mL) stimulated MC adhesion which was blunted by EC pretreatment with VCAM-1 antibody. Taken together, current data suggest that endothelial P2Y₂R/P2X₇R crosstalk could be involved with mesenteric inflammation during schistosomiasis, with a putative role of inflammasome activation, IL-1β release and VCAM-1 expression. **Conclusion:** The mesenteric endothelial P2Y₂R/P2X₇R co-activation increases leukocyte adhesion and downstream receptors signaling inflammasome-dependent releases IL-1β. **Acknowledgments:** FIOCRUZ (RJ), CNPq, CAPES, FAPERJ.

01.004 Effects of Epigallocatechin-3-Gallate on Gluconeogenesis Key-Enzymes and on Mitochondria: Potential Mechanisms Underlying its Hypoglycemic Effects. Bonetti CI, Correia BL, Souza GH, Nakanishi ABS, Comar JF, Bracht L Lab. of Hepatic Metabolism. UEM, Maringá, PR, Brazil

Introduction: Epigallocatechin-3-gallate (EGCG) is the main compound of green tea with well-described antioxidant, anti-inflammatory, and tumor-suppressing properties. In addition, several studies demonstrated its anti-obesity and anti-diabetic effects. Nonetheless, the exact molecular mechanisms underlying these effects are not well understood. **Objectives:** To investigate the direct effects of EGCG on the activities of gluconeogenesis key-enzymes and on the energy metabolism of rat liver isolated mitochondria. **Methods:** Male albino Wistar rats (200±30 g) were used. All procedures were approved by the Ethics Committee of Animal Experimentation of the University of Maringá (protocol n.2535301019). Rat liver mitochondria and microsomes were isolated by differential centrifugation and incubated with EGCG at different concentrations (10-1000 µM). **Results:** EGCG significantly reduced the activity of key gluconeogenic enzymes, namely glucose-6-phosphatase and pyruvate carboxylase. Otherwise, the activity of phosphoenolpyruvate carboxykinase was stimulated by EGCG. Mitochondrial basal respiration was stimulated by EGCG when glutamate + malate (complex I substrate) and succinate+ rotenone (complex II substrate) were used. In the presence of exogenously ADP (State III), mitochondrial respiration was significantly inhibited by EGCG, when succinate was used as substrate. State IV respiration (after ADP depletion) was stimulated by EGCG. As a consequence of both State III inhibition and State IV stimulation, the respiratory control (RC) was inhibited, especially when succinate was used as substrate. Membrane-bound enzymatic activities of the mitochondrial complexes I, II and IV were measured using disrupted mitochondria. Both complexes I and II activities were decreased by EGCG. On the other hand, complex IV was not affected by EGCG. ATPase activity measurements were done in intact mitochondria in the presence and absence of the uncoupler 2,4-dinitrophenol and in freeze-thawing disrupted mitochondria. There was a stimulus of ATPase activity in intact mitochondria at low EGCG concentrations. However, ATPase activity was reduced at higher concentrations. Reduction of ATPase activity was also observed in uncoupled and disrupted mitochondria. Mitochondrial membrane integrity was accessed by NADH-driven respiration of intact mitochondria, which was substantially increased by EGCG. Additionally, EGCG decreased real-time mitochondrial ROS production at relatively low concentrations. **Conclusion:** EGCG directly inhibits two important key-enzymes of the gluconeogenic pathway. In addition, EGCG acts both as a mitochondrial inhibitor of complexes I and II and as an uncoupling agent of oxidative phosphorylation. The uncoupling effect can be partially related to the loss of mitochondrial membrane integrity, which is probably not associated to membrane lipoperoxidation. The inhibition of gluconeogenic key-enzyme activities and the impairment of mitochondrial ATP synthesis can be two mechanisms related to the hypoglycemic action of EGCG. **Financial Support:** Coordenação de Aperfeiçoamento de Pessoal de Nível Superior (CAPES).

01.005 Evaluation of the *in vitro* Antioxidant Effect of New Compounds LQFM348 and LQFM354 in the Human Neuronal SH-SY5Y Cell Line. Campos HM¹, Ferreira PYO¹, Pagliarani B², Menegatti, R³, Ghedini PC¹ Tarrozi A² ¹UFG, Dept of Pharmacology, ²University of Bologna, Dept for Life Quality Studies, ³UFG, Faculty of Pharmacy

Introduction: Oxidative stress is involved in the pathophysiology of several health disorders, including neurodegenerative diseases (NDs), leading to membrane peroxidation, protein and DNA oxidation, and the activation of neuronal death pathways. In the search for a new drug prototype with potential use for treatment or prevention of NDs, LQFM348 and LQFM354 piperazine derivatives were synthesized in order to emphasize their antioxidant characteristics. Thus, in this work, the first *in vitro* antioxidant tests with these molecules were evaluated, aiming to provide information to support further studies. **Objective:** Evaluate the *in vitro* antioxidant and neuroprotective effects of LQFM348 and LQFM354 in the human neuronal SH-SY5Y cell line. Human neuronal SH-SY5Y cells were routinely grown in Dulbecco's Modified Eagle Medium with phenol red supplemented with 10% fetal bovine serum, 2 mM L-glutamine, 50 U/mL penicillin, and 50 µg/mL streptomycin at 37 °C in a humidified incubator with 5% CO₂. The SH-SY5Y cells were treated with the new compounds LQFM348 or LQFM354 and with the oxidative stress inducers as hydrogen peroxide (H₂O₂), tert-butyl hydroperoxide (t-BuOOH), iron sulfate (FeSO₄). The neuronal viability was assessed using the tetrazolium salt colorimetric assay; the ROS formation was evaluated with fluorescent probe H₂DCF-DA and the glutathione levels was measured using monochlorobimane. The plaques were read at multilabel plate reader (VICTOR™ X3, PerkinElmer, Waltham, MA, USA). The antioxidant activity and neuroprotection results were expressed in triplicate as a percentage + standard error of mean, comparing with the negative control cells or positive control cells. **Results:** LQFM348 and LQFM354 decreased the oxidant activity of t-BuOOH in 92.4 ± 2.35% and 94,8 ± 1.94%, respectively. In the same way, both molecules decreased ROS formation induced by H₂O₂ in 71.32 ± 6.50% and 84,3 ± 2.18%, respectively. Also, the LQFM348 and LQFM354 were able to reduce the ROS formation induced by H₂O₂ + FeSO₄ in 61 ± 1.38% and 83 ± 2.51%, respectively. In addition, the LQFM348 and LQFM354 reduced the neuronal death promoted by H₂O₂ in 44,4 ± 1.99% and 35,1 ± 5.97%, respectively. At last, the glutathione (GSH) levels were increased by the treatment with LQFM348 in 55.3 ± 2.45% and the treatment with LQFM354 does not change the GSH levels (2.47 ± 0.62%). **Conclusion:** These preliminary results showed the *in vitro* protection of LQFM348 and LQFM354 against cell damage promoted by oxidative stress. Thus, the findings corroborate the need to perform the *in vivo* effect evaluation of these molecules on experimental models associated with brain diseases and oxidative stress. **Financial Support:** CAPES and CNPQ

01.006 The Influence of Adenosine Receptor Antagonism on PDE4 and PDE8 Inhibitors Induced Airway Smooth Muscle Relaxation. Satori NA, Pacini ESA, Godinho RO. Unifesp-EPM, Div. Cellular Pharmacology, Dept of Pharmacology, São Paulo, SP, Brazil

Introduction: Elevation of intracellular cAMP is the main mechanism by which β_2 adrenoceptor (β_2 -AR) agonists and phosphodiesterase (PDE) inhibitors induce relaxation of airway smooth muscle (ASM). Previous studies from our lab have shown that the β_2 adrenoceptor agonists formoterol and fenoterol also increase the extracellular concentration of cAMP, which is converted into the bronchoconstrictor nucleoside adenosine by ectoenzymes (Pacini et al., J. Pharmacol. Exp. Ther., 366, 75, 2018; Biochem. Pharmacol., 192, 2021). The functional relevance of the extracellular cAMP-adenosine signaling was demonstrated by the ability of the adenosine receptor antagonist CGS-15943 to potentiate β_2 -AR-induced ASM relaxation (Pacini et al., 2018). Assuming that PDE 4 and PDE 8 are the predominant isoforms expressed in the ASM, in the present study, we evaluated the effect the selective inhibitors of PDE4 (roflumilast), PDE4b (A33) and PDE8 (PF-4671536) on the relaxation of rat tracheas and the impact of adenosine receptor antagonist CGS-15943 the PDE inhibitors-induced ASM relaxation. **Methods:** Isolated tracheal segments from adult male Wistar rats were pre-contracted with carbachol EC_{50} and relaxed with cumulative concentrations of salbutamol, roflumilast, A-33 and PF-4671536 in the presence or absence of 20 μ M CGS-15943 (n=5-6). The isometric contraction of these tracheal segments was measured using force transducer (FT.03; Grass Technologies, West Warwick, RI) and the relaxation responses were expressed as percentages of CCh EC_{50} contraction force (CCh EC_{50} = 0.27 \pm 0.03 μ M, n=23). **Results:** The β_2 -AR agonist salbutamol and PDE4 inhibitor roflumilast induced concentration-dependent relaxation of tracheas (salbutamol pEC_{50} = 6.93 \pm 0.10, E_{max} = 60.5 \pm 1.6%, n=6; roflumilast pEC_{50} = 4.80 \pm 0.13, E_{max} = 116.6 \pm 9.4%, n=6), while the PDE4b inhibitor A-33 and PDE8 inhibitor PF-4671536 induced about 20 to 30% relaxation of rat tracheas of only 21.64 \pm 5.67% (n=5) and 30.17 \pm 3.25% (n=6), respectively. Pre-incubation of tracheas with CSG-15943 increased by 3-fold the potency of salbutamol and by 37% the maximum relaxation promoted by salbutamol. CSG-15943 also increased the maximum relaxation of both A-33 (from 21.64 \pm 5.67% to 47.56 \pm 2.53%; n=5) and PF-4671536 (from 30.17 \pm 3.25% to 65.44 \pm 1.61%; n=6). In contrast, the adenosine receptor antagonist did not change the relaxation curve of roflumilast. **Conclusion:** The interference of CSG-15943 on salbutamol-induced relaxation supports previous studies from our lab that showed that activation of β_2 -AR with formoterol results in cAMP efflux and extracellular formation of adenosine, which in turn attenuates β_2 -AR-induced ASM relaxation. The lack of CSG-15943 effect on roflumilast-induced relaxation may be related to a low efflux of cAMP induction by this PDE4 inhibitor. However, A-33 and PF-4671536 evoked reduced relaxation response which was increased by inhibition of adenosine receptors with CSG-15943. The mechanisms responsible for the differences in responses to selective PDE4 and 8 inhibitors are being investigated in our laboratory. **Financial Support:** CAPES, CNPq 310498/2019-8 and Fapesp 18/21381-6.

01.007 The Gasotransmitter Hydrogen Sulfide (H₂S) Potentiates the *ex vivo* Secretion of α -Amylase Induced by Both Adrenergic and Cholinergic Agonists on Murine Salivary Glands. Oliveira-Alves MC, Almeida ARB, Teixeira SA, Costa SKP, Muscará MN. USP, Dpt of Pharmacology, Lab. of Biochemical Pharmacology of Free Radicals, Inflammation and Pain, Brazil

Introduction: Although the physiological relevance of H₂S has been recognized in several tissues and organs¹, its participation on salivary secretion is not definitely established, yet. We thus decided to investigate the presence and activity of H₂S-synthesizing enzymes in murine submandibular/sublingual (SM/SL) glands, as well as the effects of H₂S-donor compounds on both spontaneous and stimulated salivary activity. **Methods:** All the animal procedures were approved by the local CEUA (protocol 81/2017). Salivary SM and SL glands from female adult Swiss mice (6 wk-old, 30±3 g) were excised and the H₂S production by their homogenates was determined by the lead sulfide method in the absence or presence of the H₂S-producing enzyme inhibitors propargylglycine (PAG), b-cyanoalanine (BCA) and aminoxyacetic acid (AOAA). The expression of the H₂S-generating enzymes (CBS, cystathionine-b-synthase; CSE, cystathionine-g-liase and 3MST, 3-mercaptopyruvate sulfurtransferase) was assessed by Western blotting. Spontaneous and muscarinic (carbachol) or adrenergic (isoproterenol) stimulation of salivary secretion was analyzed *in vitro* by measuring the activity of released α -amylase, using 2-chloro-4-nitrophenol-d-maltotriose as substrate. The effects of the H₂S-donors (NaHS and Lawesson's reagent) and the H₂S-producing enzyme inhibitors (PAG and AOAA) were also studied. **Results:** Murine SM/SL gland homogenates produce H₂S, which is completely inhibited by AOAA but only partially by PAG or BCA. Western blotting analysis revealed that these glands express CSE and 3MST, but not CBS; these results were confirmed by semi-quantitative analysis by RT-PCR analysis. Carbachol-stimulated α -amylase secretion was significantly inhibited by AOAA (by 40%) but not by PAG, and was strongly stimulated by low (0.1 mM) concentrations of the H₂S donor Lawesson's reagent (by 231%). The same profile of results was obtained when the glands were unstimulated or stimulated with the adrenergic agonist isoproterenol. **Conclusions:** Murine submandibular/sublingual salivary glands produce H₂S, and exogenous donors of this gasotransmitter can significantly enhance the secretion of α -amylase, mainly when stimulated by either muscarinic or adrenergic agonists, thus suggesting that H₂S can have a physiological role on the functional activity of these glands. **Reference:** ¹Gadalla MM & Snyder SH. Hydrogen sulfide as a gasotransmitter. J. Neurochem 1996;113: 14-26. **Acknowledgements:** This study was funded by the State of São Paulo Research Foundation (FAPESP) and the Brazilian National Council for Scientific and Technological Development (CNPq); MCOA was recipient of CAPES 1711182 scholarship; SKPC and MNM are recipients of CNPq (PQ) fellowships.

01.008 The Role of Alveolar Macrophages-Expressed Plet1 In Alveolar Repair After Viral Pneumonia. Pervizaj-Oruqaj L^{1,2,3}, Selvakumar B^{1,5,6}, Ferrero MR^{1,2,3,5,6}, Cohen M⁶, Fagundez C⁶, Heiner M^{1,2,3}, Malainou C^{1,2,3}, Glaser RD², Wilhelm J^{2,3,4}, Bartkuhn M², Weiss A^{3,4}, Alexopoulos I^{1,2,3}, Seeger W^{2,3,4,5,6}, Vazquez-Armendariz AI^{1,2,3}, Herold H^{1,2,3} ¹Universities of Giessen and Marburg Lung Center, Dept of Internal Medicine, German Center for Lung Research, Giessen, Germany. ²Justus Liebig University Giessen, Inst. for Lung Health, Giessen, Germany. ³Excellence Cluster Cardio-Pulmonary Institute. ⁴Universities of Giessen and Marburg Lung Center Dept of Internal Medicine, ⁵Max Planck Institute for Heart and Lung Research, Bad Nauheim, Germany, ⁶Instituto de Investigación en Biomedicina de Buenos Aires, Buenos Aires, Argentina

Introduction: Lung tissue-resident alveolar macrophages (TR-AM) are responsible for maintenance of tissue homeostasis, also promoting epithelial regeneration after lung injury. In the present work, we describe an epithelial pro-regenerative pathway mediated by the expression of Placenta-expressed transcript 1 (Plet1) by alveolar macrophages in the context of influenza virus-induced pneumonia. **Methods:** We combined high-dimensional single-cell transcriptomics, complex lung organoid modeling, *in vivo* adoptive cell transfer, and BMDM-specific gene targeting. **Results:** We identified that Plet1 expression is induced during the resolution phase of the inflammation in a subpopulation of regenerative BMDMs, termed BMDMreg, and mediates the pro-proliferative effects of BMDMreg over epithelial progenitor cells of the alveoli. This effect was also observed in human alveolar epithelial cells treated with rPLET1. In addition, we showed that Plet1 expression on BMDMreg has a protective effect over the alveoli in the context of influenza infection, as observed by induction of epithelial proliferation and reduction of alveolar leakage. Moreover, Plet1 expression in BMDMreg and the re-emerging TR-AM pool is essential for an appropriate resolution of the inflammatory process and mice survival. Finally, samples from influenza-infected patients showed an inverse correlation between total protein concentration and PLET1 concentration in BALF, and the intratracheal administration of rPLET1 attenuated viral lung injury and rescued mice from otherwise fatal disease **Conclusion:** Plet1 pathway could represent a novel strategy to recover alveolar tissue and lung function after acute viral pneumonia. **Funding:** German Research Foundation (DFG; KFO309-284237345; SFB-TR84-114933180; SFB1021-197785619; EXC2026-390649896), the German Ministry for Education and Research (BMBF, grant IPSELON), the German Center for Lung Research (DZL), the Institute for Lung Health, and the von Behring Röntgen Foundation (grant 66-LV07). Animal experiments and the use of human samples were approved by the regional authorities of the State of Hesse (Regierungspräsidium Giessen) and by the Institutional Ethics Committee at the IBioBA Institute.

01.009 Activation of β -adrenoceptor-Adenylate Cyclase System Promotes cAMP Efflux via ABCC/MRP Transporters in Rat Vas Deferens, Prostate, Bladder and Aorta. Pacini ESA, Satori NA, and Godinho RO Unifesp-EPM, Div. Cellular Pharmacology, Dept of Pharmacology, São Paulo, SP, Brazil

Introduction: 3',5'-cyclic AMP (cAMP) is a universal intracellular second messenger that is produced in response to a variety of extracellular stimuli by activation of Gs-protein-coupled receptor/adenylyl cyclase (AC) axis. In addition to its classical intracellular function, in some cells cAMP works as an extracellular "third messenger", which depends on its efflux through ABCC transporters/ multidrug resistance associated proteins (ABCC/MRP), and its extracellular conversion to 5'-AMP and adenosine by ectoenzymes (Pacini et al., *Front. Pharmacol.* 6: 58, 2015). However, the role of Gs protein-coupled receptors and MRPs on the global extracellular cAMP efflux and contents remains to be elucidated in specific tissues/cell types, such as in vascular and non-vascular smooth muscles where purinergic signaling plays important physiological and pathophysiological roles. **Methods:** Male Wistar rats (3-month-old) were euthanized and vas deferens, prostate, bladder and aorta were isolated and kept in an organ-culture incubator containing Krebs-bicarbonate buffer at 37°C in 95% air-5% CO₂. After 60 min stabilization, tissues were stimulated with 1 μ M isoproterenol (nonselective β -agonist), 1 μ M forskolin (AC activator) or vehicle (DMSO 0.01%), for 60 min in the absence or presence of 40 μ M MK-571 (ABCC/MRP inhibitor). Then, the incubation media were collected and the extracellular cAMP concentration was determined by competitive TR-FRET immunoassay as previously described (Pacini et al., *Biochem. Pharmacol.* 192: 114713, 2021). All values were expressed as mean \pm S.E.M of "n" independent experiments. **Results:** Basal levels of extracellular cAMP were similar in vas deferens, prostate, bladder and aorta, ranging from 7.30 to 8.10 nanomolar (n=8-17) (vas deferens=8.10 \pm 0.62; prostate= 7.34 \pm 0.86; bladder= 8.09 \pm 1.43; aorta= 7.30 \pm 0.57). In all analyzed tissues, stimulation of β -adrenoceptors with isoproterenol increased 2- to 13-fold the basal levels of extracellular cAMP, whereas forskolin increased 2- to 11-fold the extracellular cyclic nucleotide (n=6-28). In addition, pretreatment of tissues with ABCC/MRP inhibitor MK-571 completely prevented the increment of extracellular cAMP levels induced by isoproterenol or forskolin (n=5-10). **Conclusion:** Our results provide evidence for a link between the β -adrenergic receptor/G protein signaling and ABCC/MRP transporters-mediated cyclic AMP efflux in vas deferens, prostate, bladder and aorta. Since the effect of isoproterenol is mimicked by forskolin, it seems that cAMP efflux is a universal mechanism triggered by high levels of intracellular cAMP. The physiologic and pharmacology role of the extracellular cAMP are under investigation in our lab. **Financial Support:** CAPES, CNPq 310498/2019-8 and Fapesp 18/21381-6. **Animal Ethics Committee:** CEUA #8359060315 and #9987150714

01.010 Thromboxane A2 Receptor (TP) Antagonism Improves Glucose Homeostasis and Lipid Profile in Obese Mice. Araújo RB, Cruz AP, Gonçalves TT, Salerno G, Leiria LO FMRP-USP, Lab. of Research in Metabolic Diseases, Pharmacology Department

Introduction: Thromboxane A2 (TXA2) is a prostanoid capable of generating biological responses in different tissues and cells through the agonism of TP receptor (*Tbxa2r*). TXA2-TP axis contribute to adipose tissue (AT) insulin resistance through boosting M1-macrophage mediated AT inflammation under obesity conditions. Therefore, rationally targeting TXA2 pathway may ameliorate obesity and related metabolic disorders. **Methods:** To test whether TXA2 antagonism could be an efficient pharmacological tool for treating diabetes, we performed an oral treatment with TP antagonist seratrodast for 10 days, using a dosage of 15 mg/kg, daily, which was estimated through the conversion of the dosage used in humans for the treatment of asthma (in Asia). We used oral metformin as a positive control (200 mg/kg) and the vehicle group received oral PB. At the day 4 of treatment, we performed a glucose tolerance test (GTT), while in the day 7 we did an insulin tolerance test (ITT). We also monitored fasting glucose and body weight during treatment. By the end of the treatment, we collected serum and tissues for further biochemical/molecular studies. **Results:** We found the treatment with TP antagonist significantly reduced body weight while improved glucose tolerance, without modifying the insulin sensitivity. Remarkably, oral treatment with TP antagonist reduced blood glucose, LDL and triglycerides, in addition to reduce the expression of *de novo* lipogenesis genes in the liver. *In vitro*, we found that the TP antagonist promoted glucose uptake into murine brown adipocytes, increased glucose-induced insulin secretion in isolated murine beta-cells and blocked glucagon-induced gluconeogenesis in human primary hepatocytes. **Conclusion:** Treatment with TP antagonist showed significant improvement in glucose and lipid metabolism *in vivo*, while our *in vitro* data indicated that its beneficial effects may happen in a cell-autonomous manner by regulating glucose metabolism in beta-cells, adipocytes and hepatocytes. **Financial Support:** CAPES, FAPESP.

01.011 Organotypic hippocampal culture as a model to study the interaction of glioblastoma with the brain microenvironment. Nóbrega AHL¹, Prado APS¹, Pimentel RS¹, Santos ARC², Valério RR², Martins MA¹, Frozza RL², Bernardi A¹. ¹IOC-Fiocruz, Lab. of Inflammation, Rio de Janeiro, Brazil; ²IOC-Fiocruz, Lab. on Thymus Research, Rio de Janeiro, Brazil

Glioblastoma (GBM) is the most common and aggressive primary brain tumor in adults, with minimally prolonged survival afforded by the current treatment that includes surgery, radiotherapy, and chemotherapy with temozolomide. [2,7] The development of new therapeutic strategies remains critical because of the poor prognosis, ineffective therapies, and recurrence [1]. Given the growing knowledge that GBMs are complex and composed of neoplastic and non-neoplastic cells, which may individually contribute to tumor formation and progression as well as to the treatment, understanding the tumor microenvironment can open new opportunities for the development of more effective therapeutic alternatives [3,6]. The present work aims to establish a model to investigate the interaction of the GBM with its microenvironment, focusing on the role of microglia. **Methods:** Organotypic cultures of hippocampus from *Wistar* rats (6-8 days old) [4,5,8] were used as non-tumor tissue and, after the 14th day of culture, were exposed to semi-confluent cells of the C6 GBM cell line for 1 h, 3 h, 6 h, 12 h or 24 h. The inflammatory mediators (TNF- α , IL-4, IL1 β , IL-6, and IL-10) released in the culture medium were evaluated by ELISA. Markers of glial alterations that could be related to neuroinflammation were evaluated in organotypic cultures by *Western blotting*. To investigate the involvement of microglia, minocycline (10 μ M) or PLX3397 (10 μ M) were used to inhibit or deplete these cells, respectively. Additionally, tumor stem cell markers (Nestin and CD133) were evaluated in GBM cells after exposure to organotypic cultures. All procedures were approved by the Animal Ethics Commission of the Oswaldo Cruz Institution (CEUA IOC-License L-011/2022). **Results:** A significant increase in TNF- α , IL-4, IL1 β , IL-6, and IL-10 cytokines levels were observed in the medium after 3 or 6 h of contact between C6 and organotypic cultures. Interestingly, we observed a significant increase of all cytokines in the hippocampal slices exposed to C6 comparing to slices without C6 contact. On the other hand, the C6 cells didn't show difference in cytokines levels, suggesting that the increase of cytokine production is derived from the non-tumoral tissue. *Western blotting* analyses showed an increase in Iba-1 immunoccontent in hippocampus slices, indicating microglial activation after contact with GBM cells. Preliminary results using minocycline and PLX3397 suggest that microglia are, at least in part, the cells responsible for the release of these cytokines and, consequently, for the neuroinflammation. Experiments are in progress to confirm this hypothesis as well as to evaluate the expression of tumor stem cell markers in GBM. **Conclusion:** Taken together, these results suggest that the contact between organotypic hippocampal slice cultures and C6 GBM can provide hints of how the microenvironment and the molecular interactions between the glioma cells and the healthy tissue drives neuroinflammation, open new roads in the developing innovative therapies to GBM. **Financing sources:** CNPq, CAPES, and FAPERJ (Grants #E-26/201.419/2021 and # E-26/202.807/2019). **Reference:** [1]Aldape, K. *Nat. Ver. Clin. Oncol.*, v. 16, p. 509, 2019. [2] Behin, A. *Lancet*, v.361, n. 9354, p. 323, 2003. [3]Charles, NA. *Glia*, v. 60, n. 3, p 502, 2012. [4] Frozza, RL. *Neurochemical Research*, v. 34, n.2 p. 295, 2009. [5] Gogolla, N. *Nat. Protocols*, v.1, n.3, p. 1165, 2006. [6] Hambadzumyan, D. *Nat Neurosci.*, v.19, n.1, p.20, 2016. [7] Sathornsumetee, S. *Cancer*, v. 110, n.1, p. 13, 2007. [8] Stoppini, L. *Journal of Neurosci. Methods*, v.37, n.2, p. 173, 1991.

01.012 Examining PARP1 Expression in MPP+ Induced SH-SY5Y Model of Dopaminergic Neuron Death. Silva LDS¹, Ferrari SSAR¹, Gomes, GMO¹, Duarte CDM¹, Schlemmer F¹, Xavier MAE¹, Titze-de-Almeida S¹, Titze-de-Almeida R¹. ¹ UnB Research Center for Major Themes, Division of Parkinson's Disease

Introduction: PARP1 (poly-(ADP ribose polymerase 1) has been implicated in dopaminergic neuron death in Parkinson's disease (PD), through the parthanatos pathway, which generates PAR polymers that enhance alpha-synuclein accumulation. Previous research has shown that PARP1 expression is regulated by microRNA 7 (miR-7), which is downregulated in the striatum of a toxin-based PD model. This study aimed to investigate PARP1 expression in SH-SY5Y dopaminergic cells injured by the neurotoxin MPP+. **Methods:** we cultured SH-SY5Y cells in DMEM media supplemented with fetal bovine serum (FBS), GlutaMAX, and an antibiotic/antimycotic solution and exposed them to MPP+ for 24 hours. Cell viability was assessed using an MTT assay after MPP+ exposure. We observed a dose-dependent decreases in cell viability (77.1%, 60%, and 43.3%) with increasing MPP+ concentrations (0.5mM, 1.0mM, and 2mM). PARP1 expression was analyzed using RT-qPCR, after RNA purification with the RNeasy Plus Mini kit (Qiagen) and reverse transcription using random primers (SuperScript First-Strand Synthesis System for RT-PCR, Invitrogen). The qPCR reaction was performed with Fast SYBR Green Master Mix (Applied Biosystems) and primers for PARP1 and the calibrator GPBP1. **Results:** our data revealed a 0.6-fold decrease in PARP1 expression in SH-SY5Y cells exposed to 1mM MPP+ for 24 hours ($p=0.0036$, Student's t test). **Conclusion:** further research, such as determining PARP1 protein expression, effects of PARP-1 inhibition on cellular fate, and quantification of miR-7, would further elucidate PARP1's role in dopaminergic cell death induced by MPP+. **Financial Support:** Fundação de Apoio à Pesquisa do Distrito Federal - FAP-DF; Conselho Nacional de Desenvolvimento Científico e Tecnológico (CNPq); Coordenação de Aperfeiçoamento de Pessoal de Nível Superior (CAPES); Ministério da Educação (MEC) - TED MEC n.9249. **Affiliation:** Research Center for Major Themes at UnB – Division of Parkinson's Disease. Centro de Pesquisa em Grandes Temas da Universidade de Brasília - UnB/FAV, Campus Darcy Ribeiro, Instituto Central de Ciências, ASS-128.

01.013 trans-Cinnamic Acid Regulates Inflammatory Response and TGF- β 1-Induced Epithelial-Mesenchymal Transition in Airway Epithelium. Fidelix MSP, Santana JR, Ferreira EGA, Barros ABB, Silva JP, Barreto EO UFAL, Lab. of Cell Biology, Brazil

Introduction: Pulmonary fibrosis is a chronic lung disease caused by progressive deterioration of lung tissue, in which elevated levels of pro-inflammatory mediators, such as IL-8, are associated with severity of pulmonary dysfunction. In response to long-term inflammation, aberrant tissue repair and epithelial-cell-to-mesenchymal-cell transition (EMT) triggers the subsequent progression of pulmonary fibrotic diseases. It is recognized that fibrotic diseases have a great impact on populational health. In addition, high levels of IL-8 have been reported as enhancer of EMT. To date, there is yet no cure for fibrosis and the available drugs are not efficient. In the attempt to search for new molecules with therapeutic potential, natural products are promising candidates. The trans-cinnamic acid is an isoform of cinnamic acid widely distributed in nature, and its potential effects on production of IL-8 and EMT is not clear in the scientific literature until now. Here, we aimed to evaluate the *in vitro* the effect of *trans*-cinnamic acid on synthesis of IL-8, and morphological and molecular aspects associated to the epithelial-mesenchymal transdiferentiation on human alveolar epithelial cell line A549 cells. **Methods:** A549 cells were grown in DMEM medium supplemented with 2% fetal bovine serum, 1% penicillin/streptomycin, 2 mM L-glutamine and maintained in a humidified incubator at 37 °C with 5% CO₂. The cytotoxic effect of *trans*-cinnamic acid (TCA, 1, 3, 10, 30, 100 and 300 μ M) was determined by MTT assay. A549 cells were pretreated with TCA (1, 10 or 30 μ M) 1 h prior to stimulation with 50 ng/mL TNF- α , and 24 h later, the IL-8 secretion was assessed using ELISA. In another set of experiments, A549 cells were stimulated with TGF- β (10 ng/mL) with or without TCA (10 ng/mL) co-treatment and the EMT phenotypic and functional features were evaluated 24h later. Morphological alterations and migratory response of TGF- β -stimulated A549 cells were evaluated by light microscopy and scratch assay, respectively. The immunofluorescence staining was performed to confirm the expression of fibronectin in TGF- β -stimulated A549 cells. Statistical differences were significant at $p < 0.05$ analysed by one-way ANOVA and Tukey's test. **Results:** Our results revealed that TCA exhibited no cytotoxic effects to any of concentrations tested after 24 h exposure. Analysis of culture supernatants showed that TNF- α -stimulated cells exhibited high levels of IL-8 (about 2-fold, $P < 0.001$) compared to non-stimulated cells. Our data showed that treatment with 1 and 30 μ M TCA inhibited, around 30% and 26%, respectively, the IL-8 secretion in TNF- α -stimulated cells. We observe that TGF- β induced changed in the morphology from epithelial-like to elongate fibroblast-like morphology, increased the expression of fibronectin (about 1.5-fold, $P < 0.01$) and increased cell migration (about 2.3-fold, $P < 0.01$). Treatment with TCA (30 μ M) caused reversion of the mesenchymal phenotype back to the epithelial phenotype. Furthermore, TGF- β -induced cell migration was inhibited by TCA treatment in approximately 68%. Notably, the elevated levels of TGF- β -evoked fibronectin production were suppressed by TCA (30 μ M). **Conclusion:** Our results suggest that TCA can inhibit IL-8 secretion in TNF- α -stimulated cells and TGF- β -induced EMT, which could serve as a promising candidate to treatment of fibrosis. **Financial Support:** CNPq, CAPES, BioproFarBA and FAPEAL.

01.014 ***In vitro* Aging Affects Epithelial Renal Cells Phenotype.** Barros GMO, Araújo LS, Almeida e Silva AC, Bagri KM, Mermelstein CS, Quintas LEM ICB-UFRJ Rio de Janeiro, Institute of Biomedical Sciences, Brazil

Introduction: Cellular aging is a degenerative and progressive process that affects all cells in the body. The loss of the body's ability to repair and regenerate tissues results in phenotypical transformations, leading to susceptibility to various diseases. As a consequence, modifications in pharmacological response may occur. The kidneys are among the most severely affected organs. A change in physiological function, such as the decrease in renal filtration rate and the accumulation of senescent cells in hypertensive patients, promotes the epithelial-mesenchymal transition (EMT), resulting in renal fibrosis. At the basolateral portion of the renal tubule epithelial cells, the transmembrane protein Na⁺/K⁺-ATPase (NKA) is an ion transporter as well as a signal transducer through protein-protein interactions when bound to selective ligands known as cardiotonic steroids (CTS). Previous results from our group have shown that bufalin, a CTS, evokes changes consistent with EMT renal proximal tubular LLC-PK1 cells. Interestingly, this phenomenon happens to higher passage (P>80), but not lower passage (P<40) cells, suggesting an increased cellular sensitivity to bufalin due to *in vitro* aging. Our objective was to evaluate phenotypical and pharmacological differences between the two cell populations. **Methods:** LLC-PK1 (porcine proximal renal tubule) cells of lower (P<40) and higher (P>80) passages were used. Cell proliferation and viability were evaluated by Trypan blue-free cells counting to 72 h in Neubauer chamber and MTT test, respectively. Cell migration/motility was evaluated by the wound healing method. NKA activity was assessed by the colorimetric detection of inorganic phosphate using Fiske and Subbarow technique. The protein expression of NKA α 1 isoform, intracellular signaling (ERK1/2, Akt, GSK3) and adhesion molecules (β -catenin, E-cadherin, occludin and vinculin) was evaluated by Western blot. Student's t test (significance: p<0.05). The data are expressed as mean \pm SEM. **Results:** P>80 cells had a greater proliferative rate and viability (1.7- and 1.5-fold higher after 72 h, respectively; p<0.05, n=5-6) compared to P<40 cells. P>80 migration rate was 2.2-fold greater than P<40 after 48 h (p<0.05, n=10). NKA activity (in μ mol Pi/mg/h: 7.4 \pm 1.2 P<40 vs 6.7 \pm 1.3 P>80; n=11) and α 1 expression were similar between both groups. ERK1/2 was 2.2-fold more active in P>80 (p<0.05, n=4), but not Akt or GSK3. The expression of adhesion proteins β -catenin, occludin and vinculin was comparable between the two groups while E-cadherin expression was very high (8.4-fold) in P>80 (p<0.05, n=5). **Conclusion:** Our findings suggest that LLC-PK1 cells from various *in vitro* passages exhibit distinct phenotypes. The enhanced proliferation, viability, and motility observed in P>80 cells might be attributed to enhanced ERK1/2 activity. On the other hand, the much higher expression of E-cadherin in P>80 is difficult to conciliate with more efficient migration, although other adhesion molecules had similar expression. Further experiments are under way to evaluate cell localization of signaling and adhesion molecules as well as the effect of bufalin on these parameters. **Financial Support:** PIBIC/UFRJ, CAPES, FAPERJ and CNPq.

02. Neuropharmacology

02.001 Effects of the Poloxamer P188 and the Dispersion P188 and Hydroalcoholic Extract of Propolis in Mice Submitted to Bilateral Occlusion of the Common Carotid Arteries. Candido G¹; Kohara NAN¹; dos Santos RS²; Bruschi ML²; Milani H¹; de Oliveira RMW¹. ¹UEM Maringá, Lab. of Pharmacology and Therapeutics, Brazil; ²UEM Maringá, Lab. of Research and Development of Drug Delivery Systems, Brazil

Introduction: Cerebral ischemia (CI) represents an important cause of disability and mortality in the world population, in addition to having a great negative impact on the costs of health systems³. Pharmacological treatments for the acute and chronic sequels of CI are still scarce. Extracts obtained from propolis have been used as healthy food and for the treatment of several cerebral diseases, including CI¹, Parkinson Disease⁴ and Alzheimer Disease⁵. Therapeutic properties of propolis include anti-inflammatory, antioxidant, and neuroprotective actions. However, the extract of propolis has low solubility in water. The molecular and adsorption properties of nonionic triblock co-polymer poloxamer 188 (P188) has been utilized in many pharmaceutical applications such as emulsion formulation². To solve the problem of low solubility of hydroalcoholic extract of propolis (HEP) in water, P188 was used as vehicle, to form a dispersion of HEP in P188 (P188/HEP). The aim of this study is to evaluate the effect of P188 as vehicle and the dispersion formed by P188/HEP. P188 has been demonstrated to have a neuroprotective effect, therefore, it is intended to first investigate the effects of P188 by itself in mice from the SHAM group, and after investigating the P188/HEP dispersion in mice submitted to bilateral occlusion of the common carotid arteries (BCCAO), a model that has been used to mimic conditions of transient CI. **Methods:** All the procedures were approved by the Ethical Committee of State University of Maringá (CEUA nº 3943160921). Male C57BL/6 mice were subjected to BCCAO for 20 minutes. Animals from the SHAM group underwent the same surgical procedures excepting for occluding the carotid arteries. The present study consisted of two experiments. First, to investigate the effect of P188: SHAM (without treatment) and SHAM + P188 (vehicle). Second, the ischemic animals were divided into four experimental groups, to evaluate the effect of the dispersion of HEP in P188 (P188/HEP), with different concentrations of the HEP: (1) BCCAO + P188 (vehicle), (2) BCCAO + P188/HEP 50 mg/kg, (3) BCCAO + P188/HEP 100 mg/kg and (4) BCCAO + P188/HEP 150 mg/kg. The treatment was performed by gavage during 7 days after reperfusion. The animals, in both experiments, were evaluated using a behavioral test battery during 15 days. Motor, cognitive and emotional functions were registered in the open field (OF) and elevated zero maze (EZM), day 7, and tail suspension test (TST), day 15. Data were analyzed by the Student t-test or ANOVA followed by Tukey's *post hoc* test. **Results:** SHAM + P188 mice exhibited decreased anxiety-like behaviors in the OF, increase in the time expended in the center of the, as compared with SHAM (without treatment) group. The treatment of BCCAO mice with the dispersion P188/HEP 150 mg/kg, resulted in increased the time expended in the open arm of EZM, as compared to BCCAO + P188 group. Furthermore, the treatment with P188/HEP 150 mg/kg decreased despair-like behavior in the TST, indicated by an increased in the latency and a decreased in the immobility time, when compared with BCCAO + P188 group. **Conclusion:** These findings suggest that short-term treatment with the P188/HEP dispersion, triggered protective mechanisms that might be involved in functional improvements in mice with BCCAO. **Acknowledgments:** CAPES, CNPq, UEM. **References:** ¹Bazmandegan, G. *Biom. & Pharm.*, v. 85, p. 503, 2017. ²Bodratti, A.M. *J. Funct. Biomater.*, 9(1), 2018. ³Dos Santos, L. B. *Braz. Jour. of Develop.*, v. 6, p. 2749, 2020. ⁴Gonçalves, V. *Nutrients*, v. 12, p. 1551, 2020. ⁵Zawia, N. H. *Free Rad. Biol. and Med.*, v. 46, p. 1241, 2009.

02.002 Autophagy and Brain Ischemia: Effects of Cannabidiol. Kohara NAN, Splendor MC, Chinen LY, Meyer E, Bonato JM, Oliveira RMMW, Milani H UEM, Lab. of Cerebral Ischemia and Neuroprotection, Maringá, PR, Brazil

Introduction: Cerebral ischemia is a condition in which cerebral blood flow is interrupted, it can be focal when a clot obstructs a cerebral vessel preventing the passage of blood to a region of the brain, or global, when the entire blood supply to the brain is blocked. Patients who survive cerebral ischemia may develop cognitive deficits, sensory and motor impairments that compromise their quality of life. Cannabidiol (CBD), one of the main non-psychotomimetic components of the *Cannabis sativa* plant, has been shown to exert neuroprotective effects in several conditions of experimental cerebral ischemia.¹ Although the pharmacological effects of CBD are not fully understood, the mechanisms associated with neuroprotection appear to involve reducing oxidative stress and neuroinflammation.² Experimental evidence indicates that the neuroprotective actions of CBD may also involve autophagic processes. This work aimed to investigate whether autophagy is involved with the neuroprotective effects of CBD after bilateral common carotid artery occlusion (BCCAO) in mice, a model of global cerebral ischemia. **Methods:** Male C57BL/6 mice underwent BCCAO surgeries for 20 min or sham. This experiment was approved by the Ethics Committee of State University of Maringá (CEUA nº 2233130521). CBD (10 mg/kg), the autophagy inducer rapamycin (RAPA; 0.25 mg/kg) and the autophagy inhibitors 3-methyladenine (3-MA; 20 mg/kg) and chloroquine (CQ; 3.5 mg/kg) were administered 1 h before and 1 h, 24 h and 48 h after the surgeries. Combined injections of RAPA, 3-MA or CQ with CBD were also performed, with 10 min intervals between injections. The animals were evaluated in the open field test (OF) five days after surgery and the analyzed parameters were distance traveled, number of entries and time in the center. In the next days, the animals were evaluated in the object location test (OLT), which had intervals of 24, 4 and 1 hour between T1 and T2. And finally, twelve days after surgery, the animals were submitted in the tail suspension test (TST) which was evaluated the latency and immobility time. The OF and TST were analyzed by one-way ANOVA, and TLO results were analyzed by two-way ANOVA. Post-hoc analysis was conducted using the Tukey's multiple comparisons test. The levels of statistical significance were set as * $p < 0.05$ and ** $p < 0.01$. **Results:** In the OF, 3-MA increased locomotor activity compared to the vehicle-treated ischemic group, whereas CQ treatment decreased locomotor activity. In TLO, CBD and RAPA attenuated BCCAO-induced spatial memory deficits. Antidepressant-like effects have been observed after the administration of CBD and 3-MA. **Conclusion:** These results suggest that autophagy activation would have beneficial effects on spatial memory in ischemic mice. Interestingly, CBD and inhibition of autophagy by 3-MA results in the antidepressant-like effects observed in ischemic animals. It is possible that the antidepressant-like effects seen with CBD and 3-MA are mediated by distinct molecular mechanisms. **References:** ^[1] CHOI, S. H. *Stroke*, v. 50, p. 2640, 2019. ^[2] JURCAU, A. *Int. J. Mol. Sci.* v. 23, p.14, 2022.

02.003 Ferulic Acid-loaded Nanostructure Prevents Morphine Reinstatement: The Involvement of Dopamine System, NRF2 and δ fosb in the Striatum Brain Area of Wistar Rats. Fontoura MB¹, Milanesi LH¹, Rossato DR¹, Da Rosa JLO¹, Burger ME² ¹UFSM, Graduate Program in Pharmacology, Brazil, ²UFSM, Dept of Physiology and Pharmacology, Brazil

Introduction: Morphine is among the most powerful analgesics and pain-relieving agents. However, its addictive properties can limit their medical use because patients may be susceptible to abuse and reinstatement. Ferulic acid (FA), a phenolic phytochemical found in a variety of foods, it has been reported to exert antioxidant and neuroprotective effects; however, its low bioavailability makes its nano-encapsulated form a promising alternative. This study aimed to evaluate the protective effects of a novel nanosystem with FA on morphine reinstatement and the consequent molecular neuroadaptations in the mesolimbic region.

Methods: Male Wistar rats (approved by the Animal Ethics Committee of the Universidade Federal de Santa Maria - 7948130516-UFSM - which is affiliated to the Council for the Control of Animal Experiments (CONCEA)) were previously exposed to morphine in conditioned place preference (CPP) paradigm, and subsequently treated with ferulic acid-loaded nanocapsules (FA-Nc) or nonencapsulated FA during morphine-preference extinction. After the treatment, animals were re-exposed to one-half dose of morphine in the CPP paradigm to induce drug reinstatement. **Results:** While morphine-preference extinction was comparable among all experimental groups, as hypothesized, FA-Nc treatment prevented morphine reinstatement. Morphine exposure increased dopaminergic markers (D1R, D3R, DAT) and Δ FosB immunoreactivity in the ventral striatum, however, FA-Nc treatment decreased D1R, D3R and Δ FosB, and increased D2R, DAT and NRF2. **Conclusion:** In conclusion, FA-Nc treatment prevented morphine-reinstatement and modified the dopaminergic neurotransmission (NRF2, and Δ FosB), indicating neuroprotective and antioxidant potential in this nanoformulation. *Work supported by FAPERGS and PROAP/PRPGP/PPG-PHARMACOLOGY/UFSM*

02.004 Diacylglycerol Kinase Inhibition Attenuates Endotoxic Fever by Regulating Prostaglandin E2 Production in Rat Hypothalamus. Assis DAS, Guimaraes NC, Gomes BRB, Sousa GLS, Teixeira DMT, Souza PEN, Veiga-Souza FH. UnB, DF, Brazil

Introduction: Systemic administration of lipopolysaccharide (LPS) induces a series of brain-controlled responses, including fever. Fever is the increase in core body temperature, a nonspecific host defense response to infectious or inflammatory insults. Using high-resolution mass spectrometry-based quantitative proteomics, we have previously reported that during LPS-induced fever, there is an upregulation of diacylglycerol kinase (DGK) β and γ isoforms in the rat hypothalamus (Firmino, M. J Proteomics, v. 187, p. 182, 2018). DGK belongs to a family of lipid protein kinases that catalyze the ATP-dependent phosphorylation of diacylglycerol to phosphatidic acid (Ma, Q. Adv Biol Regul., v. 71, p. 104, 2019). However, the functional relevance of DGKs upregulation during fever is unknown. Therefore, we investigate the effects of pharmacological inhibition of DGK in a rat model of fever. **Methods:** The procedures used in this study were approved by the Ethics Committee on the Use of Animals of the University of Brasilia (n^o 23106.010488/2021-33). Wistar rats received intracerebroventricular administration of the R59949 inhibitor 30 minutes before the intravenous injection of LPS or saline and their temperature was monitored up to 5 h. Hypothalamic Prostaglandin (PG) E2 and serum cytokines levels were determined by Elisa. The formation of reactive oxygen species (ROS) was evaluated by electron paramagnetic resonance. Statistical analysis was done by two-way ANOVA followed by Tukey post-test with $p < 0.05$. **Results:** Inhibition of DGK attenuated the increase in body temperature induced by LPS, accompanied by a decrease in hypothalamic PGE2 production. The circulating levels of interleukin 6, tumor necrosis factor α and ROS were not altered by treatment with the DGK inhibitor. **Conclusion:** These results suggest that the regulation of the balance between diacylglycerol and phosphatidic acid through DGK inhibition may be an effective modulator of fever, by a mechanism that involves the reduction of hypothalamic PGE2 production. **Financial Support:** FAPDF; Capes; CNPq; DPG/UnB.

02.005 *In silico* Drug Repurposing Identifies Potential Therapeutic Candidate for Bipolar Disorder Mood States. Mezzomo G^{1 2}, Rampelotto PH^{1 2}, Rosa PH^{1 2}, Schons T¹, Ziani PR^{1 2}, Rosa AR^{1 2 3}. ¹HCPA, Lab. of Molecular Psychiatry, Porto Alegre, Brazil; ²UFRGS, PPG in Biological Sciences: Pharmacology and Therapeutics, Instituto de Ciências Básicas da Saúde, ³Dept of Pharmacology, Instituto de Ciências Básicas da Saúde, UFRGS, Porto Alegre, Brazil

Introduction: Bipolar disorder (BD) is a chronic and severe psychiatric disorder characterized by mood disturbances. Some patients experience persistent symptoms despite pharmacological treatments, leading to cognitive and functional impairment [1,2]. Precision medicine is crucial in predicting and treating patients using biomarkers and targeted drugs. Transcriptomic technologies allow the evaluation of various biological processes associated with dysfunctional gene expression present in different diseases [2]. Therefore, transcriptomics may offer valuable insights into the molecular status of BD patients [3]. Based on the analysis of transcriptomic datasets, an *in silico* approach was used in this work to identify potential biomarkers and therapeutic candidates for BP mood states. **Methods:** Data from five microarray transcriptomic datasets obtained from the Gene Expression Omnibus repository were analyzed. All datasets were obtained from peripheral blood of BP patients and compared to healthy controls. Differential expression analysis and enrichment analysis using ToppGene was conducted to identify potential biomarkers related to BD states and candidate drugs that may modulate the transcripts. Bonferroni correction was used to determine statistical significance. We examined biomarkers and drugs having a false discovery rate adjusted p-value of less than 0.05. **Results:** A total of 118 differentially expressed genes (DEGs) common to the three mood states of BD (mania, depression, euthymia) were identified. Several microRNAs were related to these DEGs, especially those related to the microRNA-30 family (including miR-30a, miR-30b, miR-30c, miR-30d, and miR-30e) and let-7 family (including let-7a, let-7b, and let-7f), which indicates that they may be promising regulators in the development of BP and potential novel serum biomarkers for the disease. Furthermore, rosiglitazone was indicated as a potential candidate for the treatment of BD, based on drug repurposing enrichment analysis. **Conclusion:** Transcriptomic dataset analysis associated with *in silico* drug repurposing approach hold promise for identifying novel biomarkers and drugs common to the three mood states of BD. This combined approach may lead to improved therapeutic strategies and outcomes for individuals with BD. **Funding:** This study was financed by CAPES, CNPq and FIPE-HCPA. **References:** [1] Grande, I. Lancet. v. 387, p. 1561–1572, 2016. [2] Islam, AM. IMU. v. 29, p. 100881, 2022.[3] [3] Perugi, G. Int Clin Psychopharmacol. v. 34, p. 189–205, 2019. [4] Barabási, A-L. Nat. Rev. Genet., vol. 12, p. 56–68, 2011.

02.006 Immobilization and Social Isolation Stress in the Juvenile Phase Cause Different Effect in Anxious-Type Behavior in Adolescent Male and Female. Barilli LA¹; Dalben MB²; Pereira GH²; de Melo SR². ¹UEM, PPG Pharmaceutical Sciences, Brazil, ²UEM, Dpt of Morphological Sciences, Brazil

Introduction: The effect of juvenile stress on behavior and brain morphology is poorly known. Animal studies have shown that these effects are directly related to the nature of the stress paradigm, and its intensity and Frequency⁽¹⁾. However, these effects varied, and were considered maladaptive in response to neonatal emotional stress, but, paradoxically, were resilient effects in response to moderate and predictable psychological stress^(2,3). In this study we evaluated the effects of two models of stress: Social Isolation and Immobilization on anxious-like behavior in juvenile male and female mice. The analyses were obtained using the elevated plus maze test (EPM) and open field test (OFT). This study aimed to verify if stress could affect the behavioral focus in the anxious-like behavior in two stress models and if any sex differences would emerge. **Methods:** All the procedures were approved by the Ethical Committee of State University of Maringá (CEUA N^o 1281250722). Male and female C57/BL mice were randomly distributed into three groups: Control (C), Immobilization Stress (IMS), and Social Isolation (SI), kept in a sector animal house under standard conditions including controlled temperature, a 12h/12h light/dark cycle, and ad libitum food and water supplied. The stress procedures occurred for 15 consecutive days, starting at 21 days of postnatal life (P21 to P35). In the Immobilization Group for 2 hours per day (11: 30 AM – 1: 30 PM) and Social Isolation group for 24 hours per day. The animals underwent the open field test (OFT) at P36 and the Elevated Plus Maze (EPM) at P37. Before exposing the animal, the apparatus was cleaned with 70% alcohol, and the tests were recorded for 5 min and subsequently analyzed according to the analysis protocols. The collected material was evaluated using the record, for OFT we used Any Maze Software with the following parameters: total distance, center entries, center time, and center distance. For EPM we use the Anxious Index⁽⁴⁾. Data were analyzed by the Student's t-test or ANOVA followed by Tukey's post hoc test. **Results:** Male mice exhibited an increase of central entries in the OFT (p=0,0468) and immobilized females showed a lower Anxious Index in the EPM (p=0,0252). None of those changes were observed in the isolated animals. **Conclusion:** These findings suggest that 15 days of social isolation stress during juvenile did not exert a significant impact on anxiety-related behavior. However, the physical stress induced by the immobilization model resulted in a significant decrease in observed anxiety-like behavior in both female and male adolescents. **Acknowledgments:** CAPES, CNPq, UEM. **References:** ⁽¹⁾ Anisman H, Neurosci. & Biobeh. Reviews. v. 28. p. 525. 2005. ⁽²⁾ de Melo, SR Dev Neurosci. v. 44,6 p. 466. 2022. ⁽³⁾ de Melo SR. Dev Neurosci. v.40(2) p.93. 2018. ⁽⁴⁾ Cohen H. Curr. Protoc. Neurosci. Unit 9.45. Chapter 9 2013.

02.007 Effect of Oubain on Marker Expression of Neural Progenitor Cells in Dental Pulp Stem Cells. Cunha JCL¹, Coelho LDS³, Farias ERA², Fonseca MFR², Neves EPFI², Oliveira LC², Silva SS², Oliveira LLR³, Lima AP³, Valadares MC³, Leite JA². ¹UFG Goiânia PPG Biological Sciences, Dpt of Pharmacology, Brazil, ²UFG Goiânia, Dpt of Pharmacology, Brazil, ³UFG Goiânia, School of Pharmacy, Brazil

Introduction: Na⁺-K⁺-ATPase (NKA) is an important enzyme for neuronal functioning, present in the plasma membrane of most eukaryotic cells and responsible for the electrochemical gradient of sodium (Na⁺) and potassium (K⁺) ions. The structure of NKA consists of three subunits: alpha (α), beta (β) and FXYD4. α is the catalytic subunit that cleaves ATP and has binding sites for Na⁺ and K⁺; β is responsible for the insertion and localization of the enzyme in the plasmatic membrane; and FXYD has a modulatory role in catalytic activity. In mammalian cells, there are four isoforms of the α subunit: α1 is found in the lung, kidney, and nerves; α2 is present in glial cells and in skeletal and cardiac muscle; α3 is found in the brain; α4 is present in sperm and testes. Cardiotonic steroids such as oubain (OUA) represent a group of compounds that extracellularly bind to NKA, inhibiting its activity. Low concentrations of OUA are found endogenously, with evidence showing therapeutic potential in the inflammatory response and neural signaling. Dental pulp stem cells (DPSCs) have markers that enable their differentiation, such as nestin, an intermediate filament protein that appears as a marker of neural progenitor cells. Knowing that NKA is the main mechanism of neuroplasticity, the aim of this work was to verify the presence of α1 and α3 isoforms in DPSCs, as well as to evaluate the effect of OUA on nestin expression. **Methods:** Dental pulp stem cells were acquired from the ToxIn/UFG Biorepository (Ethical protocol #440.8021.0.0000.5083) and cultured in DMEM/F-12 medium with 1% antibiotic solution and 10% bovine serum. The evaluation of the presence of α1 and α3 isoforms was performed by immunofluorescence assay. To verify cell viability, the MTT assay was performed in triplicate at different concentrations of OUA (1, 10 and 100nM). Nestin expression was previously characterized in the DPSCs by flow cytometry and the cells were treated with the concentrations chosen according to the MTT assay to assess whether there is a change in expression upon exposure to OUA. **Results:** Immunofluorescence showed expression of α1 and α3 isoforms in DPSCs. It was verified that the 100nM concentration reduced cell viability by 60% (p<0.05) while the 1nM concentration showed 84% viability and 10nM showed 80% viability. Concentrations of 1 and 10nM were used to verify the expression of nestin by flow cytometry because they did not reduce cell viability: in the concentration of 1nM 38.45% of the cells showed expression and at the concentration of 10nM 44.05% showed expression, compared to the control with 33% of the cells expressing nestin (p>0.05). **Conclusion:** Our results show that DPSCs have isoforms of NKA, which can be used to evaluate compounds such as OUA that interfere with the functioning of the enzyme. OUA did not interfere with nestin expression in DPSCs, requiring further studies in differentiated three-dimensional models such as neurospheres to confirm the neuroprotective effect. **Financial Support:** CAPES. **References:** Petrushanko, IY. *Cells*, v. 11, p. 2753, 2022. Parreira, GM. *J Membr Biol.*, v. 254, p. 189-199, 2021. Mijatovic, T. *BBA - Reviews on Cancer*, v. 1776, p. 32-57, 2007. Kravtsova, VV. *Int J Mol Sci*, v. 23, article 18, 2022. Rafiee, F. *Intern. Journal of Neurosci.*, v. 130. p. 107-116, 2020. Arnaiz, GRL. *Int J Biomed Sci*, v. 10, p. 85-102, 2014. Suzuki S. *J Histochem Cytochem*, v. 58, p. 721-730, 2010.

02.009 P-coumaric Acid Derivates from Brazilian Green Propolis Attenuate Behavioral Changes, Oxidative Stress and Barriers Damage in DSS-induced Colitis Model. Cazarin CA¹, Bauer ER¹, Valachinski AW¹, Longo B¹, Basílio MI¹, Machado MS¹, Silva TFQ¹, Cury BJ¹, Venzon L¹, França TCS¹, Santos AC¹, Nunes RKS¹, Bastos JK², da Silva LM¹, de Souza MM¹.¹Univali Itajaí, PPG Ciências Farmacêuticas, Brazil; ²USP, Faculdade de Ciências Farmacêuticas, Ribeirão Preto, Brazil

Introduction: Neuropsychiatric disorders are known to be associated with comorbidities of inflammatory bowel disease (IBD). Thus, this study investigated how experimental colitis affects behavioral changes, intestinal and blood-brain barrier (BBB) integrity, and biochemical parameters in the colon and central nervous system (CNS) and measured the role of *p*-coumaric acid derivatives from Brazilian Green Propolis (BGP): artepillin C (ARC), bacarin (BAC), and drupanin (DRU), on these changes. **Methods:** Colitis were induced in Swiss female mice (30 g) aged 3 months by intake of 3% dextran sulfate sodium (DSS) for 7 days. Mice were orally treated with vehicle, ARC (3 mg/kg), BAC (3 mg/kg), or DRU (3 mg/kg) for 13 days. Behavioral parameters were assessed using novel object recognized (NOR), elevated plus maze (EPM), and tail suspension test (TST). Thereafter, oxidative, and inflammatory measurements was performed in the colon, cortex, and hippocampus samples. Gut and BBB permeability were assessed with 1% Evans blue (ethical committee: 029/22). Results were expressed as means \pm standard error of the means (S.E.M) and statistical significance was obtained by two-way analysis of variance (ANOVA). **Results:** The DSS intake promoted colitis in mice that scored 08 ± 1 points of disease activity, and treatment with ARC, BAC or DRU attenuated it ($p < 0.0001$). The colitic-vehicle group showed a decrease in object recognition index (RI) and immobility time in the TST as well as durability in the open arms of the EPM compared to the naive group ($p < 0.001$). In contrast, treatment with ARC, BAC or DRU increased RI in NOR ($p < 0.01$) and durability in the open arms of the EPM ($p < 0.05$) and decreased immobility time in TST ($p < 0.05$) compared to the colitic vehicle group. In addition, exposure to DSS decreased glutathione (GSH) ($p < 0.05$) and superoxide dismutase (SOD) activity ($p < 0.05$) in the colon, cortex and hippocampus of the colitic-vehicle treated group compared to the naive group. Treatment with ARC ($p < 0.01$), BAC ($p < 0.001$) or DRU ($p < 0.0001$) increased GSH in the colon and in parallel normalized GSH ($p < 0.05$) and SOD activity ($p < 0.05$) in the cortex and hippocampus of mice, compared to the vehicle group. Increased levels of malondialdehyde (MDA), glutathione S-transferase (GST) and myeloperoxidase (MPO) were also detected in the colon ($p < 0.01$, $p < 0.001$ and $p < 0.01$, respectively) and cortex ($p < 0.001$, $p < 0.01$ and $p < 0.05$, respectively) of mice exposed to DSS and ARC, BAC or DRU prevented these changes. Furthermore, MDA levels were increased in the hippocampus of colitic mice, which was attenuated by treatment with the compounds. Finally, colon permeability ($p < 0.0001$) and BBB ($p < 0.0001$) were increased in colitic mice compared to naive, and treatment with ARC, BAC or DRU decreased Evans blue levels in these mice ($p < 0.0001$). **Conclusion:** The results confirm the impact of colitis on CNS function and suggest that *p*-coumaric acid derivatives may be promising adjuncts in the treatment of IBD and associated neuropsychiatric comorbidities diseases. **Financial Support:** CAPES, CNPQ.

02.010 Effect of Taurine on GABA Levels in the Nucleus Accumbens of Rats Chronically Treated with Alcohol or Abstinent: A Microdialysis Study. Pulcinelli RR¹, Caletti G¹, SantAna BH¹, Nin MS², Izolan LR³, Oliveira TF⁴, Eller S⁴, Gomez R^{1,3}. ¹UFRGS, PPG Farmacologia e Terapêutica, Brazil; ²Universidade Factum, Porto Alegre, Brazil; ³UFRGS, PPG Neurociências, Porto Alegre, Brazil; ⁴UFCSPA, Porto Alegre, Dep Farmacociências, Brazil

Taurine is a positive GABAAR modulator structurally related to acamprosate, a drug licensed to prevent relapse in alcohol dependence. Chronic taurine administration increases voluntary alcohol intake in rats. However, there is no study evaluating the effect of taurine on GABA levels in the nucleus accumbens (NAcc) of chronically treated or alcohol-abstinent rats. Here, we used the microdialysis technique to investigate these effects *in vivo*. Adult male Wistar rats were allowed to choose from 2 bottles containing alcohol (20%) and vehicle solution (Alcohol group) or 2 bottles containing vehicle (Control group), 24 h/day, for 4 weeks. On day 23, half of the alcohol rats had their alcohol bottle substituted for vehicle solution (Withdrawal group). Groups were subdivided (n=6/group) to receive 100 mg/kg taurine (TAU) or saline (SAL), via i.p. once/day for 6 days. On day 20, a guide cannula was inserted into NAcc by stereotaxic surgery (A/P +1.8 mm, M/L ±1.2 mm to bregma, V/D: ±6.8 mm), and 7 days after, a probe (4 mm, CMA/12, Acton, MA) was inserted in the guide cannula and the microdialysis was performed along 5 h, with samples collected every 30 min and GABA levels determined by liquid chromatography-tandem mass spectrometry. After baseline samples collection, rats received SAL or TAU, and the effect of acute taurine on GABA efflux was observed over the next 150 min. Later, rats from withdrawal groups were exposed again to voluntary alcohol intake for 24 h. Data were tested for normal distribution by the Shapiro-Wilk test. Two-way analysis of variance (ANOVA) was used to analyze GABA baseline levels, with condition (control, alcohol, or withdrawal) and treatment (saline or taurine) as factors, followed by Bonferroni's *post hoc* test. Relative changes from baseline GABA levels throughout the microdialysis course were analyzed by Generalized Estimating Equations (GEE) followed by the Bonferroni test, with time or day as a within-subject factor, and condition, treatment, and time or day as a between-subjects factor. A P value of We found that repeated taurine administration (5 days) restored the baseline GABA levels in the NAcc of Withdrawal/TAU rats decreased by the withdrawal condition (P=0.037). On the other hand, taurine administration decreased GABA levels in Alcohol/TAU group (P=0.003). During the microdialysis, acute taurine administration increased GABA levels after 30 min in Control/TAU rats and after 60 min in Alcohol/TAU rats. However, taurine decreased GABA levels in Withdrawal/TAU rats (Pinteraction < 0.001). Alcohol intake increased four times in re-exposure Withdrawal/SAL rats and taurine treatment prevented this behavior (Pinteraction = 0.013). Our results showed that taurine effects on GABA levels were dependent on the alcohol or withdrawal condition and the acute taurine administration. The GABA restoration in the NAcc was associated with lower alcohol intake. Like acamprosate, taurine could be used as an adjunct to prevent relapse in alcohol-dependent individuals.

02.011 Effect of Celecoxib on Neurobehavioral and Oxidative Changes Induced by Systemic Exposure to Lipopolysaccharide in Male Mice, Capibaribe, VCC, Silva, DMA, Oliveira, JVS, Rebouças, MO, Coelho, DMN, Valentim JT, Juvêncio, BA, Bandeira SMA, Magalhães, LRF, Sales, ISL, Mallmann ASV, Carvalho MAJ, Aquino PEA, Sousa FCF Federal University of Ceará

Introduction: Depression is a very common mood disorder today. The pharmacological therapy currently used is still based on the monoamine theory, which has many limitations. It is suggested that depression may be associated with inflammation. In this context, Celecoxib (CLX) is widely used to relieve inflammation. The objective of this work was to evaluate the effects of CLX on neurobehavioral and oxidative changes. **Methods:** Male Swiss mice (6-9 per group) were subjected to a systemic inflammation model using LPS. For ten consecutive days, they received intraperitoneal injections of LPS at a dose of 0.5 mg/kg. From the fifth day until the tenth day, the animals were treated one hour after LPS administration with Saline (SAL), CLX (15 mg/kg), or Fluoxetine (FLU) (20 mg/kg) orally via gavage. Twenty-four hours after the last oral drug administration, the animals underwent predictive tests for depressive behavior: forced swimming test. In this test, the immobility time of the animal will be evaluated as a parameter, measured in seconds. Subsequently, the following brain areas were dissected: hippocampus (HP), prefrontal cortex (PFC), and striatum (STR). Malondialdehyde (MDA) parameters were measured to evaluate the degree of lipid peroxidation in the three brain areas. The brain homogenates were mixed with 35% perchloric acid and 1.2% thiobarbituric acid and read using the ELISA technique. The results were expressed in μg of MDA/g of tissue. The experiments were approved by the Ethics Committee for Animal Use at the Federal University of Ceará, under protocol number 5089270819. For statistical analysis, the Shapiro-Wilk test, analysis of variance (ANOVA) followed by Tukey's post hoc test, or Kruskal-Wallis followed by Dunn's post hoc test for non-parametric data, were used. The values were represented as Mean \pm Standard Error of the Mean (SEM), with significance set at $p < 0.05$. **Results:** The results show that LPS induced depressive-like behavior. The immobility time (I.T.) in the forced swimming test was significantly higher in the LPS + SAL group compared to the SAL + SAL group (LPS + SAL: 161.90 ± 19.11 ; SAL + SAL: 104.0 ± 13.06 , $P < 0.05$). Treatment with CLX was able to reverse the behavioral changes predictive of depression (LPS + CLX: 15.75 ± 4.26 ; LPS + SAL: 161.90 ± 19.1 , $P < 0.0001$). Animals that received FLU also showed significantly lower I.T. (LPS + FLU: 54.00 ± 14.36 ; LPS + SAL: 161.90 ± 19.1 , $P < 0.0001$). In the PFC, lipid peroxidation (L.P.) was significantly higher, reflecting increased MDA levels, in the LPS + SAL group compared to the group treated with SAL only (LPS + SAL: 0.52 ± 0.04 ; SAL + SAL: 0.38 ± 0.03 , $P < 0.05$). Treatment with CLX significantly decreased MDA levels after LPS exposure (LPS + CLX: 0.17 ± 0.01 ; LPS + SAL: 0.52 ± 0.04 , $P < 0.0001$). In the STR, exposure to LPS and treatment with SAL only significantly increased MDA levels compared to the SAL-treated group (LPS + SAL: 0.47 ± 0.06 ; SAL + SAL: 0.29 ± 0.02 , $P < 0.05$). Treatment with CLX significantly decreased MDA levels (LPS + CLX: 0.23 ± 0.03 ; LPS + SAL: 0.47 ± 0.06 , $P < 0.01$). MDA levels in the HP of animals in the LPS + SAL and SAL + SAL groups did not show significance. However, oral treatment with CLX after LPS exposure significantly decreased the MDA concentration (LPS + CLX: 0.19 ± 0.02 ; LPS + SAL: 0.38 ± 0.02 , $P < 0.05$). **Conclusion:** It is suggested that CLX has activity in reducing L.P. and remission of depressive behavior. **Financial Support:** CAPES, CNPQ, FUNCAP.

02.012 Disintegration of the Blood-Brain Barrier in Male BCCAO Mice. Splendor MC, Humberto M, Oliveira RMMW. UEM, Dept of Pharmacology and Therapeutics, Maringá, PR, Brazil

Introduction: Cerebral ischemia (CI) is one of the major causes of morbidity and mortality in the world. Several mechanisms are involved in the pathophysiology of IC including neuroinflammation and blood-brain barrier (BBB) desintegrity. The interruption of blood flow causes the breakdown of the BBB integrity, leading to an increase in permeability and consequent cerebral edema, neuroinflammation, and neuronal damage. The BBB is the first structure to be injured after CI¹. BBB disruption can occur within minutes to hours after CI, characterized by proteolytic degradation of tight junctions and basement membranes, endothelial bonded junctions, and increased permeability of blood-borne cell chemicals across the BBB leading to progression of additional brain damage. The underlying events of CI can affect all components of the BBB, including the loss of endothelial cells, astrocytes, pericytes, and the extracellular matrix. Thus, to study drugs that can prevent or reduce damage to the BBB, it is first necessary to carry out a time course and thus verify the period in which the damage to the BBB occurs². To evaluate the time course of the blood-brain barrier permeability in ischemic mice **Methods:** Male C57BL/6J mice, 2 and 3 months were used. Transient global cerebral ischemia was induced by bilateral occlusion of the common carotid arteries (BCCAO) for 20 minutes. To determine the period of BBB break, the animals were randomly divided into 5 groups: sham, ischemic 24, 48, 72, or 168 hours. Eight hours before sacrifice the animals were injected i.p. with a 2% solution of Evans Blue dye (EA, 0.2 mg/kg, 1 ml/kg) to observe the BBB integrity. The analysis to determine the extravasation of the BBB was performed by the Elisa technique. The results were analyzed by ANOVA followed by the Tukey post hoc test. **Results:** In all ischemic groups analyzed, there was leakage of Evans Blue, indicating increased permeability of the BBB of ischemic mice ($F_{4,58}=28.9$, $p<0.0001$). The mean and mean error in the groups were: sham (0.1037, 0.02663), 24h (0.2243, 0.02041), 48h (0.3133, 0.3133), 72h (0.1854, 0.01497) and 168h (0.1978, 0.02771). Among ischemic animals, the greatest increase in EB extravasation was detected in BCCAO mice after 168 h ($p < 0.001$). **Conclusion:** The results show that 168 hours is the best time for evaluating neuroprotective drugs aimed to reduce damage to the BBB after BCCAO.

02.013 Evaluation of TRPA1 Involvement in Oxidative and Inflammatory Processes Induced by Corticosterone in Microglial Cells (BV-2 cells). Brum GF¹; Fontana T², Pappis L³, Piton E¹; Machado AK⁴, Montagner TRS⁴; Machado AK²; Bochi GV¹ ¹UFMS Santa Maria, PPG Farmacologia, Brazil; ²UFN, Santa Maria, PPG Nanociências, Brazil; ³University of Toronto, Dpt of Pharmacology and Toxicology, Canada ⁴UFN Santa Maria, Curso de Biomedicina, Brazil

Introduction: The immune cells located in the central nervous system, especially microglial cells, play an important role in activating oxidative and inflammatory pathways commonly found in individuals with major depressive disorder (MDD). Studies have revealed the involvement of these cells in the pathogenesis of MDD, as they release neurotoxic factors when activated due to damage or stress (CALCIA et al., 2016). Corticosterone (CORT), the main glucocorticoid hormone in rodents, has a potent inhibitory effect on cell proliferation under stress conditions. Additionally, it can be cytotoxic to various cell lines, including BV-2 cells. This cytotoxic effect is associated with an increase in oxidative and pro-inflammatory mediators such as reactive oxygen species (ROS), nitric oxide (NO), and interleukins (CHANSAWHANG et al., 2022). The transient receptor potential ankyrin 1 (TRPA1) receptor belongs to a broad family of non-selective ion channels that act as sensors for oxidant compounds and inflammatory mediators. It was demonstrated that pharmacological blockade of the receptor promotes a pattern of effects like classical antidepressants (DE MOURA et al., 2014). However, the role of TRPA1 in MDD needs further investigation. Thus, the main objective of this study was to investigate the role of TRPA1 in the oxidative and inflammatory processes induced by CORT in microglial cells. **Methods:** For this, BV-2 cells were exposed to different concentrations of CORT, allicin isothiocyanate (AITC), an agonist of TRPA1, and HC-030031 (HC), an antagonist of TRPA1, for 24 hours. Additionally, the effect of AITC also was investigated at 5, 30, and 60 minutes. Subsequently, the oxidative and inflammatory status was assessed through of cell viability assays, levels of NO, ROS, and gene expression of targets of interest. **Results:** The results revealed that higher concentrations of CORT (50 and 100 μ M) induced a reduction of cell viability, increased levels of NO, ROS, and interleukin 17 (IL-17) mRNA expression. However, there were no significant differences in the mRNA expression of TRPA1, GR, and NLRP3. On the other hand, TRPA1 stimulation with AITC induced cytotoxic effects like CORT at 5 and 30 minutes, but these effects were abolished after 60 minutes. Interestingly, after 24 hours, AITC showed cytoprotective effects, suggesting a possible desensitization of the receptor. In addition, in the AITC+CORT group, the pre-incubation with AITC prevented the cell death by nuclear damage induced by CORT, but not by mitochondrial damage. Also, AITC reduced the levels of NO, ROS, and mRNA expression IL-17 induced by CORT. Similarly, the HC prevented the cell death due to nuclear damage, but not mitochondrial damage, and reduced the elevated levels of ROS and mRNA IL-17 expression caused by CORT. **Conclusion:** In conclusion, it is suggested that the oxidative and inflammatory effects of CORT in BV-2 cells appear to be partially mediated by TRPA1. **Financial Support:** CAPES. **References:** CALCIA, Marilia A. et al. Stress and neuroinflammation: a systematic review of the effects of stress on microglia and the implications for mental illness. *Psychopharmacology*, v. 233, p. 1637-1650, 2016. CHANSAWHANG, Anchana et al. Corticosterone potentiates ochratoxin A-induced microglial activation. *Biomolecular Concepts*, v. 13, n. 1, p. 230-241, 2022. DE MOURA, Juliana Cavalcante et al. The blockade of transient receptor potential ankyrin 1 (TRPA 1) signalling mediates antidepressant-and anxiolytic-like actions in mice. *British journal of pharmacology*, v. 171, n. 18, p. 4289-4299, 2014.

02.014 Pharmacologically-Enhanced Memory Destabilization allows the Impairing Effects of Reconsolidation Blockers in Male and Female Rats. Soares LA¹, Gazarini L², Bertoglio LJ¹ ¹Lab. of Neuropsychopharmacology, Dept of Pharmacology; UFSC, Florianópolis, SC, Brazil. ²UFMS, Três Lagoas, MS. Brazil

Introduction: Aversive memories allow the adaptation to a changing environment, instructing behavioral repertoire to deal with life-threatening events. Adaptive fear memories can be destabilized and gradually reconsolidated when retrieved and reactivated. On the other hand, abnormal aversive memories would be less prone to destabilization/reconsolidation, explaining their relative resistance to pharmacological interference. **Objectives:** To test a combined pharmacological intervention to overcome the resistance to impairing the destabilization-reconsolidation process of more intense and generalized aversive memories. **Methods:** Male or female Wistar rats were contextually fear conditioned with three 1.3 mA footshocks in context A and briefly re-exposed to it, without shocks, for memory reactivation. Test sessions took place in Context A to assess memory retention after reconsolidation (Test A1) and in a novel Context B to evaluate memory specificity (Test B1). Sessions were spaced apart for 24 h from each other. Each test session was repeated seven days later to assess the persistence of memory features induced herein (Tests A2 and B2). Animals received systemic injections of vehicle (VEH) or D-cycloserine (DCS; 15 mg/kg) pre-reactivation and a reconsolidation blocker, cannabidiol (CBD; 10 mg/kg), clonidine (CLO; 0.3 mg/kg) or VEH post-reactivation. Freezing behavior was quantified and used to infer treatment effects. **Results:** Males treated with DCS and CBD or CLO presented reduced freezing times when compared to VEH/VEH and DCS/VEH control groups (Test A1: DCS/CBD $p = 0.00001$; DCS/CLO $p = 0.00002$; Test A2: DCS/CBD $p = 0.00002$; DCS/CLO $p = 0.00002$); Test B1: DCS/CBD $p = 0.0001$; DCS/CLO $p = 0.0001$; Test B2: DCS/CBD $p = 0.005$ and DCS/CLO $p = 0.0001$). The results from the study using females were similar: the impairing effects of CBD and CLO on reconsolidation were only observed in animals pre-treated with DCS, in which there was also a reduction in generalized fear expression. **Conclusion:** Pre-treatment with DCS allowed the destabilization of intense and generalized fear memories and the impairing effects of CBD and CLO in both male and female rats. **Financial Support:** CAPES.

02.015 Physical Exercise Provides Beneficial Changes on Neurotrophic Factors in Brain Areas after AMPH Relapse. Rosa JLO¹, Rosa HZ¹, Segat HJ¹, Barcelos RCS¹, Roversi K¹, Rossato DR¹, Burger ME². ¹UFSM, PPG em Farmacologia, Santa Maria, RS, Brazil, ²UFSM, Depto de Fisiologia e Farmacologia, Santa Maria, RS, Brazil

In the last decades, addictive drugs abuse has grown considerably all over the world. Addiction is a serious public health problem, and the current pharmacotherapy is unable to prevent drug use reinstatement. Studies have focused on physical exercise as a promising co-adjuvant treatment on both drug withdrawal and relapse prevention. Our research group recently showed beneficial neuroadaptations in the dopaminergic system related to amphetamine-relapse prevention involving physical exercise-induced endogenous opioid system activation (EXE-OS activation). In this context, additional mechanisms were explored to understand the exercise benefits on drug addiction. Male rats previously exposed to amphetamine (AMPH, 4.0 mg/kg) for 8 days were submitted to physical exercise for 5 weeks. EXE-OS activation was blocked by naloxone administration (0.3 mg/kg) 5 minutes before each physical exercise session. After the exercise protocol, the rats were re-exposed to AMPH for 3 days, and in sequence, euthanasia was performed and the VTA and NAc were dissected. In the VTA, our findings showed increased immunocontent of proBDNF, BDNF and GDNF and decreased levels of AMPH-induced TrkB; therefore, EXE-OS activation increased all these markers and naloxone administration prevented this exercise-induced effect. In the NAc, the same molecular markers were also increased by AMPH and decreased by EXE-OS activation. In this study, we propose a close relation between EXE-OS activation beneficial influence and a consequent neuroadaptation on neurotrophins levels in the mesolimbic brain area, preventing the observed AMPH-relapse behavior. Our current findings contribute to a better understanding about the molecular basis related to physical exercise benefits in AMPH-addiction situations.

02.016 The Effects of Chronic Treatment with Semaglutide on Cerebral Vascular Inflammation in Mice with Metabolic Syndrome. Chateaubriand PHP², Curty M², Lustosa R², Baroni M², Ritta JCS³, Costa M², Figueiredo V², Obadia N^{2,3} Castro-Faria-Neto HC¹, Estado V^{1,2}. ¹IOC-FIOCRUZ, Lab. de Imunofarmacologia, Rio de Janeiro, Brasil; ²Idomed-Unesa, Rio de Janeiro, Brasil; ³Unesa, Faculdade de Farmácia, Rio de Janeiro, Brasil

Introduction: Metabolic syndrome (MS) is a cluster of risk factors that include obesity, high blood pressure, dyslipidemia, and insulin resistance. These factors are associated with an increased risk of cardiovascular disease, but they can also contribute to the onset or progression of neurodegenerative diseases due to chronic low-grade inflammation caused by obesity. Although most studies suggest that glucagon-like peptide-1 receptor agonists (GLP-1 RA), such as semaglutide, promote weight loss primarily due to their inhibitory effect on food intake, other central effects that have been described in rodents and humans encourage further clinical trials to explore potential beneficial effects on central nervous system (CNS) microcirculation. This study investigated the effects of the antidiabetic drug semaglutide on metabolic parameters and on inflammation in the cerebral microcirculation of animals in an experimental model of MS. **Methods:** Mice were fed a high-fat (HFD) or normo-lipid (ND) diet for 24 weeks, whether or not they were treated with semaglutide subcutaneously (SEMA or CONT) (n=10 per group). Metabolic, biochemical and microvascular analyzes of the brain were performed, including intravital microscopy with fluorescence, to assess the leukocyte-endothelium interaction and immunohistochemistry to analyze the expression of vascular adhesion molecules. Systemic inflammation was assessed by measuring inflammatory cytokines and adipose tissue histology. **Results:** The efficacy of semaglutide treatment as an antidiabetic and weight reducer was confirmed by the significant reduction in fasting glucose, weight, fasting insulin, leptin, and triglycerides in the HFD+SEMA group compared to the HFD+VEI group. Intravital microscopy revealed a significant reduction in leukocyte rolling and adhesion in animals treated with semaglutide, indicating an anti-inflammatory effect on the brain microcirculation. **Conclusion:** The results of the study indicate that chronic treatment with semaglutide has beneficial effects on the cerebral microcirculation in obese animals with Metabolic Syndrome (MS). These findings highlight semaglutide as a promising therapeutic approach to reduce chronic inflammation and morbidities associated with MS. However, further studies are needed to elucidate the underlying molecular mechanisms and confirm the clinical benefits of semaglutide in neurodegenerative diseases and MS. Support: FAPERJ; PIBIC-UNESA, IDOMED.

02.017 The Effects of GLP-1 Receptor Activation on Hippocampal Neuronal Integrity in Animals with Metabolic Syndrome. Curty M², Chateaubriand PHP², Lustosa R², Baroni M², Ritta JCS², Costa M², Figueiredo V², Castro-Faria-Neto HC¹, Obadia N³, Estado V^{1,2} ¹IOC-Fiocruz, Lab. de Imunofarmacologia, Rio de Janeiro, Brasi, ²Idomed-Unesa, Rio de Janeiro, Brasil. ³Unesa, Faculdade de Farmácia, Rio de Janeiro, Brasil

Introduction: Metabolic Syndrome (MS) is a chronic degenerative condition characterized by associated signs and symptoms such as systemic arterial hypertension, obesity, hyperglycemia, hypertriglyceridemia, and low HDL-cholesterol levels. The chronic low-intensity inflammation associated with visceral obesity in MS leads to the release of inflammatory cytokines, causing damage to neuronal tissue and altering the cerebral microvascular environment. These changes result in cognitive deficits and memory loss observed in advanced MS. Given this context, our study aimed to investigate the potential effects of semaglutide, an antidiabetic drug and GLP1 receptor agonist, on cerebral microcirculation and obesity, with a focus on its therapeutic potential for treating MS.

Methods: 40 C57BL/6 mice were used for the study and were housed in temperature-controlled cages (between 23-25°C) with ad libitum access to food and water. 20 animals were fed a high-fat diet (HFD) for 24 weeks, while the control group (n=20) received a normolipid diet (ND) for the same duration. At the end of 20 weeks on the high-fat diet, the mice developed MS and were treated with the antidiabetic drug semaglutide (200 µM/kg/week subcutaneously, HFD+SEMA) or saline solution (HFD+SAL) for 4 weeks (n=10 per group). Plasma levels of fasting glucose, insulin, and triglycerides were analyzed for all study groups. Brains were prepared for histological analyzes with HE staining and analyzes on the organization, thickness of the hippocampus and inflammatory infiltrates were evaluated for all groups. The slides were photographed light microscope, and the images were analyzed using the ImageJ program for assessing neuronal integrity and neurodegeneration. All experiments were carried out in accordance with the rules and approved by the Animal Ethics Committee of the Oswaldo Cruz Foundation (L-012/2021).

Results: HFD+SAL showed increased weight, glycemia, fasting insulin, and triglyceride levels compared to the control group that received the ND+SAL. In the CA1 region of the hippocampus in animals HFD+SEMA, pyramidal cells stained with HE appeared densely packed and organized in an aligned and compact manner, suggesting cellular integrity. However, animals in the HFD+SAL group exhibited disorganized and less compacted CA1 regions of the hippocampus, with spaces between cells, indicating apoptotic processes and compromised neuronal integrity in MS. These findings align with previous studies in the literature that have demonstrated cellular disorganization in the hippocampus of animals with arterial hypertension.

Conclusion: Semaglutide treatment showed beneficial effects on weight, glycemia, insulin, and triglyceride levels in MS animals. It also exhibited potential protection against hippocampal thickness reduction. These findings support semaglutide as a promising therapeutic option for MS, addressing both metabolic and neurocognitive aspects. Further research is needed to explore underlying mechanisms and long-term effects.

Support: FAPERJ; PIBIC-UNESA, IDOMED.

02.018 Investigating the Impact of Prebiotic Supplementation on Inflammation in the Cerebral Microcirculation of Animals with Metabolic Syndrome: Exploring with Intravital Microscopy. Baroni M², Curty M², Chateaubriand PHP², Lustosa R², Ritta JCS³, Costa M², Figueiredo V², Obadia N^{1,3}, Castro-Faria-Neto HC¹, Estado V^{1,2} ¹IOC-Fiocruz, Lab. de Imunofarmacologia, Rio de Janeiro, Brasil, ²Idomed-Unesa, Rio de Janeiro, Brasil. ³Unesa, Faculdade de Farmácia, Rio de Janeiro, Brasil

Introduction: The Metabolic Syndrome (MS) comprises a cluster of risk factors, including obesity, hypertension, dyslipidemia, and insulin resistance, which collectively elevate the risk of cardiovascular diseases. Current literature suggests an association between the progression of neurodegenerative diseases and MS, due to its correlation with a chronic low-grade inflammatory state. This inflammatory condition, coupled with a high-fat diet, also promotes intestinal dysbiosis, resulting in hyperactivity of innate immunity receptors that disrupt metabolic homeostasis. Additionally, it stimulates the production of hormones and neurotransmitters by the microbiota, influencing intake, immune system, and energy metabolism. The objective of this study was to assess the connection between the gut microbiome and neurodegeneration in metabolic syndrome (MS) to gain a better understanding of the impact of intestinal dysbiosis on neurodegenerative processes. To achieve this, we investigated the effects of prebiotic supplementation, specifically with short-chain fatty acids (SCFAs), in an animal model of MS. Our focus was to evaluate the interaction between leukocytes and the vascular endothelium using intravital microscopy with epi-illumination and fluorescence analysis. **Methods:** MS was induced in 20 mice by feeding them a high-fat diet (HFD) for 24 weeks, while the control group of 20 mice received a normolipid diet (ND) for the same duration. Both diets were supplemented with SCFAs as probiotics. At the end of the 24 weeks, neuroinflammation was assessed using intravital microscopy with epi-illumination and fluorescence. To visualize the cerebral microcirculation, the animals were anesthetized, and a craniotomy was performed on the left parietal bone. They were then positioned under a fluorescence microscope light beam. Subsequently, 6G rhodamine fluorophore (0.3 mg/kg) was intravenously administered to visualize the interaction between leukocytes and the vascular endothelium, enabling the evaluation of adhesion molecule expression by counting the leukocytes adhering to the venular wall. This study was approved by the Animal Ethics Committee of the Oswaldo Cruz Foundation (L-005/2021). **Results:** Supplementation with SCFAs significantly reduced body weight and fasting blood plasma glucose levels. We observed a notable decrease in brain inflammation, as evidenced by reduced leukocyte-endothelium interaction, particularly in the rolling of leukocytes in brain venules of animals receiving prebiotic supplementation compared to those on the HFD diet (HFD SAL 13.7 ± 4.5 vs HFD FOS 3.0 ± 0.8 cells/min, $p < 0.01$). **Conclusion:** MS is associated with the development of neuroinflammation. The observed reduction in brain inflammation, as indicated by the decreased leukocyte-endothelium interaction in animals supplemented with short-chain fatty acids (SCFAs), highlights the potential role of intestinal dysbiosis in neurodegenerative processes. **Support:** FAPERJ; PIBIC-UNESA, IDOMED.

02.019 Intermittent Taurine Administration Increases Alcohol Consumption in Adolescent Male Rats Exposed to the Binge Drinking Model. SantAna BH, Zilli GAL, Bastiani CS, Pulcinelli RR, Izolan LR, Leal MB, Gomez R UFRGS

Binge drinking (BD) is a usual pattern of alcohol intake among adolescents and is frequently associated with energy drinks. Taurine, an amino acid found in energy drinks, increases voluntary alcohol intake in rats after chronic administration. There is no study showing the chronic or intermittent taurine effect on alcohol intake in adolescent rats exposed to the BD model. This study aimed to evaluate the effect of different regimens of taurine administration on alcohol consumption and behavioral changes in rats exposed to the voluntary BD model. Wistar male rats, 35 days old (PN35), were exposed to four cycles of BD (PN35-59), in the dark, with free access to alcohol (20% w/v), 2 h for 3 days, followed by 4 days of withdrawal. Rats were divided into the SAL group, daily administered with saline, via ip, for 24 days; the TAU group, daily administered with taurine (100 mg/kg), via ip, for 24 days; the TAU/SAL group, administered with taurine (100 mg/kg) on the BD days (Wednesday, Thursday, and Friday) and with saline, via ip, in the other days; and the SAL/TAU group, administered with saline on the BD days and with taurine (100 mg/kg), via ip, in the other days. On PN52 day, they were exposed to the light/dark test and on PN59 day to the open field test to assess the taurine effect on anxiety-like or emotionality behaviors, respectively. Behaviors were video-recorded, and an observer blinded-to-treatments counted the time spent in the light or dark compartment, the latency to enter the dark compartment, the frequency of transitions between the compartments, and the frequency and time spent in risk assessment in the light/dark test. In the open field, the frequency of the central and peripheral crossings, rearing, and grooming behaviors and the time spent on rearing and grooming behaviors were measured. Data were tested for normal distribution by the Kolmogorov-Smirnov test. Normal distribution data were analyzed by a one-way analysis of variance (ANOVA-way), with treatments as a factor, followed by the Bonferroni post hoc test. Temporal alcohol consumption during different cycles of binge drinking was analyzed by the Generalized Estimating Equations (GEE), followed by Bonferroni, using the day as a within-subject factor, and treatment, and day as between-subjects factors. The non-parametric distribution data were evaluated by the Kruskal-Wallis test followed by the Dunn test. A P value of < 0.0001). Taurine administration did not show an anxiety-like effect or change ambulation in adolescent rats. The temporal increase in the alcohol intake associated with intermittent taurine administration is a concern if translated to humans since adolescents frequently combine binge drinking behaviors with energy drinks on the weekends. Binge drinking combined with energy drinks could increase alcohol intake and risk behaviors among youth.

02.020 A Systematic Review of the Role of Thalamic Nucleus Reuniens in Memory Acquisition and Consolidation in Lab. Rodents. Batista LP¹, Soares LA¹, Panzenhagen AC², Bertoglio LJ¹ ¹UFSC ²UFRGS

Introduction: Short- and long-term memories instruct coping strategies to recall locations and relevant cues in ever-changing environments. This systematic review brought together published data to estimate the contribution of the thalamus's nucleus reuniens (nRE) as a hub of communication and synchronization between the hippocampus and the medial prefrontal cortex during memory acquisition and consolidation. **Methods:** Rat and mice studies in which the nRE function was impaired by a permanent lesion or reversible inactivation using pharmacologic, optogenetic, and chemogenetic interventions around memory formation and reporting behavioral outcomes were included. The databases searched were MEDLINE, Scopus, and Embase. Studies purely *in vitro*, *ex vivo*, not having a control group or original data were excluded. Two reviewers, with a third available in case of divergence, performed the search and selection stages (PROSPERO number: CRD4202339942). **Results:** Eighteen articles met the inclusion criteria. Eight studies reported that pre-acquisition inactivation of the nRE hampers behavioral outcomes in tasks such as the water maze, associative object recognition, attentional shifting, and object placement. These results suggest difficulty associating local cues, increased time for spatial memory acquisition, increased freezing behavior, generalization, and lower specificity of the acquired memory. Five included studies did not reveal statistical differences indicating memory acquisition impairments. Five studies investigating the post-acquisition effects of nRE inactivation during memory consolidation were retrieved. Four studies reported deficits: whereas two studies found statistical differences in the water maze and object placement tasks for spatial memory, the other two reported changes in aversive memory in the passive avoidance task with an initial inactivation period of five minutes after the test. These results suggest that nRE inactivation may be time-dependent, leading to alterations in the early stage of memory consolidation. It was also reported that nRE inactivation after Pavlovian conditioning increased freezing and memory generalization, intensity, and persistence. One of the five studies did not show statistical differences in memory consolidation. **Conclusion:** Lesioning and inactivating the nRE lead to impairments in spatial and aversive memory acquisition and consolidation phases. These findings support the view that the nRE is a crucial brain region while memory is formed. **Financial Support:** CNPq and CAPES.

02.021 Beta-caryophyllene Exerts Protective Effect after Pilocarpine Induced-Status Epilepticus. Bariviera JL, Mallmann MP, Oliveira MS UFSM, Dpt of Physiology and Pharmacology, Santa Maria, Brazil

Introduction: Epilepsy is a common neurological disease, with an incidence 1 – 2 % worldwide (Fisher, RS. *Epilepsia*, v.58, p.52, 2017). Almost a quarter of epilepsy cases could be prevented and a lack of action to address the epilepsy treatment gap has dire consequences for people's lives and well-being. The pilocarpine epilepsy model reproduces in rodents several features of human temporal lobe epilepsy, by inducing an acute status epilepticus (SE). It is important to note that SE requires emergent, targeted treatment to reduce morbidity and mortality. Moreover, several critical events occur during the latent period that follows SE (Brophy, GM. *Neurocrit. Care.*, v. 17, p. 3, 2012; Lévesque, M. *Neurosci. Biobehav. Rev.*, v.130, p. 274, 2021). We recently demonstrated that beta-caryophyllene (BCP), a natural compound, abundant in several plants, attenuates recurrent seizure in pilocarpine induced-SE, besides, it protects blood-brain barrier from albumin infiltration. Despite that, we did not find any positive result in behavioral improvement after 24. Thus, we sought further explore the effects of BCP post-treatment on consequences of pilocarpine induced-SE seven days after the injury and repeated treatment. **Methods:** Male Wistar rats (± 28 days) were obtained from the central vivarium of Federal University of Santa Maria (UFSM – Brazil). All experimental were conducted with the approval of the institutional animal care and use committee of the UFSM (approval number 5327190319). For EEG registrations, animals were implanted with four stainless screws over de prefrontal cortex and the parietal cortex together with a ground lead positioned under de nasal sinus electrodes. SE was induced six days after the surgery procedure, it was characterized by spiking activity on EEG without return to baseline. After 1 h of SE animals received diazepam (10 mg/kg ip). BCP (100 mg/kg ip) or vehicle (NaCl 0.9% +Tween 20 0.05% ip) treatment started simultaneously with diazepam injection and was repeated at 8 h and 16 h thereafter (Mallmann, MP. *Brain Res.*, v.1784, 2022). Rats were removed from EEG 1 h after SE onset. Excitability and sensory responsiveness, and neuromotor function between epileptic and control rats are assessed seven days after pilocarpine induction, by the pick-up test and neuroscore test, respectively. To further investigate the neuroprotective effect of BCP, we evaluated the neuronal damage by immunohistochemistry. **Results:** Pilocarpine induced-SE did not significantly alter sensory response of animals after seven days as shown by Pick-up test. The neuroscore test revealed impairment of motor function after SE and BCP prevented neuromotor damage compared to vehicle-treated counterparts. SE also induced an important neuronal loss in hippocampus but not in cortex and thalamus. BCP protected against neuronal loss in CA3 and dentate gyrus hilus after seven days the pilocarpine-induced SE. Additionally, we found a strong positive correlation between neuron protection and neuromotor performance in the neuroscore test. **Conclusion:** We demonstrated that early post-treatment with BCP after SE protected against neuronal loss and motor impairments seven days thereafter. Additional studies are needed to investigate the clinical implications of these findings. This work was supported by grants from CNPq and financed in part by CAPES.

02.022 Semaglutide Improves Capillary Density and Cerebral Microvascular Function in a Mouse Model of Metabolic Syndrome. Costa M², Lustosa R², Baroni M², Curty M², Chateaubriand PHP², Ritta JCS³, Figueiredo V², Obadia N³, Faria Neto HC¹, Estado V^{1,2} ¹IOC-Fiocruz, Lab. de Imunofarmacologia, Rio de Janeiro, Brasil, ²Idomed-Unesa, Rio de Janeiro, Brasil. ³Unesa, Faculdade de Farmácia, Rio de Janeiro, Brasil

Introduction: Metabolic Syndrome (MS) is a chronic condition characterized by low-grade inflammation associated with elevated morbidity and mortality rates. It involves visceral obesity and insulin resistance, factors that amplify the production of pro-inflammatory substances such as adipocytokines. This cascade of events causes metabolic imbalances, increasing the risk of developing diabetes, cardiovascular diseases, and neurodegenerative disorders. MS also impairs microvascular dysfunction resulting in inflammation and reduced microvascular density (1, 2). Within the central nervous system, these alterations impact the neurovascular unit, contributing to endothelial dysfunction, neuroinflammation, and neuronal damage (2, 3). Current research aims to elucidate the effect of medications that can manage MS and preserve neurovascular integrity. A promising therapeutic option is GLP-1 receptor agonists, known to induce satiety, promote weight loss, and enhance insulin sensitivity. Nonetheless, their impact on cerebral microcirculation and cognitive function is yet to be thoroughly understood. Our research will explore the therapeutic potential of semaglutide in mitigating the effects of MS on cerebral microcirculation. We aim to understand whether its benefits extend beyond metabolic regulation and whether it can provide a protective function to the microvasculature of the brain. Future studies are needed to compare the potential gender differences in response to treatment. Previous studies on male diabetic rats have shown promising results, suggesting that GLP-1 agonists may have protective effects on cerebral microcirculation. **Methodology:** We randomly assigned 40 C57BL6 male mice to two groups, each fed either a high-fat diet (HFD) or a standard normolipidic diet (ND) over 24 weeks. Afterward, we further subdivided these mice into two subgroups (10 animals per subgroup) and treated them with either subcutaneous injections of semaglutide or a vehicle (SEMA or VEH) for an additional 4 weeks. We evaluated metabolic responses via biochemical techniques, and we used immunohistochemistry to assess brain structural capillary density. We prepared coronal sections with a cryostat and incubated them with isolectin IB4 to label cerebral microcirculation vessels. We used the AngioTool program, a validated resource for measuring vascular networks. We measured the following parameters: total length of cerebral capillaries, representing cerebral capillary density, and lacunarity, representing the spaces between vessels. **Results:** The HFD VEH group exhibited a significant reduction in mean vessel length ($2,37 \pm 0,1 \mu\text{m}$) as well as lacunarity in the CA1 region of the hippocampus, when compared to the ND VEH group ($3,93 \pm 0,5 \mu\text{m}$). This vascular effect, known as capillary rarefaction, indirectly represents a probable reduction in blood flow in this region. Upon analyzing the semaglutide treatment, we found that HFD SEMA group showed an increase in capillary density ($3,65 \pm 0,4 \mu\text{m}$; $p < 0,05$) and a reduction in lacunarity. **Conclusion:** Semaglutide restores cerebral microvascular density in male MS mice, emphasizing its therapeutic potential for MS-related neurodegeneration. Further research should evaluate protective effect duration and gender-specific responses. **Support:** FAPERJ; PIBIC-UNESA, IDOMED. **References:** 1-Grandl, G. Semin Immunopathol. v. 40, p. 215, 2018. 2-Obadia, N. J Neuroinflammation. v. 19, p. 104, 2022. 3- Pugazhenthii, S. Prog Mol Biol Transl Sci. v. 146, p. 243, 2017.

02.023 Semaglutide Restores Astrocytic Coverage in Cerebral Capillaries of Animals with Diet-Induced Metabolic Syndrome. Lustosa R², Baroni M², Curty M², Chateaubriand PHP², Ritta JCS³, Costa M², Figueiredo V², Obadia N^{1,3}, Faria Neto HC¹, Estato V^{1,2} ¹IOC-Fiocruz, Lab. de Imunofarmacologia, Rio de Janeiro, Brasil, ²Unesa- Idomed, Rio de Janeiro, Brasil., ³Unesa, Faculdade de Farmácia Rio de Janeiro, Brasil.

Introduction: Obesity, a significant feature of Metabolic Syndrome (MS), is a crucial factor leading to the development of chronic low-intensity inflammation. This constant inflammatory response results in neuroimmune-endocrine dysregulation. Factors such as visceral adipose tissue accumulation, increased plasma free fatty acid concentrations, tissue hypoxia, and sympathetic hyperactivity in MS may trigger the immune response. This can precipitate or exacerbate neurodegenerative diseases. The neurovascular unit, consisting of neurons, astrocytes, and endothelial cells, maintains a tight-knit relationship to ensure appropriate brain development and function. Astrocytes play a critical role in regulating cerebral blood flow and the blood-brain barrier. This study aims to evaluate the impact of chronic treatment with the antidiabetic semaglutide, a GLP-1 receptor agonist, on the astrocyte coverage in the cerebral capillaries of obese animals with MS. **Methodology:** We randomly assigned 40 C57BL6 male mice to two groups, each fed either a high-fat diet (HFD) or a standard normolipidic diet (ND) over 24 weeks. Afterward, we subdivided these mice into two subgroups (10 animals per subgroup) and treated them with either subcutaneous injections of semaglutide or a vehicle (SEMA or VEH) for an additional 4 weeks. We evaluated metabolic responses using biochemical techniques and assessed astrocytic coverage of capillaries through immunohistochemistry. The brain of each animal was dissected and processed for immunohistochemistry. Coronal sections were obtained using a cryostat and were incubated with isolectin IB4 to label cerebral microcirculation vessels, and with the primary anti-GFAP antibody to label astrocytes. We used a secondary antibody labeled with Cy3 (red) for vessels and an Alexa 488-labeled antibody (green) for astrocytes. The slides were assessed using a confocal microscope. Using the ImageJ software and the "Colocalization" tool, we measured the degree of colocalization between the astrocyte and the cerebral blood vessel. **Results:** Semaglutide treatment significantly improved astrocytic coverage in the cerebral capillaries of the cortex and hippocampus in animals that developed MS. Animals with MS that were untreated exhibited a significant reduction in astrocytic coverage in both the cortex and the CA1 region of the hippocampus, which was significantly restored with semaglutide treatment ($P < 0.001$) in the cortex and hippocampus ($P < 0.01$). **Conclusion:** This study highlights the therapeutic potential of semaglutide in improving cerebral vascular function in MS. The restoration of astrocytic coverage in the cortex and hippocampus underscores the protective role of semaglutide against neurovascular dysregulation, a common consequence of MS. Support: FAPERJ; PIBIC-UNESA, IDOMED.

02.024 Cannabidiol prevents amphetamine relapse in rats. Souza LEM¹, Rosa JLO², Metz VG², Burger ME³, Pase CS³. ¹UFSM, Centro de Ciências da Saúde, ²UFSM, PPG em Farmacologia, ³UFSM, Depto de Fisiologia e Farmacologia

Psychostimulants such as amphetamine (AMPH) are recognized by its elevated addictive potential, causing serious concerns due to positive hedonic reinforcement. Drug relapse presents a worrying situation to be managed, since in recent decades no specific pharmacological therapy has been approved for treatment of this neuropsychiatric condition. Cannabidiol is a phytocannabinoid present in *Cannabis sativa* devoid of addictive effects, which has recently emerged due to its therapeutic potential for neuropsychiatric conditions, including anxiety, depression and psychosis. In this study we investigated the possible beneficial influence of the cannabidiol (CBD) on the stress-triggered relapse behaviors in rats following development of AMPH-induced conditioned place preference (CPP). Male Wistar rats (UFSM-8850121118) received d,l-AMPH (4 mg/kg, i.p.) or vehicle in the CPP paradigm for 8 days. After the first CPP test, animals were treated with CBD (10 mg/kg, i.p.) or its vehicle for 5 days and then subjected to the forced swimming stress protocol to induce AMPH-relapse in the CPP paradigm. Behavioral findings showed that CBD treatment prevented AMPH reintegration, also exerting anxiolytic activity. While more studies are needed, these findings support the therapeutic potential of CBD in the prevention of AMPH-relapse, representing a promising candidate in the treatment of AMPH-addiction. Additional future clinical studies are needed to better understand the role of the CBD in the context of drug addiction. This study was financed by the Fundação de Amparo à Pesquisa do Estado do Rio Grande do Sul (FAPERGS) and CNPq.

02.025 Antipsychotic-Like Activity of Micronized Naringenin Particles Produced by Supercritical CO₂. Tavares VB¹, Oliveira PV², Sanaiotto O¹, Kuhn KZ¹, Daniel CF¹, Provinelli AC¹, Schio ACZ¹, Siebel AM³, Bortoluzzi A², Lanza M², Oliveira JV², Müller LG¹ ¹Unochapecó ²UFSC, UFSC ³FURG

Introduction: Schizophrenia is a psychiatric disorder associated to positive, negative and cognitive symptoms. The antipsychotic drugs available present several side effects, leading to low pharmacotherapy adherence, and are not effective to ~30% of patients. Therefore, the search for new antipsychotics is a real need. Naringenin (NAR) is a flavonoid that crosses the blood-brain barrier and has antioxidant and neuroprotective properties. However, NAR has low water solubility and, therefore, poor oral bioavailability. The micronization process decreases the size of the particles and improves the dissolution rate. Thus, the objective of this study was to obtain micronized particles of NAR (micro-NAR) and evaluate its antipsychotic-like activity. **Methods:** NAR microparticles were successfully obtained by the gas antisolvent technique using supercritical CO₂. *In vitro* dissolution rate assays confirmed that micro NAR exhibited a significant higher dissolution rate than raw NAR. *In vivo* experiments using male Swiss mice were approved by CEUA-UNOCHAPECÓ (#003/2021). Drugs used in the assays were dissolved in saline+1% Polysorbate 80 (vehicle), except micro NAR. The ketamine-induced hyperlocomotion model, predictive of positive symptoms of schizophrenia, was used. Animals were orally pretreated with vehicle (10 mL/kg), raw or micronized NAR (200 mg/kg). Afterwards, ketamine or saline were administered (i.p.) to the animals. Locomotor activity was videorecorded in an open field (OF) arena for 20 min and the distance (m), speed (m/s), number of rearings, groomings and fecal bolus were registered. ANY-Maze software was used for the analysis. Results were analyzed by one-way ANOVA followed by Tukey's test, significance for p<0.05. **Results:** One-way ANOVA revealed that ketamine induced a significant increase in distance [F(3,28) = 6.627, p=0.0016], speed [F(3,28) = 7.039, p=0, 0011] and number of rearings [F(3,28) = 9.901, p=0.0001] in OF, which can be associated with positive symptoms of schizophrenia. No effect of ketamine injection was detected on the number of groomings [F(3,28) = 0.5611, p=0.6452] and fecal bolus expelled during the OF test [F(3, 28) =1.294, p = 0.2960]. Raw NAR did not prevent hyperlocomotion, but micro NAR, administered at the same dose as raw NAR, was effective in preventing the increased distance, speed and number of grooming induced by ketamine. Furthermore, the dose of micro NAR that prevented ketamine-induced hyperlocomotion did not impair the basal locomotor activity of mice, since animals treated only with raw or micro NAR did not show differences in any locomotor parameters assessed in the OF test when compared to the vehicle-treated group. **Conclusion:** Our results demonstrate the antipsychotic-like potential of micro NAR, which is possibly related to its increased dissolution rate and, consequently, increased bioavailability, in comparison to raw NAR. **Acknowledgements:** FAPESC, CAPES, CNPq

02.026 Omega-3 (DHA) Downregulates Inflammatory State in Microglial Cell Line.

Moraes-de-Souza I¹, Moraes BPT^{1,3}, Almeida MAP^{2,3}, Bozza PT², Castro-Faria-Neto HC², Silva AR^{2,3}, Gonçalves-de-Albuquerque CF^{1,2,3} ¹Unirio, Immunopharmacology Lab., Dpt of Physiological Sciences, Rio de Janeiro, Brazil; ²IOC-Fiocruz, Immunopharmacology Lab., Rio de Janeiro, Brazil; ³UFF, PPG Neuroscience, Niterói, Brazil

Introduction: Omega-3 (ω -3) is a family of polyunsaturated fatty acids (PUFAs) mostly known for its anti-inflammatory and antioxidant properties (LAYE, 2018). Docosahexaenoic acid (DHA) is the main ω -3 PUFA in brain tissue phospholipids (AHMMED, 2020). In the Central Nervous System, microglia respond when encountering stimuli such as bacteria lipopolysaccharide (LPS) (JOFFRE, 2020). This can be a double-edged sword because microglia-mediated inflammation is necessary for brain homeostasis. However, exacerbating this process can be neurodegenerative (SALTER, 2017). Thus, DHA's beneficial effects could regulate microglia's immune response. **Methods:** BV-2 murine microglial cell line was cultured in RPMI 1640, 10% fetal bovine serum (FBS), and 1% penicillin/streptomycin at 37 °C in an incubator with 5% CO₂. Cells were plated at 5x10⁴ density per well in 24-well plates. Before treatments, cells were starved for 3 hours in a culture medium without FBS. The control group was cultured in a 2% FBS medium. Dimethyl Sulfoxide was added to the vehicle group. DHA was diluted in 2% FBS culture medium and then added to wells in a final concentration of 100 μ M or 50 μ M. Treatment with DHA was administered for 1 hour, then 100 ng/mL of O127: B8 or O127: B5 LPS was added per well until samples were collected. Enzyme-linked Immunosorbent Assay was performed to measure the production of interleukin-1 β (IL-1 β), interleukin-6 (IL-6), and macrophage migration inhibitory factor (MIF). Nitric Oxide (NO) was measured using the Griess assay, and cell viability was evaluated by measuring lactate dehydrogenase (LDH). Nuclear factor kappa B (NF- κ B) p65 subunit and p38 mitogen-activated protein kinase (MAPK) expression were analyzed by Western Blot. **Results:** The viability of BV-2 cells was reduced upon LPS challenge, but DHA treatment restored it to control levels. DHA-treated cells showed a reduction of LPS-induced production of NO, IL-6, IL-1 β , and MIF. Protein expression analysis suggests reduced LPS-induced activation of NF- κ B p65 in DHA-treated cells. **Conclusion:** Omega-3 DHA showed beneficial effects by preserving cell viability, reducing pro-inflammatory cytokines and nitric oxide production while potentially reducing activation of inflammatory signaling pathways. Hence, DHA treatment can downregulate inflammation in the BV-2 microglial cell line. **References:** AHMMED, M. K. Compr. Rev. Food. Sci. Food. Saf., v. 19, n. 1, p. 64-123, 2020. LAYÉ, S. Pharm. rev., v. 70, n. 1, p. 12, 2018. JOFFRE, C. Nut., v. 12, n. 3, p. 647, 2020. SALTER, M. W. Nat. Med., v. 23, n. 9, p. 1018, 2017. **Acknowledgments:** This research was funded by the Instituto Oswaldo Cruz—FIOCRUZ, CAPES Grant 001, PPG Neurosciences—UFF, UNIRIO, FAPERJ, and CNPq.

02.027 The γ -benzylidene digoxin derivative BD-15 reduces oxidative stress in the hippocampus and cortex induced by LPS Neves EPF¹, Fonseca MFR¹, Silva SS¹, Farias ERA¹, Ferreira PYO¹, Machado MV², Villar JAFP², Campos HM¹, Pereira RM¹, Ghedini PG¹, Barbosa LA², Leite JA¹ ¹UFG, Dept of Pharmacology, Institute of Biological Sciences, Goiânia, Brazil. ²UFSJ, Lab de Bioquímica Celular, São João Del Rei, Brazil

Introduction: Heterozygous mutations in the ATP1A3 gene encoding the neuron-specific $\alpha 3$ subunit isoform of the Na⁺/K⁺-ATPase (the sodium pump) cause distinct neurological diseases, most notably Rapid-onset Dystonia with Parkinsonism (RDP), Alternating Hemiplegia of Childhood (AHC), and Cerebellar ataxia, areflexia, pes cavus, optic atrophy and sensorineural hearing loss (CAPOS). Recent studies have shown an increase in oxidative stress in the brains of Atp1a2/Atp1a3 double homozygous knockout mice compared to the WT. The BD-15 is a synthetic cardiotonic steroids, derivate from digoxin, showing specificity for the $\alpha 3$ -isoform causing an activation of this enzyme isoform. In addition, BD-15 decreased oxidative stress in different brain regions. Accumulating evidence suggests a relationship between neurodegenerative diseases and neuroinflammation. Lipopolysaccharide (LPS) is a major bacterial TLR4 ligand that activates the innate immune response, and systemic administration of LPS can cause neuroinflammation in animal models by mechanisms involving expression of pro-inflammatory cytokines, oxidative stress, and inhibition of neurotrophic factor production. Thus, the aim of the present work was to evaluate the effect of BD-15 on oxidative stress induced by LPS in the hippocampus and total cortex of mice.

Methods: Mice were randomly divided into four groups (n=7) and each group of mice was administrated intraperitoneally (i.p.) once a day for 3 consecutive days with either vehicle (DMSO) or BD-15 (0.56 mg/kg). One hour after the last injection on day 3, mice were injected i.p. with LPS, and after 24 hours the animals were euthanized, and the hippocampus and total cortex were collected for analysis of lipid peroxidation and activity of the antioxidant enzymes superoxide dismutase (SOD) and catalase (CAT). All procedures were the research was approved by the Committee on Ethics in Animal Use (CEUA/UFG n^o 014/21). **Results:** Results showed that BD-15 treatment decreased malondialdehyde (MDA) levels by 22% (p<0.05) and 32% (p<0.05) in the hippocampus and total cortex, respectively when compared to the LPS group. Furthermore, in the hippocampus, BD-15 increased SOD activity by 47% (p<0.05) and CAT by 33% (p<0.05) when compared to the LPS group, similar results were observed for the total cortex. **Conclusion:** our results suggest that BD15 has neuroprotective activity under LPS-induced oxidative stress in the hippocampus and total cortex of mice. However, further studies are needed to better understand the influence of this new digoxin derivative on neuroinflammatory processes. **Financial Support:** CNPq

02.028 Alterations in Molecular Targets in Dopaminergic Areas of the Brain Induced by Cannabidiol in Rats Previously Exposed to Amphetamine. Rossato DR¹, Rosa JLO¹, Metz VG², Burger ME², Pase CS² ¹UFMS, PPG em Farmacologia, ²UFMS, Depto de Fisiologia e Farmacologia

Relapse is the most concerning outcome to be managed in psychostimulant drug addiction, since in recent decades no specific pharmacological therapy has been approved for the treatment of this neuropsychiatric condition. The number of publications on Cannabidiol (CBD), an abundant compound in *Cannabis sativa*, has increased remarkably over the last years and supports the view that CBD has a vast array of possible therapeutic neuropsychiatric effects. Among these possibilities, CBD's anxiolytic effects are apparently similar to those of approved drugs to treat anxiety. In this study, we evaluated molecular modifications in brain areas of rats, which were previously exposed to amphetamine (AMPH) preference and subsequently treated with CBD and challenged to drug relapse after stress episode. For this, male Wistar rats (UFMS-8850121118) received d,l-AMPH (4 mg/kg, i.p.) or vehicle in the conditioned place preference (CPP) paradigm for 8 days. After the first drug preference test, animals were treated with CBD (10 mg/kg, i.p.) or its vehicle for 5 days. Forced swimming stress protocol was used to induce relapse to AMPH-CPP. In the sequence, rats were euthanized, brains were removed and both ventral striatum (VS) and ventral tegmental area (VTA) were dissected for blotting analysis. Behavioral findings showed that CBD treatment was able to prevent AMPH-relapse. At the molecular level, the increased D1R and D2R levels, as well as the decreased DAT levels AMPH-induced in the VS were restored by CBD treatment. In the VTA, CBD restored the CB1R and NAPE-PLD levels, which were decreased by AMPH, as also, CBD decreased FAAH levels, which was increased by AMPH. Our outcomes showed preventive activity of the CBD on the stress-evoked AMPH-relapse, inducing neuroadaptations in both dopaminergic and endocannabinoid systems in brain areas. Although more research is needed, these findings support the therapeutic potential of CBD in the prevention of AMPH-relapse.

02.029 Gestational Sepsis Induces Neurovascular Alteration and Oxidative Stress in The Frontal Cortex and Hippocampus of Neonatal Mice. Granja MG^{1,3}, Alves LP^{2,3}, Moraes FM^{1,3}, Santos APA³, Siqueira MFR³, Estado V³, Silva AR³, Gonçalves-de-Albuquerque CF^{1,3}, Castro-Faria-Neto HC^{1,2,3} ¹Unirio, PPG Biologia Molecular e Celular, Brazil; ²UFRJ, PPG Imunologia e Inflamação, Brazil; ³Fiocruz, Lab of Imunofarmacologia, Brazil

Gestational sepsis can trigger a systemic inflammatory response that affects fetal brain development. Nitric oxide (NO) is a molecule that plays a crucial role in regulating the cardiovascular and immune systems, and its levels can be affected by gestational sepsis. Dysfunction of endothelial cells that express intercellular adhesion molecules (ICAM) and vascular cell adhesion molecules (VCAM) results in a pro-inflammatory response and can affect the immune cellular response and neurovascular unit. The aim of our work was to evaluate the effects of maternal sepsis on oxidative stress, neurovascular alteration, and microglia activation in the hippocampus and prefrontal cortex of neonatal mice. Pregnant mice at the 14th embryonic day were intratracheally instilled with saline 0,9% solution (control) or *Klebsiella* spp. (3x10⁸ CFU) (sepsis) and started on meropenem after 5h. The offspring were sacrificed at P2 and P8 and samples of different regions of the brain were collected for Griess method to evaluate NO production, analysis of VCAM and ICAM adhesion molecules was performed using Western Blotting. Immunohistochemistry and intravital microscopy were used to evaluate the microglia profile and microvascular unit, respectively. All the procedures were approved by CEUA-IOC L001/2022. The results revealed a significant increase in NO in the frontal cortex of the septic group at age P2 compared to the saline group. However, at the age of P8, the differences were reduced. In the analysis of the hippocampus, NO levels showed a small increase in the septic group at both ages, P2 and P8, relative to the control group. We found an increase in ICAM levels in the frontal cortex in pups at P8. In the hippocampus region, however, ICAM levels are increased in the offspring at P2, but at P8 it is not observed in the hippocampus of these animals. Analyzing the presence of VCAM in the frontal cortex it was possible to observe that, at age P2, the sepsis group showed an increase in its concentration, but at P8, VCAM levels were normalized. In the hippocampal tissue, at P2, the sepsis group showed higher VCAM concentrations, which were maintained until P8. Microglia cells were analyzed by fluorescence immunohistochemistry showing an activated profile of microglia at the sepsis group and the cerebral microcirculation was evaluated by intravital microscopy demonstrating a reduction of rolling and adhesion of leukocytes. These data suggest that maternal sepsis may be causatively related to the development of cerebral inflammation, and neurovascular dysregulation and induces oxidative stress in neonatal life. This work was supported by grants from CAPES, FAPERJ, CNPq and INCT-NIM.

02.030 Eriodictyol Protects Mice with Streptozotocin-Induced Sporadic Alzheimer Disease: In Silico, in vitro and in vivo Study. Caracas P¹, Tavares J¹, Andrade LM², Albuquerque A², Silva JHM², Andrade GM¹. ¹UFC, Dpt Center for Research and Development of Medicines, Brazil; ²Fiocruz, Lab. of Structural and Functional Biology.

Introduction: Alzheimer's Disease (AD) is a neurodegenerative disorder that causes progressive memory loss and other cognitive impairments, being the most common form of dementia and affecting 48.6 million people worldwide. However, recent research suggests that Sporadic Alzheimer's Disease (SAD) is a Type 3 Diabetes, characterized by insulin resistance in the brain, involving molecular mechanisms similar to those causing Type 2 Diabetes in peripheral tissue. Thus, intracerebroventricular (icv) injections of streptozotocin (STZ) have been used as a model of Type 3 diabetes induction and as an experimental model of SAD due to causing oxidative stress and inflammation. This work aimed to study the effects of eriodictyol (ERI), a flavonoid with already described anti-inflammatory and antioxidant activity, on cognitive deficits and neuronal damage in mice subjected to the experimental model of SAD. **Methods:** Male Swiss mice (25-35 g) received bilateral STZ injections (3 mg/kg, icv, 1.5 ml) on day 1 and 3 of the experiment and were divided into 5 groups: Control; Control + eriodictyol 4 (ERI 4); STZ; STZ + ERI (2 and 4 mg/kg). Eriodictyol (Sigma-Aldrich, EUA) treatment was carried out for 16 days, starting 1 hour after the second induction procedure. Blood glucose measurement of the animals was performed before and after the induction of SAD. **Results:** The results showed that there was no significant change in blood glucose. The treatment significantly improved the deficits in aversive, recognition and spatial memory and did not alter locomotor activity. **Conclusion:** The neuroprotective effect is probably due to an antioxidant and anti-inflammatory action via inactivation of Glycogen synthase kinase-3 beta (GSK-3) and activation of the Kelch-like ECH-associated protein 1 (Keap1)/ Nuclear Factor-Erythroid-Related Factor 2 (Nrf2) pathway, in the *in silico* experiments, which prevented the reduction of Glutathione (GSH) levels and decreased nitrite levels in the hippocampus of the animals, thus attenuating the neuroinflammatory process and insulin resistance, highlighting its potential for preventive and/or adjuvant treatment of SAD. **Financial Support:** CAPES

02.031 Effects of Low-Dose Cannabis Extract on Non-Motor Symptoms and Quality of Life in Parkinson's Disease Patients - Five Case Report. Pauli KB, Ruver-Martins AC, Silva T, Souza BL, Hollas VG, Silva EG, Nascimento FP. Unila, Lab. of Medicinal Cannabis and Psychedelic Science, Foz do Iguaçu, PR, Brazil

Introduction: Parkinson's disease (PD) is a chronic progressive neurodegenerative disorder characterized by motor alterations such as bradykinesia, tremors, and rigidity. Symptoms result from neuroinflammation and reduction of dopaminergic neurons in the substantia nigra compacta in the midbrain, as well as dysfunction of the nigrostriatal dopaminergic signaling pathway. Motor symptoms appear when approximately 60% of dopaminergic neurons are lost (GAO, *Front. Neurol.* (2017). 8, 527). Non-motor symptoms such as anxiety, depression, sleep disorders, cognitive dysfunction, and pain significantly impact the quality of life of PD patients. Available pharmacotherapy is not fully effective and causes side effects contributing to patient debilitation (FRANK, *Science* (2007). 318(5854), 1309-1312). Cannabinoid studies have shown promise as a treatment option, prompting us to evaluate the effects of an extract with low concentrations of cannabinoids on non-motor symptoms in PD patients (PERTWEE, *Br. J. Pharmacol.* (2008). 153(2), 199-215. CURRAIS, *npj Aging Mech. Dis.* (2016). 2, 16012. BILKEI-GORZO, *Philos. Trans. R. Soc. Lond., B, Biol. Sci.* (2012). 367(1607), 3326-3341).

Methods: Five patients diagnosed with idiopathic PD for at least 5 years, aged over 40, on stable levodopa treatment for 30 days, and with stage 3 or 4 according to the Hoehn & Yahr scale were selected. Two patients received an oil with a concentration of 28µg/mL of Cannabidiol (CBD) and 250µg/mL of delta-9-tetrahydrocannabinol (THC), and three received a concentration of 112µg/mL of CBD and 1000µg/mL of THC orally for 90 days. Patients were evaluated through questionnaires regarding anxiety, depression, cognitive symptoms, insomnia, sleep quality, and quality of life using the Beck Depression Inventory (BDI-II), Hamilton Anxiety Scale (HAM-A), Montreal Cognitive Assessment (MoCA), Pittsburgh Sleep Quality Index (PSQI), Insomnia Severity Index (ISI), Epworth Sleepiness Scale (ESS), and Parkinson's Disease Quality of Life Scale (PDQ-39). **Results:** All patients showed positive progress in depression scores, with some achieving improvements ranging from 8.21% to 22.16%, and one patient showed considerable improvement with a gain of 27.7%. Regarding anxiety, the majority of patients showed improvements, with gains ranging from 3.56% to 30.26%. All patients also showed increases in cognitive assessment, with three showing improvements of 3.33% to 9.99%, and one patient with a considerable improvement of 26.64%. In terms of sleep quality, the majority of patients had improvements ranging from 14.28% to 23.8%, although one patient experienced a loss of -9.52%. In excessive daytime sleepiness, there were mixed results, with some patients showing improvements of 8.32% to 12.48%, while others experienced losses of -12.48% to -16.64%. In insomnia, the majority of patients had improvements of 7.14% to 24.99%, and two patients showed considerable improvements of 28.56% to 35.7%. As for the quality of life, most patients had improvements of 8.33% to 22.44%, with one patient showing a considerable improvement of 29.49%, while two experienced losses of -2.57% and -4.49%. **Conclusion:** Low-dose cannabinoids may have a positive effect on non-motor symptoms of PD. **Financial Support:** UNILA.

02.032 Therapeutic Potential of β -Caryophyllene on the Olfactory and Anhedonic-Like Disorders Induced by a Rat Model of Parkinson's Disease. Santos JR¹, Gonçalves R², Razera A¹, Kerppes II³, Carraro E², Sampaio TB^{2,4}. ¹Unicentro, Dpt. de Farmácia, Guarapuava, Brasil, ²Unicentro, Programa de Residência multiprofissional em Atenção Primária, Guarapuava, Brasil, ³Unicentro, Dpt. de Fisioterapia, Guarapuava, Brasil, ⁴UFSM, Dpt. de Farmacologia, Santa Maria, Brasil

Introduction: Parkinson's disease (PD) is the second most prevalent neurodegenerative disorder worldwide. It is characterized by progressive degeneration of dopaminergic neurons in the nigrostriatal area. Alongside the well-known motor symptoms, PD also presents non-motor symptoms such as olfactory disturbances and anhedonia, which affect patients' quality of life. Current pharmacological treatments provide temporary symptomatic relief, mainly of motor symptoms. In this sense, evidence suggests that the endocannabinoid system may indirectly modulate the dopaminergic neurotransmission, emerging as a potential therapeutic target for PD. Therefore, this study evaluated the impact of beta-caryophyllene (BCP) treatment, a type 2 cannabinoid receptor agonist, on the olfactory and anhedonic-like disturbances induced by 6-hydroxydopamine (6-OHDA) in rats.

Methodology: 45 adult male Wistar rats (250-350g) were randomly divided into four treatment groups: (i) SHAM; (ii) BCP *per se* (100 mg/kg/day; intraperitoneal); (iii) 6-OHDA (10 μ g/hemisphere; in the dorsolateral striatum); and (iv) 6-OHDA+BCP. 6-OHDA was bilaterally injected at a dose of 10 μ g/hemisphere in the dorsolateral striatum (AP +0.2 mm; ML \pm 3.5 mm, DV -4.8 mm). SHAM and BCP groups received only vehicle. The BCP treatment was administered daily, starting on the first day after the 6-OHDA injection. Behavioral tests were conducted on the 4th and 9th days after the 6-OHDA injection to evaluate olfactory function and anhedonic-like behavior, respectively. The olfactory discrimination test (ODT) consisted of two compartments; one containing fresh bedding and the other containing the bedding from the cage where the animal was housed for 48 h (familiar compartment). The rat's investigation time in each compartment was recorded for 5 minutes to evaluate its ability to discriminate odors. In its turn, the anhedonic-like behavior was evaluated in the splash test. For this, a 10% sucrose solution was sprayed on the rat's dorsal part, and the rat was placed individually in an acrylic box. The rats were observed for 15 minutes, and the time spent on self-cleaning was recorded as a measure of self-care and motivational behavior. The use of animals in this study followed the guidelines of the Committee on Care and Use of Experimental Animal Resources and was approved by the Animal Use Committee (003/2023) of Universidade Estadual do Centro Oeste, Brazil. **Results:** In the ODT, two-way analysis of variance (ANOVA) demonstrated a main effect of 6-OHDA treatment in the percentage of time spent in the familiar compartment. Soon, 6-OHDA group showed a reduced time in the familiar compartment, as compared to the SHAM group, suggesting a deficit in the ability to discriminate odors. This reduction was attenuated by treatment with BCP. Regarding anhedonic-like behavior, evaluated in the splash test, the animals in the 6-OHDA group showed a reduction in the total self-cleaning time, indicating impairment of motivational behavior and self-care, which are characteristics of anhedonia. Of highlight, two-way ANOVA followed Tukey *post hoc* test indicated that BCP treatment reversed this 6-OHDA-induced impairment. **Conclusion:** The results suggest that BCP has promising therapeutic potential for the treatment of olfactory disorder and anhedonic-like behavior related to PD, as it improved the ability to discriminate odors and reversed the motivational deficits observed in the 6-OHDA-induced model in rats. **Financial Support:** CNPq.

02.033 Evaluation of the Antipsychotic-Like Activity of Microparticles of Naringin Obtained in Supercritical Medium. Daniel CF¹, Oliveira PV², Provenelli AC¹, Schio ACZ¹, Sanaiotto O¹, Kuhn KZ¹, Tavares VB¹, Dias JL², Aguiar GPS³, Siebel AM⁴, Oliveira JV², Müller LG¹ ¹Unochapecó ²UFSC, UFSC ³SEBRAE ⁴FURG

Introduction: One of the hypotheses of schizophrenia neurobiology postulates a hypofunction of NMDA glutamatergic receptors in GABAergic interneurons. Thus, the administration of ketamine (NMDA antagonist) mimics schizophrenia positive symptoms. Naringin is a flavanone glycoside that exhibits neuroprotective activity, but it has poor solubility in water and, therefore, low oral bioavailability. Micronization is an approach that reduces particle size and, therefore, improves properties like solubility, bioavailability, dissolution rate, and stability. In this sense, the aim of this study was to obtain microparticles of naringin and evaluate its antipsychotic-like potential. **Methods:** Naringin particles were micronized by antisolvent gas technique (GAS) using supercritical CO₂ as antisolvent and characterized by Scanning Electron Microscopy, Powder-X-ray diffraction, Differential scanning calorimetry and Fourier-transform infrared (FTIR) spectroscopy. The water dissolution rate of particles was also assessed. Ketamine-induced (10 mg/kg, i.p.) hyperlocomotion test in male Swiss mice was carried out to verify the possible antipsychotic-like effect of naringin microparticles. Mice were pretreated with vehicle (saline solution, Sham group), commercial or micronized naringin (50 or 200 mg/kg, p.o). One hour after the gavage, ketamine was injected, and the animals explored the open field arena for 30 min (acclimatization). Then, the locomotor activity was videorecorded for 20 min. The total distance traveled (m), number of rearings, groomings and the number of fecal bolus were registered. ANY-MAZE software was used for video analysis. Data were analyzed by one-way ANOVA, post-hoc Tukey (significance for $p < 0.05$). CEUA-UNOCHAPECÓ approval: 003/2021. **Results:** Naringin microparticles were successfully obtained and their specific surface area was approximately 5 times higher than the surface area of commercial naringin. Also, an increase in dissolution rate of approximately 4-fold was observed for micronized naringin compared to the commercial compound. The administration of ketamine increased the distance traveled [$F(5.56) = 8.785$, $p < 0.001$] and the number of rearings [$F(5.56) = 14.34$, $p < 0.0001$]. However, there were no effects of ketamine on the number of groomings [$F(5.56) = 1.520$, $p = 0.1794$] and fecal bolus [$F(5.56) = 2.246$, $p = 0.0634$] expelled by the animals. The administration of commercial naringin prevented hyperlocomotion only at 200 mg/kg. On the other hand, micronized naringin was able to prevent the ketamine-induced hyperlocomotion at both 50 and 200 mg/kg. **Conclusion:** Taken together, our results demonstrate that microparticles of naringin obtained by GAS using supercritical CO₂ present antipsychotic-like potential, which is probably related to its increased bioavailability, due to increased dissolution rate and specific superficial area in comparison to the commercial compound. **Acknowledgements:** UNIEDU, UNOCHAPECÓ, CAPES, CNPq, FAPESC,

02.034 Central Inhibition of PKC β Reduces Fever and Serum Cytokine Levels in Rats.

Barreto LSH, Cruz EKM, Gomes APLN, Gomes BRB, Sousa GLS, Veiga-Souza FH UnB

Introduction: Fever is an autonomic, endocrine and behavioral response coordinated by the brain in response to inflammatory conditions which trigger the synthesis of several endogenous pyrogens, such as prostaglandin (PG) E₂, interleukins (IL) 1 β , IL-6 and tumor necrosis factor(TNF)- α by the host defense cells. Lipopolysaccharide (LPS) is an endotoxin of gram-negative bacteria, widely used to induce fever in experimental models. Protein kinase C (PKC) isoforms exert regulatory activities in a variety of cellular functions, including cell growth and differentiation, gene expression, hormone secretion, among others. Evidence indicates the participation of PKC in the regulation of fever induced by LPS (Kozak et al, 1997; Thaler et al, 2009), however the isoform involved has not yet been identified. Proteomic analysis data obtained by our group demonstrated an increase in the abundance of PKC β in the hypothalamus of rats during fever (Firmino et al, 2018). Thus, the present study aimed to investigate the effect of selective inhibition of PKC β on the febrile response and hypothalamic PGE₂ production induced by LPS, as well as on the concentration of circulating inflammatory cytokines. **Methods:** The procedures used in this study were approved by the Ethics Committee on the Use of Animals of the University of Brasilia (n^o 23106.080030/2022-22). Male Wistar rats received intracerebroventricular administration of the inhibitor enzastaurin (ENZ, 0.3 – 3 ng/2 μ L) 30 minutes before the intraperitoneal administration of LPS (50 μ g/kg) or saline and their temperature was monitored up to 5 h. Hypothalamic PGE₂ and serum cytokines levels were determined by Elisa. Statistical analysis was done by two-way ANOVA followed by Tukey post-test with p<0.05. **Results:** Pre-treatment with ENZ resulted in a decrease in body temperature, accompanied by a reduction in serum levels of IL-6 and TNF- α . In contrast, there was no inhibition of hypothalamic PGE₂ production. **Conclusion:** Our data suggest the participation of PKC β in the regulation of fever induced by LPS in rats, by acting on signaling pathways downstream of PGE₂, which can reduce the thermo-effector response and the peripheral production of pro-inflammatory cytokines. Further studies are needed to confirm this hypothesis. **References:** Firmino et al, J Proteomics, v. 187, p. 182, 2018. Kozak et al, Am J Physiol, v. 273, p. R873, 1997. Thaler et al, Endocrinol. v. 150, n. 12, p. 5362, 2009. **Financial Support:** FAPDF; Capes; CNPq; DPG/UnB.

02.035 Neuroprotective Effect of LQFM219 in LPS-Challenged Rats. Fonseca MFR¹, Galvão GM¹, Neves EPFI¹, Silva SS¹, Farias ERA¹, Campos HM¹, Ghedini PC¹, Menegatti R², Leite JA¹. ¹ICB-UFG, Dpt of Pharmacology, Goiânia, Brazil; ²UFG, Lab. of Medicinal Pharmaceutical Chemistry, School of Pharmacy, Goiânia, Brazil

Introduction: In oxidative stress, there is an increase in reactive species that cause altered intracellular signaling, leading to dysregulation of the inflammatory response. The inability of antioxidant defense systems to modulate the proinflammatory response is important to development and progression of neurodegenerative diseases. In animal models of neuroinflammation, lipopolysaccharide (LPS) is used to induce the increase of pro-inflammatory cytokines and oxidative stress. LQFM219 is a molecule designed from celecoxibe (COX-2 inhibitor) and darbufelone (inhibitor of COX-2 and 5-LOX) lead compounds through a molecular hybridisation strategy. Previous studies have shown that LQFM219 has antinociceptive and anti-inflammatory potential *in vitro* and *in vivo*. Thus, the aim of the work was to evaluate the neuroprotective effect of LQFM219 on oxidative stress induced by LPS in the total cortex and hippocampus of rats. **Methods:** Male Wistar rats with 60 days old were randomly divided into five groups (n=6), each group of rats were administrated orally (gavage) with either vehicle (DMSO 10%) or LQFM219 (12.5, 25 and 50 mg/kg). One hour after treatment the animals were challenged with LPS (1 mg/kg) and after 24 hours the animals were euthanized. Serum samples were collected to determine the concentrations of pro-inflammatory cytokines TNF- α and IL-1 β . Subsequently, hippocampus and total cortex was dissected for evaluated carbonylated proteins and lipid peroxidation. All research procedures were approved by the Animal Ethics Committee (CEUA/UFG nº 016/22). **Results:** The results show that LQFM219 at doses of 12.5; 25 and 50 mg/kg reduced systemic TNF- α levels 24 hours after LPS challenge by 92.79%, 91.86% and 94.64%, respectively. When analyzing the effects of LQFM219 on oxidative stress in the hippocampus of animals 24 hours after the challenge with LPS, we observed that treatment with LQFM219 at doses of 12.5; 25 and 50 mg/kg reduced protein carbonylation by 33.33%, 57.78% and 48.89% and lipid peroxidation by 19.0%, 23.72% and 19.25% respectively. Similar results were observed for protein carbonylation and lipid peroxidation in the total cortex of animals treated with LQFM219 and challenged with LPS. **Conclusion:** Our results indicate that LQFM219 exhibits neuroprotective activity against LPS-induced oxidative stress in hippocampus and total cortex by reduction of oxidative stress, as well as reduced inflammatory parameters systemic. However, further studies are needed to better understand the influence of LQFM219 on neuroinflammatory processes. **Financial Support:** CNPq. **References:** ARAUJO, CRM. Quím. Nova, v. 38, n. 6, 2015., BATISTA, CRA. Int J Mol Sci. v. 20, n. 9, p. 2293-2323, 2019., ELSONBATY, S. Archives of Biochem. and Biophys., v. 689, 2020., ETIENNE, R. Rev. Virtual Quim., v. 13, n. 1, p. 167-191, 2021., GALVÃO, GM. Int Immunopharmacol., v. 88, 2020., GARCIA, IJP. J Cell Biochem., p. 1-11. 2018., KESHERWANI, R. Biologia (Bratisl), v. 76, p. 793-798, 2021., KIM, Y. K. Prog. Neuro-Psychopharmacol. Biol. Psychiatry, v. 64, p. 277-284, 2016., KITAZAWA, M. J Neurosci., v. 25, n. 39, p. 8843-53, 2005., LIN, TL. Frontiers in Pharmacology, v. 11, p. 554-562, 2020., LEITE, JA. Front. Pharmacol., v. 13, 2022., LEITE, J. A. et al. Scientific Reports, v. 10, n. 14180, 2020., LYMAN, M. Neurosci Res, v. 79, p. 1-12, 2014.,

02.036 Use of Cannabinoids for the Treatment of Epilepsy Associated with 1p36 Syndrome: A Case Report. Campo RM, Portilla MC, Santos FC, Novoa DA, Silva EG, Donato MF, Nascimento FP. Unila, Lab. of Medical Cannabis and Psychedelic Science, Foz do Iguaçu, PR, Brazil

Introduction: The 1p36 syndrome is a common chromosomal deletion that often causes intellectual disability, developmental delay, and epilepsy. Unfortunately, traditional treatments are often ineffective. Strong evidence links epilepsy, the endocannabinoid system (ECS) and phytocannabinoids, including cannabidiol (CBD), which shows promise in anticonvulsant treatment, and tetrahydrocannabinol (THC), which may have a synergistic effect with CBD (i.e. THC enhances the medicinal properties of CBD, while CBD attenuates the psychotropic effects of THC). We want to investigate whether treatment with cannabis extract can improve the symptoms of refractory epilepsy related to this clinical condition. **Methods:** To conduct our study, we evaluated the clinical history of a 13-year-old male patient diagnosed with epilepsy, average physiological developmental delay, dyskinetic cerebral palsy, and 1p36 deletion syndrome. **Results:** The patient had been experiencing seizures since birth and had not responded to any medication available on the national market. Due to the severity of his condition, the patient was given oral treatment with an artisanal extract of Cannabis for 223 days. The extract included various concentrations and doses of isolated CBD (20, 800, 600 or 100 mg per day) and/or CBD: THC (3.75, 5 or 20 mg per day), as well as maintaining the use of phenobarbital and diazepam in emergency cases. After the patient began treatment with the Cannabis extract full spectrum, his tonic-clonic crises and motor coordination significantly improved, and he experienced only four crises per day. When the patient took Cannabis extract with CBD: THC (1: 1), doses of isolated CBD and other anticonvulsant drugs were reduced. Additionally, he only experienced spasms upon awakening and markedly improved his quality of life. However, the patient did experience some side effects from the treatment, including laughter for 24 hours from one of the artisanal extracts of Cannabis; lack of sleep from CBD: THC 5mg/ml / 3.75mg/ml, respectively and maintenance of seizures with the isolated CBD (20mg/ml). **Conclusions:** Our study found that Cannabis extract CBD: THC (1: 1), in combination with phenobarbital, can significantly improve seizures, motor coordination, and quality of life for patients with refractory epilepsy related to 1p36 deletion syndrome and demonstrated the safety of the Cannabis medicine. Moreover, the study offers new possibilities for treating refractory epilepsy associated with 1p36 deletion syndrome with medicinal Cannabis. **Financial Support:** UNILA - PR.

02.037 Marinobufagenin Reduces Oxidative Stress in the Cortex and Hippocampus of LPS-Challenged Mice. Farias ERA¹, Lopes da Silva RR¹, Invernizzi EPF¹, Fonseca MFR¹, Silva SS¹, Campos HM¹, Pereira RM¹, Ghedini PC¹, Scavone C², Quintas LEM³, Leite JA¹
¹ICB-UFG, Dept of Pharmacology, Goiânia, Brazil. ²ICB-USP, Dept of Pharmacology, ³UFRJ, Lab. of Biochemical and Molecular Pharmacology, Rio de Janeiro.

Introduction: The biochemical integrity of the brain is crucial for the normal functioning of the central nervous system (CNS). One of the factors contributing to the biochemical degradation of the brain is oxidative stress, a process resulting from excessive production of free radicals and failure in the antioxidant response system. Oxidative stress and neuroinflammation are intrinsically related phenomena, as macrophages/microglia and astrocytes are sources of reactive oxygen species important for the development of neurodegenerative and neuropsychiatric diseases. Cardiac glycosides (CGs) are substances widely found in nature and act by binding to Na⁺/K⁺-ATPase, a transmembrane protein responsible for using the energy from ATP breakdown to transport Na⁺ and K⁺ against a concentration gradient. Marinobufagenin (MBG) belongs to the group of bufadienolides, characterized as an endogenous cardiotonic agent in mammals. Recent studies demonstrate the anti-inflammatory effect of MBG in models of zymosan-induced inflammation. Therefore, the study aimed to evaluate the neuroprotective effect of MBG in lipopolysaccharide (LPS)-induced oxidative stress in total cortex and hippocampus. **Methods:** The experimental procedures were approved by the Animal Ethics Committee of the Federal University of Goiás (CEUA/UFG Protocol No. 014/21). Swiss mice were pre-treated for 3 consecutive days with MBG (0.56 mg/kg i.p.), and 1 hour after the last day of treatment, the animals were challenged with LPS (1 mg/kg i.p.). Antioxidant parameters were evaluated in samples of the total cortex and hippocampus after euthanizing the animals, 24 hours after the LPS challenge. **Results:** MBG showed antioxidant action by decreasing lipid peroxidation by 31% and 60% and protein carbonylation by 32% and 49% in the total cortex and hippocampus respectively. Furthermore, in total cortex MBG restored the activity of catalase by 49 % and superoxide dismutase by 80% when compared with LPS group. Similar results were observed for the hippocampus. **Conclusion:** These results highlight the antioxidant potential of MBG and suggest that it is capable of reducing the oxidative effects associated with acute LPS exposure. Further additional studies are necessary to elucidate a signaling pathway induced by MBG in LPS-induced neuroinflammation. **Financial Support:** CNPq.

02.038 Protein Kinase C β Inhibition Attenuates the Production of Oxygen Reactive Species in Brown Adipose Tissue of Rats. Cajado VJ, Aguiar SCR, Gomes APLN, Sousa GLS, Souza PEN, Veiga-Souza FH. UnB

Introduction: Fever is the temporary increase in the body temperature in response to a disease or illness. The increase and maintenance of body temperature associated with fever is due to behavioral changes and autonomic responses aimed at increasing heat production and decreasing heat loss (Blomqvist & Engblom, 2018). Some studies have suggested the involvement of protein kinase C (PKC)-dependent signaling pathways in the development of fever (Kozak et al, 1997; Thaler et al, 2009), but is not clear which isoform is involved in this response. We investigated the effect of PKC β inhibitor, enzastaurin (ENZ), on the febrile response induced by lipopolysaccharide (LPS) and on the production of reactive oxygen species (ROS) in brown adipose tissue (BAT). **Methods:** Male Wistar rats received intracerebroventricular administration of ENZ 30 minutes before the intraperitoneal administration of LPS or saline and their temperature was monitored up to 5 h. ROS production was determined by electron paramagnetic resonance (EPR). The procedures used in this study were approved by the Ethics Committee on the Use of Animals of the University of Brasilia (n^o 23106.080030/2022-22). Statistical analysis was done by two-way ANOVA followed by Tukey post-test with $p < 0.05$. **Results:** The results showed that ENZ (3 ng/rat) attenuated the febrile response induced by LPS (50 $\mu\text{g}/\text{kg}$) in 38%. The administration of LPS induced an increase in the production of ROS in the BAT, which was reduced by 53% by the treatment with ENZ. **Conclusion:** Our results suggest the participation of the PKC β in the regulation of LPS-induced fever in rats, possibly by acting on signaling pathways which may reduce the efferent response and, consequently, decrease the peripheral production of ROS in the BAT, with inhibitory effects on thermogenesis. **References:** Blomqvist & Engblom, *Neuroscientist*, v. 24, p.381, 2018; Kozak et al, *Am J Physiol*, v. 273, p. R873, 1997; Thaler et al, *Endocrinol.* v. 150, n. 12, p. 5362, 2009. **Financial Support:** FAPDF; Capes; CNPq; DPG/UnB.

02.040 Social Isolation Stress Impairs Fear Extinction Recall in Mice: Effect is Reverted By a Fatty Acid Amide Hydrolase Inhibitor. Silva IP^{1,2}, Coelho AA^{1,2}, Lisboa SF¹ ¹FCFRP-USP, Dpt of BioMolecular Sciences, ²FMRP-USP, Dpt of Pharmacology

Introduction: Stress exposure and cannabinoid receptor type 1 (CB1) blockade cause deficits in the conditioned fear extinction. In contrast, increasing the endocannabinoid anandamide levels with fatty acid amide hydrolase (FAAH) inhibitors, or CB1 activation facilitate conditioned fear extinction. The transient receptor potential cation channel subfamily V member 1 (TRPV1) can also be activated by anandamide, but this activation exerts opposite effects to CB1 in defensive responses, indicating there is a balance between CB1/TRPV1 receptors. Social isolation stress might contribute to the development of psychopathologies, such as PTSD. In mice social isolation could resemble some PTSD features, such as alterations in conditioned fear processing. Therefore, the administration of a drug that facilitates CB1 signaling before the extinction session could facilitate stress-induced impairment in contextual fear conditioning. **Methods:** Male C57 mice were stressed by social isolation during 7 days or kept in groups (3 per cage), and then submitted to an inescapable footshock conditioning session (3 electrical foot-shock, 0.75 mA, 2s/each; Ugo Basile FC System, Anymaze). 24h later mice were placed in the same chamber for evaluation of freezing behavior during fear extinction acquisition (20 min / Day 2). After additional 24h the extinction recall was evaluated during 10 minutes in the same box (Day 3). Extinction recall was tested comparing the last 5 minutes of Day 2 with the first 5 minutes of Day 3. 30 minutes before re-exposure to the box in Day 2, independent groups of socially-isolated mice received URB597 (0.1, 0.3 or 1.0 mg/kg; intraperitoneally), or vehicle (10% dimethyl sulfoxide ? DMSO in NaCl 0.9%). They were evaluated 24h later in the same chamber, without drug. Prefrontal cortex and hippocampus were dissected for later analysis. All procedures were approved by the Local Animal Ethical Committee. **Results:** Vehicle-treated socially-isolated mice showed an impaired conditioning when compared to vehicle-treated grouped animals ($p < 0.05$). On Day 3, socially-isolated vehicle-treated animals showed impaired fear extinction recall, evidenced by statistical difference in the paired t Student test, between the last five minutes of fear extinction acquisition session vs. five first minutes of fear extinction recall session ($T_{16} = 2.528$, $p < 0.05$). URB597 administration attenuated this stress effect in the dose of 0.1 and 0.3 mg/kg (URB597 0.1: $T_{16} = 0.4451$, $p > 0.05$; 0.3: $T_{16} = 2.538$, $p > 0.05$), but not in the dose of 1.0 mg/kg ($T_{15} = 3.182$, $p < 0.05$). **Conclusion:** Blocking FAAH and increasing anandamide levels attenuates fear extinction impairment induced by social isolation in mice. However, when this blockage occurs more intensely, with a greater increase in anandamide levels, this effect is lost, probably because it acts on other receptors, such as TRPV1. Therefore, these mechanisms can be important targets for treatment of PTSD. Biomolecular studies will be performed for better understand the mechanisms behind these effects. **Financial Support:** CAPES, CNPq and FAPESP (2017/19731-6); FAPESP fellowship (2019/12830-4 and 2021/01656-3).

02.041 Investigation of the Antidepressant-like Activity of an Alkaloid Fraction obtained from *Psychotria nemorosa* (Rubiaceae). Provenelli AC¹, Oliveira BS¹, Hermes ME¹, Gerhard GM², Gasparetto RL², Couto CER², Klein LJ², Muller LG¹. ¹Unochapecó, PPG Environmental Sciences. ²Univali

Introduction: Depression affects about 3.8% of the world population and is characterized by depressed mood and anhedonia (WHO, 2023). Monoaminergic hypofunction is one of the hypotheses of depression neurobiology, which postulates a central decrease in serotonin, noradrenaline, and dopamine. Cimitzapine is an alkaloid that presents inhibitory activity against MAO-A *in vitro* (Klein et al., 2020) and is found in *Psychotria nemorosa*, popularly known as *Ayhuasca*. The aim of this study was to investigate the antidepressant-like effect of an alkaloid fraction from *P. nemorosa*. **Material and Methods:** Dried leaves of *P. nemorosa* (SisGen-AA26CBC) were macerated with methanol at room temperature for 3 days. To obtain the fraction enriched in alkaloids (AF), the crude methanolic extract was subjected to liquid-liquid separation with HCl and chloroform. The AF was analyzed by LC-MS, and cimitzapine was identified as its major constituent (46%). Male Swiss mice (25 - 35g) were divided by randomization (cage/liter) into experimental groups: vehicle (10 mL/kg, p.o.), fluoxetine (FLU, 30 mg/kg, p.o.) and AF (10, 30 and 100 mg/kg, p.o) (n=8/group, calculated considering $\alpha=0.05$, $\beta=0.8$). The tail suspension test (TST) was performed to analyze the immobility time (s) of the animals during the last 4 min of a 6min session (Anzollin et al., 2022). The open field test (OFT) was carried out with the minimum effective dose of the AF (10 mg/kg). The number of crossings, groomings, rearings and fecal bolus were registered for 10 min after 5 min of habituation. ANY-Maze® software was used to evaluate the behavioral parameters. Data were analyzed by one-way ANOVA, *post-hoc* Tukey (mean±SEM, significance for $p<0.05$). CEUA/UNOCHAPECÓ: #025/2022. **Results:** The administration of AF at 10 mg/kg elicited a significant reduction in the immobility time of animals (50.9±8.9s; $p=0.025$) when compared to the vehicle-treated group (90.5±6.7s), being this the AF minimum effective dose. There were no differences between the immobility time of the vehicle group and the groups treated with AF at 30 (61.0±7.3s; $p=0.152$) and 100 (121.7±10.8s; $p=0.137$) mg/kg. FLU significantly reduced mice immobility time in the TST (52.5±11.1s; $p=0.034$) in comparison to the vehicle-treated group. In the OFT, the AF at 10 mg/kg did not induce alterations in the total distance travelled (m) by the animals [vehicle: 24.57±2.24; FLU: 27.05±4.59; AF: 37.14±5.44; $p=0.13$], neither in the number of groomings [vehicle: 5.67±1.89; FLU: 1.5±0,57; AF: 1.67±0,49; $p=0.07$] nor in the fecal bolus expelled during the session. Nevertheless, a significant reduction in the number of rearings was found in the groups treated with FLU and AF [vehicle: 60.67±7.44; FLU: 27.83±6.34 ($p=0.0030$); AF: 38.83±2.81; $p=0.04$]. **Conclusion:** The AF enriched in cimitzapine presents antidepressant-like effect when acutely administered to mice at 10 mg/kg and is devoid of locomotor effects. **Acknowledgements:** UNOCHAPECÓ/UNIEDU, CAPES, CNPq. **References:** Anzollin, GS. *eJTCM*, v.12, p.309, 2022. Klein, J. J. *Nat. Prod.*, v.1463, p.71, 2016. WHO, www.who.int/news-room/fact-sheets/detail/depression, 2023

02.042 Neuroinflammation Induced by *Klebsiella pneumoniae* and the Role of PPAR- γ .

Almeida MAP¹²³, Costa MF¹², Moraes-de-Souza I¹², Moraes BPT¹²³, Bozza PT¹, Castro-Faria-Neto HC¹, Gonçalves-de-Albuquerque CF¹, Trindade P⁴, Silva AR^{1,2,3}. ¹IOC-Fiocruz, Immunopharmacology Lab., Rio de Janeiro, Brazil; ²Unirio, Immunopharmacology Lab., Dpt of Physiological Sciences, Rio de Janeiro, Brazil; ³UFF, PPG Neurosciences, Niterói, Brazil; ⁴UFRJ, Pharmacy Faculty, Dpt of Clinical and Toxicological Analyses

Introduction: Astrocytes execute numerous tasks to maintain brain homeostasis, from synapses regulation to metabolic support[1]. They also respond to inflammatory insult in several pathologies including in sepsis associated encephalopathy (SEA)[2]. Sepsis is defined as a life-threatening organ dysfunction caused by an unbalanced host response to infection[3]. SEA patients develop delirium, coma and long-term cognitive dysfunctions. Sepsis increases blood-brain barrier permeability allowing the influx of cytokines like interleukin-6, interleukin-1 β and tumor necrosis factor- α and leukocyte transmigration[4]. These events trigger glial cells to a reactive state [5]. The peroxisome proliferator-activated receptor gamma (PPAR- γ) is an important transcription factor in lipidic and metabolic regulation[6]. Thiazolidinedione drug class is a well-known antidiabetic PPAR- γ ligand[6]. Expressed in the CNS[7], the PPAR- γ activation downregulates inflammation, throughout several mechanism including inhibition of MAP kinases, nuclear factor- κ B (NF- κ B) and signal transducer and activator of transcription 3 (STAT3)[8]. **Objectives:** characterize neuroinflammation caused by *K. pneumoniae* and the effects of rosiglitazone treatment. **Methods:** Male Swiss mice were instilled with *Klebsiella pneumoniae*. Cytokines and protein expression in the brain were evaluated at 24 and 48h after insult and cerebral microcirculation 48h after insult. Mice were post-treated with 0.5 mg/kg rosiglitazone intraperitoneally. All procedures were approved by CEUA-IOC (CEUA license 028/2022). **Results:** *K. pneumoniae* increases the expression of IL-6, TNF- α , CXCL1 and CCL2 48h after instillation. Rosiglitazone was not sufficient to reduce cytokine expression. There was an increased expression of the reactive astrogliosis marker Glial fibrillary acidic protein (GFAP) at 48h. Cerebral microcirculation was affected by *K. pneumoniae*, increasing rolling and adherent leukocytes. Treatment with rosiglitazone improved cerebral microcirculation parameters. **Conclusion:** this work showed that *K. pneumoniae* induces neuroinflammation, astrocyte response and microcirculatory dysfunction 48h after insult. The treatment with rosiglitazone improved microcirculation showing that PPAR- γ may play a beneficial role in sepsis neuroinflammatory response. **Acknowledgments:** FAPERJ, CNPq, CAPES, IOC-FIOCRUZ/RJ, PPGNeuro UFF, UNIRIO. 1. Khakh, B.S. Ann. Rev. N., p.187, 2019. 2. Villarreal, A. Int. J. Mol. Sci., v.22, 2021. 3. Barichello, T. Crit. Care., v.26, p.14, 2022. 4. Tauber, S.C. Exp. Rev. Anti-infec. Ther., v.19, p.215, 2021. 5. Danielski, L.G. Mol. Neuro., v.59, p.7229 2022. 6. Carvalho, M.V.d. Int. J. Mol. Sci., v.22, 2021. 7. Warden, A. Sci. Rep., v.6, p.27618, 2016. 8. Villapol, S. Cel. Mol. Neuro., v.38, p.121, 2018.

02.044 Effects of the Enriched Environment in the Release of the Hormone Irisin and its Effects for Memory in a Mouse Model of Accelerated Aging. Malerba HN^{1,2}, Castellano M², Maia J², Marques ICS², Barrence FAC², Viel TA^{1,2} ¹ICB-USP, Graduation Course on Pharmacology, ²EACH-USP. Lab. of Neuropharmacology of Aging

Introduction: With increased longevity, there is an increase in chronic diseases that can often be debilitating. For this reason, it is expected that people are encouraged to adopt strategies to promote healthy aging. Studies are showing the benefits of enriched environment for improving memory and neuroprotection in animals and humans, which can lead to healthy longevity. Irisin is a hormone released during physical activity that is being linked to the increase in the brain-derived neurotrophic factor (BDNF) leading to memory maintenance and neuroprotection. However, little is known about the effects of the enriched environment in irisin release and brain benefits along the aging process. In this way, the objective of this work was to verify the memory and concentration of irisin in the blood of different ages senescence-accelerated mice submitted to enriched environment since early in life. **Methods:** Male senescence accelerated mice-prone (SAMP-8) were bred in our facility and submitted to enriched environment since they were 1,5 months old. Animals were separated into two groups: 1) Control SAMP-8 group (without stimulation); 2) Enriched environment SAMP-8 group (animals submitted to enriched environment, with different objects). The strategy was maintained until the animals completed 7 and 10 months of age (dead-points) and the objects were changed every 2-3 days. The evaluation of spatial memory was made with Barnes maze approximately two weeks before animals reached the endpoint. Animals were submitted to a “learning period” of 5 consecutive days followed by a memory recall one (R1) and two weeks later (R2). The irisin concentration in plasma was evaluated with a Mouse Irisin ELISA kit according to instructions of the manufacturer. **Results:** Concerning the spatial memory, it was observed that 7 months old-SAMP-8 submitted to enriched environment presented memory maintenance in R1 and R2, different from sedentary animals. 10 months old- sedentary animals could not even learn the task. On the opposite, animals submitted to enriched environment until 10 months of age could learn and remember the task, showing the preservation of memory. Blood irisin concentration was not different between 7 months of aging animals submitted or not to enriched environment. However, at 10 months of age, animals submitted to enriched environment presented an increase in 1,35 fold in blood irisin concentration ($47,87 \pm 0,91$), when compared to sedentary animals ($35,26 \pm 2,69$), $p < 0,01$. **Conclusion:** It was verified that enriched environment applied along the aging process promoted memory maintenance and increased plasma irisin concentrations in SAMP-8 animals. **Financial support:** This study was financed in part by the Coordenação de Aperfeiçoamento de Pessoal de Nível Superior – Brasil (CAPES) – Finance Code 001 and FAPESP (2020/14133-6). Malerba HN received a student ship from CNPq (168118/2018-1).

02.045 Low-Dose of Full-spectrum Cannabis sativa Oil May Improve Cognitive Impairment in Alzheimer's Disease - Cases Reports. Larentis-de-Souza B, Pauli KB, Donato MF, Nascimento FP Unila, Lab. of Medicinal Cannabis and Psychedelic Science, Clinical Trials, Foz do Iguaçu, PR, Brazil

Introduction: Alzheimer's disease (AD) is a chronic and progressive neurodegenerative disorder characterized by ongoing cognitive and functional deterioration. The epidemiology of Alzheimer's shows a global prevalence increase, especially in elderly patients. The main symptoms are cognitive, including memory loss, difficulty concentrating, language impoverishment, flawed reasoning, and decreased temporal and spatial orientation. Psychiatric and motor symptoms also occur, particularly in advanced stages. These symptoms result from a neuroinflammatory process, where an abnormal accumulation of beta-amyloid plaques and hyperphosphorylated tau neurofibrillary tangles occurs in nervous tissue. This process leads to neuronal death and progressive brain atrophy. A conclusive diagnosis is possible through a brain autopsy. Currently, the treatment of the disease involves medications and therapies aimed at attenuating cognitive deficits, delaying progression, and improving the patient's quality of life. However, even multimodal treatment offers modest benefits. The endocannabinoid system (ECS) is implicated in various physiological and pathological processes. Changes in endocannabinoid concentration and ECS dysregulation have been associated with pathological conditions, including neurodegenerative diseases, epilepsy and pain. Moreover, the phytocannabinoids delta-9-tetrahydrocannabinol (THC) and cannabidiol (CBD) are present in Cannabis sativa extract that can be used as a complementary treatment for AD because of its neuroprotective and anti-inflammatory properties. In this context, we have available AD patients that have taken full-spectrum cannabis sativa oil (CSO). **Methods:** Four patients between the ages of 70 and 94 years, including two men and two women, were evaluated in the study. They were previously diagnosed with AD, and the time since symptom onset ranged from 4 to 9 years. All patients were on prior medication treatment with acetylcholinesterase inhibitors, and three used memantine. Medications have continued without changes. Patients were using 1.5% CSO containing 1 mg of THC and 1 mg of CBD, administered once a day. The treatment duration ranged from 3 to 5 months. Mini-Mental State Examination (MMSE) Test was a tool for cognitive assessment. **Results:** All patients showed positive results, with improved performance observed through the MMSE. The first patient scored 9 points in the initial evaluation and 14 points in the second evaluation, indicating a 55.56% improvement over three months. The second patient scored 8 in the first assessment, and after two months, their score increased to 11 points, demonstrating a 37.5% improvement in performance. The third patient showed a 27.27% gain over five months, going from 11 points in the initial evaluation to 14 points in the second. The last patient exhibited a 23.53% increase in performance over five months, recording 17 points in the first assessment and 21 points in the second. Half of the patients reported side effects of daytime sleepiness, which was transient and reduced a few days after starting the Cannabis oil. **Conclusion:** Low dose of Cannabis extract rich in THC may be an exciting candidate for Alzheimer's cognitive impairment. Larger studies are necessary to extend these **Results:**

02.046 Support Social Modulates in a Sex-Dependent Way the Effects of Aversion Triggered by dPAG Chemical Stimulation on Fear and Anxiety Responses. Lima Silva AHB, Zanoveli JM UFPR Dept of Pharmacology, Curitiba, PR, Brazil

Introduction: Post-traumatic stress disorder (PTSD) is a mental health condition that can be developing after exposure to aversive traumatic events triggering inappropriate fear responses in unrelated situations. The dorsolateral column of the periaqueductal gray matter (dPAG) is a brain region that is associated with innate aversive behavioral responses, and its chemical stimulation with N-methyl-D-aspartate (NMDA) can induce an extreme fear response and facilitate processing and acquisition of fear memory and anxiety. Interestingly, evidence shows that the presence of members of the same species can modulate the processing of these emotions through the phenomenon of social support (SS). Thus, the present study investigated the influence of SS in chemically stimulated animals – male and female - into dPAG on the acquisition of conditioned place aversion and anxiety-like responses. **Methods:** Animals underwent stereotactic surgery to implant the guide cannula in the dPAG. After 1 week, during a familiarization session, the animal was exposed to explore for 10 min the apparatus constituted by three chambers linked between them with a door. In the next day, during the conditioning session (5 min), the animals were placed in one of the chosen chambers and chemically stimulated in the dPAG, with or without the presence of a conspecific (SS). Twenty-four hours after, the animals were tested for their aversion to the conditioned chamber (5 min). Finally, in the following day they were evaluated (5 min) in the elevated plus maze test to assess anxiety-like behaviors. All experiments were carried out by the University Ethics Committee under number 1509. **Results:** Animals of both sexes without SS but chemically stimulated with NMDA into dPAG presented conditioned place aversion demonstrated by the increase in the freezing time and avoidance of the aversive conditioned chamber during the test session. A sex difference was observed because the presence of SS during the aversive stimulus was able to reduce the aversive parameters in male, but not in female, indicating that in male rats the SS favors the reduction of the acquisition of a conditioned fear memory. Regarding to conspecific animals of both sexes, used as SS, they showed greater aversion to the place where they witnessed the aversive stimulus, despite not having suffered any direct aversive stimulus. All animals - both sexes - submitted to the aversive stimulation in the dPAG without SS showed a greater expression of anxiety-like behavior in the elevated plus maze test. In the presence of SS, only chemically stimulated male with NMDA showed a decrease in the anxiety parameters demonstrated by increasing in time spent in open arms. **Conclusion:** Our data indicate that there are sex-dependent differences on the capacity of the SS in modulating the effects of aversion triggered by dPAG chemical stimulation on animal behaviors related to the fear and anxiety. These results have important implications for understanding the role of SS in regulating stress and anxiety and may contribute to the development of therapeutic interventions based on SS.

02.047 The Importance of GPER in Neuroprotection and Angiogenesis in an *in vitro* Model of Ischemia due to Oxygen and Glucose Deprivation (OGD). Jucá PM, Duque EA, Munhoz C ICB-USP, Dpt of Pharmacology, São Paulo, Brazil

Introduction: Cerebrovascular diseases, including stroke, are among the leading causes of death and disability worldwide (1). The classical progression of stroke involves various mechanisms, such as oxygen and glucose deprivation and inflammation, leading to neuronal apoptosis and death (2). There are gender differences in the incidence and progression of the disease, with men being more affected and having a worse prognosis than women (3). In this context, estrogen (E2) has been shown to have a protective and antioxidant effect in numerous pathologies, including in the central nervous system (CNS) (4). Several studies have explored the role of the G protein-coupled estrogen receptor (GPER) in significant conditions such as neurodegenerative diseases and cancer (5,6). Interestingly, the activation of the GPER has been associated with tumor microenvironment revascularization, which worsens the disease prognosis. However, in the context of stroke, GPER activation could potentially restore blood flow to the affected area, thus mitigating the harmful effects of cerebral ischemia. Therefore, the current study aims to elucidate the importance of GPER activation in neuroprotective and angiogenic mechanisms in an *in vitro* stroke context. **Methods:** To this end, we conducted experiments involving human brain microvascular endothelial cells (HBMEC) lineage and primary mixed cultures derived from the frontal cortex of neonatal female rats (P1-P4, Wistar). Cell cultures were then subjected to glucose and oxygen deprivation (OGD) using a glucose-free solution containing sodium dithionite as a deoxygenating agent. We examined GPER activity by treating the cells with its selective agonist (G1; 10nM) and selective antagonist (G15; 50nM). The migratory activity and receptor expression were quantified using Wound Assay Healing and Immunofluorescence assays in HBMEC cells. Additionally, to evaluate the cytoprotective effects of GPER, we reduced its expression using a lentiviral vector (shRNA-GPER) and conducted the LDH assay. Results were expressed from a minimum of 3 independent cultures, with at least 3 replicates in each. **Results:** Our findings indicate that OGD reduces the expression of GPER in HBMECs, and treatment with G1 appears to restore it ($p=0.0856$). Nonetheless, G1 treatment reduced the migration of HBMECs after OGD ($p<0.01$), while G15 reversed this effect ($p<0.01$). Notably, GPER knockdown worsened OGD-induced cellular damage ($p<0.0001$) compared to the shRNA-scramble group, even in the presence of G1 in mixed cortical primary cells. **Conclusion:** These data suggest that GPER signaling during OGD/reperfusion is crucial for cellular protection, and the activation of this receptor via G1 appears to restore its expression after ischemic damage. However, GPER activation in endothelial cells seems to inhibit angiogenesis. **Financial support:** This work was supported by research grants from FAPESP, CNPq and CAPES. **References:** (1) JOHNSON, C. O. *The Lancet Neur.*, v. 18, n. 5, p. 439–458, 2019. (2) KURIAKOSE, D. *Int. Jour. Mol. Sci.*, v. 21, n. 20, p. 7609, 2020. (3) ROY-O'REILLY, M. *Endocrinology*, v. 159, n. 8, p. 3120–3131, 2018. (4) MCEWEN, B. S. *End. Reviews*, v. 20, n. 3, p. 279–307, 1999. (5) GUAN, J. *Neuroim.*, v. 24, n. 1, p. 60–66, 2017. (6) FILARDO, E. J. *Cli. Can. Res.*, v. 12, n. 21, p. 6359–6366, 2006.

03. Psychopharmacology

03.001 Luteolin as a Promissory Flavonoid to Improve Neurobehavioral and Gastrointestinal Changes in Autism Spectrum Disorders: Experimental Findings in Rats. Longo B, Nunes RKS, Cazarin CA, Silva TFQ, Dos Santos AC, Venzon L, Da Silva LM, Pagliochi ACS, Sievers J, Pilati SFM, De Souza MM, Da Silva LM. Univali, Postgraduate in Pharmaceutical Sciences, SC, Brazil.

Introduction: Autism spectrum disorders (ASD) are characterized by impaired social communication and restricted and repetitive patterns of behavior, interests, or activities. In addition, a large proportion of individuals with ASD suffer from gastrointestinal disorders, which contribute to neuroinflammation and exacerbate behavioral manifestations. In search of pharmacological therapies for individuals with ASD, we examined the effects of luteolin on neurological and gastrointestinal changes in an experimental model of ASD induced by prenatal exposure to valproic acid (VPA). **Methods:** Pregnant Wistar rats received VPA (600 mg/kg, i.p.) or saline on gestational day 12.5. After birth, male offspring were evaluated for neurodevelopmental from day 7 to 18. On postnatal day 23, the offspring were divided into groups and treated orally with vehicle (water plus 1% Tween, 1 ml/kg) or luteolin (10, 30, and 100 mg/kg). On postnatal day 60, social interaction, object recognition index (IR), elevated plus maze, and Open Field tests were performed. Gut and blood-brain barrier (BBB) permeability were assessed with fluorescein isothiocyanate dextran and Evans blue, respectively. After euthanasia, oxidative and inflammatory parameters were examined in the ileum, colon, cortex, and hippocampus. Histological analyses were performed in the ileum, colon, and hippocampus (CEUA/UNIVALI: 034/22p). **Results:** Animals prenatally exposed to VPA showed poorer performance in neurodevelopmental tests compared to the saline group. Similarly, 60 days postnatally, the vehicle group showed decreased social interaction time, IR, dwell time in open arms, and impaired locomotor and exploratory activity ($p < 0.05$ vs. VPA-non exposed group). On the other hand, luteolin treatment increased social interaction time and reversed all behavioral deficits observed in the IR, elevated plus maze, and open field tests caused by prenatal VPA exposure ($p < 0.05$ vs. vehicle group exposed to VPA). VPA exposure increased gut and BBB permeability compared with the saline group in 124% and 50%, which was attenuated by luteolin. Luteolin treatment also increased glutathione availability in the hippocampus and colon and reduced malondialdehyde and myeloperoxidase levels in all tissues studied compared with vehicle exposed to VPA ($p < 0.05$). In addition, luteolin attenuated hippocampal and intestinal mucosal microscopic damage, avoided the decrease in the intestinal muscle layer, and normalized mucin levels compared with the VPA-exposed vehicle group ($p < 0.05$). Animals in the vehicle group showed weight loss at day 60 compared with the saline group, which was prevented by luteolin treatment ($p < 0.05$). **Conclusions:** Prenatal exposure to VPA induces neurobehavioral and gastrointestinal disturbances in the offspring of rats, indicating the existence of a gut-brain connection in this model that was attenuated by luteolin. Thus, luteolin is an interesting therapeutic source in the search for treatments that improve central and peripheral changes associated with ASD. **Financial Support:** Coordenação de Aperfeiçoamento de Pessoal de Nível Superior (CAPES).

03.002 Potential Antidepressant-like Effect of *Centella asiatica* Extract and Active Compound Madecassic Acid in Animals Submitted to Material Deprivation and Social Isolation. Bertollo AG¹, Kreuz K¹, Medeiros J¹, Mingoti MED¹, Silva BV¹, Cassol JV¹, Dallagnol P¹, Narzetti RA¹, Roman Junior WA², Bohnen LC², Ignacio ZM¹. ¹UFFS; ²Unochapecó

Introduction: Major depressive disorder (MDD) is one of the most prevalent forms of psychiatric disorder. It is the leading cause of disability worldwide and causes loss in people's quality of life. The etiology is not well understood, but research indicates that stress in childhood and lack of social support in adult life contribute to the development of the disorder. An animal model of maternal deprivation (MD) mimics chronic stress in childhood, and social isolation (SI) in young adulthood is a behavioral model that tends to potentiate the effects of MD in rodents. Several individuals are refractory to classic treatments, so it is necessary to study new therapeutic strategies. *Centella asiatica* is a medicinal plant with antioxidant, anti-inflammatory and neuroprotective potential, mechanisms that contribute to the fight against the pathophysiology of MDD, and therefore has antidepressant potential. This study aimed to evaluate the effect of the hydroalcoholic extract of *Centella asiatica* and the active compound madecassic acid on depressive-like behavior in adult rats submitted to MD in the first days of life and SI in a young life. **Methods:** This research was approved by the Ethics Committee on Animal Use (CEUA), UFFS, SC, Brazil, under protocol 1912270922. The animals were divided into five groups (N = 10 for each group) for both males and females: Stress-free control + vehicle (Stress-free control); MD + SI + vehicle (Negative control); MD + SI + Escitalopram (positive control) 10 mg/kg; MD + SI + *Centella asiatica* extract 30 mg/kg; MD + SI + madecassic acid 10 mg/kg. The animals were subjected to MD 10 days after the first day of birth. At 50 days of age, they started the SI protocol for 30 days, and at the end of that period, they were submitted to chronic treatment for 14 (fourteen) days, according to the objective of each group. At the end of the treatment, the animals were submitted to protocols of locomotor activity in the open field and behavioral despair in the forced swimming test. The data were analyzed using ANOVA and Tukey's test ($p < 0.05$). **Results:** In both male and female groups, the MD and SI protocol induced depressive-like behaviors at statistically significant levels, and *Centella asiatica* extract and the active compound madecassic acid reversed depressive-like behaviors. **Conclusion:** These results suggest that *Centella asiatica* and madecassic acid has potential antidepressant action, at least partially, through an anti-inflammatory and antioxidant profile. **Financial Support:** FAPESC and UFFS. **Acknowledgement:** FAPESC and UFFS.

03.003 Affinity of Antidepressants to dDAT: Is More Aromatic Rings Better? Triches FF¹, Triches F², Oliveira CL¹ ¹CCB-UFSC, Lab. of Behavioral Neurobiology, Brazil; ²CFM-UFSC Dept of Mathematics, Brazil

Molecular docking methods are often used in structure-based virtual screening on large molecular libraries. Ensemble-docking is a computational method to evaluate protein-ligand binding properties by docking a target ligand with multiple versions of a macromolecule. This study aims to evaluate the binding properties of a series of antidepressants with the available versions of the crystallized *D. melanogaster* dopamine transporter (dDAT). An experiment conducted dockings of 1576 ligands (26 antidepressants plus 1550 decoys) with 11 dDAT structures in three different programs (Autodock Vina, DockThor and Gold). The molecules were downloaded from the following database: antidepressants (InChI code) from ZINC; structure of ten crystallized dDATs from RCSB-PDB; a theoretical structure of dDAT from AlphaFold; decoys (using the SMILE code of antidepressants) from DUD-E. Results of ensemble dockings for each pair ligand-dDAT were combined by applying three different consensus techniques (ECR, ECR+MS, LF). Consensual results were organized into a ranking of ligands “from the best to the worst pose in the binding site” or “from the lowest to the highest affinity to dDAT”. The consensual rankings were validated using the receiver-operator-characteristic (ROC). This calculation revealed how many antidepressants (true positive) were listed on the first 1%, 2%, 5%, 10%, 20% or 50% of the dataset. Independent of the type of consensus, the number of true positive ligands in the first 1% to 10% of the dataset was low (maximum 7.7%). In the range between 20% to 50% of the dataset, the LF had slightly better performance than another consensus (ECR: 34,62% to 80,77%; ECR+MS: 42,31% to 80,77%; LF: 46,15% to 84,62%). A decoy derivative of the antidepressant paroxetine occupied the top position in all rankings. The worst positions were occupied by decoys derived from fluvoxamine (ranking ECR or ECR+MS) and mirtazapine (ranking LF). Top-ranking ligands have more aromatic rings than the low positions indicating that the complexity of their structure plays a role in the interaction with dDAT. Understanding the interaction of different antidepressant molecules with dDAT reinforces the use of flies as an animal model in neuropsychological research. **Financial Support:** CNPq and CAPES

03.004 Effects of Inflammatory Preconditioning on Behavior, Molecular and Oxidative Parameters in Mice Subjected to Chronic Restraint Stress. Piton E¹, Pereira GC¹, Viero FT¹, Arboit F², Andrade LG², Portela Junior VVM², Guilherme Vargas Bochi¹, ¹UFSM Santa Maria, PPG Farmacologia, Brazil, ²UFSM Santa Maria, PPG Medicina Veterinária, Brazil.

Introduction: Major depressive disorder (MDD) is one of the most prevalent psychiatric disorders worldwide, however its pathophysiology remains poorly understood. It is known that stress is an important factor in the pathophysiology of MDD. In addition, it has already been verified that patients with MDD have high levels of inflammatory markers. Therefore, both physical stress and inflammatory stress represent good animal models for the induction of depressive-like behavior. Thus, the aim of this study was to evaluate the impact of an inflammatory stimuli on behavioral alterations induced by chronic restraint stress. **Methods:** Forty Swiss male mice (25-30 g, at 6-8 weeks), approved by the UFSM Animal Care and Use Committee (3601271021/2021) were used. The animals were segregated into 4 groups: Vehicle + control (VEH+CON), Vehicle + lipopolysaccharide (VEH+LPS), Vehicle + chronic restraint stress (VEH+CRS) and lipopolysaccharide + chronic restraint stress (LPS+CRS). The CRS was performed daily 6 hours for 28 days. Intraperitoneal injection of LPS (830 µg/Kg/10mL) or saline solution (10 mL/Kg) occurred before the onset of CRS. During the protocol, body weight and coat state were evaluated. After 24 hours of the last CRS session, the animals were submitted to two days of behavioral tests, including the Tail Suspension Test (TST) and Forced Swimming Test (FST) and 24 hours later they were euthanized to remove brain structures and blood. **Results:** The LPS+CRS and VEH+CRS groups had higher scores in the coat state ($p=0.0037$; $p<0.0001$), indicating a reduction in self-care behavior, as well as a reduction in body weight ($p=0.0006$; $p=0.0122$), compared to the VEH+CON group. In the TST, the LPS+CRS animals exhibited a longer immobility time ($p=0.0482$), while in the FST there was a reduction in the climbing time in the LPS+CRS and VEH+CRS groups ($p=0.0022$; $p=0.0207$), in relation to the VEH+CON group. There were no differences between groups in plasma corticosterone levels, as well as in oxidative parameters, since LPS+CRS didn't change catalase, superoxide dismutase and myeloperoxidase activity, nor hydrogen peroxide levels. As for gene expression, through quantitative Polymerase Chain Reaction (qPCR), there was a reduction in the expression of GFAP, an astrocyte marker, in the LPS+CRS group ($p=0.0216$), and LPS+CRS, VEH+CRS and VEH+LPS groups showed an increase in the expression of IBA-1, a microglial activation marker, in the prefrontal cortex (PFC) ($p=0.0224$; $p=0.0040$; $p=0.0204$), compared to the VEH+CON group, but in relation to BDNF, no differences were observed. **Conclusion:** The LPS+CRS model induced increased immobility and demotivation, reduced self-care and body weight, suggesting more pronounced behavioral changes than the CRS model alone. Furthermore, the increased expression of IBA-1 suggests a central immune response, while the reduction of GFAP may indicate atrophy/loss of functional capacity of astrocytes in the LPS+CRS group. However, further studies are needed to characterize appropriate experimental models for the study of MDD. **Financial Support:** FAPERGS.

03.005 Repeated Treatment with Sodium Butyrate Attenuated Deficits of Contextual Fear Extinction Induced by Social Defeat Stress in Mice. Coelho AA^{1,2}, Souza-Junior FJC^{1,2}, Lisboa SF² ¹FMRP-USP, Dept of Pharmacology, Ribeirão Preto, Brazil ²FMRP-USP, Dept of BioMolecular Sciences, School of Pharmaceutical Sciences of Ribeirão Preto, USP, Brazil

Introduction: Exposure to severe traumatic stressors can result in neuropsychiatric disorders, particularly post-traumatic stress disorder (PTSD). In PTSD, impairment of fear extinction (FE) is a key factor. The endocannabinoid (eCB) system, extensively described as a stress buffer system, facilitates the FE process in animal models and humans and is dysregulated in PTSD patients and animal models of PTSD. Stress-induced epigenetic changes, particularly in the histone acetylation pattern by increased activity of histone deacetylases (HDACs) enzymes can regulate the expression of the eCB system mediators. In this work, we aimed to investigate if an HDAC inhibitor, sodium butyrate (NaB), during stress prevents its long-term effects on fear memory. **Methods:** For that, NaB (25, 50, and 100 mg/kg) was systemically administered to mice before each session of the repeated social defeat stress (RSDS) protocol (6 days, 2 hours per day) and the animals were submitted to behavioral tests. All procedures were approved by the local Animal Research Ethical Committee (approval 21.1.526.60.9). **Results:** RSDS-induced hypolocomotion in the open field test (OFT) and social avoidance in the social avoidance test (SAT) on the day after the end of the stress. One-week later RSDS induced FE impairment in the contextual fear conditioning (CFC) protocol, which consisted of one conditioning session (3 shocks of 0,7mA, 2 sec each), followed 24h later by an extinction learning session (30 min without shocks), and a recall session (10 min without shocks) a day later. NaB treatment induced anxiogenic and anxiolytic effects in the OFT, depending on the dose. There was no drug effect on SAT. In the CFC, NaB attenuated the RSDS-induced FE impairment in a dose-dependent way. **Conclusion:** Our present data indicate that inhibition of HDACs during stress with NaB can prevent long-lasting fear extinction impairment (PTSD-like behavior) in mice. Although the mechanisms are still unclear, brain areas (prefrontal cortex and hippocampus) were collected for later evaluation of global and specific sites' histone acetylation levels and their association with eCB-related genes. **Financial Support:** The São Paulo Research Foundation (process: 2021/01656-3 and 2017/19731-6).

03.006 Effects of Ayahuasca on the Extinction of Contextual Aversive Memories in Rats.

Werle I, Nascimento LMM, Bertoglio LJ UFSC, Dept of Pharmacology, Florianópolis, Brazil

Introduction: Aversive memories and anxiety responses are necessary for animals' defense and survival. The extinction of aversive memories is a representative process of behavioral adaptation, as the neutral, inhibitory memory formed can suppress the original aversive memory. It has been studied in rodents due to similarities with cognitive behavioral therapies in the clinic. Scientific evidence suggests that the serotonergic system regulates the extinction of aversive memories. Ayahuasca (AYA) is a beverage obtained from the decoction of *Psychotria viridis* leaves and *Banisteriopsis caapi* bushes, which contain substances that enhance serotonergic function, especially the serotonergic type-2 receptor agonist N,N-dimethyltryptamine (DMT). This work aimed to investigate the effects of AYA on the extinction of recent and remote contextual aversive memories and its influence on the expression of exploratory and defensive behaviors related to anxiety using adult male Wistar rats. **Methods:** The elevated plus-maze (EPM) paradigm was used to assess parameters related to anxiety and general exploration activity one and twenty-four hours after oral treatment with AYA (containing 0.1, 0.3, or 1.0 mg/kg of DMT) or vehicle solution (water). A contextual aversive conditioning protocol was used in the experiments related to the extinction of aversive memories. Context A-conditioned animals were treated with AYA (0.3 mg/kg of DMT, orally) one hour before the extinction session (context A) and subsequently tested to assess extinction retention (context A), generalization (context B), and reinstatement (context A) of the memory. In all tests, the freezing behavior was quantified and used to infer treatment effects. **Results:** No significant differences among groups suggested that AYA does not alter anxiety-related and general exploration behaviors at this dose range. A single administration of AYA reduced freezing expression relative to the control group during the extinction session, but the groups did not differ in the fear extinction retention test. To assess whether the difference observed during the extinction session was due to changes in anxiety or general exploration, animals conditioned to the context were treated with AYA and submitted to the EPM, in which there were no differences relative to the control group, suggesting that changes in general anxiety or exploration did not accompany that effect. When we repeated the association of AYA with the extinction session twice, on consecutive days, there was a reduction in the freezing times in the AYA group in comparison to controls during extinction sessions and the extinction retention test for both 1 and 21-day-old memories. There were no changes in freezing expressed in a neutral, unconditioned context. As predicted, the groups returned to expressing similar freezing levels following the reinstatement of the original memory. **Conclusions:** These results suggest that AYA containing DMT 0.3 mg/kg may enhance rats' extinction of recent and remote contextual aversive memories. **Financial Support:** Conselho Nacional de Desenvolvimento Científico e Tecnológico, Coordenação de Aperfeiçoamento de Pessoal de Nível Superior, and FAPESP.

03.007 Involvement of the Endocannabinoid System in the Effect of Cocaine on the Conditioned Place Preference Test: A Systematic Review and Meta-Analysis. Santos AC, Iglesias LP, Moreira FA ICB-UFMG, Lab. of Neuropsychopharmacology, Dept of Pharmacology, Belo Horizonte, MG, Brazil

Introduction: Drugs of abuse, such as cocaine, are psychoactive substances capable of inducing physiological and behavioral changes, with the potential to cause addiction by interacting with the brain reward system. The endocannabinoid system modulates brain mechanisms underlying reward and contextual memory - a key factor in the process from initial use of the drug to addiction. The aim of this study is to elucidate the involvement of the endocannabinoid system in the effects of cocaine in the conditioned place preference test (CPP), through a systematic review and meta-analysis. **Methodology:** The search for articles was carried out on 06/04/2021, by two independent reviewers, as well as the following steps. The PubMed/Medline and Scopus databases were used to search for scientific articles using the terms? ("conditioned place preference" AND cocaine) AND (cannabinoid* OR endocannabinoid*)?. The PICOS strategy was used to precisely define the eligibility criteria, being Population (P): Adult mice or rats as experimental subjects; Intervention (I): Acute administration of THC and CBD phytocannabinoids, synthetic cannabinoids, CB₁ and CB₂ agonists and antagonists and endocannabinoid hydrolysis inhibitors without intervention prior to administration or testing; Comparison (C): Vehicle administration; Outcome (O): Variable time spent on the cocaine-paired side of the CPP; Study Design (S): Original experimental preclinical studies evaluating the involvement of CB₁ and CB₂ receptors in the reward effects of cocaine in the CPP test. The tabulation of the data of interest was done in an *Excel* spreadsheet and the graphically expressed data were extracted using the WebPlotDigitizer program. Regarding the statistical analysis, the meta-analysis is being carried out using the RStudio statistical software. **Results:** Of the 125 articles found, 16 were included, containing a total of 74 experimental groups to be analyzed. **Conclusion:** The meta-analysis is being developed, therefore, there are no quantitative results to evaluate. **Financial Support:** Fundação de Amparo à Pesquisa do Estado de Minas Gerais.

03.008 Antidepressant-like Effect of the Hydroalcoholic Extract of *Solidago chilensis* and Quercitrin in Rats Submitted for Stress of Maternal Separation. Bohnen LC¹, Lindemann H¹, Buzatto MV¹, Capoani GT¹, Lopes MCB¹, Kunst FM¹, Ansolin LD¹, Bertollo AG², Medeiros J², Ignacio ZM², Gutiérrez MV³, Roman Junior WA¹ ¹Unochapecó, ²UFFS ³Universidad the Sonora, México

Introduction: Evidence suggests that childhood stress is associated the brain damage and depressive symptoms. In rodents, maternal separation (MS) mimics early life stress and is used as a model for prospecting new antidepressant agents. In this context, this study aims to evaluate the involvement of inflammatory and oxidative stress markers, in the effects of hydroalcoholic extract from *Solidago chilensis* (HESc) and the compound isolated quercitrin (QRT), on antidepressant-like behavior of rats submitted for MS. **Methods:** The HESc was obtained by maceration (5 days) and a sample (50 g) was submitted to the separation funnel with solvents of crescent polarity. The ethyl acetate fraction was fractionated at column rendering the compound QRT. The chemical study was performed in chromatographic (HPLC) and spectrometric analyses (ESI-IT-MSⁿ). The *in vivo* experiments were approved in CEUA-Unochapecó (002/2021). The animals were submitted to MS (10 days) after the birth. At sixty days of age, the rats were divided into groups (n=10) and submitted the chronic treatment for 14 days (p.o): MS + vehicle (Veh, water); MS + escitalopram (ESC, 10 mg/kg); MS + HESc (50 mg/kg); MS + quercitrin (QRT, 10 mg/kg). Also, there was a group without stress + vehicle (Naïve, N). After the treatments, the animals were submitted the open field test (OFT) and forced swim test (FST). After euthanasia, biochemical analyzes were performed in the hippocampus and serum. **Results:** The chemical analyses identified nine polyphenolic compounds in HESc, including quercitrin (x mg ou %). In OFT the group MS (Veh group) showed increased crossings compared to the N, which were decreased in HESc and ESC groups compared with Veh. On the other hand, HESc and QRT increased the swimming time in TSF, showing an antidepressant-like behavior. Veh group increased levels of inflammatory cytokines in the hippocampus and serum myeloperoxidase (MPO), and the treatments maintained these values at baseline levels. Veh also reduced non-protein thiol levels (NPSH) in the hippocampus, and QRT and ESC reversed this condition. In addition, QRT and ESC reduced thiobarbituric acid reactive substances (TBARS) levels in the hippocampus and serum. As expected, the interleukin-1 β (IL-1 β) had a considerable increase in the Veh group and the treatments decreased the levels of this inflammatory marker. Furthermore, HESc and QRT reduced IL-6 levels in the hippocampal. **Conclusion:** The results together suggest that HESc and quercitrin present an antidepressant-like effect and the pharmacological mechanism involves the modulation of inflammatory and stress oxidative markers as well as the reduction of neuroinflammatory cytokines in the hippocampus and serum. **Financial Support:** UNIEDU/FUMDES. **Acknowledgment:** UNOCHAPECÓ and UNIEDU/FUMDES.

03.009 Effectiveness of Prototypic Antidepressants in the Forced Swimming Test: A Stratified and Network Meta-Analysis. Martins T, Bolzan JA, Triches FF, Costa JEM, Eckert FB, Lino de Oliveira C UFSC, Dpt of Physiological Sciences, PPG in Pharmacology, Florianópolis, Brazil, ²UFSC, Florianópolis, Brazil

Introduction: Reviews of the literature indicate that prototypic antidepressants reduced the immobility time of rodents in the forced swimming test (FST). This study aims to compare the efficacy of different prototypic antidepressants in the FST. **Methods:** Systematic review and meta-analysis were conducted according to a preregistered protocol (PROSPERO, CRD42020200604). Meta-analyses (random-effects model) used data from 200 articles (k=561 studies) randomly selected from the library with 2560 references reporting the immobility time of rodents treated with antidepressants before the FST. Data were extracted from the full text by one reviewer, and checked by another, for the estimation of combined effect sizes and 95% confidence intervals (CES, Hedges g [CI95%]). Data were stratified according to species (k=326/n=5126 mice; k=235/n=3640 rats) and further divided into subgroups of interventions (pharmacological class, compounds, via of administration). Subsets of homogeneous studies (same species, strain, phenotype, FST protocol) were pooled in the Network meta-analysis (NMA). NMAs were conducted with data from studies in mice (k=11/n=252) or rats (k=55/n=807), calculating a p-score (ps) per antidepressant in each species. The ps is the probability of a given compound being more effective than the others in the network. The higher the ps, the higher effectiveness. The CINeMA tool was used to assess the reliability of the NMA, varying from very low, low, moderate, and high. **Results:** Stratified meta-analysis indicated that antidepressants decreased immobility time in the FST with a very large, significant, but inconsistent estimate of CES (mice: 1.84 [1.66; 2.03], Z=19.6, p < 0.0001, I²=82.8%, p < 0.0001, $\tau^2=2.07$; rats: 1.44 [1.25; 1.62], Z=15.2, p < 0.0001, I²=79.7%, p < 0.0001, $\tau^2=1.53$). Except for the tetracyclic antidepressants in rats (0.73 [-0.3; 1.76], k=9), the CES of other classes of antidepressants were medium to huge, in favour of intervention, and significant. Stratified by compounds, CES varied in magnitude and significance in mice (from clomipramine 0.05 [-0.61; 0.7], k=9 to tramadol 7.2 [1.21; 13.2], k=3) and rats (from amoxapine, -0.36 [-1.1; 0.39], k=3 to desvenlafaxine, 2.86 [1.62; 4.1], k=3). Except for “subcutaneous injection in mice” (0.17 [-0.2; 0.55], k=18) or “oral diet in rats” (0.64 [-0.2; 1.48], k=4), the CES of others via of administration were very large, in favour of intervention, and significant. Vehicle and five (imipramine, amitriptyline, nortriptyline, fluoxetine and citalopram) or nine (imipramine, desipramine, fluoxetine, mianserin, amitriptyline, citalopram, fluvoxamine, clomipramine and amoxapine) antidepressants were included in the NMA of mice or rats, respectively. According to the ranking, imipramine was the most effective compound in mice (-4.19 [-6.91; -1.48], ps=0.87) or rats (-1.76 [-2.31; -1.20], ps=0.88). Citalopram was the lowest effective compound in mice (0.29 [-4.88; 5.46], ps= 0.25) and amoxapine in rats (0.38 [-0.88, 1.64], ps=0.11). The confidence in the results of the NMA was moderate. **Conclusion:** Summarising, many monoaminergic antidepressants reduce the immobility in mice and rats in the FST, independent of the rodent strains, pharmacological class or via of administration. Even though the results indicate imipramine as the more efficacious antidepressant in the FST, these results are limited to the small sample size, heterogeneity and confidence. Nevertheless, this methodology seems promising for future analysis with a more abundant amount of data. **Financial Support:** CAPES.

03.010 How Antidepressants Affect Flies' Behavior? A Systematic Review. Eckert FB¹, Triches FF¹, Costa JEM¹, Suman PR², de Toni DC³, Marino-Neto J⁴, Lino de Oliveira C¹. ¹UFSC, Dpt of Physiological Sciences, PPG in Pharmacology, Florianópolis, Brazil; ²BCCF-UFRJ Rio de Janeiro, Brazil; ³UFSC Florianópolis, Dpt of Cellular Biology, Embryology and Genetics, Brazil; ⁴UFSC Florianópolis, Institute of Biomedical Engineering, Brazil

Introduction: *Drosophila melanogaster*, also known as the fruit fly, is a model organism in neuroscience, including psychopharmacology. Here, the aim was to answer the following question: how do antidepressants affect flies in behavioral assays? **Methods:** A systematic review (PROSPERO CRD42020225423) was conducted to answer this question using the information in the available literature. **Results:** The search in four databases ("PubMed", "Web of Science", "Scopus", "EMBASE"), using a combination of terms related to the population (flies of any sex, age, lineage), intervention (monoaminergic antidepressants) and outcome (behavioral assays), returned 169 articles. After screening with predefined eligibility criteria, 12 articles were included in the review (k= 144 studies). Ten articles (k= 132 studies) were eligible for data extraction of control or intervention groups (mean, standard error or deviation, sample size) to the calculations of the individual (ES) or combined (CES) effect sizes (standardized mean difference, Hedges g), and confidence intervals (95% CI). Most studies were in adult flies (k= 121) and less in larvae (k= 15). In larvae, studies used mostly desipramine (k=8) or fluoxetine (k=5) in locomotion assays (k=13). Only the studies using fluoxetine were qualified for the CES calculations (k=5). Conclusively, fluoxetine treatment reduced the distance (k=1, g= -1.12, 95% CI [-1.9; -0.34]), body contractions (k=2, g=-3.27, 95% CI [-17.25; 10.72] and feeding behaviors in larvae (k=2, g= -2.54, 95% CI [-4.88; -0.20]. In adult flies, studies were made in males (k=47), females (k=38), a mixture of sexes (k= 33) or not specified sex (k=3). Fluoxetine was the most prevalent drug administered to adult flies (k=101 studies). Courtship was the most prevalent behavioral assay (k=84), followed by the forced swimming test (FST, k= 26 studies). Despite being an important assay to predict the efficacy of antidepressants in laboratory rodents, the sucrose preference appeared only in five studies in adult flies. The effect of fluoxetine varied according to the dose, outcome, and stress conditions the adult flies were exposed. In courtship assays, fluoxetine increased mating (k=54, g= 0.05, 95% CI [-0.08; 0.1955] and courtship latencies (k=54, g= 0.34, 95% CI [0.16; 0.52]) in unstressed flies. In the FST, fluoxetine treatment of unstressed flies decreased the immobility latency inconclusively (k= 17, g=-0.09, 95% CI [-0.26; 0.08]). Two studies applying the same assays to measure sucrose preference, observed that flies treated chronically with fluoxetine (10 µM) preferred sucrose when chronically stressed (g=2.55, 95% CI [0.32; 4.79]; g=3.37, 95% CI [0.67; 6.07]), and the opposite occurred to unstressed flies (g= -1.36, 95% CI [-3.04; 0.31]; g=-0.42, 95% CI [-1.83; 1]). Conversely, stressed adults acutely treated with a higher dose of fluoxetine (10 mM) preferred sucrose less than controls (k=1, g=-0.34, 95% CI [-1.15; 0.47]). **Conclusion:** Present results indicate that flies, like rodents, respond to antidepressant treatment and could be useful organisms to study the mechanism of these drugs. The wide estimate of 95% CI of the CES in the behavioral assays indicated that more studies are necessary to conclude about the effects of fluoxetine, or other antidepressants, especially in adult flies. So, the current evidence about the effects of antidepressants on flies' behavior is still incipient, and this field lacks new studies to fill the knowledge gaps. **Acknowledgments:** CAPES, CNPq, and FAPERJ.

03.011 The Activity of Phosphodiesterase 4 Favors Extinction Instead of Reconsolidation – The Potential Involvement of PKA and proBDNF. Sohn JMB^{1, 2}, Cardoso NC¹, Raymundi AM¹, Prickaerts J², Stern CAJ¹ ¹UFPR, Dpt. of Pharmacology, Curitiba, Brazil; ²University of Maastricht, Dpt. of Psychiatry and Neuropsychology, The Netherlands.

Introduction: Traumatic memories play a role in posttraumatic stress disorder (PTSD) development. Short or prolonged memory retrieval may induce reconsolidation or extinction, respectively. Phosphodiesterase 4 (PDE4), an enzyme expressed in the dorsal hippocampus (DH), hydrolyzes the cAMP thus limiting the PKA-induced CREB phosphorylation (pCREB) and BDNF expression, which are involved in fear memory processing. The mechanisms underpinning the switch between reconsolidation and extinction are undetermined. Uncovering them would advance the development of better treatments for PTSD. We aimed to test the hypothesis that PDE4 activity in the DH might control these processes. **Methods:** Male Wistar rats with guide-cannulas to the DH underwent contextual fear conditioning. After 24 h, independent groups were exposed to a short retrieval and 5 min later received roflumilast (ROF; PDE4 inhibitor; 9 ng/0.5µL/side) or vehicle (VEH) into the DH. To assess the treatment effect, the rats were exposed, 1 and 10 days later, to Test A1 and Test A2 (3 min) and freezing time was assessed. H89 (PKA inhibitor, 10 µM/0.5 µL/side) was administered before the treatment with ROF to assess the PKA role in ROF effects. Also, other groups received ROF after retrieval and anisomycin (ANI; 2 ng/0.5 µL/side) after Test A1. The expression of CREB/pCREB, pre-proBDNF, proBDNF, and mature BDNF in the DH were analyzed by western blot. The samples were collected 90 min after retrieval or Test A1 of animals treated with VEH or ROF i.p. (0.1 mg/kg) 5 min after retrieval. The data are expressed as mean ± SEM and were analyzed by one-, two-way or repeated-measures ANOVA followed by the Newman-Keuls post-hoc. The local ethics committee approved all procedures (#1436). **Results:** The PDE4 inhibition in the DH did not change the freezing time in Test A1. In Test A2, ROF-treated group presented a significant reduction in freezing compared to control (ROF: 19±4; VEH: 60±6; n=9/group). This effect depended on memory retrieval (VEH: 48±7; ROF: 53±5; n=9/group), Test A1 (VEH: 53±6; ROF: 45±7; n=8/group) and was spared after a reinstatement session (VEH: 41±6; ROF: 34±6; n=8/group). The PKA or protein synthesis inhibition abolished the ROF effect in Test A2 (H89-ROF: 50±7; VEH-ROF: 20±5; n=8-9 and ROF-ANI: 44±9; ROF-VEH: 19±4; n=7/group). H89 or ANI did not induce per se effects (VEH-VEH: 55±6; VEH-ANI: 47±8 and H89-VEH: 37±7; VEH-VEH: 46±3; n=7-8). These data suggest that extinction facilitation underlies the ROF effect instead of reconsolidation disruption. The treatment with ROF did not change the pCREB/total CREB ratio expression in the DH after retrieval (VEH: 270±28; ROF: 270±32; n=13/group). After Test A1, it enhanced proBDNF expression (VEH: 75±12; ROF: 127±19; n=11-12) without changing pre-proBDNF (VEH: 117±13; ROF: 112±11) or mature BDNF (VEH: 114±15; ROF: 94±8) in the DH, suggesting an involvement of proBDNF on ROF effects. **Conclusion:** Inhibiting PDE4 in the DH after a short retrieval session changes the memory fate from reconsolidation to extinction. This effect depends on PKA and is associated with an increase in proBDNF expression without changing the CREB activity in the DH. **Financial Support:** CAPES/NUFFIC and CNPq

03.012 Influence of *Aloysia citriodora* Palau (Cedron Paraguay) (Verbenaceae) Extract and its Main Fraction on Behavioral Performance in Experimental Models of Anxiety and Depression Induced in Mice. Martinez PEY, Báez WJA, Díaz DAI, Universidad Nacional de Asunción, Depto de Farmacología. Facultad de Ciencias Químicas, San Lorenzo, Paraguay

Introduction: *Aloysia citriodora* Palau (Verbenaceae) is an aromatic plant popularly used for medicinal purposes in Paraguay. It is attributed to properties against fever, digestive discomfort, insomnia, and anxiety, and as a "tranquilizer" among others. The objective of this study was to evaluate the influence of oral administration of the crude extract and the butanolic fraction obtained from *A. citriodora* on behavioral parameters of mice subjected to induced anxiety and depression.

Materials and Methods: The methodology used is an experimental design using adult Swiss albino male mice, subjected, on the one hand, to the elevated plus-maze tests associated with the hole board test, and on the other hand, the forced swimming test associated with caudal suspension as validation procedures of its popular use as an anxiolytic and antidepressant.

Results: Qualitative chemical studies of the crude extract detected the presence of flavonoids and polyphenols, among others. Exploratory chromatography of the crude extract and the butanolic fraction revealed the presence of verbascoside. The behavior of mice in the open arms of the elevated plus-maze (permanence time and the number of entries) was significantly increased by oral treatment with 50, and 150 mg/kg of the crude extract of *A. citriodora*, compared to vehicle-treated groups and compatible with the anxiolytic effect. In the same sense, 0.5 mg/kg of diazepam induced a significant increase in the permanence time and number of entries in the open arm, thus validating the method used. However, the main butanolic fraction did not induce significant changes in the frequency of entry or in the time spent in the open arms of the plus-maze compared to the vehicle-treated group. On the other hand, repeated administration in a 24-h period (24, 18, and 1 h before the swimming test) with doses of 6, 17, 50, and 150 mg/kg p.o., of the crude extract of *A. citriodora*, caused a marked decrease in the time of immobility of the mice subjected to the tests of forced swimming (FST) and tail suspension (TST), compared to the vehicle-treated group, respectively. The repeated administration in a 24-h period (24, 18, and 1 h before the FST) of the butanolic fraction (3, 9, and 27 mg/kg) induced a significant reduction in the immobility time of groups of mice exposed to FST and TST. In the same sense, repeated doses of imipramine (32 mg/kg, i.p.) in 24 h caused a significant decrease in immobility time in both tests, thus validating the test used.

Conclusion: Based on these results, it is concluded that the crude extract of *A. citriodora* significantly increases behaviors consistent with an anxiolytic effect in mice using the elevated plus-maze. Likewise, the crude extract and the butanolic fraction of *A. citriodora* significantly increase the immobility time in the forced swimming and tail suspension tests, compatible with an antidepressant effect. These results encourage further studies to elucidate the mechanism of action and identify whether verbascoside or another active ingredient (s) is/are potentially responsible for the actions detected in this study.

03.013 Disruption of Fear Memory Reconsolidation by Δ^9 -Tetrahydrocannabinol Involves Hippocampal CB1 and PPAR γ Receptors and Microglia Activation. Raymundi AM¹, Sohn JMB¹, Guimarães FS², Bertoglio LJ³, Stern CAJ¹. ¹UFPR, Dpt of Pharmacology, Curitiba, Brazil, ²FMRP-USP Ribeirão Preto, Dpt of Pharmacology, Brazil, ³UFSC, Dpt of Pharmacology, Florianópolis, Brazil

Introduction: Impairing fear memory reconsolidation effectively reduces fear responses and has been proposed as a treatment for post-traumatic stress disorder. We reported that an ultra-low dose of Δ^9 -tetrahydrocannabinol (THC) administered before retrieval impairs reconsolidation, an effect that requires the dorsal hippocampus (DH). THC is a partial agonist of cannabinoid type-1 (CB1) and type-2 (CB2) receptors with affinity to peroxisome proliferator-activated receptor gamma (PPAR γ). PPAR γ activation often underlies microglial activity in males. Here, we aimed to investigate whether and how the THC treatment after fear memory retrieval impairs reconsolidation in rats. We also examined potential sex-related differences and the engagement of hippocampal CB1, CB2, and PPAR γ receptors, as well as the involvement of microglia activation. **Methods:** To induce reconsolidation, fear-conditioned male Wistar rats underwent a short retrieval session in the conditioned context. Immediately after, they received THC (0.002 or 0.3 mg/kg i.p.) or vehicle (VEH). The animals were exposed to Test A₁ after 24 h to assess the treatment effects. In experiment 2, immediately after retrieval, male rats were pre-treated with VEH, AM251 (CB1 receptor antagonist; 0.5 nmol/0.5 μ l/side), AM630 (CB2 receptor antagonist; 0.1 nmol/0.5 μ l/side), or GW9662 (PPAR γ antagonist; 32 pmol/0.5 μ l/side) into the DH and received VEH or THC (0.002 mg/kg i.p.). In experiment 3, male rats were pre-treated with minocycline (microglia inhibitor; 10 μ g/0.5 μ l/side) into the DH and received THC (0.002 mg/kg i.p.) or VEH immediately after retrieval. Lastly, fear-conditioned female rats received THC (0.002 mg/kg i.p.) or VEH immediately after retrieval. The percentage of freezing time was assessed as a fear memory index. Data were expressed as mean \pm SEM and analyzed by repeated-measures or two-way repeated-measures ANOVA followed by Newman-Keuls post-hoc. All procedures were approved by the UFPR ethics committee (#1526). **Results:** In males, the administration of THC 0.002, but not 0.3, significantly reduced freezing times in Test A₁ compared to controls (41.4 \pm 7.1 vs. 72.9 \pm 2.9; n=8-10/group), suggesting a reconsolidation impairing effect. The effect of THC 0.002 in Test A₁ (30.6 \pm 4.6) was prevented by AM251 (68.9 \pm 2.8) and GW9662 (55.9 \pm 5.4) but not by AM630 (37.9 \pm 6.1; n=6-10/group). Pre-treatment with minocycline also prevented (63.9 \pm 3.4) the effect of THC 0.002 (34.0 \pm 4.2; n=9-10/group), suggesting that CB1 and PPAR γ receptors, as well as microglia activation, underlie the THC effect. In females, the administration of THC 0.002 did not change freezing behavior in Test A₁ compared to controls (58.5 \pm 5.6 vs. 62.7 \pm 4.6; n=12-15/group), indicating no impairments in memory reconsolidation. **Conclusion:** The ultra-low dose of THC-disruptive effect in reconsolidation depends on hippocampal CB1 and PPAR γ receptors, as well as microglial activation. This effect is CB2 receptor-independent and sex-specific, suggesting that this dose of THC might engage mechanisms to reduce fear responses that are more relevant to male than female rats. **Financial Support:** CNPq, Fundação Araucária and FAPESP.

03.014 Doxycycline Induces Rapid Antidepressant-Like Effects Through Reduction of Nitric Oxide Levels. Sales AJ¹, Del Bel EA², Gomes FV¹, Joca SRL³, Guimarães FS¹ ¹FMRP-USP, Dpt of Pharmacology, Ribeirão Preto, Brazil, ²FORP-USP, Dpt of Basic and Oral Science, Ribeirão Preto, Brazil, ³Aarhus University, Dpt of Biomedicine, Denmark.

Introduction: Tetracyclines, including doxycycline and minocycline, have shown neuroprotective, anti-inflammatory, and antidepressant-like effects. Previous study demonstrated that a subantimicrobial dose of doxycycline (10 - 50 mg/kg) reverts the behavioral and inflammatory responses in mice submitted to the lipopolysaccharide model of depression. However, the molecular mechanisms involved in the antidepressant action of doxycycline are not yet completely understood. Doxycycline inhibits the expression of nitric oxide (NO) which is increased by stress exposure. The inhibition of inducible NO synthase (iNOS) induces antidepressant-like effects in forced swimming test (FST). However, there is currently no data about the involvement of NO levels in the antidepressant-like effects of doxycycline. Therefore, the aims of this study were: i) to investigate the behavioral effect induced by acute doxycycline in FST and chronic unpredictable stress (CUS), and ii) the effects of doxycycline associated with NO donor (sodium nitroprusside, SNP) and iNOS inhibitor (1400W) in mice FST. **Methods:** Male mice (8 weeks) received i.p. injection of saline or doxycycline (10, 30 and 50 mg/kg), alone or combined with SNP (0.1, 0.5 and 1 mg/kg) or 1400W (1, 3 and 10 µg/kg), and 30 minutes after were submitted to the FST. In CUS, the animals were stressed daily (one stressor by day) for 21 days and received i.p. injection of saline or doxycycline on days 8 or 21. On day 22, the animals were submitted to the sucrose preference test (SPT) followed by FST. **Results:** Doxycycline (50 mg/kg) prevented and attenuated the behavioral effects of mice submitted to the CUS, increasing the sucrose preference, and decreasing the immobility time in the FST, compared to the control stressed mice. Doxycycline alone (50 mg/kg) or associated (30 mg/kg) with 1400W (1 µg/kg) induced an antidepressant-like effect in the FST, which was prevented by SNP (1 mg/kg) pretreatment. **Conclusion:** Altogether, our data suggest that the reduction of NO levels could be related to acute doxycycline treatment resulting in rapid and sustained antidepressant-like effects in mice. **Financial Support:** FAPESP (process number: 2023/09557-0).

03.015 Cannabigerol Prevents Behavioral Impairments Induced by Psychotomimetic Drugs in Animal Models for Schizophrenia. Pedrazzi JFC¹, Hallak JEC¹, Zuardi AW¹, Del-Bel EA^{1 2}, Guimarães FS³, Crippa JA¹ ¹FMRP-USP, Dept of Neurosciences and Behavioral Sciences, Ribeirão Preto, SP, Brazil, ²FORP-USP, Dept of Basic and Oral Biology, Ribeirão Preto, SP, Brazil, ³FMRP-USP, Dept of Pharmacology, Ribeirão Preto, SP, Brazil

Introduction: The constant search for new pharmacologically active compounds, especially those that do not exhibit toxic effects, intensifies the interest in plant-based ingredients and their potential use in pharmacotherapy. Cannabigerol (CBG) is a phytocannabinoid found in the plant *Cannabis sativa*, which, like cannabidiol (CBD), is not psychotomimetic and is devoid of intoxicating effects. CBG is a biologically active compound that is present in much smaller quantities and, in its acid form, is a precursor to other phytocannabinoids. Over the years, our research group has observed that CBD shows antipsychotic effects in diverse behavioral protocols. For example, in animal models related to schizophrenia-positive symptoms CBD reduced stereotyped and hyperlocomotion induced by psychotomimetic drugs. CBD also restores deficits in prepulse inhibition of the startle response (PPI). This behavioral change is proposed to reflect the impaired sensorimotor gating in individuals with schizophrenia. PPI disruption can be induced by drugs that facilitate dopaminergic- or inhibit glutamatergic-neurotransmissions, such as amphetamine (AMPH) or dizocilpine (MK-801), an N-methyl-d-aspartate (NMDA) receptor antagonist. Moreover, MK-801 promotes behavioral alterations in social interaction and novel object recognition (NOR) tests. These tests have been widely used to study changes related to negative symptoms and cognitive deficits of schizophrenia, respectively. **Objective:** This study aimed to assess whether CBG acutely has an antipsychotic-like profile in different animal models related to schizophrenia symptoms induced by AMPH or MK-801. **Methods:** 8-week-old male Swiss mice were used, which independently underwent other experimental protocols. The tests were: prepulse inhibition test (PPI), open-field, social interaction, and NOR. Treatments were administered acutely via the intraperitoneal route. d-amphetamine (AMPH, Sigma-Aldrich, USA) was dissolved in 0.9% sterile saline. Cannabigerol (CBG, BSPG Laboratories, United Kingdom) was dissolved in Tween 80 to a final concentration of 2% (v/v) and in 0.9% sterile saline. MK-801 (Sigma-Aldrich, USA) was dissolved in 0.9% sterile saline. In the experimental protocols, four different doses of CBG were generally used (1, 3, 10, and 30 mg/kg). The PPI and open-field protocols used AMPH (5 mg/kg). MK-801 was tested in a dose of 0.5 mg/kg for the PPI protocol, while in Social Interaction and NOR protocols, the dose was 0.2 mg/kg. PPI test results were evaluated by repeated measures ANOVA with the treatment as the independent factor and the prepulse intensity as a repeated measure. Two-way ANOVA evaluated open-field, social interaction and NOR test **Results:** Duncan's post hoc test ($p < 0.05$) revealed specific differences between test treatments. All experiments were conducted under CONCEA guidelines. **Results:** Systemic CBG in low doses attenuated the AMPH's disruptive effects on PPI and open-field tests. In addition, also at low doses, pre-treatment with this compound attenuated the impairments in the social interaction test and NOR induced by MK-801. **Conclusion:** The results of this work are unprecedented and suggest that CBG exhibits antipsychotic-like effects in preclinical trials. Furthermore, CBG showed low-dose therapeutic effects, indicating that it may be more potent than CBD and a promising compound for clinical use. **Support:** FAPESP; CNPq; CAPES; NAPNA; USP.

03.016 Preventive Treatment with Pro-Resolving Lipid Mediator Resolvin D5 (Rvd5) and its Precursor Docosahexaenoic Fatty Acid (DHA) Induces Anxiolytic-Like Effect in Male Rats.

Zanoveli JM, Silva AHBL, Matos JHB UFPR, Dept of Pharmacology, Curitiba, PR, Brazil

Introduction: Anxiety disorders are categorized as a set of pathologies with specific diagnostic criteria based on signs and symptoms. It is known that stress is one of the causal factors for the occurrence of anxiety disorders and that preclinical studies indicate that chronic or even acute stress can induce a more expressive and lasting anxiety response in laboratory animals. Thus, the aim of the present study was to investigate behavioral anxiety responses of male rats submitted or not to an acute restraint stress (ARS, 2 hours; Experiment 1) and whether the treatment with DHA and RvD5, neuroprotective compounds, would be able to prevent the anxiety-like responses (Experiment 2). In both experiments we evaluated, one week after the end of the treatments, whether the effects of the procedures were lasting or not. For this, we used the light-dark transition (LDT) test. **Methods:** In Experiment 1, the animals were acclimated for 3 days before the beginning of the procedures, on the 4th day half of them were exposed to ARS (stressed animals – S animals) and half were not (non-stressed animals – NS animals). Twenty-four hours after, the S and NS animals were submitted for 5 min to the elevated plus maze test (EPM) to assess anxiety-like parameters and in the sequence, they were tested for exploratory activity in the open field test (OFT) for 5 min. One week later, the animals were evaluated in the LDT test and anxiety parameters were quantified. In Experiment 2, only S animals were pretreated for 8 consecutive days with RvD5, DHA or Vehicles (Saline or Oil) after acclimatization, while NS animals were pretreated only with their respective vehicles. On the eighth day, 2 hours after the last injection, half of the animals were subjected to ARS (S animals) and half of them were not (NS animals). The doses used for DHA were: 100 mg or 400 mg/kg diluted in oil and for RvD5 were: 1, 3 or 10 ng/animal diluted in sterile saline. The behavioral tests follow the same procedure described above. All experiments were conducted by the Ethics Committee of the University under number 1443. **Results:** In Experiment 1, S animals presented a more prevalent anxiety-type response in most parameters evaluated in the EPM and OFT, without alteration in the exploratory activity of the animals. Interestingly, the effect of the ARS was long-lasting because 1 week after, the S animals showed a more expressive anxious-like behavior when evaluated in the LDT test. Regarding to Experiment 2, the treatment with DHA (in the two doses used) and RvD5 (1 ng/animal), was able to prevent the anxiety-like responses during EPM and OFT, without changing the exploratory activity of the animals. Preliminary results indicate that the treatments present a lasting anxiolytic-like effect, since this effect was maintained 1 week after the end of the treatment. **Conclusion:** Our data show that ARS was able to act as a short- and long-term anxiety-inducing factor. The treatment with RvD5 and its precursor DHA produced anxiolytic-like effect, indicating that this effect is long-lasting, at least for 1 week after the end of treatments. Studying these neuroprotective compounds can contribute to developing prophylactic therapies to combat anxiety related to stress. **Acknowledgments:** We thank CAPES-Brasil (CAPES - Financial Code 001) for the grant and CNPq for the productivity grant (Process No. 303863/2020-0).

03.017 Spermidine Prevents the Reinstatement of Alcohol Conditioned Place Preference. Silva A.A1, Henriques GM1, Rocha VN1, Dias Júnior BC 1, Santos AA 1, Oliveira-Lima AJ1, Marinho EAV1, Rubin MA2, Mello CF³ ¹UESC, Dept of Health Sciences, Ilhéus, BA, Brazil. ²UFMS, Dept of Biochemistry, Center of Natural and Exact Sciences, ³UFMS, Dept of Physiology and Pharmacology, Center of Health Sciences, Santa Maria, RS, Brazil

The aim of this study was to investigate whether spermidine alters extinction and reinstatement of ethanol-induced conditioned place preference (CPP) in mice. Adult female Swiss mice were injected with alcohol (1.8 g/kg, i.p.) and placed in one compartment (drug-associated compartment) for 10 min in four alternate days to induce CPP. Animals were subjected to a post-conditioning test to confirm CPP. The animals received vehicle or spermidine (SPD) at the doses of 3, 10 or 30 mg/kg, and were placed in the drug-associated compartment for 10 min in 4 alternate days. On the following day, a post-treatment test was performed. One day later, alcohol re-exposure was performed in the alcohol-paired compartment, followed by a post-reexposure test, carried out in the next day. In a second experiment, after conditioning, animals were treated with vehicle, the N-methyl-D-aspartate (NMDA) receptor polyamine binding site antagonist arcaine (ARC, 0.1 mg/kg), SPD (10 mg/kg) or the association of both (ARC+SDP) in the drug-associated compartment. Similar to experiment 1, animals were then sequentially subjected to alcohol re-exposure and a post-reexposure test. In both experiments alcohol induced place preference. Spermidine did not alter CPP extinction but prevented the reinstatement of CPP induced by alcohol reexposure. In the second experiment, arcaine prevented the effect of spermidine on alcohol-induced CPP reinstatement. The results suggest that SPD may facilitate the reconsolidation of conditioning memory, disrupting CPP. This effect seems to involve the polyamine binding site at the NMDA receptor, because it is prevented by ARC. These data encourage the use of spermidine as adjunct therapy for alcohol abuse disorders, particularly to prevent relapse.

03.018 Evaluation of the Anticonvulsant Potential of Synthetic Cannabinoid Compounds in a Seizure Model Induced by Pentylentetrazole in Zebrafish (*Danio rerio*).

De Souza MM¹, Souza FL¹, Valachinsk AW¹, Teixeira NC¹, Costa BG¹, Escortegonha Pollo, LA², Biavatti, MW² ¹NIQFAR/Univali, Chemical Pharmaceutical Research Center, Brazil, ²PPGFAR-UFSC, Graduate Program in Pharmacy, Brazil

Introduction: Epilepsy is a chronic and devastating brain disease characterized by an imbalance of excitatory and inhibitory processes, resulting in unpredictable, unprovoked, recurrent seizures. So far, pharmacological intervention is the main treatment, since only few people are considered suitable for a ketogenic diet or surgical intervention. Unfortunately, the marketed antiseizure drugs control seizures in only about 70% of the patients. Moreover, a considerable number of patients also experience mild to moderately severe side effects, and cannabidiol (CBD) obtained from *Cannabis sativa* has been an interesting alternative making the investigation of the anticonvulsant potential of compounds with a chemical structure similar to CBD interesting options in the management of epilepsy. The aim of the present study is to evaluate the anticonvulsant effects of synthetic cannabis compounds. **Methods:** For that, groups of Zebrafish (*Danio rerio*) were pre-treated with 06 synthetic cannabinoic compounds LP171-175, LP26 and LP258 (1 mg/L), CBD (0.5mg/L) and Diazepam 75mg/L (40 min) and exposed to 20mM pentylentetrazole (PTZ) per 20 min being filmed. During this time, the following were analyzed: latency for clonic seizures, number of events, animal mortality up to 24 hours after exposure to PTZ. At the end of the experiments, the animals were euthanized, their brains collected for biochemical experiments of oxidative stress. All experimental procedures were submitted to the Ethics Commission for Animal Use at UNIVALI (CEUA) and approved with opinion CEUA-002/21. **Results:** The results showed that only the compounds LP1171, LP1195 and LP206 statistically promoted an increase in seizure latency compared to the vehicle, with effects similar to CBD and DZP. All treatments promoted a reduction in the number of crises and mortality of the animals, with the compound LP1-175 and DZP being the most protective. In addition, attenuated treatments also prevented oxidative stress in fish, decreasing lipid peroxidation and increasing oxidative protein activity. Unlike what was observed in the DZP group, they did not affect the general swimming activity of the fish, suggesting different mechanisms of action. **Conclusions:** The data together suggest that the evaluated compounds may be interesting pharmacological targets for the treatment of epilepsy. **Financial support** - CNPq/FAPESC

03.019 Mice Infected with *Plasmodium berghei* ANKA Strain and Healed with Antimalarial Drugs Present Late Cognitive Impairment. Dias QM, Noletto TG, Passos TG, da Silva, AC, de Oliveira, LM. Fiocruz-Rondonia, Lab. de Neuro e Imunofarmacologia

Introduction: Post-malaria neurological syndrome is a neglected condition with a broad clinical spectrum that may involve cerebellar and cognitive motor disorders. The clinical manifestations of the syndrome can occur with a latency of several days to weeks (approximately 2 months), after the cure of malaria with the use of antimalarials. Pathophysiology is still unknown and causes significant damage to the quality of life of affected individuals. The present study experimentally evaluated the manifestations and late alterations in spatial memory of C57BL/6 mice cured of *Plasmodium berghei* ANKA infection. **METHOD.** All experiments using mice were proved for the Ethics Committee (approval number 08/2021). The study used murine malaria induced by intraperitoneal injection (ip) of the 10⁶ red blood cell parasite with the *Plasmodium berghei* ANKA strain in adult male C57BL/6 mice. On days 5, 13, and 19 after infection. From day 6 to day 12 after infection, the animals were treated with the antimalarial combination chloroquine (25 mg/ Kg; ip) + primaquine (0,72 mg/ Kg; ip). On the sixth day after the end of antimalarial treatment (18th day after infection), the animals cured of malaria (parasitemic clearance) were evaluated in the Y-maze for spatial memory. **RESULT.** The results show that the animals developed infection with *Plasmodium berghei* ANKA, as evidenced by the increase in blood parasitemia the fifth day after infection. The effectiveness of antimalarial treatment was confirmed by the suppression of parasitic forms in the peripheral blood. Weight and blood glucose did not change significantly during the study. In the Y-maze test, we observed that control animals (uninfected and untreated) or animals treated with antimalarials and not infected with *Plasmodium berghei* showed a significant increase in preference for the new arm, compared to the other arms. However, the animals that were cured of *Plasmodium berghei* ANKA did not show preference for the new arm compared to the other arms. **Conclusion:** The lack of preference for new arms in the Y-maze test indicates that mice treated and healed of *Plasmodium berghei* infection had late spatial memory impairment. This result did not appear to occur due to changes in weight and blood glucose. **Financial Support:** PROEP FIOCRUZ RO. **Acknowledgments:** Oswaldo Cruz Foundation (Fiocruz RO) for Financial Support

03.020 Validation of an Experimental Protocol to Generate a Traumatic-Like Memory in Male and Female Rats. Nascimento LMM, Soares LA, Bertoglio LJ. UFSC Florianópolis, Dpt of Pharmacology, Brazil

Introduction: Humans exposed to a threatening or stressful event may develop post-traumatic stress disorder (PTSD). Studying aversive memories using contextual aversive conditioning provides insights into the mechanisms underlying such responses. This experimental approach involves associating a neutral stimulus (context) with a biologically relevant stimulus (shock), which triggers defensive responses (e.g., freezing). The first stage of memory formation corresponds to the first contact with a specific information or situation, referred to as acquisition. The information obtained is still labile and malleable, requiring gradual stabilization through the consolidation process. After consolidation, the memory is no longer subject to interventions. However, when evoked and reactivated, a contextual aversive memory with an adaptive character can be destabilized and restabilized (reconsolidated) to maintain or adjust the memory over time. On the other hand, when the formation of aversive memories is dysfunctional, generalized fear and extinction deficits can be expressed. **Objective:** To validate an experimental protocol generating traumatic memories in rats by modulating shock intensity. **Methodology:** Adult male and female rats (CEUA/UFSC n^o 7819200422) were conditioned with three electric shocks of different intensities (0.7, 1.0, or 1.3 mA). Memory persistence and generalization were assessed in subsequent test sessions. Freezing behavior, an indicator of aversive memory, was quantified as a percentage of the time. Results were expressed as mean \pm standard error of the mean. Repeated measures ANOVA was adopted when re-exposures to the same context were performed. The Newman-Keuls post hoc test was used to determine differences with a statistical significance ($p < 0.05$). **Results:** Males in the group conditioned with a shock intensity of 1.3 mA presented significantly increased ($p < 0.0001$) freezing times compared to 0.7 mA and 1.0 mA groups when exposed to context B (Tests B1 and B2 performed seven days apart). Females in the group conditioned with a shock intensity of 1.3 mA presented increased freezing ($p < 0.0001$) compared to 0.7 mA and 1.0 mA groups during exposure to both context A (Tests A1 and A2 performed seven days apart) and context B (Tests B1 e B2). **Conclusion:** These findings validate an experimental protocol to generate a traumatic-like memory in male and female rats and suggests that relatively high shock intensities generate more intense and generalized memories, particularly in females. This experimental protocol helps investigate mechanisms underlying aversive memory formation and stability, providing valuable insights into the processes involved in PTSD and the potential factors that influence its development, paving the way for further research aimed at developing targeted interventions for individuals with PTSD. **Financial Support:** CNPq

03.021 *In Silico* Characterization of Novel Biological Markers and Potential Therapeutic Candidates for Bipolar Disorder: A Computational Approach. Schons T¹, Ziani PR^{1,2}, Rosa PH^{1,2}, Mezzomo G^{1,2}, Rampelotto PH^{1,2}, Rosa AR^{1,2,3} ¹HCPA, Lab. of Molecular Psychiatry, Porto Alegre, Brazil, ²ICBS-UFRGS, PPG in Biological Sciences: Pharmacology and Therapeutics, Porto Alegre, Brazil, ³ICBS-UFRGS, Dept of Pharmacology, Institute of Basic Health Sciences, Federal University of Rio Grande do Sul, Porto Alegre, Brazil

Introduction: Bipolar Disorder (BD) is a chronic psychiatric illness characterized by alternating mood episodes, and it's associated with cognitive and functional impairment [1,2]. The diversity of BD presents a challenge in conducting research on the fundamental causes and implementing consistent treatment strategies. Developing new drugs is expensive and time-consuming; however, with the help of bioinformatics, drugs already approved for other clinical conditions can be redirected [3]. Previously, we systematically reviewed the literature to find biological markers for BD. In this study, we aim to update this review and identify potential therapeutic candidates for BD [4] using an *in silico* approach. **Methods:** Through a systematic search strategy, we collected and identified all proteins differentially expressed in proteomic studies of peripheral fluids (plasma and serum) from patients with BD compared to healthy controls. Initially, the list of differentially expressed proteins was expanded in STRING [5]. Only curated knowledge and experimental evidence were used as the source of interaction data in such analysis, and the confidence score was fixed at 0.7. This procedure keeps only interaction with high confidence. Enrichr [6] and Toppfun [7] were then used for protein enrichment analysis with *Homo sapiens* as a background. We applied the Bonferroni correction to determine the statistical significance of the results. We specifically focused on biomarkers and drugs with an adjusted p-value < 0.05. **Results:** We identified 47 differentially expressed proteins from 11 articles included in this work, which increased to 237 after the network expansion in STRING. The main biological function identified was ubiquitin activity, important for regulating biological processes. The main biological process was the cytoplasmic translation, related to the protein synthesis in the cytoplasm. In addition, several microRNAs associated with BD (e.g., miR-92a-3p, miR-615-3p, miR-16-5p, miR-193b-3p) indicate they may be new biomarkers for the disease. Furthermore, drug repurposing analysis identified different drug candidates for BD, including laevadosin (a mixture of nucleotides and nucleosides), the antineoplastic agent nocodazole, and the anti-inflammatory nimesulide, but none of them had been specifically tested for this psychiatric condition. Another drug identified was the antidepressant nefazodone, which is commonly used for treating BD. **Conclusion:** Proteomics data analysis in conjunction with *in silico* drug repurposing method shows potential in discovering new biomarkers and drugs associated with BP. This integrated approach can potentially enhance therapeutic strategies and outcomes for individuals affected by BD.

Funding: This study was financed by Capes, CNPq and FIPE-HCPA. **References:** [1] Rodrigues, J. E. International Journal of Molecular Sciences V. 23, Issue 10, 2022. [2] Rosa, A. R. Acta Psychiatrica Scandinavica, 125, 335–341, 2012. [3] Pushpakom, S. Nature Reviews Drug Discovery, v. 18, p. 41–58, 2018. [4] Ziani, P. R. Clinical Psychopharmacology and Neuroscience, 20, 211–227, 2022. [5] Szklarczyk D, et al. Nucleic Acids Res., v. 47, p. 607–613, 2019. [6] Kuleshov, M.V., et al. Nucleic Acids Res., v. 44, p. 90–97, 2016. [7] Chen, J., et al. Nucleic Acids Res., v. 37, p. 305–311, 2009.

03.022 Changes in Hippocampal Activity and C-FOS Expression in Female Offspring Exposed to SSRI Prenatal Treatment. Aquino ACQ, Freitas, AKMSO, Freitas-Junior, RAO UFRN, Centro de Ciências da Saúde, Natal, Brasil

Selective Serotonin Reuptake Inhibitors (SSRIs) are medications prescribed to treat depression, anxiety, and some personality disorders (1-3). The use of SSRIs during pregnancy can cause problems for the offspring, due to the possibility of these drugs crossing the placental and blood-brain barrier (2). Potent prenatal display, therefore, may involve behavioral impairment and persist into adulthood (1,3). Serotonergic overexpression during embryonic development can lead to changes and support in the engineered circuits that control cognitive and emotional behavior, although subcortical and cortical information processing is state-dependent, including subcortical limbic areas (1,3). This work examined how prenatal exposure to fluoxetine affects memory, anxiety, and depressed behavior in fluoxetine-treated female rat offspring. Wistar rats (*Rattus norvegicus*) were used, divided into three groups: Control (Naive), treated with water (Vei) and Fluoxetine (Flx). The treated dose of Flx for each pregnant woman was 10 mg/kg/day, according to data extracted from other studies, daily, from the thirteenth day of pregnancy until the end of the 21-day period of pregnancy. After the period of birth and sexing, the female offspring were observed throughout the experiment, checking their body weight and behavioral tests were performed when they reached 90 days of age, followed later by immunohistochemical analysis. offspring in several training and testing tasks, using devices that assess aspects related to behavioral and cognitive aspects (open field, discriminative avoidance and context-conditioned fear), as well as neurochemical evaluation of c-fos expression in the offspring's hippocampus. The study showed that an embryonic exposure to fluoxetine affected aversive memory performance but did not affect anxiety and depression behavior. Furthermore, there was an increase in C-fos positive cells in CA1 and CA3 after discriminative avoidance training in the Flx group compared to the Naive and Vei groups. The results point out that fluoxetine can lead to mnemonic alterations during pregnancy. However, additional analyzes, including other neurochemical markers, are needed to define the delay in the development of microcircuits and impairment of specific neuropeptide markers for cortico-limbic structures. but no anxiety and depression behavior. Furthermore, there was an increase in C-fos positive cells in CA1 and CA3 after discriminative avoidance training in the Flx group compared to the Naive and Vei groups. The results point out that fluoxetine can lead to mnemonic alterations during pregnancy. However, additional analyzes, including other neurochemical markers, are needed to define the delay in the development of microcircuits and impairment of specific neuropeptide markers for cortico-limbic structures. but no anxiety and depression behavior. Furthermore, there was an increase in C-fos positive cells in CA1 and CA3 after discriminative avoidance training in the Flx group compared to the Naive and Vei groups. The results point out that fluoxetine can lead to mnemonic alterations during pregnancy. However, additional analyzes, including other neurochemical markers, are needed to define the delay in the development of microcircuits and impairment of specific neuropeptide markers for cortico-limbic structures. Animal Research Ethics Committee: CEUA-UFRN 045/2019. Kepser LJ. *behav. Brain. Res.*, v.15, p.3, 2015. Lisbon, SF. *pharm.*, v. 80, p.49, 2007. Millard, SJ. *Neurosci. Biobehav.*, v. 80, p.743, 2017.

03.023 Antagonism of TRPV1 Receptors Associated with FAAH Inhibition is Necessary to Facilitate the Impaired Fear Extinction in iNOS Knockout Mice. Ferreira BF¹, Sato Y¹, Marques APA¹, Fronza MG¹, Lisboa SFS². ¹USP, Dpt of Pharmacology, Ribeirão Preto, Brazil, ²USP, Dpt of Biomolecular Sciences, Ribeirão Preto, Brazil

Introduction: iNOS KO mice present impaired contextual conditioned fear extinction and increased NOS activity and endocannabinoid system dysregulation in the prefrontal cortex (PFC). A fatty acid amide hydrolase (FAAH) enzyme (which degrades anandamide) inhibitor or a nNOS inhibitor attenuated the behavioral changes observed in these animals. CB1 and TRPV1 receptors mediate anandamide effects, oppositely modulating the contextual fear conditioning (CFC) expression, possibly involving NMDA/NO pathway. In the present study, we aimed to investigate whether TRPV1 receptors antagonism, alone or associated with FAAH inhibition, attenuates the behavioral deficits observed in iNOS KO mice in the CFC. **Methods:** Male C57Bl/6J and iNOS KO mice (8 weeks old) received three footshocks (0.75mA, 2s each) in the conditioning box. After 24h, mice received intraperitoneal injections of the TRPV1 antagonist SB366791 (SB, 0.1-1.0 mg/kg/10ml), the TRPV1 antagonist/FAAH inhibitor AA-5HT (0.1-1.0 mg/kg/10ml) or vehicle 30min before re-exposure to the box for evaluating extinction acquisition for 20 min. 24h later, the recall of extinction memory was assessed for 5 min. After the extinction recall, a group of untreated animals was euthanized for qPCR and western blot analysis of TRPV1, CB1, and nNOS in PFC. **Results:** iNOS KO mice presented impaired extinction of fear memory. Treatment with the lowest doses of SB and AA-5HT (0.1 mg/kg) facilitated fear extinction acquisition in iNOS KO mice. Nevertheless, only AA-5HT attenuated the freezing behavior of iNOS KO in the extinction recall session. TRPV1, but not CB1 or nNOS, mRNA was reduced in iNOS KO mice. In addition, there was a trend towards increasing protein expression of nNOS. **Conclusion:** Overall, our data showing that iNOS KO mice present impaired fear extinction and that SB, but not AA-5HT, failed to facilitate the recall of the extinction memory suggests that the sole blockage of TRPV1 receptors is not sufficient to facilitate extinction retrieval, requiring additional CB1 receptors activation by FAAH inhibition. **Financial Support:** FAPESP (2017/19731-6); CAPES fellowship.

03.024 Effects of Ayahuasca to Treat Symptoms of Pathological Grief: A Case of Series.

Spicigo CC, Pereira VG, Hirata F, Silveira GO, Yanomine M, Donato MF, Fermino FA, Nascimento FP Unila, Foz do Iguaçu, PPG Bioscience, Brazil; PR; ²USP São Paulo, Dpt of Pharmaceutical Sciences, Brazil

Introduction: Ayahuasca is obtained from the decoction of two plants, Banisteriopsis caapi(BC) and Psychotria viridis(PV). The former contains reversible monoamine oxidase (MAO) inhibitors such as harmine, harmaline and tetrahydroharmine (THH). These harmines inhibit the breakdown of monoamines, reducing the metabolism of neurotransmitters, helping to maintain normal levels of these compounds. PV contains the psychedelic tryptamine N,N-dimethyltryptamine (DMT), responsible for the drink's psychoactive effects. Pathological grief (PL) has a prevalence of 2.5% in the world, the main difference between the normal process of grief and a pathological process would be time, the person has persistent symptoms of grief, impairing their quality of life and functionality, for a period of twelve months. Ayahuasca is being tested in LP as it has demonstrated therapeutic potential in various psychiatric pathologies. **Methods:** The objective of this study was to investigate whether ayahuasca could promote a therapeutic effect for 5 patients with symptoms of pathological mourning, as well as on secondary aspects such as quality of life, sleep, depressive symptoms, resignification of the loss, and intensity of the hallucinogenic experience and perception of mystical experience. The present study presents a series of cases with qualitative and quantitative descriptive and prospective methodology with the objective of evaluating the effectiveness of the use of ayahuasca in the treatment of patients with pathological mourning. Ayahuasca was administered in liquid form, orally, with a dose of 0.36 mg/kg of DMT and the other components and their respective concentrations were: harmine - 1.97 mg/kg, harmaline - 0.21 mg/kg and tetrahydroharmine - 1.15 mg/kg. Each patient was his own control, where we compared symptoms before treatment and 7, 30 and 365 days after. **Results:** Patients on average had an improvement of 48.23% in terms of grief, as assessed on the Prolonged Mourning Assessment Questionnaire (PG13), after 365 days. Regarding depressive symptoms, four of the five patients showed improvement greater than 29%, in these 4 patients ranging from 29.63% to 69.23% of improvement, using the Montgomery-Asberg Depression Rating Scale (MADRS), compared with your initial data. Four patients had improvement in sleep, the positive variation was from 21.45% to 45.45%, 30 days after treatment, through the Pittsburgh Sleep Quality Index (PSQI-BR). The resignification of mourning was evaluated using a scale that measured the improvement in the interpretation of the loss. The resignification scores vary between 0 and 100, where 0 means not having resignified the loss and 100 means total reframing. Improvement was evident in patients 5, 3, 1 and 4, who achieved improvement in the scale score of 25; 32; 49 and 65 points, respectively, after 365 days of treatment. **Conclusion:** This study shows that ayahuasca reduced symptoms related to grief, as well as depression and sleep quality. Furthermore, these effects were observed up to 1 year after a single administration of ayahuasca.

03.025 Evaluation of the Effect of the Hydroalcoholic Extract of *Heteropterys tomentosa* on Memory in Mice. Almeida Filho OP¹, Pires JCB², Santana JVS², Freitas-Júnior RAF³, Buccini DF¹, Munhoz CD¹, Moreno SE¹ ¹USP, Dpt Pharmacology, PPG pharmacology, Brasil; ²UCDB, PPG Biotechnology, ³UFMS PPG Biotechnology

Introduction: Plant extracts have garnered significant attention in the realm of memory dysfunctions owing to their potential neuroprotective and cognitive-enhancing qualities. Numerous plant extracts have been extensively researched for their impact on memory and have exhibited promising outcomes. Notably, plant extracts possess neuroprotective properties, shielding brain cells against damage induced by oxidative stress, inflammation, and other detrimental factors. *Heteropterys tomentosa*, a plant traditionally employed in Brazilian folk medicine, is recognized for its medicinal properties, including antioxidant and anti-inflammatory activities. However, studies investigating its comprehensive properties, particularly its influence on memory and other neurodegenerative diseases, remain limited.

Objective: Evaluation of the effect of the hydroalcoholic extract of *H. tomentosa* (H.E.H.t) on memory behavior in mice and *in vitro* antioxidant properties. **Methodology:** A hydroalcoholic extract (H.E) (70% alcohol; 30% water) of *H. tomentosa* was prepared. Male Swiss mice were divided into six groups: (a) untreated control group, (b) control group treated with scopolamine (1 mg/kg), (c) H.E H.t (1 mg/mL), (d) H.E H.t (1 mg/mL), (e) H.E H.t (5 mg/mL), and (f) H.E H.t (10 mg/mL) + scopolamine (1 mg/kg), 24h before behavior tests. Memory were evaluated through the novel object recognition, the time of interaction with the familiar and novel object was evaluated, and Morris water maze experiments, (CEUA 003/2019),. The antioxidant activity of the plant extract was evaluated using the DPPH radical scavenging method. Data were statistically analyzed using one-way ANOVA, and differences were considered significant for a P value < 0.05. **Results:** For the Morris water maze experiment, the memory capacity to find a platform in an apparatus is evaluated. No statistical differences were found when observing the number of entries and the time spent in the platform's quadrants. However, mice were treated with H.EH.H.t at 1mg/mL and 5mg/mL demonstrated longer latency times compared to the scopolamine-treated groups. In the novel object recognition test the interaction time between two objects is evaluated, with one of the objects being already familiar to the animal, mice treated with H.EH.H.t at 1mg/mL, 5mg/mL, and 10mg/mL displayed shorter interaction times with familiar objects and higher recognition rates of novel objects in comparison to the control group. Furthermore, the antioxidant activity of E.EH.H.t extract was found to be similar to ascorbic acid (positive control), inhibiting 50% of the DPPH radical at a concentration of 60mg/mL. **Conclusion:** The treatment with H.E.H.t appears to modulate the behavior related to object recognition memory and spatial memory in Swiss mice. Additionally, the data suggest antioxidant activity of the plant extract and also indicate that the treatment is not toxic to the organism. These findings highlight the importance of additional studies on the impact of phytotherapeutics on behavior, offering potential for the development of biopharmaceuticals. However, biochemical assays are required to observe changes in pathways that may trigger behavioral alterations. **Financial Support:** CAPES

03.026 Association between Emotional State and Salivary Cortisol Concentration of Active and Non-Active Elderly Humans. Maia J¹, Pereira AAR¹, Castellano M¹, Malerba HN^{1,2} Marques ICS¹, Viel T^{1,2} ¹EACH-USP, Lab. of Neurofarmacology of Aging, Brazil; ²ICB-USP

Introduction: Research focused on the multifactorial aging process has addressed the concepts of senescence and senility. However, despite the considerable number of existing theories, many mainly aim to identify factors capable of negatively influencing the aging process. Recent studies indicate that stressful stimuli throughout one's life, also called chronic stress, are correlated with an increase in cortisol, consequently increasing the inflammatory response and suppressing the immune system, unbalancing the relationship between pro and anti-inflammatory cytokines. Therefore, the objective of this study was to verify the influence of social interaction and low-grade physical activity on self-perception of stress and depression using scales and on the concentration of cortisol in the saliva of the studied groups. **Methods:** The sample size for this study (n= 60) was determined based on the percentage of elderly people (60+) in the city of Americana (SP). From this sample, 30 individuals, who did not practice any type of physical activity were included in the control group (G1), and 30 individuals, that were physically active participated in the ATIVAidade project, were included in the experimental group (G2). ATIVAidade is a project that aims to improve quality of life through social interactions and physical activities and these people were involved with this project for at least 3 months prior to the survey. The participants answered questionnaires to verify stress level (Perceived Stress Scale - PSS) and depression (Depression Scale - CES-D). After that, they were asked to collect saliva samples in the morning period for three days in a row. The analysis of salivary cortisol was performed with an Elisa kit according to instructions of the manufacturer. EACH/USP ethics committee: 5.048.571. **Results:** Regarding the PSS scale, even though both groups showed high levels of stress according to the test scorecard, there were no differences between them (G1, 18.66±9.45; G2, 17.56±7.51, p= 0.7171). On the CES-D scale, G1 showed signs of the presence of depression scoring above the cutoff points of the scale (>12), while G2 scored below, however there was no difference between them (G1 16.38±10.66; G2 10.84±9.08; p=0.0802. Despite the lack of difference in the qualitative analysis of stress and depression, the salivary cortisol analysis showed a significant decrease in G2 by 7.3-fold (12.71±14.01ng/mL) when compared to G1 (93.83±156.1ng/mL), p=0.004. **Conclusion:** Although the groups showed no difference in the PSS and CES-D self-perception scales, we could observe that the biological marker of stress used, cortisol, had a significant reduction in expression in the active group. Thus, the findings correlate social interaction and the practice of physical activity as potent regulators of stress in the body, which can improve the quality of life and modulate the brain health of the elderly. **Financial Support:** FAPESP2020/14133-6

03.027 Chlorpromazine Hydrochloride Liposomes is Safe in Alternative Models and Decreases the Catatonic Effect of the Free Drug in Mice. Ferreira JGJ¹, Rez TG¹, Ayres TA¹, Barbosa E¹, Rodrigues GZP¹, Verza SG¹, de Mattos CB¹, Dallegrave E², Morisso FDP¹, Gehlen G¹, Charão MF¹, Betti AH¹. ¹Feevale, Institute of Health Sciences, Brazil; ² UFCSPA, Porto Alegre, Brazil

Introduction: Chlorpromazine is used in the treatment of schizophrenia; however, it has a cautious use, due to its side effects, especially catalepsy. In this context, liposomes emerge as a potential strategy to improve this concern. Then, the aim of this study was to evaluate the behavior of liposomes containing chlorpromazine hydrochloride on catalepsy test, as well as its potential toxicity *in vivo*, using alternative models, such as *Caenorhabditis elegans* and the OECD Acute Toxicity Protocol, number 423. **Methods:** Liposomes containing chlorpromazine hydrochloride were developed by lipid film hydration method and were characterized for particle size, zeta potential, polydispersity index, pH and content. All tests were performed using 4 groups of treatments: (1) control solution (vehicle), (2) liposomes containing chlorpromazine hydrochloride (10 mg/kg), (3) white liposomes (without the drug), (4) free drug (10 mg/kg); and were previously approved by Feevale Animal Research Ethical Committee (protocol n° 01.17.057). The liposomes potential toxicity was first evaluated in an alternative model, using the nematodes *C. elegans*. Development and survival were analyzed in the wild strain N2 and the acute oral toxicity in adult Balb/C mice, nulliparous females (n=3). Feed consumption and body mass were evaluated for 14 days. Pharmacological evaluation was performed by following the catalepsy curve (n=6/group). **Results:** Liposomes had a milky appearance, with mean particle size of 204.25 ± 11.70 and 200.26 ± 5.23 , polydispersity index of 0.21 ± 0.01 and 0.20 ± 0.06 , zeta potential of -40.55 ± 5.50 and -21.88 ± 9.93 , and pH of 6.27 ± 0.14 and 5.68 ± 0.36 , for white liposome and chlorpromazine hydrochloride liposome, respectively. In the pharmacological evaluation, liposomes containing chlorpromazine did not induce catalepsy during the 7 hours evaluated, differing from the free drug, which induced catalepsy. Regarding the toxicity evaluated in the *C. elegans*, the free drug affected the nematode development and significantly decreased their survival at the concentrations above 0.25 and 0.50 mg/mL, differing from the liposome, that affected only the development. Acute treatment in mice did not show any sign of toxicity (eyelid ptosis, piloerection, hypothermia, posterior or anterior train paralysis), as well as changes in body mass and feed consumption during the whole period evaluated. **Conclusion:** This study evidenced a reduction in an important side effect of chlorpromazine when liposomated, without any important toxicity in alternative models. However, further studies are necessary to evaluate the effectiveness and security of this inedited formulation. **Financial Support:** CAPES and Feevale University.

04. Inflammation and Immunopharmacology

04.001 **Development of an Anti-Inflammatory Gel Containing the Extract of an Agave Genus Agro-Industrial Waste Associated with a Polyphenol.** Ferreira FY¹, Fracasso JAR², Costa LTS², Ximenes VF³, Paes JTR¹, Dos Santos L¹ ¹UNESP Assis, Dpt of Biotechnology, Brazil; ²Unesp Araçatuba, PPG of Science, Brazil; ³Unesp Bauru, Dpt of Chemistry, Brazil

Introduction: Brazil has the greatest biodiversity on the planet and is the second largest agricultural producer in the world, consequently, one of the largest generators of agro-industrial waste. Studies that use plant residues as a source of new medicines are extremely necessary in several aspects, such as: health, environmental, social and economic preservation. In this respect, studies carried out in our laboratory have already shown that the extract obtained from the residue of *Agave sisalana* (sisal) has anti-inflammatory activity. Aiming at enhancing this activity and developing a herbal medicine with effective therapeutic activity, the association of this extract with tannic acid, a natural polyphenolic compound, was carried out. In the literature, the pharmacological activities of isolated tannic acid are elucidated, but its association is insufficiently researched, and nothing is known about the effects of a topical product containing sisal and tannic acid. Therefore, this study aimed to develop and analyze the anti-inflammatory and toxicological profile *in vivo* of the gel containing sisal residue extract (SE) and tannic acid (TA). **Methods:** Initially, the phytochemical profile of the SE was evaluated, then the cytotoxicity (CT) and anti-inflammatory activities (AA) of the association of SE with TA. In the phytochemical evaluation of SE, the cobalt chloride method was used to measure saponins. In *in vitro* studies, SE associated with TA, respectively, were analyzed at concentrations (mg/mL) of: 0.1/0.01 (A1); 0.2/ 0.02 (A2); 1/0.1 (A3) and 2/0.2 (A4). CT was evaluated by the MTT method. To determine the AA, the methods of inducing hemolysis and macrophage spreading were used, with hypotonic solution NC (negative control) and dexamethasone (0.1 mg/mL) as the positive control (CP). The *in vivo* AA of the gel containing 20 mg/g SE for 2 mg/g tannic acid was determined in mice (Protocol CEUA 004/2022) by the method of induction of edema by carrageenan (CPE), with the carbopol-based formulation as the NC and dexamethasone 1 mg/g (CP). **Results:** The quantitative dosage of saponins for SE was 43.0±0.3 mg of quijalla saponins equivalent to one gram of dry extract. In the cytotoxicological profile evaluation, only ES and A1 didn't showed cytotoxicity with 105.2 and 76.5 percent of cell viability, respectively. In the *in vitro* anti-inflammatory evaluation, all concentrations showed effective anti-inflammatory activity when compared to PC, the A4 showed the best result in both assays, with 95.86 percent of inhibition of hemolysis and 82 percent of inhibition of spreading. Subsequently, during the evaluation of *in vivo* topical acute inflammation, using the paw edema method, it was possible to verify that the association obtained results similar to dexamethasone gel at 4 and 6 h of treatment, respectively (p<0.05) **Conclusion:** It is concluded that SE has high levels of saponins, which must be responsible for the AA. The A4 association presents expressive AA activities, and potentiated the previous results of SE and TA alone. The gel containing the association presents AA similar to PC, commonly used in clinical medicine.

04.002 Evaluation of Oxidative Stress Parameters in Patients with Systemic Lupus Erythematosus. Sampaio AMKV¹, Safraid GF², Petreceli RR³, Bulegon JS³, Vida RL², Correa GL¹, Brucker N^{1,2,3}. ¹UFMS, Dpt of Pharmacology and Physiology, Brazil; ²UFMS, PPG in Pharmacology, Brazil; ³UFMS, PPG in Pharmaceutical Sciences, Brazil

Introduction: Systemic lupus erythematosus (SLE) is a chronic, multisystemic, inflammatory disease of unknown cause and autoimmune nature, characterized by the presence of various autoantibodies. The alterations caused by autoantibodies can lead to an imbalance between reactive substances due to excessive cellular activation resulting in oxidative stress. The objective of this study was to evaluate biomarkers of oxidative stress in SLE patients and compare them with healthy controls. **Methodology:** Twenty SLE patients (LP group) undergoing outpatient treatment in the city of Santa Maria-RS and twenty healthy controls (HC group) participated in this study. Ethics committee approved and registered this study under number CAAE: 52583721.1.0000.5346. Blood samples were collected by venipuncture, with and without anticoagulant, and subsequently centrifuged, analyzed or stored at -80°C. The plasma was assessed to evaluate lipid peroxidation (TBARS)¹ and vitamin C levels² by spectrophotometry. Non-protein thiols³ and DNA damage were assessed in erythrocytes by spectrophotometry and comet assay⁴, respectively. Statistical analysis was performed using GraphPad Prism. **Results:** The results of oxidative stress biomarkers were (mean ± SEM) in LP and HC respectively: MDA 1.32 ± 0.24 mM and 1.31 ± 0.7 mM; non-protein thiols: 205.4 ± 18.61 mM, 220.7 ± 14.94 mM; vitamin C: 18.38 ± 1.8 µg Vit C/ml, 19.51 ± 2.01 µg Vit C/ml; Tail DNA: 16.37 ± 2.5%, 13.58 ± 1.27%; p>0.05. Correlation was observed between levels of non-protein thiols and vitamin C (r=0.346, p=0.031). **Conclusion:** Our study observed no significant differences in oxidative stress biomarkers between lupus patients and healthy controls. However, a correlation between levels of vitamin C and non-protein thiols was observed. Vitamin C is only obtained through diet, and this may indicate that antioxidant consumption may improve the endogenous antioxidant system, especially against the oxidation of -SH groups⁵. Further investigations are required to understand the oxidative stress in lupus patients. **Funding:** CAPES. **References:** 1. Grotto, D. J Pharm Biomed Anal., v.43, p. 619, 2007. 2. CDC. USDHHS, p. 17, 1979 3. Benzie, IFF. Anal. Biochem., v. 82, p. 70, 1996 4. Ellman, GL. Arch. Biochem. Biophys., v. 82, p. 70, 1959. 5. Paniz, C., Clin. Biochem., v. 40, p. 1367.

04.003 Type 1 Diabetes Did Not Modify Zymosan-Induced Arthritis in Mice. Barbosa BLSS, Guimarães FV, Carttman L, Chaves AS, Cotias AC, Martins MA, Silva PMR, Carvalho VF IOC-Fiocruz Lab. of Inflammation, Rio de Janeiro, Brazil

Introduction: Diabetes mellitus (DM) is a chronic metabolic disease characterized by hyperglycemia. Patients with type 1 diabetes have a higher prevalence of juvenile idiopathic arthritis, a disease characterized by an accumulation of inflammatory cells into the joints, causing swelling, local pain, limitations of movement, and, in some cases, damage of bones and cartilage, than non-diabetic ones. Thus, our objective was to investigate whether diabetes induced by alloxan could interfere with zymosan-induced arthritis in mice. **Methods:** Diabetes was induced by a single intravenous injection of alloxan (65 mg/kg) into male C57 Black/6 mice. Arthritis was induced by intra-articular injection of zymosan (500 µg/joint) on days 7 and 14 after diabetes induction, and the analyses were performed 7 days after the last challenge with zymosan. The parameters analyzed included: i) body weight; ii) blood hyperglycemia; iii) joint oedema; iv) joint leukocyte infiltration, v) bone mineral density (microcomputed tomography -PerkinElmer GX2 microCT). The analysis of the bone microarchitecture was performed using the Analyze 14.0 software. **Results:** We showed that alloxan-induced hyperglycemia paralleled to loss of body weight, characterizing the development of diabetes. In addition, we noted that diabetic mice presented a significantly reduction in the bone mineral density (BMD) of the bones comprising the joint (femur and tibia) as compared to non-diabetic mice, in a clear association with an increase in blood neutrophil/lymphocyte ratio. In addition, zymosan-induced oedema and leucocyte infiltration, including neutrophils and mononuclear cells, in the joint of non-diabetic mice. Diabetic mice, provoked with zymosan, exhibited similar levels of blood glucose, body weight, blood neutrophil/lymphocyte ratio, and BMD of the bones that comprise the joint as compared to diabetic mice injected with vehicle. Finally, diabetes did not modify zymosan-induced oedema (4.3 ± 0.1 mm and 4.8 ± 0.09 mm, mean \pm SEM, n = 6) and leukocyte accumulation, either neutrophils (504 ± 212 and $398 \pm 230 \times 10^3$ /cavity, mean \pm SEM, n = 6) or mononuclear cells ($130 \pm 46 \times 10^3$ /cavity and $97 \pm 41 \times 10^3$ /cavity, mean \pm SEM, n = 6). **Conclusion:** Our findings show that alloxan-induced diabetes did not modify inflammation triggered by zymosan in joints of C57 Black/6 mice, probably because this is a model of monoarthritis, and not the complex condition of systemic polyarthritis. **Financial Support:** FIOCRUZ, CNPQ, FAPERJ, INCT-NIM, CAPES, JICA.

04.004 Astrocytes Respond to Different Inflammatory Stimuli. Almeida, M.A.P^{1,2,3}, Costa, M.F^{1,2}, Moraes, B.P.T^{1,2,3}, Bozza, P.T¹, Castro-Faria-Neto, H.C¹, Gonçalves-de-Albuquerque, C.F^{1,2,3}, Trindade, P.⁴, Silva, A.R^{1,2,3}. ¹IOC-Fiocruz, Immunopharmacology Lab., Rio de Janeiro, Brazil; ²Unirio, Immunopharmacology Lab., Dept of Physiological Sciences, Rio de Janeiro, Brazil; ³UFF, PPG in Neurosciences, Niterói, Brazil; ⁴UFRJ, Dept of Clinical and Toxicological Analyses, Pharmacy Faculty, Rio de Janeiro, Brazil

Introduction: Functional astrocytes responsive to the inflammatory response can be obtained from induced pluripotent stem cells (iPSCs)(1,2). Reactive astrogliosis is characterized by alterations or loss of morphology in astrocytes exposed to a stressor stimulus (3). Sepsis causes glial activation (4) and is characterized by a large production of cytokines, causing hemodynamic and metabolic problems(5). Inflammation has a great impact on the Central Nervous System (CNS) leading to acute and chronic damage (6). It is known that injuries to the central nervous system trigger NF- κ B signaling in astrocytes, inducing an increase in cytokine production and expression of intermediate filaments. Reactive astrocytes have impaired metabolic functions and release cytokines, which perform neuroprotective or neurotoxic functions (7). The nuclear factor kappa B (NF- κ B) is a regulator of several genes that mediate immune and inflammatory responses and its activation results in the phosphorylation of pathways such as NF- κ B p65 and p38 (8,9). **Methods:** For the identification of molecular and cellular phenotypes associated with astrogliosis, human astrocytes derived from iPSC cells were exposed to pro-inflammatory stimuli such as TNF- α and LPS, in a plate culture medium for three different conditions and subsequently evaluated through laboratory tests such as western blotting. **Results and Conclusion:** The analyzes of our research suggest that astrocytes were able to respond to TNF- α stimulation by increasing NF- κ B (p65) and p38 phosphorylation. Furthermore, we analyzed whether the presence of FBS at different concentrations was able to modulate the response to LPS. Preliminary analysis suggests that the presence of serum in the culture may help in the response of these cells, possibly increasing the phosphorylation of p65 and p38. **Acknowledgments:** FAPERJ, CNPq, CAPES Grant 001, IOC-FIOCRUZ/RJ, Post-Graduate Program in Neurosciences (UFF), UNIRIO, UFRJ. **Financial Support:** CAPES, CNPq, FAPERJ, IOC, FIOCRUZ. **References:** 1. Yan, Y. Stem Cells Transl Med., vol.2, p.862, 2013 2. Pasca, AM. Nat Methods, vol.12, p.671, 2015 3. Buffo A. Proc Natl Acad Sci U S A., v.105, p.3581, 2008 4. 14. Moraes, C. Pharmaceuticals., v.14, p.416 2021 5. Vachharajani, VT. J Leukoc Biol., v.96, p.785 2014. 6. Danielski, L.G. Mol. Neuro., v.59, p.7229 2022. 7. Trindade, P. Glia., v.68, p.1396, 2019 8. Zhang, J, Toxicology., v.336, p.17, 2015 9. Yao, Y. Biomed Rep., v.13, p.51 2020

04.005 Phosphodiesterase 4 is Involved in cAMP Degradation Induced by Prostaglandin E2 and Endothelin-1 in the Hypothalamus. Amateckes JA, Costa RA, Zampronio AR UFPR Curitiba, Dpt of Pharmacology, Brazil

Introduction: Fever is one of the most important responses against infectious and/or inflammatory agents and begins with the production of endogenous pyrogens, which in turn generates central mediators such as prostaglandin E2 (PGE2) and endothelin-1 (ET-1) (Zampronio et al., *Temperature (Austin)*, 2: 506, 2015). It is known that PGE2 exerts its action on inhibitory EP3 receptors by reducing cAMP. The EP3 receptors are extensively found in gamma-aminobutyric acid (GABA) neurons in the pre-optic area of the hypothalamus. The inhibition of these neurons activates descending pathways responsible for increasing the body temperature observed during fever (Morrison & Nakamura, *Annu Rev Physiol*, 81: 285, 2019). It is not known if central mediators of fever such as ET-1, which acts independently of PGE2 synthesis, also produce fever by reducing cAMP. ET-1 acts on ETB receptors to produce fever and these receptors can also be inhibitory. The degradation of cAMP into 5'AMP takes place through the activity of the enzyme phosphodiesterase (PDE). PDE4 isoform is highly expressed in the mammal's brain (Bhat et al., *Pharmacol Res* 160: 105078, 2020) but it is not known if this isoform is responsible for the degradation of cAMP in the hypothalamus. The aims of this study were to evaluate if a) the PDE4 was the isoform involved in the degradation of cAMP during PGE2-induced fever using Roflumilast, a PDE4 inhibitor; and b) if the febrile response induced by ET-1 was also dependent on cAMP reduction. **Methods:** Male Wistar rats (90 days) were used. An intracerebroventricular (i.c.v.) guide cannula was implanted in the lateral ventricle for drug administration and remote temperature recorders implanted in the peritoneal cavity temperature measurement. Roflumilast (30µg, i.c.v., 2 µl) or vehicle (saline) were administered alone or 30 min before the pyrogen. The febrile response was induced by PGE2 (250 ng, i.c.v.) or ET-1 (1 pmol, i.c.v.). Experiments were conducted at an ambient temperature of 28°C. Experimental protocols were approved by CEUA-BIO/UFPR #1392. **Results:** The i.c.v. administration of PDE4 inhibitor Roflumilast alone did not change the body temperature of the animals. The i.c.v. administration of PGE2 and ET-1 induced a significant febrile response of 38,03°C and 38,06°C, respectively, when compared to the vehicle-treated animals. Pre-treatment of the animals with Roflumilast abolished the febrile response induced by PGE2 and significantly reduced the fever induced by ET-1. **Conclusion:** The results suggest that PDE4 is the main PDE involved in the metabolism of cAMP in the hypothalamus during fever. In addition, similarly to PGE2, ET-1 seems to exert an inhibitory action in cAMP production to induce fever. **Financial Support:** CNPq and UFPR.

04.006 The Therapeutic Potential of *Arrabidaea chica* Verlot (Bignoniaceae) in Pulmonary Sepsis. Brito MASM^{1,2,3}, Chagas MSS^{1,2}, Moragas-Tellis CJ³, Silva AR², Behrens MD³, Gonçalves-de-Albuquerque CF^{1,2} ¹Unirio Rio de Janeiro, Dpt of Physiological Sciences, Brazil, ²IOC-Fiocruz, Rio de Janeiro, Immunopharmacology Lab., Brazil, ³Farmanguinhos, Natural Products Lab., Rio de Janeiro, Brazil

Introduction: Pneumonia is an inflammatory disease of acute or chronic manifestation caused by several etiological agents, as *Pseudomonas aeruginosa*, an opportunistic pathogen that cause severe infections in immunosuppressed patients (1,2). Considering the increase in microbial resistance to medicines, the search for new therapeutic alternatives is relevant. Medicinal plants stand out as potential sources of new drugs with antimicrobial activity. Various plant species already used by the population as anti-inflammatory, antimicrobial, and wound healing are present in the National List of Medicinal Plants of Interest to the Brazilian Unified Health System (Rennisus) (3). *Arrabidaea chica* (Humb. & Bonpl.) Verlot (Bignoniaceae) is widely found in Brazil, mainly in the Amazon region (4), and is one of the plants in Rennisus. Studies show that this plant extracts have antioxidant, analgesic, anti-inflammatory, antimicrobial, antiangiogenic, anti-Trypanosoma, and anti-Leishmania action (5, 6, 7, 8). We evaluated the effect of a crude extract of *A. chica* (CEAC) in a murine pneumonia model induced by *P. aeruginosa*. **Methods:** All experimental procedures were approved by the Ethics Committee of Animal Experiments of IOC (protocol: L054/2015). The hydroalcoholic extract (7: 3) of leaves of *A. chica* (CEAC) was obtained by maceration. *P. aeruginosa*, strain PA01 (PA), was cultured in solid culture medium tryptic soy agar (TSA), and a colony was selected and transferred to Luria-Bertani Broth (LB) liquid medium. Male Swiss mice were instilled intratracheally with 107 CFU of the bacterium. Five hours later, the animals were treated orally with crude extract (50, 100, and 200 mg/kg). The survival rate of the animals was evaluated for 4 days. **Results:** The doses of 100 and 200 mg/kg of the CEAC reduced the accumulation of total leukocytes, number of neutrophils, and mononuclear cells, when evaluated in blood, and 100 mg/kg was the most effective. In BAL, the same effect of reducing the total leukocyte and neutrophil accumulation was observed for both doses. The 100 mg/kg dose promoted a potent reduction in neutrophil accumulation. The reduction effect of mononuclear cells was similar in both concentrations. Treatment with *A. chica* extract also reduced the pulmonary edema. **Conclusions:** Our findings suggest that CEAC, in 100 and 200 mg/kg doses, features anti-inflammatory and antibacterial activities by reducing pulmonary edema, CFUs, and total leukocyte influx. **Financial Support:** CNPq, CAPES, FAPERJ, Farmanguinhos, IOC, FIOCRUZ and UNIRIO. **References:** 1. BAYES, HK. *Sci. Rep.*, v.6, 35838, 2016; 2. PETROCHEILOU, A. *Glob. Pediatr. Health*, V.6, 2333794X1773846, 2017; 3. BRASIL, Rennisus, 2009; ALVES, MSM. *Rev. Bras. Farmacogn.*, v. 20, p. 215, 2010; 4. MICHEL, AFRM. *J. Ethnopharmac.*, n. 165, p. 29, 2015; 5. MIRANDA, N. *Photodiagn. Photodyn. Ther.*, v. 19, p. 256, 2015; 6. MORAGAS-TELLIS, CJ. *Mol.*, v. 25, p. 3547, 2020; 7. SILVA-SILVA, JV. *Pharmace.*, v. 15, n. 3, p. 331, 2020; 8. VASCONCELOS, CC. *Int. J. Mol. Sci.*, v. 20, p. 4717, 201

04.007 Evaluation of the Anti-inflammatory and Antinociceptive Effect of the Aqueous Extract of *Allophylus edulis* (A.St-Hil., Cambess. & A. Juss.) Radlk. Leaves. Fava de Souza M¹, Santos SM¹, Faoro JAM¹, Oliveira Junior PC², Narcizo LL³, Santos JM¹, Silva ME¹, Passos BP³, Rhoden SL³, Formagio ASN^{1,3} ¹UFGD, PPG in Health Sciences, ²Rede Pró-Centro Oeste, PPG in Biotechnology and Biodiversity, ³UFGD, PPG in Biodiversity and Environment

Introduction: *Allophylus edulis*, a South American tree known as vacum, has been used in folk medicine to treat inflammation (Körbes, 1995). It has hepatoprotective and negative ionotropic potential, and its essential oils have anti-inflammatory, antioxidant and antimycobacterial properties (Trevizan et al., 2016; Piekarski-Barchik et al., 2021; Santos et al., 2021). However, the aqueous extract's anti-inflammatory and antinociceptive effects are unknown. This study aims to evaluate the aqueous extract of *A. edulis* leaves for its antioxidant, anti-inflammatory and antinociceptive potential due to its traditional medicinal use.

Methods: Fresh leaves of *A. edulis* ((SisGen-A51F665) were collected in the city of Dourados, MS, Brazil, and submitted to infusion and lyophilization. The aqueous extract was subjected to quantification of constituent contents and to measure the antioxidant activity using the lipid peroxidation (linoleic acid/ β -carotene test) and free radical scavenging (DPPH) method as described by Hayat et al. (2020) and Miller (1971). The anti-inflammatory activity of the aqueous extract (3, 30 or 100 mg/kg, i.g.) was evaluated by the method of paw edema induced by carrageenan (300 μ g/paw), complemented with tests of mechanical hyperalgesia and acetone-induced allodynia (Winter et al., 1962; Sufka et al., 1998); while the antinociceptive activity was induced by formalin (20 μ L at 2.5%). Differences between groups were analyzed by ANOVA followed by the Newman-Keuls post-test. **Results:** The aqueous extract revealed 177.56 \pm 6.16 mg GAE/g (total phenolic compounds), 37.29 \pm 0.18 mg QE/g (flavonoids), 5.22 \pm 0.11 mg QE/g (flavonols) and 37.78 \pm 1.12 mg EC/g (condensed tannins). Antioxidant activity showed an IC₅₀ of 27.88 \pm 0.002 μ g/ml and 117.9 \pm 0.50 μ g/ml by free radical scavenging method and lipid peroxidation, respectively. The evaluation of the aqueous extract showed an anti-inflammatory effect at the tested doses. After 4 hours of carrageenan injection, the *in vivo* effect of oral administration on carrageenan-induced inflammation showed a mean inhibition of 59.7% of paw edema. While, in this same period, the positive control, dexamethasone (1 mg/kg) showed an inhibition of 72.4%. The dose of 30 mg/kg showed the greatest inhibitions in the tests of acetone-induced allodynia (61.9%) and mechanical hyperalgesia (83.2%) after 4 hours of carrageenan injection. A characteristic two-phase pattern was observed after formalin injection. The treated groups did not differ statistically from the control in the neurogenic phase and had an average inhibition of 20.6% in the inflammatory phase.

Conclusion: In conclusion, the aqueous extract demonstrated a significant amount of total phenolic compounds, flavonoids, flavonols, and condensed tannins, along with antioxidant and anti-inflammatory properties. **Financial Support:** CAPES - Finance Code 001 and FUNDECT.

Ethics committee approval: CEUA/UFGD Protocol n^o 05/2021. **References:** Hayat, J. et al. Heliyon 6, e05609, 2020. Körbes, VC. Plantas medicinais. 48. ed., p. 188, 1995. Miller, HE. J. Am. Oil Chem. Soc. v. 45, p. 91, 1971. Piekarski-Barchik, AS. et al. Chem. Biodivers, 2021. Santos, S.M. et al. J. Ethnopharmacol. v. 267, p. 113495, 2021. Sufka, KJ. et al. Eur. J. Pain. v. 2, p. 358, 1998. Trevizan, L.N.F. et al. J. Ethnopharmacol. v. 192, p. 510, 2016. Winter, C.A. et al. Proc. Soc. Exp. Biol. Med., v. 111, p. 547, 1962. **Acknowledgments**

The authors express their gratitude to the Federal University of Grande Dourados, FUNDECT and CAPES for financial support.

04.008 Effects of Cyanidin 3-Glucoside on some Immunoregulatory Properties of Mesenchymal Stem Cells. Freitas S¹, Makiyama EN¹, Neves BRO¹, Gonçalves, CES¹, Borelli P¹, Fock RA¹ ¹USP Dpt of Clinical and Toxicological Analyses, PPG Pharmacy: Physiopathology and Toxicology, Brazil.

Introduction: Mesenchymal stem cells (MSCs) hold promises for the treatment of various diseases, such as cancer, autoimmune, inflammatory and infectious diseases [1]. They regulate the immune system and produce various soluble substances [2]. Anthocyanins, natural pigments of some vegetables and fruits, have bioactive properties [3-4]. In this study, we investigated whether anthocyanin cyanidin-3-glucoside (CY3G), known for its anti-inflammatory action, would affect the immunoregulatory properties of MSCs. **Methods:** The mesenchymal stem cell line used was C3H/10T1/2 (CCL-226™, ATCC®), which was cultivated and supplemented with 50µM of CY3G, and was also stimulated with Lipopolysaccharide (LPS). The murine cell line RAW 264.7 (TIB-71™, ATCC®) and splenic lymphocytes from C57BL/6 mice were cultivated in the presence of C3H/10T1/2 conditioned medium. This study was performed following its approval by the institutional animal care committee (CEUA-FCF Protocol #627). The protein expression of NFκB, STAT3 and PCNA was evaluated in MSCs by Western blotting, on the other hand, in RAW 264.7 cells and in splenic lymphocytes the expression of NFκB was evaluated. The secretome of all these strains were analyzed by ELISA assay. **Results:** We verified a decrease in the production of IL-1β, an increase in the production of nitric oxide (NO) and a reduction in the activation of NFκB on MSCs. RAW 264.7 cells exposed to the conditioned medium of MSCs showed lower production of IL-1β, IL-6 and IL-12, in addition to decreased NFκB expression. In splenic lymphocytes, we observed a decrease in IL-2 production and an increase in IL-10. **Conclusion:** The CY3G modulates the immunoregulatory properties of MSCs, promoting an immunosuppressive profile and affecting immune system cells. **References:** [1] Ragni, E. et al. Stem Cell Res. Ther. v.11, p.2-19, 2020; [2] Li, N.; Hua, J. Cell. Mol. Life Sci.v. 74, p. 2345-2360, 2017; [3] Mazza, G.; Francis, F. J. Crit Rev Food Sci Nutri. v.35, p.341, 1995; [4] Ferrari, D. et al. Toxicol. Lett. v. 264 p. 51-58, 2016. **Financial Support:** CNPq (130475/2021-1), and FAPESP.

04.009 Evaluation of Cannabinoid Receptor Modulation in the Activation of Human Peripheral Neutrophils. Correa AMC^{2,3}, Pádua TA², Seito LN², Silva PRO², Santos SOS², Henriques MGMO^{1,2,3} ¹IBRAG-UERJ, Lab. of Cellular and Molecular Pharmacology, Dept of Cell Biology, Rio de Janeiro, Brazil, ²Fiocruz-Farmanguinhos, Lab. of Applied Pharmacology,, Rio de Janeiro, Brazil ³UERJ-IBRAG - PPG in Biosciences

Introduction: The mammalian endocannabinoid system (ECS) is primarily responsible for maintaining homeostasis. The ECS directly influences several functions related to the central and peripheral nervous system and is also involved in several pathophysiological diseases such as cancer, cardiovascular, pulmonary and infectious diseases. Cannabinoid compounds that bind to cannabinoid receptors B1 (CB1) and B2 (CB2) have been an important focus of study for possible anti-inflammatory treatments. Neutrophils are considered key cells in the development of infectious or non-infectious lung inflammatory diseases. In this context, CB1 and CB2, have been reported to modulate neutrophil activity in inflammatory diseases. However, the mechanisms of neutrophil activation modulated by CB1 and CB2 receptors are still unclear. **Aim:** This work aims to study the effect of activation of cannabinoid receptors in the mechanisms of neutrophil activation and migration. **Methods:** For this, peripheral human neutrophils were isolated from 3 different volunteers, treated with different concentrations [0.1-100 µM] of CB1 (ACEA) or CB2 (JWH133) agonist and their viability was evaluated using live/dead kit (ThermoFisher-Far red). The expression of CB2 in unstimulated and stimulated human neutrophils with different stimuli such as PMA [5 nM], FMLP [10 µM] and TNF-α [10 ng/mL] + IL-8 [10, 25 and 50 ng/mL] was evaluated by western blotting. To investigate how ACEA [0.1-100 µM] or JWH133 [0.1-100 µM] alters the peripheral human neutrophils migration and NETosis, these cells were stimulated with IL-8 and PMA, respectively. Neutrophil migration was induced by IL-8 [12 ng/mL] stimulation and evaluated using Transwell® (0.3 µm). NETosis process was induced by PMA stimulation [5 nM] and quantified NETs by Sytox-Green® (ThermoFisher) fluorescence formed. **Results:** Neutrophil viability was ≥ 90% in all treatments concentrations of CB1 and CB2 agonists. The expression of CB2 was observed with all stimuli evaluated. Pre-treatment with ACEA [0.1-100 µM] or JWH133 [0.1-100 µM] indicated a tendency to modulate the neutrophil migration dependent on the tested volunteer but were not statistically significant. We observed that the pre-treatment with CB2 agonist, JWH133 at [1-10 µM] concentrations was able to reduce the release of NETs (p≤0,05) after 4 hours of stimulation with PMA [5 nM], whereas CB1 agonist, ACEA, in all concentrations tested, was not able to significantly modulate this response. **Conclusion:** These results indicate a potential modulation of neutrophil activation by CB2 receptor. As perspectives, we intend to evaluate whether the activation of CB1 and CB2 receptors alter the behavior of neutrophils and the development of acute lung injury in murine experimental models and the molecular mechanism of this effect. This study was approved by the Research Ethics Committee from FIOCRUZ, CEP-CAAE: 56727722.6.0000.5248. **Financial Support:** CNPq, FAPERJ, CAPES

04.010 Sexual Dimorphism in Hypothalamic Serotonin Levels During Systemic Inflammation. Costa RA, Amateck JA, Zampronio AR ¹UFPR, Dpt of Pharmacology, Curitiba, Brazil;

Introduction: Systemic inflammation is usually caused by infections that may lead to organ dysfunction. The disease is characterized by fever, hyperalgesia, hypolocomotion, loss of appetite, and drowsiness, known as sickness syndrome and sickness behavior. In the model of endotoxemia by lipopolysaccharide (LPS) injection, a milder systemic inflammatory response, previous studies have shown a reduction in hypothalamic serotonin (5-HT) levels during the febrile response, which would facilitate the increase in prostaglandin levels in male rats (Mota *et al.*, *Brain Behav Immun*, 66: 372, 2017). Previous studies have also shown that females have a lower febrile response than males (Coelho *et al.*, *Inflammation*, 44: 321, 2021). The aim this study was to evaluate if, concomitantly with the different febrile response, male and female rats show differences in hypolocomotion, a sickness behavior, and in hypothalamic 5-HT levels. Hypothalamic levels of dopamine (DA) were also evaluated. **Methods:** Male and female Wistar rats (90 days) received remote temperature recorders in the peritoneal cavity. After 7 days, the animals were transferred to a room at 28°C and received LPS (*E. Coli*, 0111: B4, 100 µg/kg, i.p.) or saline and body temperature was evaluated for 5 h. At the end of this period, the animals were submitted in the open field test and then the hypothalamus was collected for 5-HT, DA and its metabolites 5- hydroxy-indole acetic acid (5HIAA) and 3,4-Dihydroxyphenylacetic acid (DOPAC) dosage by high performance liquid chromatography (HPLC). This study was approved by the Animal Research Ethics Committee of the Federal University of Paraná (No. 1444/2022). **Results:** Confirming previous results, LPS induced a febrile response in both male and female rats but the febrile response in females was lower than in males. In the open field, LPS injection significantly reduced the number of crossings, the distance traveled, and velocity in males and females when compared to saline-treated animals. However, no difference was seen between male and female rats. LPS administration induced a significant reduction of 5-HT (20%) and its metabolite 5HIAA (25%) in the hypothalamus in males. In females, unlike males, a significant increase in the levels of 5-HT (85%) and 5HIAA (72%) in the hypothalamus was observed after LPS injection. Moreover, DA and DOPAC hypothalamic levels were similarly increased (25% and 50%, respectively) in both male and females after LPS injection. **Conclusion:** Our findings showed an important sexual dimorphism in the levels of 5-HT and its metabolite in the hypothalamus during the endotoxemia: while in males there is a reduction, in females there is an increase in these levels. This difference may be related to the lower febrile response observed in females. No differences were observed in hypolocomotion or in the levels of other neurotransmitters such as DA. The understanding of these differences is important for a better control the systemic inflammation. **Financial Support:** CNPq and UFPR.

04.011 Potential Role of Thrombin and PAR-1 in Lung Fibrosis Caused by Silica Particles in Mice. Souza, LM¹, Ferreira, TPT¹, Martins, MA¹, Lagente, V², Silva, PMR¹ ¹IOC-Fiocruz, Lab. of Inflammation, Rio de Janeiro, Brazil

Introduction: Silicosis is an occupational disease characterized by a chronic inflammatory component, which later culminates in collagen deposition and granuloma formation. Pieces of evidence indicate the existence of high levels of enzymes involved in the coagulation cascade, such as thrombin, in patients with lung fibrotic diseases, acting on its active site PAR-1. Epithelial cells are shown to be critical targeted cells in the silicosis progression, based on their ability to secrete inflammatory and profibrotic factors. In this study, we investigated the potential involvement of thrombin and its active site PAR-1, in the development of lung fibrosis induced by silica particles in mice, emphasizing epithelial cells as possible targets. **Methods:** Human lung epithelial cell lineages A549 and CALU-3 were stimulated with silica particles (30 - 300 μ L) and thrombin (10 U/mL), and 24 h later the supernatant was recovered for quantification of cytokines IL-8 and IL-6 by ELISA. Male Swiss-Webster mice were instilled with intranasal silica (10 mg/50 μ L) and controls received the same volume of sterile saline. The analyses were made 28 days post-silica and included: i) pulmonary mechanics and airways hyper-reactivity to methacholine measured by whole-body invasive plethysmography (Finepointe, Buxco System); ii) collagen deposition and granuloma formation evaluated in the lung tissue by classical histological techniques (H&E and *Picrus sirius*); iii) thrombin and PAR-1 were evaluated by ELISA and Western blot, respectively. All experimental procedures were performed in accordance with the guidelines of the Committee on Use of Laboratory Animals of the Oswaldo Cruz Foundation (L-001/19A2). **Results:** Incubation with silica particles activated both epithelial cell lines "in vitro", and the highest concentration (300 μ g/mL) increased the levels of IL-8 in A549 and IL-6 in CALU-3. Likewise, thrombin led to the production of IL-8 and IL-6 in A549 and CALU-3, respectively. Confirming previous data, we noted that mice challenged with silica particles, at 28 days, exhibited a significant increase in basal levels of lung resistance and elastance as well as airways hyper-reactivity to aerosolization with methacholine, as compared to controls. A marked inflammatory response, collagen deposition, and granuloma formation were detected in the lungs of silica-challenged mice, phenomena that paralleled with increased levels of thrombin and PAR1. **Conclusion:** Our findings show that silica and thrombin can produce inflammatory (IL-8) and profibrotic cytokines (IL-6) in epithelial cells. Intranasal silica induces a decrease in lung function and fibrosis in mice, phenomena associated with higher levels of thrombin and its active site PAR-1. Altogether, these data suggest that thrombin may be considered a potential target for fibrotic diseases, though additional experiments are needed to clarify the role of thrombin/PAR1 in silicosis. **Financial Support:** FIOCRUZ, FAPERJ, CNPq, CAPES, Brazil.

04.012 Anti-Inflammatory Potential of Gamma Terpinene in a Zymosan-Induced Arthritis

Model. Silva GHO, Amaral CF, Rocha EMT, Cuman RKN, Silva-Comar FMS UEM Lab. of Inflammation, Brazil

Introduction: Medicinal plants and their isolated compounds have been largely used in the pharmaceutical, cosmetic and food industries in reason of their various pharmacological and biological properties [1]. Gamma terpinene (GT), a monoterpene, is an important chemical constituent of the essential oils of many medicinal plants that show anti-inflammatory, antioxidant and antimicrobial activity. With respect specifically to the anti-inflammatory activity, GT was able edema and neutrophil migration reducing, possibly by modulation of the Prostaglandin-E2/Interleukin 10 (PGE2/IL-10) and inhibiting the cytokines pro-inflammatory production. [2,3,4]. The aim of this study was to evaluate the GT effect in the zymosan-induced arthritis experimental model. The experimental protocols were approved by the Ethical Committee in Animal Experimentation of the State University of Maringá (CEUA/UEM–No.7379190922). **Methods:** Joint inflammation was induced by an intra-articular injection of zymosan (200µg/cavity) in 10µL sterile saline. One hour before zymosan injection, the mice were orally treated with vehicle (Tween 80 – 2%) or GT at the doses of 25, 50, 75 or 100 mg/kg. Six hours later, the animals were euthanized by anesthetic overdose for measurement knee joint swelling and leukocytes count. Articular edema was evaluated by measurement of the diameters of the left joints using a digital caliper. **Results:** Rheumatoid arthritis is a musculoskeletal disorder that affects mainly the peripheral joints and it is associated with pain, reduced range of movement, tenderness and inflammation. In the zymosan-induced arthritis in mice the synovial tissue inflammation is marked by massive cellular recruitment, mainly of PMN cells, as neutrophils [5,6]. The pre-treatment with GT at doses 50, 75 and 100 mg/kg was able to inhibit the migration of leukocytes into the synovial cavity in 82.5%, 75.9% e 75%, respectively. In addition, GT, at the same doses, joint edema formation reduced (73.8%, 53.45% and 49.8%, respectively) at 6 hours after arthritis induction. **Conclusion:** This study showed that GT have potential anti-inflammatory effect by reduce leukocyte migration and knee edema. However, studies are needed to elucidate the mechanisms by which GT acts on inflammatory processes, which may contribute to the validation of this compound and help in the treatment of inflammatory diseases in the future. **References:** [1] Ramsey, JT. J Biol Med. v. 93, p. 291-305, 2020. [2] Giweli, A. Mol. v. 17, p. 5, 2012. [3] Hanafi, RS. Nat Prod J. v. 4, p. 1, 2014. [4] Ramalho, TR. Planta Med. v. 82, p. 15, 2016. [5] Rocha, FAC. Ver BrasReumatol. v. 43, n. 4, p. 206-17, 2003. [6] Harris, ED. New Eng J. v. 322, n. 18, p. 1277-1289, 1990. **Acknowledgments:** To CAPES and CNPq for the support and incentive to research.

04.013 Effects of Gamma Terpinene on the Inflammatory Response. Amaral CF¹, Silva GHO¹, da Rocha EMT², Cuman RKN³, Silva-Comar FMS³. ¹UEM, PPG in Health Sciences, Maringá, PR, Brazil; ²UEM, PPG Pharmaceutical Sciences, Maringá, PR, Brazil; ³DFT-UEM Dpt of Pharmacology and Therapeutics, Maringá, PR, Brazil

Introduction: The gamma-terpinene (GT) is a monoterpene found in the essential oil of several plants, such as: *Eucalyptus* genus, *Cuminum cuminum*, *Coriandrum sativum*, *Satureja thymbra*¹. This compound has been reported to present analgesic, antimicrobial and anti-inflammatory activity. This study investigated the effect of GT on the inflammatory response. Specifically, it was evaluated *in vitro* leukocyte chemotaxis, phagocytic activity and *in vivo* leukocyte migration. **Methods:** Chemotaxis *in vitro* was realized in Boyden chambers using leukocytes from the peritoneal cavity of mice with zymosan-induced peritonitis. The cells were incubated with GT at concentrations of 3, 10, 30 and 90 µg/mL for 30 min and fMLP was the chemotactic agent. The phagocytosis assay was performed with GT at the same concentrations. *In vivo* cell migration was performed by the intravital microscopy method and the tested GT doses were 25, 50, 75 and 100 mg/kg. The experimental protocols were approved by the Ethical Committee in Animal Experimentation of the State University of Maringá (CEUA/UEM - protocol number 8218160922). **Results:** The acute inflammation is a process characterized by a vascular response and initial recruitment of polymorphonuclear cells, typically neutrophil, and the migration and accumulation of neutrophils at the inflammation site are crucial for host defense. However, uncontrolled inflammation accompanied by the excessive migration of leukocytes has unfavorable effects on the course of tissue healing due to proteolytic enzymes release and reactive oxygen species production². In the process of chemotaxis, cells are attracted by the chemotactic gradient to the site of inflammation, performing their defense function. However, this response can have an unbalanced outcome, hence the importance of drugs that act at this stage of inflammation³. To verify the direct effect of GT on *in vitro* leukocyte chemotaxis, the study was performed using fMLP as chemotactic agent. It was observed that GT (30 and 90 µg/mL) inhibited the neutrophil (50% and 57%, respectively) in response to fMLP stimulation. The similar results was observed in the phagocytic assay, obtaining a result of 72% and 81% reduction. Mechanisms by which the GT decreases the leukocyte migration to the inflammatory site were investigated using intravital microscopy system. GT, at dose of 100 mg/kg, caused a significant reduction of leukocytes rolling (65%) and adherent leukocytes (55%). **Conclusion:** In conclusion, the results showed that GT presents anti-inflammatory activity as demonstrated by the inhibition in the leukocyte recruitment and decreased phagocytic activity. **Acknowledgments:** This study was financed in part by the Coordenação de Aperfeiçoamento de Pessoal de Nível Superior – Brasil (CAPES) - Finance Code 001. **References:** [1] Ramalho, T.R. *Planta Med*, 82 (15): 1341-5, 2016. [2] Ciepiela, O. *Respiratory Physiology and Neurobiology*, 1098-1102, 2015. [3] Ley, K. *Immunology*, 678–89, 2007.

04.014 Studies on the effects of ethanol on allergic lung inflammation. Bohrer GP¹, Oliveira MA¹, Moriya HT², Marianno P¹, Melhado IVS¹, Alves VF¹, Teixeira SA¹, Kiataki LGS¹, Ribeiro MR¹, Muscará MN¹, de Sá Lima L¹, Scavone C¹, Camarini, R¹, Tavares de Lima, W¹
¹ICB-USP, Dept. of Pharmacology, São Paulo, Brazil. ²USP, Dept. of Telecommunication and Control Engineering, São Paulo, Brazil

Introduction: Asthma is a chronic inflammatory disease of the airways in which the presence of mast cells, eosinophils and neutrophils among others is observed. Asthma induces damage to the bronchial epithelium, airway hyperreactivity and structural changes that lead to airway remodeling (BARNES PJ, 1989). Excessive consumption of ethanol is a public health problem and studies show that ethanol can aggravate the pulmonary inflammatory condition observed in pneumonia and acute respiratory distress syndrome (ARDS) (BARNES PJ, 1989; MARTORELL et al., 1993). Despite the above, the effects of ethanol consumption on the profile of the pulmonary allergic response, such as that triggered in asthma, are still not fully understood (PAWANKAR, 2013). **Methods:** Male Swiss mice (18 weeks) were submitted to two ethanol ingestion protocols for twenty-four days (30%, v/v, by gavage): 1) binge drinking type: the intake of high doses of ethanol (5g/kg) for three days followed by four days without ingestion, 2) chronic ingestion: the intake of 2.5 g/kg during twenty- four consecutive days. The control group received an equivalent volume of water. Four days after starting the protocols, the animals were ovalbumin (OVA) - sensitized (day 0, i.p) and OVA challenged (days 14, 21 and 28, i.n). On the twenty- ninth day, after the last challenge, the number of cells recovered in bronchoalveolar lavage (BAL), and respiratory mechanics (flexiVent) were evaluated. **Results:** Our data indicated that animals with allergic lung inflammation showed an increase in total cells compared to non-allergic animals (OVA-H₂O: $115.12 \pm 24.84^*$ versus PBS-H₂O: $19.00 \pm 1.22 \times 10^4$ cells/mL, n=8). The same occurred with the number of eosinophils (OVA-H₂O: $43.29 \pm 5.44^*$ versus PBS-H₂O: $0.01 \pm 0.01 \times 10^4$ cells/mL, n=8). Exposure to ethanol did not alter the total cell count in the BAL of allergic animals however, it increased the number of eosinophils (binge drinking: $58.73 \pm 3.86^*$, n=5; Chronic alcohol: $57.83 \pm 3, 26^*$, n=6 versus OVA - H₂O: $43.29 \pm 5.44 \times 10^4$ cells/mL, n=8). Allergic animals showed increased lung resistance (RL) compared to non-allergic animals when challenged with methacholine (OVA-H₂O: $1.70 \pm 0.58^*$, n=5 versus PBS-H₂O: 0.63 ± 0.06 cm H₂O. s/ml, n=4). When allergic animals received ethanol intermittently or chronically, there was a decrease in RL compared to the allergic group that was not exposed to ethanol (Binge drinking: $0.47 \pm 0.042^*$, n=5; Chronic alcohol: $0.67 \pm 0.08^*$, n=5 versus OVA-H₂O: 1.70 ± 0.58 cm H₂O.s/mL, n=5). *P<0.05. **Conclusion:** Ethanol exposure appears to worsen allergic lung inflammation due to the increased number of eosinophils in the BAL. On the other hand, it decreases airway hyperreactivity in allergic mice. Although preliminary, our data suggest the interference of ethanol in allergic lung inflammation as well as in airway hyperreactivity in an asthma model. **Financial support:** CNPq and Capes. **References:** 1 - BARNES, P. J. *The J of allergy and clinic immunol*, v. 83, p. 1013, 1989. 2 – MARTORELL et. al. *An Esp Pediatr*, v. 39, p. 116, 1993. 3 - PAWANKAR, R. *Braz J Allergy Immunol*, v. 1, p. 4., 2013.

04.015 Release of Neutrophil Extracellular Traps (NETs) Contributes to Silica-Induced Lung Fibrosis in Mice. Ferreira GC¹, Guimarães FV¹, Pires TC², Foguel D², Schneider A³, Cunha FQ³, Martins MA¹, Silva PMR¹. ¹IOC-FIOCRUZ, Lab. de Inflamação, ²IBBqM-UFRJ, ³FMRP-USP

Introduction: Activated neutrophils participate in innate immunity through several mechanisms, including the formation and release of neutrophil extracellular traps (NETs), structures playing a role in the host defense. Silicosis is an occupational lung disease triggered by silica particles, characterized by an inflammatory component associated with granulomatous fibrogenesis in the lung. In this study, we investigated the role of NETs in silica-induced pulmonary fibrosis in mice. **Methodology:** Murine neutrophils stimulated with silica particles (300 µg/mL) “in vitro” were evaluated for the release of NETs. Swiss Webster mice, in addition to C57/Bl-6 as wild type (PAD4-WT) and PAD4 gene knockout (PAD4-KO) mice were used. Animals were instilled with intranasal silica (10 mg), and both the initial (7 days) and late (28 days) phases were evaluated. Treatment with DNase I Pulmozyme® (40 µg/animal), intranasally, started 6 h after silica challenge and was maintained, daily, for 7 consecutive days with the analyzes being performed 1 day or 20 days after the last dose - initial and late phase, respectively (license L001/19-A2). **Results:** Murine neutrophils challenged with silica “in vitro”, showed an increase in extracellular DNA staining as compared to those incubated with medium (controls), an indicative of the release of NETs. Mice instilled with silica showed increased airway resistance and lung elastance, a response exacerbated after methacholine aerosolization. A marked leukocyte infiltration, mainly of neutrophils, and an increase in the lactate dehydrogenase (LDH) concentration were detected in the bronchoalveolar lavage, 7 days after silica challenge. At 28 days, the levels of myeloperoxidase (MPO) were increased in the lung of silicotic mice, an indicative of neutrophil influx. Lung fibrosis and granuloma formation were detected in silica-challenged mice, with maximal response being noted at 28 days. Treatment with Pulmozyme® reversed the decrease in lung function (resistance and elastance) and reduced neutrophil infiltration and granuloma formation in silicotic lungs. PAD4-KO mice, when instilled with silica, showed a similar profile of inflammation and fibrosis when compared to PAD4-WT mice. **Conclusion:** Our data show that silica promote neutrophil infiltration and release of NETs in the lungs of mice, in parallel to tissue fibrosis and granuloma formation. Treatment with DNase I Pulmozyme® improved lung function and reduced granuloma formation, suggesting the role of NETs in the development of fibrosis. PAD4 deficiency did not interfere with silica-induced lung fibrosis, indicating that NETs formation seems to be independent of PAD4 histone citrullination. As LDH levels are higher in silicotic mice, we may propose that NETs formation might be accounted for by neutrophil necroptosis triggered by silica particles. Altogether, our findings suggest that NET inhibition may represent a potential therapeutic target for silicosis. **Financial Support:** FIOCRUZ, FAPERJ, CNPq, CAPES (Brazil).

04.016 Effect of the Tyrosine Kinase Inhibitor Bosutinib on Sepsis-Induced Brain Dysfunction. Cunha CMCD^{1,2,3}, Moraes BPT^{1,2,3}, Abreu VHP^{1,2}, Soares GVM^{1,2}, Moraes-de-Souza IM^{1,2}, Almeida MAP^{1,2,3}, Estado V³, Sayão PGF^{1,2}, Souto HA^{1,2}, Bozza PT², Castro-Faria-Neto HC², Silva AR^{2,3}, Gonçalves-de-Albuquerque CF^{1,2,3} ¹Unirio, Immunopharmacology Lab, Dept of Physiological Sciences, Rio de Janeiro, Brazil, ²IOC-Fiocruz, Immunopharmacology Lab, Brazil, ³ UFF, PPG in Neurosciences, Niterói, Brazil

Introduction: Sepsis-associated brain dysfunction occurs in about 70% of septic patients and contributes to worse prognosis and mortality; its pathophysiology includes glial hyperactivation, impairment in blood perfusion, and vascular and neuronal damage (1,2). The Src-family kinases (SFK) is a family of protein kinases that regulates as chemotaxis, cell adhesion and migration, cytokine secretion, and endothelial permeability. SFK inhibition attenuates leukocyte and endothelial responses exacerbated in inflammatory reactions (3-6). Bosutinib is a multiple kinase inhibitor clinically used in treating chronic myeloid leukemia with a potent effect on SFK (7). Bosutinib may regulate sepsis's systemic and cerebral immune response. **Methods:** Swiss mice (25 - 30g) were divided into 4 groups: Sham + Bosutinib; Sham + Vehicle; cecal ligation and puncture (CLP) + Bosutinib and CLP + Vehicle. The CLP were subjected to a polymicrobial sepsis model, and sham had the cecum just exteriorized. The treatments were performed orally 30 min before and 6 h after surgery with bosutinib (3 mg/kg) or vehicle. 24 h after CLP, mice clinical signs were observed and represented as clinical score. The anesthetized animals were submitted to cardiac perfusion and had their brains collected for the quantification of TNF- α , IL-1 β , IL-6 and VEGF by enzyme-linked immunosorbent assay (ELISA), or to intravital microscopy and laser speckle, to evaluate cerebral leukocyte-endothelial adhesion, capillary density, cerebral blood perfusion. The number of animals per group ranges from 3 to 9 and the results come from two independent experiments. All experimental procedures were approved by the Ethics Committee on the Use of Animals of IOC (L015/2015) and of UNIRIO (2019/03). **Results and Conclusion:** Bosutinib improved sepsis survival and decreased severity after CLP, significantly reduced sepsis-induced levels of pro-inflammatory cytokines and VEGF. Leukocyte rolling and adhesion in septic mice increased, while the mice treated with bosutinib showed less leukocytes in rolling and adhesion when compared to untreated septic mice. Functional capillary density decreased in septic mice. Bosutinib treatment increased the number of perfused capillaries when compared to the untreated CLP group, reversing capillary rarefaction. These results show that bosutinib reduced brain damage caused by sepsis, immunomodulating neuroinflammation, and mitigating neurovascular changes. **Funding:** FAPERJ, UNIRIO, CAPES Grant 001, IOC, FIOCRUZ, PPGNeuro. **References:** 1. Gofton, TE. *Nat. Rev. Neurosci.*, v. 8, p. 557, 2012. 2. Catarina AV. *Mol Neurobiol.* V.58, p.2770, 2021 3. Lowell, CA. *Cold Spring Harb. Perspect. Biol.* v. 3, p. a002352, 2011. 4. Byeon, SE. *Mediators Inflamm.*, v. 2012, 2012. 5. Liu, G. *Arterioscler Thromb Vasc Biol*, v. 31, p. 1342, 2011. 6. Baruzzi, A. *Cell. Mol. Life Sci.*, v. 65, p. 2175, 2008. 7. Houry, H. *Blood*, v. 119, p. 3403, 2012.

04.017 The Specialized Pro-Resolving Mediator Maresin 2 Accelerates the Wound Healing Process in a Murine Model of Dorsal Skin Lesion. Pierotti SM, Semeão LO, Saraiva-Santos T, Zaninelli TH, Bertozzi MM, Ritter PD, Franciosi A, Ferraz CR, Ferrante LF and Casagrande R UEL, Londrina, PPG Health Sciences, Brazil

Introduction: Maresin 2 (MaR2) is one of the last described specialized pro-resolving lipid mediators (SPMs). Although it reduces phagocytosis of zymosan and neutrophil recruitment, it is not known whether these anti-inflammatory actions can be used to treat skin wounds. Unsuccessful healing of wounds is responsible for several complications and high mortality rates, and this aggravating factor increases in the case of pre-existing disease, infections, and nutritional deficiencies. The aim of this study was to analyze the effects and mechanisms of action of the SPM MaR2 on wound healing in a murine model of dorsal skin wounds. **Methods:** The experiments were performed in adult hairless mice (HRS/J), or in C57BL/6 background LysM e-GFP/+ mice. The animals were divided into groups (sham, control wound without treatment and wound treated with MaR2), each group with a total of 6-8 animals per experiment. The dorsal skin was pinched at midline and a 5 mm dermal biopsy punch (0.1963cm² total area) was used to create two full-thickness excisional skin wounds, symmetrically positioned in the dorsum of mice. Treatment started after wound induction using intraperitoneal treatment with MaR2 for 7 days. After that the lesioned skin was collected with 6 mm biopsy punch and processed for each of the analyses. Values are presented as the mean ± standard error of the mean (SEM) and statistical evaluation was performed with GraphPadPrism® software. Parametric 1-way ANOVA followed by Tukey's multiple comparison test was performed to compare differences between 3 or more groups, and or non-parametric Mann-Whitney test or Wilcoxon rank sum test was used for pair-wise comparisons of groups. A value of p <0.05 was considered statistically significant. Experimental procedures were approved by the Animal Welfare Board of Londrina State University (CEUA-UEL process #15654.2019.33). **Results:** Treatment with 100 pg/animal of MaR2 accelerated the healing process showing higher efficiency in lesion closure (152%), decreased inflammatory histopathological changes (30%), neutrophil recruitment (MPO [46%] and migration of LysM-eGFP positive cells [42%]), decreased levels of inflammatory cytokines (IL-1β [33%] and TNF-α [99%]) and mRNA expression of MMP-1 (72%), MMP-9 (97%) and TIMP-1 (76%). **Conclusion:** The results of our study suggest the lipid mediator MaR2 as a promising therapeutic approach to improve skin wound healing. **Financial Support:** This work is supported by grants from National Council for Scientific and Technological Development (CNPq, Brazil), Fundação Araucária (PRONEX grant and PBA grant). Soraia Mendes Pierotti acknowledges Master's Degree Scholarship from Coordination for the Improvement of Higher Education Personnel (CAPES, Brazil). **References:** CHATTERJEE, A. *PLoS ONE*, v. 9, n. 11, 2014. DENG, B. et al. *PloS one*, v. 9, n. 7, p. e102362, 2014. JADAPALLI, JK. *The FASEB Journal*, v. 32, n. 10, p. 5227, 2018. LANDÉN, NX. *Cellular and Molecular Life Sciences*, v. 73, n. 20, p. 3861–3885, 2016. LAWTON, S. *Nurs. Times*, v. 115, p. 30-33, 2019. MEDEIROS, AC. *Journal of surgical and clinical research*, v. 7, n. 2, p. 87-102, 2016. NORLING, LV. *The Journal of Immunology*, v. 186, n. 10, p. 5543–5547, 2011. POTEKAEV, NN. *Journal of Clinical Medicine*, v. 10, n. 24, p. 5947, 2021. REIS, MB. *PLoS ONE*, v. 12, n. 7, p. 1–15, 2017. SERHAN, CN. *Nature*, v. 510, n. 7503, p. 92–101, 2014. SIPKA, T. *Free Radical Biology and Medicine*, v. 192, p. 200–212, 2022. YU, C. *Molecular Immunology*, v. 146, p. 78-86, 2022.

04.018 PI3K γ Inhibition Drives Lymphocyte Polarization Towards a TH2 Phenotype AND Attenuates Irinotecan-induced Intestinal Mucositis. Cajado AG¹, Rangel GFPR¹, Choquenaira-Quispe C¹, Freitas GL¹, Maia IFVC¹, Silva RL¹, Da Silva FDM¹, Alencar NMN¹, Alves APNN¹, Hirsch E², Wong DVT¹, Lima-Junior RCP¹ ¹UFC, ²Università degli Studi di Torino, Italy

Introduction: Mucositis is a common side effect of irinotecan-based cancer treatment (IRI). The upregulation of inflammatory cytokines during mucositis drives the inflammatory response promoted by IRI. Phosphatidylinositol-3-kinase gamma (PI3K γ) is widely expressed in leukocytes and its inhibition has been considered a promising therapeutic strategy for controlling inflammatory and autoimmune disorders. We then analyzed whether PI3K γ inhibition alters the inflammatory cytokines profile in the model of IRI-induced intestinal mucositis. **Methods:** Male C57BL/6 mice (20-22g, n=6-9/group) received vehicle (1% DMSO, 10 ml/kg, p.o.), IRI (120 mg/kg, one injection/day/four days, i.p.) alone or combined with AS-605240 (a PI3K γ selective inhibitor, 10 mg/kg, p.o./six days). On day seven after the first dose of IRI, the severity of diarrhea was determined. After animals' euthanasia, ileum samples were obtained for analyzing inflammatory parameters, which included: gene expression of *Tgfb*, *Cxcl1*, *Il12b*, *Ifng*, *Il33* and *Il4*, IL-1 β and IL-6 cytokine levels. We counted goblet cells stained with Alcian's Blue and PAS. Additionally, villus/crypt ratio and histological scores were analyzed. We used One-way ANOVA or Kruskal-Wallis test followed by the Bonferroni or Dunn's post-test for statistical analysis, accepting a P<0.05. **Results:** IRI-associated intestinal injury was confirmed by the increased gene expression of *Tgfb* (65-fold), *Cxcl1* (10-fold), *Il12b* (4-fold), *Ifng* (5 fold), and *Il33* (53 fold). Notably, PI3K γ inhibition reduced the expression of *Tgfb* (47%) and *Cxcl1* (12%). *Il4* expression increased in the AS-605240+IRI group, while the expressions of *Il12b*, *Ifng*, and *Il33* remained unaltered vs. IRI. Remarkably, PI3K γ inhibition reduced IL-1 β (13 \pm 2.3) and IL-6 (23 \pm 3.1) levels vs. the IRI group (IL-1: 43 \pm 5.7 and IL-6: 58 \pm 8.4). This cytokine balance suggested the activation of a Th2 response profile, which is in agreement with the increased acidic (10.5 \pm 4.6 vs. 8.7 \pm 0.6) and neutral (14.3 \pm 0.6 vs. 8.3) goblet cells in the group treated with AS-605240. The anti-inflammatory response promoted by the PI3K γ inhibition attenuated the morphometric alterations (increased villus/crypt ratio vs. IRI), histopathological damage (AS-605240+IRI: 1[1-2]) vs. the IRI (2[1-2]), and diarrhea scores (PI3K γ inhibitor: 1[1-2] vs. IRI: 2[1-3]). **Conclusion:** PI3K γ inhibition attenuates intestinal damage in the irinotecan-induced mucositis model, probably by altering the inflammatory cytokine balance favouring a Th2 profile. **Financial Support:** CNPq, Capes, and Funcap.

04.019 SARS-CoV-2 Spike Glycoprotein Ectodomain Induces Gut Inflammation, Luminal Hydroelectrolyte Imbalance, and Impairs Mucosal Integrity in a Novel Murine Model. Nascimento RR¹, Aquino CC¹, Sousa JK^{1,4}, Cajado AG¹, Gadelha KKL¹, Rocha JA², Medeiros JVR², Magalhães PJC¹, Gois BM³, Wong DVT¹, Lima-Junior RCP¹, Lima AAM¹, Engevik AC⁵, Nicolau LAD², Vale ML¹ ¹UFC, Dpt of Physiology and Pharmacology, Fortaleza, Brazil, ²UFDP, Biotechnology and Biodiversity Center Research, Parnaíba, Brazil, ³UFR, Faculty of Health Sciences, Rondonópolis, Brazil; ⁴University of Virginia School of Medicine, Division of Infectious Diseases & International Health, Charlottesville, USA; ⁵Medical University of South Carolina, Dpt of Regenerative Medicine and Cell Biology, Charleston, USA.

Introduction: SARS-CoV-2 is the virus responsible for Coronavirus Disease 2019 (COVID-19). In addition to the classic respiratory symptoms, studies have reported the incidence of gastrointestinal (GI) symptoms, including nausea/vomiting, abdominal pain, and diarrhea. However, limited experimental models exist to understand the pathophysiology of COVID-19 in the GI tract. Thus, the inoculation of SARS-CoV-2 Spike glycoprotein ectodomain (Spike) into intestinal loops would serve as an experimental tool to study this pathobiology in the GI tract. **Methods:** For this, male C57BL/6 mice (n=6) (20 to 25g; CEUA-NPDM/UFC n°07070322-0) were used. After anaesthesia, Spike (5µg/loop) or PBS (control; C) was inoculated into intestinal loops. After 4 hours, the mice were euthanized, and the loops were collected and weighed. Intestinal fluid was collected for chloride measurement. Gut samples were processed for myeloperoxidase (MPO) activity, histomorphometric analysis, immunohistochemistry (Paneth cells and Muc2+), gene expression (Il6, Il10, Tlr2, Tlr4, Cldn, Ocln, and Tjp1 targets), Western Blotting (IL-1β, IL-6, TNF-α, claudin, and occludin), and contractility. **Results:** Inoculation of Spike into intestinal loops increased wet weight (Spike: 109.20 ± 8.62 vs. C: 68.67 ± 4.21 mg/cm), MPO (Spike: 14.59 ± 1.50 vs. C: 4.44 ± 0.28 U/mg tissue), and chloride secretion in intestinal fluid (Spike: 0.075 ± 0.006 vs. C: 0.043 ± 0.001 mEq/L). Histological analysis demonstrated that Spike increased inflammatory infiltrate, epithelial changes, and destruction of mucosal histoarchitecture (Spike: 6.25 ± 0.12 vs. C: 3.36 ± 0.12), decreased Paneth cells (Spike: 20.3% vs. C: 30.8% Paneth/crypt), and muc2+ production (Spike: 0.041 ± 0.002 vs. C: 0.059 ± 0.004 pixels). Spike significantly increased Il6 (294-fold higher compared to C), Il10 (4-fold higher compared to C), Tlr2 (4-fold higher compared to C), and Tlr4 (3-fold higher compared to C) gene expression, as well as protein expression of IL-1β (Spike: 1.25 ± 0.07 vs. C: 0.70 ± 0.06 kDa), IL-6 (Spike: 2.10 ± 0.11 vs. C: 1.63 ± 0.07 kDa), and TNF-α (Spike: 1.09 ± 0.09 vs. C: 0.83 ± 0.02 kDa). Additionally, Spike increase of Cldn (5-fold higher compared to C), while decrease Ocln (Spike: 0.58 ± 0.12 vs. C: 1.13 ± 0.25) and Tjp1 (Spike: 0.57 ± 0.10 vs. C: 1.05 ± 0.11) gene expression. Protein expression of claudin (Spike: 1.06 ± 0.06 vs. C: 1.30 ± 0.06 kDa) and occludin (Spike: 4.93 ± 0.32 vs. C: 12.08 ± 1.60 kDa) was also decreased by Spike. Finally, electromechanical contractile effects were reduced in the Spike group (Spike: 0.12 ± 0.02 vs. C: 0.21 ± 0.45g). **Conclusion:** The Spike promoted changes in the gut mucosa, characterized by: 1) Secretory effect in the intestinal lumen, 2) Exacerbated inflammatory response, 3) Histological alterations, and 4) Impairment of intestinal integrity. **Financial Support:** CAPES, CNPq, and FUNCAP.

04.020 Anti-inflammatory and Antinociceptive Effects of *Dipteryx alata* Leaves. Santos JM¹, Souza MF¹, Santos SM¹, Oliveira-Junior PC², Brait DRH¹, Narcizo LL³, Rhoden S³, Silva ME¹, Marangoni JA¹, Borges JT¹, Passos BP³, Trichez VDK¹, Formagio ASN¹. ¹UFGD, PPG Health Sciences, Dourados, Brazil, ²UFGD, PPG Biotechnology and Biodiversity, Dourados, Brazil, ³UFGD, PPG Biological and Environmental Sciences, Dourados, Brazil

Introduction: *Dipteryx alata* (Fabaceae) is a tree species found in Latin American countries, known as “baru” (Carvalho et al, 2023). *D. alata* leaves are used in folk medicine for the treatment of inflammation and pain (Ribeiro et al, 2017), however, without scientific evidence. In this sense, we aimed to evaluate the anti-inflammatory and anti-hyperalgesic potential of the aqueous extract of *D. alata*. **Methods:** Leaves were collected in Dourados/MS, Brazil. A specimen was deposited in the herbarium of the UFGD (n° 7619). Plant material was washed, dried, and pulverized in a knife mill. Leaves powder was infused in distilled water at 80 °C (1: 10, w: v) for 15 minutes, filtered, and lyophilized to obtain the aqueous extract of *D. alata* leaves (AE-DA, 17.0% yield). The study protocol was approved by the UFGD Ethics Commission on Animal Use (n° 14/2021). Swiss mice (50 days old, 30-35 g) were obtained from Bioterio Central-UFGD and kept under a 12-hour light/dark cycle, humidity 50 ± 5%, 22 ± 2 °C, and provided water and food ad libitum. For the carrageenan-induced pleurisy assay, thirty animals were housed (n=6) and orally treated with vehicle (water), AE-DA at doses of 3, 30, or 100 mg/kg, or dexamethasone (1 mg/kg). After 1 hour, pleurisy was induced with 1% carrageenan (100 µL, intrapleural), as described by Vinegar et al (1973). For the assay of CFA-induced edema and hyperalgesia, animals were housed (n=5/group) and orally treated with vehicle (water), AE-DA at doses of 30 or 100 mg/kg, or prednisolone (3 mg/kg). After 1 hour, the animals received an intraplantar injection of 30 µL Complete Freund’s Adjuvant - CFA (oil suspension containing inactive *M. tuberculosis*) in the right paw. In the other hind paw, 30 µL saline solution of 0.9% was injected for control. After 3 and 4 hours of CFA injection, edema was measured with a paw plethysmometer (PANLAB Harvard), and mechanical hyperalgesia was determined by the Von Frey test (Insight®, EFF 301, digital analgesimeter) (Santos et al, 2021). Data are expressed as the mean ± standard error of the mean. Differences (P<0.05) among groups were evaluated by one-way ANOVA followed by the Tukey test. **Results:** animals treated with AE-DA at doses of 3, 30, and 100 mg/kg showed a significant reduction in leukocyte migration of 10.53, 40.18, and 85.17%, respectively. Dexamethasone, in turn, showed 92% inhibition of leukocyte migration. The oral administration of AE-DA at doses of 30 and 100 mg/kg showed a decrease in the edema formation of 35.3 and 58.5% (3 hours) and 33.3 and 55.5% (4 hours), respectively. Prednisolone reduced edema by about 88%, at 3 and 4 hours after CFA injection. Additionally, animals treated with AE-DA showed significant anti-hyperalgesic effect, with reductions of 71.4 and 76.2% (30 mg/kg) and 78.6 and 82.1% (100 mg/kg), respectively, at 3 and 4 hours after CFA injection. While, prednisolone inhibited mechanical hyperalgesia in 83.4 and 86.1%, respectively, at 3 and 4 hours after CFA injection. **Conclusion:** *Dipteryx alata* leaves have anti-inflammatory and anti-hyperalgesic properties in the acute phase, confirming their traditional use in the treatment of pain and inflammatory conditions. **References:** Carvalho, CS. Jd. Bot. RJ [Online, Flora do Brasil], pág 1, 2023. Ribeiro RV. J Ethnopharmacol., v. 205, pág 69, 2017. Santos, E. J. Ethnopharmacol., v. 278, pág. 114308, 2021. Vinegar, JF. Exp. Biol. Med., v. 143, pág. 711, 1973.

04.021 **Effect of β -myrcene Treatment on Leukocyte Activity *in vitro* and *in vivo*** da Rocha EMT¹, Amaral CF¹, Silva GHO¹, Silva IVM¹, Batistela VR¹, Silva-Comar¹, Cuman RKN¹ UEM

Introduction: β -Myrcene (MYR) is an abundant monoterpene that occurs as a major constituent in many plant species, being a popular flavoring and flavoring agent (food additive) used in the manufacture of foods and beverages. The main reported biological properties of β -myrcene are anxiolytic, antioxidant, anti-aging, anti-inflammatory and analgesic properties. The inflammatory response is activated against some tissue injury or infectious process, where a systemic infectious process can cause an inflammatory response [1]. **Methods:** *In vitro* chemotaxis was performed in Boyden chambers using leukocytes from the peritoneal cavity of mice with zymosan-induced peritonitis. Cells were incubated with MYR at concentrations of 3, 10, 30 and 90 μ g/mL for 30 minutes and fMLP was used as a chemotactic agent. Polymicrobial infection was induced using the cecal ligation and puncture (CLP) method [2]. To evaluate the effect of MYR on the *in vivo* inflammatory response, male mice of the C57BL/6 strain were used in an experimental sepsis model of cecal ligation and perforation CLP. Six hours after induction of sepsis, the peritoneal cavity was washed with sterile saline and an aliquot of the wash was diluted in Turk's liquid for total leukocyte count. Later slides were prepared with the peritoneal lavage and fixed to perform the differential count. For the *in vivo* tests, the animals (n=6-8) were pre-treated with MYR at doses of 50, 100 and 200 mg/kg, orally. **Results:** MYR treatment decreased leukocyte migration *in vitro* (3 mg/ml: 3%; 10 mg/ml: 28%; 30 mg/ml: 62%; 90 mg/ml: 73%). The volume of inflammatory exudate in the peritoneal cavity was increased in all experimental groups when compared to the SHAM group (Sham: 0.49 \pm 0.02 mL; CLP: 0.99 \pm 0.05 mL; MYR 50 mg/kg: 0.90 \pm 0.08; MYR 100 mg/kg: 0.91 \pm 0.05; MYR 200 mg/kg: 0.84 \pm 0.05, *P<0.05). The results indicated a significant increase of 451% (P<0.05) in the number of leukocytes recruited to the peritoneal cavity in the CLP group of animals (CLP: 10.371* \pm 2.599 cells/mm³, *P<0.05) compared to the SHAM (1.881 \pm 285 cells/mm³), due to an increase (46%) in polymorphonuclear cells. Treatment with MYR at doses of 100 and 200 mg/kg promoted a reduction in the total number of leukocytes (46% and 45%) in relation to the CLP group (5.619 \pm 1.204 and 5.665 \pm 811, respectively, #P<0.05). Treatment with MYR at a dose of 50 mg/kg (4%; 9.910 \pm 1276, #P<0.05) did not reduce the number of migrated cells. **Conclusions:** The results obtained indicate that MYR has an effect in reducing the number of migrated cells in the systemic inflammatory response, evaluated in sepsis (CLP model). **Reference:** [1] Cavalcante, H. A. *Inflammation*, 43, 193-203, 2020. [2] Rittirsch, D. *Nature Protocols*, v. 4, n. 1, p. 31–36, 2008. **Acknowledgments:** Capes, CNPQ.

04.022 **Methyl Gallate Effect on Chikungunya Arthritis in Mice.** Oliveira TAL¹, Correa LB¹, Pereira LM¹, Nunes PCG², Azeredo EL², Rosas EC¹. ¹Fiocruz-Farmanguinhos, Lab. of Applied Pharmacology. Institute of Drug Technology, Brazil; ²IOC-Fiocruz, Lab. of Viral Immunology, Brazil

Introduction: Chikungunya virus (CHIKV) infection induces a disease called Chikungunya, which is commonly associated with joint pain. At present, no specific therapy is available for CHIKV infection. Methyl gallate (MG), is a phenolic compound found in some medicinal plants, and it has been recognized for its anti-inflammatory and antioxidant properties in previous studies. In fact, MG reduced the inflammation in the knee joint inhibiting the leukocyte infiltration and the production of pro-inflammatory cytokines as well as chemokines. The objective of this study was to assess the effect of MG in the CHIKV infection *in vitro* and *in vivo*. **Methodology:** Vero cells were previously treated with different concentrations of MG (10-100 μ M) and after 24- and 48 hours cell viability was evaluated by MTT. Following this, CHIKV-infected Vero cells were pre-treated with MG (100 μ M), and a reverse transcription-polymerase chain reaction (RT-PCR) was performed to analyze the viral infection. To assess the action of MG on joint inflammation induced by CHIKV, kinetics from 0 to 9 days were studied, where on day 0, CHIKV was inoculated subcutaneously in the ventral side of the foot with 10^5 p.f.u. of CHIKV diluted in PBS to a volume of 20 μ l in C57BL/6 mice. Mock-infected mice were inoculated with PBS alone. In the kinetics study the animals were submitted to euthanasia at different times to evaluate paw edema, cells count from blood and lymph nodes, cytokines quantification and the inflamed paws were removed for further analysis. **Results:** Our results showed that MG not reduced cell viability at a concentration of 100 μ M and did not alter the infection of Vero cells *in vitro*. The study of kinetics in C57BL/6 mice showed an increase in paw diameter from 6 h on, reaching its peak on the seventh day after CHIKV inoculation. An increase in inguinal lymph node cells was observed, which was maximum on the fifth day after infection in mice that received CHIKV compared to Mock. Mice treatment with MG (10 mg/kg/animal) showed a reduction in inguinal lymph node cells. Regarding the quantification of CXCL-1/KC and IL1 β in the inguinal lymph nodes, there was no significant difference. **Conclusion:** Our results suggest that paw injection of CHIKV in mice induced an inflammatory reaction that was reduced after pretreatment with methyl gallate.

04.023 Supression by Gold Nanoparticles (AuNPs) of Lung Fibrosis Target by Bleomycin in Mice. Ferreira, GG; Guimarães, FV1; Fernandes, AJM; Pires, ALA; Arantes, ACS; Janinni-Sá, YAP; Martins, MA; Silva, PMR. IOC-Fiocruz, Laboratory of Inflammation. RJ, Brazil

Introduction: Idiopathic pulmonary fibrosis (IPF) is a chronic and progressive disease, characterized by infiltration of inflammatory cells, hyperplasia of alveolar epithelial cells, recruitment of fibroblasts and subsequent fibrosis, representing a challenge for health services due to the lack of effective therapy. Gold nanoparticles (AuNPs) show anti-inflammatory properties, being a good therapeutic option for lung disorders. IN this study we investigated the effect of therapeutic administration of AuNPs on lung inflammation and fibrosis induced by bleomycin in mice. **Methods:** Anesthetized female C57/BL6 mice were challenged by oropharyngeal aspiration with a single dose of bleomycin (0.06 U/40 μ L sterile 0.9% saline/animal). Control animals received the same volume of sterile saline. AuNPs (0.05 - 1.5 μ g/mL) were aerosolized every two days, from day 14 to 20 post-bleomycin, and the analyzes performed 1 day after the last administration. The following parameters were analyzed: i) lung function and airway hyper-reactivity by invasive whole-body plethysmography; ii) leukocyte infiltration in the bronchoalveolar lavage (BAL); iii) morphological analysis by standard histological techniques (H&E and Masson's trichrome staining); iv) quantification of fibrosis by Ashcroft scale and collagen by Sircol and western blot; v) oxidative stress markers by biochemical analysis; and vi) quantification of cytokines and chemokines by ELISA. All experimental procedures were approved by the Committee on Use of Laboratory Animals of Oswaldo Cruz Foundation (license L001/19-A2). **Results:** We showed that mice challenged with bleomycin exhibited an increase in the airways resistance and lung elastance, as well as hyperreactivity to methacholine aerosolization. In parallel, an increase in the leukocyte infiltration was noted in the BAL of bleomycin-challenged mice, mainly of polymorphonuclear neutrophils. Consistent with the morphological assessment, the modified Aschcroft score was significantly increased in lung tissue of bleomycin-challenged mice. Collagen content quantified by Sircol confirmed the induction of lung fibrosis by bleomycin, with type I collagen predominating as compared to the type III. Increased production of reactive oxygen species (ROS), decreased activity of antioxidant enzymes (SOD and CAT) and increased levels of malondialdehyde (MDA) together with higher levels of the transcription factor NRF2 were detected after bleomycin challenge. In addition, increased levels of cytokines (IL-6, IL-1 β e TGF- β) and chemokines (KC, MCP-1 and MIP-1 α) were shown in the fibrotic lungs. The therapeutic administration of AuNPs restored respiratory function and attenuated the pulmonary fibrosis condition by reducing the levels of type I collagen. We also observed a decrease in the production of cytokines and chemokines, recovery of the activity of the antioxidant enzyme CAT, reduction of MDA levels and increase of the NRF2 transcription factor. **Conclusion:** Our findings show that treatment with AuNPs reduced inflammatory and fibrogenic components in the lung of mice challenged with bleomycin, suggesting that AuNPs seem to constitute a promising therapeutic approach for application in fibrotic lung diseases such as IPF. **Financial Support:** FIOCRUZ, FAPERJ, CNPq, CAPES (Brazil).

04.024 Role of Glucocorticoid-Induced Leucine Zipper in a Pre-Clinical Model of Pneumonia caused by *Pseudomonas aeruginosa*. Carvalho AFS¹, Cardoso C², Lara ES¹, Augusto IL³, Caixeta RS³, Zaidan I^{2,7}, Montuori-Andrade ACM^{2,8}, Lima EBS¹, Carneiro FS¹, Monteiro AHA², Queiroz-Junior CM⁴, Russo RC⁵, Bruscoli S⁹, Teixeira MM⁶, Sousa LP^{1,2,3}. ¹UFMG Belo Horizonte, PPG Clinical and Toxicological Analysis, Brazil, ²UFMG Belo Horizonte, PPG Pharmaceutical Sciences, Brazil, ³UFMG Belo Horizonte, Dpt of Clinical and Toxicological Analysis, Brazil, ⁴UFMG Belo Horizonte, Dpt of Morphology, Brazil, ⁵UFMG Belo Horizonte, Dpt of Physiology and Biophysics, Brazil, ⁶UFMG Belo Horizonte, Dpt of Biochemistry and Immunology, Brazil, ⁷USP Ribeirão Preto, Dpt of Cellular and Molecular Biology, Brazil, ⁸USP Ribeirão Preto, Dpt of Immunology, Brazil, ⁹University of Perugia, Dpt of Medicine and Surgery, Italy.

Introduction: *Pseudomonas aeruginosa* is one of the main causatives agent of ventilator-associated pneumonia (VAP) promoting a significant increase in morbimortality and longer stay in the intensive care unit. The inflammatory response is essential to ensure bacterial clearance, but need to be spatially and timely regulated in order to prevent tissue damage. Emerging studies have highlighted the role of the pro-resolving mediator glucocorticoid-induced leucine zipper (GILZ) on modulating host responses to ensure pathogen control and prevent tissue damage during infections. Here, we have evaluated the role of GILZ during pneumonia caused by *P. aeruginosa*. **Methods:** C57BL/6 wild-type or GILZ deficient mice (GILZ^{-/-}) were anesthetized with ketamine/xylazine (80 mg/kg and 10 mg/kg, respectively) and acute lung injury (ALI) was induced by intranasal instillation of 10⁶ CFU of *P. aeruginosa* (strain PAO1). Control mice received saline (mock infection). Kinetics of the infection were carried out at five different time points to harvest bronchoalveolar lavage (BAL), blood and lung samples to analyze inflammatory parameters, bacterial load and tissue damage. In a therapeutic protocol, PAO1-infected mice were treated with a cell-permeable GILZ fusion protein - TAT-GILZ (0.2 mg/kg, i.p.), empty TAT (0.1 mg/kg, i.p.) or vehicle (DMSO 0.6% at 12 and 24 hours post infection (hpi). Samples were harvest 48 hpi, in order to evaluation of the same parameters. **Results:** GILZ^{-/-} mice show more severe ALI, characterized by higher neutrophilic infiltration and lower monocytes/macrophage in the airways, accompanied by defective efferocytosis, delayed bacterial clearance, and pronounced lung damage as compared to WT-littermates. Administration of TAT-GILZ to PAO1-infected mice increased macrophages numbers in the airways associated to increased efferocytosis and reduced lung damage. Noteworthy, TAT-GILZ improved the lung function during pneumonia compared to the vehicle and TAT groups. **Conclusion:** Herein, we present role of endogenous GILZ for control inflammatory response, bacterial dissemination and tissue damage. Conversely, exogenous TAT-GILZ administration reduced inflammation, and lung damage/dysfunction during pneumonia induced by *P. aeruginosa*. Further studies applying different therapeutical protocol and association with antibiotics are still needed to identify the mechanisms by which TAT-GILZ exerts its functions in this infectious context. **Financial Support:** National Institute of Science and Technology in Dengue and host-microbial interactions, a programme grant (465425/2014-3) from FAPEMIG, APQ-03221-18; CAPES, 23038.003950/2020-16; and CNPq, PQ-306789/2018/3.

04.025 **Effect of Diabetes on the Neutrophil Release from the Bone Marrow.** Pacheco, FS¹, Chaves, AS¹, Insuela, DBR¹, Souza, LM¹, Brasiel, PGA¹, Silva, PMR¹, Martins, MA¹, Neto, HCF², Carvalho, VF¹. ¹IOC-Fiocruz, Lab. of Inflammation, ²IOC-Fiocruz, Immunopharmacology Lab., Rio de Janeiro, Brazil

Introduction: It is well known that bone marrow function is deficient in diabetes and that diabetic animals and patients present blood neutrophilia[1]. However, the mechanisms involved with neutrophil release from the bone marrow in diabetes is elusive. During neutrophil release from bone marrow, there is an overexpression of CXCR-2 in neutrophils surface in association with an increase in its ligands, including CXCL-1/KC and CXCL-2/MIP-2 [2,3]. Our objective was to evaluate the impact of diabetes on the neutrophil release from the bone marrow. **Methods:** Diabetes was induced by a single injection of alloxan (65 mg/kg, i.v.) in fasted male *Swiss-Webster* mice, and the analysis were performed after 21 days. We evaluated CXCR-2 expression on neutrophil surface and the levels of CXCL1/KC and CXCL2/MIP-2 in the bone marrow using flow cytometry and ELISA, respectively. **Results:** Diabetes-induced an increase in the number of mature neutrophils in bone marrow in parallel to blood neutrophilia compared to non-diabetic mice. We analyze showed a reduction in the CXCR-2 expression in bone marrow neutrophil surface from diabetic mice compared to non-diabetic mice. Nevertheless, we did not observe changes in the CXCL1/KC and CXCL2/MIP-2 levels in the bone marrow of diabetic mice compared to non-diabetic mice. **Conclusion:** These results indicate a failure in the neutrophil release from bone marrow of diabetic mice. **Financial Support:** CNPq, Capes, Faperj, Fiocruz, and Jica CEUA: L-027/2016 e L001/2019 **References:** 1. Rankin, SM. *J Leukoc Biol.*, v. 88, p. 2, 2010. 2. Wengner AM, Pitchford SC, Furze RC, Rankin SM. *Blood.*, v.111, p.1, 2008. 3. Loius M, Fukda S. *Experimental Hematology.*, v.34, p. 8, 2015.

04.026 Development and Evaluation of the Antimalarial Activity of Lipid Core Nanocapsules (LNC) Containing Lumefantrine and Artemether in Experimental Cerebral Malaria Model. Moraes, BPT^{1,2,3}, Silva, KP⁴, Rodrigues, SO^{2,3}, Moraes-de-Souza, I^{2,3}, Almeida, MAP^{1,3}, Estado, V³, Bozza, PT³, Castro-Faria-Neto, HC³, Ferrarini, SR⁴, Silva, AR^{1,3}, Gonçalves-de-Albuquerque, CF² ¹UFF, PPG in Neuroscience, ²UFRJ, Immunopharmacology Lab., Rio de Janeiro, Brazil, ³IOC-Fiocruz, Immunopharmacology Lab., Rio de Janeiro, Brazil ⁴UFMT, PPG in Health Sciences, Sinop, Brazil

Introduction: Cerebral malaria (CM) is the most aggressive complication caused by *Plasmodium falciparum*, with a mortality rate of 20% of CM cases. Patients are currently treated using artemisinin combination therapy. Artemether-lumefantrin (AL) is one of the first-line recommendations of WHO. However, the increase in drug resistance is the major treatment obstacle. Thus, new therapeutic strategies for antimalarial drugs to reduce resistance and increase therapeutic efficiency are needed. Nanosystems have advantages in developing new pharmaceutical formulations, including reduced toxicity and administered dose, increased bioavailability, and controlled drug release. We used an experimental CM (ECM) model to assess the antimalarial effects of LNCs containing AL. **Methods:** Drug-free (LNC_{BL}) and drug-containing (LNC_{AL}) suspensions of LNCs were developed by interfacial deposition of the preformed polymer and characterized for their average nanoparticle diameter by photon correlation spectroscopy analysis. Laser diffraction was used to confirm the equivalent sphere diameter (d_{4.3}) means and particle size distribution (Span). For the ECM model, C57Bl/6 mice were inoculated with 10⁵ *Plasmodium berghei* ANKA infected red blood cells (iRBC) i.p. Mice were treated by gavage with LNC_{BL} and LNC_{AL}, AL on its free form, EtOH or Chloroquine (CQN) on 5-7 days post-infection (dpi). We evaluated the antimalarial effects of LNC_{AL} compared to AL in survival, parasitemia, and clinical score on 5-7 dpi. To assess the inflammatory status of the brain, the cytokines were quantified through ELISA. Intravital image microscopy of the brain was performed to evaluate the leukocyte rolling and adhesion. This project was approved by the Ethics in Animal Research Committee/IOC (L-022/2020). **Results:** To investigate the effects of the LNC_{AL} in an ECM model, we treated animals on 5-7 dpi. Mice treated with LNC_{AL} survived 100%, a higher effect than the CQN and AL groups. Parasitemia and clinical score were accessed in 5-14 dpi. LNC_{AL} completely abolished parasitemia by 10 dpi and decreased clinical scores. During CM hepatosplenomegaly is a common feature due its close relation to developing the immune response and eliminating iRBCs. LNC_{AL} treatment positively correlated with the spleen/liver/body weight index. CM hallmarks are acute systemic inflammation and secretion of cytokines and chemokines and sequestrated iRBC in the brain microvasculature. Levels of inflammatory markers IL-6, TNF- α , IL-1 β , KC, and MCP1 were reduced by LNC_{AL} treatment. Intravital microscopy revealed that LNC_{AL} reduced leukocyte rolling and adhesion even compared with AL. **Conclusion:** LNC_{AL} was successfully developed and characterized and showed better results than the AL in measured parameters in ECM. Funding: FAPERJ, UNIRIO, CAPES, IOC, FIOCRUZ.

04.027 Annexin A1/FPR-2 Axis promotes Resolution of Inflammation during Experimental Bacterial Pneumonia. Lara ES¹, Carvalho AFS¹, Cardoso C², Zaidan I^{2,7}, Grossi L², Carneiro FS¹, Caixeta RS³, Augusto IL³, Montouri-Andrade ACM^{2,8}, Queiroz-Junior CM⁴, Russo RC⁵, Costa VV⁶, Teixeira MM⁶, Tavares LP⁹, Sousa LP^{1,2,3} ¹UFMG, PPG Clinical and Toxicological Analysis, Belo Horizonte, Brazil, ²UFMG, PPG Pharmaceutical Sciences, Belo Horizonte, Brazil, ³UFMG, Dpt of Clinical and Toxicological Analysis, Belo Horizonte, Brazil, ⁴UFMG, Dpt of Morphology, Belo Horizonte, Brazil, ⁵UFMG, Dpt of Physiology and Biophysics, Belo Horizonte, Brazil, ⁶UFMG, Dpt of Biochemistry and Immunology, Belo Horizonte, Brazil, ⁷USP, Dpt of Cellular and Molecular Biology, Ribeirão Preto, Brazil, ⁸USP, Dpt of Immunology, Ribeirão Preto, Brazil, ⁹Harvard University, Dpt of Medicine, Massachusetts, USA

Multidrug-resistant Gram-negative bacteria are the main causes of pneumonia in the nosocomial environment. The inflammation of the airways and lung parenchyma triggered during pneumonia is necessary for bacterial clearance, but must be spatially and temporally regulated to prevent further tissue damage and bacterial dissemination. We have shown that activation of the pro-resolving axis mediated by Annexin A1 (AnxA1) and its FPR (Formyl Peptide Receptor)-2 receptor control the inflammatory response and bacterial dissemination during pneumococcal pneumonia. Herein, we have evaluated the role of the AnxA1/FPR-2 axis in the inflammatory response caused by pneumonia induced by the Gram-negative bacteria *Escherichia coli*. For that, AnxA1 or FPR-2/3 knockout (KO) mice and wild-type (WT) controls were intranasally infected with 3×10^6 CFU of *E. coli* (ATCC25922) and euthanized 24 hours post infection (hpi) for evaluation of inflammatory parameters and lung bacterial load. In separate experiments, WT animals infected with *E. coli* were treated 8 hpi with the AnxA1 peptidomimetic Ac₂₋₂₆ and euthanized 24 hpi for evaluation of the same parameters. All procedures were approved by the Ethics Committee of the Universidade Federal de Minas Gerais (CEUA, protocol number: 262/2018). We show that AnxA1 and FPR-2/3 KO mice exhibited exacerbated neutrophilic inflammation, higher bacterial dissemination, decreased apoptosis/efferocytosis counts in airways, accompanied of intense lung damage and dysfunction compared to WT mice. In addition, FPR-2/3 KO mice exhibited higher lethality rates to *E. coli*-induced pneumonia compared to WT mice. Interestingly, administration of Ac₂₋₂₆ at the peak of *E. coli*-induced pneumonia decreased neutrophilic inflammation, increased apoptosis/efferocytosis counts alongside improvement of bacterial clearance in the airways and lungs, an effect also associated with increased numbers of macrophages in Ac₂₋₂₆ treated animals. In summary, the engagement of the AnxA1/FPR-2 axis is an important mechanism for resolution of lung inflammation and bacterial clearance during pneumonia caused by *E. coli*. The AnxA1 peptidomimetic Ac₂₋₂₆ was effective in this infectious model and can constitute a new adjunctive therapeutic strategy for the treatment of infectious lung diseases.

04.028 Topical Anti-inflammatory Activity of Gel Based on *Momordica charantia* L. in a Model of Monoarthritis Induced by Complete Freund's Adjuvant. Moreira FAS¹, Silva ACA¹, Pinheiro S¹ Santos BLB¹, Sousa Neto BP¹, Rufino ADD¹, Almeida FRC¹, Cornélio ML², Sousa MC¹, Oliveira FA¹ ¹UFPI, Medicinal Plants Research Center, Teresina, Brazil. ²UFPB, Lab. of Cosmetic Technology, Dept of Chemical Engineering, Brazil

Introduction: Rheumatoid arthritis is characterized as a systemic autoimmune inflammatory disease that affects the synovial membrane of the joints. The usual pharmacological treatment consists of the use of non-steroidal anti-inflammatory drugs, glucocorticoids and disease-modifying anti-rheumatic drugs. However, these drugs have several adverse effects, such as gastric irritation, immunosuppressive activity, ulcer formation and reduced glomerular filtration rate. To this end, topical formulations were developed, which offer advantages such as safety and a lower risk of drug interactions. With the need for new therapeutic options, formulations based on medicinal plants have been studied. Among the variety of medicinal plants with biological actions, *Momordica charantia* L. is mentioned, which is associated with several activities, including antiviral, antitumor, anti-HIV and antioxidante. An *in vitro* study carried out with macrophages (RAW 264.7 treated with LPS) of the methanolic extract of *M. charantia* L. concluded that the triterpenoids momordicin I and TCD exert anti-inflammatory activity through the modulation of the synthesis of Nitric Oxide, inhibition of the activity of TNF- α , IL-6 and IKK/NF κ B signaling pathway. Carrying actives in formulations for topical use is advantageous, as it allows local action, avoids the first-pass effect, is easy to apply and has greater adherence to treatment. In the present work, the anti-inflammatory potential of a gel formulation based on the glycolic extract of *Momordica charantia* L. (Gel MCH) was investigated in rats by topical route (v.t.). **Methods:** Initially, the animals were divided into four groups of 8 animals each (N=8) and then sensitized with 50 μ of Complete Freund's Adjuvant (CFA, *Mycobacterium tuberculosis* 1mg/ml) at the base of the tail. Twenty-one days after sensitization, the animals received a dose of 50 μ of CFA in the tibiotarsal joint, then were treated with Vehicle (1.5% carbopol gel v.t.), MCH Gel (200 mg/kg v.t.) or Diclofenac (4 mg/kg v.t.) for 14 days. Joint swelling was measured daily using a caliper and joint capacity was assessed using a disability meter. In the end, the test animals were euthanized and then blood was collected to measure IL-6 and TNF- α cytokines using ELISA kits (CEUA /UFPI protocol No. 697/21). **Results:** The Gel MCH formulation (200 mg/kg) reduced ($p < 0.05$) edema by 37.12% in the first 5 hours of observation, reaching a reduction of 36.2% over the days of treatment. MCH gel (200 mg/kg) was also able to decrease paw elevation time and plasma concentrations of IL-6 ($p < 0.05$) and TNF- α ($p < 0.05$) compared to the group vehicle treated only. **Conclusion:** The results obtained demonstrate that the formulation based on *M. charantia* L. exerts a topical anti-inflammatory action, evidenced by the reduction of joint edema, improvement of joint capacity over the days of observation and reduction of IL-6 and TNF- α concentrations plasma. **Financial Support:** CAPES, UFPI.

04.029 Immunomodulatory Activity of Red Propolis on Human Monocytes and its Killing Activity on Methicillin-Resistant *Staphylococcus aureus* (MRSA). Ripari N, Sartori AA, Honorio MS, Bastos JK, Sforcin JM. UNESP-Botucatu, Dept of Chemical and Biological Sciences, Institute of Biosciences, Brasil.

Introduction: Previously, we noticed the red propolis extract (RPE) activity on methicillin-resistant *Staphylococcus aureus* (MRSA) strains, and a synergistic antimicrobial action of RPE in combination with Imipenem (IMI) (Ripari et al., 2013). Aim: The aim of this study was to evaluate these same MRSA inhibitory concentrations of RPE and RPE + IMI on human monocytes, evaluating cell viability, cytokine production (TNF- α , IL-1 β , IL-6, IL-8, IL-10) and cell surface markers (TLR-2, TLR-4, HLA-DR and CD80). We also evaluated the killing capacity of monocytes on the MRSA standard strain ATCC 33591. Material and **Methods:** This study was approved by the Ethics Committee of the Botucatu Medical School, UNESP (CAAE 35248620.0.0000.5411). Blood of healthy donors was collected for separation of mononuclear cells by FicollPlaque Plus. Afterwards, the cells were treated with monoclonal antibodies for monocyte selection using the MACS® Monocyte Isolation Kit II Human. Monocytes (5.105/well) were incubated with MRSA inhibitory concentrations of RPE (15.62 $\mu\text{g/ml}$), IMI (250 $\mu\text{g/ml}$), or RPE+IMI at 25% of their inhibitory concentrations (15.62 and 62.5 $\mu\text{g/mL}$, respectively) for 18 h. DMSO (5%) and LPS (0.1 $\mu\text{g/ml}$) were used as controls. Cell viability was analyzed by the MTT method, cytokines by ELISA and surface markers by flow cytometry. To assess the killing percentage, monocytes treated for 18h were further challenged with MRSA (1 monocyte: 4 bacteria) for 3h and lysed with distilled water for incubation on Brain Heart Infusion (BHI) agar for 24h for colony forming unit (CFU/ml) count. **Results:** Bacterial inhibitory concentrations of RPE or RPE+IMI did not affect monocyte viability. All cytokines were suppressed by RPE; however, RPE+IMI increased their production. Likewise, HLA-DR and TLR-2 were down-regulated by RPE, and up-regulated by RPE+IMI. IMI alone significantly increased TLR-4 monocytes expression. RPE induced a higher killing activity than DMSO or LPS, but RPE+IMI showed no difference. **Conclusion:** RPE at inhibitory concentrations for MRSA did not exert cytotoxicity on monocytes indicating a selective toxicity. RPE decreased the production of pro-inflammatory cytokines and down-regulated surface markers. On the other hand, the combination of RPE+IMI modulated the pro-inflammatory state on monocytes both in membrane markers and cytokines. These data indicate that red propolis could mitigate chronic inflammation caused by MRSA infection; on the other hand, the combination of propolis with imipenem can kill the bacteria directly and help the immune system to fight it by up-regulating cytokines and surface markers. **References:** Ripari, N., Pereira, AFM, Júnior, AF, Rall, VLM, Aldana-Mejía, JA, Bastos, JK, & Sforcin, JM *Journal of Applied Microbiology*, v. 134(2), p. 80, 2023. **Financial Support:** FAPESP (2017/04138-8) e CAPES

04.030 Glucagon Resolves Lipopolysaccharide-Induced Lung Neutrophilic Inflammation in Mice. Insuela DBR¹, Ferrero MR¹, Chaves AS¹, Coutinho DS¹, Magalhães NS², Silva AR³, Silva PMR¹, Martins MA¹, Carvalho VF¹ ¹IOC-Fiocruz, Lab. of Inflammation, Rio de Janeiro, Brazil; ²IOC-Fiocruz, Lab. of Hospital Infection Research, Rio de Janeiro, Brazil; ³IOC-Fiocruz, Lab. of Immunopharmacology, Rio de Janeiro, Brazil; University of Rio de Janeiro, Rio de Janeiro, Brazil

Introduction: Resolution is an active physiological process that limits the inflammatory response and thus prevents the development of chronic inflammation. In the lungs, failure of the resolution phase plays a central role in the pathophysiology of some diseases. Previously, we demonstrated that glucagon (GLU) has anti-inflammatory properties, but its effect on inflammation resolution remains elusive. In this study, we evaluated the pro-resolution effect of GLU in a murine model of lung neutrophilic inflammation induced by LPS. **Methods:** Male A/J mice were obtained from Oswaldo Cruz Foundation breeding colony and used in accordance with the guidelines of the Ethic Committee on Use of Laboratory Animals of the Oswaldo Cruz Foundation, Licenses L-027/2016. Neutrophils isolated from bone marrow were stimulated with LPS (100 ng/mL) for 24h *in vitro* and the expression of GLU receptor (GcgR) was evaluated by flow cytometry. In *in vivo* study, mice were challenged with LPS (25 µg/µL, i.n.) and analyses were made 24 h after. Treatment with GLU (1 µg/Kg, i.n.) was realized 4 h after LPS provocation. GcgR expression in the lung was evaluated by immunohistochemistry. The inflammatory response was analyzed through bronchoalveolar lavage (BAL). The levels of GLU, IL-1β, TNF-α, TGF-β1 and PGE2 in airways were measured by ELISA. Neutrophil apoptosis in the BAL was assessed by cell morphology. Bax and Bcl-2 expression in lung was quantified by western blot. Airway hyperreactivity (AHR) to methacholine was evaluated through an invasive barometric plethysmography. **Results:** LPS increased the percentage of neutrophils expressing GcgR *in vitro*. In addition, instillation of LPS led to neutrophil infiltration into the airways and increased GcgR expression by inflammatory cells, without modifying GLU levels in the lung. As given 4 h post-LPS, GLU decreased neutrophil accumulation in lung and BAL 24 h after LPS provocation ($0.11 \times 10^5 \pm 0.03$; $13.33 \times 10^5 \pm 1.84$; $8.06 \times 10^5 \pm 0.99$ neutrophils in BAL of saline, LPS and LPS plus GLU, respectively; mean \pm SEM; n = 6; p<0.05). This effect of GLU on lung neutrophilic inflammation occurred in parallel with an increase in the percentage of apoptotic neutrophils in the BAL, a rise in the levels of the pro-apoptotic Bax protein and a decrease in the expression of the anti-apoptotic Bcl-2 protein in the lung. GLU also reduced the levels of the proinflammatory cytokines IL-1β and TNF-α while elevated the amount of the pro-resolving mediators TGF-β1 and PGE2 in the airways. Finally, GLU inhibited AHR to methacholine in mice provoked with LPS. **Conclusion:** GLU accelerated the resolution of lung neutrophilic inflammation induced by LPS in mice, by reducing neutrophil recruitment, inducing apoptosis of these cells and increasing the levels of the pro-resolving mediators PGE2 and TGF-β1 in the airways. **Financial Support:** CAPES, FAPERJ and CNPq.

04.031 Effect of JMXiBn, a Non-Anesthetic Bupivacaine Analogue, on a Murine Model of Asthma Marked by Steroid Resistance. Cotias AC, Serra MF, Azevedo CT, Costa JCS, Bernardi A, Carvalho, VF, Cordeiro RSB, Silva PMR, Martins MA IOC-Fiocruz, Lab. de Inflamação, ²Farmanguinhos-Fiocruz, RJ, Brazil

Introduction: Glucocorticoids (GCs) are the most effective anti-inflammatory drugs of asthma treatment, although adverse effects and resistance are limiting factors. Several studies have indicated that nebulization of the local anesthetic lidocaine can control the disease in patients with difficult-to-treat asthma. Although adverse effects associated to the blockade of bronchodilator neurogenic reflexes are important barriers of lidocaine drug repositioning as an antiasthmatic therapeutic agent. In this work, we investigated the antiasthmatic effect of JMXiBn, a local anesthetic bupivacaine derivative designed to present anti-inflammatory and bronchodilator action, but with limited local anesthetic action. **Methods:** The effectiveness of JMXiBn was tested in *in vitro* systems, including GH3 cells, evaluating Na⁺ current (patch clamp), and analyses of lymphocytes proliferation and apoptosis. In *in-vivo* analyses, we used A/J mice sensitized on days 0 and 7 by a suspension of Al(OH)₃ and ovalbumin (OVA) given subcutaneously, and challenged intranasally, once a week, for 9 consecutive weeks, starting on the second-week post-sensitization. Budesonide (BUD) (7.5 mg/mL, aerosol), JMXiBn (2.5; 5 e 10 mg/kg, aerosol), both BUD (7.5 mg/mL, aerosol) plus JMXiBn (2.5 mg/mL, aerosol) or vehicle for 7 consecutive days, only during the last week of OVA provocations. Airway hyper-reactivity (AHR), lung leukocyte infiltration, extracellular matrix deposition, mucus exacerbation, cytokines generation and oxidative stress parameters were evaluated 24 h after the last challenge. Western blotting was used to investigate Nrf2 and PI3K δ expression in the lung tissue. The Committee on Use of Laboratory Animals of the Oswaldo Cruz Institute (license L002-2020-A3; Rio de Janeiro, Brazil) approved all protocols and experimental procedures involving animals. **Results:** We observed that JMXiBn Na⁺ channel blockade potency was 60-fold lower than that of bupivacaine, drastically reducing local anesthetic activity. In addition, JMXiBn was more potent than bupivacaine in inhibiting lymphocyte proliferation and survival *in vitro*. Allergen challenge promoted airway hyper-reactivity, pulmonary remodeling, mucus exacerbation and increased levels of inflammatory mediators, as well as reduced catalase activity and increased lipid peroxidation. Treatment with JMXiBn improved all these parameters in GCs resistant asthma model, while budesonide was not effective. Furthermore, there was a substantial increase in the oxidative imbalance, which seemed to contribute to reduction of antioxidant defenses (catalase activity and expression of Nrf2) and increased PI3K δ expression. All these changes were clearly sensitive to JMXiBn, but not to bupivacaine, under conditions where GC treatment was inactive. Moreover, JMXiBn reactivated sensitivity to GC following co-administration, probably due to the reduction of oxidative stress and elevated PI3K δ expression, in parallel with increased expression of Nrf2, which has been linked in close-dependent manner to GC refractoriness. **Conclusion:** These results suggest that JMXiBn is a means of achieving the beneficial effect of lidocaine on difficult-to-treat asthma without the anesthetic effect. **Financial Support:** FAPERJ, CNPq, PDTIS and CAPES, Brazil.

04.032 Evaluation of Ouratein D as Potential Therapeutic Alternative in the Coronavirus-Induced Infection. Monteiro AHA¹, Montuori-Andrade ACM¹, Cardoso C¹, Souza JAM¹, Carvalho AFS², Lara ES², Zaidan I¹, Lima EBS², Augusto IL³, Caixeta RS³, Rocha MP¹, Costa VV⁴, Teixeira MM⁴, Braga FC¹, Sousa LP^{1,2,3} ¹UFMG, PPG Pharmaceutical Sciences, Belo Horizonte, Brazil ²UFMG, PPG Clinical and Toxicological Analysis, Belo Horizonte, Brazil ³UFMG, Dpt of Clinical and Toxicological Analysis, Belo Horizonte, Brazil ⁴UFMG, Dpt of Biochemistry and Immunology, Belo Horizonte, Brazil

Introduction: The model of severe acute respiratory syndrome (SARS) induced by the betacoronavirus MHV-3 mimic, yet with some limitations, the inflammatory condition observed in clinical cases of severe COVID-19, which presents a complex and robust inflammatory response. In this study, we have evaluated the effect of oral and systemic administration of Ouratein D, a component of the extract of *Ouratea spectabilis* that show anti-inflammatory and antimicrobial activities, as a potential therapeutic alternative in inflammatory and antiviral response, morbidity and mortality induced MHV-3 infection. **Methods:** We used 6-week-old male C57BL/6 WT mice infected intranasally (i.n.) with 3×10^3 PFUs of MHV-3. After 12, 24, 36 and 48 hours post infection (hpi), the mice were treated with vehicle (Saline + propylene glycol for i.n. or DMSO intraperitoneally) or Ouratein D (1 mg/kg/animal, by gavage or intraperitoneally). Mice were euthanized three days after infection and samples harvested for analysis of the inflammatory profile in bronchoalveolar lavage, lung damage and viral loads in tissues. Another group of mice was used to evaluate the lethality rates after Ouratein D treatment of MHV-infected animals. To this, mice were infected with 1×10^2 PFUs of MHV-3 (i.n.) and treated with vehicle or Ouratein D by 12, 24, 36, 48, 60, 72, 84, 96, 108 and 120 hpi (1 mg/kg/animal, by gavage). **Results:** Treatment with Ouratein D reduced the infiltration of leukocytes into the alveoli of mice, compared to untreated animals, which was mainly characterized by the decrease of macrophages and lymphocytes numbers. Ouratein D treatment of infected mice also reduced lung edema, as evaluated by quantification of total protein. Noteworthy, Ouratein D treatment partially rescued the lymphopenia characteristic of MHV-3 infection. In keep with the lower numbers of mononuclear cells found in the airways of Ouratein D-treated mice, we found decreased levels of the mononuclear cells-chemoattractant chemokine CCL2 and increased IL-10 levels in the lungs, alongside reduced levels of the pro-inflammatory cytokine IL-6 and the chemokine CXCL1 in plasma. Interestingly, Ouratein D treatment decreased the viral titers in lung, heart and spleen of MHV-infected mice, compared to vehicle-treated mice. Notably, administration of Ouratein D could rescue approximately 30% of mice from MHV-induced lethality **Conclusion:** Our data suggest that treatment with Ouratein D was efficient in protecting the host by modulating the inflammatory response and reducing the viral load, presenting possible antiviral potential.

04.033 Anti-inflammatory Role of Annexin A1 during Chikungunya Infection: Implications for Therapeutic Intervention. Araújo S^{1,3}, Costa VRM¹, Gonçalves MR¹, Santos FM¹, Queiroz-Júnior CM¹, Lima EBS², Perretti M⁵, Costa VV^{1,3}, Teixeira MM^{1,4} ¹ICB-UFMG, Drug Research and Development Center, Belo Horizonte, Brazil, ²FF-UFMG, Dpt of Clinical and Toxicological Analysis, ³UFMG, PPG in Cell Biology, Dpt of Morphology, ⁴ICB-UFMG, Dept of Biochemistry and Immunology, ⁵Queen Mary University of London, UK

Introduction: Host immune responses play a crucial role in the pathogenesis and severity of Chikungunya virus infection (CHIKV). However, the potential contribution of failure in endogenous inflammation resolution pathways to the disease has not been thoroughly explored. Annexin A1 (AnxA1), a pro-resolving protein that interacts with its G-coupled receptor FPR2, is expressed in various cell types, including leukocytes, and is known to regulate inflammation and maintain immune homeostasis. We hypothesized that inadequate engagement of AnxA1 in CHIKV infection may contribute to the cytokine storm and development of CHIKV-induced arthritis. **Methods:** AnxA1 knockout (KO) or wild-type (WT) mice were inoculated with 1×10^6 PFU of CHIKV via the subcutaneous route. Alternatively, WT mice were prophylactically or therapeutically treated with the AnxA1 mimetic peptide AC2-26 (150 µg/animal, i.p.). Mechanical hypernociception, paw edema, quantification of inflammatory mediators, immune cell accumulation (MPO), viral titers, and tissue histopathology were evaluated (CEUA UFMG 135/2019). **Results:** CHIKV infection induced increased AnxA1 expression in the footpad of WT mice. AnxA1 KO mice exhibited uncontrolled inflammation, characterized by increased levels of MPO, CXCL1, and IL-6, as well as enhanced accumulation of CD11b⁺Ly6G⁺ cells in the paw at 2 dpi. Increased accumulation of type 1 conventional dendritic cells (cDCs1) and CD8⁺ T cells at 7 dpi was observed in AnxA1 KO mice compared to infected WT littermates. AnxA1 deficiency was associated with increased viral clearance in the organs and aggravated paw tissue damage, while virus-induced hypernociception and paw edema remained unaffected. Similar disease phenotypes were observed in Fpr2/3 KO mice, indicating that the anti-inflammatory effects of AnxA1 are dependent on FPR2 engagement. On the other hand, administration of Ac₂₋₂₆ reduced CHIKV-induced inflammation in WT mice, as evidenced by decreased levels of MPO, CXCL1, and IL-6 in the footpad. AC₂₋₂₆ administration also decreased the accumulation of CD11b⁺Ly6G⁺ cells in the paw and the percentage of CD4⁺ T cells in the popliteal lymph node of CHIKV-infected mice, resulting in a reduction in CHIKV-induced paw edema and mechanical hypernociception. **Conclusion:** Collectively, these findings suggest that AnxA1 plays a significant role in CHIKV infection and propose targeting the AnxA1-FPR2/ALX pathway as a potential therapeutic approach for controlling acute inflammation caused by the virus. **Funding:** This research was supported by the Fapemig Hospedeiro em Dengue Project (project SUB 1 125036-1), the Medical Research Council in the United Kingdom (Newton project MR/No17544/1), the National Institute of Science and Technology in Dengue and Host-microorganism Interaction (INCT dengue) (Grant 465425/2014-3), and CAPES, Brazil – (project MCTI/CNPq/CAPES/FAPS 16/2014).

04.034 Effect of Transplantation of Interleukin-4 Programmed Macrophages in Severe Acute Respiratory Syndrome Induced by Murine Betacoronavirus. Felix FB¹, Beltrami VA¹, Martins DG¹, Sousa LP², Teixeira MM³, Pinho V¹. ¹ICB-UFMG, Dpt of Morphology, Belo Horizonte, Brazil; ²FF-UFMG, Dpt of Clinical and Toxicological Analysis, Belo Horizonte, Brazil; ³UFMG, Dpt of Biochemistry and Immunology, Belo Horizonte, Brazil

Introduction: Alternatively activated macrophages or M2 can be achieved *in vitro* by several stimuli, including IL-4. This macrophage phenotype possesses anti-inflammatory properties and play a critical role in tissue repair and wound healing. Transplantation of IL-4-programmed macrophages is an immunomodulatory therapy to enhance tissue repair and constitute a putative treatment for inflammatory diseases. Here, our objective was to investigate whether exogenous administration of IL-4-programmed macrophages could mitigate the inflammatory response and serve as a cell transfer treatment for managing lung dysfunction induced by the betacoronavirus (MHV-A59) infection. **Methods:** Mice were intranasally inoculated with MHV-A59 (10^3 PFU), known to induce a robust inflammatory response in the lungs. Bone marrow cells were isolated and differentiated into macrophages, and then polarized toward an M2-like phenotype using recombinant murine IL-4. The IL-4 programmed macrophages (1×10^6 cells/mouse) were administered to the mice via intravenous tail vein injection, either in a single dose on day 3 post-infection (pi) or two doses on days 3 and 4 pi. Mice were euthanized on day 5 pi, and bronchoalveolar lavage (BAL) was harvested to evaluate inflammatory leukocytes. The lung tissue was examined to assess chemokine production, histopathological changes, and viral load. Animal Ethics Committee under protocol 123/2023. **Results:** Treatment with IL-4-programmed macrophages reduced lung damage, viral load, and excessive production of the proinflammatory cytokines IFN- γ , IL-6, TNF and IL-1 β induced by MHV-A59 infection. In addition, IL-4-programmed macrophage transplantation reduced total leukocytes and neutrophil numbers in BAL. However, there were no change in protein levels in the BAL and numbers of circulating leukocytes in the blood. **Conclusion:** Transplantation of IL-4 programmed macrophages show beneficial effects in mitigating the inflammatory response induced by MHV-A59 infection. **Financial Support:** This work was supported by grants from National Institute of Science and Technology in Dengue and Host-Microbial Interactions, a program grant from Conselho Nacional de Desenvolvimento Científico e Tecnológico (CNPq), Fundação de Amparo à Pesquisa do Estado de Minas Gerais (FAPEMIG, Brazil), Coordenação de Aperfeiçoamento de Pessoal de Nível Superior (CAPES, Brazil).

04.036 Plasmin Modulates the Inflammatory Response and Reduces Lung Damage in Experimental Pneumococcal Pneumonia. Cardoso C¹, Carvalho AFS², Lara ES², Zaidan I¹, Grossi L¹, Montuori-Andrade ACM¹, Augusto IL³, Caixeta RS³, Carneiro FS², Queiroz-Junior CM⁴, Felix FB⁴, Teixeira MM⁵, Braga FC¹, Tavares LP⁵, Sousa LP^{1,2,3}. ¹UFMG Belo Horizonte, PPG Pharmaceutical Sciences, Brazil; ²UFMG Belo Horizonte, PPG Clinical and Toxicological Analysis, Brazil; ³UFMG, Dpt of Clinical and Toxicological Analysis, Belo Horizonte, Brazil; ⁴UFMG, Dpt of Morphology, Belo Horizonte, Brazil; ⁵UFMG Belo Horizonte, Dpt. of Biochemistry and Immunology, Brazil; ⁶Dpt. of Medicine, Harvard Medical School, Boston, USA

Introduction: Emerging studies have highlighted the role of Plasminogen/Plasmin system in key steps of inflammation resolution, including neutrophil apoptosis, efferocytosis and macrophage recruitment and reprogramming. Recently, we have shown that Plg/Pla prevent sepsis severity by modulating local and systemic inflammation and collateral organ damage. Here, we investigated the effect of Pla in a pre-clinical model of pneumococcal pneumonia.

Methods: Male BALB/c mice were intranasally infected with 10⁵ CFU of *S. pneumoniae* (ATCC 6303 serotype 3) and then treated with Pla (10 µg/mouse, i.p.) or vehicle, 12 h post-infection (hpi). Mice were euthanized at 24 or 48 hpi and bronchoalveolar lavage (BAL) was collected to analyze inflammatory/resolving parameters (leukocyte infiltration, neutrophil apoptosis, efferocytosis, cytokines/chemokines and total proteins levels) and bacterial load. Plasma levels of IL-6 and CXCL1 chemokine were also evaluated. Lungs were harvested for myeloperoxidase and histological analyzes. Alveolar macrophages after Pla-instillation were measured by flow cytometry. The pan-caspase inhibitor zVAD-FMK was administered to Pla-treated infected mice. Lethality rates induced by pneumococcal pneumonia were determined after 12h- and 24h- of Pla-treatment. **Results:** Regardless of the applied protocol, Pla-treatment during pneumococcal pneumoniae decreased neutrophilic infiltration in the airways alongside lower CXCL1 levels and higher neutrophil apoptosis. There were increased numbers of monocytes/macrophages associated with higher efferocytosis rates, without modify bacterial loads in BAL. In addition, there were decreased levels of TNF, IL-6, IL-1β in BAL and IL-6 and CXCL1 in plasma in both protocols applied. Treatment with Pla decreased pneumococcus-induced lung damage, mainly in protocol 2, decreasing the infiltration of leukocytes in lung parenchyma and overall histopathological score. Noteworthy, Pla-instillation induced increased numbers of alveolar macrophages (SiglecF⁺/F4/80⁺) in the alveoli. Administration of zVAD-FMK impaired Pla-induced resolution of neutrophilic inflammation, suggesting apoptosis is an underlying mechanism of Pla-induced resolution of pneumococcal pneumonia. Finally, treatment with plasmin rescued 20% of the mice from the lethality induced by pneumococcus. **Conclusion:** In summary, our data suggest that plasmin modulates the inflammatory response in airway and lung parenchyma, protecting animals from lung damage and lethality induced by pneumococcus by promoting caspase-dependent resolution of neutrophilic inflammation. **Financial Support:** National Institute of Science and Technology in Dengue and host-microbial interactions (465425/2014-3), FAPEMIG, APQ-03221-18; CAPES, 23038.003950/2020-16; and CNPq, PQ-306789/2018/3.

04.037 The Investigational New Mexiletine Derivative JME-209 Inhibits Exacerbation on Lung Inflammation and Bronchoconstriction in Mice Subjected to Cigarette Smoke Inhalation and H1N1 Infection. Gomes HS, Coutinho DS, Cotias AC, Ferreira TPT, Almeida MD, Lopes RR, Nobrega MECG, Santos HBS, Arantes ACS, Carvalho VF, Silva PMR, Martins MA IOC-Fiocruz Lab. of Inflammation, Rio de Janeiro, Brazil

Influenza A (H1N1) virus is a common cause of acute exacerbation of chronic obstructive pulmonary disease (COPD), while cigarette smoking is COPD's major risk factor in many countries. Much of COPD's mortality and health care costs are accounted for by acute exacerbations, characterized by difficult-to-control episodes of increased symptoms and airflow obstruction. The local anaesthetic mexiletine antagonizes bronchospasm in animal models and patients, but adverse side effects related to local anaesthesia of the airways limited its efficacy. We report here the impact on acute exacerbation of lung Inflammation triggered by influenza virus in cigarette smoke-exposed mice of JME-209, 1-([1,1'-biphenyl]-4-aryloxy)-2-propanamine, a novel mexiletine analogue optimized to present reduced local anaesthetic activity and improved bronchodilator and anti-inflammatory properties. **Methods:** A/J female mice were exposed to cigarette smoke inhalation for four consecutive days and infected with H1N1 (PRN, 300 PFU) on day 3. We gave JME-209 treatment (3 mg/kg, oral) twice, 1 h and 24 h post-infection. Lung resistance, leukocyte accumulation and tissue peroxidation levels (MDA values) were performed 24 h after the last cigarette smoke exposure. All procedures involving the use of experimental animals were previously approved by FIOCRUZ's ethics committee CEUA – L002/2020-A3. The data were analyzed using parametric one-way ANOVA with post-hoc Turkey test (significance for $p < 0.05$). **Results:** We found that Penh values (an indicator of airway resistance) (mean \pm SEM) either from mice subjected to cigarette smoke (Cs) alone (0.6 ± 0.44) or H1N1 infection alone (0.9 ± 0.26) were significantly inferior to those values observed in mice subjected to the combination of insults (CsH1N1) (1.3 ± 0.14). Concerning airways and lung neutrophilic infiltration and oxidative-stress-induced lung tissue damage indexes, statistically significant upregulations were also noted. Treatment by JME-209 of CsH1N1 mice inhibited exacerbated values on Penh (1.3 ± 0.1 vs 0.9 ± 0.7 , $n=8$, $p=0.03$), neutrophils accumulation in the airways (60 ± 7 vs $25.4 \pm 3.9 \times 10^4$ cells/BAL, $n=8$, $p < 0.0001$), neutrophils infiltrate in the lungs (MPO values) (0.5 ± 0.07 vs 0.2 ± 0.5 , $n=8$, $p=0.001$ D.O/right lung) and tissue oxidant stress (MDA values) (1.32 ± 0.13 vs 0.6 ± 0.07 , $n=7$, $p=0.0002$ η Mol/mg ptn). **Conclusion:** These findings suggest that JME-209 oral treatment could be an effective therapy for controlling acute exacerbations of respiratory diseases such as COPD. **Financial Support:** CAPES, CNPq and FAPERJ.

04.038 Effect of Ylang-ylang (*Cananga odorata*) Essential Oil on the Hyperalgesia, Edema Formation and Histopathological Alterations in Zymosan-Induced Arthritis Model. Lossavaro PKMB, Bonfá IS, Lencina JS, Felipe JL, Fernandes MML, Ferreira JV, Toffoli-Kadri MC, Silva-Filho SE UFMS, Pharmaceutical Sciences, Food and Nutrition College, PPG Pharmaceutical Sciences, Campo Grande, Brazil

Introduction: The use of anti-inflammatory drugs becomes limited in therapy due to the adverse effects. Several biological activities have been described for Ylang-ylang essential oil (YEO). The aim of this study was to evaluate the effect of YEO on edema formation, mechanical hyperalgesia and cartilage destruction in zymosan-induced arthritis model.

Methods: Swiss male mice were orally treated with YEO (50, 100 and 200 mg/kg), dexamethasone (1 mg/kg) or vehicle (saline solution and Tween 1%) (n=5-7 animals/group). One hour after pre-treatment, 200 µg of zymosan diluted in 10 µL of sterile saline were injected into the mice joint cavity of the right knee. Mechanical hyperalgesia was evaluated at 3 and 4 hours after arthritis induction, using a digital analgesimeter (Von Frey, Insight®). The knee joint edema formation was evaluated at 4 and 6 hours after arthritis induction, using a digital micrometer. Histological analysis was performed 7 days after zymosan-induced arthritis (animals were treated daily with YEO at dose of 200 mg/kg). The right knee joint was collected and sent for histological analysis. The experimental protocol was approved by the Animal Research Ethical Committee of the UFMS, under registration 1.182/2021 CEUA/UFMS.

Results: The zymosan injection induced mechanical hyperalgesia at 3 and 4 hours. In these times, only the YEO treatment (200 mg/kg) reduced mechanical hyperalgesia in 52.38% and 81.75%, respectively, compared to control group. The YEO treatment at doses of 50 and 100 mg/kg did not significantly reduce the mechanical hyperalgesia in any tested times. The YEO treatment showed anti-inflammatory activity, promoting a significant reduction in knee edema formation at doses of 100 and 200 mg/kg, in all tested times. The dexamethasone treatment promoted a reduction of mechanical hyperalgesia and knee edema formation in all-time points tested. In histological analysis, discontinuity the surface the cartilage, disorientation of chondrocytes columns, cells death, proliferation (clusters) and hypertrophy were observed in the arthritic animals. The YEO (200 mg/kg) and dexamethasone treatment, for 7 days, promotes a reduction of cartilage damage to grade 1, where the cartilaginous surface is intact, with a homogeneous matrix. **Conclusion:** YEO has anti-inflammatory activity, reducing knee joint edema formation, mechanical hyperalgesia and reduced cartilage destruction in mice submitted to zymosan-induced arthritis model. **Financial Support:** CNPq and CAPES.

04.040 Plasmin decreases Neutrophil Migration and reduces Adhesion to Inflamed Endothelium. Carneiro FS¹, Sugimoto MA², Zaidan I¹, Lara ES¹, Cardoso C³, Carvalho AFS¹, Caixeta RS⁵, Cooper D², Gonçalves WA⁴, Pinho V⁴, Perretti M², Sousa LP^{1,3,5} ¹UFMG Belo Horizonte, PPG Clinical and Toxicological Analysis, Brazil ²University of London, William Harvey Research Institute, London ³UFMG, PPG Pharmaceutical Sciences, Belo Horizonte, Brazil, ⁴UFMG, Dpt. of Morphology, Belo Horizonte, Brazil, ⁵UFMG, Dpt. of Clinical and Toxicological Analysis, Belo Horizonte, Brazil

Introduction: The Plasminogen/Plasmin (Plg/Pla) system is associated with a variety of biological activities beyond the classical dissolution of fibrin clots, including cell migration, tissue repair and inflammation. Inflammation is an evolutionarily conserved response that guarantees the maintenance of tissue homeostasis through resolution - an active process mediated by molecules named pro-resolving mediators. Despite the classical view of the Plg/Pla system, emerging studies have revealed its actions in key steps of inflammation resolution, including reduction of pro-inflammatory mediators, decrease of neutrophil numbers and enhancing their apoptosis and efferocytosis, and recruitment with further reprogramming of monocytes/macrophages toward resolving phenotypes. Given the importance to control of neutrophils numbers and function in order to avoid further tissue damage, here we have investigated the role of Pla to modulate features of neutrophil such as migration, adhesion and rolling to inflamed endothelium. **Methods:** To explore the role of Pla on neutrophil migration, human neutrophil were pre-treated with Pla (4ug/mL) or Pla+TXA (tranexamic acid, a Pla-binding site inhibitor) and subjected to chemotaxis assay in 24-well transwell plates using fMLP or IL-8 as chemoattractants or control medium. *In vivo* experiments were carried out using C57BL/6 male mice pre-treated or not with Pla for 1h, followed by intraarticular (i.a) or intrapleural (i.pl.) challenge with LPS (500 ng) for further 6 h. Exudates were harvested to count leukocytes. The evaluation of neutrophil adhesive properties were performed *in vitro* by flowing Pla-treated neutrophils on HUVEC monolayers or *in vivo* by intravital microscopy of Pla-treated inflamed knee. **Results:** Our data show that Pla reduced neutrophil chemotaxis toward IL-8 or fMLP. Interesting, the Pla-effect on neutrophil chemotaxis was inhibited by TXA, denoting a dependency of Pla-binding to cell surface. Accordingly, pre-treatment of mice with Pla, decrease neutrophil migration to the pleural or articular cavities. Notably, Pla reduced firm adhesion to inflamed endothelium *in vitro* and decreased adhesion and rolling to the inflamed knee. **Conclusion:** The data obtained so far shown an unrecognized effect of Pla inhibiting neutrophil migration and neutrophil-endothelial interactions, in which can minimizing the deleterious effects of neutrophils during overwhelming inflammation. The underlying mechanism deserve further elucidation. **Financial Support:** FAPEMIG, CAPES and CNPq. **Research Ethics Committee Statement:** The study was approved by the Committee on Ethics in the Use of Animals (CEUA), protocol number 3/2019, of the Federal University of Minas Gerais (UFMG). Study in the lab of prof MP was approved by East London & The City Local Research Ethics Committee (05/Q0603/34 ELCHA, Londres, Reino Unido).

04.041 Sepsis Modulates Expression of Endogenous Deoxyribonucleases Related to the NETs Clearance in Mice. Costa VF, Galant LS, Ramos AS, Rodrigues FC, Oliveira-Leandro Maísa, Schneider AH, Almeida C J L R, Wanderley CW, Cunha FQ. FMRP-USP

Introduction: Sepsis is characterized as life-threatening inflammatory dysfunction in response to an infection, which can lead to death. Neutrophil extracellular traps (NETs) are net-like structures composed of neutrophil proteins on a DNA scaffold. The clearance of NETs is mediated by deoxyribonucleases (DNases), which degrade this backbone. Studies carried out by our research group show an increase in the concentration of NETs in the plasma of patients with sepsis. In addition, several studies show that the degradation of NETs by recombinant DNases improves the outcome of animals with sepsis. **Objective:** Analyze the modulation of DNase activity and the expression of these enzymes in healthy or in septic mice. **Methodology:** Using the cecum ligation and puncture (CLP) model, we analyzed the mortality caused by sepsis and the levels of cytokines in the plasma of the animals. Also, we evaluated NETs levels and DNase activity in spleen, liver, systemic circulation and peritoneal cavity. In addition, we analyzed the expression of DNases 1, and γ genes in spleen, liver, and peritoneal lavage. **Results:** The CLP model of sepsis provided the mortality of 100% of the animals within 48 hours after the procedure and increased the levels of cytokines TNF- α , IL-1 β and IL-6 in the plasma of CLP animals. NETs levels were increased in the circulation, spleen, liver and peritoneal lavage of animals with sepsis. The DNase activity of the animals with sepsis increased in the lavage and in the circulation after the procedure, while in the spleen and liver did not show any difference. In the spleen, a reduction in the expression of all DNases analyzed was observed, in contrast, in the liver, there was an increase in the expression of DNase 1 and γ , in the peritoneal lavage, a reduction in the expression of DNase γ was observed. **Conclusions:** During sepsis, there is modulation of gene expression of the main DNases involved in NET clearance. In some compartments, enzymes capable of degrading DNA are released, these enzymes can have bacterial origin. Although there is an increase in DNase activity in some compartments during sepsis, this increase is not sufficient to reduce NET concentrations to physiological levels. However, further studies are needed to verify the clearance of NETs during sepsis. **Financial Support:** CNPq, CAPES and FAPESP.

04.042 The Specialized Pro-Resolving Mediator, Resolvin D5, Protects the Skin from Oxidative Stress Induced by UVB Irradiation. Semeão LO, Pierotti SM, Saito P, Pinto IC, Ferrante LF, Kumagai CM, Rodrigues CCA, Vale DL, Melo CPB, Trambaioli BM, Santos KMM, Alves MG, Radoski RE, Casagrande R, UEL, PPG Health Sciences, Londrina, Brazil

Introduction: The skin is the largest organ of the human body summing up about 16% of the body mass. It provides a protective physical barrier between the body and the environment. External environment treats include ultraviolet (UV) irradiation, which causes oxidative stress (OS), resulting from an imbalance between reactive oxygen species (ROS) production and antioxidant defense mechanisms. OS initiates an inflammatory response involving cytokine production, metalloproteinase 9 (MMP-9) activity and formation of skin edema. On the other hand, inflammation can be actively reduced by specialized pro-resolution lipid mediators (SPM) such as resolving D5 (RvD5). RvD5 is a SPM derived from docosahexaenoic acid that reduces cytokine production and oxidative stress in response to lipopolysaccharide. Whether RvD5 has a similar activity in UVB skin inflammation is unknown, thus, determining it was our aim in the present study. **Methods:** Hairless mice were randomly assigned into six groups (n=6 per group). RvD5 doses were prepared with saline solution and administrated by intraperitoneal route to mice 1h before and 7h after UVB irradiation dose of 4.14 J/cm². The UVB-induced inflammation and OS were evaluated by skin edema (standard area skin punch), catalase activity, ability to reduce iron (FRAP), ability to scavenge the radical ABTS (ABTS), reduced glutathione levels (GSH); superoxide anion production (NBT assay); cytokine levels were quantitated by ELISA, and MMP-9 activity was determined by enzymography. Each assay was performed with samples collected at time points indicated in the results section, which were previously standardized by our laboratory. The results were expressed as mean ± standard error mean and analyzed using the GraphPadPrism® software (p<0.05). Ethical approval by the institutional board number was: CEUA-UEL # 11146.2016.97. **Results:** We started our study with samples collected 12h after irradiation since there is significant induction of skin edema and depletion of skin endogenous antioxidant defenses. At 12h, RvD5 reduced UVB-triggered skin edema (3, 10 and 30pg/mouse with inhibition of 0%, 97% and 100%, respectively). For FRAP (90%), ABTS (100%) and GSH (43%), only the dose of 30pg/mouse was active in all tests, thus, this dose was selected for the next assays. RvD5 also reduced the activity of MMP-9 activity (61%). At 2h after UVB irradiation, it is characteristic to observe a depletion of catalase activity, which was prevented by 60% by RvD5 treatment. At 4h after UVB irradiation, it is characteristic to observe superoxide anion and cytokine (IL-1beta, TNFalpha, IL-10 and TGFbeta) production, which were abolished (100% inhibition) by RvD5 treatment. **Conclusion:** The results demonstrate that treatment with RvD5 reduces a wide range of parameters applied to evaluate UVB skin inflammation and oxidative stress. Therefore, RvD5 is a novel potential therapeutic molecule to counteract the deleterious effects of UVB irradiation in the skin. **Financial Support:** Fundação Araucária, CNPq and CAPES

04.043 Histological Analysis of the Effect of Nanoencapsulated Diclofenac Associated with Iontophoresis on Rat Joints with CFA-Induced Arthritis. Santos WP¹, Cherem KNN¹, Dornelles FN¹, Souza-Silva E¹, Lemos-Senna EMT², Tonussi CR¹ ¹LANEN-CCB-UFSC, Nociception Neurobiology Lab., Florianópolis, SC, Brazil. ²CCS-UFSC, Pharmacotechnical Lab., Health Sciences Center, Florianópolis, SC, Brazil

Introduction: Rheumatoid arthritis (RA) is a chronic inflammatory disease affecting 1.5-2% of the population and causes the progressive joint destruction, leading to articular pain and stiffness [1]. Nonsteroidal anti-inflammatory drugs (NSAIDs) are commonly used to alleviate pain symptoms and rigidity; however, their prolonged use can result in gastrointestinal, hepatic, renal, and cardiovascular adverse effects [2]. Nanocarriers containing diclofenac (solid lipid nanoparticles, SLN, and nanoemulsions, NE) have been developed to optimize local drug delivery and reduce adverse effects. This study evaluated the transcutaneous iontophoretic administration of nanocarriers-containing diclofenac in a model of arthritis in rats.

Methods: Arthritis was induced in the animals by injecting complete Freund's adjuvant (CFA, 50 µL, 5 mg/mL, *Mycobacterium tuberculosis*) into the tibiofemoral joint [4]. After 23 hours of CFA injection, transdermal application of SLN and NE containing diclofenac (413.8 and 783.4 µg/mL, respectively), with or without iontophoresis (3.95 mA.min) [5], was performed. Additionally, another group of animals received free diclofenac intravenously (25 µg/kg). Eight days after the procedures, the animals were euthanized, and the joints were collected for morphological analysis. Histological sections were observed under bright-field images at 40x magnification using an Olympus BX41 microscope, and the images were analyzed using ImageJ software [6] to measure the thickness and count of chondrocytes in femur and tibia cartilage. **Results:** In the control groups, CFA promoted synovitis, cartilage degeneration, and bone remodeling. Groups systemically treated with free diclofenac, and locally with SLN and NE containing diclofenac associated with iontophoresis presented a preserved number of chondrocytes and cartilage thickness, similar to the naive group. **Conclusion:** The present data support that transcutaneous iontophoresis of nanoencapsulated diclofenac had beneficial effects on the morphology of periarticular tissues, such as articular cartilage and the synovial membrane, similar to the effects observed with intravenous treatment. The study was approved by the Local Animal Research Ethical Committee (CEUA/UFSC, No.1914250220/2020). **Acknowledgments:** Taciane Stein da Silva, Prof. Anicleto Poli, the Multiuser Laboratory of Studies in Biology (LAMEB/UFSC), the Interdisciplinary Laboratory for the Development of Nanostructures (LINDEN/UFSC), and CAPES/CNPq (financial support). **References:** [1] Abhishek, A. Osteoarthritis Cartilage, v. 21. p.1229, 2013. [2] Klinge, SA. Phys. Sportsmed., v. 41, p. 64, 2013. [4] Gomes, RP. Rev. Bras. Reumatol., v. 54, p. 83, 2014. [5] Motta, AF. Life Sci., v. 73, p. 1995, 2003. [6] Schneider, C. Nat Methods, v. 9, p. 671, 2012.

04.044 Food Restriction during Pregnancy Increases Susceptibility to Infections in Adult Offspring by Compromising the Alveolar Macrophages Activity. Azevedo GA¹, Negreiros NGS², Soares AW¹, Lippi BK², Candido CS², Landgraf MA³, Landgraf RG². ¹Unifesp-EPM, Dpt. of Medicine, São Paulo, Brazil. ²Unifesp-Diadema, Dpt. of Pharmaceutical Sciences, Brazil. ³Unip-Santos, Brazil

Introduction: Maternal food restriction during pregnancy induces morphological and metabolic fetal adaptations and predisposes to metabolic diseases and defective inflammatory response, in offspring. This study aimed evaluate the phenotypic profile of macrophages from low birth weight (LBW) rats, induced by intrauterine food restriction, to elucidate the reason why animals get more infections. **Methods:** Pregnant female Wistar rats were subjected to 50% calorie-protein food restriction during gestation, the control group that received feed ad libitum. After the birth of the offspring, we monitored the weight and size of the animals on days 1, 5, 10, 15 and 20 of life. At 12 weeks of age, male offspring rats were euthanized to obtain macrophage cells to evaluate the phenotypic profile (M1 and M2) by flow cytometry, for evaluation cytokines, phagocytic activity and microbicidal capacity of alveolar macrophages incubated with *Saccharomyces cerevisiae*. **Results:** Malnutrition during gestation caused a drop in fetal birth weight (LBW) compared with offspring from control group (normal body weight at birth-NBW). The count of colony forming units, was significantly higher in LBW than NBW group. LBW group showed defective phagocytic activity because the number of yeasts phagocytosed by alveolar macrophages is lower than the NBW group. Cytokine IL-10 was significantly higher in LBW without stimulation and after 4 hours with yeast, an increase in IL-6 is not observed, as occurs in the control group. The M1 and M2 profile was analyzed by flow cytometry and the preliminary results showed no significant difference between the groups in alveolar macrophage cells without stimulation. **Conclusion:** low birth weight induced by maternal malnutrition during pregnancy prejudices phagocytic activity of alveolar macrophages and might compromises immune response and increase susceptibility to infections. **Financial Support:** FAPESP (2019/05242-9, 2020/16020-4), CNPq and CAPES – Finance Code 001

04.045 Effects of Obesity and Ovaries Removal on Expression of Glucocorticoid Receptor in Lung of Mice Submitted to Mixed Asthma. Suaiden-Schmidt A¹, Ribeiro MR¹, Oliveira MA¹, Moriya HT³, Duque-Almeida E¹, Dragunas G¹, Munhoz CD¹, Donato Júnior J², Santana Melhado IV¹, Riffo-Vasquez Y⁴, Tavares-de Lima W¹ ¹ICB-USP, Dept. of Pharmacology, ²ICB-USP, Dept. of Physiology and Biophysics, ³EP-USP, Dept. of telecommunication and Control Engineering, ⁴Institute of Pharmaceutical Science, King's College London, UK.

Introduction: Obesity is a worldwide public health problem characterized by excessive accumulation of body fat, inducing a chronic low-grade inflammation. Postmenopausal obese women are prone to worsening asthma. Asthma is a chronic inflammatory disease and is characterized by cell migration, epithelial damage, hyperreactivity and airway remodeling. Bronchodilators and glucocorticoids are the first choice to pharmacological management of asthma whereas glucocorticoid resistance may be found in obese menopausal asthmatic women. Here, we study seek to identify the role of obesity and reduced circulating levels of female sex hormones on translocation of glucocorticoid receptors in the lung of female mice submitted to the mixed asthma model. **Methods:** Female Balb/c mice (20-35g) were maintained on a conventional diet (CD) and a high-fat diet (HFD) for a period of ten weeks. The groups were divided into control and experimental which were sensitized (ip) and challenged (intranasal) with ovalbumin (OVA 1.2 mg/mL adsorbed in 75 μ L of Complete Freund's Adjuvant, ip). Afterwards, lung mechanics (flexiVent) was conducted. The lung inflammation was quantified counting the cells recovered in bronchoalveolar lavage (BAL). We also performed ovaries removal (OVx) and the false manipulation (Sham-OVx). Cytosolic and nuclear lung expression of GC receptors were evaluated by Western Blot. Data are expressed as mean \pm SEM and were analyzed by Student's t-test or two-way ANOVA followed by Bonferroni post-test (Graphpad Prism 7.0; * $p < 0.05$). **Results:** HFD significantly increased the weight of mice (CD: 6.1 ± 0.3 g vs HFD: 11 ± 0.6 g, * $p < 0.05$, n=10). Obese OVx mice reduced uterine weight (Sham OVx: 0.15 ± 0.01 mg, n=10 vs OVx: 0.02 ± 0.001 *mg n=10, * $p < 0.05$, and the vaginal smears identified as distreous phase. HFD-OVA challenge increased the cells recovered in BAL (total: PBS: 5.55 ± 0.45 vs OVA: 91.27 ± 5.22 , $\times 10^4$ cells/mL, * $p < 0.05$), neutrophils (PBS: 0.02 ± 0.01 vs OVA: 30.74 ± 2.50 , $\times 10^4$ cells/ml n=10, * $p < 0.05$) and eosinophils (PBS: 0.04 ± 0.03 vs OVA: 31.0 ± 2.76 , $\times 10^4$ cells/ml n=10, * $p < 0.05$). OVA challenge induced an increased airway resistance (Rn) to methacholine in HFD-OVx mice (3.27 ± 0.58 * vs HFD- Sham OVx: 1.10 ± 0.070 * n=8, cm/ H₂O.s/mL, * $p < 0.05$). Expression (densitometry) of GR in lung of HFD-OVA-OVx mice (0.36 ± 0.116 %, n: 5) significantly reduced ($p < 0.05$) in comparison to HFD OVA-Sham OVx mice (0.63 ± 0.17 % n=5). Our data also showed a reduced ($p < 0.05$) translocation of GR in HFD-OVA-OVx mice as compared to HFD-OVA-Sham OVx mice (0.96 ± 0.57 vs 3.41 ± 0.59 %* $p < 0.05$). **Conclusion:** Our data suggestive that the upon obesity the expression and translocation of GR in the lung in mixed asthma are negatively modulated by sex hormones. Ethics Committee: (6141100720/2020/CEUA). **Financial Support:** CNPq and CAPES.

04.046 Paroxetine Reduces Adrenergic Receptor Internalization. Rodrigues FC^{1,2}, Galant LS^{1,2}, Kanashiro A^{1,2}, Borges FV^{1,2}, Duarte DA³, Costa Neto CM³, Pupo AS⁴, Cunha FQ^{1,2}
¹FMRP-USP, Dept. of Pharmacology, Brazil; ²FMRP-USP, Center of Research in Inflammatory Diseases, Brazil; ³FMRP-USP, Dept. of Biochemistry and Immunology, Brazil; ⁴IBB-Unesp-Botucatu, Dept of Biophysics and Pharmacology, Brazil

Introduction: Sepsis is a critical condition characterized as a deregulated immune response from the host against an infection. One prominent feature observed during sepsis is the increased concentration of plasmatic catecholamines, including Noradrenaline and Adrenaline. These molecules bind to α and β -adrenergic receptors, which are classified as G-Protein Coupled Receptors (GPCRs). Activation of these signaling pathways leads to the decoupling of G β / γ subunits, thereby initiating intracellular mobilization of ions calcium and subsequently promoting vasoconstriction and an increase in heart rate. Furthermore, this process is associated with elevated activity of G-Coupled Receptor Kinase 2 (GRK2), which contributes to GPCRs internalization. However, in sepsis, the efficacy of circulating catecholamines in inducing cardiac and smooth muscle contraction within blood vessels is reduced, leading to vasoplegia. Additionally, septic patients exhibit down-regulation of adrenergic receptors, turning vasoconstrictor administration ineffective in improving mortality outcomes. Notably, it is known paroxetine, a selective serotonin re-uptake inhibitor, is capable of selectively bind to GRK2 active domain, inhibiting its action and can increase murine cardiomyocyte contractions. **OBJECTIVES:** Therefore, the present study aims to demonstrate the potential of paroxetine in attenuating the internalization of α 1-A adrenergic receptors (α 1-AR), both *in vivo* and *in vitro*. **Methods:** To perform *in vivo* assays, mice were submitted to Cecum Ligation and Punction (CLP) and treated with paroxetine 6h hours after surgery. At 12 hours the heart was collected, stained in slides and incubated with anti- α 1-AR to perform immunofluorescence (IF). To measure internalization *in vitro*, we performed Bioluminescence Resonance Energy Transfer (BRET) based assay with HEK-293 cells transfected with α 1-AR-RLucII and KRas-GFP plasmids, pre-treated with paroxetine for 30 minutes and stimulated with norepinephrine at the moment of Δ ebBRET reading. **Results:** Our IF shows that paroxetine reduced α 1-AR mean of fluorescence intensity (MFI) levels in heart tissue, with 12 hours collection, of mice CLP-induced treated with ertapenem, when compared to mice treated only with ertapenem. This data provides that paroxetine administration was capable of reducing α 1-AR internalization *in vivo*. Therefore, *in vitro* BRET based assay shows that pre-treatment with increasing concentration has avoided α 1-AR negative BRET signals variation in cells stimulated with norepinephrine, when compared to norepinephrine control group. The data contributes to showing that paroxetine was capable of avoiding α 1-AR internalization *in vitro* in a concentration dependent manner. **Conclusion:** Although more investigation is needed, our data sustain the hypothesis that paroxetine can reduce internalization in cardiomyocytes from CLP-induced mice, which may contribute to the recovery of adrenergic molecules efficacy in sepsis vasoplegia. Therefore, BRET-based assay contributes to show that paroxetine's α 1-AR reducing internalization is concentration-dependent and could be a novel drug treatment for sepsis at clinics. **FINANTIAL SUPPORT:** This study was fomented by the governmental agencies Coordenação de Aperfeiçoamento de Pessoal de Nível Superior (CAPES), Conselho Nacional de Pesquisa e Desenvolvimento (CNPq) and Fundação de Amparo e Pesquisa do Estado de São Paulo (FAPESP), as well for Center of Research in Inflammatory Diseases (CRID). This work follows the norms of Animal Use Ethics Consil (CEUA-FMRP), N^o 241/2019.

04.047 Effect of Free and Nanostructured Omega 3 in Animals Challenged with Lipopolysaccharides (LPS) in the Lung. Santos FS^{1,2,3}, Moraes BPT^{1,2,4}, Silva KP⁵, Almeida MAP^{1,2,4}, Costa MF^{1,2}, Moraes-de-Souza I^{1,2}, Cunha CMCD^{1,2,4}, Bozza PT², Kaue FS^{1,2,3}, Brito MAMS¹, Castro-Faria-Neto HC², Ferrarini, SR⁴, Silva, AR^{1,2,4}, Gonçalves-de-Albuquerque CF^{1,2,3,4} ¹Unirio, Immunopharmacology Lab., Department of Physiological Sciences, Federal, Rio de Janeiro, Brazil, ²IOC-Fiocruz, Immunopharmacology Lab., Rio de Janeiro, Brazil, ³UFF, Postgraduate Program in Science and Biotechnology, Niterói, Brazil, ⁴UFF, PPG in Neurosciences, ⁵UFMT Post-Graduate Program in Health Sciences, Sinop, Brasil

A variety of diseases that culminate in lung inflammation, alveolar damage and pulmonary edema are called Acute Respiratory Distress Syndrome (ARDS) (LUYT et al.,2020). The effects of the lipid mediators of omega 3 eicosapentaenoic acid (EPA) and docosahexaenoic acid (DHA) may have the ability to promote a reduction in the number of cells related to inflammation by regulating tissue infiltration, exhibiting potent anti-inflammatory actions (Schwab et al., 2007; FERNANDES, 2020). The nanoencapsulation of polyunsaturated fatty acids is a promising system to promote the maintenance of their nutraceutical properties, protection against their oxidation, thus improving therapeutic efficacy (VIEIRA, et al., 2020). In this work we proposed that supplementation with nanostructured omega 3 DHA has a beneficial and protective effect on inflammatory lung disease induced by the component of Gram-negative bacteria LPS. **Methods:** Experimental model: Swiss male mice were submitted to intratracheal instillation of LPS. These animals received a intraperitoneal pre-treatment with nanostructured omega 3 (NanoDHA) 24 h before the instillation with LPS. The experimental model was approved by the Animal Experimentation Ethics Committee of IOC (CEUA-IOC) under license L-005/2023. Collection of bronchoalveolar lavage (BAL): One day after the exposure to LPS, the mice were eutanized and the BAL collected for total and differential leukocyte counts and protein measurement. Statistical Analysis: Data were analyzed by analysis of variance (one-way ANOVA) followed by the Bonferroni test, with p values < 0.05 considered significant. **Results:** We observed a significant decrease in the number of leukocytes in the NanoDHA+LPS compared to the LPS group, characterized by a significant decrease in the number of mononuclear cell. NanoDHA also decreased the total protein content, as compared to LPS group. **Conclusion:** Preliminary results show a significant reduction in accumulation of the main cells linked to inflammatory processes in bronchoalveolar lavage and protein extravasation. These effects encourage further analysis to better understand how nanostructured omega 3 affects the inflammatory process in the lung. Research on preventive and therapeutic measures is relevant in the current global health scenario. **References:** 1. LUYT, Intensive care medicine, v. 46, p. 2168-2183, 2020. 2. SCHWAB. Nature, v. 447, n. 7146, p. 869-874, 2007. 3. FERNANDES, Programa de Pós-Graduação em Ciência da Saúde, 2020. 4. VIEIRA, Maiana da Costa et al. Revista de Nutrição, v. 33, 2020. **Acknowledgments:** UNIRIO, IOC, FIOCRUZ, CAPES, PPBI, PPGNeuro, FAPERJ and CNPq.

04.048 Fetal Programming by in utero Food Restriction: Implications in The Response to Inflammatory Bowel Disease. Soares AW¹, Azevedo GA¹, Candido CS², Lippi BK², Negreiros NGS², Landgraf MA³, Landgraf RG². ¹Unifesp-EPM, Dpt. of Medicine, São Paulo, Brazil, ²Unifesp-Diadema, Dpt. of Pharmaceutical Sciences, Brazil. ³Unip-Santos, Brazil

Introduction: Inflammatory bowel disease (IBD) is a chronic and inflammatory condition that affects the intestine, being classified into ulcerative colitis (UC) and Crohn's disease (CD). Nowadays, there is an increase in the incidence of IBD, especially in developing countries. Dietary restriction during pregnancy, in addition to impairing fetal growth, exposes the fetus to high concentrations of maternal glucocorticoids, and this intrauterine environment can program the development of diseases in adult life. Changes in nutrient availability during the intrauterine period could lead to epigenetic changes, increasing susceptibility to chronic diseases in adult life. Considering that the epigenetic mechanisms are crucial in the cellular response to the environment and to endogenous stimuli, as they contribute to the stability of the chromatin structure, to the integrity of the genome, to the modulation of the expression of tissue-specific genes, among others, we formulate the hypothesis that molecular mechanisms, including epigenetic alterations resulting from global malnutrition, are involved in the attenuation of the inflammatory response already observed by our group. **Methods:** After fetal programming and offspring weaning, the animals were divided into 4 groups: 02 control groups; Normal Birth Weight (NBW), Low Birth Weight (LBW) and 02 groups that underwent disease induction; NBW+DSS and LBW+DSS. Experimental acute colitis was induced in male Wistar mice by administering 3% DSS in the drinking water for six days. Body weight, the consumption of water and feed, and the presence of blood in the stool were monitored. On the 7th day, the animals were euthanized, and the colon removed for cytokines and pro-inflammatory proteins analysis. **Results:** Although there was no statistical difference in the percentage of weight loss, feed, water and water+DSS consumption between the groups, we observed that the Clinical Disease Activity Index was higher for the NBW+DSS group compared to the others and correlated significantly with pathological changes in the acute phase of the disease. This can be confirmed with the increase in COX-2 expression observed in the same group. **Conclusion:** The results indicate that NBW (normal birth weight) animals have a more intense experimental intestinal inflammatory response. The discrepancy in clinical signs of the disease contributes to a complex scenario of adaptations and metabolic changes, which may increase the risk of secondary chronic diseases often seen in inflammatory bowel diseases (IBD). **Financial Support:** FAPESP (2020/16020-4), CNPq and CAPES.

04.049 Evaluation of the anti-inflammatory effect of hydrogen sulfide (H₂S) donor on experimental asthma in mice submitted to precocious ovulation. Francelino Alves V¹, Melhado IV², Ribeiro MR¹, Prata de Oliveira J¹, Dallazen JL¹, Kiataki LGS¹, Teixeira SA¹, Oliveira MA¹, Frajblat M⁴, Caliendo G³, Severino B³, Moriya H T², Muscara MN¹, Pereira Costa SK¹, Tavares-de-Lima W¹ ¹ICB-USP, Dept. of Pharmacology, São Paulo, Brazil, ²EP-USP, Dept. of Telecommunication and Control Engineering, São Paulo, Brazil, ³University of Naples, Dept of Pharmacy, School of Medicine, Napoli, Italy, ⁴UFRJ, Brazil

Introduction: Asthma is a chronic inflammatory airway disease with a high prevalence in women after puberty. Clinical evidence indicates that women who had early menarche (before 8 years old) are more prone to develop asthma. In previous cohort studies, lung inflammation was increased in women that developed early menarche. In previous studies of our laboratory, we found that precocious ovulation (PO) exacerbated the murine allergic lung inflammation. Glucocorticoids (GC) are used in pharmacological asthma management although the risk of side effects and resistance to GC treatment are also described. H₂S donors hybrid drugs represent an opportunity to reduce the adverse effects of glucocorticoids in asthma.

Objective: To Evaluate the effects of the treatment with 4-hydroxy-thiobenzamide (TBZ), an H₂S donor and hybrid molecule [H₂S donor and prednisone (Pred)] on lung inflammation and respiratory mechanics of female mice upon PO. **Methods:** Induction of precocious ovulation: Female Balb/C mice (21 days old) received 5 IU of eCG (ip) and 2 days after 5IU of hCG by the same route, referring to the first of three cycles of administration. The animals were sensitized with ovalbumin (OVA) 24 h after the end of the 3rd cycle of induction (day 0). OVA challenges were performed by intranasal route (days 14, 21 and 28) Before the challenges (30 min), the animals were treated with equimolar doses of Pred (5,5 mg/kg), hybrid molecule (9,1 mg/kg) or TBZ (3,6 mg/kg) by gavage and 24 h after de last OVA-challenge the studies were carried out. Respiratory mechanics parameters were determined using FlexiVent (SCIREQ® Montreal, Quebec, Canada) after methacholine (MCh) provocation. Lung inflammation was characterized by cells present in bronchoalveolar lavage (BAL). Data are expressed as mean ± SEM and were analyzed by two-way ANOVA followed by Tukey post-test (*p<0.05). **Results:** BAL of allergic mice under PO (PO-OVA), revealed a significant increase in total cells compared to animals under PO challenged with PBS (PO-PBS), (PO-OVA: 183.00±39.65* (n=8) vs PO-PBS: 24.62±4.44, x 10⁴ cells/mL (n=8)). PO-OVA treated with Pred, TBZ or Hybrid molecule presented a significant reduction of total cells (X10⁴ /ml) compared to control animals (PO-OVA: 183,00 ± 39.65 vs PO-OVA-Pred: 35.25 ± 12.42* (n=6), PO-OVA-TBZ: 81.71 ± 11.30* (n=7) and PO-OVA-Hybrid molecule: 61.47 ± 14.61* (n=8). Eosinophils count also increased in the PO-OVA group relative to PO-PBS group (PO-OVA: 146.00±35.74* vs PO-PBS: Not detected). The PO-OVA groups treated with Pred, TBZ or Hybrid molecule showed a significant decrease in the number of eosinophils (PO-OVA: 146.00 ± 35.74 versus PO-OVA Pred: 26.51 ± 11.17*, PO-OVA-TBZ: 63.57 ± 10.01* and PO-OVA-Hybrid molecule: 40.03 ± 10.26* x 10⁴ cells/mL). Lung resistance of PO-OVA revealed a significant increase in comparison to PO-PBS animals (PO-OVA: 5.38± 1.08 (n=11) vs PO-PBS: 1.33 ± 0.12* (n=13) cmH₂O.s/mL). Mice treated with Pred, TBZ or Hybrid molecule, showed a significant decrease in RL (PO-OVA: 5.38± 1.08 vs PO-OVA-Pred: 1.94± 0.17* (n=8), PO-OVA-TBZ: 3.30 ± 0.35* (n=7) and PO-OVA-Hybrid molecule: 2.78±0.48* (n=8) cmH₂O.s/mL). **Conclusion:** Our data suggest that the hybrid molecule and TBZ demonstrate potential therapeutic effects to improve lung inflammation and lung hyperreactivity in allergic mice submitted to precocious ovulation. Besides, the hybrid molecule could constitute an alternative to asthma management preventing adverse effects of glucocorticoids. **References:** Corvino, A. J. Adv. Res., v. 35, p. 267, 2022. Macsali, F. Am J Respir Crit Care Med., v. 183, p. 8, 2011. **Financial Support:** CAPES and CNPq.

04.050 Assessment of Nicotine Lung Harmful Effects Triggered by Electronic-Cigarette Aerosol Exposure in Mice. Nobrega MECG, Cotias AC, Gomes HS, Lopes RR, Arantes ACS, Coutinho DS, Carvalho VF, Silva PMR, Martins MA IOC-Fiocruz, Lab. of Inflammation, Rio de Janeiro, Brazil

Introduction: Nicotine, a substance with a psychoactive and addictive effect, has potent pharmacological activities when inhaled. There is a rapid increase in electronic nicotine delivery systems (ENDS) under the argument that they could help minimize the harmful effects of tabagism. However, little is known about nicotine's effects on the lung airways. Our study aimed to compare the potential inflammatory impact of electronic cigarette (e-cig) aerosol, with or without nicotine, on the pulmonary airways of mice in a short-term condition of E-cig aerosol exposure. **Methods:** C57BL/6 female mice (6 - 8 weeks) were exposed to e-cig aerosol, for 1 h per day for 4 consecutive days. The system comprised a whole-body rodent exposure chamber into which aerosol from commercial e-liquid, infused or not with nicotine (20 mg/mL), generated by an ENDS device, was pumped. Mice were subjected to 160 E-cig puffs, 70 mL volume of aerosolized nicotine e-liquid using a cigarette smoke generator system commercially available (Data Sciences International, USA). Leukocyte counting in blood and bronchoalveolar lavage (BAL), lung tissue oxidative stress measurements, airway hyper-reactivity and some mechanical respiratory parameters (obtained via non-invasive whole body plethysmography technique) were evaluated 24 h after the last E-cig aerosol exposure. All protocols and procedures involving the use of animals were approved by the Oswaldo Cruz Institute Laboratory Animal Use Committee (license number: L002-2020-A3; Rio de Janeiro, Brazil). **Results:** Following aerosolized methacholine (150 mg/mL), mice exposed to nicotine-enriched aerosol presented reduced respiratory frequency rate (356.5 ± 22.56 breaths per minute (BPM) to 287.4 ± 22.11 BPM; mean \pm SEM, $n=5$; $p \leq 0,005$) and expiration peak (6.1 ± 0.7 mL/sec to 3.6 ± 0.2 mL/sec; $n=5$; $p \leq 0,005$), accompanied by increased expiration time (0.12 ± 0.01 sec to 0.19 ± 0.02 sec; $n=5$, $p \leq 0,005$), compared to those mice subjected to atmospheric (atm) air. In addition, aerosolization with nicotine, but not without nicotine, led to airway hyper-reactivity and leucocyte accumulation into the bronchoalveolar space (140.6 ± 29.0 cells $\times 10^3$ /BAL to 297.5 ± 38.9 cells $\times 10^3$ /BAL; $n=5$; $p \leq 0,005$) and lung tissue oxidative damage (0.28 ± 0.04 MDA/ protein mg to 0.71 ± 0.09 MDA/ protein mg; $n=5$; $p \leq 0,005$) 24 h after the fourth e-cig aerosol exposure session. Both aerosols, with and without nicotine, caused a significant decrease in the lung tissue catalase activity (5.5 ± 1.4 U/ protein mg in animals subjected to atm air to 1.0 ± 0.1 U/protein mg and 2.2 ± 0.2 U/protein mg, respectively; $n=5$; $p \leq 0,005$). **Conclusion:** Exposure to aerosol puffs generated by e-liquid containing 20 mg/mL nicotine for a short time (1 h per day for four consecutive days) is enough to demonstrate that the stimulus of inhaled nicotine is most likely able to promote harmful lung changes, such as leukocyte infiltration, airway hyper-reactivity and lipid-oxidative damage, all of which recognized as pivotal pathological features of tabagism. **Financial Support:** CNPq, FAPERJ and CAPES.

04.051 Identification of Interleukin-13 (IL-13) as a Biomarker in Workers Exposed to Silica Dust. Ferreira TPT¹, RIBEIRO PC², Arantes ACS¹, Guimarães FV¹, Castro-Faria-Neto HC³, Martins MA¹, Castro HA² Silva PMR¹ ¹IOC-Fiocruz, Lab. of Inflammation, ²ENSP-FIOCRUZ, Center for Studies on Workers Health and Human Ecology, ³IOC-Fiocruz, Lab. of Inflammation, Rio de Janeiro, Brazil Rio de Janeiro, Brazil

Introduction: Occupational exposure to respirable crystalline silica is one of the most common and serious risks. Silicosis is a progressive, irreversible, and incurable fibrotic lung disease. Interleukin 13 (IL-13) is a profibrotic cytokine responsible for Th2 responses in humans. In this study we evaluated the potential involvement inflammatory cytokines, mainly focusing on IL-13, as biomarkers in silica-exposed subjects. The reactivity of peripheral blood leukocytes was also evaluated “in vitro”. **Methods:** A total of 60 subjects were included in the study, 29 workers exposed to silica particles and 31 unexposed volunteers as controls. Major respiratory symptoms (dyspnea and coughing), including smoking habits and former work exposure, were recorded on a standardized questionnaire. Plasma samples from the individuals were obtained, and cytokines/chemokines were determined by antibody-based multiplex immunosorbent assay kit. Peripheral blood mononuclear cells (PBMC) and polymorphonuclear neutrophils (PMN) were isolated and, then incubated with phorbol-12-myristate-13-acetate (PMA, 40 µg/mL), LPS (1 µg/mL) and silica (300 µg/mL) “in vitro”. Quantification of cytokines, reactive oxygen species (ROS) and neutrophil extracellular traps (NET) were performed by ELISA, intracellular probe CM-H2DCFDA and Sytox Green, respectively. This study was approved by the Clinical Research Ethics Committee of Sergio Arouca National School of Public Health/FIOCRUZ (CAAE: 46140821.8.3001.5248), and consent was signed by each participant. **Results:** Symptoms of exposed workers to silica dust included coughing and dyspnea. Increased levels of the cytokine IL-13 were detected in the plasma of silica-exposed workers as compared to the unexposed volunteers. IL-7, MIP-1alpha, IP-10 and eotaxin levels were also elevated in the exposed workers. Based on “in vitro” assays, we showed that PBMC from exposed workers spontaneously released higher levels of IL-6, than those from unexposed controls. Activation with LPS, but not silica particles, increased IL-6 production in PBMC from exposed workers, though there was no difference in comparison to those from the controls. In line, we found that ROS generation and NET release were spontaneously elevated in the PMN from silica-exposed workers. Activation with PMA or LPS, but not silica, increased ROS production, with more pronounced response detected in cells from the exposed workers. For NET, when PMN from exposed workers were activated with PMA and LPS, they showed lower response as compared to those from controls. No difference was noted when comparing the response of PMN from both exposed and controls, under conditions of silica stimulation. **Conclusion:** Our results show, for the first time, the presence of increased levels of the cytokine IL-13 in the plasma of silica-exposed workers. Moreover, blood PMNs showed a primed state characterized by elevated ROS production and NET release, suggesting that IL-13 and/or neutrophils might be considered as biomarkers in the case of workers exposed to respirable silica dust. **Financial Support:** FIOCRUZ, FAPERJ, CNPq.

04.052 The Role of the Renin-Angiotensin System on the Hyperactivity of the Hypothalamus-Pituitary-Adrenal Axis in a Mouse Model of Type 1 Diabetes. Chaves AS, Magalhães NS, Silva PMR, Martins MA, Carvalho V IOC-Fiocruz, Lab. of Inflammation, Rio de Janeiro, Brazil Rio de Janeiro, Brazil

Introduction: Diabetes Mellitus (DM) is a chronic metabolic disease characterized by reduced insulin production and increased levels of glucocorticoid hormones (GC) [1]. Chronically, increased circulating GC levels are related to the development of diabetes comorbidities, including impaired wound healing, and neuropathy [1,2]. The hyperactivity of the hypothalamus-pituitary-adrenal (HPA) axis in DM occurs in parallel to the hyperstimulation of the renin-angiotensin system (RAS), since diabetic individuals have increased circulating levels of angiotensin (Ang) II [3]. Thus, our objective was to investigate the role of the RAS in the hyperactivity of the HPA axis in diabetic animals. **Methods:** Diabetes was induced by a single intravenous injection of alloxan in male Swiss-Webster mice, and the animals were treated with the ACE inhibitor, Captopril, AT₁ antagonist, Olmesartan, AT₂ antagonist, PD123319, and/or AT₂ agonist, CGP42112A, for 14 consecutive days, starting 7 days after diabetes induction. **Results:** Our results show that the treatment with Captopril reduced plasma Ang II (7.17±2.12; 7.12±0.943; 18.1±2.39; 8.78±1.25 of non-diabetic plus saline, non-diabetic treated with Captopril, diabetic plus saline and diabetic treated with Captopril, respectively; mean ± SEM; n=6; p<0.05) and corticosterone levels (349±51.9; 345±69.7; 2282±389; 659±120 of non-diabetic plus saline, non-diabetic treated with Captopril, diabetic plus saline and diabetic treated with Captopril, respectively; mean ± SEM; n=6; p<0.05). Furthermore, Olmesartan also reduced HPA axis hyperactivity by reducing plasma corticosterone levels (340.6±75.73; 732.2±134.6; 28304±1854; 10650±1827 of non-diabetic plus saline, non-diabetic treated with OLM, diabetic plus saline and diabetic treated with OLM, respectively; mean ± SEM; n=7; p<0.05). The ACE inhibitor and AT₁ antagonist reduced the steroidogenesis machinery by reducing the expression of 11βHSD1, StAR and MC2R in the adrenals of diabetic animals. In parallel, we observed, in the pituitary gland of diabetic mice, that ACE inhibitor decreased the expression of GR, POMC and the number of ACTH positive cells. In addition, we showed that AT₁ antagonist reduced ACTH expression in the pituitary of the diabetic mice. We also observed that AT₂ antagonist blocked the inhibitory properties of Olmesartan on the corticosterone production in diabetic animals. Treatment with AT₂ agonist was not able to alter the expression of StAR and MC2R in the adrenals of diabetic mice, but the treatment reduced the circulating levels of corticosterone (1024±382; 496±335; 12187±2850; 4554±1009 of non-diabetic plus saline, non-diabetic treated with CGP, diabetic plus saline and diabetic treated with CGP, respectively; mean ± SEM; n=5; p<0.05). In conclusion, our findings show that RAS modulation through ACE inhibitor, AT₁ blocker or even AT₂ agonist were able to inhibit the HPA axis hyperactivity in diabetic mice. Therefore, the repositioning of ACE inhibitors or ARBs, and even the use of AT₂ agonists are interesting therapeutic strategies for the treatment of diabetes comorbidities associated with hypercortisolism. **References:** 1 Torres, RC; Prevatto, JP; Martins, MA; Silva, PM, Frias, VC. Type-1 diabetes HPA axis to the disease complications. J Diabetes Metab [internet]. 2013; 2 Burford N, Webster N, Cruz-Topete D. Hypothalamic-Pituitary-Adrenal Axis Modulation of Glucocorticoids in the Cardiovascular System. Int J Mol Sci [Internet]. 2017 Oct 16;18(10): 2150.

04.053 IL10-Induced STAT3/NFκB Crosstalk Modulates Pineal and Extra-Pineal Melatonin Synthesis. Córdoba-Moreno MO, Markus RP, Fernandes PACM USP, Dept of Physiology, São Paulo, SP, Brazil

Introduction: Immune-pineal axis activation adjusts relevant processes in assembling immune responses (Markus, RP. *Int. J. Mol. Sci.*, v. 22, p. 12143, 2021). NFκB activation by pro-inflammatory cytokines inhibits the pineal while inducing immune-competent cells' melatonin synthesis. Cytokines activating de JAK/STAT pathways, such as IFN-γ (Barbosa-Lima, LE. *J. Pineal Res.*, v. 67, p. e12599, 2019) and IL10 (Córdoba-Moreno MO. *Sci. Rep.*, v. 10. P. 4799, 2020), modulate melatonin synthesis in the pineal, bone marrow (BM), and spleen. The stimulatory effect of IFN-γ upon the pineal gland depends on STAT1/NFκB interaction (Barbosa-Lima, LE. *J. Pineal Res.*, v. 67, p. e12599, 2019), but the mechanisms controlling IL10 effects on melatonin synthesis remain unclear. **Methods:** Here, we evaluated the roles of STAT3 and NFκB activation by IL10 (3 - 100 ng/mL) upon the expression of melatonergic enzymes (Serotonin N-Acetyltransferase, SNAT; and Acetylserotonin O-Methyltransferase, ASMT), N-acetylserotonin (NAS) and melatonin synthesis by rats' pineal gland, BM, spleen, and peritoneal cells. ASMT, SNAT, (P)STAT3 and NFκB expression and cellular localization were determined by image-associated flow-cytometry (AMNIS flowsight) and the functional roles of the transcriptional factors were assessed using specific blockers (PDTC for NFκB, and Curcubitacin I for STAT3). NAS and melatonin production were determined by ELISA or HPLC. All procedures were approved by the CEUA of the Institute of Biosciences (license numbers 207/2014 and 253/2016) **Results:** The results show that IL10-induced interactions of (P)STAT3 with specific NFκB dimmers lead to different effects upon the melatonergic system depending on the cell type analyzed. IL10 increases the pineal's ASMT, NAS, and melatonin content via nuclear translocation of NFκB/STAT3. In BM, the nuclear translocation of STAT3/p65-NFκB complexes increases ASMT expression and melatonin content. Increased PSTAT3/p65-NFκB nuclear translocation in the spleen enhances (P)SNAT expression and melatonin content. Conversely, in peritoneal cells, IL10 leads to NFκB p50/p50 inhibitory dimer nuclear translocation, decreasing (P)SNAT expression and melatonin content. **Conclusion:** IL10's effects on melatonin production are cell-dependent and controlled by differential interactions between NFκB subunits and (P)STAT3. The data open the possibility for further investigations assessing variations of IL10 levels and downstream pathways during immune responses as critical regulatory factors adjusting pineal and extra-pineal synthesis of melatonin. **Financial Support:** FAPESP: 2010/52687-1; 2013/13691-1 and CNPq: 3778555/2013-8; 304637/2013-0; 480097/2013-5.

04.054 Anti-Inflammatory Potential of Uvaol in Human Epithelial Cell Line A549 Via *in-vitro* and *in-silico* Approaches. Santana JR, Barros ABB, Ferreira EGA, Viana RS, Silva JP, Barreto E UFAL

Introduction: Uvaol, a triterpene present in olives and virgin olive oil, has been shown anti-inflammatory and immunomodulatory properties which have exhibited interesting similarities with the effects of glucocorticoids (GCs). To investigate the potential mechanisms of this triterpene, we used *in vitro* and *in silico* approaches to evaluate the activation of the glucocorticoid receptor (GR). **Methods:** A549 cells were grown in DMEM medium supplemented with 2% fetal bovine serum, 1% penicillin/streptomycin, and 2 mM L-glutamine and maintained in a humidified incubator at 37°C with 5% CO₂. Uvaol and TNF- α were purchased from Sigma Chemical (St Louis, MO, USA). Cells were pre-treated with uvaol (1 and 10 μ M) 1 h before stimulation with 50 ng/mL TNF- α for 24 h. Pro-inflammatory cytokines secretion was evaluated by ELISA. Additionally, cell viability was measured by MTT assay. The molecular docking and molecular dynamic simulations of GR-ligand complexes formed between the ligand binding domain of GR with cortisol (a natural steroid) or uvaol were carried out. Statistical differences were significant at $p < 0.05$ analyzed by one-way ANOVA and Tukey's test. **Results:** Exposure of A549 cells to TNF- α induced a marked increase in the secretion of IL-6 (about 32-fold, $P < 0.001$) and IL-8 (about 10-fold, $P < 0.001$) after 24 h. TNF- α -stimulated A549 cells and treated with uvaol at 1 and 10 μ M exhibited a reduction in the secretion of the inflammatory mediators IL-6 (in 37% and 46%, respectively) and IL-8 (in 53% and 62%, respectively). Dexamethasone, used as a reference drug (1 μ M), also inhibited the secretion of IL-6 (65%) and IL-8 (57%). The concentrations used for uvaol had no significant influence on cell viability. *In-silico* molecular docking simulation showed that uvaol present stable interaction to the active site of GR showing a binding affinity of -7.3 Kcal/mol to GR, while the natural ligand cortisol binding affinity by GR was of -7.0 Kcal/mol. **Conclusion:** Our findings suggest that the uvaol inhibited the TNF- α -induced inflammatory response by a mechanism that affects the secretion of IL-6 and IL-8. Molecular docking calculations gave an indication that uvaol could interact with GR and act as a glucocorticoid receptor modulator against inflammation. **Financial Support:** CNPq, CAPES, BioproFar-BA, and FAPEAL.

04.055 Evaluation of the Potential of Angiotensin 1-7 - MAS Receptor Agonist - as a Therapeutic Alternative in Coronavirus-Induced Infection. Lima EBS¹, Zaidan I¹, Monteiro AHA², Cardoso C², Carvalho AFS¹, Lara ES¹, Souza JAM¹, Augusto IL³, Caixeta RS³, de Oliveira LC³, Costa VV⁴, Teixeira MM⁴, Sousa LP^{1,2,3}. ¹UFMG, PPG Clinical and Toxicological Analysis, Belo Horizonte, Brazil, ²UFMG, PPG Pharmaceutical Sciences, Belo Horizonte, Brazil, ³UFMG, Dpt. of Clinical and Toxicological Analysis, Belo Horizonte, Brazil, ⁴UFMG Belo Horizonte, Dpt. of Biochemistry and Immunology, Brazil

Introduction: Exacerbated inflammatory response plays a crucial role in the progression and severity of acute respiratory syndrome (SARS) induced by the murine betacoronavirus MHV-3. The viral infection triggers a robust inflammatory response, leading to acute lung injury and significant impairment of the respiratory function. After lung infection, the virus spread systemically resulting in high viral loads in multiple organs and severe systemic disease, in which causes the death of all mice within 6-7 days post-infection (dpi). In this study, we have evaluated the effect of systemic administration of Angiotensin-(1-7)-[Ang-(1-7)], a peptide of the contra-regulatory arm of the Renin-Angiotensin System (RAS) endowed with anti-inflammatory and pro-resolving properties, on the overwhelming inflammation and tissue damage induced by MHV-3 infection. **Methods:** We used 6-week-old male C57BL/6 WT mice infected intranasally (i.n.) with 3×10^3 PFUs of MHV-3. After 12-, 24-, 36-, and 48-hours post-infection (hpi) (short protocol) or by 12/12 h until 96h (long protocol) mice were treated with vehicle (Saline + or DMSO intraperitoneally, i.p.) or Ang-(1-7) (30ug/kg/animal, i.p.). Mice were euthanized three or five days after infection and samples were harvested for analysis of the inflammatory profile in bronchoalveolar lavage. Another group of mice was used to evaluate the lethality rates after Ang-(1-7) treatment of MHV-infected animals. To this, mice were infected with 1×10^2 PFUs of MHV-3 (i.n.) and treated with vehicle or Ang-(1-7) by 24, 48, 72, 96, and 120 hpi (30ug/kg/animal, i.p.). **Results:** Treatment with Ang-(1-7) reduced leukocyte infiltration into the alveoli of mice, compared to untreated animals, which was mainly characterized by a decrease in mononuclear cells in both protocols applied. Additionally, Ang-(1-7) treatment reversed the pronounced blood lymphopenia characteristic of MHV-3 infection at the 3dpi and decrease the systemic levels of IL-6 at 5dpi, without effect in virus titers in lungs. Notably, the administration of Ang-(1-7) was able to rescue approximately 50% of mice from MHV-induced lethality and also resulted in a recovery of 20-25% of body weight compared to untreated animals with Ang-(1-7). **Conclusion:** Our data suggest that treatment with Ang-(1-7) was effective in protecting the host by modulating the inflammatory response, reducing mortality, and promoting weight recovery. **Financial Support:** CAPES, 23038.003950/2020-16; CNPq, PQ-306789/2018/3. and Fapemig, BPD-01010-22/ 30338.

04.056 The Immunoregulatory Function of Mesenchymal Stem Cell on Macrophages is Affected by Zinc. Makiyama EN, Freitas S, Fock RA FCF-USP, Dept of Clinical and Toxicology Analyses, School of Pharmaceutical Sciences, University of São Paulo, São Paulo, Brazil

Introduction: Mesenchymal stem cell (MSCs), also known as mesenchymal stromal cells, are important pluripotent cells that can differentiate into osteoblast, chondrocyte, adipocyte, have abilities of self-renewal and regulates the hematopoietic niche [1, 2]. Nowadays, much has been discussed of their therapeutic capacity, the immunomodulatory activity acting on the regulation of inflammation producing growth factors, cytokines and chemokines. Otherwise, there are highlights the search for compounds that have the ability to increase the immunomodulatory potential of MSCs [3, 4]. It's known that micronutrients have immunomodulatory effects and softens the effects of many diseases, and deficiency of micronutrients like zinc (Zn) can promote immune dysfunctions and infections [5, 6]. In this way, this study aims to understand immunomodulatory aspects of MSCs that may be influenced by the action of Zn. **Methods:** MSCs of mice lineage called C₃H₁₀T_{1/2} (ATCC CCL-226), was treated with and without Zn²⁺ and stimulated or not with 1,25µg/mL of LPS. After 24 hours the supernatants were collected and measured the levels of nitric oxide (NO); Interleukin 6 (IL-6) and Transforming growth factor beta 1 (TGF-β1). Additionally, to attempt whether the factors secreted by MSCs plays some role in the production of inflammatory cytokines of other immune cells, we evaluated mice lineage macrophages (Raw264.7; ATCC TIB-71) stimulated with LPS for 24h, and then was measured the level of IL-6; Interleukin 12 (IL-12). **Results:** We observed that Zn reduced the production of NO in MSCs. Additionally, when MSCs are stimulated with LPS the amount of IL-6 produced the production is lower in cells cultivated with Zn. About the production of TGF-β1, no differences were observed between groups. When Raw264.7 cells were stimulated with LPS and cultivated with the supernatant from MSCs was possible to observe that the supernatant from MSCs cultivated with Zn has the potential to reduce the production of IL-6 and IL-12 by these macrophages. **Conclusion:** At the time we can conclude MSCs treated with Zn have potential to reduce inflammatory cytokines, also acting as immunosuppressive on Raw264.7 cells, with ability to reduce the production of IL-6 and IL-12 by these cells when stimulated with LPS. **References:** [1] Wang, S. *J. of Hematol. Oncol.* V.5 P.19 2012; [2] Wang Y. *Nature Immunology* Vol.15 p. 1009-1016. 2014.; [3] Wang Y. *Nature Immunology* Vol.15 p. 1009-1016. 2014; [4] Wang Y. *Nature Immunology* Vol.15 p. 1009-1016. 2014; [5] Dhawan, M. *Annals of Med. And Surg.* V.77 P.1 2022. ; [6] Jiang, W. *Cell Proliferation.* V.53, P.1, 2020. **Funding Support:** Conselho Nacional de Desenvolvimento Científico e Tecnológico CNPq and Fundação de Amparo à Pesquisa do Estado de São Paulo FAPESP

05. Pain and Nociception Pharmacology

05.001 *In Silico* and *in vivo* Analysis of Terpinolene's Antinociceptive Mechanisms in Neuropathic Pain Induced by Paclitaxel. Cavalcante KDM¹, Acha BT^{1,2}, Pimentel VD², Ferreira PMP^{1,2}, Sousa DP³, Almeida FRC², Dittz D^{1,2}. ¹UFPI, Lab. of Experimental Cancerology, Brazil, ²UFPI, PPG Pharmacology, Brazil; ³UFPB, Lab. of Pharmaceutical Technology, Brazil

Introduction: Nociceptive pain is triggered by persistent stimuli, as in cancer treatment. Hence, neuropathic pain derived from chemotherapy-induced peripheral neuropathy (CIPN) is one of its main complications. This condition is the main dose-limiting side effect of taxanes such as paclitaxel (PTX) and negatively affects patients' quality of life, limiting cancer treatment. Natural molecules such as terpinolene (TPO) have shown to demonstrate antinociceptive activity in neuropathic pain induced by the partial sciatic nerve ligation model. This work aimed to evaluate the antinociceptive activity of TPO in a murine model of PTX-induced neuropathic pain. **Methods:** In Swiss mice, neuropathic pain was induced by administration of PTX (2 mg/kg, i.p.) for 4 consecutive days. Then, animals were treated daily with TPO (50, 100, and 200 mg/kg, p.o), vehicle (2% Tween 80 and 0.9% NaCl, p.o.) or pregabalin (10 mg/kg, p.o.) up to 11 days. Mechanical nociception was assessed by the von Frey test in neuropathic pain induction, and acute and sub-acute TPO antinociceptive activity evaluation. In order to verify molecular interactions between TPO with target receptors involved in neuropathic pain, molecular docking studies were performed using AutoDockVina and BIOVIA Discovery Studio. Finally, the antinociceptive mechanism of TPO was also verified through the measurement of superoxide dismutase (SOD), glutathione reductase (GSH) and malondialdehyde (MDA) assay. **Results:** The subacute treatment with TPO as well as the positive control pregabalin significantly (*p<0.05) increased the mechanical nociceptive thresholds in neuropathic animals. TPO at 200 mg/kg showed the best result by approaching threshold levels of the Sham group and increasing 30 times (17th and 19th days) the mechanical nociceptive threshold of neuropathic animals when compared to the vehicle group (negative control) (*p<0.05). Molecular docking analysis showed that TPO has favorable interactions with the type 3 serotonin receptor (5-HT₃) (*p<0.05) and the $\alpha 2\delta$ subunit of voltage-gated calcium channels when compared with its control ligands, bufotenin and pregabalin. TPO (200 mg/kg) also restored GSH levels in the animal's serum. Its antinociceptive effect was reversed by pretreatment with naloxone, ketanserin, ondansetron, L-arginine and glibenclamide, suggesting the role of opioid and serotonergic system, L-arginine/nitric oxide pathway and K⁺-ATP channels. **Conclusion:** TPO displays antinociceptive activity by increasing mechanical nociceptive threshold of animals with CIPN and showed favorable molecular interactions with 5-HT₃ receptor and $\alpha 2\delta$ subunit of voltage-gated calcium channels. Moreover, serotonergic and opioid systems, K⁺-ATP channels as well as L-arginine/nitric oxide pathway are involved in TPO antinociceptive mechanisms in CIPN. **Support:** CAPES and CNPq.

05.002 Antinociceptive and Antioxidant Activities of Terpinolene in a Paclitaxel-Induced Neuropathic Pain Model and its Antiproliferative Effect on Human Breast Cancer Cells.

Paixão MS¹, Acha BT^{1,2}, Cavalcante MSC^{1,2}, Ferreira PMP^{1,2}, Sousa DP³, Almeida FRC², Dittz D^{1,2}. ¹UFPI, Cancerology Lab. - Federal University of Piauí, Brazil, ²UFPI PPG Pharmacology, Brazil,

Introduction: Chemotherapy-induced peripheral neuropathy (CIPN) is an adverse effect of most antitumor agents such as paclitaxel (PTX) and negatively impacts patient's quality of life. Bioactive molecules from natural products such as Terpinolene (TPO) show potential properties of reducing chemotherapy-induced peripheral neuropathy. In this study, we investigated the antinociceptive and antioxidant activity of TPO in neuropathic pain induced by PTX coupled with its antiproliferative effect against human breast cancer cells. **Methods:** CIPN was induced in swiss mice through the administration of PTX (2 mg/kg, i.p.) for 4 consecutive days. Then, animals were treated daily with TPO (50, 100 and 200 mg/kg, p.o.), vehicle (2% Tween 80 and 0.9% NaCl, p.o.) or pregabalin (10 mg/kg, p.o.) for 11 days. Mechanical (von Frey test), cold (acetone test) and thermal (hot plate test) nociception was assessed in CIPN, as well as in the evaluation of acute and sub-acute antinociceptive activity of TPO. GSH and MDA levels and SOD activity were quantified in serum of animals treated with TPO (200 mg/kg). The viability of normal human breast cells (MCF-10A), human breast tumor cells (MDA-MB-231) and neuroblastoma (U-87) as well as pharmacological interaction (isobologram analysis) between TPO and PTX against MDA-MB-231 was evaluated by resazurin assay. **Results:** TPO (50, 100 or 200 mg/kg) increased by up to 5-folds the mechanical nociceptive thresholds of animals, 180 and 240 min after treatment (acute protocol), compared to animals of vehicle group (*** $p < 0.001$). Moreover, the treatment with TPO (100 and 200 mg/kg) and pregabalin for 11 days (sub-acute protocol) promoted a significant increase in the mechanical, cold and thermal nociceptive threshold, compared with vehicle group (* $p < 0.05$) attaining threshold levels similar to sham animals. PTX reduced by 60% GSH levels, compared to the negative control group. In contrast, TPO (200 mg/kg) and pregabalin restored GSH levels, with values closer to sham group ($p < 0,05$). TPO or PTX did not alter MDA levels and SOD activity. The half-maximal inhibitory concentration (IC-50) of TPO on MDA-MB-231 cells was 338.5 $\mu\text{g/mL}$ and $> 1000 \mu\text{g/mL}$ in normal breast (MCF-10) and glioblastoma (U87) cells. Association of TPO and PTX showed synergic activity in reducing the MDA-MB-231 viability. **Conclusion:** TPO exhibits acute and subacute antinociceptive activity and restored GSH levels in CIPN induced by paclitaxel. Additionally, terpinolene demonstrate cytotoxicity and selectivity against triple negative breast cancer cells and acts synergically with paclitaxel in reduction of tumor cell viability. **Support:** CAPES and CNPq. **CEUA UFPI:** Protocol N° 736/2022

05.003 Effect of Maresin 2 Treatment on Neuropathic Pain, Depression, and Anxiety Associated with Experimental Diabetes. Oliveira G¹, Ferreira MV¹, Bonfim JPC¹, Verri WAJ², Zanoveli JM¹, Cunha JM¹. ¹UFPR, Dpt of Pharmacology, Curitiba, Brazil, ²UEL, Dpt of Patology, Londrina, Brazil,

Introduction: Neuropathy (DN) is the most prevalent complication of diabetes and often manifests as pain, one of the most incapacitating symptoms. Moreover, diabetic patients are more likely to develop psychiatric disorders, such as depression and anxiety which can further reduce the quality of life. The clinical management of these complications is a challenge due to their complex pathophysiology, which may involve common mechanisms such as neuroinflammation. Maresin 2 (MaR2), a pro-resolving lipid mediator, has exhibited antinociceptive, anti-inflammatory, and pro-resolving effects in models of inflammatory pain. However, the effects of MaR2 on diabetic animals remain unknown, which is the aim of this study. **Methods:** Experimental diabetes was induced by a single intraperitoneal injection of streptozotocin (STZ; 60 mg/kg) in male Wistar rats (weighing 180-240g). Animals with blood glucose levels equal to or greater than 250mg/dL were considered diabetic. Five experimental groups were conducted: normoglycemic treated with vehicle (NGL-VEH), diabetic treated with vehicle (DBT-VEH), or MaR2 (1, 3, 10 ng/rat i.p) from day 14 to day 27 of the experiment. Mechanical allodynia was assessed by an electronic Von Frey test (VFT) before STZ injection (baseline) and from day 14 to day 27 after STZ. The open-field test (OF), Elevated Plus-Maze (EPM), and the modified Forced Swim Test (mFST) were conducted on the 28th, 29th, and 31st, respectively. All experimental procedures were approved by Institutional Ethics on Animal Use (CEUA-BIO-UFPR #1108). **Results:** Compared to the NGL-VEH group, the DBT-VEH group exhibited: 1) an increase in blood glucose (403%); 2) a decrease in weight gain (79,7%); 3) a significant decrease in mechanical threshold (58,8%), starting 14 days after STZ and peaking at 4th week; 4) a decrease in locomotor parameter when evaluating the number of crossings in the OF; 5) Decrease in time spent on open arms (52%) and an increase in time spent on closed arms (18,7%) in the EPM; 6) Decreased mean counts when the swimming behavior was assessed in mFST (10,6%). When compared to the DBT-VEH group, only the experimental group treated with the highest dose of MaR2 (10 ng) showed a significant difference (15%) when the mechanical threshold was evaluated in the VFT. MaR2 treatment did not alter locomotor behavior when the number of crossings was evaluated in the OF. None of the doses of MaR2 was able to reduce anxious-like behavior in the EPM test, nor antidepressant activity in mFST. **Conclusion:** Our data, although partial, demonstrate an antinociceptive effect of MaR2 over the mechanical allodynia associated with experimental diabetes, without impairing locomotor behavior. Although no antidepressant or anxiolytic-related effects were observed after MaR2 treatment, further studies are necessary to comprehend its effects on diabetic neuropathy and other complications related to diabetes.

05.004 Effect of Zinc Dietary Restriction and Supplementation on Pain and Inflammation in Mice CFA Model. Silva MC, Poblete LS, Matias DO, Lima LMTR, Miranda ALP. UFRJ, Faculty of Pharmacy, Rio de Janeiro, Brazil

Introduction: Zinc (Zn) is the second most abundant metal in the human body and essential in physiological processes of the neurological and immune systems. The dyshomeostasis of essential metals such as Zn is related to changes in the inflammatory, immune and behavioral responses. Recent evidences shown a relevant role of Zn in inflammatory processes, such as effects in reducing the levels of pro-inflammatory cytokines, after oral administration of Zn, mainly TNF- α , and pain, reducing paclitaxel induced neuropathic pain (Yusuf S et al, Iran J Microbiol, 11, 2019; Luo J et al, J Neurosci, 38, 2018), and in addition, patients with chronic myofascial pain have lower intracellular stores of zinc and selenium and inadequate intake of these nutrients (Barros-Neto JA et al, PLoS One, 11(10), 2016). Recently, we have shown that a zinc restricted diet leads a pain signalling disruption promoting nociceptive but not inflammatory pain in weaned mice (Lima CKF et al, An Acad Bras Cien, 2023). **Objectives:** To evaluate the impact of dietary zinc restriction and supplementation on a model of subchronic pain and inflammation induced by Complete Freund's Adjuvant (CFA) in mice. **Methods:** Animals, divided in three groups ($n_{total}=9/group$), were submitted to 6 weeks of dietary zinc intervention: control diet (30 mg/kg of Zn), zinc deficient diet (11 mg/kg of Zn) and zinc enriched diet (150 mg/kg of Zn) (CEUA/UFRJ 086/21). CFA (20 μ l) was injected into mice right hind paw at the beginning of the 5th week to induce inflammation. Pain and inflammation parameters were analyzed for 2 weeks after CFA injection through behavioral experiments: mechanical hyperalgesia (von Frey filaments), Heat Thermal Hyperalgesia (Hargreaves), paw thickness (edema) and open field locomotor test. Euthanasia was done on the 15th day and plasma, plantar tissue, sciatic nerve, spinal cord were collected to further biochemical and histological analyzes such as protein dosages, TNF, MPO, IL-10, IL-6 and IL-1B. **Results:** The Zinc-deficient diet led to a lower body weight gain in the group of male animals compared to the control and zinc-supplemented groups. No difference between groups was observed for female. Differences in response to painful mechanical stimuli are also observed between males and females submitted to CFA. In all groups CFA induced intense mechanical (basal $1.85\pm 0.15g \times 0.14\pm 0.06g$; $*p<0.05$) and heat thermal hyperalgesia, and an increase in paw area (mm^2) for at least 7 days. Zn-deficient diet induced a more pain sensitive and inflammatory state of the animals, and the supplementation was not able to prevent inflammation by CFA. No difference was observed comparing with control diet group for the intervention period studied. **Conclusions:** Experiments carrying out biochemical analyses of inflammatory mediators and a study for a longer period of intervention are in course in view to better understand the modulation of inflammation by zinc and the benefit of a zinc supplementation for a long term. **Financial Support:** CAPES, CNPq, PIBIC/CNPq, FAPERJ.

05.005 *Schinus terebinthifolius* Essential Oil and its Main Component Delta-3-Carene Induce Antinociception Via Serotonergic Receptors. Santana GCS¹, Lima AA², Souza TA³, Silva MS³, Soares MBP^{2,4}, Viana MDM¹, Villarreal CF¹ ¹UFBA, School of Pharmacy, Salvador, Brazil, ²Fiocruz, Gonçalo Moniz Institute, Salvador, Brazil ³UFPB, João Pessoa, Brazil ⁴SENAI-CIMATEC Salvador, Brazil

Introduction: *Schinus terebinthifolius* Raddi. (Anacardiaceae) is a flowering plant species from South America. In Brazil, it occurs in the Atlantic Forest of the Northeast region, where it is popularly known as "pink pepper" (Lima, 2020). Its essential oil (EO) has been traditionally used by inhalation for control of painful conditions. However, the analgesic properties of this EO have not yet been scientifically proven. The present study evaluated the antinociceptive effect of *S. terebinthifolius* EO and its major compound, investigating its possible mechanism of action. **Methods:** Phytochemistry analysis of EO was carried out by gas chromatography coupled to mass spectrometry. For *in vivo* assays, Swiss male mice (CEUA IGM/FIOCRUZ 003-2022) were used. Mice were treated with saline 0.9% (control group) or *S. terebinthifolius* EO (Akã Essential Oils, 150-600 μ L) by inhalation route (Donatello, 2020). Morphine (5 mg/kg, intraperitoneal route) was the reference drug. The thermal nociceptive threshold was evaluated in the tail flick test (Leite-dos-Santos, 2012). To avoid misunderstanding, motor impairment was assessed by rota-rod test. The major compound in the EO was also evaluated in the tail flick test (1.5-25 mg/kg; orally). To study the mechanism of action, functional antagonism assays were performed with naloxone (non-selective opioid receptor antagonist; 1 mg/kg), yohimbine (α 2-adrenergic receptor antagonist, 2 mg/kg), or methysergide (non-selective serotonergic receptor antagonist; 5 mg/kg) by intraperitoneal route in the same model experimental. **Results:** Phytochemical analysis revealed Delta-3-Carene as the major compound (76.93%) of *S. terebinthifolius* EO. In the tail flick test, inhalation treatment with EO increased the nociceptive threshold at doses of 300 and 600 μ L. Motor alterations were not observed in any dose assessed by rota-rod test, which validates antinociceptive effect. For Delta-3-Carene, antinociceptive effect was observed up to 6.25 mg/kg - dose with maximum effect at 1.5h. In the functional antagonism assay, the antinociceptive effect of EO was reversed by pre-treatment with methysergide, but not with naloxone or yohimbine, suggesting that the mechanism of action of this essential oil involves serotonergic pathways. Corroborating this hypothesis, the antinociceptive effect of Delta-3-Carene was also reversed by methysergide. In fact, the serotonergic system is involved in pain processing and endogenous analgesia, representing an important target for the development of analgesics. **Conclusion:** The results demonstrated the antinociceptive effect of *Schinus terebinthifolius* EO, suggesting that this effect may be mediated, at least in part, by its major compound delta-3-carene acting in serotonergic pathways. This study is the first demonstration of the antinociceptive effects of *S. terebinthifolius* EO by inhalation route. Data presented here reinforce the traditional use of *S. terebinthifolius* for painful conditions. **Financial Support:** CNPq (INCT-RENNOFITO 465536/2014-0); CAPES (código 001); FAPESB (BioproFar-BA, PIE0009/2022). **Acknowledgment:** Akã Oils Essentials. **References:** Donatello, NN. *J. Neuroimmunol.*, v.15, p. 340, 2020. Leite-dos-Santos, GG. *Toxicon*, v. 60, p. 1005, 2012. Lima, MDCL. *Zebraf.*, v.17, p.112, 2020.

05.006 Pharmacological Effects of Cannabidiol in the Nitroglycerin (NTG)-Induced Migraine in Mice. Amaral FKCW¹, Stern CAJ¹, Nassini R², De Logu F², Silva RR¹, Rosa Filho SP¹, Werner MFP¹ ¹UFPR, Pharmacology, ²UNIFI, Clinical Pharmacology

Introduction: Migraine is a common and highly disabling neurobiological disorder. The pathophysiology is still not well understood, and the pharmacotherapy is not suitable for most patients, making evident the importance of studying new therapeutic approaches. Based on extensive research regarding the pharmacological properties of Cannabidiol (CBD) in addition to the treatment of epilepsy, CBD has become a promising research option for migraine therapy. Since there are few studies investigating the effect of isolated CBD and the possible mechanisms of action involved in migraine models, herein we investigated the pharmacological activity of CBD in NTG-induced migraine in mice. **Methods:** Male Swiss mice were treated intraperitoneally (i.p.) with vehicle (0.9 % saline) or cannabidiol (CBD) at doses of 1,3,10 and 30 mg/kg concomitantly with NTG 10 mg/kg or vehicle, 1 h before the assessment of periorbital mechanical allodynia (PMA). PMA was evaluated during 4 h, by applying von Frey monofilaments using the up and down method. To study the modulation of CBD in the NTG-induced PMA related to migraine mechanisms, mice were pretreated i.p. with nitric oxide synthase inhibitor (L-NAME, 40 mg/kg, 1 h); antagonist of CB1 receptors (AM251, 1 mg/kg), antagonist of CB2 receptors (AM630, 1 and 10 mg/kg), antagonist of 5-HT_{1A} receptors (WAY100135, 10 mg/kg), antagonist of PPAR_γ receptors (GW9662, 3 mg/kg) or vehicle via i.p. 30 min before concomitant application of CBD (10 mg/kg) and NTG or vehicle (i.p.). All values represented the 2nd h of PMA as well as by the pain face, or, so-called mouse grimace scale (MGS). **Results:** NTG evoked a sustained PMA reaching 94.92% at 2h (vehicle 0.77 ± 0.12 g), which was completely blocked by L-NAME (127.30%). In the dose-response experiments NTG elicited PMA at 2 h (96%), (vehicle: 1.10 ± 0.15 g) and CBD at doses of 1,3,10 and 30 mg/kg significantly reduced the PMA induced by GTN in 63%, 34%, 132% and 4%, respectively. Then, the dose of 10 mg/kg of CBD was chosen for all experiments. Further, mice pretreated with AM251 (1 mg/kg), AM630 (1 and 10 mg/kg) and WAY100135 (10 mg/kg) impair CBD-induced analgesia in GTN-provoked PMA by 96.70%, 87.95% and 68.66% and 88.57%, respectively, when compared to their respective control groups (GTN + vehicle). However, the PPAR_γ receptor antagonist did not revert the CBD-induced analgesia (100.45%) in GTN-provoked PMA (94.20%) (vehicle 0.89 ± 0.13). Additionally, we found significantly lower MGS scores in CBD 1 and 10 mg/kg, as well as in PPAR_γ receptor antagonist group when compared to NTG group (1.68 ± 0.47) (control: 0.08 ± 0.03). **Conclusion:** Our findings has been proven that CBD is effective against NTG-induced migraine. In addition, the blockade of CB1, CB2 and 5HT_{1A} receptors, indicate that multiple mechanisms may be involved with the effects of CBD in the NTG model of acute migraine in mice. More studies are needed to explore the underlying mechanisms of CBD for migraine treatment. **License number of ethics committee:** CEUA/BIO-UFPR: 1458. **Financial Support:** CAPES - Finance Code 001.

05.007 Evaluation of TRPV4 Channel Participation in a Type I Complex Regional Pain Syndrome Induced Nociception Model in Mice. Ruviaro NA¹, Rodrigues P², Peres DS², Frare JM², Trevisan G¹ ¹UFMS, PPG Biological Sciences: Toxicological Biochemistry, Brazil. ²UFMS, PPG Pharmacology, Brazil

Introduction: Complex regional pain syndrome type I (CRPS-I) is a common disabling pain condition that can occur after surgery, fractures, and limb trauma. One of the most common causes is through ischemia/reperfusion injury (Kessler, *NeuroRehabilitation*, v. 47, p. 253, 2020). Currently, there is still no adequate pharmacological treatment for CRPS-I chronic pain, making it necessary to search for new pharmacological targets. A possible target is the transient vanilloid potential receptor 4 (TRPV4) which is involved in the mechanisms that cause neuropathic and inflammatory pain (Iannone, *Neurosci. Lett.*, v.18, p.136380, 2022). The TRPV4 receptor is a non-selective calcium channel found in CNS cells, such as neurons and astrocytes, and is activated by mechanical stress, thermal and osmotic stimuli, and which can also be activated by endogenous chemical factors (Kumar, *Mol Neurobiol.*, v.55, p.8695, 2018). Thus, the present study aimed to evaluate the participation of the TRPV4 channel in an induced nociception model of CRPS-I in mice. **Methods:** Different behavioral tests were performed including von Frey (mechanical stimulus), acetone (cold thermal stimulus), hot plate (hot thermal stimulus), rotarod, open field, hind paw edema determination, and nest-building behavior. All tests were measured after the onset of post-ischemia chronic pain (CPIP, a model of CRPS-I). The induction of CPIP was performed by hind paw transient ischemia and reperfusion (De Prá, *Eur. J. Pharmacol.*, v.14. p.859, 2019). Briefly, after anesthesia, a nitrile O-ring was positioned around the mice left limb proximal to the ankle joint to act as a tourniquet for 2 hours. Then, after the O-ring removal, mice fully recovered within 30–60 minutes of reperfusion. Control mice were under anesthesia, and the O-ring was cut so that it only loosely surrounded the ankle without occluding the blood flow to the right hind paw. C57BL/6 male animals were used and test measurements were performed before (baseline) and on days 1, 5, 10 and 15 post-induction. Moreover, in the 15th day, the antinociceptive effect of a TRPV4 antagonist (HC-067047, 10 mg/kg, i.p) was also evaluated. All animals used were previously approved by Animal Research Ethical Committee of Federal University of Santa Maria (CEUA n°5749300620). **Results:** CPIP animals showed mechanical allodynia and thermal hypersensitivity from day 1 post-induction forward, compared to the control group, reaching the nociception peak of mechanical allodynia on the 15th day. Hind paw edema was observed in CPIP animals after reperfusion. The administration of HC-067047 showed an antinociceptive effect of 3h for thermal hypersensitivity and up to 2h for mechanical allodynia in CPIP animals. In addition, daily treatment with the receptor antagonist (HC-067047, 1 mg/kg, i.p) post-induction forwards, also showed antinociceptive effect on CPIP animals. No alterations in locomotor activity were observed. **Conclusion:** In conclusion, it was possible to demonstrate that the TRPV4 channel is involved in induced nociception in a mouse model of complex regional pain syndrome type I. **Financial Support:** CNPq and CAPES program.

05.008 Paclitaxel Induces Neurotoxicity in Human Sensory Neuron-Like Cell. Schiess MC¹, Silva GSA¹, Bufalo MC², Zambelli VO¹ ¹IBu, Lab. of Pain and Intracellular Signalization, Sao Paulo, SP, Brazil, ²IBu, Centre of Excellence in New Target Discovery, Sao Paulo SP, Brazil

Introduction: Paclitaxel (PTX) is a chemotherapy drug widely used to treat solid cancer. However, it frequently causes peripheral neuropathy, resulting in sensory abnormalities and pain in patients receiving treatment for cancer (Martin LG, Einstein, v. 9, p. 538, 2011). Mechanistically, PTX binds to and stabilize microtubules and, consequently, interrupts axonal transport, leading to an insufficient supply of ATP and increased oxidative stress. However, the molecular mechanisms involved in PTX-induced neurotoxicity in sensory neurons and, consequently, for the development of pain is unknown. Considering that culturing primary cells from the dorsal root ganglia requires a significant number of animals, we aimed to characterize the PTX-induced neurotoxicity in a model of human sensory neuron-like cells, derived from the neuroblastoma SH-SY5Y cell line. **Methods:** Sensory neurons-like cell were obtained from the culture and differentiation of SH-SY5Y cells in the presence of all trans-retinoic acid (10 μ M) and brain derived neuron factor (50 ng/mL). Cells were seeded in 75 cm³ flasks until 80% of confluence and 7x10³ neurons were transferred to 96 well plates in collagen matrix (100 mg/mL) for differentiation. The neurotoxic effect was evaluated in mature neurons treated with paclitaxel (0.025, 0.1, 0.25, 0.5, 1.0, 2.5 5.0 and 10.0 μ M) or control groups (culture media, DMEM/F12; culture media + vehicle). Cell viability was assayed by lactate dehydrogenase (LDH) release and inhibition of 3-(4, 5-dimethylthiazol-2-yl)2,5-diphenyl-tetrazolium bromide (MTT) reduction. **Results:** Increasing concentrations of PTX (0.5, 2.5 and 10.0 μ M) do not induce neurotoxicity when evaluated by MTT, 24h after incubation. However, 48h after PTX incubation, the concentrations of 0.5, 2.5, and 10.0 μ M decreased the neuron viability (80.2 \pm 2.9%*, \pm 1.4%*, 82.5 \pm 2.5%* vs 100%, respectively), when compared with control groups (*p<0.05, n=12, One-way ANOVA, Post-Test Tukey). Moreover, 72h of incubation with 0.5, 2.5, 5.0 e 10.0 μ M of PTX impaired the neuron viability (75.6 \pm 3.9%*, 66.4 \pm 5.5%*, 65.9 \pm 4.3%*, 56.4 \pm 3.3%* vs 100%, respectively) (*p<0.05, n=8, One-way ANOVA, Post-Test Tukey). Sensory neuron-like cells treated with PTX (0.5, 2.5, 5.0 and 10.0 μ M) displayed increased LDH leak, when compared to neurons treated with vehicle in 48h of incubation (~3.9 \pm 46.0* fold, 3.5 \pm 40.2* fold, 3.1 \pm 53.1* fold, 3.2 \pm 49.0* fold, respectively) (*p<0.05, n=6, One-way ANOVA, Post-Test Tukey) and 72h (~5.6 \pm 44.6* fold, 6.0 \pm 10.8* fold, 6.1 \pm 4.8* fold, 5.7 \pm 8.3* fold, respectively) (*p<0.05, n=3, One-way ANOVA, Post-Test Tukey). **Conclusion:** Our findings indicate that PTX induces neurotoxicity in sensory neurons-like cells. We established a useful model for studding the molecular mechanism involved in chemotherapy-induced neuropathy and, perhaps, for the management of painful conditions. **Financial Support:** FAPESP (n^o 2022/02779-4; n^o 2021/14831-8)

05.009 The role of the meningeal lymphatic system in the development of neuropathic pain. Castro RS, Anibal CES, Pigatto GR, Cunha TM FMRP-USP, Dept of Pharmacology, Ribeirão Preto, Brazil

Introduction: Neuropathic pain is characterized as a type of chronic pain resulting from an injury to the nervous system. The mechanisms involved in neuropathic pain are complex and involve peripheral and central phenomena. Some types of peripheral nerve injuries direct infiltration and activation of immune cells not only to the site of injury, but may also act to activate and recruit immune cells to the dorsal root ganglia of the spinal nerve (DRG) and to the spinal cord. A system of lymphatic vessels has recently been characterized in the meninges, with a postulated role in brain "cleaning" by draining cerebral fluid, during tissue homeostasis, the meninges support numerous immune sentinel cells, and in injury-induced inflammatory conditions. From the CNS, infections, autoimmunity or even neurodegeneration, immune cells derived peripherally or from the bone marrow of the skull bones infiltrate the parenchyma and alter the immune landscape within the meninges. As the meninges were considered an immune-privileged site, we hypothesized that modulation of the lymphatic system could affect neuropathic pain. To test this hypothesis, we will study the role of the meningeal lymphatic system under the nociceptive and inflammatory mechanisms of neuropathic pain. **Methods:** C57BL/6 (local ethics committee CEUA-FMRP/USP 096/2020) mice were submitted to the spared nerve injury (SNI) model of neuropathic pain, and behavioral tests were performed on days 3, 7 and 14. Next, the meninges were harvested from control and SNI groups 3, 7, and 14 days after SNI induction, processed and analyzed for qRT-PCR for the lymphatic markers, Lyve1, Prox1, and Vegfr3 genes normalized to Gapdh mRNA expression and the control group. Data were analyzed by Two-way ANOVA with a significance level set at 0.05. **Results:** Preliminary results showed that, over the time of evaluation, the gene expression of lymphatic vessel markers varied at different time points after SNI. Lyve1 and Vegfr3 expression increased significantly on day 14 after SNI (Two-ANOVA, Bonferroni's posttest, n=6, p<0,05) compared to days 3 and 7 after SNI, while Prox1 peaked at 3 days upon SNI induction (Two-way ANOVA, Bonferroni's test, n=6, p<0,05). **Conclusion:** Thus, preliminary results show a distinction regarding the role of lymphatic vessels in the development and maintenance of neuropathy. Therefore, further approaches are needed to determine the contribution of the lymphatic system in the onset and progression of neuropathic pain. **Financial Support:** Conselho Nacional de Desenvolvimento Científico e Tecnológico (Cnpq)

05.010 Study and Development of New Candidates for Anti-Inflammatory and Antinociceptive Drugs that Inhibit the P2X7 Receptor. Salles JP¹, Galvão RMS¹, Faria RX², Miranda ALP¹ ¹ LEFEx-UFRJ, Brazil; ²LAPSA-FIOCRUZ, Brazil

Introduction: Inflammation is an important mechanism that involves vascular and cellular components and a variety of soluble substances that aims to remove the response-inducing stimulus and initiate local tissue recovery. The ionotropic receptor P2X7 plays a significant role in inflammation and pain. The extracellular ATP binding to the receptor leads to cytokines release, such as IL-1b, IL-6, and TNF-a, which might promote cell death. Studies have reported P2X7 receptor involvement in the pathophysiology of several inflammatory diseases, in which its inhibition is a promising pathway since current treatments are associated with severe adverse effects. In this context, new selective P2X7 inhibitors with high potency in humans are needed. **Methods:** In this work, we selected two synthetic substances that exhibited high potency to functionally inhibit P2X7R *in vitro*. We investigated the action on acute and chronic models of inflammatory pain in *Swiss Webster* adult mice of both sexes (CEUA/UFRJ 054/22). In the 2.5% formalin-induced hyperalgesia model, the animals were divided into 5 groups: vehicle, indomethacin, morphine, PMM 75-17, and PMM 100-17. The tested substances were administered orally at 0,1, 1, and 10 mg/kg 1 hour before intraplantar stimulation. The time that the animal remained licking the injected paw was registered. In the Complete Freund's Adjuvant (CFA) model, mice were injected in the right hind paw and mechanical allodynia was evaluated by von Frey filaments for 14 days. Treatments were performed daily with vehicle or tested substances. On the 15th day, euthanasia was performed, and tissue was collected for histological analysis and quantification of inflammatory mediators. **Results:** Screening in the formalin 2.5% model showed that substances significantly inhibited pain-related behavior when compared to the control groups (vehicle and indomethacin) ($p < 0.0001$) in doses of 1 mg/kg and 10 mg/kg. PMM 75-17 exhibited significant antinociceptive effects (60%) in 1 mg/kg and 10 mg/kg doses ($n=12$; $p < 0,0001$). Studies on subchronic inflammatory model induced by CFA are being conducted. **Conclusion:** Treatment with the candidate for P2X7R antagonists decreased hyperalgesia induced by formalin, showing promising anti-inflammatory effects. **Financial Support:** CAPES, CNPq, FAPERJ. **References:** Cavillon, JM. *Inflam: From Mol. and Cell. Mech.* v. 1, p. 1517, 2017; Ren, WJ. *Purinergic Signal.* v. 18, p. 83, 2022; Andrejew, R. *Front. Mol. Neurosci.* v. 13, p. 124, 2020; Savio, LEB. *Front. Pharmacol.* v. 9, p. 52, 2018; Mathiesen, O. *Acta Anaesthesiol Scand.* v. 58, p. 1182. 2014.

05.011 Advanced Oxidation Protein Products (AOPPs) are Involved in Nociception and Neuroinflammation in a Relapsing-remitting Experimental Autoimmune Encephalomyelitis Model in Mice. Rodrigues P¹, Vieiro FT¹, Frare JM¹, Peres DS¹, Stein CS², Brum ES³, Silva AM⁴, Dalenogare DP¹, Moresco RN², Oliveira SM³, Ferreira J⁴, Pillat MM¹, Bochi GV¹, Trevisan G¹ ¹UFMSM, Graduated Program in Pharmacology, Santa Maria, RS, Brazil. ²UFMSM, Graduated Program in Pharmaceutical Sciences, Santa Maria, RS, Brazil. ³UFMSM, Graduated Program in Biological Sciences, Santa Maria, RS, Brazil, ⁴UFSC Graduated Program in Pharmacology, UFSC, Florianópolis, SC, Brazil

Introduction: Relapsing-remitting multiple sclerosis (RRMS) pathophysiology is unclear and frequently causes neuropathic pain (Katsara, M. Med. Chem. v. 14, p. 104, 2018). Nociception is detected in experimental autoimmune encephalomyelitis (EAE) models associated with transient potential receptor ankyrin 1 (TRPA1) and NADPH oxidase (Nox) activation. The acute treatment with apocynin (APO), an unspecific Nox inhibitor, reduce the neuropathic-like symptoms in relapsing-remitting EAE (RR-EAE) model (Dalenogare, D. P. Exp. Neuro. v. 328, p. 113241, 2020). Nox induces myeloperoxidase (MPO) activation, leading to advanced oxidative protein products (AOPPs) formation which activates TRP causing pain (Ding, R. Redox. Biol. v. 10, p. 1, 2016). However, there is no TRPA1 antagonist available in the clinic to treat the MS neuropathic pain. In this context, Nox inhibitors have been tested in phase II clinical trials to treat neuropathic pain in diabetes patients (Reutens AT, Contemp Clin Trials. 2020). Therefore, we propose to evaluate if the APO repeated treatment reduces the nociceptive symptoms of the RR-EAE-induced mice due to the AOPPs levels modulation.

Methods: Adult C57BL/6 female mice (n^o9746010620) were immunized with MOG_{35?55} 200 ?g, and QuilA 45 ?g, s.c. and two doses of pertussis toxin 1 ng/?l i.p. (Dalenogare, D.P. Exp. Neuro. v. 328, p. 113241, 2020). We initiated APO treatment 100 mg/kg i.g. 20 days after RR-EAE induction and repeated the injection daily through 15 days (Li, YQ., Acta. Pharmacol. Sin. v. 34, p. 352, 2013). The tests were conducted after passed 3h of the APO treatment to avoid the acute antinociceptive effect. We assessed the clinical score, mechanical (von Frey test) and cold allodynia (acetone test), grip test (neuromuscular performance), rotarod (locomotor activity) on days 7-35 post-induction and the nest building test (spontaneous pain) at 34 to 35 day. We measured AOPPs levels or Nox/MPO activity in the prefrontal cortex, hippocampus, and spinal cord, and cytokines in plasma samples. We also evaluated the gene expression of Mog, Iba-1, Gfap, Olig-1, IL-4 and IL-10 by PCR in the prefrontal cortex, hippocampus, and spinal cord. Data are expressed as mean±SEM and analysed according to the parametric or non-parametric assumption with p<0.05. **Results:** APO treatment reverted the mechanical and cold allodynia, and reduced the clinical score (<0.0001), spontaneous nociception (0.0181), and paw strength (0.0003) after RR-EAE-induction without weight or locomotor change. The APO treatment reduced the disease score of the RR-EAE-induced mice (<0.0001). The AOPPs and Nox/MPO activity increased in the central nervous system structures and plasma was reverted by APO treatment in all samples (<0.0001). The RR-EAE-induced mice had an increase level of IL-17, IFN-?, TNF-?, and IL-6 (0.0240) in plasma without change after APO treatment, but the IL-4 and IL-10 were increased after APO treatment (0.0057). The APO treatment reverted the demyelination, astrocyte, and glial activation in the spinal cord and prefrontal cortex, and the demyelination in the hippocampus (0.05). **Conclusion:** We demonstrated that AOPPs accumulation is involved in the neuroinflammation and neuropathic-like pain in the RR-EAE model. We have also observed the AOPPs levels reduction after APO repeated treatment may be due to the modulation of MPO/Nox. In addition, the APO treatment restored the myelin and reduce neuroinflammation which generated the RR-EAE clinical score reduction. Hence, compounds that modulated the AOPPs formation pathway could represent a therapeutic complement for MS patients. **Funding:** We wish to acknowledge fellowships received from the Conselho Nacional de Desenvolvimento Científico (CNPq) and Coordenação de Aperfeiçoamento de Pessoal de Nível Superior (CAPES). Ph.D. fellowship to P.R from CAPES [process #88887.501568/2020-00]. G.T is the recipient of a fellowship from CNPq [process #303531/2020-7] and a research grant from Fundação de Amparo à Pesquisa do Estado do Rio Grande do Sul (FAPERGS) [process #21/2551-0001935-2].

05.012 Investigation of the Mechanisms of Antinociceptive Action of α -Phellandrene through Molecular Docking and its Toxicity to U87 Cell Lines. Pinheiro-Neto FR¹, Pereira SAP¹, Acha BT¹, Ferraz SLNS¹, Gomes LS¹, Cavalcante MLS¹, Freitas GBL¹, Dittz-Júnior D², Ferreira PMP², Cavalcante MLS², Almeida FRC² UFPI

Introduction: α -Phellandrene (α -Phel), 5-isopropyl-2-methyl-1,3-cyclohexadiene, is a cyclic monoterpene first isolated from *Eucalyptus phellandra* (now called *E. radiata*). It is also present in the essential oils of cúrcuma (54%), *B. sacra* (42%), *E. elata* (35%) and *E. dips* (17%). The substance is safe and approved by the Food and Drug Administration (FDA) as a food additive. Current studies show *in vitro* cytotoxic capacity of α -Phel against *In vitro* proliferation assays revealed cytotoxic action upon murine cells of B-16/F-10 and S-180, with CI50 values of 436.0 (335.7–566.4 μ g/ mL) and 217.9 (169.7–279.7) μ g/mL, respectively., as well as inhibition of tumor growth *in vivo* (47.3 to 82.7%), besides direct decrease in peritumoral tissue in the subaxillary region. In addition, this monoterpene decreases mechanical sensitivity in mice bearing S-180 under acute or subacute treatment (25 and 50 mg/kg). The aim of this work was to investigate possible mechanisms of antinociceptive action through molecular docking and its toxicity to glioblastoma cells (U87). **Methods:** α -Phel was designed and optimized in terms of its three-dimensional structure for its lowest energy conformation (according to parameters of modified classical mechanics) using the ACD/ChemSketch software, version 14.0. Using the AutoDockTools software, rotational, ligand and target bonds were detected and defined as rigid. Gasteiger charges and polar hydrogens were also included. α -Phel was anchored to each of the proposed binding sites using Molegro and DS Viewer software using Moldock SE algorithm calculation, 30 runs, maximum interaction of 1500 in order to assess the type of possible interactions between α -Phel and the receptors. The viability of glioblastoma cells of the U87 lineage was evaluated by the resazurin assay. In a 96-wells plate, 100 μ L of 4×10^3 cells, suspended in DMEM supplemented with 5% FBS, were added to each well, and incubated at 37°C and 5% CO₂ for 24 hours. The culture medium was discarded and replaced with 100 μ L of complete medium with different concentrations (1.953125 – 1000 μ g/mL) of α -Phel. **Results:** α -Phel, similarly to other substances, exhibited negative binding energy in the molecular docking study with binding energies of -74.20, -68.75, -76.96, -73.22, -32.06, -59.40, -105.37 Kcal/mol, for TRPV1, μ and δ opioid, histamine H1 GABA-A, VEGF and PPAR-GAMA receptors, respectively, which indicates a strong and stable interaction between α -Phel and molecular targets and supports the hypothesis that this substance has probable anticancer, antimetastatic and analgesic activity. α -Phel also showed cytotoxicity against U87 cells in a concentration-dependent manner starting at a 31.25 μ g/mL. **Conclusion:** This result converges with the molecular docking findings and encourages further studies on the anticancer potential of the α -Phel. **Financial Support:** CAPES, UFPI.

05.013 Collagen-Derived Advanced Glycation End-Products Sensitize Human Sensory Neuron-Like cells to Capsaicin-Induced Calcium Influx. Silva GSA¹, Bufalo MC², Souza MM², Chudzinski-Tavassi AM^{2,3}, Pico G¹, Zambelli VO¹. ¹IBu, Lab. of Pain and Signaling, São Paulo, Brazil; ²IBu, Center of Excellence in New Target Discovery, São Paulo, Brazil; ³IBu, Innovation and Development Lab., Innovation and Development Center, São Paulo, Brazil

Introduction: Increased collagen-derived advanced glycation end-products (AGEs) are consistently related to painful diseases, including osteoarthritis, diabetic neuropathy, and neurodegenerative disorders. Recently, our group showed that human sensory-like neurons differentiated from SH-SY5Y cell lines display pro-nociceptive functions, such as, substance P release and transient receptor potential vanilloid 1 (TRPV1) up-regulation. Here, we sought to investigate whether the glycation process sensitizes sensory neurons-like cells to capsaicin excitation and activates nociceptive signaling pathways. **Methods:** Sensory neurons-like cell were obtained from the differentiation of SH-SY5Y cells, incubated with extracellular collagen matrix (ECM- 100 µg/mL), all trans-retinoic acid (10 µM) and brain derived neuron factor (50 ng/µL). The pro-nociceptive environment was mimicked by incubating cells with glycated extracellular matrix (ECM-GC). Cell viability was assayed by inhibition of 3-(4, 5-dimethylthiazol-2-yl)2,5-diphenyl-tetrazolium bromide (MTT) reduction. Calcium influx was evaluated by the fluo-8 calcium assay kit, incubated with capsaicin (0.1-10 µM). At the end of the experiment, KCL (100 µM) was used to determine the maximum fluorescence and cell responsiveness. Changes in the intracellular Ca²⁺ influx were determined by the peak fluorescence intensity minus baseline fluorescence intensity. Data were expressed as mean values ± SEM. In addition, the levels of proteins involved in pro-nociceptive signaling and cell death, such as activating transcription factor 3 (ATF3) and B-cell lymphoma 2 (Bcl2) were quantified by western blot. **Results:** The glycation process does not interfere with cell viability. Furthermore, the analysis of calcium influx in sensory neuron-like cells shows that glycation process increases capsaicin-induced calcium influx (52.13%) when compared with cells treated with normal collagen, suggesting that AGEs potentiate capsaicin-induced excitation. Moreover, sensory neuron-like cells treated with ECM-GC displayed increased levels of ATF-3 and Bcl2 (40.78% and 27.63%, respectively), when compared to ECM-NC. **Conclusion:** These data indicate that glycation hypersensitizes sensory neuron-like cells, triggering pro-nociceptive and pro-neurodegenerative signaling. Together, our results suggest that we established a functional model that can be useful for screening candidates for the management of painful conditions. **Financial Support:** Fundação de Amparo à Pesquisa de São Paulo (FAPESP 2021/14831-8; 2022/08417-7 AND GlaxoSmithKline 2015/50040-4; 2020/13139-0).

05.014 The Antinociceptive Action of Isopulegol Involves Neuronal Plasma Membrane Stabilization leading to GABAergic Neuroinhibition in Detriment of Glutamatergic Excitation in the Rat Spinal Cord. Próspero DFA¹, Pereira SAP¹, Acha BT¹, Cavalcante MLS², Dittz-Júnior D², Ventura T³, Lobo MGB³, Ferreirinha F³, Correia-de-Sá P³, Almeida FRC¹ ¹UFPI, Lab. of Pain Pharmacology, ²Lab. of Experimental Cancerology, Teresina, Brazil. ³University of Porto, Lab. of Pharmacology and Neurobiology, School of Medicine and Biomedical Sciences Abel Salazar (ICBAS), Porto, Portugal.

Introduction: Isopulegol (ISO) is a monoterpene alcohol present in essential oils from various plants, such as *Corymbia citriodora*, *Achillea abrotanoides* and *Mentha canadensis*. Studies with ISO have shown a dose-dependent antinociceptive effect in the glutamate test, as well as in several other acute pain assays. Atropine, a non-selective muscarinic receptor antagonist, reversed the ISO antinociceptive action. These results suggest that the analgesic effect of ISO is mediated by the CNS, given that the main site of action of cholinomimetics in analgesia is the spinal cord. In this study, we aimed at investigating the cytotoxicity of ISO on U87 cells and erythrocytes and its modulatory effect on neurotransmitter release in the rat spinal cord. **Methods:** Wistar rats (180g) and U87 glioblastoma cells were used. Experimental procedures were approved by the Ethics Committee and the Animal Welfare Responsible Organism (ORBEA/ICBAS-UP N^o224/2017). U87 cells viability was assessed by the resazurin assay in a 96-wells plate filled with 100 μ L of 4×10^3 cells/well. ISO (1.953125-500 μ g/mL) was tested by replacing the culture medium with the desired concentration of the drug. The action of ISO on plasma membrane stability was evaluated *in vitro* using a hypotonic hemolysis prevention assay in rat erythrocytes. The modulatory effect of ISO (0.3, 1 and 3 mM) on KCl-evoked [³H] GABA (gamma-aminobutyric acid) and [¹⁴C] Glutamate release was tested in nerve terminals (synaptosomes) isolated from the rat spinal cord. Western blot analysis showed that synaptosomes isolated from the rat spinal cord were highly enriched in the presynaptic neuronal marker, synaptophysin (1: 1000), with almost no contamination by GFAP (1: 500), the glial fibrillary acidic protein, compared with the total cell lysates. **Results:** ISO (IC₅₀ 305.4 μ g/mL) reduced the proliferation of U87 glioblastoma cells. ISO (1 and 3 mM) partially prevented hypotonic hemolysis of rat erythrocytes. With regard to neurotransmitter release, ISO (1 and 3 mM) favored the release of [3H] GABA by 19.35% compared to the control group while decreasing the output of [14C]Glutamate (0.3; 1 and 3 mM) by 59.7, 80.4 and 86%, respectively, from synaptosomes depolarized with KCl (30 mM) from the rat spinal cord (* $p < 0.05$). **Conclusion:** Preliminary data suggest that the antinociceptive action of ISO involves stabilization of neuronal plasma membranes leading to neurotransmitters release unbalance, thus favouring GABA-mediated inhibition in detriment to glutamatergic excitation. The antiploriferative activity of ISO observed in the human glioblastoma cell line U87 may be a promising effect in the clinical treatment of cancer, however, more studies should be done to elucidate such mechanisms. **Financial Support:** CAPES, UFPI. The work made at ICBAS-UP was partially supported by FCT (UIDB/04308/2020 and UIDP/04308/2020).

05.015 Analgesic Efficacy of the Slow-Releasing Hydrogen Sulfide (H₂S) Donor, GYY4137 and the Polysulfide, Dimethyl Trisulfide in Postoperative Pain Model: Role of Transient Receptor Potential Ankyrin 1. Dallazen JL^{1,2}, Horváth AI^{2,3}, Tékus V², Hajna Z², Alsou'b DFB², Helyes Z^{2,3,4}, Pintér E^{2,3,4}, Costa SKP¹. ¹ICB-USP, Dept Farmacologia, Brazil, ²Dept Pharmacology and Pharmacotherapy, Medical School, University of Pécs, Hungary, ³National Laboratory for Drug Research and Development, Budapest, Hungary, ⁴Eötvös Loránd Research Network, Chronic Pain Research Group, University of Pécs, Hungary

Introduction: Postoperative pain affects about 80% of patients submitted to surgical intervention with few safe therapeutic options available (Gan TJ. *J Pain Res*, v10, p2287, 2017). The Transient Receptor Potential Ankyrin 1 (TRPA1) channel is activated by the slow-releasing H₂S donor (GYY4137) and polysulfide dimethyl trisulfide (DMTS), which in turn leads to analgesia via release of inhibitory mediators and/or sensory desensitization (Bátaí IZ. *Front Endocrinol*, v9, p55, 2018). This study aimed to investigate the effects of GYY4137 and DMTS in a murine postoperative pain model with emphasis on the involvement of the TRPA1 channel. **Methods:** Plantar incision surgery (PIS) was performed in male C57BL/6, TRPA1-deficient (TRPA1 KO) and wild-type (TRPA1 WT) mice (8–12 weeks old; license BA02/2000-62/2022). Before and 24h after PIS, mechanonociceptive and thermonociceptive thresholds were determined by dynamic plantar aesthesiometry and hot plate, respectively, and paw volume by plethysmometry. Later, mice were intraperitoneally treated with GYY4137 (80, 260 and 800 µmol/kg), DMTS (80, 260 and 400 µmol/kg), or vehicle (VEH), and measurements were repeated 1, 3, and 5 h after treatments. The same parameters were measured in PIS-TRPA1 WT and KO mice using the effective dose of GYY4137 or DMTS and paralleled by detecting neutrophil myeloperoxidase (MPO) activity by *in vivo* luminescence imaging and blood perfusion by Laser Speckle. **Results:** PIS induced mechanical and thermal hyperalgesia, and paw edema in VEH-treated animals compared to the sham group. GYY4137 at 260 and 800 µmol/kg inhibited mechanical and thermal hyperalgesia compared to the VEH-treated group. DMTS at 400 µmol/kg reversed the mechanonociceptive threshold, without altering the thermonociceptive threshold at any tested dose. PIS-induced paw edema was reduced by GYY4137 and DMTS in all tested doses. The analgesic effect of either GYY4137 (800 µmol/kg) or DMTS (400 µmol/kg) was absent in TRPA1 KO mice, but the anti-edematogenic effect was unaffected. The MPO activity in the operated paws of TRPA1 KO mice was significantly lower as compared to TRPA1 WT mice. Whilst GYY4137 treatment reduced the increased MPO activity in operated paw of TRPA1 WT mice, it further enhanced MPO activity in TRPA1 KO mice. DMTS reduced MPO activity in TRPA1 WT mice, without affecting this parameter in TRPA1 KO mice. TRPA1 WT and KO mice exhibited increased blood perfusion in the operated paw, which were restored to the basal levels by GYY4137 and DMTS. **Conclusion:** The analgesic effects of GYY4137 or DMTS are modulated by the TRPA1 channel, whilst the anti-inflammatory actions are not. **Financial Support:** CAPES (001); CNPq (142343/2020-0; 200357/2022-0; 312514/2019-0); Hungarian research grants EGA-16; Eötvös Loránd Research Network; Hungarian Brain Research Program-3; National Laboratory of Drug Research and Development.

05.016 Therapeutic Effects of β -Caryophyllene on Oxaliplatin-Induced Neuropathy in Mice: Analysis of Antinociceptive, Anti-Inflammatory and Redox Modulation Activity.

Agnes, JP¹, Schran, RG², Ferreira J², Goldoni FC³, Benvenuti L³, Santin JR³, Quintão NLM³, Zanotto-Filho A¹ ¹UFSC, Lab. de Farmacologia e Bioquímica do Câncer, PPG em Farmacologia, Depto de Farmacologia, Florianópolis, SC, Brasil, ²UFSC, Lab. de Farmacologia Experimental, PPG em Farmacologia, Depto de Farmacologia, Florianópolis, SC, Brasil, ³Univali, Lab. Farmacologia e Toxicologia, PPG em Ciências Farmacêuticas, Itajaí, SC, Brasil

Oxaliplatin (OXA) is commonly used in colorectal cancer treatment, but it often leads to OXA-induced neuropathy (OIN). OIN is caused by platinum adducts forming in neuronal DNA, resulting in oxidative damage and neuroinflammation. Symptoms include paresthesia, dysesthesia, cold hypersensitivity, and spontaneous pain. OIN's chronicity may necessitate changes in therapy, such as dose reduction and longer intervals between cycles of chemotherapy, which can lead to reduced cytotoxic activity and tumor resistance. We investigated the effects of β -caryophyllene (BCP) in a mouse model of OIN. BCP has anti-inflammatory properties via CB2 receptors and recently demonstrated redox modulation capabilities by reducing reactive oxygen species (ROS) and oxidative damage. We hypothesized that BCP treatment would alleviate oxidative damage, neuroinflammation, and hyperalgesia induced by OXA. Female Swiss mice were used (CEUA-UFSC nº 1670201021) to establish the OIN model, received 5 mg/kg of OXA every 48 hours for 14 days. BCP was administered orally at doses ranging from 25 to 100 mg/kg/day concurrently with OXA. We also investigated the effects of BCP (100 mg/kg) after OIN was established. The involvement of CB2 receptors in BCP's antinociceptive response was assessed using the CB2 antagonist SR144528 and the synthetic CB2 agonist GW405833. Mechanical and thermal nociception were evaluated using the von Frey filaments test and cold plate test, respectively. At the study termination, the spinal cord was collected for ELISA analysis of IL-1 β , TNF, and 4-hydroxynonenal levels, as well as oxidative damage quantification (TBARS) and ROS measurement (DCFH-DA). BCP treatment effectively reduced mechanical and cold hyperalgesia in both concurrent and post-induction neuropathy models. The CB2 antagonist inhibited BCP's mechanical antinociceptive activity, while the CB2 agonist showed similar effects to BCP, suggesting CB2 receptor involvement. These findings highlight CB2 as a potential target for OIN treatment. BCP treatment also reduced IL-1 β and TNF levels in the spinal cord, indicating anti-inflammatory effects. Additionally, BCP reduced ROS levels and lipid peroxidation, demonstrating its redox modulation activity. In conclusion, BCP treatment effectively reduced hyperalgesia in a mouse model of OIN, both during concurrent OXA treatment and after neuropathy induction. CB2 receptors partly mediate BCP's antinociceptive effects, as observed with the CB2 antagonist. BCP also reduced neuroinflammation, oxidative damage, and lipid peroxidation in the spinal cord. This study was supported by funding from CNPq and CAPES, with technical support from LAMEB-UFSC (multi-user laboratory).

05.017 The Antinociceptive Effect of Cannabinoid Receptor Agonists is Enhanced in Aspirin-Triggered Lipoxin A4 Treated-Diabetic Rats, Ferreira MV¹, Jesus CHA², Bonfim JC¹, Oliveira G¹, Liebl B¹, Verri-Junior WA³, Zanoveli JM¹, Cunha JM¹ ¹UFPR, Dept of Pharmacology, Curitiba, PR, Brazil; ² Indiana University, Dept of Psychological and Brain Sciences, Bloomington, IN, USA; ³UEL, Dept of Pathology, Londrina, PR, Brazil

Introduction: Neuropathy is the most common complication of diabetes, and often manifests as painful symptoms including spontaneous pain, hyperalgesia, and allodynia. Current pharmacological approaches for managing diabetic neuropathy are ineffective, posing a clinical challenge. Cannabinoids have shown beneficial effects in pain management, and lipoxin A4, a specialized pro-resolving lipid mediator, has demonstrated positive modulation of the CB1 receptor. Combining drugs offers potential advantages of lower doses, minimizing side effects, and maximizing therapeutic effects. However, the interaction between aspirin-triggered lipoxin A4 and cannabinoid agonists in diabetic neuropathic pain remains unexplored, which was the aim of this study. **Methods:** Experimental diabetes was induced by a single injection of streptozotocin (STZ; 60 mg/kg; i.p) in male Wistar rats (weighing 180-240g). The experimental groups were: normoglycemic control rats treated with vehicle (NGL-VEH), diabetic rats treated with VEH (DBT-VEH) or ATL (1 or 3ng/rat; i.p.) starting 14 days after STZ and lasting until the 32nd. On days 28th and 32nd diabetic rats (treated with VEH or ATL) received an acute intrathecal injection of VEH or cannabinoid receptor agonists ACEA or JWH-133 (at doses of 10 or 30µg/10µL). Mechanical allodynia was assessed by an electronic Von Frey test (VF) and was performed one day before STZ injection (basal) and again on the 14th, 22nd, 28th, and 32nd days after STZ. In the 28th and 32nd VF was assessed before treatment and 30, 60, 120, and 180 minutes after i.t. treatment with cannabinoid receptor agonists. All experimental protocols were approved by Institutional Ethics on Animal Experimentation (CEUA-BIO-UFPR #1418). **Results:** When compared to NGL-VEH rats, diabetic animals developed a significant reduction of the mechanical threshold (58,31%) which starts on the 14th day after STZ. When compared to the DBT+VEH group; 1) DBT groups treated with ATL (1 and 3ng) have a significant increase in mechanical threshold (17% and 16,9% respectively); 2) DBT groups pre-treated with VEH plus ACEA or JWH-133 (10 or 30 µg) had a significant increase in mechanical threshold (15,26% or 14,91%; 15,66% or 18,22%, respectively). The sub-chronic treatment with ATL (3 ng) significantly increased the antinociceptive effect of ACEA or JWH-133 (only at a dose of 30 µg and 1 hour after treatment) over the mechanical allodynia in diabetic rats (37,38% or 38,79%, respectively). **Conclusion:** Although not fully explored in this study, our data suggest that the ATL treatment may interact with both cannabinoid receptors, improving the mechanical allodynia associated with experimental diabetes in rats. Furthermore, this is the first time in literature that a specialized pro-resolving lipid mediator is combined with a CB2 receptor agonist and shown an interaction. However, more studies are needed to characterize how this interaction occurs. **Support:** CAPES (Finance Code 001), Pronex (Contract 014/2017.; Protocol 46843.484.37488.23052016).

05.018 TRPA1 Modulates Nociception in a Model of Migraine-Like Behavior Caused by Unpredictable Sound Stress in Mice. Viero FT¹, Rodrigues P¹, Nassini R², Geppetti P², Trevisan G¹ ¹UFMS, Graduate Program in Pharmacology, Santa Maria, RS, Brazil. ²University of Florence, Dept of Health Science, Clinical Pharmacology and Oncology, Florence, Italy.

Introduction: Migraine represents one of the most significant causes of disability worldwide and has a higher prevalence in female patients (Feigin, VL. *Lancet Neurol.*, v.19, p.10, 2020). Stress, such as sound stress, is frequently reported as a migraine trigger (Kelman, L. *Cephalalgia.*, v.27, p.8, 2007), but the underlying mechanisms are not fully understood (Dina, O. *Eur J Pain.*, v.15, p.4, 2011). In addition, available therapies often do not provide complete pain relief or have several side effects. Thus, there is a need for new pharmacological targets to treat migraine, such as transient ankyrin receptor potential 1 (TRPA1) blockage (Spekker, E. *Int J Mol Sci.*, v. 700, p.24, 2023). TRPA1 channel is a pro-algesic receptor, expressed in trigeminal nociceptors, and is sensitive to oxidative stress common in migraine (Ladini, L. *Int J Mol Sci.*, v.23, p.19, 2022). Thus, the study aimed to investigate the role of the TRPA1 receptor in the model of migraine-like behavior following the induction of unpredictable sound stress in male and female mice and to explore possible pathology mechanisms. **Methods:** Male and female adult C57BL/6J mice (20–30 g) were used: littermate wild-type (*Trpa1*^{+/+}) and TRPA1-knockout (*Trpa1*^{-/-}) mice (25–30 g, 5–8 weeks). The protocols employed in our study were approved by Committee for Animal Care of the University of Florence (1194/2015-PR). The mice were exposed to unpredictable sound stress for 3 days non-consecutive for 30 minutes. Non-stressed animals were placed in the sound chamber but without exposure to the sound stimulus (Khasar, G. *J Pain.*, v.10, p.4, 2009). We assessed the grimacing pain behavior (spontaneous nociception), periorbital and hind paw mechanical thresholds (von Frey test), and open field (exploratory/locomotor behavior) on the day 7th post-stress induction (Viero, F. *Front. Pharmacol.*, v.13, p.14, 2022). Calcitonin gene-related peptide (CGRP) levels were evaluated in plasma samples. Nitric oxide, H₂O₂, and IL-6 levels were measured in plasma, brainstem, and trigeminal ganglion. Data were expressed as mean±SEM and analyzed according to the parametric or non-parametric assumption with p<0.05. **Results:** TRPA1 deletion prevented the periorbital (<0.0001), hind paw mechanical allodynia (0.0068), and spontaneous nociception (0.0004) after migraine induction in either male or female mice. TRPA1 deletion also prevented the CGRP increase in stressed mice plasma (0.0023). Furthermore, migraine-induced mice have an increase of IL-6 (0.0047), NOx (<0.0001), H₂O₂ (0.0021) in plasma levels, similarly occurring in the brainstem and trigeminal ganglion. The nociceptive, behavioral, and biochemical alterations detected in this model were mostly shown in female stressed mice. The migraine phenotype was abolished completely in TRPA1 deleted mice, thus highlighting the essential role of the channel in such mechanism. **Conclusion:** The major finding of the present study is the strict correspondence between mediators TRPA1 agonists that provoke migraine in patients and evoke periorbital, hind paw allodynia, and spontaneous nociception in mice. Furthermore, our data showed that mice females had higher levels of IL-6, CGRP, NOx, H₂O₂ mediators than stressed males, which could be one of the possible reasons for the higher prevalence of the experience in female patients. Our data also showed that the TRPA1 pathway contributes to unpredictable sound stress-evoked migraine-like behavior. **Financial support** Fellowships from the Conselho Nacional de Desenvolvimento Científico (CNPq).

05.019 Impaired Mitochondrial Dynamics Contributes to Paclitaxel-Induced Peripheral Neuropathy. Martins BB¹, Hösch N¹, Ferreira J², Zambelli VO¹ ¹IBU, Lab. of Pain and Signaling, São Paulo, Brazil; ²ICB-USP, Dpt. of Anatomy, São Paulo, Brazil

Introduction: Paclitaxel is a chemotherapy drug used primarily for the treatment of breast and ovarian cancer. However, it frequently causes peripheral sensory neuropathy, resulting in sensory abnormalities and pain in patients receiving treatment for cancer. Mechanistically, PTX binds to and stabilize microtubules and, consequently, interrupts axonal transport, leading to an insufficient supply of ATP and increased oxidative stress. Mitochondria exist as a dynamic and heterogeneous network that undergoes continuous fusion and fission processes. GTPases such as mitofusins 1 and 2 (Mfn1 and Mfn2), and dynamin-related protein 1 (Drp1) that control mitochondrial fusion and fission, respectively, are vital for the regulation of plasticity mitochondria. Studies demonstrate a causal correlation between the impairment of mitochondrial bioenergetics metabolism and the development of chemotherapy-induced peripheral neuropathy. However, whether mitochondrial fusion-fission are important for bioenergetics metabolism in sensory neurons and, consequently, for the development of pain is unknown. Therefore, the aim of this work is to investigate the role of mitochondrial dynamics in paclitaxel-induced neuropathy. **Methods:** The neuropathy was induced by paclitaxel (4 mg/kg, ip.), with 4 injections on alternate days, in wild-type C57BL/6 mice weighing 20–22 g. The mechanical nociceptive threshold was detected by von Frey filaments and cold allodynia by the acetone test. To assess motor function and coordination the rotarod test was performed. The protein expression of mitochondrial fusion (Mfn-2) and fission (Drp-1) was detected by Western Blot in samples from the dorsal ganglion of the spinal cord (DRG). Mitochondrial morphology was evaluated by transmission electron microscopy of the DRG. The behavioral, biochemical and imaging assays were performed at 7, 28 and 42 days after paclitaxel. The procedures were approved by the Animal Care Committee, Butantan Institute. **Results:** Paclitaxel reduces the mechanical nociceptive threshold (hypernociception) when compared to vehicle-treated mice, with peak at day 21 ($80 \pm 7,5\%$, $*p < 0.05$, $n=8/\text{group}$), returning to baseline levels at day 42 after treatment. Moreover, paclitaxel increases the nociceptive response to acetone (cold allodynia), with peak at day 21 ($93 \pm 42\%$, $*p < 0.05$, $n=8/\text{group}$). Moreover, no cold allodynia was detected at days 28 and 42. Paclitaxel treated mice exhibited normal motor activity relative to vehicle treated mice throughout the study. Interestingly, the expression levels of the Drp1 (fission) in DRG increases at 28 after paclitaxel ($54 \pm 16\%$, $*p < 0.05$, $n=8-6/\text{group}$). However, paclitaxel does not change the Mfn2 (fusion) levels. Supporting the biochemical data, the electron microscopy of the DRG demonstrates extensive mitochondrial swelling and fragmentation on the day 28 after paclitaxel, when compared to the vehicle group. Mild mitochondrial alterations were detected at days 7 and 42. **Conclusions:** Together, we show that excessive mitochondrial fission at DRG contributes to the development of paclitaxel-induced neuropathy. This study reveals Drp1 as a potential target for the neuropathic pain treatment. **Financial Support:** FAPESP (2021/14831-8) CAPES (001) Fundação Butantan.

05.020 Study of New Natural Derivatives Inhibitors of the P2X7 Receptor in Inflammatory Pain and Arthritis in Mice. Galvão RMS^{1,2}, Salles JP^{2,3}, Miranda ALP², Faria RX^{1,4} ¹IB-UFF, Graduate Program in Science and Biotechnology, Brazil, ²UFRJ, Lab. of Studies in Experimental Pharmacology, Brazil, ³UFRJ, Graduate Program in Pharmacology and Medicinal Chemistry, Brazil, ⁴IOC, Lab. for Environmental Health Assessment and Promotion, Brazil

Introduction: The ionotropic purinergic receptor P2X7 subtype (P2X7R), activated by extracellular ATP, is widely distributed in mammalian cells. A brief exposure to ATP induces the influx of cations, such as Ca²⁺, Na⁺, and K⁺, through plasma membrane. When activated, P2X7R is responsible for releasing cytokines, such as IL-1 β , IL-6, and TNF- α , that can lead to cell death. The therapeutic control of inflammation by P2X7R antagonism or modulation has been extensively explored and studied for the treatment of autoimmune diseases, such as rheumatoid arthritis (RA). Once the current treatments are palliative and have several associated adverse effects, the search for new therapeutic molecules to treat RA, with *in vivo* efficacy, are with great interest. **Objective:** In this work, we selected two substances present mainly in two essential oils that exhibit high inhibition potency of P2X7R activation *in vitro* and investigated the action on pain and reduction of RA in mice after oral administration. **Methods:** *Swiss Webster* adult mice of both sexes were used (CEUA/UFRJ 055/22). In the 2.5% formalin-induced hyperalgesia model, the animals were divided into 5 groups: vehicle, indomethacin, morphine, substance β , and N. The test substances were administered at 0,1, 1, and 10 mg/kg doses, 1 hour before intraplantar stimulation. The time that the animal remained licking the injected paw was timed. In the model of Complete Freund's Adjuvant (CFA) induced sub-chronic inflammatory joint pain, mice right hind paw was injected with 20 μ l of CFA, and mechanical allodynia was evaluated by von Frey filaments for 14 days. Treatments were performed daily with vehicle or test substance. On the 15th day, euthanasia was performed, plasma and other tissues were collected for histological analysis and quantification of inflammatory mediators. **Results:** Screening in the formalin 2.5% model showed that substances β and N significantly inhibited inflammation at doses of 1 and 10 mg/kg, with 60.5% and 71.1% of antinociceptive effect in the second phase of the formalin test, respectively compared to the DMSO 1% control (vehicle) (n=4-6; p<0.05). Treatment with both substances at a dose of 1 mg/kg significantly increased the nociceptive threshold of CFA-induced mice (n=13; p<0,05). Treatment with N substance also reduced paw edema in the CFA model. Cream formulations of these two substances are in development and will be tested for their analgesic and anti-inflammatory effects. **Conclusion:** Treatment with P2X7R antagonists decreased edema, pro-inflammatory and pro-algesic effects induced by formalin and CFA, indicating that P2X7R is an important pharmacological target for the development of new therapies for the treatment of chronic inflammatory diseases like arthritis. **Financial Support:** CAPES, CNPq, FAPERJ. Cao, F. *Autoimmun. Rev.*, v. 18, p. 767, 2019 Figliuolo, VR. *Cytometry A.*, v.85, p. 588, 2014 Lister, MF. *J. Inflamm.*, v.4, 2007 Mrid, RB. *Biomed. Pharmacother.*, v. 151, 2022 Rivas-Yáñez, E. *Int. J. Mol. Sci.*, v. 21, p. 4937, 2020 Rocha, SB. *Adv. Rheumatol.*, v. 59, 2019

05.022 Anti-inflammatory and Antinociceptive Activity of the Hydroalcoholic Extract of *Heteropterys tomentosa* in Mice. Freitas-Júnior RAF², Ferraz GB², Almeida-Filho OP¹, Santana JVS², Moreno SE², Buccini DF, Munhoz CD¹ ¹ICB-USP, Lab. of Neuronal Endocrine Pharmacology and Immune Modulation, Dept of Pharmacology, São Paulo, Brazil, 2UCDB, Lab. of Pharmacology, Biotechnology Program, Mato Grosso do Sul, Brazil

Introduction: Inflammation and pain play a significant role in the development of various pathological conditions. Modulating these processes can enhance pain management strategies and help prevent inflammation-related disorders. The study of plant extracts, particularly *Heteropterys tomentosa*, holds great importance in addressing pain and inflammation. Exploring the therapeutic potential of phototherapeutics allows for the development of alternative treatments with potentially fewer side effects, thereby contributing to better pain management and an improved quality of life for individuals dealing with these conditions. **Aim:** The aim of this study is to investigate the anti-inflammatory and antinociceptive potential of the hydroalcoholic extract of *H. tomentosa* in mice. **Methods:** In this study, we utilized the hydroalcoholic extract (H.E. *H.t*) (70% alcohol and 30% water) of *H. tomentosa*. To evaluate the anti-inflammatory effect of extract, Swiss mice were subjected to the neutrophil migration test in the abdominal cavity. For the assessment of nociception, the acetic acid-induced abdominal writhing test (0.8%) was conducted (CEUA 003/2019). Statistical analysis of the data was performed using one-way ANOVA, and differences were considered significant for a P-value of less than 0.05. **Results:** At a concentration of 50 mg/mL, the H.E.H.t demonstrated a 43.82% inhibition of neutrophil migration compared to the group treated with carrageenan. Additionally, the treatment exhibited a 58.46% decrease in the number of writhing responses in the acetic acid-induced abdominal writhing test compared to the control group (saline). **Conclusion:** In conclusion, the extract appears to possess anti-inflammatory and antinociceptive activity, suggesting the need for further assays to investigate the activation of biochemical pathways related to inflammation and pain. **Financial Support:** CNPq and CAPES

06. Cardiovascular and Renal Pharmacology

06.001 Evaluation of Long-Term Hemodynamic Response in Wistar Rats Treated with Topiramate During Childhood. Oliveira GR, Silva KGN, Bonancea AM, Miguel MVO, Pelosi GG UEL, Dpt of Physiological Science, Brazil

Introduction: Topiramate (TOP) is an antiepileptic drug prescribed for children over 2 years of age. The administration of antiepileptic drugs has been associated with cardiovascular dysfunction. However, there is limited data on literature about the long-term effects of TOP on the cardiovascular system. According to the Developmental Origins of Health and Disease (DOHaD) concept, early-life exposures to adversities may lead to long-term impairments in individuals healthy. This study aimed to evaluate the hemodynamic response to vasoactive drugs in adult rats treated with TOP during childhood. **Methodology:** Wistar rats from the central care unity of State University of Londrina were used in the present work and all experiments were approved by the ethics committee (CEUA nº 100/2018). After mating, gestational day 0 (GD-0) was determined. After birth, postnatal day 0 (DPN-0) was identified, and the rats were separated by sex into four groups: female control group (CTR^f) (n=7), male control group (CTR^m) (n=12), female TOP group (TOP^f) (n=6), and male TOP group (TOP^m) (n=12). From DPN-16 to 28, the TOP groups received TOP treatment (41 mg/kg/day) via gavage, while the CTR groups received tap water via gavage. Femoral artery and vein cannulation were performed for the groups on DPN-85 for females and DPN-120 for males. After a 24-hour recovery period, the hemodynamic response to intravenous administration of vasoactive drugs phenylephrine (Phe; 50 µg/ml/kg, iv; 0.34 ml/min), and sodium nitroprusside (NPS; 50 µg/ml/kg, iv; 0.8 ml/min) was analyzed. **Results:** Intravenous infusion of Phe resulted in a dose-dependent pressor response in both CTR^f and TOP^f groups, as well as in CTR^m and TOP^m groups, with no significant differences between CTR^f and TOP^f or CTR^m and TOP^m groups. The infusion of NPS resulted in a dose-dependent depressor response in all groups without significant differences between CTR^f and TOP^f or CTR^m and TOP^m groups. (Female curve: Interaction: $p=0.6748$; $F(10, 110)=0.7514$; Concentration: $p<0.0001$, $F(10, 110)=85.38$; Treatment: $p=0.7443$; $F(1, 11)=0.1119$. (Emax: CTR^f: 64.30 ± 7.353 mmHg; TOP^f: 56.06 ± 2.913 mmHg; $p=0.3493$; $t=0.9775$) (EC50: CTR^f: 0.5345 ± 0.0367 µg/kg; TOP^f: 0.5337 ± 0.0168 µg/kg; $p=0.9854$; $t=0.0187$). CTR^f; n=7. TOP^f; n=6. (Male curve: Interaction: $p=0.5740$; $F(10, 220)=0.8574$; Concentration: $p<0.0001$, $F(10, 220)=85.61$; Treatment: $p=0.8139$, $F(1, 22)=0.05677$. (Emax: CTR^m: 67.66 ± 30.34 mmHg; TOP^m: 44.37 ± 3.965 mmHg; $p=0.4546$; $t=0.7612$) (EC50: CTR^m: 1.737 ± 0.2065 µg/kg; TOP^m: 1.534 ± 0.03551 µg/kg; $p=0.3432$; $t=0.969$). CTR^m; n=12. TOP^m; n=12. The infusion of NPS caused a dose-dependent depressor response in the animals with no statistically significant differences observed between the CTR^f and TOP^f or CTR^m and TOP^m groups. (Female curve: Interaction: $p=0.9988$; $F(10, 110)=0.1487$; Concentration: $p<0.0001$, $F(10, 110)=73.21$; Treatment: $p=0.5045$, $F(1, 11)=0.476$. (Emax: CTR^f: -59.15 ± 6.013 mmHg; TOP^f: -3862.42 ± 8.26 mmHg; $p=0.7502$; $t=0.356$) (EC50: CTR^f: 0.929 ± 0.04 µg/kg; TOP^f: 0.905 ± 0.056 µg/kg; $p=0.7281$; $t=0.3566$). CTR^f; n=6. TOP^f; n=7. (Male curve: Interaction: $p=0.7585$; $F(10, 220)=0.6627$; Concentration: $p<0.0001$, $F(2, 271)=103.1$. **Conclusion:** Administration of TOP during childhood did not change the hemodynamic response in adult rats in long-term. Funding: CAPES.

06.002 Elastase-2 Deletion Impact on Cardiac Remodeling by Angiotensin II Infusion in Mice Models. Kovacs HZ¹, Mestriner F¹, Dugaich VF¹, Dantas PB¹, Nakagi VS², Ribeiro MS¹, Becari C^{1,3} ¹FMRP-USP, Division of Vascular and Endovascular Surgery, Dept of Surgery and Anatomy, ²FMRP-USP, Dept of Physiology, Ribeirão Preto, SP, Brazil. ³FOB-USP, Dept of Biological Science, Bauru-SP, Brazil

Introduction: Angiotensin II (AngII) is a peptide that plays a role in systemic blood pressure, but has also been related to deleterious effects, such as cardiac abnormal remodeling, autonomic impairment, and abdominal aortic aneurysm (AAA). Elastase 2 (ELA-2) is an enzyme that forms locally ang II, and its knockout has been demonstrated to protect against AAA development. We sought to investigate if the Elastase-2 deletion could prevent other deleterious effects related to AngII infusion. **Methods:** Male wild type (C57bl/6, WT) and ELA-2 knockout (CELA-2aTm1Bdr; ELA-2KO) mice were either treated with saline (WT+Sal, ELA-2KO+Sal) or angiotensin II (2.28g/g/min, WT+AngII, ELA-2KO+AngII) for twenty-eight days by subcutaneously mini-pumps infusion. Echocardiography in B-Mode was performed with Vevo 2100 equipment to obtain Ejection Fraction (EF), Left Ventricular end-systolic diameter (LVIDs) and Heart Rate (HR). Mice were anesthetized during the exams with isoflurane (5% v/v for induction and 2% v/v for maintenance). Data were expressed as mean \pm standard error of mean, and unpaired t-tests were performed to determine statistical significance. A value of $p < 0,05$ was considered significant. **Results:** Before treatment, WT and ELA-2KO mice did not differ in EF, LVIDs and HR. After 14 days, treatment with Ang II induced a decrease in LVIDs in WT (WT+sal, n=5 vs WT+AngII, n=4, $p=0,02$) and ELA-2KO (ELA-2KO+Sal, n=4 vs ELA-2KO+AngII, n=5, $p=0,0012$) groups, and an increase in EF in ELA-2KO group (ELA-2KO+Sal vs ELA-2KO+AngII, $p=0,0135$), whereas EF in WT groups were similar. HR was also similar among groups. After 28 days, both groups treated with Ang II maintained a reduction in LVIDs (WT+Ang II n = 4 vs WT+Sal n = 5, $p = 0,01$; ELA-2KO+Ang II n = 5 vs ELA-2KO+Sal n = 4, $p=0,017$). The EF was still increased in ELA-2KO treated with Ang II (ELA-2KO+Ang II vs ELA-2KO+Sal, $p = 0,011$), and was also increased in WT treated with Ang II (WT+Ang II vs WT+Sal, $p = 0,048$). HR was similar among groups. **Conclusion:** These data indicate that the knockout of ELA 2 could not prevent progression to cardiac remodeling, but prevented autonomic impairment in knockout mice. **Financial Support:** This study was funded by the Fundação de Amparo à Pesquisa do Estado de São Paulo (Fapesp, grants n. 2017/21539-6; 2018/23718-8; 2020/03308-0; 2022/02162-7), CNPq-Pibic, CAPES, Faepa.

06.003 Analysis of Renin and Angiotensin Converting Enzyme 2 in Aorta from Human Abdominal Aortic Aneurysm. Francisco DF¹, Dugaich VF¹, Mestriner F¹, Corsi C¹, Campos LCB¹, Couto AES¹, Vasconcelos J¹, Jordani MC¹, Ribeiro MS¹, Becari C². ¹FMRP-USP, Division of Vascular and Endovascular Surgery, Dpt of Surgery and Anatomy, Ribeirão Preto, SP, Brazil; ²FOB-USP, Dpt of Biological Science, Bauru, SP, Brazil

Introduction: Abdominal aortic aneurysm (AAA) is a degenerative disease, marked by a chronic inflammatory process, with loss of muscle cells and degradation of the extracellular matrix, which results in a gradual weakening of the vessel wall and rupture if not treated on time. The renin-angiotensin system (RAS) has a relevant role both in physiological events and in the pathogenesis of cardiovascular diseases. Two main counterregulatory axes are described, the angiotensin-converting enzyme (ACE)/angiotensin II/AT1 receptor axis being responsible for inflammation, proliferation, and vasoconstriction and the beneficial axis composed of angiotensin-converting enzyme 2 (ACE-2), angiotensin 1 -7 and MAS receptor responsible for the anti-inflammation, vasodilator and antiproliferative action. The imbalance of these axes is involved in the pathogenesis of AAA and has been the focus of study to understand the progression of this disease better. Therefore, we sought to analyze Renin and ACE-2 in the aortic tissue of control patients and patients with AAA. **Methods:** In the study group are 21 patients diagnosed with infrarenal AAA of degenerative etiology, eligible for correction through conventional open surgery, who were admitted to the Vascular and Endovascular Surgery Outpatient Clinic of HCRP-USP after authorization through the consent term. In the control group, 13 individuals diagnosed with brain death were included after authorization through the informed consent signed by the donor's family. Aortic tissue samples were obtained during conventional repair surgery for the AAA group and during organ harvesting for the control group. ACE-2 and Renin analyzes were performed by enzyme immunoassay (ELISA). Data are mean \pm SEM. Mann-Whitney test was used to analyze continuous variables. The significance level adopted was $p < 0.05$. All statistical analyzes were performed using the GraphPadPrism program. The project was approved by the Ethics and Research Committee of the HCRP-FMRP-USP (CAAE: 82879518.6.0000.5440). **Results:** ACE-2 concentration is decreased in the aortic tissue of patients in the AAA group compared to the control group ($p < 0.05$) which indicates that this RAS axis is regulated negatively in the AAA group. Tissue renin showed no statistical difference between the control and AAA groups. However, interestingly, we observed that renin tends to present higher concentrations in the tissue of the AAA group, indicating the overactivation of the RAS in these patients. **Conclusion:** Our data demonstrate that ACE-2 is decreased in AAA. Confirming that the beneficial axis of the RAS (ACE-2) is downregulated in the aortic tissue of patients with AAA. This result contributes to the study of new therapeutic targets to limit the progression of the disease and formulate less invasive methods for the treatment of AAA. **Funding:** FAPESP (grants n. 2017/21539-6; 2018/23718-8, 2022/02162-7), CAPES, CNPq, FAEPA.

06.004 Upregulated Hexosamine Pathway contributes to Aneurysmal Vascular Lesion.

Hosomi N^{1,2,3}, Silva JF^{1,4}, Alves JV¹, Costa R^{1,5}, Mestriner F^{6,7}, Nguyen TAV², Becari C^{6,7}, Yanagisawa H^{2,8}, Tostes R¹ ¹FMRP-USP, Dpt of Pharmacology, Brazil, ²TARA-University of Tsukuba Life Sciences Center for Survival Dynamics, Ibaraki, Japan, ³University of Tsukuba, School of Medicine and Health Sciences, College of Medical Science, Ibaraki Japan, ⁴University of Arizona, Dpt of Physiology, Tucson, USA, ⁵UFJ, Academic Unit of Health Sciences, Brazil, ⁶FMRP-USP, Dpt of Surgery and Anatomy, Brazil, ⁷FOB-USP, Dpt of Biological Sciences, Brazil, ⁸University of Tsukuba, Faculty of Medicine, Ibaraki Japan.

Introduction: An aortic aneurysm (AA) is an enlargement in the wall of the aorta, the main blood vessel carrying blood from the heart to the body. Most AA develops silently without symptoms and can result in sudden death due to aortic rupture with around a 20% chance of survival. Although worldwide about 200,000 people die from AA each year, the underlying molecular mechanism is still unknown and there are no effective medications to prevent its progression. Glycosylation of serine and threonine residues of nuclear and cytoplasmic proteins with O-linked β -N-acetylglucosamine (O-GlcNAcylation) is implicated in cardiovascular pathophysiological processes, but its role in AA remains unknown. Abnormal activation of cofilin-1, a member of the cofilin family of proteins essential for remodeling and disassembling actin filaments, promotes the progression of ascending AA in mice. Considering that cofilin-1 is modified by O-GlcNAc, we hypothesized that O-GlcNAcylation of cofilin-1 leads to cytoskeleton disassembly, contributing to aneurysmal vascular lesion. **Methods:** We used aortic samples from endothelial cell (EC)- and smooth muscle cell (SMC)-specific fibulin-4 (Fbln4) knockout mice (ECKO and SMKO, respectively). SMKO, but not ECKO mice exhibit postnatal thoracic AA with elastic fiber disruption. Aortic samples from patients with abdominal aortic aneurysm (AAA) lesions were also used. Expression of O-GlcNAc, OGT (O-GlcNAc transferase), and cofilin-1 was determined by western blot. O-GlcNAcylated-cofilin-1 was determined by immunoprecipitation. Cultured arterial SMCs were treated with Thiamet-G (OGA inhibitor, 1 μ M for 24 h) or vehicle (PBS). O-GlcNAc-modified proteins, SMC migration (scratch assay) and proliferation (PCNA content), and actin assembly (phalloidin fluorescence microscopy) were evaluated. All experiments were performed following the guidelines of the National Council for Animal Experimentation Control and approved by the Ethics Committee on Animal Use (protocol #106/2019) and Research Ethics Committee (protocol CAAE: 82879518.6.0000.5440) of the University of São Paulo, Ribeirao Preto campus. P <0.05 was considered statistically different. **Results:** Expression of total O-GlcNAc-modified protein and OGT was increased in ascending aorta of Fbln4 SMKO mice, but not Fbln4 ECKO mice, compared with control mice (O-GlcNAc: 2.83 ± 0.68 vs. 0.87 ± 0.13 and OGT: 0.31 ± 0.06 vs. 0.13 ± 0.02). In cultured SMC, Thiamet-G increased O-GlcNAc-modified proteins compared to vehicle-treated SMC (2.37 ± 0.13 vs. 0.75 ± 0.05), accelerated the scratch closure, and reduced phalloidin signal. There was no change in SMC PCNA content in Thiamet-G-treated cells. O-GlcNAc-modified Cofilin-1 was found in human samples of AAA. **Conclusion:** Human and mouse aneurysmal lesions exhibit increased content of O-GlcNAc-modified proteins. Increased O-GlcNAc may contribute to SMC dysfunction by cofilin-1-dependent mechanisms and actin disassembly. **Financial Support:** FAPESP (2013/08216-2, 2018/15192-6 to RC Tostes and 2017/21539-6 to C Becari) and FAPESP-Tsukuba SPRINT 2018 (to RC Tostes and H Yanagisawa).

06.005 Nebivolol Prevents Redox State Changes Induced by Cyclophosphamide in Mouse Heart. Marchetti BM, Pimenta GF, Dourado TMH, Tirapelli CR EERP-USP, Lab. of Cardiovascular Pharmacology,

Introduction: Cyclophosphamide (CYP) is a nitrogen mustard widely used in the treatment of cancer. However, its toxic effect in multiple organs limits its therapeutic use. CYP-induced cardiotoxicity occurs in 20-25% of patients receiving the drug. The mechanism by which CYP induces its toxic effect involves different cellular pathways, the main one being increased oxidative stress. In this scenario, the enzyme nicotinamide adenine dinucleotide phosphate [NAD(P)H] oxidase plays an important role in mediating the detrimental effects of CYP on the heart, acting as the main source for the generation of reactive oxygen species (ROS). Cytoprotective compounds are used to improve the quality of life of patients taking CYP. Nebivolol is a third-generation β -blocker that promotes antioxidant effect by reducing the expression of the enzyme NAD(P)H oxidase. Considering that oxidative stress is a central element of CYP-induced cardiac toxicity and that nebivolol has broad antioxidant action, the hypothesis of the present study is that nebivolol will prevent CYP-induced cardiac damage.

Methods: Male C57Bl/6 mice (20-22g) were divided in 4 groups: control, CYP, nebivolol, and CYP-nebivolol. The animals were treated for 5 days with nebivolol (10 mg/kg/day, gavage), and the last dose was administered one hour after CYP injection (300 mg/kg, i.p.). In the left ventricle, the level of superoxide anion (O₂⁻) was assessed by lucigenin chemiluminescence and the concentration of malondialdehyde (MDA) colorimetrically. Catalase and superoxide dismutase (SOD) activity were measured colorimetrically. Nitrite concentration, reduced glutathione (GSH), and plasma CK-MB concentration were assessed. The results were analyzed by Two-way ANOVA followed by Bonferroni post-test. The study was approved by the local CEUA (EERP/USP; 20.1.304.22.2). **Results:** CYP increased generation of O₂⁻ (RLU/mg protein) (n=6-8; C: 54±6.7; CYP: 266.1±36.5*; NEB: 146.6±37.8; CYP+NEB: 133.8±14.7) and the concentration of MDA (mmol/mg protein) (n=5-7; C: 2.3±0.8; CYP: 5.8±0.9*; NEB: 4.1±0.6; CYP+NEB: 4.6±0.5) in the left ventricle, and nebivolol prevented these responses. The activity of antioxidant enzymes SOD (%inhibition/mg protein) (n=6-8; C: 41.6±6.3; CYP: 42.9±3.3; NEB: 33.7±2.7; CYP+NEB: 35.7±3.9) and catalase (U/μl/mg protein x 10⁴) (n=6-8; C: 4.3±0.5; CYP: 3.5±0.1; NEB: 3.8±0.3; CYP+NEB: 3.4±0.1) were not changed after treatment with CYP. Nebivolol treatment decreased GSH concentration (μg/mg protein) (n=6-8; C: 42.8±1.7; CYP: 33.7±3.0; NEB: 22.9±2.1*; CYP+NEB: 43.3±2.4) and increased nitrite concentration (μmol/mg protein) (n=5-7; C: 4.4±0.4; CYP: 2.9±0.2; NEB: 5.7±0.8*; CYP+NEB: 2.8±0.4). Plasma concentration of CK-MB (U/l) (n=5-8; C: 774.9±35.0; CYP: 741.1±56.9; NEB: 765.9±49.9; CYP+NEB: 651.9±96.5) showed no significant differences among experimental groups. **Conclusion:** CYP promotes alteration of the redox state in the heart and nebivolol acted as an antioxidant to decrease the generation of O₂⁻ and the consequent lipoperoxidation. **Financial Support:** FAPESP - Fundação de Amparo à Pesquisa do Estado de São Paulo **References:** BHATT, L. et al. J Ayurveda Integr Med., 8: 62-67, 2017. VALE, G. T. et al. Eur J Pharmacol, 799: 33-40, 2017. IMBABY, S. et al. Hum Exp Toxicol, 33(8): 800-13, 2014.

06.006 Activation of Vascular Autophagy as a Counter-Regulatory Mechanism in Aldosterone-Induced Vascular Dysfunction: Role of Protein O-GlcNAcylation. Rodrigues D¹, Costa RM¹, Vargas P^{1,2}, Barros PR¹, Oliveira-Neto JT¹, Machado MR¹, Freitas-Filho EG³, Hosomi N¹, Okada LY¹, Martins NS², Bonato VD², Cunha LD³, Tostes R¹ ¹FMRP-USP, Depto. of Pharmacology, ²FMRP-USP, Depto. of Biochemistry and Immunology, ³FMRP-USP, Cellular and Molecular Biology and Pathogenic Bioagents

Introduction: Autophagy is a complex catabolic process that recycles intracellular cargo to maintain cell homeostasis. Autophagic flux can be activated as an adaptive mechanism to cope with stress and is implicated in cardiovascular dysfunction. O-GlcNAc (O-glycosylation with N-acetylglucosamine) is a post-translational modification that regulates intracellular processes including autophagy. **Hypothesis:** Considering that proteins linked to the regulation of autophagy are modified by O-GlcNAc, this study aims to determine whether O-GlcNAcylation induced by aldosterone regulates autophagy in the vascular system. **Methods:** Analyses of differentially expressed (DE) genes in human adrenocortical carcinoma (ACC) samples and adjacent normal tissues were analyzed from publicly available data (GSE accession number: 19776). Human endothelial cells (EA.hy926) were treated with aldosterone (100 nM) and protein O-GlcNAcylation and autophagic flux were evaluated via western blot. These parameters were also analyzed in the thoracic aortas of 12-week-old male C57BL/6 mice treated with aldosterone (600 µg/kg/day) for 14 days via osmotic mini-pump infusion. **Results:** Aortas of animals treated with aldosterone displayed increased O-GlcNAc levels. Autophagy markers (LC3-II, p62 and Beclin1) were all decreased in the aortas from aldosterone-treated mice suggesting hyperactivation of the autophagic flow. *In vitro*, EA.hy926 cells treated with aldosterone for 24 or 48 hours showed an increase in LC3-II content, indicative of autophagic flux activation. The same was observed for the O-GlcNAcylation of proteins. 141 DE genes in ACC samples were identified as targets of O-GlcNAc modification and 2 of them are linked to autophagy (OGT and TBC1D5). Ongoing experiments in the aortas of mice treated with aldosterone are being conducted to evaluate autophagy via immunofluorescence. Also, in mice vascular smooth muscle cells (MOVAS cell line) on culture, we are analyzing the effects of aldosterone on autophagy and protein O-GlcNAcylation. **Conclusion:** With these data, we suggest that activation of autophagic flux in response to aldosterone may be interconnected with vascular protein O-GlcNAcylation and may represent a novel mechanism by which aldosterone induces vascular dysfunction. **Financial Support:** FAPESP, CAPES and CNPq.

06.007 Proteomics and Therapeutic Responsiveness in Preeclampsia. Pinto-Souza CC¹, Rossini BC², Dos Santos LD², Sandrim VC¹ ¹IBB-Unesp-Botucatu, Dept of Biophysics and Pharmacology, PPG Biotechnology, Botucatu, SP, Brazil, ²IBTEC-Unesp-Botucatu, Botucatu, SP, Brazil

Introduction: Preeclampsia (PE) is a hypertensive syndrome of pregnancy, characterized by target organ damage, related to a high incidence of cardiovascular sequelae. Women diagnosed with the disease take antihypertensive drugs, however, about 40% of patients do not respond to this treatment, precisely those who have the worst clinical outcomes. Through the proteomic strategy, we intend to 1) compare the profile of proteins expressed in responsive (20.0 ± 2.0 years) and non-responsive (18.5 ± 3.1 years) patients to antihypertensive therapy divided into two pools (each one with a number of four) from non-depleted plasma samples; 2) investigate which proteins are differentially expressed between groups and 3) find out which signaling pathways are altered between the subtypes and whether they are associated with the endothelium. Thus, in order to highlight the pathophysiological mechanisms involved in the disease and the search for potential biomarkers. Ethical conduct of research: We have obtained approval for all human investigations (CAAE: 37738620.0.0000.5440), **Methods:** We performed protein quantification by Bradford, quality control by one-dimensional electrophoresis and tryptic digestion for breaking peptide bonds. Pattern Lab, Uniprot, Panther, String, and Reactome software were used for bioinformatics analysis. **Results:** We identified 131 total proteins. Of which, 124 were identified in responders and 105 in non-responders. Furthermore, 98 are common in both groups. About 26 proteins were found uniquely in the responder group and some of them are associated with immune and complement pathways. While in the non-responder group, 7 proteins were detected only in it and they were also connected with the defense mechanism, although no significant functional enrichment was detected. Furthermore, considering a fold change of 2.0, there were 16 differentially expressed proteins, 1 up-regulated and 15 down-regulated comparing non-responsiveness versus responsiveness. Most of them modulate the immune system (immunoglobulin heavy variable 3-23 and 3-48; pregnancy-specific beta-1-glycoproteins 1, 3 and 7; pregnancy zone protein); integrates inflammatory processes (apo B-100; ApoL-I; serum amyloid A-4) or the complement system (Complements C1qB; C1s; C4-A; C4-B; C5; component C8 gamma chain and complement C9). **Conclusion:** These findings emphasize the divergence of the pathophysiological mechanisms between the two subtypes of the disease, since the under regulated circulating proteins are those that act in the protection of the endothelium, demonstrating the connection between the pathogenesis of PE and alterations in the inflammatory and defensive processes. And so, helping to explain the complexity and clinical consequences of this hypertensive disorder. Funding: Coordination for the Improvement of Higher Education Personnel (CAPES) [financial code 001]; National Council for Scientific and Technological Development (CNPq) [315026/2021-9 - CNPq PQ2] and São Paulo Research Foundation (FAPESP) [Nº2021/12010-7] and [Nº 2022/07605-4].

06.008 Cecal Slurry as a Research Model for New Pharmacological Therapies for Sepsis-Induced Cardiovascular Dysfunction. Delfrate G, Assreuy J, Fernandes D UFSC, Dpt of Pharmacology, Florianópolis Brazil

Introduction: Sepsis leads to organ dysfunction due to a dysregulated host response to an infection. Treatment of this condition is challenging, representing the main cause of death from infection in hospitals. Septic shock is characterized by severe and persistent hypotension, leading to reduced organ perfusion and death. Experimental models are useful to clarify the mechanisms of injury and to point to new pharmacological targets. In this context, cecal ligation and puncture (CLP) is the most used model to induce sepsis but its major drawbacks are its invasiveness and high variability. It consists of opening the abdominal cavity, exposing the colon, reducing its lumen, perforating it and spillover cecal contents. This model demands surgical training, anesthesia, and animal suffering. An alternative method is the cecal slurry (CS) model, which consists of the intraperitoneal injection of a suspension of cecal contents. However, CS model is much less explored in the literature, limiting its application. Therefore, the aim of this study was to standardize CS model in rats, as well as to evaluate whether it reproduces the cardiovascular dysfunction observed in sepsis, compared to CLP model.

Methods: Male Wistar rats (90-100 days of age; 300-400 g) were submitted to sepsis by CLP under anesthesia (isoflurane 3%) as previously described (Rittirsch, D. *Nat. Protoc.*, v. 4, p. 31, 2009) or by CS (1 g/kg i.p. of cecal contents of donor rats, without anesthesia). Both septic groups received the same analgesic (tramadol, 10 mg/kg i.p.) and volume replacement protocols (NaCl 0.9% 37°C, 50 mL/kg s.c.). Naive animals (no intervention) were used as controls. Mean arterial pressure (MAP) was measured through a pressure-transducer coupled catheter (Powerlab 8/30) inserted into the carotid artery of anesthetized animals. Renal blood flow was measured by a laser probe connected Doppler blood flow monitor (Moor Instruments) placed over the kidney. Vascular reactivity was evaluated in aortic rings. All analyzes were performed 24 h after sepsis induction. **Results:** Hypotension was observed in CLP (75.9 ± 7.2 mmHg) and CS (64.1 ± 12 mmHg) groups compared to control rats (101.1 ± 13.7 mmHg) ($n = 10-11$; one-way ANOVA; $p < 0.05$). MAP response to angiotensin II (10 pmol/kg) was lower in CLP (12.3 ± 7.6 mmHg) and CS (8.7 ± 4.6 mmHg) groups compared to control (32.7 ± 10.4 mmHg; $n = 10-11$; ANOVA; $p < 0.05$). Response to phenylephrine (10 nmol/kg) was reduced in CS (29.6 ± 12.3 mmHg) compared to controls (44.78 ± 11 mmHg), but not in CLP (31.6 ± 14.7 mmHg) group ($n = 10$; ANOVA; $p < 0.05$). Renal blood flow was also decreased in CS (264.2 ± 131.1 perfusion units; PU) compared to control (373.3 ± 50.44 PU), but not in CLP (314.4 ± 85.61 PU) group ($n = 10-11$; ANOVA; $p < 0.05$). Concentration-response curves to phenylephrine in isolated aorta rings showed decreased vascular reactivity in the CLP (2.12 ± 0.6 ua) and CS (AUC 2.4 ± 0.4 ua) groups compared to control (AUC 3.26 ± 0.5 ua) ($n = 8$; ANOVA; $p < 0.05$). **Conclusion:** CS model consistently reproduced the hemodynamic dysfunction and vascular hyporeactivity to vasoconstrictors induced by sepsis. This study represents an important contribution for the refinement of experimental sepsis, as it shows a less invasive and highly reproducible model. **Financial Support:** FAPESC, CAPES, CNPq.

06.009 Basal Release and Action of 6-Nitrodopamine from Human Popliteal Artery and Vein *in vitro*. Lima AT, Oliveira LFG, Britto-Júnior J, Campos R, De Nucci G FCM-Unicamp, Dept of Pharmacology, Campinas, São Paulo, Brazil

Introduction: Human umbilical cord vessels[1], aortic rings from *Chelonoidis carbonarius*[2] and *Pantherophis guttatus*[3] present basal release of 6-nitrodopamine (6-ND), as detected liquid chromatography coupled to tandem mass spectrometry (LC-MS/MS). The release of 6-ND is reduced when the vessels are incubated with the NO synthase inhibitor L-NAME, and in these tissues 6-ND acts as a selective dopamine D₂-like-receptor antagonist. Here it was evaluated whether human peripheral vessels release 6-ND, as measured by LC-MS/MS, and its action on pre-contracted vessels. **Methods:** Participants who have undergone surgery for leg amputation in the Hospital Santa Casa de Misericórdia (Sorocaba-SP) were asked to sign an informed consent. The clinical procedure was approved by the local IRB. The human popliteal artery and vein were removed, with special care not to damage the endothelial layer or to over distend the vessels during the procedure. The vessels were placed in a container with Krebs-Henseleit's solution (KHS; pH 7.4, 95%O₂: 5%CO₂) at 8°C. Artery and vein rings were suspended vertically between two metal hooks in 10-mL organ baths containing KHS, continuously gassed with a mixture of 95%O₂: 5% CO₂ (pH 7.4) at 37°C. In endothelium-intact and endothelium-denuded rings pre-treated with L-NAME (100 µM), the preparations were pre-contracted with U-46619 (3 nM). After a sustained contraction was obtained, cumulative concentration-response curves to 6-ND and to the selective D₂ antagonist L-741,626 (10 pM–300 nM) were performed. The relaxation responses were expressed as percentage of the contractile response. **Results:** Basal release of 6-ND from popliteal artery (n=7) and vein rings (n=4) were 1.0±0.3 and 1.4±0.2 ng/mL, respectively, which was reduced in L-NAME treated rings (0.4±0.1 and 0.4±0.2 ng/mL, respectively). 6-ND caused concentration-dependent relaxations of artery (pEC₅₀ 8.17±0.02 and E_{max} 66.78±3.23%) and vein (pEC₅₀ 8.26±0.09 and E_{max} 83.24±9.84%) and L-741,626 caused concentration-dependent relaxations of artery (pEC₅₀ 8.73±0.28 and E_{max} 58.08±8.85%) and vein (pEC₅₀ 9.12±0.17 and E_{max} 68.66±6.73%) which were significantly reduced in endothelium-denuded artery and vein rings, but unaffected by pre-treatment of the artery and vein rings with L-NAME. **Conclusion:** 6-ND is a novel endothelium-derived catecholamine released by human popliteal artery and vein rings, where it acts as a potent vasodilator by blocking dopamine D₂-like receptors. **Acknowledgments:** ATL thanks FAPESP for PhD fellowship (2021/13593-6). JBJ thanks FAPESP for post-doctoral fellowship (2021/14414-8). GDN thanks FAPESP (2019/16805-4) and CNPq (303839/2019-8). [1] Britto-Júnior J, Coelho-Silva WC, Murari GF, Serpellone Nash CE, Mónica FZ, Antunes E, De Nucci G. 6-Nitrodopamine is released by human umbilical cord vessels and modulates vascular reactivity. *Life Sci.* 2021 Jul 1;276: 119425. doi: 10.1016/j.lfs.2021.119425. [2] Britto-Júnior J, Campos R, Peixoto M, Lima AT, Jacintho FF, Mónica FZ, Moreno RA, Antunes E, De Nucci G. 6-Nitrodopamine is an endogenous selective dopamine receptor antagonist in *Chelonoidis carbonaria* aorta. *Comp Biochem Physiol C Toxicol Pharmacol.* 2022 Oct;260: 109403. doi: 10.1016/j.cbpc.2022.109403. [3] Lima AT, Dos Santos EX, Britto-Júnior J, de Souza VB, Schenka AA, Campos R, Moraes MO, Moraes MEA, Antunes E, De Nucci G. Release of 6-nitrodopamine modulates vascular reactivity of *Pantherophis guttatus* aortic rings. *Comp Biochem Physiol C Toxicol Pharmacol.* 2022 Dec;262: 109471. doi: 10.1016/j.cbpc.2022.109471.

06.010 Protein SUMOylation is involved in Renal Resistance against Ischemia after Hemorrhagic Shock. Oliveira FRMB¹, Soares ES¹, Ramos HP¹, Lättig G², Harms C², Cimarosti HI¹, Sordi R¹. ¹UFSC, PPG Pharmacology, Florianópolis, Brazil; ²Charité Hospital, Center for Stroke Research, Germany.

Introduction: Hemorrhagic shock (HS) is a condition associated with multiple organ dysfunction (MOD) and death. Excessive bleeding followed by reperfusion causes a damage known as ischemia-reperfusion injury [1]. The precise mechanisms of MOD are not completely elucidated. It is well known that severe cell stress may lead to increased small ubiquitin-like modifier (SUMO) levels, and several SUMO targets are involved in organ protection [2]. The hypothesis of our study is that SUMOylation increases after HS to protect the organ against ischemia. In this study we investigated the degree of renal and hepatic damage associated with HS as well as temporal changes of SUMOylation in these organs. **Methods:** Male Wistar rats were given tramadol (10 mg/kg, s.c.) and ketamine and xylazine (100 and 10 mg/kg, i.p., respectively). The left femoral artery and vein were cannulated, and blood was withdrawn at a rate of 1 mL/min until mean arterial pressure (MAP) reached 40 ± 2 mmHg. The animals were kept at this MAP target for 90 min and, then, reperfused with the previously shed blood. Two, 6 or 24 h after reperfusion, blood, kidney, and liver were harvested, and parameters of organ damage and SUMO1/2/3 profile were investigated. False-operated animals were used as controls (n = 10/group). The role of SUMOylation after hypoxia/reoxygenation injury was investigated in mutated human kidney cells (HK-2) overexpressing SUMO1 or SUMO2 and subjected to oxygen and glucose deprivation (OGD). CEUA/UFSC: 7396250219. **Results:** HS animals exhibited hypotension and increased heart rate. General markers (CK and LDH) as well as hepatic markers (AST and ALT) showed progressive elevation for up to 24 h. Conversely, markers of renal function (urea and creatinine) increased 2 h after the shock and returned to baseline values within 24 h. The kidneys exhibited reduced oxidative stress due to enhanced antioxidant mechanisms (free sulfhydryl, glutathione reductase, and catalase) compared to the liver. Activation of apoptotic proteins (caspase-3 and 8) and histological damage were observed in the liver while no changes were found in the kidneys. In contrast, dot-blot showed that global levels of SUMOylation (mainly SUMO2/3) were increased in the kidneys. Western blot revealed alterations in (de)SUMOylation in different bands of renal tissue while no changes were detected in the hepatic tissue. The number of propidium iodide (PI)-positive HK-2 cells increased after OGD when treated with a SUMOylation inhibitor (35.3 ± 2.0 vs. 76.6 ± 7.0). Conversely, overexpression of SUMO1 (PI = 40.4 ± 16.8) or SUMO2 (PI = 32.9 ± 8.1) reduced cell death compared to the control vector (PI = 76.0 ± 12.7). **Conclusions:** Systemic organ failure in HS persisted for at least 24 h. While liver injury markers increased over time, we observed a reduced kidney damage which was associated with an increased global SUMOylation in this organ. The inhibitor of SUMOylation increased the death of renal cells, while the overexpression of SUMO1 and SUMO2 induced cell protection. These findings suggest that SUMOylation of proteins is, at least in part, involved in renal resistance to ischemia after HS. **Financial Support:** CAPES and CNPq. **References:** [1] Wu et al, Cell. Physiol. Biochem. v.46, p.1650, 2018 [2] Lee et al, Open Biol. v.27, p. 950, 2007

06.011 External Quality Assessment from the Systematic Review and Meta-Analysis about the Effects of Antidepressants on Blood Pressure of Male and Female Rats. dos Santos TM, Linder AE ¹UFSC, Dpt of Pharmacology, Florianópolis, Brazil

Introduction: Failures in the transparency of methodological reporting in basic research bring uncertainty regarding biases related to selection (allocation concealment), performance (randomization and blinding during the experiment), detection (randomized and blinded evaluation of the result), attrition (reporting of incomplete or of selected results) and other biases. This prevents the proper and effective evaluation of methods and results, impairing the internal quality of the studies that indicates whether the study results can be truly attributed to the effect of the intervention and not to other factors, such as uncontrolled biases. This omission of important information may be the reason why the assessment of the internal quality of the articles included in an unpublished systematic review and meta-analysis on “the effects of antidepressants on blood pressure in male and female rats” using the “Risk of Bias” tool. – Systematic Review Center for Laboratory Animal Experimentation” (RoB – SYRCLE) points to a general unclear risk of bias. Another important factor that can also generate inconclusive results is the external quality assessment, which qualifies the reports on the execution and publication of the studies. Based on this, we tested the hypothesis that the external quality assessment is as unclear as the internal quality assessment of basic studies.

Methods: For this purpose, the external quality assessment of the articles included in the systematic review and meta-analysis above reported was performed by a single reviewer with a checklist adapted from CAMARADES (Collaborative Approach to Meta-Analysis and Review of Animal Data from Experimental Studies) containing 10 items that were judged as “yes”, “no” and “unclear” (in the same way the internal quality was assessed) according to their variations.

Results: From the included publications (n=44), the majority were peer-reviewed (~97%, n=43), reported species/strain (~97%, n=43), age or weight (~100%, n=44), sex of the animals (~90%, n=40) and the blood pressure measurement protocol (~90%, n=40). Half of the publications used some guide for the use of animals (50%, n=22) and just over half of the publications reported compliance with animal welfare regulations (~68%, n=30). Approximately 52% (n=23) of publications reported less than three conditions of housing in Bioterium; ~20% (n=9) from three to five conditions and ~27% (n=12) reported none. Only ~27% (n=12) of the publications declared possible conflicts of interest and none of the studies reported having performed a sample calculation. Among the options of responses “yes”, “no” and “unclear”, the adapted CAMARADES tool generated less “unclear” responses (58 out of 440) than the RoB-SYRCLE tool (302 out of 440). **Conclusion:** Overall, our findings may be due to the fact that the items from CAMARADES are more explicit about the type of information to be assessed. **Financial Support:** Coordenação de Aperfeiçoamento de Pessoal de Nível Superior (CAPES).

06.012 Effects of Chronic Treatment with *Alpinia zerumbet* Leaf Extract on Cardiovascular changes in the Model of Renovascular Hypertension 2 Kidney, 1 Clip.

Menezes MP¹, Santos GP, Silva DLB, Gouveia JF, De Oliveira BC, Cavalheira MA, Silva EM, Soares RA, Da Costa CA, De Bem GF, Resende AC, Ognibene DT. UERJ, Dept of Pharmacology, Rio de Janeiro, Brazil

Introduction: Renovascular hypertension is secondary to renal artery stenosis, leading to hyperactivation of the renin-angiotensin system, generating several physiological changes, such as cardiovascular remodeling and oxidative stress. *Alpinia zerumbet* is a plant native to East Asia and found in abundance along the Brazilian coast. Popularly known as *Colonia*, it is widely used in folk medicine for its antihypertensive, anxiolytic, and diuretic properties. **Objective:** This study aimed to investigate the possible cardiovascular effects of *Colonia* leaf extract (AZE) in a model of renovascular hypertension, two kidney, one clip (2K1C). **Methodology:** 45-days-old male Wistar rats (CEUA UERJ: 001/2021) were anesthetized with isoflurane (4% for hypnosis + 1 L/min of O₂; 2% for maintenance + 0.8 L/min of O₂) and, after laparotomy, a silver clip with a diameter of 0.20 mm was inserted around the left renal artery, generating the 2K1C group. Sham rats were submitted to laparotomy to be used as controls. After the surgery, the groups were divided into those treated or not with AZE (50 mg/kg/day in drinking water) for 7 weeks. During treatment, systolic blood pressure (BP) was measured once a week by caudal plethysmography. The animals were then anesthetized with isoflurane (4% for hypnosis + 1 L/min of O₂; 2% for maintenance + 0.8 L/min of O₂) and the blood was collected through the puncture of the abdominal aorta. Thoracic aorta and heart were collected for morphometric analysis and the mesenteric arterial bed (LAM) was isolated and coupled to an organ perfusion system to assess its responsiveness to vasoactive agents. Plasma and heart homogenate were used to assess the oxidative damage to lipids, observing the levels of malondialdehyde (MDA), as well as the activity of the antioxidant enzymes Catalase (CAT), Glutathione Peroxidase (GPx) and Superoxide Dismutase (SOD) through spectrophotometry. **Results:** Treatment with AZE impaired increasing SBP in the 2K1C+AZE group (mm Hg; 2K1C+AZE: 128±3/ 2K1C: 195±12.3; n=15). In addition, the treatment prevented the promotion of hypertrophy in the intima-media layer of the thoracic aorta (µm; 2K1C+AZE: 95.9±4.8/ 2K1C: 133.1±5.8; n=6), the left ventricular (mm; 2K1C+AZE: 2±0.08/ 2K1C: 3.1±0.11; n=6), and intraventricular wall remodeling (mm; 2K1C+AZE: 2±0.07/ 2K1C: 2.9±0.17; n=6) as well as the narrowing of the left ventricular lumen (mm²; 2K1C+AZE: 5±0.27/ 2K1C: 3.7±0.19; n=6). Also, the treatment prevented the reduction of antioxidant enzymes activities in plasma (CAT [U/mg ptn] - 2K1C+AZE: 1.53±0.23/ 2K1C: 0.52±0.18; SOD [U/mg ptn] - 2K1C+AZE: 95.47±12.7/ 2K1C: 33.09±7.6; GPx [U/mg ptn] - 2K1C+AZE: 0.010±0.0004/ 2K1C: 0.006±0.0003; n=6) and in the heart homogenate (CAT - 2K1C+AZE: 0.49±0.05/ 2K1C: 0.22±0.03; SOD - 2K1C+AZE: 43.27±4.9/ 2K1C: 20.21±0.9; n=6) and also prevented the increase in MDA levels in plasma (nmol TBA/mg ptn - 2K1C+AZE: 0.18±0.017/ 2K1C: 0.29±0.05; n=6) and heart homogenate (2K1C+AZE: 0.04±0.002/ 2K1C: 0.06±0.004; n=6). On the other hand, AZE treatment did not improve vascular dysfunction in this model. **Conclusion:** Thus, this study shows that AZE treatment is able to prevent the development of hypertension and cardiovascular remodeling in the 2K1C model, which may be related, in part, to the improvement of oxidative stress. **Financial Support:** CAPES and FAPERJ.

06.013 The Resveratrol during Pregnancy and Lactation Reduces Oxidative Stress, Matrix Metalloproteinase (MMP)-2 Activity, and Hypertension in Adult Offspring. Neves VGO, Gomes BQ, Rocha EV, Mello MM, Assis VO, Tirapelli CR, Castro MM FMRP-USP, Dept of Pharmacology

Increased matrix metalloproteinase (MMP)-2 activity and oxidative stress are associated with hypertension in spontaneously hypertensive rats (SHR). MMP-2 activity contributes to hypertrophic arterial remodeling in hypertension. Resveratrol reduces both oxidative stress and MMP-2 activity in some cardiovascular disease. Knowing that treatment with resveratrol during pregnancy and lactation is important to reduce the systolic blood pressure (SBP) in the adult life, we tested the hypothesis that a diet rich in resveratrol during this period in SHR rats reduces oxidative stress and MMP-2 activity in the aortas of offspring, thus reducing the development of hypertrophic vascular remodeling and arterial hypertension in adulthood. SHR and WKY female rats (180g) were treated with resveratrol, 4g/kg, during pregnancy and lactation. The offspring were separated by gender and studied at the end of 12 weeks (CEUA-USP 052/2021). It is important to note that the offspring did not receive treatment with resveratrol after weaning. SBP was analyzed by tail-cuff plethysmography and aortas were analyzed by gel and *in situ* zymography, DHE for oxidative stress, DAF for nitric oxide (NO), and morphological analysis with H&E. Statistics were performed by two-way ANOVA with Tukey's post-test ($p < 0.05$). Both male and female SHR rats had significantly higher blood pressure than WKY at 12 weeks. Resveratrol, however, reduced this in both male and female SHR ($n=13$; $p < 0.05$). There was an increase in oxidative stress in the aortas of male and female SHR rats and resveratrol was able to reduce it only in the female ($p < 0.05$; $n=6$). Resveratrol also increased NO availability and reduced *in situ* gelatinolytic activity in the aorta of SHR offspring in both genders ($n=6$; $p < 0.05$). Finally, we noted that the hypertrophic vascular remodeling occurred specially in the aortas of male SHR offspring and resveratrol seems to attenuate it ($p=0.06$). In conclusion, resveratrol during pregnancy and lactation contributed to attenuate high SBP and MMP-2 activity in the aortas of both male and female adult offspring. **Financial Support:** CAPES, FAPESP, CNPq and FAEPA.

06.014 Potentiation by 6-Nitrodopamine of the Chronotropic Effect of Dopamine, Noradrenaline, and Adrenaline in the Rat Isolated Atria. Fuguhara V, Britto-Júnior J, Lima AT, Antunes E, De Nucci G Unicamp, Dpt of Pharmacology, Campinas, Brazil

Introduction: 6-nitrodopamine is released from rat isolated atria, and is 100 times more potent than noradrenaline and adrenaline, and 10,000 times more potent than dopamine as positive chronotropic agent(1). 6-nitrodopamine release is not affected by pre-incubation with tetrodotoxin, indicating that is not released by nerve terminals. Inhibition of either phosphodiesterase 3 or phosphodiesterase 4 in the rat and mouse causes sinoatrial tachycardia(2) but does not potentiate the tachycardia elicited by catecholamines(3). Here we investigate the interaction of 6-nitrodopamine with the classical catecholamines in the rat isolated right atria rate (RIAR). **Methods:** Male Wistar-rats were euthanized by isoflurane overdose and the right atrium was mounted between two metal hooks in 10-mL custom designed glass chambers containing Krebs-Henseleit's solution, continuously gassed with a mixture of 95% O₂ : 5% CO₂ at 37°C using a heated circulator. Tissues were allowed to equilibrate under a resting tension of 10mN for one hour, and the isometric tension was registered using a PowerLab system(1). **Results:** Incubation with dopamine (1pM, Panel A; n= 6), noradrenaline (1pM, Panel B, n= 4), and adrenaline (1pM, Panel C; n= 5), did not increase the atrial frequency. 6-nitrodopamine (0.01pM) also had no effect on the atrial frequency (not shown), however co-incubation of 6-nitrodopamine (0.01pM) with either dopamine (1pM, Panel A; n= 4), noradrenaline (1pM, Panel B; n= 6), and adrenaline (1pM Panel C; n= 5) resulted in significant increases in rat isolated atria rate, which persisted for at least 30min after washout of the agonists. Co-incubation of dopamine (1pM) with 1pM of either noradrenaline (Panel D, n= 4) or adrenaline (Panel E, n= 4) did not result in significant increases in RIAR. Co-incubation of noradrenaline (1pM) with 1pM of adrenaline (Panel F, n= 4) also failed to cause significant increases in atrial frequency. **Conclusion:** The remarkable synergism exhibited by 6-nitrodopamine on the positive chronotropic effect induced by catecholamines indicate that 6-nitrodopamine has a different mechanism of action than that proposed for beta-adrenoceptor stimulation (increase in adenylate cyclase activity). The finding reinforces the idea that 6-nitrodopamine may be important therapeutic potential for both acute and chronic heart failure. **Financial Support:** grant 2022/07737-8, 2021/14414-8, 2021/13593-6, 2017/15175-1, 2019/16805-4, São Paulo Research Foundation (FAPESP) and CNPq (303839/2019-8). **References:** 1. Britto-Júnior, J. Life Sci., v. 307, p. 1, 2022. 2. Galindo-Tovar, A. Naunyn-Schmied Arch Pharmacol., v. 379, p. 379, 2009. 3. Kaumann, AJ. Naunyn-Schmied Arch Pharmacol., v. 380, p. 421, 2009.

06.015 Elastase-2, an angiotensin II forming enzyme, is upregulated in human abdominal aortic aneurysm. Dugaich VF¹, Mestriner F¹, Carlos Corsi¹, Franco D¹, Vasconcelos J¹, Jordani MC¹, Ribeiro MS¹, Becari C². ¹FMRP-USP, Div. of Vascular and Endovascular Surgery, Dept of Surgery and Anatomy, Ribeirão Preto, SP, Brazil. ²FOB-USP, Dept of Biological Science, Bauru, SP, Brazil

Introduction: The abdominal aortic aneurysm (AAA) is a pathological dilation of the abdominal aorta that can lead to death as a cause of the rupture and bleeding. The AAA main risk factors are being old, men, and having smoking habits. Other risk factors can include hypertension, hyperlipidemia, and family history. This disease has no pharmacological treatment other than repair surgery. The Renin-Angiotensin System (RAS) regulates the cardiovascular system and has been implicated in the pathogenesis of AAA. Elastase-2 (ELA-2) is an enzyme that generates angiotensin-II (Ang II) in arteries and contributes to resistance arteries and vascular remodeling in animal models. Our group demonstrated that Elastase-2 Knockout (ELA-2KO) mice ELA-2KO mice might be less susceptible to develop an aorta dilation in AAA induced by Angiotensin II (Ang II) infusion in mice models. Therefore, Elastase-2 is a candidate factor that contributes to the formation and/or development of AAA. We sought to investigate the expression of Elastase-2 in the AAA human aorta. **Methods:** Aortic tissue from AAA patients (n=22) was collected during conventional AAA repair surgery, while control aortas were obtained from organ donors (n=10). Clinical data were also collected from both patient groups. Protein expression and RNA quantification for Elastase-2 codify gene CELA2a was analyzed by Western Blotting and qPCR. This project was approved by the Ethic Committee (CAAE: 82879518.6.0000.5440). **Results:** Our AAA cohort consisted mostly of males (77.27% AAA vs. 60% Control, p=0.4), smokers or ex-smokers (90.91% AAA vs. 30% Control, p=0.001) and most of them had hypertension (81.82% AAA vs. 50% Control, p=0.09). Analysis of mRNA expression by qPCR in the AAA group (n=7) showed that CELA2a was upregulated (p=0.0012) compared with the control group (n=6). Elastase-2 (CELA2a) protein expression by western blotting was upregulated (p=0.03) in the AAA group (n=14) compared with the control group (n=7). **Conclusion:** Our data show, for the first time, that Elastase-2 expression in the human aorta, and is up-regulated in AAA human patients. Our data are showing that Elastase-2 contributes to the development of the aneurysm and aorta dilation, similar to what our research group previously showed in ELA-2 KO mice models. Supported by: FAPESP (grants n. 2017/21539-6; 2018/23718-8, 2022/02162-7).

06.016 6-Nitrodopamine and 6-Cyanodopamine are Released by Human Washed Platelets. Campos R¹, Mathias-Netto FC¹, Nash CES¹, Moraes MO², Moraes MEA², De Nucci G³ ¹UNICAMP, Dept of Pharmacology, Campinas, Brazil, ²UFC Fortaleza, Dept of Pharmacology, Brazil, ³USP, Dept of Pharmacology, São Paulo, Brazil

Introduction: 6-Nitrodopamine is a novel catecholamine that is released from vascular tissues, such as human umbilical cord vessels, aortic rings from *Chelonoidis carbonarius* (Britto-Jr et al., 2022), *Pantherophis guttatus* (Lima et al., 2022) and from *Callithrix* spp (Britto-Jr., 2023). 6-Nitrodopamine (6-ND) has been previously identified as an endogenous substance with dopamine antagonistic properties (Britto-Jr et al., 2022). This study aims to identify its role in platelet aggregation. **Methods:** Liquid Chromatography couple to mass spectrometry was used to quantify catecholamines from washed platelet samples. Optical aggregometry was used to identify the role of 6-ND, 6- CyanoDopamine, Dopamine, known receptor subtype selective dopaminergic agonists and antagonists have in ADP, collagen and thrombin stimulated aggregation to identify any inhibitory or potentiator role of 6-ND. Aggregations were carried out in human Plasma Rich Platelets (PRP) and washed platelets. All subjects gave written informed consent, and the State University of Campinas (UNICAMP) ethics committee approved the clinical protocol (Approval Number 00812918.0.0000.5404). **Results:** Platelets released 6-Nitrodopamine and 6- CyanoDopamine upon stimulation by thrombin (0.1 U) or collagen (1ug/mL) (n=5 for each group). 6-Nitroadrenaline, 6- Bromo Dopamine and 6-NitroDopa were not detected (n=5 for each group). 6-ND does not cause or inhibit platelet aggregation and does not affect ADP, Collagen or Epinephrine induced PRP aggregation or Thrombin-induced washed platelet aggregation. Curiously, 6-ND potentiates the aggregation induced by U-46619. 10 µM Dopamine is sufficient to potentiate ADP and Collagen induced aggregation at subthreshold concentrations. 6-ND reduces dopamine potentiation of ADP and Collagen induced aggregation. Haloperidol and the D3 receptor antagonists PG01037 and SB277011A reduce the potentiation induced by dopamine but not basal ADP and collagen potentiation. Sumanriole, a selective D2 agonist, potentiated aggregation which was blocked by 6-ND. **Conclusion:** The data demonstrates that platelets released 6-Nitrodopamine and a new catecholamine, 6- Cyanodopamine. 6-ND acts as a D2/D3 receptor antagonist. Given that both dopamine and 6-ND are released by the vascular endothelium, 6-ND modulates platelet reactivity and may play a protective role against thrombosis involving vascular dysfunction. **Financial Support:** Rafael Campos (2022/08232-7) and Gilberto De Nucci (2019/16805-4) thanks FAPESP. **References:** Britto-Jr, J. CBP, Part C., v.260, p.10940, 2022 Lima, AT. CBP, Part C., v.262, p. 109471, 2022 Britto-Jr, J. Braz.J. Biomed. Res, v.53, e12622, 2023

06.017 Basal Release and Smooth Muscle Relaxation Induced by 6-Nitrodopamine in Isolated Mouse Urinary Bladder, Urethra and Prostate. Oliveira MG¹, Britto-Júnior J, Chiavegatto S², Monica FZ¹, Antunes E¹, Zatz R³, De Nucci G¹ ¹Unicamp, ²ICB-USP, ³FM-USP

Introduction: 6-Nitrodopamine (6-ND) is an endogenously produced product of the nitric oxide (NO)-dependent nitration of dopamine. Growing evidence shows its key role as a potent mediator of *in vivo* and *in vitro* chronotropism in rats, as well as its spasmogenic activity in the vas deferens of both rats and humans. However, the production, release, and function of 6-ND in the tissues of the urinary tract is still unknown. Therefore, the aim of this study was to investigate whether 6-ND is released from the mouse urinary bladder and to evaluate its relaxing actions on smooth muscle in the mouse bladder, urethra, and prostate *in vitro*.

Methods: Experiments were conducted in adult male control (C57BL/6), eNOS *-/-*, iNOS *-/-* and nNOS *-/-* knockout mice. After euthanasia, urinary bladders were isolated and maintained in 1 mL of Krebs-Henseleit solution for 30 min (37 °C). Basal release of 6-ND was assessed in the supernatants by liquid chromatography with tandem mass spectrometry (LC-MS/MS). A pool of four bladders was used to constitute each experimental sample. In another series of experiments, concentration-response curves to 6-ND were conducted in two different conditions: one under baseline conditions to assess its potential contractile effect, and the other in tissues pre-contracted with carbachol (10 µM) for bladder and prostate, and vasopressin (1 µM) for the urethra, to evaluate relaxation. The data represent the mean ± SEM, with n representing the number of animals. Statistical analysis was performed using t-tests. All protocols had the approval of the ethics committee (5959-1/22, 6087-1/22 and 6067-1/22; CEUA/UNICAMP). **Results:** Urinary bladders from control mice exhibited a basal release of 6-ND, as detected in the supernatants by LC-MS/MS (1.97 ± 0.45 ng/mL, n = 22). The release was significantly lower in bladders from nNOS *-/-* mice (0.37 ± 0.10 ng/mL, n = 8, p = 0.021), but not from eNOS *-/-* (1.74 ± 1.2 ng/mL, n = 5) or iNOS *-/-* (0.99 ± 0.31 ng/mL, n = 8), suggesting nNOS is the isoform responsible for 6-ND synthesis in mouse urinary bladder. *In vitro* experiments showed no significant contractile effects of 6-ND in the assessed tissues. Conversely, cumulative addition of 6-ND promoted concentration-dependent relaxations in all evaluated tissues. The maximal response (E_{max}) to 6-ND were 56 ± 5.0 % for bladder, 27 ± 1.5% for urethra and 57 ± 9.5% for prostate, respectively (n = 6). Moreover, 6-ND exhibited high potency, producing 50% of the maximum relaxation at the picomolar range. However, further exploration is needed to detect 6-ND release in other vesical tissues understand the underlying mechanisms responsible for 6-ND-induced relaxation in these tissues. **Conclusion:** The release of 6-ND may represent a novel mechanism by which NO can independently modulate smooth muscle reactivity, irrespective of cGMP production. Investigating the effects of 6-ND could provide valuable insights into its pathophysiological importance and therapeutic potential. **Financial Support:** Fapesp 2019/16805-4.

06.018 Loss of Beta-2 Adrenergic Receptor S-Nitrosylation Protects Against Myocardial Ischemia Reperfusion Injury. Rosales TO¹, Roy R¹, Gao E², Premont RT³, Stamler JS³, Koch WJ¹. ¹Duke University School of Medicine, Dept of Surgery, Durham, NC, USA; ²Temple University, Center for Translational Medicine, Philadelphia, PA, USA; ³Case Western Reserve University School of Medicine, Institute for Transformative Molecular Medicine, Cleveland, OH, USA; University Hospitals Cleveland Medical Center, Harrington Discovery Institute, Cleveland, OH, USA

Background: Myocardial infarction (MI), caused by ischemia-reperfusion (I/R) injury, remains the leading cause of morbidity and mortality worldwide. Signaling through G protein-coupled receptors (GPCRs), such as Beta-adrenergic receptors (BARs), plays a critical role in heart function and pathology. Under pathogenic conditions, myocardial BAR dysfunction contributes to pathogenesis progression by excessive signal uncoupling and receptor desensitization, which in turn, leads to myocyte death and contractility defects. It has been shown that the activation of B2ARs, an important BAR isoform in the heart, mediates myocyte survival and can exert cardioprotective effects against I/R injury. On this matter, nitric oxide (NO) is a key regulator of B2AR responses. NO binding to protein cysteine thiols (AKA S-nitrosylation) can alter target protein activity, localization, partner binding, or stability. It has been reported that B2AR S-nitrosylation at Cys265 drives receptor desensitization and caveolar internalization, whereas B2AR lacking the S-nitrosylation site, exhibits prolonged signaling. Therefore, we aimed to investigate the role of SNO-B2AR in cardiac signaling and acute myocardial dysfunction after I/R injury. **Methods:** Female and male wild-type (WT) C57BL/6 mice and genetically engineered mice lacking the B2AR S-nitrosylation site (B2AR-C265S knock-in (KI) mice) were submitted to myocardium injury by coronary artery ligation. Myocardial injury was induced with 60 min of ischemia, followed by 24 h of reperfusion. Mice were submitted to increasing doses of isoproterenol (ISO) (0.5, 1, 5 and 10 ng) to determine *hemodynamic parameters*. *In vivo* experiments, molecular and biochemistry assays were performed 24 h after I/R surgery. Appropriate statistical analyses were performed according to each experimental data set (Student's t-test or ANOVA). **Results:** Our results show that: i) B2AR-C265S KI responses to ISO were increased when compared to B₂AR WT; ii) I/R-induced infarct size was reduced in B2AR-C265S KI (32%) compared to B2AR WT (57%), whereas infarct area at risk did not change among the groups; iii) Ejection fraction (EF), left ventricular (LV) mass and Fractional shortening (FS) did not change 24 h after I/R surgery. **Conclusions:** Our data show that mice with B2AR lacking the S-nitrosylation site exhibit prolonged receptor response. Moreover, B2AR-C265 KI mice displayed attenuated infarct size in a mouse model of acute myocardial I/R injury. The preservation of B2AR density and/or functionality in the heart may help to explain the cardioprotection observed in B2AR-C265S KI mice. Thus, S-nitrosylation is a central mechanism in B2AR signaling and may contribute to novel therapeutic interventions to promote cardioprotective signaling, shedding new light on pathogenesis and mechanisms of cardiac injury/repair with translational potential.

06.019 AT1r Expression in Abdominal Aortic Aneurysm and Angiotensin II Receptor Blockers Treatment Impact in Human Tissue. Vasconcelos JL¹, Dugaich VF¹, Francisco DF¹, Mestriner F¹, Corsi C¹, Couto AES¹, Becari C², Ribeiro MS¹. ¹FMRP-USP, Division of Vascular and Endovascular Surgery, Dept of Surgery and Anatomy, Ribeirão Preto, SP, Brazil. ²FOB-USP, Dept of Biological Science, Bauru-SP, Brazil

Introduction: Hyperactivity of the Renin-Angiotensin System is associated with the emergence and growth of Abdominal Aortic Aneurysms (AAA). An important component of this pathway is the AT1 receptor, which is involved in cell growth, proliferation, pro-inflammatory activity, angiogenesis, and fibrosis. Due to its plurality of actions, it has been identified as a therapeutic target using angiotensin II receptor blockers (ARB). We sought to investigate the effect on tissue expression of AT1r in the presence of an aortic aneurysm and the impact of chronic ARB administration in humans. **Methods:** We collected human tissue samples from the aorta during AAA corrective surgery (n=10), and control samples were obtained through organ donation (n=6). Tissue expression of AT1r was quantified using Western Blotting (WB). ARB treatment analysis was based on previous use by patients of this medication due to cardiovascular comorbidities. The ARB drug was Losartan and was administered 50mg (n=2) and 100mg (n=3) once a day, according to medical indications due comorbidities management. The chronic use of ARB was obtained through analysis of medical records, identifying patients submitted to aneurism correction and in ARB treatment pre-surgical in previous medical appointments. These patients have similarities in age, comorbidities, sex, and aneurysm size with each other as well as the control group. Protocol approved by the Human Ethics Committee (CAAE: 82879518.6.0000.5440). **Results:** The AAA group presents an expression of AT1r upregulated, about the control group ($p=0.05$). By evaluating only the samples from the AAA group and dividing them according to the previous use of medications, we obtained the following results: The group in which patients were treated before surgery with Losartan (BRA) did not show alteration in aorta AT1r expression compared to the group that did not receive this medication ($p=0.15$). **Conclusion:** According to the data, there is an overexpression of the AT1 receptor in the tissues of patients with abdominal aortic aneurysms. The chronic losartan treatment did not interfere with aorta AT1r expression compared to those who did not receive the medication. **Funding:** This research was supported by Conselho Nacional de Desenvolvimento Científico e Tecnológico (CNPQ), Fundação de Amparo à Pesquisa do Estado de São Paulo (Fapesp, grants n. 2017/21539-6; 2018/23718-8; 2020/03308-0; 2019/11485-1, 2022/02162-7), CAPES, Faepa.

06.020 Diuretic activity of crude ethanol and saponin-rich extracts of *Solanum sisymbriifolium* Lam. in rats. Arrúa WJ, Ibarrola DA, Hellión-Ibarrola MC, Duarte JG, Galeano Universidad Nacional de Asunción, Facultad de Ciencias Químicas, Dept of Pharmacology, Paraguay

Introduction: *Solanum sisymbriifolium* Lam. is a native perennial plant with chemical characteristics of therapeutic importance. It is used for its antihypertensive and diuretic biological activities in Paraguayan traditional medicine. For this reason, the aim of the study was to evaluate the effect of acute oral administration of doses of the ethanol (EESs) and saponin-rich (SSs) extracts obtained from the root of *Solanum sisymbriifolium* Lam. on the diuresis profile of rats. **Methods:** The diuretic activity was determined using 36 male Wistar rats, randomly distributed into the following six groups: Control group that received saline solution 0.1 mL/100 g of body weight; Diuretic group that was treated with 20 mg/kg of furosemide (F20 mg/kg); two groups treated with the crude ethanolic extract of *S. sisymbriifolium* with doses of 50 and 100 mg/kg (EESs50 mg/kg and EESs100 mg/kg, respectively); and two groups were treated with the extract enriched in saponins with doses of 1 and 10 mg/kg (SSs1 mg/kg and SSs10 mg/kg, respectively). All substances were orally administered, and animals were placed in metabolic cages individually for a period of 24 hours. The diuretic activity of the extracts was determined by measuring urine volume, urinary electrolyte, urine pH and glomerular filtration rate. The urine output measured at 5 h and 24 h, electrolyte concentration, pH and glomerular filtration rate were measured at 24 hours duration. Data were analyzed by one way ANOVA followed by Dunnett's test. The work protocol was evaluated and approved by the Institutional Ethics Committee according to CEI 869/2022. **Results:** The findings indicated that both doses of crude ethanol and saponin-rich extracts of *S. sisymbriifolium* Lam. significantly increase diuresis after 24 hours of treatment. Urinary pH was not affected by treatment. On the other hand, a significant increase in the urinary elimination of sodium and chloride was observed without affecting the elimination of potassium with all the doses of the extracts used. In addition, a significant increase in the glomerular filtration rate was evidenced. **Conclusion:** This study confirms the ethnopharmacological use of *S. sisymbriifolium* Lam. as diuretic agent. Both the ethanolic and saponin-rich extracts presented natriuretic and saluretic effects. In addition to an increase in the glomerular filtration rate, this supports its diuretic effect. The diuretic activity of the extracts of *S. sisymbriifolium* may be due to the presence of active molecules of saponins. The better diuretic effect was observed in the SSs which contain more concentration of saponins. Furthermore, these diuretic effects support the potential antihypertensive effect of this plant species. **References:** Hakim E.M., *J Ethnopharmacol.*, v.273, pag. 113942, 2021 Hozaien H.E., *Nat Prod Res*, v. 33, pag. 1832-1833, 2019 Ibarrola D.A., *J Ethnopharmacol.*, v. 298, pag. 115605, 2022 Kau S.T., *J Pharmacol Methods*, v. 11, pag. 67-75, 1984 **Financial Support:** This research did not receive any specific grant from funding agencies in the public, commercial, or not-for-profit sectors.

06.021 The Influence of C3a on Matrix Metalloproteinase (MMP)-2 Activity and Oxidative Stress in Angiotensin-II-induced Hypertension. Ramos LVR, Mello MM, Castro MM FMRP-USP, Dept of Pharmacology.

Introduction: Hypertension is associated with inflammation, increased cytokine concentrations and exacerbated immune responses. Increased levels of angiotensin II contribute to intensify the effects of the complement system, C3a and C5a, in their receptors at the vasculature. The activation of the complement system decreases the levels of Foxp3 and inhibits the immunosuppressive actions of regulatory T cells in angiotensin II models of hypertension. Furthermore, increased levels of C3a contributes to trigger oxidative stress and increase the expression of matrix metalloproteinase (MMP)-2 in rat aortas with aneurysm, an important protease that contributes to arterial remodeling in many cardiovascular diseases. We analyzed whether increased C3a levels contributes to trigger oxidative stress and MMP-2 activation in mice aortas, thus contributing to vascular remodeling and dysfunction in hypertension. **Methods:** C57BL/6 mice were submitted to a surgery where minipumps containing angiotensin II (1 mg/kg/day) or vehicle were subcutaneously implanted. Mice were treated with the C3aR antagonist (SB290157), at 1 mg/kg/day intraperitoneally, every other day for 14 days (CEUA-USP 1204/2023). Tail-cuff plethysmography was done every two days after minipumps implantation for measuring systolic blood pressure (SBP). The aortas were collected to analyze MMP-2 activity by gel and *in situ* zymography and oxidative stress production by immunofluorescence of DHE. Statistics were performed by two- or one-way ANOVA followed by Tukey's post-test. $p < 0.05$ was used. **Results:** The SBP was higher in the angiotensin II mice compared to Sham and Sham+SB290157 (143.5 ± 4.7 vs. 104.8 ± 2.4 and 114.3 ± 4.6 ; $p < 0.05$; $n=7$). Treatment with the antagonist of C3a notably decreased it (118.0 ± 4.7 ; $p < 0.05$; $n=8$). MMP-2 levels were measure by immunofluorescence and higher levels were detected in the aortas of angiotensin II mice (vs. controls; $p < 0.05$; $n=5-6$). Afterwards, *in situ* and gel zymography, MMP-2 activity was increased in the aortas of angiotensin II mice (vs. controls; $p < 0.05$; $n=5$) and the SB290157 was able to decrease it ($p < 0.05$; $n=5-6$). Lastly, the production of oxidative stress was also evaluated in the aortas by DHE. There was an increase in the production of oxidative stress in the aortas of hypertensive mice and the SB290157 significantly reduced it (57.4 ± 2.7 vs. 39.4 ± 3.4 ; $p < 0.05$; $n=5$). **Conclusion:** treatment with the antagonist of C3aR, SB290157, reduced the accentuated SBP in angiotensin II mice in addition to reduce oxidative stress and MMP-2 activity in the aortas. We are next evaluating whether these mechanisms contribute to cause vascular remodeling and dysfunction in hypertension. **Financial Support:** CNPQ/ FAPESP/ CAPES/ FAEPA

06.022 **Effects of Beta-Caryophyllene in the Cecal Slurry Model of Sepsis.** Mariot LN¹, Queiroz LY¹, Delfrate G¹, Alves GF², Nardi GM, Sordi R¹ ¹UFSC, PPG in Pharmacology, ²UniTO, PPG in Pharmaceutical and Biomolecular Sciences

Abstract: Sepsis is defined as a dysregulated response of the organism to an infection, and evolution to organ dysfunction. The acute renal manifestation associated with sepsis involves a decrease in global renal blood flow and secondary tubular epithelial cell death, or acute tubular necrosis. It has been shown that the endocannabinoid system is effective as a therapeutic target for some pathologies, as it modulates the immune and cardiovascular systems. Recent studies show that activation of cannabinoid receptor type 2 (CB₂) increases renal perfusion by a direct vascular effect. The aim of this study was to investigate the effect of a CB₂ receptor agonist in sepsis. **Methods:** Male Swiss mice were subjected to cecal slurry (CS) model of sepsis through the injection of 350 μ L of a cecal solution prepared from the cecal contents of a donor mice. Sham animals (350 μ L of PBS; i.p.) were used as controls. Vehicle (peanut oil) or β -caryophyllene (β C; CB₂ agonist; 50 mg/kg) was administered (v.o.) 6 h after sepsis induction for 7 days. Mean arterial pressure (MAP) was measured through a pressure-transducer coupled catheter (Powerlab 8/30) inserted into the carotid artery of anesthetized animals. Renal blood flow was measured by a laser probe connected to a Doppler blood flow monitor (Moor Instruments) placed over the kidney. Temperature, body mass, score of severity and food consume was evaluated by 7 days. **Results:** Hypotension was observed in CS (86.4 \pm 16.3 mmHg) when compared to control mice (125.56 \pm 12.9 mmHg). Renal blood flow was also decreased in CS (199.3 \pm 51.2 perfusion units; PU) compared to control (363.1 \pm 84.4 PU). Compared with sham, CS group showed body mass loss (sham: 1 \pm 5%; CS: 11 \pm 5%), decrease of food intake (sham: 8; CS: 4.9 \pm 0.6g), high sepsis severity score (sham: 0; CS: 4 \pm 1), hypothermia 6 h after model induction (sham: 35 \pm 1 $^{\circ}$ C; CS: 32 \pm 1 $^{\circ}$ C), and recovery of the temperature in 7 days (sham: 35 \pm 1 $^{\circ}$ C; CS: 36 \pm 1 $^{\circ}$ C). CS + vehicle group had a more significant body mass loss, in addition to less food intake compared to CS + β C group (veh: 17 \pm 3% and 1,1 \pm 0,2 g; β C: 11 \pm 3,5% and 4,25 g, respectively). No effect of β C administration was observed on score of severity, hypothermia in 6 hours or temperature in 7 days. **Conclusion:** Sepsis was associated with hypotension, renal blood flow reduction and body mass loss when compared to sham animals. β C improved some parameters such food ingestion and body weight. Additional data are still necessary to better elucidate the effect of β C in sepsis. **Financial Support:** CAPES, CNPq. **References:** Pressly J. D., Soni H., Park F., *Phys. Genom.* v. 1; p. 90–96, 2019. Starr ME, Saito H. *Aging Dis* v. 5, p. 126–136, 2014.

06.023 Evaluation of the Late Effects of Topiramate Treatment during Childhood on Baroreflex Control in Male and Female Rats. Miguel MVO, Silva KGN, Bonancea AM, Oliveira GR, Pelosi GG ¹UEL, Dpt. of Physiological Sciences, PPG of Physiological Sciences, Brazil

Introduction: Exposure to environmental factors can affect the body in a variety of ways, such as neurochemical, structural, and physiological changes, and can have long-term health consequences. This relationship is linked to the concept of the Origin of the Development of Health and Disease (DOHaD). In the present study, we investigated the treatment with Topiramate (TOP), an antiepileptic drug prescribed to treat epilepsy and prevent migraines, on cardiovascular function of adulthood rats. **Methods:** All protocols were approved by the ethics committee on the use of animals of the State University of Londrina (n^o 100/2018). Wistar male and female rats were used in this study. After mating, the offspring were divided into two experimental groups: the control group (CTR), which received water, and the TOP group, which was submitted to oral administration of the TOP (41 mg/kg/day). The administration was performed by gavage since the postnatal day 16, extending until the postnatal day 28. In adulthood, specifically from postnatal day 85 for estrus-phase female rats and from postnatal day 120 for male rats, catheterization of the femoral artery and vein was performed. After a period of 24 hours, cardiovascular records were collected for analysis and infusions of vasoactive drugs such as sodium nitroprusside (NPS - 50 μ g/ml/kg) and phenylephrine (Phe - 50 μ g/ml/kg). The analysis of the baroreflex using sigmoid curves was characterized by certain parameters, namely, (I) P1 and P2, which is the lowest and highest plateau of the curve, respectively, (II) the heart rate range (HR) and (III) the gain. Two-way ANOVA was used for statistical analysis, followed by Tukey's post-test. **Results:** According to the parameters derived from the baroreflex sigmoid curve of adult female rats after administration of TOP in childhood, a statistically significant difference in baroreflex gain was observed. Gain (CTR^F=-1.427 \pm 0.1582; TOP^F=-2.402 \pm 0.2247; p=0.0033*; t=3.662), P1 (CTR^F=-73.84 \pm 10.13; TOP^F=-100.7 \pm 12.25; p=0.1163; t=1.705), P2 (CTR^F=95.02 \pm 37.50; TOP^F=101.8 \pm 43.98; p= 0.8110; t=0.245) and HR range (CTR^F=168.9 \pm 24.75; TOP^F=205.5 \pm 18.65; p= 0.2751; t=1.149 CTR^F n=7, TOP^F n=6). In addition, the administration of TOP in female rats did not promote long-term changes in the tachycardiac slope, (slope CTR^F=-2.553 \pm 0.6379; slope TOP^F=-2.313 \pm 0.7016; p=0.8205, t=0.2324), however there was an increase in the bradycardiac slope of the TOP female rats (slope CTR^F=-2.164 \pm 0.3034; slope TOP^F=-3.221 \pm 0.3639; p=0.0458*; t= 2.251; CTR^F n=7, TOP^F n=6) when compared to the CTR group. The male rats showed no significant difference in all the parameters derived from the sigmoid curve. Gain (CTR^M=-1.406 \pm 0.1370; TOP^M=-1.479 \pm 0.1479; p=0.7204; t=0.3621), P1 (CTR^M= -81.14 \pm 37.50; TOP^M=-88.17 \pm 43.98; p= 0.9204; t=0.1217), P2 (CTR^M= 92.19 \pm 37.11; TOP^M=99.21 \pm 41.40; p=0.9006; t=0.1262) and HR range (CTR^M=173.5 \pm 15.52; TOP^M=187.5 \pm 16.08; p=0.5353; t=0.6290; CTR^M n=13, TOP^M n=13). Similarly, the administration of TOP in childhood in male rats did not change the tachycardiac slope (slope CTR^M=-2.617 \pm 0.3469; slope TOP^M=-2.834 \pm 0.3625; p=0.6519, t=0.4569), the bradycardiac slope (slope CTR^M=- 2.270 \pm 0.3408; slope TOP^M=-2.569 \pm 0.4273; p=0.589; t= 0.547; CTR^M n=13, TOP^M n=13) when compared to the CTR group. **Conclusion:** The use of TOP in childhood did not change baroreflex responses in male rats. However, in female rats, there was an increase in bradycardiac response indicating that TOP treatment during childhood modulate baroreflex activity in the long term. **Financial Support:** CAPES

06.024 Methylene Blue Preserve the Microcirculation and Reduces Death in Rat Sepsis.

Dantas PB¹, Mestriner F¹, Dugaich VF¹, Barbosa JM¹, Fagundes A¹, Couto AES¹, Becari C², Evora P¹, Ribeiro MS¹ ¹FMRP-USP, Dept of Surgery and Anatomy, Ribeirão Preto, SP, Brazil, ²FOB-USP, Dept of Biological Sciences, School of Dentistry of Bauru, University of São Paulo, Bauru-SP, Brazil

Introduction: Sepsis is a serious medical condition that occurs when the body responds to an infection in an exaggerated way, causing a widespread inflammation that can lead to damage in multiple organs and systems of the body. Sepsis can cause extensive inflammation throughout the body that can lead to low blood pressure, high respiratory rate, and intense leukocyte activation in the vessels, resulting in microcirculation disbalance accompanied by organ multiple failure. Sepsis mortality is high, and new and old drugs are being studied to help maintain hemodynamic stability as methylene blue (MB). MB has been used to increase the blood pressure in sepsis showing to be efficient in rebalancing circulatory integrity in physiological patterns. We sought to investigate methylene blue treatment in the sepsis survival rate and mesenteric microcirculation preservation. **Methods:** Adult male Hannover rats weighing between 200-250g from University of São Paulo-Ribeirão Preto Campus (USP) were treated by intravenous bolus with MB (4 mg/kg) or saline. Mild sepsis was induced by CLp with 4 holes, moderate sepsis with 10 holes, and severe sepsis with 20 holes in the cecum using a 16-gauge needle. The rats' groups were: I) Mild Sepsis+Saline (n=21), II) Mild sepsis+MB (n=21), III) Moderated sepsis+saline (n=26), IV) Moderated sepsis+MB (n=28), V) Severe sepsis+saline (n=18), VI) Severe sepsis+MB (n=20). The rat's survival was evaluated during 9 days after surgery and expressed as the percentage of animals surviving by the log-rank test (X², chi-square). Intravital microscopy was performed to evaluate the integrity of the mesenteric microcirculation by analyzing the leukocyte rolling and adhesion by lipopolysaccharide (LPS) sepsis model. LPS was administered intraperitoneal and treatment with intravenously MB by femoral vein. The leukocyte rolling and adhesion were quantified by intravital microscopy in rats that received the following treatment: I) Saline (n=5), II) LPS+Saline (n=6), III) MB + Saline (n=5), IV) LPS+MB (n=7), V) MB+LPS (n=5). **Results:** MB treatment significantly improved survival rate in severe sepsis. Severe sepsis groups treated with MB had a survival rate of 30% after 9 days (p=0.02) However, all severe sepsis rats' groups that received saline died along 9 days of surgery. Interestingly, MB treatment did not change survival rate in the mild and moderate sepsis groups compared with saline groups, respectively. The rats that received LPS showed an accentuated improvement of leukocyte adhesion and rolling in mesenteric vessels compared with the saline group. Rats that received only MB had similar results to the control group. Although, when rats received LPS and were treated with MB (after or before LPS), the leukocytes adhered and rolled in the mesentery diminished significantly (p< 0,001) similarly to the control group. **Conclusion:** Our data suggest that MB was able to reduce mortality in the severe sepsis and leukocyte migration. MB might be a beneficial drug for the protection of microcirculation.

06.025 FoxO1 O-GlcNAcylation on Vascular Endothelial Function. Pedersoli CA¹, Silva-Neto JA¹, Duarte DA¹, Gonçalves DAP², Silva NLE³, Silva JFG¹, Gasparini MV⁴, Machado MR¹, Gonçalves TT¹, Bressan AFM¹, Ketteluch IC³, Navegantes LC⁵, Carneiro FS¹, Tostes RC¹. ¹USP, Dpt. of Pharmacology, Ribeirão Preto, Brazil; ²UFMG, Dpt. of Physical Education, Belo Horizonte, Brazil; ³FMRP-USP, Dpt. of Dept of Biochemistry and Immunology; ⁴FMRP-USP, Dpt. of Cellular and Molecular Biology and Pathogenic Bioagents, Brazil; ⁵ FMRP-USP, Dpt. of Physiology, Brazil

Introduction: FoxO1 is an intracellular transcriptional factor related to insulin/glucose signaling. FoxO1 is regulated by post-translational modifications such as phosphorylation and O-GlcNAcylation (O-GlcNAc), where a moiety of N-acetyl-glucosamine (GlcNAc) is attached to serine and threonine residues. This process is increased in cells from humans and experimental models of diabetes mellitus. Increased O-GlcNAc leads to changes in location, structure, traffic and function of proteins, including the FoxO1 molecule. This posttranslational modification is catalyzed by two enzymes: OGT that attaches, and OGA that removes the O-GlcNAc modification. Thiamet-G (TMG) is a pharmacological tool used to artificially increase O-GlcNAc in animals and cells by OGA inhibition. In the vasculature, increased O-GlcNAc content alters the function of proteins such as eNOS, impairing endothelial function. Likewise, overactivation of the transcription factor FoxO1 contributes to oxidative stress and reduces nitric oxide (NO) bioavailability in the endothelial cell, processes that lead to blood vessel damage. Hypothesis: We hypothesized that the O-GlcNAc modification of FoxO1 increases its activity leading to endothelial dysfunction. **Methods:** Human umbilical vein endothelial cells (HUVEC) were used to evaluate the levels of O-GlcNAcylation after treatment with TMG. O-GlcNAc-modified proteins were determined by immunoblot; calcium transients induced by histamine were determined using the cell permeant FLIPR probe. Experiments were performed in the presence of vehicle or AS1842856, a FoxO1 inhibitor. Human embryonic kidney 293 cells (HEK293T) were transfected with Foxo1-Rluc, a FoxO1 construct that allows the detection of FoxO1 translocation; and the content of O-GlcNAcylated-FoxO1 was determined by immunoprecipitation. Concentration-response curves to acetylcholine (ACh) were performed in aortic rings of db/db mice, which are spontaneously diabetic and their respective controls (db/+). The efficacy (Emax) and potency (pD₂) of this vasorelaxant agonist were determined. **Results:** Thiamet-G increased the content of O-GlcNAcylated proteins [(arbitrary units-AU) 191±39, p<0,05] in relation to control 64±14] in both cell lines, increasing transcriptional activity of FoxO1 [(fluorescence ratio-FR) control: 1,33±0,18; TMG: 2,02±0,35]. Inhibition of FoxO1 activity increased histamine-induced calcium signal [(arbitrary unit of fluorescence-AUF) control: 93310±4250; TMG: 89512,2±3852,4; AS1842856: 104633,2±3791; AS1842856 + TMG: 115735,7±5398] in HUVEC. Isolated aortic rings of the db/+ mice showed a relaxation of 70,4% of the initial tone to ACh, while the aortas of the db/db relaxed 57,5% (p=0,14; n=8) in response to ACh. ACh pD₂ was decreased in the db/db group [6.3±0.2 in the db/+ vs. 5.3±0.6 in the db/db (p=0,28; n=8)], i.e. isolated aortic rings of db/db mice, which are spontaneously diabetic and have a higher content of O-GlcNAcylated proteins [(AU) 153.5±35.5] when compared to control aortas (87.0±26,2). **Conclusion:** High levels of O-GlcNAc-modified proteins increase FoxO1 activity in HEK293T. FoxO1 inhibition leads to increased calcium signaling. These phenomena allow us to infer that overactivation of FoxO1 is present in conditions linked to high O-GlcNAc protein levels, such as in arteries from diabetic animals, and may represent a mechanism for vascular injury in this disease. **Financial Support:** FAPESP (2021/04378-4), CAPES e CNPq. Approved by the Ethics Committee on Animal Use (CEUA FMRP-USP 072/2020).

06.026 Endothelium-Dependent and -Independent Vasorelaxant Effect of Estriol in Rat Thoracic Aorta. Batista RAO¹, Rocha IR¹, Sousa CM¹, Silva CM¹, da Silva Filho FA¹, Oliveira-Porfiro LM² and Oliveira TS¹ ¹UFVJM, Dept of Pharmacy, Lab. of Experimental Pharmacology, Diamantina, MG, Brazil. ²UEG-Itapuranga, Itapuranga, GO, Brasil.

Introduction: Hormone replacement therapy (HRT) with estrogen has cardioprotective effects for younger or early postmenopausal women, having a beneficial effect on the cardiovascular system, reducing coronary heart disease and all-cause mortality [1-2]. Knowing that estrogen is a pharmaceutical preparation commonly used in HRT and considering its health benefits [3], the present study was designed to investigate the vascular effects of estriol (E3) in thoracic aorta of rats, elucidating the mechanisms underlying the impact of estrogen. The study of E3 in vascular function may contribute to a better understanding of the potential benefits of estrogen-based therapies in the management of cardiovascular disease in postmenopausal women. **Methods:** The vasorelaxant effect of E3 was evaluated in preparations of rings from the thoracic aorta of male Wistar rats (200-300g) using organ chambers. Concentration-response curves (1 μ M - 1mM) were constructed in aortic rings pre-contracted with phenylephrine with endothelium-intact or -denuded. Relaxation responses in intact endothelial rings were performed in the presence of the nitric oxide synthase inhibitor L-NAME (100 μ M), the cyclooxygenase inhibitor Indomethacin (10 μ M) or the non-selective blocker of K⁺ channels TEA (1mM). All experiments were conducted in accordance with the National Council for the Control of Animal Experimentation (CONCEA) and were approved by the local Research Ethics Committee (Protocol CEUA/UFVJM n^o 09/2022). Data are presented as mean \pm SEM of 8 different experiments and analyzed by Student's t-test or one-way ANOVA statistical tests where appropriate. P values \leq 0.05 were considered significant. **Results and Discussion:** E3 promoted concentration-dependent relaxation in endothelium-intact and -denuded aortic rings (E_{max} = 59.90 \pm 3.41% and 29.75 \pm 1.46%, respectively). Incubation with the nitric oxide synthase inhibitor (L-NAME) or the non-selective K⁺ channel blocker (TEA) reduced E3 relaxation (E_{max} = 42.36 \pm 0.92% and 51.30 \pm 2.75%), showing involvement of NO pathway and K⁺ channel in the vasorelaxant effect of E3. On the other hand, inhibiting the cyclooxygenase pathways using indomethacin enhances the vasorelaxant effect caused by E3 (E_{max} = 86.38 \pm 5.75%) and another level of experiments will begin to study this possible synergistic effect. The results suggest that the vasorelaxant effect of E3 is endothelium-dependent and -independent. Endothelium-dependent mechanism is mediated by activation of NO pathway and K⁺ channel and better study of of the cyclooxygenase pathways to characterize a possible synergic effect, since the effect in the presence of indomethacin was increased. Together, these results suggest that the vasorelaxant effect of E3 is endothelium-dependent and -independent. The endothelium-dependent mechanism is mediated by the activation of the NO pathway and the K⁺ channel and a synergistic effect with indomethacin needs to be investigated to elucidate the contribution of cyclooxygenase pathways. **Financial Support:** Coordenação de Aperfeiçoamento de Pessoal de Nível Superior (CAPES) and Fundação de Amparo à Pesquisa do Estado de Minas Gerais (FAPEMIG) - APQ-02841-21. **References:** [1] R.D. Langer, H.N. Hodis, R.A. Lobo, M.A. Allison, Hormone replacement therapy - where are we now? Climacteric: the journal of the International Menopause Society 24(1) (2021) 3-10. [2] R.D. Langer, The evidence base for HRT: what can we believe? Climacteric: the journal of the International Menopause Society 20(2) (2017) 91-96. [3] B.R. Bhavnani, F.Z. Stanczyk, Pharmacology of conjugated equine estrogens: efficacy, safety and mechanism of action, The Journal of steroid biochemistry and molecular biology 142 (2014) 16-29.

06.027 The Deletion of Elastase-2, an Angiotensin-II Forming Enzyme, Changes Typical Abdominal Aortic Aneurysm Phenotype in Mouse Model. Mestriner F¹, Ribeiro MS¹, Couto AES¹, Dugaich VF¹, Kovacs HZ¹, Francisco DF¹, Corsi CAC¹, Vasconcelos JL¹, Bruch P¹, Melo MMB², Neto J², Nakagi VS¹, Costa RM², Castro MM², Tostes R², Becari Christiane^{2,3}
¹FMRP-USP, Division of Vascular and Endovascular Surgery, Dept of Surgery and Anatomy
²FMRP-USP, Dept of Pharmacology, Ribeirão Preto, SP, Brazil. ³FOB-USP, Dept of Biological Science, Bauru-SP, Brazil

Introduction: Elastase-2 (ELA-2) is an enzyme that generates angiotensin-II (Ang II) in arteries and contributes to resistance arteries and vascular remodeling in animal models. It has also been shown that continuous infusion of Ang II induces aortic remodeling, systemic hypertension, and impaired smooth muscle cell (SMC) function, which may play a role in the pathophysiology of abdominal aortic aneurysms (AAA). Therefore, we aimed to investigate the role of ELA-2 in aortic contractility, hypertension, and wall remodeling induced by Ang II infusion using a mouse model of AAA. **Methods:** Male C57bl/6 (WT) and ELA-2 knockout (CELA-2aTm1Bdr; ELA-2 KO) mice were treated with saline or Ang II for twenty-eight days via subcutaneous infusion. The mice were divided into four groups: WT treated with saline (WT+SAL), ELA-2KO treated with saline (ELA-2KO+SAL), WT treated with Ang II (WT+Ang II), and ELA-2KO treated with Ang II (ELA-2KO+Ang II). Vascular ultrasonography (US) was performed before and after treatment to confirm the development of AAA. Morphological parameters, including collagen and elastin assays, as well as immunofluorescence imaging for inflammatory mediators and metalloproteinase activity, were assessed. ROS activity was analyzed by DHE fluorescence intensity for biochemical analysis. Aortic contractility after Ang II infusion was measured using myography assays to understand the overall tensile strength and structural integrity of the aortic wall. Statistical analyses were performed using the Mann-Whitney test, one-way ANOVA, and two-way ANOVA. This study was approved by CEUA (n.131/2019). **Results:** ELA-2KO mice did not develop AAA in the Ang II infusion model. The most dilated aortas were detected in the WT+Ang II group. In contrast, the ELA-2KO group, infused with the same dose of Ang II for the same duration, exhibited significantly reduced cross-sectional aortic dilatation at the infrarenal position ($p < 0.0001$) compared to the WT+Ang II group. The aorta from the WT+Ang II group showed higher remodeling activity compared to the WT+Saline group. Remodeling hypotrophy, high levels of ROS, increased gelatinolytic activity, and differences in aortic contractility and relaxation were observed, with all these parameters being down-regulated in the ELA-2KO+Ang II group compared to the WT+Ang II group. **Conclusion:** These findings demonstrate that Elastase-2 plays a significant role in the pathophysiology of AAA, as evidenced by differences in key parameters associated with AAA development. Targeting the enzyme Elastase-2 could be a potential therapeutic approach to prevent AAA development. **Supported by:** FAPESP (grants n. 2017/21539-6; 2018/23718-8 2020/03308-0)

06.028 Administration of Chloroquine during Pregnancy Does Not Alter the Hemodynamic Response of Offspring in Adulthood. Bonancea AM, Miguel MVO, Oliveira GR, Pelosi GG. ¹UEL, Dpt. of Physiological Sciences, Brazil

Introduction: The use of chloroquine (CQ) during pregnancy is of concern because it can cause cardiotoxic effects due to high cumulative doses, mainly conduction disturbances, arrhythmia, heart failure, and ventricular hypertrophy. Although CQ is considered safe in pregnancy, its use in this condition is still controversial, since CQ crosses the placenta and can be deposited in fetal pigmented tissues. The intrauterine environment should provide optimal conditions for fetal development, therefore, the DOHaD theory states that exposure to adversity early in life can cause disease late in life. Therefore, we aimed to evaluate the effects of intrauterine QC exposure in the offspring on the hemodynamic response to vasoactive drugs. **Methods:** Wistar rats provided by the central animal care unity of the State University of Londrina were subjected to the mating protocol. After pregnancy confirmation, the rats were separated into a control group, treated with water, and a CQ 24 mg/kg/day, CQ 48 mg/kg/day and CQ 72 mg/kg/day groups that received treatment from gestational day 15 to 21. The male offspring at adulthood underwent femoral artery and vein cannulation surgery and, one day after, the hemodynamic response to vasoactive drugs was evaluated with the infusion of phenylephrine (PHE) (50 µg/ml/kg) and sodium nitroprusside (NPS) (70 µg/ml/kg). **Results:** Intravenous administration of PHE caused a dose-dependent pressor response, showing no statistical difference when compared between the CTR group and CQ doses (PHE curve: Interaction: $p=0.7123$; $F(30, 360)=0.8389$; Concentration: $p<0.0001$; $F(10, 360)=225.3$; Treatment: $p=0.3855$; $F(3, 36)=1.043$). (Emax: CTR: 45.38 ± 3.2 mmHg, $n=8$; CQ 24mg: 44.29 ± 3.793 mmHg, $n=14$; CQ 48mg: 51.57 ± 3.951 mmHg, $n=9$; CQ 72mg: 46.64 ± 6.445 mmHg, $n=9$; $p=0.6799$). (EC50: CTR: 0.5076 ± 0.02617 µg/kg, $n=8$; CQ 24mg: 0.5475 ± 0.02881 µg/kg, $n=14$; CQ 48mg: 0.5479 ± 0.02573 µg/kg, $n=9$; CQ 72mg: 0.5876 ± 0.04191 µg/kg, $n=9$; $p=0.4524$). Similarly, NPS infusion caused a dose-dependent depressant response in rats, without showing statistically significant differences when comparing the CTR and CQ dose groups. (NPS curve: Interaction: $p=0.8477$; $F(30, 400)=0.7338$; Concentration: $p<0.0001$; $F(10, 400)=262.4$; Treatment: $p=0.1578$, $F(3, 40)=1.827$). (Emax: CTR: -53.17 ± 10.62 mmHg, $n=9$; CQ 24mg: -59.14 ± 12.2 mmHg, $n=16$; CQ 48mg: -46 ± 7.063 mmHg, $n=10$; CQ 72mg: -48.17 ± 8.355 mmHg, $n=9$; $p=0.8075$). (EC50: CTR: 1.241 ± 0.1158 µg/kg, $n=9$; CQ 24mg: 1.257 ± 0.1069 µg/kg, $n=16$; CQ 48mg: 1.251 ± 0.06914 µg/kg, $n=10$; CQ 72mg: 1.246 ± 0.0781 µg/kg, $n=9$; $p=0.9995$). **Conclusion:** We can conclude that the administration of CQ during pregnancy with the doses used in this study presents a safe profile in the context of DOHaD, since the offspring had no changes in cardiovascular function related to hemodynamics in the long term.

06.029 Sepsis-Induced Differential Electrocardiographic Changes in Male and Female Rats Hahmeyer MLS, Silva-Santos, JE ¹UFSC, Dpt. de Farmacologia, Brazil

Introduction: Cardiovascular dysfunction is a hallmark of sepsis, a life-threatening syndrome associated with the host's dysregulated immune response to an infection. Acute heart failure can worsen the prognosis of septic patients. Although the generation of heartbeats in a synchronized rhythm depends on electrical stimulus propagation from the sinus node through cardiac cells, the influence of sex on electrocardiographic (ECG) parameters in experimental models of sepsis remains to be investigated. We hypothesized that cardiac electric conduction is differentially impaired in male and female rats subjected to the cecum ligation and perforation (CLP) model of sepsis. **Methods:** Male and female Wistar rats (90-120 days) were anesthetized with ketamine/xylazine (20/100 mg/kg, i.p.) for subcutaneous electrode insertion and lead II ECG traces assessment. One day after, the animals were anesthetized with isoflurane and subjected to non-occluding (one transfixated hole) CLP. All animals received tramadol (10 mg/kg; 1 and 13 h after CLP) to prevent pain (CEUA/UFSC: 4585200422). At 6 and 24 h after the CLP, the animals were anesthetized with ketamine/xylazine, and the ECG was recorded again. The baseline ECG data was used as a control pattern. The results were analyzed using ANOVA or Student *t* test. **Results:** No differences existed between male and female rats in any ECG segment evaluated before sepsis induction. CLP resulted in reduced RR intervals with increased heart rate in males and females, as found at 6 and 24 h after the surgery. Prolonged QT intervals were found in male and female rats at 6 h but only in females at 24 h after the CLP. Moreover, the QRS duration (QRSd) was unaltered in males and reduced in females at 6 h, but while septic females presented normal QRSd, a higher QRSd was found in males at 24 h after CLP. The P wave amplitude was unaltered in male rats during sepsis, but it was significantly reduced in female rats from 0.073 ± 0.005 mV to 0.037 ± 0.011 and 0.046 ± 0.003 mV at 6 and 24 h after CLP. Additionally, both PR segment and P wave duration were reduced in septic females (for instance, from 0.049 ± 0.001 and 0.026 ± 0.002 s to 0.042 ± 0.002 and 0.014 ± 0.001 s at 24 h after CLP, respectively). However, male septic rats displayed no changes in PR length, and the P wave duration was reduced only at 24 h after CLP. **Conclusion:** Our results confirm that sepsis results in ECG abnormalities that can be consistently measured in anesthetized rats subjected to CLP. Moreover, the changes differed between male and female animals once females displayed short PR interval and regular QRS complex despite the increased heart rate. Understanding how these differences impact heart recovery or continuous dysfunction during the septic state can outline new approaches for treating this condition. **Financial Support:** CAPES (001) and CNPq (405538/2021-9 and 312637/2021-7)

06.030 Reduction of Sirtuin 1 Expression in Perivascular Adipose Tissue of the Thoracic Aorta During Aging in SAMP-8 Mice. Alves AS, Marques BVD, Akamine EH ICB-USP, PPG Pharmacology, Brazil

Introduction: Vascular aging increases the risk for cardiovascular disease. Perivascular adipose tissue (PVAT) produces mediators that regulate the function and other aspects of blood vessels, and PVAT dysfunction plays a role in vascular changes. The PVAT surrounding the thoracic aorta (TA) has brown adipocytes (BA), and the shift to a white phenotype of the PVAT from TA may be involved in the dysfunction of this tissue that is seen with aging. Sirtuin 1 (SIRT1) is capable of activating transcription factors that stimulate biogenesis and mitochondrial function in cultured lineage adipocytes, and this appears to be important in the emergence of BA. The hypothesis of the present study is that SIRT1 reduction promotes dysfunction/reduction of mitochondrial biogenesis, leading to the loss of the brown phenotype and TA PVAT dysfunction in aging. The aim of the study was to evaluate the expression of SIRT1, mitochondrial genes (UCP-1 and citrate synthase), and mitochondrial biogenesis markers (NRF-1, NRF-2, TFAM) in the TA PVAT of young and old mice. **Methods:** SAMP-8 mice, which show accelerated aging, were used at 3 (3M) and 8 (8M) months (CEUA: 5624120821). The mRNA expression for SIRT1 and biogenesis markers was evaluated by quantitative PCR, and the results were obtained by calculating $2^{-\Delta\Delta Ct}$ and presented as arbitrary units (A.U). Results represent mean \pm standard error of mean. Statistical analysis was performed using the unpaired Student T-test, and the significance value was $p < 0.05$. **Results:** For the SIRT1 gene, we observed a reduction in the expression of its mRNA in the PVAT of aged SAMP-8 animals compared to the younger ones (3M: 1.12 ± 0.21 ; 8M: 0.57 ± 0.11 ; A.U.; N=6; $p < 0.05$). The mRNA expression of the mitochondrial genes UCP-1 (3M: 1.54 ± 0.50 ; 8M: 1.78 ± 0.36 , A.U.; N=6; $p > 0.05$) and citrate synthase (3M: 1.21 ± 0.30 ; 8M: 0.79 ± 0.33 , A.U.; N=6; $p > 0.05$) and the mRNA expression of the mitochondrial biogenesis markers NRF-1 (3M: 1.08 ± 0.17 ; 8M: 1.08 ± 0.23 , A.U.; N=6; $p > 0.05$), NRF2 (3M: 1.27 ± 0.27 ; 8M: 1.80 ± 0.27 , A.U.; N=6; $p > 0.05$) and TFAM (3M: 1.25 ± 0.38 ; 8M: 1.02 ± 0.24 , A.U.; N=6; $p > 0.05$) in TA PVAT were not different between young and old mice. In TA, mRNA expression for SIRT-1 (3M: 0.34 ± 0.23 ; 8M 0.14 ± 0.05 , A.U.; N=6; $p > 0.05$), UCP-1 (3M: 0.37 ± 0.30 ; 8M: 0.82 ± 0.34 ; A.U. N=6; $p > 0.05$), NRF-1 (3M: 0.37 ± 0.11 ; 8M: 0.27 ± 0.06 ; A.U.; N=6; $p > 0.05$), and NRF-2 (3M: 1.26 ± 0.30 ; 8M: 2 ± 0.32 ; A.U.; N=6; $p > 0.05$) showed no statistically significant difference between ages. **Conclusion:** The reduction in mRNA expression of the SIRT-1 is apparently not associated with the reduction in mRNA expression of mitochondrial genes and markers of mitochondrial biogenesis, and this phenomenon does not occur in the same way in the adjacent TA. **Financial Support:** FAPESP, Capes, CNPq 88887.645566/2021-00.

06.031 Vascular Effects of Hydrogen Sulfide (H₂S)-Donors: Mitochondria as New Targets. Marques LAC, Teixeira SA, Costa SKP, Muscará MN USP-ICB Farmacologia São Paulo SP Brazil

Introduction: Previous studies show that both the spontaneous H₂S donor sodium hydrosulfide (NaHS) and the mitochondria-targeted H₂S-donor AP39 cause vasorelaxation, both *in vitro* and *in vivo*. Regarding AP39, experiments performed in cultured endothelial cells revealed that at least some of its effects include protection from oxidative stress, thus evidencing that despite the similar vascular effects of these H₂S donors, critical differences must exist between them in terms of the mechanisms activated by the released H₂S. In this way, in this study we aimed to assess the mechanisms involved in the vasorelaxing activities of AP39 and NaHS on mouse mesenteric arteries *in vitro*. **Methods:** The experimental protocol was approved by the local ethics committee for animal experimentation (CEUA/ICB N° 7759060218). C57BL/6 male mice were euthanized under anesthesia (isoflurane 5% in O₂) and first-order mesenteric arteries were isolated. Artery rings (2-mm) were mounted on a wire myograph for isometric tension registry. Phenylephrine(Phe)-induced contraction in the presence of different concentrations of AP39 (10, 30, and 100 nM) and NaHS (10, 30, and 100 μM) was assessed. The vasorelaxation elicited by both compounds was assessed in rings with preserved (E+) or denuded (E-) endothelium. The participation of the NO-cGMP pathway was assessed by adding L-NAME (100 μM) or ODQ (10 μM), and the involvement of K⁺ channels was characterized by adding TEA (3 mM), apamin (5 μM) or glibenclamide (10 μM). The involvement of endogenous H₂S was assessed by adding AOAA (10 mM). The expression of the H₂S-producing enzymes (CSE, CBS, and 3MPST) was analyzed in the mesenteric artery homogenates by Western blot. E_{max} and pA₂ values were obtained from the concentration-response curves. Differences among the groups were analyzed by one-way ANOVA followed by the Bonferroni's test for multiple comparisons; values of P<0.05 were considered as statistically significant. **Results:** Both H₂S-donors reduced Phe-induced constriction in a concentration-dependent manner, although AP39 was more potent than NaHS. On the other hand, the vasorelaxant responses to both AP39 and NaHS were attenuated after endothelium removal (AP39 E_{max} E+=72.5±4.6% vs. E-=34.8±2.0%; P<0.001; NaHS E_{max} E+=84.0±7.7% vs. E-=47.1±5.7%; P<0.01) or in the presence of either L-NAME (AP39 E_{max}=27.0±4.5%, P<0.001; NaHS E_{max}=44.0±7.0%, P<0.001) or ODQ (AP39 E_{max}=22.9±3.4%, P<0.001; NaHS E_{max}=33.0±4.4%, P<0.001). Both H₂S-donors activate K⁺ channels, as demonstrated by the interference observed in the presence of TEA (AP39 E_{max}=38.6±4.6%, P<0.001; NaHS E_{max}=45.8±4.7%, P<0.01) and apamin (AP39 E_{max}=52.0±4.8%, P<0.001; NaHS E_{max}=45.0±3.0%, P<0.01), but KATP were only involved in the NaHS response (E_{max}=42.5±7.6%, P<0.01). Although the arteries express CSE, CBS, and 3MPST (as detected by Western blotting), the addition of AOAA did not interfere with the vasorelaxation induced by either of the H₂S donors. **Conclusions:** The different vasorelaxing mechanisms of AP39 and NaHS evidence the relevance of the H₂S release profile and the intracellular target. Studies on the molecular pathways involved in vascular cells following the selective release of H₂S on mitochondria are currently in progress. **Financial Support:** FAPESP (2019/14051-2), CNPq (140309/2022-5), and CAPES (Finance Code 001). **References:** ZHAO, W. et al., Am. J. Phys. 283, 474, 2002, DONOVAN, K. et al., Vasc. Phar., v.93, 20, 2017, GHEIBI, S. et al., Bioch. Phar., v.149, 42, 2018, TOMASOVA, L. et al., N.O., v.46, 131, 2015, GERO, D. et al., Pharm. Res. v.113, 2016, LATORRE E. et al., Aging. v.19, 10, 2018

06.032 Glycolytic Profile of CD4⁺ T Cells and Cardiac Hypertrophy and Increased Blood Pressure in a Mouse Model of Gender-Affirming Hormone Therapy (GAHT). Oliveira-Neto JT¹, Santos JD¹, Oliveira CV², Cebinelli GCM², Machado MR¹, Souza FM⁴, Rodrigues D¹, Soares HAS⁴, Silva MC⁴, Silva CAA³, Santana da Silva J⁴, Fazan-Júnior R³, Cunha FQ², Farias-Filho JCA², Tostes, RC¹ ¹FMRP-USP, Dept. of Pharmacology, ²FMRP-USP, Dept. of Immunology, ³FMRP-USP, Dept. of Physiology, ⁴Fiocruz, Bi-Institutional Research Platform in Translational Medicine

Introduction: Testosterone is used in gender transition by transmasculine people and, although safe, increases cardiovascular risk, with pro-hypertrophic effects in the heart. Testosterone also increases glycolytic pathways. Effector CD4⁺ T cells contribute to cardiac remodeling, and metabolic changes modulate CD4⁺ T cells function, with glycolytic metabolism favoring Th17 differentiation. In the present study, we test the hypothesis that testosterone, in a gender-affirming hormone therapy (GAHT) mouse model, induces cardiac dysfunction by increasing the glycolytic metabolism in Th17 lymphocytes. Thus, we evaluated whether testosterone in female mice increases glycolytic metabolism in CD4⁺ T cells, enhancing Th17 differentiation, and leading to cardiac dysfunction. **Methods:** *In vitro*, naive CD4⁺ T cells (CD44^{Lo}/CD62L^{Hi}) were purified from lymph nodes and spleen of female C57BL/6 (WT) mice, differentiated into Th17 or regulatory T (Treg), in the presence of vehicle or increasing concentrations of testosterone. *In vivo*, 8-week-old female WT, IL-17Ra knockout (-/-) and Rag1^{-/-} mice received testosterone cypionate (48 mg.kg⁻¹.week⁻¹) or vehicle for 8 weeks. Ventricular function and structure were determined by echocardiogram and histomorphometric analyses. Expression of p-PKM2^{Tyr105} and p-STAT3^{Tyr705} was determined by Western blot and arterial pressure (BP) by carotid cannulation. All protocols were approved by the Ethics Committee on Animal Use (CEUA-FMRP/USP, – Protocol number: 1026/2021). **Results:** *In vitro*, testosterone enhanced skew toward Th17 profiles, whereas bunted to Treg. Testosterone increased IL-17 gene expression, effector cytokine of Th17 cells, and Pkm2 gene expression and protein content in CD4⁺ T cells. *In vivo*, testosterone-treated female WT mice showed cardiac hypertrophy and dysfunction, characterized by increased intraventricular septum, ejection fraction and shortening fraction - systole; and reduction in left ventricular internal diameter and left ventricular volume - systole. Effects not observed in Rag1^{-/-} mice. However, there was an increase in cardiac output in WT and Rag1^{-/-} mice treated with testosterone; and increased cardiac p-PKM2^{Tyr105} and p-STAT3^{Tyr705} protein content. After 24 weeks, testosterone increased blood pressure in female mice. Testosterone did not change blood pressure in females Rag1^{-/-} or IL-17Ra^{-/-}. However, adoptive transfer of CD4⁺ T cells to Rag1^{-/-} restored increasing BP induced by testosterone. **Conclusion:** Testosterone favors Th17 differentiation and has a potential role in altering the glycolytic metabolism of CD4⁺ T cell, induces cardiac hypertrophy, and, in a long-term, increases BP in female mice. These findings point out important targets that may be used as markers of cardiovascular risk in transmasculine people on GAHT. **Financial Support:** FAPESP, CAPES and CNPq.

06.033 Estrogen has a Protective Role Against Endothelial Glycocalyx Shedding caused by SARS-CoV-2 Infection. Machado MR¹, Potje SR², Costa TJ¹, Benatti NR³, Martins Júnior RB⁴, Costa RM⁵, Tostes RC¹ ¹FMRP-USP, Dept. of Pharmacology, Brazil, ²UEMG, ³HC-FMRP-USP, ⁴FCFRP-USP, ⁵UFJ

Introduction: SARS-COV-2 infection promotes endothelial dysfunction in patients with COVID-19 and male patients are at greater risk of developing serious complications than females. The endothelial glycocalyx is a key regulator of vascular homeostasis. The plasma from hospitalized patients with COVID-19, but not from healthy individuals, promotes glycocalyx degradation. Sex hormones have a considerable effect on the regulation of the immune response and endothelial function. **Objective:** to evaluate whether estrogen prevents endothelial glycocalyx degradation promoted by SARS-CoV-2 infection. **Methods:** All procedures were approved by the National Research Ethics Committee (CONEP: 30816620.0.0000.5440). A cohort of 159 hospitalized patients with a confirmed diagnosis of COVID-19 and healthy subjects was included in this study. Patients with COVID-19 (C) were divided into the following experimental groups: women of childbearing age (MJ), postmenopausal women (MM), and men (M). In addition, control healthy individuals (H) were included in the respective groups. The serum levels of IFN- γ , IL-1 β , IL-6 TNF- α , heparan sulfate and heparanase were determined. Human umbilical vein endothelial cells (HUVECs) were treated with serum from COVID-19 patients and healthy subjects for 1 hour. Then, cell viability assays, and measurements of H₂O₂ by amplex red, NO by DAF fluorescent probe, and ROS generation by lucigenin were performed. HUVECs were treated with physiological concentrations of estrogen and testosterone before being infected with SARS-CoV-2. RT-PCR was used to assess viral load and glycocalyx structure was evaluated by transmission electron microscopy. **Results:** Patients with COVID-19 exhibited high levels (in pg/ml) of IFN- γ [(mean; SEM) C; 51.8; H; 1.2 \pm 10.2), TNF- α (C: 27.6; H: 1.5 \pm 7.6) and IL-6 (C: 65.3; H: 0.6 \pm 19.2), but not of IL-1 β (0; 0.8 \pm 0.3), versus healthy individuals. Men exhibited higher levels of IL-6 (M: 31.5 \pm 5.3; MM: 48.2 \pm 11.3; MJ: 5.3 \pm 1.6) and TNF- α (M: 45.1 \pm 9.7; MM: 24.6 \pm 7.7; MJ: 16.5 \pm 5.4) compared to women with COVID-19. Serum from COVID-19 patients did not alter the viability of healthy endothelial cells (H: 97.9 \pm 2.8; MJ: 94.5 \pm 1.9; MM: 94.5 \pm 2.4; M: 91.3 \pm 1.1), but reduced H₂O₂ (H: 98.6 \pm 4.4; MJ: 57.9 \pm 1.9; MM: 59.3 \pm 2.4; M: 60.3 \pm 1.14) and NO (H: 122.1 \pm 3.8; MJ: 95.4 \pm 2.9; MM: 93.7 \pm 3.1; M: 83.3 \pm 2.5). Patients with COVID-19 exhibited higher levels of heparan sulfate (C: 1628; H: 709.6 \pm 124.2) and heparanase (C: 8652.8; H: 3377.5 \pm 1557) versus healthy individuals. Men and postmenopausal women exhibited higher levels of heparan sulfate (M: 1858.4 \pm 138.8; MM: 1532 \pm 124.2; MJ: 1067 \pm 74.20) and heparanase (M: 6909 \pm 749.3; MM: 13365 \pm 2164; MJ: 4303 \pm 811) compared to women with COVID-19. Serum from postmenopausal women and men with COVID-19 increased ROS generation (H: 110.2 \pm 3.9; MJ: 102.7 \pm 4.5; MM: 147.7 \pm 11.1; M: 148.4 \pm 7.2) in healthy endothelial cells. HUVECs treated with estrogen had a significantly lower viral load than cells infected with SARS-CoV-2, in the presence of mock or testosterone [Mock: 0.0 \pm 0.0; SARS-Cov-2 (MOI-2): 6.9 \pm 0.3; E2+ SARS-Cov-2: 3.9 \pm 0.1; T+ SARS-Cov-2: 4.9 \pm 0.1] and treatment with estrogen but not testosterone maintained the structure of the glycocalyx. **Conclusion:** Serum from postmenopausal women and men with COVID-19, containing increased pro-inflammatory cytokines, promotes shedding of the endothelial glycocalyx. Estrogen reduces viral load in endothelial cells infected with SARS-Cov-2 and protects against glycocalyx degradation. **Financial Support:** CAPES, CNPq, CRID-CEPID.

06.034 Experimental Model of Acute Kidney Injury Induced by *Apis mellifera* Venom. Nogueira-Souza PD¹, Romanelli, MA², Siqueira BH¹, De Almeida MM¹, Gomes-da-Costa PI¹, Lara LS², Melo PA¹ ¹ICB-CCS-UFRJ, Lab. de Farmacologia das Toxinas, Farmacologia e Química Medicinal, Rio de Janeiro, Brazil; ²ICB-CCS-UFRJ, Lab. de Farmacologia Renal, Farmacologia e Química Medicinal, Rio de Janeiro, Brazil

Introduction: The africanized bees *Apis mellifera* have rapid reproduction, high ability to form swarms and are very aggressive. These animals are associated with many cases of accidents in humans and animals due to mass attacks and have been considered a public health problem in Brazil. The symptoms developed by victims can be local or systemic, and in some cases can cause rhabdomyolysis, cardiac, respiratory, and renal failure. Acute kidney injury (AKI) can occur after mass attack by different mechanisms, including the direct effects of venom components, and indirect toxico-isquemic effects. One of these toxico-isquemic effects is a consequence of rhabdomyolysis induced by bee venom, which occurs in 33 to 50 % of all cases. So, the aim of this study is to establish and characterize the acute AKI by *Apis mellifera* venom in mice by perimuscular administration at a dose by 5 mg/kg. **Methods:** To realize this project, mice (25 - 30 g - IVB n°001/20) were divided into 4 groups, being (1) Control 24 h, (2) Bee venom 24 h, (3) Control 48 h and (4) Bee venom 48 h. These animals were allocated in metabolic cages after venom perimuscular injection, and were euthanized after 24 or 48 h, according to the experimental group. First was analyzed the physiological and muscular parameters: water intake and urinary volume, and the muscular parameter creatinocinase (CK) content and myeloperoxidase (MPO) activity on *extensor digitorum longus* muscle, respectively. After were evaluated the renal function parameters proteinuria, blood urea nitrogen and urinary and plasmatic creatinine. Most of these parameters were analyzed through biochemical kits. **Results:** The results obtained showed that there are no differences between the water intake into the 4 groups. The animals of CTRL 24 h group produced less urine than BV 24 h. No difference was observed in the volume of urine produced between the 48 h groups. The CK content on EDL muscle is totally reduced in Bee Venom groups (24 h and 48 h), compared to CTRL 24 h and 48 h groups, respectively. The animals of BV groups showed MPO activity extremely bigger compared to CTRL groups, in both hours evaluated. The proteinuria was statistically higher only in BV 24 h compared to CTRL 24 h and BUN was smaller in BV group, either in 24 or 48 h. The urinary creatinine was different only between 24 h groups and there is no difference in plasmatic creatinine in the 4 groups. **Conclusion:** The results showed that *A. mellifera* venom can cause acute kidney injury when injected in a muscular way and further studies must be developed to understand the mechanism involved in this renal injury. **Financial support:** CAPES, FAPERJ, CNPq

06.035 Wedelolactone Reverts Acute Kidney Injury Resulting from *Bothrops jararacussu* Envenomation. Romanelli MA¹, Nogueira-Souza PD¹, Chaves JO², Brito ES², Pinto HMC², Albernaz LCS², Gonzalez SR², Melo PA², Lara LS¹. ¹UFRJ, Dpt. of Pharmacology and Medicinal Chemistry, Rio de Janeiro, Brazil; ²UFRJ-Macaé, Phamacology Lab, Brazil

Introduction: Snakebites are considered neglected tropical diseases by the World Health Organization. Bothrops snakes are responsible for almost 90% of snakebites in South America, representing a serious public health problem in tropical countries due to their high morbidity and mortality. Acute kidney injury (AKI) is defined as the sudden loss of kidney function in hours or days and is one of the main complications resulting from snakebites. Wedelolactone (WED) is a metabolite derived from *Eclipta prostrata* leaves, capable of neutralizing the myotoxic, proteolytic and hemorrhagic activities of *B. jararacussu* venom and its toxins, being a treatment option for kidney damage resulting from envenomation. **Methods:** Male Wistar rats weighing between 100 and 120 g were divided into 8 experimental groups (n = 8-12; CEUA 009/22): (1) Control (Ctrl), which received 0.9% NaCl solution intramuscularly (im); (2) Ctrl+WED: received doses of 2, 5 and 10 mg/kg of WED im; (3) *B. jararacussu* (Bj): received 3.5 mg/kg of venom (im); (4) Bj+WED: received 3.5 mg/kg of Bj (im) and, 2 hours after intoxication, were treated with doses of 2, 5, or 10 mg/kg of WED (im). After the respective treatments, the animals were allocated, in metabolic cages for 24 hours (with water and food *ad libitum*) for urine collection to assess urinary volume (VU) and water intake (IA). Then, the rats were euthanized for collection of kidneys and plasma. Plasma samples were used to measure plasmatic creatinine (PCre) and blood ureic nitrogen (BUN), while in urine samples proteinuria and glomerular filtration rate were evaluated. The left renal pole of the right kidney was used for renal histological analysis, such as hematoxylin eosin (HE) while with the right renal pole a renal homogenate was made and from this, evaluation of the activity of renal sodium transporters. **Results:** The urinary volum (UV) increased in the Bj group when compared to Ctrl group and the WED 5 mg/kg dose was the only able to reserve this effect. In Bj group, there was an increase in plasmatic creatinine (PCre) and blood ureic nitrogen (BUN), an increase in proteinuria and in the Glomerular Filtration Rate (GFR). All parameters were reverted using WED treatment. Histological evaluation (n = 3/group) of HE staining demonstrated renal damage in the Bj group: tubular necrosis, glomerular atrophy, glomerular segmentation and epithelial denudation, all prevented by treatment with WED 5.0 mg/kg. On the other hand, WED was not able to revert local muscle damage caused by venom administration. Furthermore, (Na⁺+K⁺)ATPase (NKA) activity increased in the Bj group and WED at 5 mg/kg was able to revert this effect. Finally, Na⁺-ATPase activity also increased in the poisoned group, but this effect was not reverted. **Conclusion:** WED mainly at 5 mg/kg seems to revert AKI resulting from *Bothrops* envenomation. However, it is necessary to evaluate the signaling pathways involved in the development of AKI so that it is possible to estimate which action negotiations are involved in this process. Financial support: CAPES, CNPq, FAPERJ. **References:** ROMANELLI, MA. *Toxicon*. v. 199, p.117, 2021. HOSTE, EA. *Nat. Rev. Nephrol.* v. 14, p. 607, 2018. MELO, PA. *Toxicon*. v. 32, p. 595,1994.

06.036 **Characterization of Acute Kidney Injury (AKI) Induced by *Bothrops jararaca* Venom.** Guerrero TN¹, Romanelli MA², Gomes DS², Nascimento MLS¹, Brigido MC¹, Lara LS¹, Zingali RB². ¹UFRJ, Medicinal Biochemistry Institute, Brazil; ²UFRJ, Dpt. of Pharmacology and Medicinal Chemistry, Brazil

Introduction: Every year about 2.5 million people are victims of snake bites. In Brazil, the most medically relevant snake is the *Bothrops jararaca*. The symptoms of envenomation are acute inflammation at the bite site and bleeding disorders, which can lead to kidney failure and death. Despite kidney failure being the main cause of death after poisoning, the kidney damage is not completely understood and needs to be well studied in *in vivo* models. Thus, the objective of this work is to characterize the acute kidney injury induced by *Bothrops jararaca* venom in rats. **Methods:** Three doses of venom (3.5, 6 and 8 mg/kg) were tested. The control group received 0.9% saline solution. The venom was injected intramuscularly into male Wistar rats (CEUA: n°128/18). After the injection, the animals were kept in metabolic cages and the following parameters were analyzed after 24h: extent of muscle damage and kidney damage (urinary creatinine, proteinuria, plasma creatinine, blood urea nitrogen (BUN) and renal tissue histology). **Results:** All animals presented a hemorrhagic lesion at the injection site, the extent of the lesion was dose-dependent. Biochemical parameters indicated kidney damage: proteinuria increased 2.7-fold at the dose of 6 mg/kg; BUN increased about 1.5-fold and plasma creatinine increased about 2-fold at the three doses tested. Histological analyzes showed the following changes that occurred in a dose-dependent manner: atrophy and glomerular segmentation; Bowman's capsule space distention; interstitial edema; hemorrhage; collagen deposition in the cortical and medullary region. **Conclusion:** the occurrence of acute kidney injury was observed in a dose-dependent manner as demonstrated by decay in kidney function and confirmed by histological findings. Thus, here an *in vivo* model of kidney injury by *B. jararaca* venom was established for future work. **Financial Support:** CNPq, CAPES and FAPERJ.

06.037 Basal Release of 6-Cyanodopamine 6-Nitrodopamine and 6-Nitroadrenaline from *Callithrix* spp. Isolated Ventricles. Santos Júnior GQ¹, Britto-Júnior J¹, Campos R¹, Nyamkondiwa KL², Klugh KL², Peterson LW², De Nucci G^{1,3} ¹FCM-Unicamp, Dept of Pharmacology, Campinas, Sao Paulo, Brazil; ²Rhodes College, Dept of Chemistry, Memphis, Tennessee, USA; ³ICB-USP, Dept of Pharmacology, Institute of Biomedical Sciences, University of Sao Paulo, Sao Paulo, Brazil

Introduction: 6-Nitrodopamine is released from rat isolated atria and is one hundred times more potent than noradrenaline and adrenaline, and ten thousand times more potent than dopamine, as a positive chronotropic agent (1). The released 6-nitrodopamine is reduced when the atria are pre-incubated with the nitric oxide synthase inhibitor L-NAME and when the atria are obtained from animals chronically treated with L-NAME (1). Here it was evaluated whether *Callithrix* spp. isolated ventricles release other related catecholamines such as 6-nitrodopamine and 6-nitroadrenaline and an unrelated catecholamine, 6-cyanodopamine.

Methods: *Callithrix* spp were anesthetized with ketamine and xylazine (80 mg/kg; IM and 10 mg/kg; IM, respectively) after sedation with propofol (30 mg/kg; IV). The animals were euthanized by exsanguination. The heart was removed, the ventricles separated and suspended separately in a 5 mL organ bath containing Krebs-Henseleit's solution (KHS) containing ascorbic acid (3 mM), and continuously gassed with a mixture (95% O₂/ 5% CO₂) at 37 °C for 30 min. Following contamination with 6-nitrodopamine-d₄, used as internal standard, an aliquot (1mL) of KHS was injected into a solid phase extraction cartridge and the catecholamines were eluted with 0.8mL of acetonitrile/water (90: 10;v/v). The eluate was evaporated under nitrogen at 60°C, reconstituted in acetonitrile/water (50/50;v/v) and 3µL injected into an HPLC apparatus coupled to tandem mass spectrometry. The limit of quantitation was 0.1ng/mL (2). 6-cyanodopamine was synthesized as previously described (3). 6-Nitrodopamine, 6-nitrodopamine-d₄ and 6-nitroadrenaline were obtained from Toronto Research Chemicals (Toronto, Canada). **Results:** The developed and validated method was applied to the evaluate the basal release of catecholamines from *Callithrix* spp. isolated ventricles. From the *Callithrix* spp. isolated ventricles, it was detected the basal release of 6-nitrodopamine (4.27±0.80ng/mL), 6-cyanodopamine (0.22±0.05ng/mL) and nitroadrenaline (1.50±0.ng/mL) were detected by LC-MS/MS. **Conclusion:** This first identification of 6-cyanodopamine and 6-nitroadrenaline in a biological system reveals the existence of a novel family of endogenous catecholamines. **References:** 1. Britto-Júnior J, de Oliveira MG, Dos Reis Gati C, Campos R, Moraes MO, Moraes MEA, Mónica FZ, Antunes E, De Nucci G. 6-Nitrodopamine is an endogenous modulator of rat heart chronotropism. *Life Sci.* 2022 Oct 15;307: 120879. doi: 10.1016/j.lfs.2022.120879. 2. Campos R, Pinheiro DHA, Britto-Júnior J, de Castro HA, Mendes GD, Moraes MO, Moraes MEA, Lopes-Martins RÁB, Antunes NJ, De Nucci G. Quantification of 6-nitrodopamine in Krebs-Henseleit's solution by LC-MS/MS for the assessment of its basal release from *Chelonoidis carbonaria* aortae in vitro. *J Chromatogr B Analyt Technol Biomed Life Sci.* 2021 Mar 22;1173: 122668. doi: 10.1016/j.jchromb.2021.122668. 3. Rote, JC, Malkowski SN, Skyler Cochrane C, Bailey, Peterson LW. Catechol reactivity: Synthesis of dopamine derivatives substituted at the 6-position. *Synthetic Communications.* 2017;47;5: 435-441.

07. Endocrine, Reproductive and Urinary Pharmacology

07.001 Nebivolol Prevents Cyclophosphamide-Induced Oxidative Stress in The Bladder. Jesus CPS, Pimenta GF, Tirapelli CR EERP-USP, Pharmacology Lab

Introduction: Cyclophosphamide (CYP) is a prodrug, whose metabolism needs to undergo hepatic oxidation, giving rise to cytotoxic compounds with antitumor effect. However, this reaction also generates toxic products such as acrolein, which is directly related to redox imbalance, causing hemorrhagic cystitis by increasing levels of reactive oxygen species (ROS) in the bladder as well as in other tissues¹. Nebivolol (NEB) acts as an antioxidant by inhibiting NAD(P)H oxidase and by direct superoxide ($O_2^{\cdot-}$) scavenging action, reducing ROS production, decreasing the degree of lipoperoxidation and tissue damage². We hypothesized that treatment with NEB would prevent changes in the redox state in the bladder promoted by CYP. **Methods:** Adult male C57BL/6 mice (20-25 g) were distributed in 4 groups: control (CTL), CYP, NEB and NEB+CYP. Mice were treated for 5 days with NEB (10 mg/kg/day, gavage)³ and the last dose of the β -blocker was administered 1h before injection of CYP (300 mg/kg, i.p.)². After 24 h of administration of CYP, animals were euthanized for collection of the bladder, kidneys, thymus and blood. The bladder was removed and weighed to assess edema. Lucigenin chemiluminescence was determined with the aim of detecting the production of $O_2^{\cdot-}$ by the enzyme NAD(P)H oxidase. The concentration of malondialdehyde (MDA) was determined colorimetrically using the curve for MDA as a reference. Concentration of reduced glutathione (GSH) was determined colorimetrically. **Results:** There was a reduction in the weight of animals treated with CYP and the ratio between the bladder and the weight of the animals showed that CYP causes bladder edema (bladder/weight in mg;n=24-28),(CTL: 1.3 ± 0.06 ;NEB: 1.2 ± 0.03 ;CYP: $2.3\pm 0.11^*$;CYP+NEB: $2.2\pm 0.09^*$). The mice treated with CYP showed lower consumption of water (mL;n=23)(CTL: 28.7 ± 1.58 ;NEB: 22.9 ± 1.50 ;CYP: $23.5\pm 1.58^*$;CYP+NEB: $17.7\pm 1.20^*$) and feed (g;n=23) compared to NEB and control (CTL: 16.0 ± 0.45 ;NEB: 14.0 ± 0.45 ;CYP: $14.5\pm 0.28^*$;CYP+NEB: $12.1\pm 0.66^*$). The results of the lucigenin assay (RLU/mg protein) showed that the use of NEB as an antioxidant prevented the increase in $O_2^{\cdot-}$ concentration caused by CYP in the bladder (n=9-13;CTL: 581.5 ± 74.5 ;NEB: 523.5 ± 61.0 ;CYP: $1181.0\pm 193.8^*$; CYP+NEB: 479.4 ± 132.4), renal cortex (n=5-6;CTL: 6136.6 ± 1050.0 ; NEB: $2379.1\pm 203.5^{**}$;CYP: $9223.4\pm 811.9^*$;CYP+NEB: 5450.6 ± 416.4), and thymus (n=5-8;CTL: 365.6 ± 54.1 ;NEB: 445.7 ± 26.9 ;CYP: $944.7\pm 209.9^*$;CYP+NEB: 635.3 ± 92.8). NEB also prevented the increase in MDA concentration (mol/mg protein) in the bladder (n=7-8;CTL: 4.2 ± 0.2 ;NEB: 4.9 ± 0.2 ;CYP: $8.3\pm 1.4^*$;CYP+NEB: 4.7 ± 0.4) and thymus (n=5-11;CTL: 2.8 ± 0.2 ;NEB: $2.4\pm 0.2^*$;CYP: $4.0\pm 0.2^{**}$;CYP+NEB: 3.3 ± 0.3) caused by CYP. **Conclusion:** NEB prevented both CYP-induced increase in ROS production and lipoperoxidation not only in the bladder, but also in the thymus and kidney, suggesting that NEB promoted a broad-spectrum cytoprotective effect with potential clinical relevance. **Financial Support:** Capes and CNPq. **References:** 1.IQUBAL, A. et al. Life Sci., v. 218, p. 112-131, 2019; 2.VALE, G. T.et al. Can. Jou. of Phy. and Pha. doi: 10.1139/cjpp-2019-0143; 3.OLIVEIRA,M.G. doi: 10.3390/antiox12010092.

07.002 Impact of Intravascular Hemolysis on Functional and Molecular Changes in the Urinary Bladder: Implications for Overactive Bladder in Sickle Cell Anemia. Silveira THR¹, Pereira DA¹, Pereira DA¹, Calmasini FB², Costa FF³, Silva FH¹. ¹USF Bragança Paulista, Lab. of Multidisciplinary Research, Brazil, ²Unifesp, Brazil, ³Unicamp, Hematology and Hemotherapy Center, Brazil

Introduction: In sickle cell disease (SCD), the primary mechanism underlying overactive bladder (OAB) appears to be due to reduced nitric oxide (NO) bioavailability, which leads to detrusor overactivity, a component of OAB [1-3]. Intravascular hemolysis, a defining characteristic of SCD, results in the release of hemoglobin into the plasma. This circulating, cell-free hemoglobin diminishes the bioavailability of nitric oxide (NO). Our hypothesis is that the heightened levels of plasma hemoglobin due to intravascular hemolysis could potentially contribute to detrusor overactivity in SCD. Therefore, the current study is designed to examine the impact of intravascular hemolysis on the contractile responses of the detrusor smooth muscle (DSM) using a murine model of intravascular hemolysis. **Methods:** Intravascular hemolysis was induced in C57BL/6 mice by intraperitoneal injection of phenylhydrazine (PHZ) [REF]. Mice were injected with PHZ at 50 mg/kg and then reinjected with 50 mg/kg 8h later. Mice were killed in an isoflurane chamber four days after the first injection with PHZ. Strips of detrusor were mounted in isolated organ baths, and contractile response to carbachol (CCh; 1 nM -100 μ M), KCl (1-300 mM) α,β -methylene ATP (1, 3 and 10 μ M), and electrical field stimulation (EFS; 1-32 Hz) were measured. Statistical comparisons were made using Student's unpaired t-test. **Results:** Plasma hemoglobin was significantly higher in PHZ compared to control mice (12 ± 1 and 3 ± 1 μ M, respectively; $P<0.001$), indicating intravascular hemolysis in PHZ-treated animals. Carbachol maximal contractile responses (E_{max}) were significantly higher ($P<0.05$) in the PHZ group compared to the control (1.5 ± 0.2 and 0.9 ± 0.1 mN/mg, respectively; $n=6$). KCl-induced E_{max} contractions were significantly higher ($P<0.05$) in the DSM from PHZ compared to WT mice (1.7 ± 0.2 and 0.8 ± 0.1 mN/mg, respectively). Likewise, the DSM contractions to EFS and α,β -methylene ATP were significantly ($P<0.05$, $n=6$) increased in PHZ mice compared with control mice. **Conclusion:** Our study shows intravascular hemolysis leads to increased DSM contractions, indicating that PHZ mice exhibit an overactive bladder phenotype. It is likely that hemoglobin act to inactivate nitric oxide, thus reducing the amount of bioavailable nitric oxide, which favors detrusor overactivity. **Financial Support:** FAPESP - 2022/10548-2. **Approval of the Human Research Ethics Committee:** 03.02.2021. **References:** 1. CLAUDINO, M. A. Urinary Bladder Dysfunction in Transgenic Sickle Cell Disease Mice. PLOS ONE, 10(8), e0133996, 2015., 2. IACOPUCCI, A.P.M. Intravascular hemolysis leads to exaggerated corpus cavernosum relaxation: Implication for priapism in sickle cell disease. FASEB JOURNAL, v. 36, p. 1-5, 2022., 3. KARAKUS, S. Urinary dysfunction in transgenic sickle cell mice: model of idiopathic overactive bladder syndrome. American Journal of Physiology-Renal Physiology, 317(3), F540-F546, 2019. ARAKUS, S. Urinary dysfunction in transgenic sickle cell mice: model of idiopathic overactive bladder syndrome. American Journal of Physiology-Renal Physiology, 317(3), F540-F546, 2019.,

07.003 The Effects of Hypothyroidism Progression Over the Melatonergic System in the Reproductive Tract of Male and Female Rats. Paiva RVN^{1,2}, Mondes PHL¹, Brandão BJ¹, Sant'Anna JN¹, Santos MEF¹, Santos LC², Markus RP³, Fernandes PACM³, Silva JF², Tamura EK¹. ¹UESC, Dpt. of Health Sciences, Chronobiology Research Group, Ilhéus, Brazil; ²UESC, Dpt. of Biological Sciences, Center for Research in Reproduction and Endocrinology, Ilhéus, Brazil; ³USP, Dpt. of Physiology, Lab. of Chronopharmacology, São Paulo, Brazil

Introduction: Thyroid dysfunctions have been considered one of the principals endocrinopathies that compromise human and animal health. For example, hypothyroidism is associated with several complications related to the reproductive system. On the other hand, melatonin is a natural indolamine considered as a regulatory molecule in many pathophysiological processes, including a regulatory role of the reproductive system. The melatonin effect in the pathophysiological context of hypothyroidism is still controversial and based in a few studies. Therefore, this work aimed to investigate the progression of hypothyroidism in the melatonergic system in the reproductive organs of adult rats.

Methods: Adult Wistar rats, males (n=72) and females (n=72), were separated into control and hypothyroid groups. The hypothyroidism was induced with orogastric administration of propylthiouracil (PTU, 1mg/animal) and the control group received a vehicle (3mL/animal), during 3 or 15 days. Euthanasia occurred at three different time points, 6 hours after lights on (ZT6), before lights off (ZT11,5), and 6 hours after lights off (ZT18). Blood, pineal gland, and reproductive organs (testicles, epididymis, vesicular gland, prostate, ovaries, and uterus) were collected. Plasma was used to measure the free thyroxine (T4) by ELISA. The pineal gland, left testicle and left ovary to assess gene expression of *Aanat* and *Asmt* (biosynthetic melatonin enzymes) through RT-qPCR, and the right testicle, right ovary, and uterus for histomorphometric measurement. Animals were weighed at the beginning and at the end of the treatment, including the sexual organs. All the procedures were approved by the UESC animal ethics committee (N°26/21). **Results:** The results showed that hypothyroidism was confirmed by T4 reduction. In relation to gene expression of *Aanat* and *Asmt* in the pineal gland of male rats, there is a reduction in the expression of *Aanat* in 3 and 15 days of treatment on the ZT18, while in females this enzyme expression has increased in 3 days and a decrease of *Asmt* was also observed with 15 days. On the sexual organs was verified in males an increased expression of *Asmt* in 15 days (ZT6), and in females increased *Aanat* expression at 3 and 15 days (ZT11,5). At the ovaries, was verified a reduction of antral follicles within 15 days of treatment. Regarding the weight of the sexual organs, a reduction of epididymis and prostate was observed in males within 3 and 15 days of treatment, respectively. **Conclusion:** Studies investigating melatonin and hypothyroidism are few and controversial. Our finding points to alterations in the melatonergic system during the progression of hypothyroidism in the reproductive tract of male and female rats. These results contribute to new knowledge and consequently to possible future treatments in reproductive dysfunction. **References:** Belviranli, M. *Cell Biochem. Funct.*, v. 26, p. 19, 1 jan. 2008. Johnson, CA. *Clin Tech Small Anim Pract.*, v. 3, p. 129, 2002. Tordjman, S. *Cur Neuropharmacol.*, v. 15, p. 434, 2017.

07.004 Impacts of Cesarean Section on The Gut Microbiome in the Long Term and Consequent Effects on the Individual's Vulnerability to DEHP. Santiago MSA¹, Nogueira LS¹, Avellar MCW², Perobelli JE¹ ¹Unifesp-Baixada Santista, Depto de Ciências do Mar ²Unifesp-EPM. Depto de Farmacologia

Introduction: The gut microbiome (GM) performs many critical roles for the host, such as modulation of the immune and endocrine system, regulation of organs' physiology, and metabolism of xenobiotics. Many factors can disrupt the GM composition, being the birth pathway - vaginal delivery (VD) or cesarean section (CS) - the main factor in the neonate. However, there is no information about the long-term impacts of CS on GM, as well as about the potential systemic implications of this GM disruption. This study aims to assess the long-term effects of CS on GM composition and evaluate whether an altered GM resulting from CS leads to increased vulnerability to the reproductive toxicity of the DEHP (Bis(2-ethylhexyl)phthalate). **Methods:** Male Wistar rats were born via VD or CS, followed by cross-fostering procedure, being called VDCF and CS. One additional group of VD was not submitted to cross-fostering, being called VD. On postnatal day (PND) 1 (n=6-7/group), PND21 (n=6-7/group), and PND90 (n=5-10/group), animals were euthanized and distal colon were collected under sterilized conditions for GM composition analysis by bacterial 16S rRNA gene high-throughput sequencing (Illumina MiSeq/HiSeq). In addition, to assess the individual's vulnerability to DEHP, animals from each group (VDCF, CS, and VD) were distributed into control (c, received only corn oil) and treated (t, received 48 mg/kg/day of DEHP). Treatment occurred from PND25 to PND90, by gavage. The age of preputial separation was recorded. On PND90, biometric parameters, epididymis and testis histopathology, and sperm motility and morphology analysis were performed. Ethics Committee Approval #2428081021/CEUA-Unifesp. **Results:** On PND1, CS presented different bacterial diversity and relative abundance, when compared to VD and VDCF. On PND21, the GM differed especially in relative abundance among the three groups. On PND90, alterations in the diversity and relative abundance were observed in both comparisons: birth pathways as the only factor (VDc x VDCFc x CSc) and birth pathways associated with DEHP exposure (c groups compared to their respective t groups). The age of preputial separation, the biometric parameters, and the sperm motility and morphology on PND90 were comparable among all experimental groups. In the initial segment and cauda of the epididymis, CSc showed a reduction in the amount of spermatozoa in the lumen, compared to VDc. Also, the initial segment showed reduced interstitium and lumen proportion when comparing VDCFc x VDc and CSc x VDCFc, respectively. In testicular histopathology, a higher occurrence of seminiferous epithelial detachment was observed in the CSt when compared to CSc, VDt and VDCFt. **Conclusion:** Similar to humans, the birth pathway was also responsible for altering the GM composition of rats at birth (PND 1), which was partially restored after lactation (PND 21). On PND 90, differences in bacterial diversity and relative abundance were observed, both in control groups, suggesting a long-term impact of CS only, but also on treated groups, suggesting an altered vulnerability to DEHP of individuals born via CS. The histopathological findings in the testis suggested impaired spermatogenesis due to CS associated with DEHP exposure, while results from epididymal histopathology indicate effects of the birth pathway, not associated with DEHP exposure. The next steps of the present study will allow us to deeper investigate the mechanisms of reproductive and endocrine impacts of CS and DEHP exposure. **Financial Support:** FAPESP, CAPES, Cnpq

07.005 Effect of Vitamin D on Metabolic Control Parameters and Lipid Peroxidation Markers in an Experimental Model of Type 2 Diabetes Mellitus. Brito AKS, Macedo JL, Oliveira ASSS, Santos MVDR, Silva ILC, Campos AJR, Queiroz CRT, Bastos FGT, César ESL, Mendes AVS, Almeida JOCS, Santos AA, Arcanjo DDR, Martins MCC UFPI, Dpt of Biophysics and Physiology, Brazil

Diabetes mellitus (DM) is a disease characterized by hyperglycemia resulting from defects in insulin secretion and/or action. Vitamin D is an important steroid in calcium and phosphorus metabolism, and has been reported to have positive effects on glycemic control and lipid profile in DM. This study evaluated the effect of vitamin D administration on parameters of metabolic control and lipid peroxidation in an experimental model of type 2 diabetes mellitus (DM2). Male Wistar rats (n=35) aged 08 to 12 weeks and with body weight between 180 to 200 g, were randomly assigned to groups of seven animals, treated for 28 days from confirmation of DM: Normal control (NC) and diabetic control (DC) received only vehicle (sunflower oil), diabetics treated with metformin 150 mg/kg (MET), diabetics treated with vitamin D at doses of 0.25 µg/kg/day (Vit D 0.25) and 0.50 µg/kg/day (Vit D 0.50) orally. DM2 was induced by a hyperlipidic diet for 35 days and administration of streptozotocin (30 mg/kg) diluted in citrate buffer pH 4.5 on day 36 intraperitoneally. The animals in the CN group received only citrate buffer. All experimental protocols were approved by the Ethics Committee on Animal Use (CEUA) of the Federal University of Piauí (number 660/2020). There was no difference between the groups in lipid profile parameters (Total Cholesterol (TC), Triglycerides (TG) and HDL-c) and atherogenic indices (TG/HDL-c and TC/HDL-c). The fasting glycemia of the vitamin D treated groups, showed significantly lower mean values (410.60±28.55; 403, 90±31.68) when compared to the CD (513.90±17.98) (p<0.05). The Vit D 0.50 group showed a significant reduction in mean random capillary blood glucose values (427.9±17.65) when compared to the CD group (528.9±28.66) (p<0.05). As for lipid peroxidation markers, both vitamin D-treated groups had significantly lower plasma concentrations of malondialdehyde (MDA) (9.53±0.28; 8.48±1.09) compared to the CD and MET groups (13.67±0.33; 12.76±0.30) (p<0.05). Myeloperoxidase (MPO) activity were significantly lower in the vitamin D supplemented groups (7.14±0.62; 5.30±0.58) when compared to CD (10.41±1.05) (p<0.05). Vitamin D treatment, at the doses and treatment time used here, resulted in improved glycemic control, evidenced by reduced random capillary blood glucose, as well as reduced lipid peroxidation, although they produced no change in the lipid profile. Thanks to Fundação de Amparo à Pesquisa do Estado do Piauí - FAPEPI and Programa de Pesquisa para o SUS - PPSUS for the financial support.

07.006 Chronic Treatment with Guanosine, a Guanine-Based Nucleoside, Improved Prostate Hypercontractility and Corpus Cavernosum Relaxation in Obese Mice. Passos GR; Gomes ET; Ghezzi AC; Antunes, E; Mónica FZ. FCM-UNICAMP, Dept of Translation Medicine, Faculty of Medical Sciences, University of Campinas

Introduction: Guanosine, a guanine-based nucleoside, has demonstrated neuroprotective (Coelho et al., 2022) and antiplatelet effects (Burnstock et al., 2015) in previous studies. A prior study showed that adding guanosine (0.1-1 mM) *in vitro* led to relaxation of the corpus cavernosum. Additionally, guanosine (100 µM, 30 min) enhanced the relaxation induced by sodium nitroprusside, acetylcholine or tadalafil in isolated CC from healthy mice, resulting in higher intracellular levels of cyclic guanosine monophosphate (cGMP) (Nicoletti et al., 2020). This study aimed to investigate the effects of chronic oral guanosine treatment on the smooth muscle reactivity of both the corpus cavernosum and prostate from obese mice. **Methods:** Animals were fed either a standard or high-fat diet from the seventh to the nineteenth week of life. In their fifteenth week, they were randomly allocated into three groups: 1) Lean; 2) Obese; and 3) Obese undergoing guanosine treatment (60 mg/kg, in the drinking water, for 4 weeks). Lean and obese groups received filtered water. After euthanasia, the prostate and corpus cavernosum were isolated for functional and molecular assays. The data represent the mean ± SD, with *n* representing the number of animals used in each protocol. Statistical analysis was performed using t-tests or one-way ANOVA as appropriate. All protocols had the approval of the ethics committee (5865-1 CEUA/UNICAMP). **Results:** Obese mice exhibited a significant increase ($p < 0.05$) in total body weight (50.7 ± 3.3 g, $n = 5$) and prostate weight (22.3 ± 1.9 g, $n = 6$) compared to lean mice (27.2 ± 2.2 g and 14.8 ± 1.4 mg, for body and prostate weights, respectively, $n = 5$). Guanosine treatment did not affect these parameters (50.8 ± 4.0 g; 18.2 ± 4.7 mg, for body and prostate weights, respectively, $n = 6$). Obese animals exhibited a hypercontractile prostate in response to phenylephrine (3.98 ± 1.04 mN, $n = 5$, $p < 0.05$) compared to lean mice (1.57 ± 0.40 mN, $n = 5$), and this effect was reversed by guanosine treatment (2.19 ± 1.17 mN, $n = 6$, $p < 0.05$). In another set of experiments, concentration-response curves to phenylephrine were conducted in tissues pre-treated (30 min) or not with either the soluble guanylate cyclase inhibitor (ODQ, 10 µM), adenosine A2A receptor antagonist (ZM241385, 1 µM) or adenosine A2B receptor antagonist (MRS, 1 µM). Pre-incubation with these substances completely reversed ($n = 5$, $p < 0.05$) the inhibitory response induced by guanosine treatment. The expression of phosphorylated (p)-VASP(Ser157) was lower in the prostate of the obese group ($n = 5$) compared to lean ($n = 5$), but the treatment did not affect with this parameter. The relaxation induced by transmural stimulation, acetylcholine and sodium nitroprusside was significantly lower ($p < 0.05$) in isolated corpus cavernosum from obese mice ($n = 5$) compared to lean ($n = 5$). Oral treatment with guanosine significantly improved the relaxing responses compared to untreated obese mice. In the corpus cavernosum, the protein expression of p-VASP(Ser239), but not p-VASP(Ser157), was significantly lower in the obese mice compared to lean ($n = 5$). Guanosine treatment led to an increase in p-VASPSer239 expression. **Conclusion:** The four-week guanosine treatment regimen ameliorated the hypercontractile state of the prostate and erectile function in obese mice. This improvement in the prostate appears to be partially mediated by the activation of the adenosine A2 receptor. **Financial Support:** FAPESP 2022/11621-5, 2017/15175-1

07.007 A 2-Week Treatment with 5-Azacytidine Improved the Hypercontractility State in Prostate from Obese Mice: Role of the Nitric Oxide-Cyclic Guanosine Monophosphate Signaling Pathway. Ghezzi AC¹, Passos GR¹, Oliveira MG¹, Oliveira AL¹, Mendonça GRA^{2,3}, Mello G¹, Antunes E¹, Monica FZ¹ ¹FCM-Unicamp, Dept of Translation Medicine, Campinas, Sao Paulo, Brazil. ²FCM-Unicamp, Dept of Pathology, Campinas, Sao Paulo, Brazil. ³ANM, Young Leadership Physician Program, Rio de Janeiro, RJ, Brazil

Benign prostatic hyperplasia (BPH) is characterized by an increase in prostate volume and contraction. Downregulation of the nitric oxide (NO)-cyclic guanosine monophosphate (cGMP) signalling pathway contributes to prostate dysfunction. Previous studies in cancer cells or vessel have shown that epigenetics mechanisms control the gene and protein expression of the enzymes involved in the production of NO and cGMP. This study aims to evaluate the effect of a 2-week treatment of 5-azacytidine (5-AZA), a DNMT inhibitor, on the prostate function of mice fed with a high-fat diet. Mice were fed with chow diet (carbohydrate: 70%; protein: 20%; fat: 10%) or high-fat diet (HFD) (carbohydrate: 29%; protein 16%; fat: 55%) for 12 weeks. Control and obese mice were treated with 5-Azacytidine (0,5 mg/kg, daily by intraperitoneal injection) or its vehicle from the 10th to 12th. Functional, histological and biochemical assays were carried out. The results were presented with Mean±SD, N= number of animals used in each protocol. Obese mice presented a significant reduction in epithelial cells and an increase in glandular lumens compared to the control. The treatment with 5-AZA completely reversed these alterations. No significant difference was observed in the stromal cells in all studied groups (HE - %epitélio CTL-Veh: 40,724±9; CTL-AZA: 40,834±6; HFD-Veh: 24,104±9*; HFD-AZA: 38,228±10; %lúmen CTL-Veh: 37,352±7; CTL-AZA: 39,523±6; HFD-Veh: 54,07±15*; HFD-AZA: 38,417±14; %estroma CTL-Veh: 21,923±7; CTL-AZA: 19,642±8; HFD-Veh: 18,958±7; HFD-AZA: 23,354±7) *P<0.05 (HFD-Veh ≠ all groups). Immunohistochemistry for alpha-actin, a marker for smooth muscle and myofibroblasts was carried out. A significant increase in the expression of alpha-actin was observed in obese mice. The treatment with 5-AZA reversed this increase (A4-actin: CTL-Veh: 17,682±2,60; CTL-AZA: 19,595±3,698; HFD-Veh: 23,162±4,562*; HFD-AZA: 12,623±2,443) *P<0.05 (HFD-Veh ≠ all groups). NO-cGMP is considered the main inhibitory mediator in the prostate. Therefore, inhibitors of nitric oxide synthase (L-NAME, 1 µM, 30 min) or soluble guanylate cyclase (ODQ, 10 µM, 30 min) were incubated in isolated prostate from all studied groups. The *in vitro* concentration used of L-NAME or ODQ did not significantly affect the pharmacological parameters of Phe in both CTL and HFD groups. On the other hand, L-NAME and ODQ completely reversed the inhibitory response induced by the 5-AZA treatment in prostate from obese mice (Emax PHE: CTL-Veh: 1,93±0,50; CTL-L-NAME: 2,95± 0,27; CTL-AZA: 2,43±0,27; CTL-AZA-L-NAME: 3,20±0,30; HFD-Veh: 4,51±0,32; HFD-L-NAME: 4,63±0,44; HFD-AZA: 3,15±0,43#; HFD-AZA-L-NAME: 4,40±0,57); #P<0.05 (HFD-AZA ≠ HFD-Veh; HFD-L-NAME and HFD-AZA-L-NAME). (EMAX PHE: CTL-Veh: 1,93±0,23; CTL-ODQ: 2,36±0,45; CTL-AZA: 2,03±0,45; CTL-AZA-ODQ: 2,42±0,33; HFD-Veh: 3,93±0,44; HFD-ODQ: 3,87±0,53#; HFD-AZA: 2,57±0,59#; HFD-AZA-ODQ: 3,57±0,51) #P<0.05 (HFD-AZA ≠ HFD-Veh; HFD-ODQ and HFD-AZA-ODQ). The treatment with 5-AZA significantly increased the intracellular levels of cGMP CTL-Veh: 0,058±0,011; CTL-AZA: 0,060±0,130; HFD-Veh: 0,038±0,007*; HFD-AZA: 0,058±0,0123 *P<0.05 (HFD-Veh ≠ all groups). On the other hand, there is no difference in the intracellular levels of cAMP (CTL-Veh: 22,128±4,628; CTL-AZA: 20,656±10,069; HFD-Veh: 12,265±5,581; HFD-AZA: 16,167±6,262) *P<0.05 (HFD-Veh ≠ all groups). In conclusion, our study paves the way to develop or repurpose therapies that increased the prostate cGMP levels, improving prostate function in BPH. This work was supported by Fundação de Amparo à Pesquisa do Estado de São Paulo (FAPESP; grant number 2019/19490-4)

07.008 Experimental Pharmacology of Liraglutide and Empagliflozin: Impacts on Metabolism and Brain Microcirculation in Type 2 Diabetes. Estado V¹, Costa d'Avila J², Santana Carlos A², dos Santos Silva I², Mafra Moreno², Chateaubriand PHP³, Figueiredo V³, Caire de Castro Faria H¹, Azeredo Siqueira R³ ¹IOC-Fiocruz, Lab. of Immunopharmacology,, ²Unig, ³Unesa- Idomed, Rio de Janeiro, Brazil

Introduction: Type 2 diabetes is a highly prevalent chronic disease associated with microvascular dysfunction and increased risk of brain disorders. Antidiabetic drugs such as empagliflozin, a SGLT2 inhibitor and liraglutide, a GLP-1 receptor agonist reduce body weight and blood glucose, decreasing cardiovascular risk. Liraglutide and empagliflozin have shown benefits in improving metabolic parameters, but their effects on brain microcirculation in diabetes are unknown. This study aimed to evaluate the effects of liraglutide and empagliflozin on metabolism and brain microcirculation in diabetic rats. **Methods:** Type 2 diabetes was induced in male Wistar rats (n=40) using a high-fat diet and low-dose streptozotocin. Liraglutide (100 µg/kg s.c.) and empagliflozin (10 mg/kg oral) treatments started one week after streptozotocin injection and lasted five weeks. Body mass, food intake, oral glucose tolerance test (OGTT), brain microcirculation, and histological analysis were assessed. **Results:** T2D rats showed increased body mass, while liraglutide-treated groups exhibited weight reduction. OGTT indicated improved glucose tolerance in all treated groups. Intravital microscopy revealed increased leukocyte adhesion and rolling in cerebral microvessels of T2D rats, which were normalized in both treated groups. Empagliflozin demonstrated superior glycemic control, while liraglutide showed better weight reduction. Both treatments reduced leukocyte rolling and adhesion in brain microvessels of diabetic rats, with empagliflozin being more effective in preventing microvascular rarefaction. **Conclusions:** Combining liraglutide and empagliflozin provides additional benefits in diabetes. Empagliflozin effectively prevents brain microvascular rarefaction, while liraglutide promotes weight reduction. These findings suggest the potential of these drugs in managing metabolic and microvascular complications in type 2 diabetes.

07.009 Neonatal Overnutrition causes Opposite Effects on Biometric Parameters and Glucose Homeostasis in a Model of Intrauterine Growth Restriction. Peixe CMS¹, Lorenzon F¹, Gregorio T², Santos LC², Santangelo E¹, Baptista G³, Santos GJ², Lima FB²
¹UFSC, Dpt. of Physiological Sciences, Florianópolis, ²UFSC Florianópolis, PPG multicenter in Physiology Sciences, Brazil, ³UFSC, PPG Pharmacology, Florianópolis, Brazil

Introduction: Prenatal exposure to excessive levels of synthetic glucocorticoids, such as dexamethasone (DEX) leads to fetal programming, resulting in intrauterine growth restriction (IUGR) and long-term impairment in metabolism. Due to the IUGR causing low birth weight, infant formulas are introduced sooner than ideally, as a means to compensate for this problem. However, since the postnatal period is critical for development, this energy overload in a crucial stage result in neonatal overnutrition and alterations in the energetic metabolism. Thus, we aimed to explore the impact of neonatal overnutrition in biometric parameters and glucose homeostasis in animals exposed to a model of IUGR induced by DEX. **Methods:** Pregnant Wistar rats were treated with DEX (0.1 mg/kg in the drinking water, D) or vehicle (C) during gestational days 14 to 19. On postnatal day 3 (PND3), the litters were adjusted to 10 (normal litter, NL) or 4 (small litter, SL) pups. The four groups composed of the male offspring were C+NL, C+SL, D+NL and D+SL (n=9-11/group). Animals were weighed at birth, every three days during lactation and then every two weeks until postnatal week 14 (PNW14), when fasting blood glucose was measured, along with the intraperitoneal glucose tolerance test (50% glucose solution [2g/kg b.m.], ipGTT). **Results:** Prenatal DEX resulted in low birth weight (4.93 ± 0.41 vs 5.70 ± 0.53 ; $p<0.0001$ [g]) and reduced lactational weight (g), while litter reduction led to increased body mass. The interaction of DEX and litter mitigated weight gain during the lactation period (PND9: C+NL= 14.86 ± 1.18 ; C+SL= 17.55 ± 2.89 ; D+NL= 13.23 ± 7.73 ; D+SL= 13.69 ± 2.40 ; Interaction $p=0.0356$; Litter $p=0.0033$; DEX $p<0.0001$). In adulthood, litter reduction increased the body mass (g), whereas prenatal exposure to DEX caused a persistent reduction of body weight (PNW14 C+NL= 358 ± 18 , C+SL= 404 ± 18 , D+NL= 352 ± 18 , D+SL= 358 ± 25 ; Interaction $p=0.0043$; litter $p=0.0005$; DEX $p=0.0004$). Fasting glucose (mg/dL) was lower in animals who underwent both prenatal DEX and neonatal overnutrition (C+NL= 106 ± 6 , C+SL= 111 ± 6 , D+NL= 108 ± 4 , D+SL= 102 ± 6 ; $p=0.0195$). However, after glucose challenge, litter size alone and its interaction with DEX resulted in higher levels of glycemia at 60 and 120 min, respectively (t60 C+NL= 215 ± 56 , C+SL= 216 ± 58 , D+NL= 189 ± 54 , D+SL= 286 ± 89 ; $p=0.0482$; t120 C+NL= 146 ± 16 , C+SL= 142 ± 23 , D+NL= 129 ± 11 , D+SL= 157 ± 28 ; $p=0.0498$). Correspondingly, the interaction of both factors also raised the area under the curve ([AUC] C+NL= 12826 ± 5381 , C+SL= 10697 ± 5059 , D+NL= 9309 ± 4252 , D+SL= 17064 ± 7717 ; $p=0.0209$). **Conclusion:** We demonstrated that prenatal exposure to excessive levels of DEX coupled with neonatal overnutrition disrupts glucose homeostasis, but can be metabolically protective by attenuating weight gain. **Financial Support:** Capes, CnPQ.

08. Respiratory and Gastrointestinal Pharmacology

08.001 **Antiulcerogenic Activity of Hesperetin and Carveol in Animal Models.** Pessoa MMB¹, Pessôa MLS¹, Alves VP, Silva ML, Araruna MEC, Alves Junior EB, Batista LM UFPB

Introduction: In recent years, numerous plant species and their isolated compounds, including terpenes and flavonoids such as carveol and hesperetin, have exhibited promising effects in the context of peptic ulcers, as demonstrated in animal model studies. Carveol is a monoterpene commonly found in the essential oils of various plants, such as *Rosmarinus officinalis* (Rosemary). Hesperetin, on the other hand, is a flavonoid found in citrus fruits like oranges. In light of this, the present study aimed to assess the anti-duodenal ulcer and gastric healing activity of these compounds in animal models. **Methods:** Male Wistar rats (*Rattus norvegicus*) weighing 180-250g were utilized for the animal experiments. To evaluate the duodenal antiulcerogenic activity of hesperetin and carveol (both purchased from SIGMA-ALDRICH), the animals were treated with tween 80 5% (negative control), lasoprazole 30 mg/kg (positive control), or various doses of hesperetin and carveol (25, 50, 100, and 200 mg/kg). Duodenal ulcers were induced using hydrochloric cysteamine following the protocol by Szabo et al. (The Am. J. of Phat, v. 93, p. 273, 1978). To evaluate the healing activity in a chronic gastric ulcer model, gastric ulcers were induced using acetic acid based on the protocol by Okabe and Amagase (Biol. And Pharm. Bulletin, v. 28, p. 1321-1341 2005). The ulcerative lesion area was determined using the ulcerative lesion index (ILU). Various antioxidant models were also evaluated, including reduced glutathione (GSH) (Faure, Birkhäuser Basel, v.1 p. 237, 1995), malondialdehyde (MDA), myeloperoxidase (MPO) (Krawisz, Gastroenterology, v. 87, p. 1344, 1984), and superoxide dismutase (SOD) (Sun et al., Clin Chem. v. 34, p. 497, 1988). Additionally, the cytokines interleukin-1 beta (IL-1?), interleukin-6 (IL-6), tumor necrosis factor-alpha (TNF-?), and interleukin-10 (IL-10) were assessed according to Kendall et al. (Planta, v. 159, p. 505, 1983). The results were considered significant when $p < 0.05$. **Results:** The results indicate that oral administration of hesperetin and carveol at doses of 25, 50, 100, and 200 mg/kg significantly reduced (p **Conclusion:** In conclusion, these findings suggest that hesperetin and carveol possess duodenal antiulcer activity, gastric healing activity, and low toxicity when administered in repeated doses. These effects are likely associated with the involvement of the antioxidant system and immunomodulation. **Acknowledgements:** CNPq / UFPB / PGPNSB / IpeFarM. **Ethics Committee (Animal Use Ethics Committee/UFPB):** 1774211455

08.002 Immunoregulatory, antioxidant, anti-secretory and cytoprotective activity of farnesol involved in gastroprotection. Pessôa MLS, Pessoa MMB, Alves VP, Silva ML, Batista LM UFPB

Introduction: Farnesol, which is a product of natural origin, belonging to the class of sesquiterpenes, is widely found in propolis, in the essential oils of aromatic plants. The main objective of this work was to verify the gastroprotective activity of farnesol in the ethanol-induced ulcer model and to investigate the mechanisms involved in this action. **Methods:** For experimental procedures with animals, male Wistar rats (*Rattus norvegicus*) weighing 180-250g were used, and the farnesol used was obtained on a synthesis scale, purchased from Sigma Aldrich. To evaluate the gastroprotective activity of farnesol, the animals were treated with tween 80 5% (negative control), carbenoxolone 100 mg/kg (positive control) or farnesol 25, 50, 100 and 200 mg/kg) the ulcer protocol was used gastric ulcer induced by absolute ethanol (Morimoto et al., *The Jap J. of Phar*, v. 57, p. 495, 1991). For evaluation of antiseecretory activity, the animals were submitted to pylorus ligation and treated (v.o and i.d) (Shay, *Gastroenterology*, v. 5, p. 43, 1945.), The area of the ulcerative lesion was determined by the ulcerative lesion index (ILU). To evaluate the cytoprotective mechanisms, the participation of sulfhydryl groups (SHs) was investigated (Matsuda et al., *Life Sciences*, v. 65, p. 27, 1999), participation of nitric oxide (NO) (Sikiri et al., *European Journal of Pharmacology*, v. 332, p. 23-33, 1997) of ATP-dependent potassium channels (KATP) (Olinda et al., *Phytomedicine*, v. 15, p. 327, 2008), determination of mucus concentration (Rafatullah et al., *Gastroenterology*, v. 2, p. 245, 1990) and participation of prostaglandins (Rodrigues et al., *Gastroenterology*, v. 3, p. 34, 2010). The antioxidants evaluated were reduced glutathione (GSH) (Faure, *Birkhäuser Basel*, v.1 p. 237, 1995.), malondialdehyde (MDA), myeloperoxidase (MPO) (Krawisz, *Gastroenterology*, v. 87, p. 1344, 1984.) and superoxide dismutase (SOD) (Sun et al., *Clin Chem*. v. 34, p. 497, 1988). The cytokines evaluated were interleukin-1 beta (IL-1?), interleukin-6 (IL-6), tumor necrosis factor alpha (TNF-?) and interleukin-10 (IL-10)(Kendall et al., *Planta*, v. 159, p. 505, 1983). The test was considered significant when $p < 0.05$. **Results:** In the ethanol-induced ulcer protocol, farnesol (25, 50, 100 and 200 mg/kg, p.o.) showed a gastroprotective effect in 73%, 92%, 97% and 98%, respectively, of inhibition of the ulcerative lesion in comparison to the control group (tween 80 5%). In the experimental protocol of pylorus ligation (gastric juice containment), farnesol (100 mg/kg, v.o. and i.d.) reduced ILU in both pathways, did not change pH in both pathways, H⁺ concentration and volume gastric juice orally. However, it reduced the concentration of H⁺ and the volume of gastric juice via the intraduodenal route. Previous administration of NEM blockers (blocker of sulfhydryl groups), L-NAME (NO synthesis inhibitor), glibenclamide (KATP channel blocker) and indomethacin (cyclooxygenase inhibitor), reduced the gastroprotection exerted by farnesol, in addition to increased gastric mucus in the stomach tissue, suggesting the participation of these pathways in its gastroprotective activity. In addition to having antioxidant effects by increasing the concentration of GSH and SOD activity and reducing MDA levels and MPO activity, it also demonstrated anti-inflammatory and immunomodulatory effects by reducing the cytokines IL-1?, IL-6 and TNF-? and increase the anti-inflammatory cytokine IL-10. **Conclusions:** Thus, it was possible to conclude that farnesol has a gastroprotective activity involving immunoregulatory, antioxidant and antiseecretory activity in the gastric mucosa in animal models. **Acknowledgments:** CAPES/UFPB/PgPNSB/IPeFarM. **Committee for Ethics in the Use of Animals (UFPB):** Protocol n° 9667170122.

08.003 Araucaria Brown Propolis Hydroalcoholic Extract, but not Junicedric Acid from this Extract, Promotes Gastroprotection in Rodents. Cury BJ¹, Venzon L¹, Silva HFT¹, Makowieski LP¹, Jerônimo DT¹, Silva LM¹, Farias T¹, Kenupp JB², Santos MFC³, Silva LM¹. ¹Univali, PPG in Pharmaceutical Sciences, Itajaí, SC, Brazil; ²Unifran, Research Center in Exact and Technological Sciences, Franca, SP, Brazil; ³FCFRP-USP, Ribeirão Preto, Brazil

Introduction: The different types of propolis have a wide therapeutic potential, and factors related to the place of origin, the type of collecting bee, and the form of the extract influence these activities. Although brown propolis has been used in folk medicine for centuries, including for gastric disorders, brown propolis from *Araucaria* sp. has only recently been discovered. Therefore, the present study aimed to investigate the antiulcer potential of the hydroalcoholic extract of brown *Araucaria* propolis (EHPMA) at doses of 30, 100, and 300 mg/kg (p.o.) or 30 mg/kg (i.p.) and junicedric acid (AJ, 3 and 10 mg/kg, p.o.) isolated from this propolis (SisGen: A0BD757). **Methods:** For this purpose, the gastric lesion was induced in mice by acidified ethanol (0.1 ml/10 g) and pyloric ligation was performed in rats to verify gastric antisecretory activity. Histological, histochemical, oxidative, and inflammatory parameters were quantified in gastric mucosa, and mice exposed to acidified ethanol-induced ulceration were pretreated with NEM, L-NAME, yohimbine, or indomethacin. Anti-*Helicobacter pylori* potential was evaluated in vitro, as were cytotoxic effects and fibroblast proliferation (CEUA UNIVALI 029-19p). **Results:** It was found that the dose of 100 mg/kg (p.o.) EHPMA was the only one that promoted gastroprotection and in parallel increased GSH levels and the activity of CAT and SOD in the ulcerated gastric mucosa, in addition to decreasing MPO and MDA levels compared to the vehicle-treated ulcer group. The extract at a dose of 100 mg/kg did not show antisecretory activity, but pretreatment with L-NAME, NEM, indomethacin, or yohimbine abolished the gastroprotective capacity of the extract, indicating the involvement of nonprotein sulfhydryl compounds, type 2 adrenergic receptors, prostaglandins, and nitric oxide in the observed effect. In addition, treatment with EHPMA (100 and 300 mg/kg) increased mucin staining of the gastric mucosa compared with the vehicle group. Histological findings also showed that EHPMA (100 mg/kg) was able to prevent tissue damage or structural loss of the tissue barrier and reduce edema and inflammatory infiltrates. At concentrations of 1 or 10 µg/ml, the extract showed no cytotoxicity in fibroblasts and no anti-*H. pylori* effect in vitro, and the minimum inhibitory concentration was greater than 1000 µg/ml. AJ has no gastroprotective effect at the doses tested. **Conclusions:** Overall, this study contributed to the validation of the anti-ulcer activity of *Araucaria* brown propolis and showed that it is a promising natural resource for the development of new strategies for the treatment of gastric ulcers. It was also demonstrated that junicedric acid is not an important bioactive compound for this effect. **Financial Support:** CAPES and CNPQ.

08.004 Hydroalcoholic Extract of Araucaria sp Brazilian Brown Propolis alleviates Ulcerative Colitis induced by TNBS in Rats. Cury BJ¹, Jerônimo DT¹, da Silva LM¹, Farias T¹, França TCS¹, Dos Santos AC¹, Andriolo, IRL¹, Santos MFC², Kenupp JB³, da Silva LM¹. ¹Univali, PPG in Pharmaceutical Sciences, Itajaí, SC, Brazil; ²Unifran, Research Center in Exact and Technological Sciences, Franca, SP, Brazil; ³FCFRP-USP, Ribeirão Preto, Brazil

Introduction: Currently, pharmacological treatment of ulcerative colitis (UC) aims to promote and maintain remission of the disease, but a cure cannot be achieved. Alternative practices have gained attention in the treatment of chronic diseases, including apitherapy, where propolis has been highlighted for its therapeutic properties. The brown propolis of *Araucaria sp.* from the state of Paraná is rich in diterpenes, a class of secondary metabolites that possess anti-inflammatory properties. Despite the diterpene content and the fact that other Brazilian propolis have been shown to have an anti-inflammatory effect on the intestine, the potential of brown propolis from *Araucaria* in the treatment of inflammatory bowel diseases is still unknown. Therefore, the aim of this study was to investigate the anti-inflammatory effect of brown propolis from *Araucaria sp.* in rats with TNBS-induced colitis. **Materials and Methods:** The cytotoxic effect of the hydroalcoholic extract (HEPMA, 10, 30, and 100 µg/ml) was studied in IEC6 cells. In the *in vivo* tests, animals were treated orally for 5 days with vehicle (1% DMSO, 1 ml/kg), dexamethasone (25 mg/kg, s.c.), or HEPMA (30, 100, and 300 mg/kg, p.o). On the 4th day of treatment, the animals received a single dose of TNBS (150 mg/kg) intracolically, and they were euthanized on the 6th day after the start of treatment. The weight of the animals was recorded throughout the experimental period. Subsequently, macroscopic, and microscopic damage as well as GSH and MDA levels and the activity of the enzymes GST, CAT, SOD and MPO were measured (SisGen: A0BD757). **Results:** HEPMA reduced IEC-6 cell viability at 100 µg/ml, but oral treatment with HEPMA at doses of 100 and 300 mg/kg decreased colonic lesions induced by TNBS instillation in rats. Moreover, the extract increased acidic and neutral mucin concentrations. In parallel, administration of HEPMA decreased MDA concentrations and restored basal levels of GSH and SOD, CAT and GST activity in the colon. In addition, a dose-dependent inhibition of MPO activity was observed (LogIC₅₀=1.9). The dexamethasone-treated group showed significant animal weight loss but lower MDA concentrations, and GST activity was like baseline levels. In contrast, the activity of the enzymes SOD, CAT, and MPO increased, and GSH concentrations were like those of the vehicle group. **Conclusion:** This study shows that HEPMA may be promising in the search for therapies for inflammatory bowel disease, as it acts by reducing oxidative and inflammatory damage, especially by neutrophils.

08.005 Doxycycline Reduces Inflammation in Lung and Gut in a Murine Model of Acute Respiratory Distress Syndrome. Santos AA, Oliveira TD, Dias KT, Tavares-de-Lima W, Rodrigues SFP. USP, Dpt of Pharmacology, Brazil

Introduction: Acute respiratory distress syndrome (ARDS) is a disease with rapid onset and is featured by an excessive acute inflammatory process in the lung, resulting in alveolar edema and subsequent tissue hypoxia. It is often observed in diseases like pneumonia, sepsis, and more recently, the coronavirus disease 19 (COVID-19). The pathogenesis of ARDS involves the neutrophils and monocytes trafficking to the lung tissue, massive release of inflammatory and oxidant mediators, and proteases, including matrix metalloproteinases (MMPs), which contribute to the loss of surfactant, epithelial and endothelial cells apoptosis, alveolar edema, difficulty in gas exchange, and high rate of morbidity and mortality. Distant tissues, like the gut, can play a role in the ARDS pathogenesis as well (lung-gut axis). Despite the use of artificial ventilation and corticosteroids as only strategies to combat ARDS, part of patients does not respond to this treatment. In this context, we have tested doxycycline (Dox), a tetracycline with MMPs inhibitory activity, in an experimental model of ARDS. **Methods:** ARDS was obtained by an intratracheal (I.T.) injection of peptidoglycan (PPG) and lipoteichoic acid (LTA) in C57Bl/6 mice (CEUA protocol #9737280921), which was repeated 24h later. As control, distilled water was I.T. injected. Dox treatment (20 mg/kg) was orally performed 2h and 24h after injection of PPG/LTA. **Results:** ARDS mice showed enhanced number of cells in the bronchoalveolar lavage fluid (BALF) (364.1 +/- 15.97) compared to the control group (12 +/- 1.0) (P<0.05). These cells were mainly constituted of neutrophils. Dox treatment reduced the number of cells in the BALF (248.6 +/- 24.32) (P<0.05, N=7). Increased protein concentration was observed in the PPG/LTA BALF compared to the control group, and it was not reduced by Dox treatment. More leukocyte rolling (11.93 +/- 0.71/min) (P<0.05) was observed in the gut venules of ARDS mice compared to the control group (5.12 +/- 0.32), but not on those treated with Dox (7.75 +/- 0,18) (N=7). An increased malondialdehyde concentration was observed in the PPG/LTA BALF compared to the control group, and it was not reduced by Dox treatment. **Conclusion:** Dox treatment reduces leukocyte presence in lung and gut and does not change reactive oxygen species levels in lung in an experimental model of ARDS. **Financial Support:** FAPESP #2020/07212-7; #2022/13258-5; CAPES: #88887.704584/2022-00

08.006 Gold Nanoparticles Reduced Lung Inflammation in a Murine Model of Acute Respiratory Distress Syndrome. Oliveira, TD, Santos, AA, Oliveira, MA, Tavares-de-Lima, W, Rodrigues, SF. USP, Dpt of Pharmacology, Sao Paulo, Brazil

Introduction: The acute respiratory distress syndrome (ARDS) is a disease that progresses quickly and is characterized mainly by pronounced lung edema and hypoxemia that lead to high morbidity and mortality rates. It is in great part observed in diseases like sepsis, pneumonia and, most recently, by the coronavirus disease 19 (COVID-19). The pathogenesis of ARDS is complex and involves excessive inflammatory response, which leads to alveolar-capillary barrier damage and consequent edema. Moreover, it is observed neutrophils, monocytes and epithelial cells infiltration in the lung parenchyma and release of proinflammatory mediators, such as cytokines, proteinases, reactive oxygen and nitrogen species (RONS), and coagulation factors, which are greatly responsible for the endothelial and lung epithelial cells death, which further enhances the alveolar-capillary barrier permeability and contribute to the difficulty in gas exchange, and high rates of morbidity and mortality. The gut-lung axis seems to play a role in the pathophysiology of ARDS as well, probably by increasing the intestinal permeability and bacterial translocation to the lungs. It was demonstrated that 20 nanometers size citrate-capped gold nanoparticles (cit-AuNP) reduce inflammation and oxidative stress and diminish intestinal permeability or bacterial translocation in experimental models of local acute insult. Therefore, we aimed to test the efficacy of cit-AuNP in diminishing the pulmonary alterations in a murine model of ARDS and their's effects on intestinal inflammatory parameters in mice with ARDS as well. **Methods:** ARDS was obtained by an intratracheal (I.T.) injection of peptidoglycan (PPG) and lipoteichoic acid (LTA) in C57Bl/6 mice (CEUA protocol #9737280921), which was repeated 24h later. As control of ARDS, distilled water was I.T. injected. Cit-AuNP treatment was intravenously performed 2h and 24h after injection of PPG/LTA. **Results:** ARDS mice showed enhanced number of cells in the bronchoalveolar lavage fluid (BALF) compared to the control group (400.9+/- 53.62 vs. 28.36+/- 2.070, $P < 0.001$). These cells were mainly constituted of neutrophils. Cit-AuNP treatment reduced the number of cells in the BALF (184.1+/- 27.30, $P < 0.0005$) (N=8). ARDS mice also showed enhanced concentration of proteins in BALF, and cit-AuNP treatment reduced this protein concentration (N=6). However, lung histological analysis demonstrated that ARDS mice presented higher tissue damage compared to control group (N=5), and cit-AuNP treatment did not correct this parameter. Furthermore, respiratory mechanics analysis showed that ARDS mice presented higher tissue damping (G) and elastance (H) than control group (N=4), and cit-AuNP treatment did not change this phenotype. **Conclusion:** Cit-AuNP treatment reduced lung inflammation in ARDS-induced mice but did not reduce histology damage. **Financial Support:** FAPESP 2020/07212-7, CAPES: #88887.816548/2023-00.

08.007 **ASK1 Regulates Bleomycin-induced Pulmonary Fibrosis.** Valenca SS 1-2, Dong BE 2, Gordon EM 2, Sun RC 3, Waters CM 2. ¹ICB-UFRJ, Brazil; ²University of Kentucky, Dept of Physiology, USA; ³University of Kentucky, Dept of Neuroscience, USA

Introduction: Pulmonary fibrosis (PF) is an abnormal remodeling of cellular composition and extracellular matrix that results in histological and functional alterations in the lungs. Apoptosis signal regulating kinase-1 (ASK1) is a member of the mitogen activated protein (MAP) kinase family that is activated by oxidative stress and promotes inflammation and apoptosis.

Methods: Ask1 knockout mice (Ask12/2) and C57BL/6Jmice were purchased from The Jackson Laboratory. All mouse lines were housed with food/water ad libitum, and weight was recorded daily. Male mice between 3 and 6months of age received intratracheal instillation of a single dose of 0.3 U/kg of bleomycin. Control mice received saline intratracheally. In other experiments, mice were treated daily with 20 mg/kg selonsertib (Selleck Chemicals) by oral gavage starting 8 days after bleomycin instillation. Control mice were given vehicle (ethanol: water) by oral gavage on the same schedule. At the experimental endpoint (22 d), lung function measurements were made, followed by the collection of BAL fluid (BALF) and lung tissue. The Institutional Animal Care and Use Committee for the University of Kentucky approved all animal procedures. **Results:** Here we show that bleomycin-induced PF is reduced in Ask1 knockout mice (Ask12/2) compared with wild-type (WT) mice, with improved survival and histological and functional parameters restored to basal levels. In WT mice, bleomycin caused activation of ASK1, p38, and extracellular signal regulated kinase 1/2 (ERK1/2) in lung tissue, as well as changes in redox indicators (thioredoxin and heme-oxygenase-1), collagen content, and epithelial–mesenchymal transition markers (EMTs). These changes were largely restored toward untreated WT control levels in bleomycin-treated Ask12/2 mice. We further investigated whether treatment of WT mice with an ASK1 inhibitor, selonsertib (GS-4997), during the fibrotic phase would attenuate the development of PF. We found that pharmacological inhibition of ASK1 reduced activation of ASK1, p38, and ERK1/2 and promoted the restoration of redox and EMT indicators, as well as improvements in histological parameters. **Conclusion:** Our results suggest that ASK1 plays a central role in the development of bleomycin-induced PF in mice via p38 and ERK1/2 signaling. Together, these data indicate a possible therapeutic target for PF that involves an ASK1/p38/ERK1/2 axis. **Financial Support:** Supported by the National Heart, Lung, and Blood Institute grants HL131526 and HL151419.

08.008 **Antioxidant and healing activities of *Melipona compressipes fasciculata* (Smith, 1854) stingless bee pot pollen in *in vitro* and *in vivo* models.** Neves JA¹, Sousa MC¹, Silva FV¹, Viana AFSC², Fernandes HB¹, Moreira FAS¹, Santos BLB¹, Oliveira RCM¹ ¹UFPI, ²UFC

Introduction: Brazil has the greatest diversity of stingless bees in the world and among these stands out *Melipona compressipes fasciculata* (Smith, 1854). Bee pollen is the product resulting from the agglutination of floral pollen, nectar and salivary enzymes of bees. In hives, there are biochemical changes and conversion of bee pollen into "pot pollen" or "stingless bee bread" (SBB), with high nutritional value and different chemical compounds of botanical origin and relevant presence of phenolics (anti and prooxidants), but it is less studied. In this sense, the aim was to evaluate the antioxidant and healing activities, after palynological and toxicological characterization of SBB pot pollen. **Methods:** Samples of SBB were collected from hives in the rainy (SBB1) and dry (SBB2) seasons. The evaluation of the healing effect occurred through the model of gastric ulcers induced by acetic acid in rats. **Results:** The palynological characterization showed that the samples are monofloral, with a predominance of pollen types of *Mimosa pudica* L. and *Mimosa caesalpiniiifolia* Benth., respectively. By the toxicological bioassay in *Artemia salina* L., the LC50 were: SBB1 = 1159.0 and SBB2 = 1134.0 µg/mL, being non-toxic. The total phenolic content of the extracts was SBB1 = 9.32 and SBB2 = 6.59 mg of gallic acid equivalent/g. The phenolic profile, by HPLC and HPLC-MS/MS, revealed, in both samples, compounds with reported antioxidant and gastroprotective activities, such as caffeic acid, quercetin, myricetin and naringenin, with SBB2 showing a greater presence of these. *In vitro* antioxidant activity was SBB1 = 62.93 and SBB2 = 58.86% DPPH reduction, with no significant difference between samples (Student's t test, p < 0.05). In a model of gastric ulcer induced by acetic acid in rats, oral treatment for 7 days with SBB2 at all doses (3, 8 and 24 mg/kg) significantly reduced ulcer volume and increased healing by 36, 85 and 97%, respectively, when compared to the vehicle group. This treatment with SBB2 (at all doses) did not cause alterations in weight gain and organ weight, and in terms of biochemical parameters, it also reduced markers of liver damage, glycemia and increased HDL. SBB2 (24 mg/kg) stimulated gastric tissue regeneration, increased levels of SH-NP groups (103%), decreased MDA levels (84%) and increased the percentage of collagen fibers. **Conclusion:** With this, it is concluded that the pot pollen of *M. compressipes fasciculata* studied is monofloral, non-toxic, presents phenolics, antioxidant and healing activities, possibly by potentiating mucosal defenses, improving the biochemical profile and does not cause signs of toxicity in rats, being a potential agent for use in the prevention and/or treatment of gastric ulcer, with viable application in biotechnological, food and/or pharmaceutical products.

08.009 Mechanisms Involved in the Inflammatory Response of Bradykinin in Presence of LPS in the Bronchoalveolar Lavage Model in Mice. Dutkevicz N, Silva ALM, Signori L, Schlemper SRM, Schlemper V., UFFS, Realeza Veterinary Medicine Course, Brazil

Introduction: Bradykinin (BK) and lysyl-BK (kallidin) are vasoactive peptides, which are generated in plasma and tissues from kininogens by the actions of kallikreins. Once released, kinins act at their specific B1 and B2 membrane receptors to exert several physio-pathological effects. **Methods:** The present study investigated the agonist effect of BK receptors induced via respiratory tract inflammation by LPS in BALB/C mice. The animals received BK (10 nMol/mL) by inhalation for 3 minutes in a specific chamber. The B2 receptor antagonist HOE-140 (D-Arg-[Hyp³Thi⁵,DTic⁷,Oic⁸]-BK) (10 nMol/ml) and the B1 receptor antagonist DALBK (des-Arg⁹[Leu⁸]-BK (300 nMol/ml) were administered via nasal instillation in mice that received intraperitoneal LPS (20 µg) 24 hours before. After 2 hours the animals were euthanized and the bronchoalveolar lavage (BAL) was obtained to analyze the total cell count (TCC) and differential cell count (DCC). **Results:** The group treated with DALBK showed a significant decrease in the TTC number (maximum inhibition 45,4% ± 3.8) in comparison with LPS + BK group, as well as showing more macrophages (68.83% ± 2.94) than lymphocytes (29.33% ± 2.88), and a low number of neutrophils (1.17% ± 0.30) and basophils (0.67% ± 0.42). When compared to the LPS + BK group, the HOE-140 group showed a maximum inhibition in the total number of leukocytes of 29.9% ± 4.1, 52.83% ± 7.36 of macrophages, 43% ± 7, 81 lymphocytes, 2.33% ± 0.55 neutrophils and 1.83% ± 0.94 basophils. **Conclusions:** The leukocyte migration to the airway lumen allowed for the investigation of the role of kinins in chronic inflammatory processes in the airways of rodents. In general, the observations made in this study indicate the use of B1 and B2 receptor antagonists for respiratory chronic diseases such as asthma. **Financial Support:** Fundação Araucária - PR

08.010 Evaluation of the Antidiarrheal Activity and Motility Effects of Hesperetin in Animal Models. Alves VP¹, Pessoa MMB², Pessôa MLS¹, Batista LM¹ ¹UFPB, Dpt. of pharmaceutical Sciences, Paraíba, Brazil

Introduction: Diarrhea is a gastrointestinal disorder in which there are changes in the number of bowel movements (three or more in a 24-hour period) and in the consistency of the stool (semi-solid or liquid). This disorder has a multifactorial etiology and can be classified as infectious when triggered by microorganisms and non-infectious when caused by drugs, for example. Therapy can be non-pharmacological by replacing water and electrolytes or pharmacological. However, this therapy has limitations, among which we can mention the high rate of recurrence, high cost of hospitalizations and adverse effects, in this context natural products arise, especially medicinal plants, due to their therapeutic potential, variety of active molecules and its cultural context. Hesperetin is a natural compound of the flavonoid class that can be found in citrus fruits, such as *Citrus x sinensis*. The objective of this study was to evaluate the antidiarrheal activity and the effects on motility (transit and emptying) related to this flavonoid. **Methods:** The animals used for this study were male Swiss mice (*Mus musculus*) aged 6 – 8 weeks, weighing between 28 and 35g. The animals were maintained at a temperature of 23 ± 2 °C, with a 12-hour light and dark cycle. For the evaluation of antidiarrheal activity, the castor oil-induced diarrhea protocol was used (Awouters C. J. et al. *J. Pharm. Pharmacol.* 30, 41-45, 1978). For gastric emptying, the protocol for assessing effects on gastric emptying was used (Scarpignato, C. A. et al. *Arch. Int. Pharmacodyn. Ther.* 246, 286-294, 1980). And for intestinal transit, the protocol used was transit induced by castor oil (Stickney, J. C. and Northup D. W. *Proc. Soc. Exp. Biol. Med.* 101, 582-583, 1959). For the statistical analysis of the results, ANOVA was used followed by Dunnett's test (mean \pm standard deviation) followed by Tukey's post-test. **Results:** Hesperetin (obtained from Sigma-Aldrich) showed antidiarrheal activity, oral pretreatment with loperamide (positive control - 5 mg/kg) and hesperetin at doses of 100 and 200 mg/kg promoted an inhibition percentage of 83%, 77% and 69%, respectively, when compared to the negative control group (0.9% saline – Vehicle 10 mL/Kg). For gastric emptying, the animals treated with saline had a gastric emptying rate of 96.9%, whereas for the groups treated with loperamide and hesperetin (doses of 25, 50, 100 and 200 mg/kg) it promoted a reduction of 75.7%; 68.3%; 33.3%; 24.5% and 23% respectively when compared to the negative control. In the evaluation of intestinal transit, the negative control group presented a percentage of transit of 98.8%, whereas loperamide and flavonoid (doses of 50, 100 and 200 mg/kg) promoted a reduction of motility to 21%; 37.8%; 20.4% and 22.4% respectively, when compared to the negative control. **Conclusions:** Thus, from the results, it can be concluded that hesperetin has antidiarrheal activity and antimotility effect by reducing intestinal transit and gastric emptying. **Acknowledgements:** CNPq / UFPB / PGPNSB / IpeFarM.

08.011 Evaluation of Acute Toxicity, Antidiarrheal Activity and Gastrointestinal Motility of Gamma-Terpinene in Animal Models. Silva ML, Pessoa MMB, Pessoa MLS, Alves VP, Araruna MEC, Alves Junior EB, Batista LM UFPB

Introduction: Diarrhea is an intestinal disorder characterized by a decrease in stool consistency, which becomes semi-solid or liquid and an increase in the frequency of bowel movements to three or more times in a 24-hour period. Gamma-terpinene is a monoterpene present in the volatile essential oil present on *Melaleuca alternifolia*. The aim of the present study is to evaluate the toxicity, antidiarrheal activity and effects on motility (transit) related to this terpene. **Methods:** The animals used for this study were male Swiss (*Mus musculus*) mice, with ages between 6 to 8 weeks and weighing between 25 and 35 grams, they were acclimatized to a temperature of $23 \pm 2^\circ\text{C}$ and kept in light-dark cycle of 12/12 hours. For the assessment of toxicity, gamma-terpinene was administered at different doses (300 and 2000 mg/kg), followed by behavioral evaluation of the animals, following the protocol established by OECD. Guideline, p.423-423, 2001.; Almeida et al, *Rev Bras Farm.* v.80, p.72-76, 1999. For the evaluation of the antidiarrheal activity, gamma-terpinene was administered in different doses (25, 50, 100 and 200 mg/kg) and the control group received loperamide in the dose of 5 mg/kg, following the castor oil induction protocol recommended by Awouters CJ. et al. *J. Pharm. Pharmacol.* v.30, p.41-45, 1978. And for intestinal transit, the animals also received the gamma-terpinene in different doses (25, 50, 100 and 200 mg/kg) and for the control group was administered loperamide in the dose of 5 mg/kg, following the castor oil induction protocol recommended by Stickney, JC. and Northup DW. *Proc. Soc. Exp. Biol. Med.* v.101, p.582-583, 1959. For the statistical analysis, was used mean \pm standard deviation for parametric data and median (minimum and maximum values) for non-parametric data, the tests were performed by ANOVA, followed by Dunnet or Tukey post test. **Results:** In the evaluation of toxicity, the animals submitted to the administration of gamma-terpinene at a dose of 300 mg/kg showed behavioral changes (grooming and tremors), compared to the control group (Tween 80 5%), and at a dose of 2000 mg/kg, two animals died. The monoterpene also presented antidiarrheal activity at a dose of 200 mg/kg, with 36% of inhibition, when compared to the control group that presented 82% of inhibition. The gamma-terpinene promoted the reduction of gastrointestinal motility, by reducing the transit, to 60% at a dose of 200 mg/kg, when compared to the control group, that presented 40% of reduction. **Conclusions:** Thus, the results about the present study, it can be concluded that gamma-terpinene have low toxicity, with DL50 of 2.500 mg/kg, antidiarrheal activity, and antimotility effect by reducing intestinal transit. **Acknowledgements:** CNPq / UFPB / PGPNSB / IpeFarM.

08.012 Hydroalcoholic Extract from *Aloysia citriodora* and Verbascoside Promote Gastroprotection Through Mucosal Protection and Modulation of Inflammatory and Oxidative Stress Markers. Buzatto MV¹, Gomes DB¹, Miorando D¹, Somensi LB², Silva, LM², Roman-Junior, WA¹ ¹Unochapecó ²UNIVALI

Introduction: The species *Aloysia citriodora* Palau (Verbenaceae), known as erva-luisa, is native to Brazil and the leaves are popularly used to treat fever and digestive disorders. However, the gastric protective effect has not yet been evaluated. In this context, this work aims to investigate the gastroprotective effect of *A. citriodora* and its major compound, verbascoside. **Methods:** The hydroalcoholic extract of *A. Citriodora* (HEAc) was obtained by maceration. A sample was submitted to partition with solvents of increasing polarity. The ethyl acetate fraction was subjected to fractionation on a silica gel liquid column with yielding of verbascoside. The chemical analysis were performed through spectroscopic analysis of ¹H-NMR, ¹³C-NMR and MS (ESI). For the antioxidant activity, the EHAc was evaluated by decreasing the absorbance of 2,2 diphenyl-1-picryl-hydrazyl (DPPH). The experiments were approved under protocol 004/04/CEUA/2021. For the acute gastroprotective evaluation in rats, ethanol and indomethacin ulcers were induced in the groups: Vehicle (Veh), carbonexolone (Carb, 200 mg/kg), HEAc (3, 30, or 300 mg/kg) or VBS (30 mg/kg). Naïve (N) was not induced. The stomach lesions were analyzed macroscopically and histologically. Samples of stomachs were used for biochemical analyses of malondialdehyde (MDA), myeloperoxidase (MPO), catalase (CAT), superoxide dismutase (SOD), glutathione S-transferase (GST) and reduced glutathione (GSH). In order to evaluate the possible pharmacological mechanisms involved in gastroprotection, the acid antsecretory activity was evaluated. **Results:** The phytochemical analysis showed a high yield of VBS which was identified through spectroscopic study. In *in vitro* antioxidant activity, the EHAc presented an EC₅₀ of 25.59 mg/ml, a more efficient result than the standards, gallic acid and quercetin (30.72 and 36.42 mg/ml, respectively). In acidified ethanol-induced ulcers, HEAc 30 or 300 mg/kg showed a reduction of 28,92% and 52,99%, respectively, and VBS showed a reduction of 36,18%, both compared with Veh. In indomethacin-induced ulcers, HEAc 30 or 300 mg/kg reduced 52 and 79% compared with Veh, VBS reduced 87% compared with the same group. These results were corroborated with the histological and histochemical analysis. In ethanol-induced ulcers, HEAc 30 and 300 mg/kg increased GSH and GST. VBS reduced MDA and MPO values. In indomethacin-induced ulcers, VBS increased GSH, GST and SOD, the HEAc 30 and 300 mg/kg increased CAT levels. HEAc and VBS caused decrease in the gastric volume and acidity, maintaining the peptic activity values close to the physiological. **Conclusion:** The results observed to validate the popular use of *A. citriodora*. The HEAc and verbascoside present gastroprotective activity and the pharmacological effects are related to the reduction of pro-inflammatory markers and oxidative stress. **Acknowledgments:** UNOCHAPECÓ, CNPq.

08.013 *Uncaria tomentosa* a Medicinal Plant with Gastroprotective and Gastric Healing Properties in Rats: Histological, Biochemical Analysis and Use of Ultrasound. Simomura VL¹, Buzzato MV¹, Miorando D1, Somensi LB², de Oliveira BMM¹, Steffler AM¹, Veloso JJ¹, Barrichello A¹, Kunst FM¹, Ansolin LD¹, Vidal-Gutiérrez M³, da Silva LM⁴, Roman Junior WA¹. ¹Unochapecó, ²Uniarp, ³University of Sonora, ⁴Univali

Introduction: *The Uncaria tomentosa* (Willd DC.), is native to the Amazon rainforest where it is known as cat's claw. Its popular use is extensive among Peruvian and Brazilian tribes, mainly for the treatment of inflammations and gastrointestinal disorders. However, studies that evaluate the gastroprotective potential have not yet been performed. This work aims to investigate the gastroprotective and gastric healing effects of barks from *U. tomentosa*.

Methods: The extractive method (decoction) aims to mimic the popular use of the plant and the phytochemical analysis was performed by mass spectrometry (ESI-IT-MSⁿ). The experiments *in vivo* were approved under protocol CEUA n° 17/2020. For the gastroprotective evaluation in rats, ethanol and piroxicam ulcers were induced in the groups: Vehicle (Veh, water), Omeprazole (Ome, 20 mg/kg), EAUt (30, 60, or 120 mg/kg). Naïve (N) was not induced. The stomach lesions were analyzed macroscopically, and histological and histochemical analyses were performed. In order to evaluate the possible pharmacological mechanisms, the acid antisecretory activity was evaluated. In the gastric healing model, 80% acetic acid was instilled in the serous layer and the treatments were administered for 7 days: Veh, Ome (20 mg/kg). or EAUt (60 mg/kg). N was not induced nor treated. In order to monitor healing, ultrasound examinations were performed. The stomachs were removed and evaluated macroscopically and histologically. In addition, myeloperoxidase (MPO), catalase (CAT), superoxide dismutase (SOD), and glutathione (GSH) analyses were performed.

Results: The chemical study pointed to twelve compounds among them, the mitraphylline alkaloid which is considered the marker for the species. In ethanol-induced ulcers, animals that received EAUt 30, 60, or 120 mg/kg demonstrated a reduction in the ulcerated area (56.46, 31.59, and 39.82% respectively), compared to the vehicle group ($p < 0.01$). In piroxicam ulcers, EAUt 30, 60, or 120 mg/kg presented a reduction in the ulcerated area of 65.18, 82.59, and 69.30% respectively. These results were corroborated by the histological, histochemical analysis, and ultrasound analysis. The administration of EAUt at doses of 60 and 120 mg/kg did not change the volume, the total acidity of the gastric secretion. In the gastric healing evaluation, EAUt decrease the lesion area by 64.8% compared with Veh ($p < 0.0001$), and the ultrasound and histological images corroborated the obtained **Results:** No significant results were obtained for EAUt against the analyzed antioxidant enzymes (GSH, CAT, SOD). However, the EAUt treatment reduced MPO activity by 54.3% compared to the vehicle group. **Conclusion:** EAUt presents gastroprotective and gastric healing effects mediated by preserving the mucosa and reducing inflammation. These activities possibly are related to the presence of alkaloids and polyphenolic compounds in the extract. Financial Support/Acknowledgment: Community University of Chapecó Region Unochapecó; Uniedu/FUMDES.

08.014 **Extracts of *Baccharis dracunculifolia* DC and Brazilian Green Propolis Ameliorates Ethanol- and Lps-induced Liver Injury in Mice.** Santos AC¹, França TCS¹, Pilati SFM¹, Kenupp JB², da Silva LM¹ ¹Univali, PPG in Pharmaceutical Sciences, SC, Brazil, ²FCF-USP, Ribeirão Preto, Brazil

Introduction: Extending the ethnopharmacological validation of the hepatoprotective potential of *B. dracunculifolia* and in continuity with previous studies, this study aimed to evaluate the hypothesis that hydroalcoholic extracts *B. dracunculifolia* (HEBD) and green propolis (HEGP) reduce liver damage in exposed mice to ethanol and lipopolysaccharide (LPS). **Materials and Methods:** Swiss mice were divided into 8 groups (n=6): Vehicle, silymarin (200 mg/kg), HEBD (30, 100, or 300 mg/kg), and HEGP (30, 100, or 300 mg/kg) and treated orally once daily for 10 days. Concurrent oral ethanol (30%) was administered once daily for 10 days, followed by a single administration of LPS (2 mg/kg, intraperitoneally) one day before euthanasia. Liver and blood samples were then collected for histological and biochemical measurements. In parallel, mice (n=6) received vehicle or extracts (100 or 300 mg/kg, p.o.) during the same treatment period and were not exposed to ethanol/LPS (CEUA: 016/20 p) (SisGen: A0BD757). **Results:** HEBD and HEGP at a dose of 30 mg/kg decreased GOT serum levels, and both extracts at all doses tested decreased GPT serum levels in mice exposed to ethanol/LPS. The liver injury impaired antioxidant defenses in mice, as evidenced by a 46% decrease in GSH levels and a 38% and 87% decrease in GST and CAT activity, respectively, which was accompanied by a twofold increase in MDA in the liver. Treatment with HEBD or HEGP prevented these changes in oxidative parameters, however, HEBD did not prevent the increase in MDA levels. In addition, MPO and NAG activity, as well as the levels of IL -6 and IL -10, were increased in the livers of mice exposed to ethanol/LPS compared with the untreated group (p<0.05). Treatment with HEGP and HEBD reduced MPO and NAG activity and levels of IL -6 and IL -10 compared with mice exposed to ethanol/LPS (p<0.05). Mallory bodies and inflammatory infiltrate were detected in the liver parenchyma of mice exposed to ethanol/LPS and this change was minimized by treatment with both extracts. However, animals treated with HEBD still showed hydropic degeneration in hepatocytes. Furthermore, no signs of hepatic toxicity were observed in healthy animals treated with the extracts. **Conclusion:** The beneficial potential of the hydroalcoholic extracts of *B. dracunculifolia* and BGP in chronic ethanol- and LPS-induced liver injury was experimentally confirmed. Both extracts achieve the described effects probably due to their antioxidant activity and inhibitory activity against leukocyte migration and cytokine secretion. However, preparations obtained from green propolis may be more promising in the treatment of liver diseases. **Financial Support:** CAPES and CNPq.

08.015 *Spirulina (Arthrospira) platensis* prevents Oxidative Stress, Inflammation and Damage to Contractile Reactivity in the Ileum of Rats fed a Hypercaloric Diet. Diniz AFA¹, Ravilly RAA¹, Claudino BFO², Francelino DMC², Alves-Júnior EB¹, Barros BC¹, Lacerda-Júnior FF¹, Ferreira PB¹, Alves AF^{1,3}, Batista LM^{1,3}, Silva BA^{1,3} ¹PPgPNSB-CCS-UFPB ²CCS-UFPB ³DCF-CCS-UFPB

Introduction: Obesity is characterized by an energy imbalance caused by caloric intake and expenditure, being a risk factor associated with a wide range of pathophysiological conditions, including gastrointestinal diseases (LOPES et al., BrazJHealthRev, v5, p578, 2022). In recent years, it has been shown that overexpression of oxidative stress and pro-inflammatory cytokines is a mechanistic link between obesity and cellular functions in animals and humans. In this sense, studies have focused on the potential nutritional and antioxidant value of natural foods of mineral, animal and vegetable origin, such as algae, capable of neutralizing the adverse effects of oxidative stress (GIL-CARDOSO et al., MolNutrFoodRes, v61, 2017). Thus, *Spirulina (Arthrospira) platensis (SP)* stands out, an alga with anti-inflammatory and antioxidant activities (ABDEL-MONEIM et al., SaudiJournalofBiolSci, v29, p1197, 2022). The objective is to evaluate the preventive effects of SP supplementation on oxidative stress, interleukin-1 (IL-1?) levels, as well as the involvement of the NADPH oxidase pathway in changes in contractile reactivity in the ileum of rats fed a hypercaloric diet. **Methods:** The rats were divided into a group fed a standard diet (SD), a hypercaloric diet (HCD) and/or fed a hypercaloric diet and supplemented simultaneously with SP 25 mg/kg (HCD + SP25), after 8 weeks of treatment the ileum was collected for the analyses. Results were expressed as mean and standard deviation of the mean and analyzed by one-way ANOVA followed by Tukey's post-test ($p < 0.05$, $n=5$). **Results:** It was observed that in the HCD group there was underproduction of antioxidant enzymes as well as overexpression of oxidative stress in the ileum, curiously this damage was prevented by the alga. Similarly, the rats in the HCD group had high levels of IL-1, such an increase was avoided in the HCD + SP25 group. Such results were confirmed by the involvement of the NADPH oxidase pathway, through its inhibition by the alga in the HCD+SP25 group. **Conclusions:** It is evident, therefore, that SP prevents the increase in oxidative stress and the inflammatory profile in the ileum of obese rats, by negatively modulating the NADPH oxidase pathway, making it a promising therapeutic alternative in the treatment of inflammatory bowel diseases aggravated by obesity. Research approval: CEUA/UFPB (2352101019). **Financial Support:** CNPq, CAPES, PROEX. - Concelho Federal de Farmacia – CFF - INCT- RENNOFITO/CNPq

08.017 Hydrogen Sulfide improves Intestinal Epithelial Cell Barrier under Inflammatory Stimulus. Prata de Oliveira J^{1,3}, Wallace J², Muscara, MN¹, Costa, SKP¹, Denadai-Souza, A³
¹ICB-USP, Depto de Farmacologia, Brazil; ²University of Calgary, Dept of Physiology and Pharmacology, Canada; ³KU Leuven, Lab. of Mucosal Biology, Dept of Chronic Diseases, Metabolism and Ageing, Belgium

Introduction: The non-steroidal anti-inflammatory drugs (NSAIDs) are globally the most widely used and prescribed medications however, its use can promote intestinal damage, encompassing issues such as bleeding and ulceration (1). In parallel, the new endogenous gasotransmitter, hydrogen sulfide (H₂S) as well as donors of H₂S, have been shown to exert anti-inflammatory and cytoprotective properties (2) but the mechanisms involved in triggering this condition are not well established. This study was undertaken to evaluate the protective effect of the hydrogen sulfide-releasing derivative of ketoprofen (ATB-352) in comparison to its parent molecule ketoprofen in the cellular integrity of the intestinal epithelial barrier.

Methods: Intestinal epithelial cell lineages Caco-2/TC7 and HIEC-6 (5% CO₂, 37°) were subjected to IFN- γ (2.5 ng/ml; 3 h) stimulation and further exposed to TNF- α (10 ng/ml) or vehicle (culture medium) for a total period of 24 hours. Cells were then exposed to ketoprofen (100 μ M), ATB-352 (150 μ M), the H₂S portion donor 4-HTBZ (50 μ M) or vehicle for 72 hours, and the cellular viability was measured via the ATP-release assay. Caco-2/TC7 cells were placed in transwell plates for the evaluation of epithelial barrier integrity. Briefly, Trans Epithelial Electrical Resistance (TEER) was quantified using the EVOM device, whereas the paracellular permeability was evaluated by assessing the translocation of FITC-dextran (3 kDa) from the apical to basolateral poles. Mean \pm SEM, p

Results: IFN- γ and TNF- α stimulation led to a reduced cellular viability (< ATP-release) in HIEC-6 cells (p

Conclusion: ATB-352 and 4-HTBZ in Caco-2/TC7 and HIEC-6 cells, in contrast to ketoprofen, applied at the same equimolar concentrations are devoid of toxic effects against the non-simulated intestinal epithelium. In the context of inflammation, 4-HTBZ reversed intestinal epithelial barrier disruption caused by inflammatory cytokines. Ongoing RNA sequencing experiments will provide insights towards the molecular mechanisms underlying the protective effect of H₂S.

Financial Support: CNPq (312514/2019-0) and CAPES (88887.694612/2022-00).

References: Costa, SKP. Antioxid Redox Signal, v. 33, n. 14, p.1003- 2020. doi: 10.1089/ars.2019.7884. Lee, MW. Clin Geriatr Med., v. 37, n. 1, p. 31, 2021. doi: 10.1016/j.cger.2020.08.004.

08.018 *Sonchus oleraceus* promotes Gastroprotection in Rodents Via Antioxidant, Anti-Inflammatory, and Antisecretory Activities. Vecchia CAD¹, Serpa PZ¹, Locateli G¹, Miorando D¹, Ferraz CV¹, Buzatto MV¹, Gutiérrez MV², Somensi LB³, Silva LM⁴, Roman Junior WA¹ ¹Unochapecó, ²Unesp, ³Uniarp, ⁴Univali

Introduction: Gastric ulcer is an epithelial tissue injury caused by an imbalance in gastric homeostasis between aggressive agents (acid secretion, ROS, and pepsin), and protective factors (mucosal barrier, HCO₃⁻ and antioxidant agents). Pharmacological treatment, although effective, is associated with certain adverse side effects, and ulcer recurrence. *Sonchus oleraceus* L. (Asteraceae) is an edible and medicinal plant popularly used to treat stomach aches throughout the world. However, the gastroprotective effect has not yet been evaluated. In this context this study was designed to be the first experimental investigation of the gastroprotective mode of action of this species. **Methods:** The project was registered in the National System for the Management of Genetic Heritage and Associated Traditional Knowledge (SisGen, #A01709D). The hydroalcoholic extract of *S. oleraceus* (HES) was obtained by maceration (5 days). The HES was submitted to phytochemical analyzes (ESI-IT-MSⁿ) and quantification of flavonoid. The experiments *in vivo* were approved in CEUA (#020/2017). For the acute gastroprotective evaluation in mice, ethanol and indomethacin ulcers were induced in the groups: Vehicle (Veh), Carbenoxolone (Cbx, 200 mg/kg), HES (3, 30, or 300 mg/kg). Naïve (N) was not induced. The stomach lesions were analyzed macroscopically and histologically. Antioxidant biochemical analyzes were performed of glutathione (GSH), superoxide dismutase (SOD), catalase (CAT), glutathione-S-transferase (GST), Myeloperoxidase (MPO) and tumor necrosis factor alpha (TNF- α). The gastric secretion and pepsin activity was assayed by method of pylorus ligation, in rats treated with Veh, Omeprazole 20 mg/kg or HES 300 mg/kg. **Results:** The chemical analyzes showed high amount flavonoids in HES (6,7%), and the spectrometric assay indicated the presence of nine compounds among them, glycosylated phenolics and aglycones. In ethanol-induced ulcers, HES 30 and 300 mg/kg showed reductions in the size of the ulcerated area (71 and 72%, respectively) compared with the veh. In indomethacin ulcers, the reduction was 70 and 57%, respectively. The gastroprotective effects were corroborated by histological and histochemical analyses. HES showed positive results in maintaining the antioxidant activity, avoiding depletion of SOD and GSH activity. In addition, HES decreased the activity of MPO and TNF levels, increased pH, and reduction in gastric acidity as well as the activity of pepsin. **Conclusion:** HES has gastroprotective effects mediated via an enhancement of antioxidant defenses, and preservation of mucosa, in parallel with a reduction in the inflammatory process. These effects are probably associated with the presence of flavonoids in HES. **Financial Support:** CAPES. **Acknowledgment:** UNOCHAPECÓ and CAPES.

08.019 Hydroalcoholic Extract of *Arrabidaea chica* and 3'-Hydroxy-Carajurone-Rich Subfraction Promote Gastroprotection and Gastric Healing Effect in Rodents. Miorando D¹, Steffler AM¹, Veloso JJ¹, Buzatto MV¹, Simomura VL¹, Kunst FM¹, Ferraz CV¹, Vidal-Gutiérrez M², Somensi LB³, Silva LM³, Roman Junior WA¹. ¹Unochapecó, Dpt of Pharmacognosy; ²University of Sonora, Dpt of Chemistry; ³Univali, Dpt of Pharmacology

The species *Arrabidaea chica* (Humb. & Bonpl.) B. Verl (Bignoniaceae), known as crajiru, is native to Brazil. The leaves are popularly used to treat inflammation and digestive disorders. However, the pharmacological mechanism of the gastric protective effect of the plant has not yet been fully elucidated. This work aims to investigate the mode of action gastroprotective and gastric healing effect of *A. chica*. This research is registered in the SisGen (AA6E1F9). The leaves of *A. chica* were collected in Caibi (26°57'10"S 53°13'58"W) in February 2021 and deposited in Herbarium (#4929). The hydroalcoholic extract of *A. chica* (HEAc) was obtained by maceration (7 days). A sample of HEAc (28.9 g) was submitted to partition and the dichloromethane fraction was subjected the liquid column chromatography (Sephadex® LH-20). The Subfraction 3 (SfAc3) presented the highest yielding of polyphenolic compounds and was submitted for spectrometric analyzes (ESI-IT-MSⁿ). The experiments *in vivo* were approved in CEUA n°17/2021. For the acute gastroprotective evaluation, ethanol and piroxicam ulcers were induced in the groups: Vehicle (Veh), Omeprazole (Ome 30 mg/kg), HEAc (10, 30 or 100 mg/kg) or SfAc3 (30 mg/kg). Naïve (N) was not induced. The stomach lesions were analyzed macroscopically and histologically. In order to evaluate pharmacological mechanisms, the acid antsecretory activity and ulcer induction in mice pretreated with N-ethylmaleimide (NEM) or N-ω-nitro-L-arginine methyl ester (L-NAME) was evaluated. In the gastric healing model, 80% acetic acid was instilled in the serous layer and the treatments occurred for 7 days: Veh, Ome or HEAc (both 30 mg/kg). N was not induced nor treated. Ultrasound examinations were performed to assess healing progress. The stomachs were evaluated macroscopically and histologically. Myeloperoxidase (MPO), catalase (CAT), superoxide dismutase (SOD) and glutathione (GSH) analyzes were performed. The chemical analysis identified 14 polyphenolic compounds in HEAc and 5 in the SfAc3 (3'-hydroxy-carajurone, majority). In ethanol-induced ulcers, HEAc 30 and 100 mg/kg showed a reduction of 58% and 53%, respectively, and SfAc3 82%. In piroxicam ulcers, 92% and 90%, respectively, and SfAc3 77% both compared with Veh. These results were corroborated with the histological analysis. HEAc and SfAc3 caused decrease in the gastric volume and acidity, maintaining the pH and peptic activity values close to the physiological. It was also observed the influence of the nitric oxide and sulfhydryl groups in the gastroprotection in both treatments. In the gastric healing evaluation, occurred an acceleration of the process in 69% of HEAc compared with Veh. The ultrasound and histological images validate the results along with the positive results in MPO and CAT analysis. HEAc and SfAc3 exhibits a gastroprotective and gastric healing effect mediated by decrease of acidity, preservation of the mucosa, involvement of nitric oxide and sulfhydryls, reduction of oxidative stress and inflammation. The effects can be related to the polyphenolic compounds identified. **Financial Support:** FAPESC. **Acknowledgment:** UNOCHAPECÓ.

08.020 Low Doses of Cannabidiol Reduces Inflammation and Pain, Improves Mice Welfare, and Regulates Cortical Serotonin Levels on DSS-induced Colitis. Naidek AF, Luz BB, Stern CAJ, Werner MFP UFPR, Pharmacology Dept

Introduction: Ulcerative colitis (UC) is an inflammatory bowel disease that affects the colon, causing pain, inflammation, and diarrhea, and it has implications for well-being, potentially leading to anxiety and depression. Due to the lack of effective treatments for UC, it is imperative to explore and develop new therapeutic approaches. Recently, there has been a growing interest in cannabidiol (CBD), a phytocannabinoid with analgesic, anti-inflammatory, anti-oxidative, and anxiolytic effects. In this study, we investigated whether low doses of CBD can improve the colonic symptoms of UC and the welfare of the animals. **Methods:** Colitis was induced by 5% Dextran Sulfate Sodium (DSS) in the drinking water for five days, being replaced by tap water in the last two days, completing the 7-day protocol. Female Swiss mice were orally treated with CBD at 0.01, 0.1, and 1 mg/kg. The Disease Activity Index (DAI) was observed daily by changes in weight loss, stool consistency, and blood presence in the stool. Mechanical abdominal hypersensitivity was measured using Von Frey filaments. Elevated plus maze (EPM) and nest-building tests were performed in order to evaluate the welfare of the animals and the Anxiolytic-like behavior. On the eighth day, all mice were euthanized, and the colon tissue and prefrontal cortex were extracted. The histological bowel sections were stained with hematoxylin-eosin (HE) to assess histological changes. Myeloperoxidase (MPO), TNF- α , IL-10, and Glutathione (GSH) levels were measured in the colon. In the prefrontal cortex tissue, the 5-HT levels were measured using high-performance liquid chromatography (HPLC-ED). **Results:** The DAI score in the CBD-treated mice showed an average decrease of 34% on day six compared to the DSS group (5.26 ± 0.492). Furthermore, histopathological analyses revealed that none of the CBD treatments protected the architecture nor preserved the mucins against DSS-induced colitis. Abdominal hypersensitivity was reduced, especially on day six, where the CBD 0.01 mg/kg (37%), 0.1 mg/kg (35%), and 1 mg/kg (27%) treatments decreased the frequency of response to the filament, compared to the DSS group (65.33 ± 4.70 %). For MPO, CBD 0.01 and 0.1 mg/kg treatments decreased neutrophil infiltration by 52 and 48.5%, respectively, compared to the DSS group (7.98 ± 0.97 mO.D./mg of protein). CBD at all doses significantly reduced TNF- α levels, with the higher reduction observed with CBD 0.1 mg/kg (75%) compared to the DSS group (12.49 ± 4.18 pg/mg of protein). Additionally, CBD treatments at doses of 0.01 mg/kg and 0.1 mg/kg restored GSH levels by 54% and 56%, respectively, compared to the DSS group. The serotonin levels in the prefrontal cortex increased by 129% in the CBD 0.1 mg/kg group compared to the DSS group (23.57 ± 3.61 ng/g of tissue). The EPM test revealed that CBD 0.1 mg/kg increased the percentage of time spent in the open arms by 83% compared to the DSS group (11.54 ± 1.74 %). Additionally, all CBD doses showed an increased score in the nest-building test compared to the DSS group. **Conclusion:** Regardless of whether CBD did not improve the remission rates of UC, new perspectives of therapeutic approaches were offered. Our findings showed that beyond anti-inflammatory, analgesic, and antioxidant effects, low doses of CBD also promote welfare, possibly through modulation of serotonin levels in the prefrontal cortex. **License number of ethics committee:** 1353. **Financial Support:** CAPES—Finance Code 001. **Acknowledgments:** Gisele O. Guaita (HPLC-ED).

08.021 Fluoxetine Accelerates Gastric Healing in Male Rats, But Not in Ovariectomized and Sexually Intact Female Rats. Silva TFQ, Silva, Cazarin CA, Longo B, Nunes RKS, Cury BJ, Santos AC, França TCS, Venzon L, Silva LM Univali Postgraduate in Pharmaceutical Sciences, SC, Brazil

Introduction: It is known that serotonin (5 - HT) not only plays a role in mood disorders but also affects gastrointestinal tract function. Interestingly, studies have demonstrated the gastroprotective effect of selective serotonin reuptake inhibitors (SSRIs) such as fluoxetine. However, the gastric healing effects of SSRIs remains unknown, as does whether there is a gender dimorphism in this effect. Therefore, in this study, the gastric healing effect of fluoxetine was investigated in male and female rats. **Methods:** Gastric ulcers were induced in anesthetized male and female Wistar rats by the instillation of 80% acetic acid into the gastric serosa. After two days of induction, they received oral vehicle, omeprazole (20 mg/kg), or fluoxetine (0.17 and 1.7 mg/kg) once daily for seven days. On the tenth day after ulcer induction, the animals were euthanized, and the ulcerated tissue was collected for morphological and biochemical studies. To investigate the effect of fluoxetine on gastric secretion, pyloric ligation was performed in male and female rats. Finally, to verify the role of sex hormones in the effect of fluoxetine, the acetic acid-induced ulcer model was performed in ovariectomized rats. All protocols were approved by CEUA/UNIVALI (019/20p and 019/22). **Results:** Fluoxetine treatment reduced ulcer area in male rats at oral doses of 0.17 and 1.7 mg/kg compared with the vehicle-treated ulcerated group. However, no reduction in gastric lesion area was observed in female animals after treatments with fluoxetine. The microscopic analysis confirmed these data and showed that fluoxetine treatments increased histochemical staining for mucins in the gastric mucosa of male rats. Mucosal ulceration decreased GSH availability in both male and female rats, and fluoxetine administration did not reverse this effect. MDA levels and MPO activity were increased in ulcerated mucosa and decreased only in fluoxetine-treated males. In addition, fluoxetine treatment (0.17 and 1.7 mg/kg) did not decrease acidity, volume, or peptic activity in male and female rats subjected to pyloric ligation. Moreover, the administration of fluoxetine to ovariectomized rats failed to accelerate gastric healing in rats. **Conclusion:** These results highlight the gastric healing potential of fluoxetine, which modulates protective mechanisms such as the mucus barrier and antioxidant defenses in male but not in female rats. Furthermore, the lack of gastric healing efficacy in females does not appear to be directly related to sex hormones. Importantly, the sex-specific approach used in this study will contribute to comprehensive studies that consider sex differences in the serotonergic system in gastric ulcer healing and consider drugs such as fluoxetine as agents of choice in male depressed patients with gastric ulcers in the future. **Financial Support:** CAPES, CNPQ, FUMDES/UNIEDU, Santa Terezinha and Mais Econômica Drugstore

08.022 Esophagoprotective Effect of Lemon Gum, a Biopolymer from *Citrus x Latifolia*, on Experimental Gastroesophageal Reflux Disease in Rats. ¹Teixeira LFLS, ¹Silva KC, ¹Gomes IAB, ¹Oliveira AP, ¹Pacheco G, ¹Sousa GC, ¹Lopes ALF, ²Franco AX, ¹Ribeiro FOS, ³Freitas RA, ¹Silva DA, ¹Medeiros JVR, ¹Nicolau LAD ¹UFDFPar, ²UFC, ³UFPR

Introduction: Gastroesophageal Reflux Disease (GERD) is a prevalent condition that affects approximately 20% of the Western population and can present with erosions in the esophageal mucosa, a phenotype known as erosive esophagitis (EE). Therapeutic alternatives should be considered since standard treatment partially fails in all disease phenotypes, including EE. We aimed to evaluate the esophagoprotective effect of lemon tree gum (LG), a biopolymer obtained from *Citrus x latifolia*, on erosive esophagitis in rats. **Methods:** Male Wistar rats (230-250g) were used in this study. All procedures were approved by the local ethics committee (Protocol #018/20). The animals were divided into six groups: (1) sham; (2) EE; (3) EE + commercial alginate (v.o.); and (4-6) EE + GL (3, 30 and 90 mg/kg, p.o.). After euthanasia, esophageal samples were collected to evaluate myeloperoxidase (MPO) activity, malondialdehyde (MDA) and glutathione (GSH) dosages and the evaluation of changes in histopathological parameters. Finally, the quartz crystal micro balance technique (QCM-D) was performed to evaluate the interaction of LG with Mucin-2. Statistical values were performed considering the significant difference when $p < 0.05$. **Results:** As for the levels of MPO, in the groups with EE there was an increase of $(1.375 \pm 0.1095 \text{ U MPO/mg of tissue})$ when compared with the sham group $(0.3183 \pm 0.03087 \text{ U MPO/mg of tissue})$. Furthermore, pretreatment with LG at a dose of 30 mg/kg decreased $(0.2857 \pm 0.1597 \text{ U MPO/mg of tissue})$ MPO activity. For MDA, in the groups with EE there was an increase $(765.6 \pm 152.4 \text{ mmol MDA/g of tissue})$ when compared with the sham group $(217.7 \pm 8.395 \text{ mmol MDA/g of tissue})$, while the pre-treatment with LG 30 mg/kg decreased $(285.2 \pm 31.94 \text{ mmol MDA/g tissue})$. Regarding glutathione, the EE group reduced its levels $(104.4 \pm 6.470 \mu\text{g GSH/g of tissue})$ when compared to the sham group $(181.4 \pm 14.0 \mu\text{g GSH/g of tissue})$, but pretreatment with LG preserved $(165.0 \pm 5.05 \mu\text{g GSH/g tissue})$ GSH levels. LG reduced total scores [3 (0-8)] of histopathological parameters in rats with EE compared to the group that did not receive protective solution [10 (6-12)]. By reading the histological slides, it was seen that LG reduced (1.05 ± 0.43) the amount of mast cells in the submucosa of the esophagus when compared to the group with EE (6.00 ± 0.89) . QCM-D showed satisfactory interaction between LG and Mucin-2 due to the rapid adsorption on the sensors, as evidenced by the decrease in the resonance frequency, which is related to mass absorption and the increase in dissipation, associated with the slight increase in viscoelasticity of the layer formed in that region. **Conclusion:** Our results demonstrate the esophagoprotective potential of LG due to its ability to prevent inflammatory events and oxidative stress, as well as to reduce damage to the esophagus of rats with erosive esophagitis according to histopathological analyses. Therefore, LG is a biopolymer of interest for the study of GERD therapy. **Financial Support:** CNPq and CAPES.

09. Natural Products and Toxinology

09.001 A Novel Method of Isolating Snake Venom Metalloproteinases P-I from the Venom of *Bothrops jararaca*. Rodrigues MAF¹, Sousa EP¹, Galizio NC¹, Serino-Silva C¹, Grego KF¹, Tanaka-Azevedo AM¹, Morais-Zani K¹. ¹IBu, Dpt of Herpetology, Brazil

The Brazilian Department of Health states that 70% of the registered snakebites in Brazil are caused by the species *Bothrops jararaca*, from the Viperidae family. Hemorrhagic activity, coagulopathy, local edema and tissue necrosis are the most common symptoms caused by *Bothrops* envenomation, and the treatment used for these snakebites is the specific antivenom according to the bites severity and snake genus. *Bothrops* venom is predominantly composed of proteins, with the Snake Venom Metalloproteinases (SVMPs) representing an important part of those. The SVMPs are divided into SVMP P-I, P-II and P-III, with the P-I group being found in the vast majority of *Bothrops* species, in comparison with the other two. This greater predominance indicates that the P-I has a more relevant role on the envenoming than other SVMPs, therefore analyzing this toxin subfamily may be important for a better knowledge about the proteins biological and biochemical functions, pathophysiological functions, and consequently, the antivenom improvement. Taking this into consideration, the objective of the present work is to isolate and characterize the SVMP P-I from *Bothrops jararaca* venom. The partial purification of SVMP P-I from *Bothrops jararaca* venom was achieved by two chromatographic steps, using gel filtration and ion exchange chromatography. The isolation process was evaluated by Sodium Dodecyl Sulfate-PolyAcrylamide Gel Electrophoresis (SDS-PAGE). Firstly, the Superdex 75 was used for a gel filtration chromatography, and the obtained fractions were read on the Spectra-Max at a wavelength of 280nm, resulting in four major peaks. The chromatographic fractions were evaluated by a 15% acrylamide concentration SDS-PAGE, that indicated one peak with the highest concentration of SVMP P-I. Then, this peak was submitted to an ionic exchange chromatography on HiTrap Q Fast Flow. The resulting fractions were read at 280 nm as before mentioned, indicating two major peaks. The fractions composing these peaks were analyzed on a 15% acrylamide SDS-PAGE. The toxin eluted at peak 2 showed protein bands mostly in the range between 25 and 37kDa. Since the molecular mass of SVMP P-I is between 20 and 30kDa, there was a partial isolation of the SVMP P-I from *B. jararaca* venom. This work is supported by FAPESP (2020/07268-2; 2021/07627-5, 2023/00949-2), CNPq (309995/2022-1), Secretaria de Estado da Saúde de São Paulo and Fundação Butantan.

09.002 Enzymatic and Neuromuscular Activities of *Crotalus durissus ruruima* (Viperidae: Crotalinae) Venom and Neutralization by Therapeutic Antivenom *in vitro*. Demico PJ¹, Oliveira IN¹, Torres-Bonilla KA², Hyslop S², Moura-da-Silva AM³, Rocha AM⁴, Maciel JB⁴, Sartim MA⁴, Pucca M⁴, Monteiro WM⁴, Floriano RS¹. ¹Unoeste, Lab of Toxinology and Cardiovascular Research, Presidente Prudente, Brazil; ²FCM-Unicamp, Campinas, Dpt of Translational Medicine, Brazil; ³IB, Lab of Immunology, São Paulo, Brazil; ⁴UEA, Graduate Program in Tropical Medicine, Manaus, Brazil

Introduction: The South American rattlesnake (*Crotalus durissus terrificus*; CDT) causes most rattlesnake bites in southeastern and southern Brazil, with *C. d. cascavella*, *C. d. collilineatus* and *C. d. ruruima* (CDR) being important in other regions. Envenoming by CDT may cause renal failure and peripheral neuromuscular paralysis, with CDT antivenom being the main treatment. Little is known of the neurotoxicity of CDR venom and its neutralization by antivenom. In this work, we compared the enzymatic profiles of CDT and yellow (y) and white (w) CDR venoms and their neuromuscular activity and neutralization by antivenom *in vitro*.

Methods: CDT venom was from the state of São Paulo, CDR venoms were from the state of Roraima, and CDT antivenom was from the Instituto Butantan. Phospholipase A₂ (PLA₂), L-amino acid oxidase (LAO), proteolytic, and esterase activities were assayed colorimetrically. Phrenic nerve-diaphragm (PND) preparations from male Swiss mice (30-40 days old) were mounted in a Ugo Basile myographic system for indirect stimulation, with muscle twitches recorded using LabScribe4 software. The results were expressed as the mean ± SD. **Results:** CDRy venom had higher LAO (DA_{435nm}/min: 9.4±0.8, n=3) and proteolytic (DA_{440nm}/min: 1.5±0.04, n=3) activities than CDRw and CDT, whereas CDRw had higher PLA₂ (DA_{425nm}/min: 7.0±0.7, n=3) and esterase (DA_{410nm}/min: 4.6 ± 0.7, n=3) activities. CDRw and CDT venoms had similar LAO (DA_{435nm}/min: 1.2±0.4 vs. 2.0±0.2, respectively, n=3) and proteolytic (DA_{440nm}/min: 0.09±0.02 vs. 0.11±0.05, respectively, n=3) activities, whereas CDRy and CDT had comparable esterase activity (DA_{410nm}/min: 2.3±0.4 vs. 1.7±0.3, respectively, n=3). In PND, CDRy venom (3-100 ug/ml, n=4) caused intense neuromuscular facilitation within 40 min and complete blockade after 80-120 min. CDRw venom (3-100 ug/ml, n=4 each) caused discreet facilitation, with full neuromuscular blockade after 80-110 min. CDRy and CDRw venoms caused similar blockade (50%: 64±4 and 51±3.5 min for 10 ug of venom/ml, respectively, n=3; 90%: 86±4.5 and 85±4 min for 10 ug of venom/ml, respectively, n=3) and were more potent than CDT venom (50% and 90% blockade: 79±4.3 min and 106±5.5 min for 10 ug of venom/ml, n=3). CDT antivenom: venom ratios of 1: 1.5 and 3: 1.5 (vol/w) neutralized the neurotoxicity of CDRy and CDRw venoms (10 ug/ml, n=4 each) and the initial facilitation by CDRy venom. **Conclusions:** CDR venom has a similar enzymatic profile to CDT venom, but with variations in the activities. CDRy and CDRw venoms cause neuromuscular blockade that is neutralized by antivenom in a manner similar to CDT venom. **Financial Support:** São Paulo State Research Foundation (FAPESP, grant no. 2022/05878-3 and 2023/01961-6).

09.003 Preliminary Analysis *in vitro* of the Phytochemical, Anti-Inflammatory and Cytotoxic Profile of the Extract of a Plant of the Arecaceae Family Aiming the Future Development of a New Herbal Medicine. Meschick CG¹, Fracasso JAR², Ximenes V³; Verri-Junior WA⁴; Dos Santos L^{1,2} ¹ UNESP-FCL-ASSIS, Dpt of Biotechnology, Brazil; ²FOA-UNESP, PPG of Science, Brazil; ³ UNESP-FC-Bauru, Dpt of Chemistry, Brazil; ⁴UEL, Dpt of Pathological Sciences, Brazil

Introduction: The Amazon rainforest is considered a world heritage site and its biodiversity is threatened by rampant deforestation due to agriculture and industry. Therefore, it's necessary to seek strategies to ensure its preservation, such as the sustainable use of its biodiversity. A native plant to be mentioned is that of the Arecaceae family, a palm tree endemic to the Amazon region, which has high local ethnopharmacological value. Furthermore, it's known that synthetic drugs for the treatment of inflammation have several side effects and their use is excessive because a prescription isn't necessary for their acquisition. In these contexts, the objective of this project is to study the phytochemical profile and anti-inflammatory activity of the extract obtained from this plant. **Methods:** The scientific name of the plant under study will not be described because this research will result in a patent. The fruit was obtained from the city of Altamira, state of Pará (latitude: 3°11'41" S; longitude: 52°12'33" W) and this study was registered in SisGen under license n°. A1E6868. The quantitative dosage of phenols was performed using the Folin-Ciocalteu method. The quantitative dosage of flavonoids was based on the complexation of this metabolite with AlCl₃. The characterization of flavonoids was performed using HPLC. To determine the anti-inflammatory activity, were performed the stabilization of the HRBC membrane after induction of hemolysis test, the phagocytosis tests on slide and spreading with immortalized macrophages of the RAW 264 lineage. The cytotoxicity of the extract was evaluated by neutral red uptake assay, with the same cells. **Results:** The extract showed, in 1 g of dry extract, a concentration of total phenols of 145 ± 3.1 mg of gallic acid equivalents and 9 ± 1.9 milligrams equivalent to quercetin for flavonoids. The characterization of flavonoids identified the presence of catechin in the extract. In the evaluation of the anti-inflammatory activity, the extract promoted, respectively, the following results at the tested concentrations of 10, 30 and 100 µg/ml: 86.73%, 87.59% and 89.69% of hemolysis inhibition, 95.13%, 96.98% and 96.16% inhibition of phagocytosis and 51.43%, 53.61% and 54.82% inhibition of spreading. In the cytotoxicity analysis, all tested concentrations (100 to 1600 µg/mL) did not reduce cell viability by more than 30% and the higher concentration did not differ significantly (p<0.05) from the negative control. **Conclusion:** The extract showed high concentrations of total phenols, as well as flavonoids, the main constituent of the extract being catechin. When compared to the results in the literature, it was possible to verify that the extract presented potent anti-inflammatory action *in vitro* and did not show cytotoxicity. In summary, the results have shown to be promising for the future use of this extract as an anti-inflammatory herbal medicine. The next step is to carry out *in vivo* studies in accordance with ANVISA RDC40 regulations. **Financial Support:** Fundação de Amparo à Pesquisa do Estado de São Paulo (FAPESP).

09.005 Methyl Cinnamate Regulates TGF- β -Induced Fibroblast Activation through a SMAD3 Dependent Mechanism. Barros ABB, Ferreira EGA, Fidelix MSP, Carmo JOS, Silva JP, Santana JR, Barreto E UFAL, Lab. of Cell Biology, Brazil

Introduction: Fibroblasts are key effector cells in tissue remodeling. They persistently remain active in fibrotic diseases, which results in progressive deposition of extracellular matrix (ECM). Transforming growth factor- β (TGF- β) is a central mediator in tissue fibrosis, inducing the expression of ECM-related genes through canonical (TGF- β /SMADs) and non-canonical (TGF- β /p38/JNK/Rho) pathways. Methyl cinnamate (MC), a hydroxycinnamic acid derivative, has been shown to have several pharmacological properties by affecting distinct molecular intracellular signaling pathways. Thus, given the lack of information about its effects on fibroblasts, we decided to examine the antifibrotic effects of methyl cinnamate on *in vitro* TGF- β -induced fibroblast activation. **Methods:** Murine L929 fibroblasts were grown in DMEM medium supplemented with 2% fetal bovine serum, 0.02% penicillin/streptomycin, 2 mM L-glutamine and maintained in a humidified incubator at 37 °C with 5% CO₂. Then, L929 cells were treated with methyl cinnamate (MC, 0.1, 1, and 10 μ M), and 24 h later cell viability was measured by MTT assay. In another set of experiments, L929 cells were stimulated with TGF- β 1 (10 ng/mL) with or without MC (10 μ M) co-treatment and, 24h later, cell migration was measured through a scratch assay. Laminin and Smad3 (phospho-smad3) were identified through Immunofluorescence using NIH ImageJ software. All the reagents and chemicals were purchased from Sigma Chemical (St Louis, MO, USA). Statistical differences were significant at $p < 0.05$ analyzed by one-way ANOVA and Tukey's test. **Results:** Methyl cinnamate did not affect cell viability. Our data shows, for the first time, that the treatment with 10 μ M MC decreased, around 53%, the TGF- β -induced fibroblast migration. The treatment with MC (10 μ M) also inhibited 25% of the TGF- β -induced elevated laminin levels. Mechanistically, MC attenuated the nuclear immunostaining of phospho-Smad3 induced by TGF- β in L929 fibroblasts. **Conclusions:** Taken together, our data suggest that methyl cinnamate can regulate fibroblast functions by decreasing its migration and laminin production via inhibition of the TGF- β /Smad3 pathway. **Financial Support:** CNPq, CAPES, BioproFar-BA and FAPEAL.

09.006 Protective Effect of Polysaccharides from Fruit Byproduct on 5-Fluorouracil-Induced Intestinal Mucosal Damage. Schiebel CS¹, Oliveira NMT¹, Braga LLVM¹, Silva KS¹, Abboud KY², Cordeiro LMC², Ferreira DM¹. ¹FPP, PPG em Biotecnologia Aplicada à Saúde da Criança e do Adolescente, Curitiba, Brazil; ²UFPR, Dept of Biochemistry and Molecular Biology, Curitiba, Brazil

Introduction: One of the most common toxic effects of oncologic treatment is intestinal mucositis, a complication that affects up to 100% of patients, depending on the treatment regimen. Chemotherapy-induced mucositis (CIM) is a complex gastrointestinal problem in which the protective intestinal barrier is disrupted, resulting in severe inflammation, injury, and ulceration. 5-Fluorouracil (5-FU) is widely used for a variety of tumors. Although it has great clinical efficacy, studies show that 20 to 50% of patients develop CIM (SOUGIANNIS et al, 2021). Various treatment strategies are used to minimize the adverse effects of 5-FU (e.g., pain, vomiting, and diarrhea) and to improve the patient's tolerance to oncologic treatment. However, CIM remains a clinical challenge, treatment adherence is difficult, and not all patients respond to available therapeutic approaches (YSABELLA et al, 2015). Therefore, the search for new alternatives for the prevention and treatment of CIM remains necessary. In this sense, the food processing industry produces large amounts of waste every year. This type of products has a high added value because they are easily accessible and inexpensive, and because they contain bioactive compounds known for their interesting biological activities. Here, we investigated the protective effect of polysaccharides extracted from fruit byproducts (here referred to as FBP) against intestinal toxicity induced by 5-FU. **Methods:** Human epithelial colorectal adenocarcinoma cells (Caco-2) and human gingival fibroblasts (HGF) were cultured. 5-FU (50 mg/mL) was used to induce toxicity. FBP (100 - 300 µg/mL) was used to test the protective potential against 5-FU-induced toxicity. The rate of cellular metabolic reduction was determined using Prestoblu. Scratch assay was used to investigate the healing potential of FBP. Mitomycin C was used to inhibit cell proliferation and analyze the mechanism of FBP on wound healing. Permeability assay (transwell permeable supports) was used to study the effect of FBP on epithelial barrier integrity. Kruskal-Wallis followed by Dunn post-test, one- or two-way ANOVA followed by Bonferroni posttest for multiple comparisons were used to compare differences between groups. Differences with $p \leq 0.05$ were considered statistically significant. **Results:** 5-FU significantly decreased the rate of cellular metabolic reduction and significantly increased paracellular permeability. Treatment with FBP (300 µg/mL) was able to prevent the cellular toxicity induced by 5-FU. In addition, FBP prevented the increase in paracellular permeability promoted by 5-FU. FBP was also able to accelerate wound closure. Mitomycin C inhibited cell proliferation, and in the presence of mitomycin C, FBP was also able to accelerate wound healing. **Conclusions:** This study demonstrates that FBP can protect Caco-2 and HGF cells from 5-FU-induced toxicity. Although further studies are needed, this study highlights the biotechnological potential of FBP for the development of adjuvant therapies for the treatment of chemotherapy-induced mucositis. **Financial Support:** This work was supported by Capes (Finance Code 001), the Instituto de Pesquisa Pelé Pequeno Príncipe, and CNPq (Grant numbers: 302195/2022-0 to DMF and 404717/2016-0, 310332/2015-0 and 307314/2018-9 to LMCC). **References:** SOUGIANNIS, A.T. *Am. J. Physiol. Gastrointest. Liver Physiol.*, v. 320, p. 712, 2021. YSABELLA, Z.A. *Curr. Oncol. Rep.*, p. 1, v. 1, 2015.

09.007 Apitoxin or Melittin Applied to the Zusanli Acupoint (E36) Induced Long Lasting Analgesia in Neuropathic Pain Model in Rats. Boaventura de Oliveira AM¹, Silva DF¹, Sant'Anna MB¹, Silva, JRT³, Marques-Porto R², Picolo G¹ ¹IBu, Lab. of Pain and Signaling, Brazil; ²IBu, Lab. of Development and Innovation, Brazil; ³Unifal, Lab. of Neuroscience, Neuromodulation and Study of Pain, Brazil

Introduction: Chronic Pain is a multifactorial disease that affects 20% of the worldwide population, and it is a leading source of suffering since it interferes with daily routine. According to ICD-11, it is defined as “pain that persists or recurs for more than three months” and is difficult to treat. One type of chronic pain is neuropathic pain which is related to a lesion or disease affecting the somatosensory system. Despite the various pharmacological treatments available for the clinical control of this disease, none of them promote the complete reversal of the painful condition, and in some cases induce several side effects. Due to this fact, integrative and complementary practices, such as acupuncture, have been indicated for these patients to promote the improvement of the quality of life and reduction of the painful sensation. Among the techniques present in acupuncture, pharmacopuncture, the application of drugs in acupoints, combined with Apitoxin has been gaining prominence considering its antinociceptive potential. However, few studies have been executed to ensure the applicability of this treatment and to investigate the possible pathways involved in analgesia. Then, our aim was to evaluate the antinociceptive effect of the apitoxin injected in E36 acupoint in the control of neuropathic pain. **Methods:** Neuropathy was induced by the chronic constriction of sciatic nerve (CCI). On the fifteenth day, pharmacopuncture was performed with Apitoxin and Melittin (the majority compound of Apitoxin). Mechanical (Von Frey filaments) and cold sensitivity tests (acetone test) were applied. Naloxone, a non-selective opioid receptors agonist, was subcutaneously administered to evaluate the participation of the endogenous opioid in analgesia mediated by pharmacopuncture. **Results:** CCI induced hypernociception observed 7 and 14 days after surgery. Pharmacopuncture (apitoxin and melittin) induced an increase in the mechanical nociceptive threshold of the animals observed after 30 min, which remains for four and five days, respectively. Additionally, in acetone test, similar results were observed, demonstrating the protective potential of the toxin against thermal allodynia. The analgesic effect promoted by pharmacopuncture was blocked by naloxone, indicating the participation of opioid pathway. **Conclusion:** The performance of pharmacopuncture proves to be attractive as a complementary therapy in patients who suffer from chronic pain due to the potential and lasting of its effect. The results suggest the participation of the endogenous opioids pathway in the observed analgesia. Further studies are still necessary to analyze other potential mechanisms related to the therapeutic action of this technique.

Financial support: nº 2013/07467-1

09.008 Presynaptic Excitatory Action of a Fraction Isolated from *Bothrops bilineatus smaragdinus* (Viperidae: Crotalinae) Venom in Mouse Phrenic Nerve-Diaphragm Preparation. Couceiro FYGM¹, Pacagnelli FL¹, Torres-Bonilla KA², Hyslop S², Lomonte B³, Floriano RS¹. ¹Uneste Presidente Prudente, Lab of Toxinology and Cardiovascular Research, Brazil; ²FCM-Unicamp, Dpt of Translational Medicine, Campinas, Brazil; ³University of Costa Rica, Clodomiro Picado Institute, Costa Rica

Envenomation by *Bothrops* snakes is generally characterized by inducing renal injury, haemostatic disturbance, and hypotension which are mediated by a variety of enzymes such as L-amino acid oxidase, C-type lectin, serine protease, metalloprotease, and phospholipase A₂ (PLA₂). *Bothrops bilineatus smaragdinus* is an Amazonian arboreal viper occasionally involved in human envenomation. *B. b. smaragdinus* venom is characterized by inducing an intense neuromuscular facilitation followed by blockade in mammalian isolated nerve-muscle preparation. In this study, we purified a fraction potentially involved in the typical facilitation neuromuscular by *B. b. smaragdinus* venom in mammalian nerve-muscle preparation *in vitro* and examined its influence on peripheral neurotransmitter release using mouse phrenic nerve-diaphragm (PND) preparation. Crude venom was fractionated by gel filtration using a TSKgel® G2000SWXL column coupled to a HPLC Shimadzu SCL-10AVP system. Fractions obtained by gel filtration were subjected to residual neuromuscular activity in mouse PND preparation using an Ugo Basile S.R.L. 4400 myographic system. PLA₂ activity of the fractions was determined on an artificial substrate (4-nitro-3-octanoyloxybenzoic acid) by spectrophotometry. Evoked (EPPs) and miniature end-plate potentials (MEPPs) were determined by conventional electrophysiology techniques. Gel filtration revealed eight fractions (Peaks: P1–P8) from crude venom, with the fraction P8 presenting intense neuromuscular facilitation. Fraction P8 exhibited concentration-dependent neuromuscular facilitation producing an increase of ~48% (for 5.9 mg/ml) and ~125% (for 15.6 mg/ml) in twitch amplitude in PND preparation (values compared to basal twitch amplitude considered as 100% of response), reached in 120- and 75-min incubation, respectively ($p < 0.05$ compared to control preparations, $n = 3$). Fraction P8 did not show catalytic activity for PLA₂. Fraction P8 (15.6 mg/ml) produced significant increase in the frequency of MEPPs from 15 min onwards [MEPPs/min: from 8.7 ± 2.9 (basal) to 75.7 ± 7.1 ($t_{30 \text{ min}}$), $p < 0.05$, $n = 4$]. In addition, fraction P8 (15.6 mg/ml) significantly increased the amplitude of EPPs [EPP/mV: from 7.5 ± 2.3 (basal) to 28.6 ± 9.2 ($t_{30 \text{ min}}$), $p < 0.05$, $n = 4$]. These findings indicate that fraction P8 is directly related to neuromuscular excitatory effect previously observed with *B. b. smaragdinus* crude venom in mammalian nerve-muscle preparation *in vitro*, most likely stimulating acetylcholine release from motor neuron terminals. **Financial Support:** This work was funded by São Paulo Research Foundation (grant no. 2020/04287-6).

09.009 Proteomic and Functional Comparison of Different Venom Phenotypes of *Bothrops jararaca* Snakes Regarding the Abundance of Metalloproteases. Sousa EP, Galizio NC, Serino-Silva C, Vidueiros JP, Grego KF, Tanaka-Azevedo AM, Morais-Zani K. IBU São Paulo, Dpt of Herptology, Brazil

Snake venoms are the most studied animal toxins. The variability in venom composition has been described not only within and interspecies, but also according to sex, age and geographic distribution. The *Bothrops* genus is responsible for 90% of snakebites in Brazil, with their venom having three main activities: proteolytic or necrotizing, coagulant and hemorrhagic. The resulting clinical aspects from the envenoming from the bites of this genus can be characterized by important local manifestations, owing to the action of different families of toxins, including metalloproteases (SVMP). These enzymes are involved in several pathophysiological processes, such as the development of edema, degradation of extracellular matrix components, hemorrhage, degradation of factors of the coagulation cascade and platelet aggregation inhibition. In general, SVMPs are the most abundant component among *Bothrops* venoms, as is the case of the *Bothrops jararaca* species, in which it corresponds to about 25% of the venom. However, in a recent study carried out by our group, it was verified by high-performance liquid chromatography (HPLC) that some individuals of this species have poor amounts of SVMP, which reflects in a lower proteolytic activity on collagen. In addition, this variability regarding SVMP content may influence the pathophysiology of the envenomation caused by this species. Based on this finding, the objective of this work was to analyze 54 individuals of the species *B. jararaca* of state of São Paulo in order to establish possible venom phenotypes regarding SVMP abundance, and, therefore, contribute to the understanding of how the SVMP variability affects envenomation regarding to lethality and hemorrhagic activity. By HPLC analyses, it was possible to identify four possible venom phenotypes in relation to the content of SVMPs, and while 76% of the individuals displayed the two expected standard peaks related to this toxin family, 11% expressed only the first one, 4% only the second, and 9% showed no relevant HPLC peaks. These evidence were subsequently corroborated by SDS-PAGE, where the same four phenotypes identified according to electrophoretic profile. As expected, the assays measuring the degradation of type II collagen showed variation among the phenotypes, with those who were lacking the second or both peaks being the most deficient in their activities. We hope the current work will help our understanding regarding the SVMP role in the hemorrhagic effects, a severe factor in snakebite accidents. This work was supported by FAPESP (2020/07268-2; 2021/07627-5), CNPq (309995/2022-1), Secretaria de Estado da Saúde de São Paulo and Fundação Butantan.

09.010 Effect of Mesalazine in an Animal Model of DSS-Induced Ulcerative Colitis. Rosa Filho, SP, Amaral FKCW, Brito MSC, Silva, RR, Werner MFP UFPR, PPG Farmacologia, Brazil

Introduction: Mesalazine (5-ASA) is a drug used to treat ulcerative colitis. It acts locally by reducing colon inflammation and is effective for mild to moderate cases. However, there are few studies in literature evaluating the effect of 5-ASA in animal models. This study aimed to investigate if 5-ASA can be considered an adequate control drug for acute colitis model using Swiss mouse strain. **Methods:** Colitis was induced by 5% of dextran sodium sulfate (DSS) dissolved in drinking water for 5 days followed by 2 days of water. Female Swiss mice were orally treated once daily with vehicle (1% carboxymethyl cellulose solution, 1 ml/kg) or 5-ASA (50, 100 or 200 mg/kg), and disease activity index (DAI) was monitored. The mechanical allodynia was measured using von Frey filaments (0.008, 0.02, 0.07, 0.16 and 0.6 g). After 7 days colons were collected, measured, homogenized for quantification of myeloperoxidase (MPO) and also processed for histological analyses. **Results:** The DSS group had a significant weight reduction on the sixth day (-6.76%) that lasted until the eighth day (-11.45%) when compared to the control group. Likewise, for the DAI, the DSS group began to register a score with a significant difference from the sixth day to the seventh and eighth days (3.20 ± 0.573 ; 5.30 ± 0.844 and 7.50 ± 0.269 DAI respectively) when compared to the control group. The treatment with failed to prevent weight loss or improvement of the DAI when compared to the DSS group. The DSS group had a 17.80% reduction in colon length when compared to the control group (10.08 ± 0.20 cm). No 5-ASA dose prevented colon shortening compared to the DSS group. The DSS group also reduced the score of nest building test in 42.35% when compared to the control group (4.85 ± 0.143). Administration of DSS increased abdominal mechanical allodynia with the 0.6 g filament by 150% on the sixth day and on the eighth day by 210 %, when compared to the control group. In contrast, on the sixth day, treatment with 5-ASA at 50, 100 and 200 mg/kg reduced abdominal mechanical hypersensitivity with the 0.6 g filament by 80%, 28% and 48% respectively. Similarly, at the eighth day, 5-ASA at 50 and 100 mg/kg reduced abdominal mechanical allodynia by 58% and 45% respectively, when compared to the DSS group. As expected, DSS increased MPO values by 279% when compared to the control group (2.04 ± 0.51 O.D./mg of protein). The treatment with 5-ASA did not achieve significant changes at 100 and 200 mg/kg (4.76 ± 1.22 and 5.22 ± 1.44 O.D./mg of protein, respectively) when compared to the DSS group (7.78 ± 1.17 O.D./mg of protein). For the histological analyses, the DSS group showed colonic destruction with significant histopathological shortening of length (48%) in the mucosa when compared to the control group (C: 214.96 ± 9.56 μ m). **Conclusion:** While 5-ASA showed some reduction in the mechanical allodynia, it did not reduce the main inflammatory markers in this animal model. Therefore, it was shown that 5-ASA proved to be an inadequate control drug for acute colitis model using Swiss mouse strain in the tested doses. **License number of ethics committee:** 1476. **Financial Support:** CAPES—Finance Code 001; UFPR.

09.011 Divergent Roles for Adenosine Receptors in the Hypotension Caused by *Bothrops jararacussu* (Jararacussu) Snake Venom in Anesthetized Rats. Varón JCG, Torres-Bonilla KA, Pereira BB, Dias L, Hyslop S Campinas, Dpt of Translational Medicine (Section of Pharmacology), Unicamp, Brazil

Introduction: Many snake venoms contain enzymes capable of releasing and metabolizing precursors of adenosine, and more than 20 years ago Aird (*Toxicon*, v. 40, p. 335, 2002) suggested that adenosine present in snake venoms or released endogenously may play a role in venom-induced hypotension and prey immobilization. Venom enzymes such as phospholipases A₂ and snake venom metalloproteinases can cause myonecrosis and hemorrhage, leading to the release of intracellular ATP that can be converted to ADP, AMP and adenosine to contribute to venom-induced hypotension. In this work, we examined the role of adenosine receptors A₁, A_{2A}, A_{2B} and A₃ in the hypotension caused by *Bothrops jararacussu* (jararacuçu) snake venom in anesthetized rats. **Methods:** Male Wistar rats were anesthetized with isoflurane and cannulated for hemodynamic measurements, with the parameters being monitored continuously (LabChart v.7 software, ADInstruments). Venom (obtained from the Centro de Extração de Toxinas Animais - CETA, Morungaba, SP, Brazil) and receptor antagonists (from Sigma Chemical Co., St. Louis, MO, USA) were injected i.v. in 100 µl of 0.9% NaCl, with the antagonists being injected 20 min before venom. The experimental protocols were approved by an institutional Committee for Ethics in Animal Use (CEUA/UNICAMP, protocol nos. 4996-1/2018 and 5616-1/2020). **Results:** A non-lethal dose of venom (0.2 mg/kg, i.v.) caused transient hypotension that was maximal after 1 min (~50% reduction) and returned to normal after 1 h (n=6); a higher dose (0.4 mg/kg, i.v.) caused progressive hypotension, with marked bradycardia and respiratory failure, with the rats dying within 5 min (n=6). Pretreatment with the A₁ antagonist DPCPX (0.3 mg/kg, i.v.) markedly potentiated the hypotension with the non-lethal dose and produced a profile similar to that for the lethal dose of venom, with the rats dying within 5 min (n=6). A similar potentiation of the hypotension and lethality was seen with the A₃ antagonist MRS1523 (1 mg/kg, i.v.), with death occurring slightly later (~10 min, n=6). In contrast, pretreatment with the A_{2A} antagonist ZM 241385 (100 µg/kg, i.v.) and A_{2B} antagonist PSB 603 (500 µg/kg, i.v.) did not potentiate the hypotension or lethality, but enhanced the subsequent recovery. Pretreating the rats with adenosine, as a bolus injection (1.2 mg/kg, i.v.) or infusion (3 µg/kg/min, i.v.), did not affect the hemodynamic responses to venom. Pretreating the rats with atenolol (4 mg/kg, i.v.), a selective Beta₁-adrenergic antagonist, markedly potentiated the venom-induced hypotension and produced a profile similar to that seen with the lethal dose of venom, whereas an infusion of dopamine (10 µg/kg/min, i.v.) protected rats against the hemodynamic, cardiac and respiratory alterations and death associated with the lethal dose of venom (0.4 mg/kg, i.v.). **Conclusion:** These findings show that adenosine acting through A₁ and A₃ receptors has a protective role against venom-induced hypotension and lethality, whereas the A_{2A} and A_{2B} receptors do not contribute to the acute hypotension but may enhance the recovery from hypotension. **Financial Support:** This work was supported by CAPES (JCGV and KATB; Finance code 001) and CNPq (BBP and SH; grant no. 313273/2018-9).

09.012 Evaluation of Pyroligneous Extracts in Glioblastoma Cells. Bastos-Cavalcante CM¹, Silva JKS¹, Varjão MTS¹, Ferreira SCA¹, Santos ESR¹, Ximenes-Silva A², Queiroz AC¹, Moura-Neto V³, Solleti JI⁴, Bispo MD⁴, Moreira MSA¹ ¹UFAL, Pharmacology and Immunity Lab., ²UFAL, Lab. of Electrophysiology and Brain Metabolism, ³UFRJ Lab. of Biomedicine of the Brain, ⁴UFAL, Lab. of Process Separation and Optimization Systems

Glioblastoma Multiforme (GBM) is a primary malignant glial tumor of the Central Nervous System (CNS) associated with high morbidity and mortality rates worldwide due to its high degree of proliferation and invasiveness, where patient survival is around 15 months. Therefore, the search for alternative drugs for the treatment of GBM is urgent. In this sense, pyrolysis is a technique for obtaining extracts through the thermochemical process of transforming biomass into a pyroligneous extract, basically composed of acids, alcohols, aldehydes, ketones, phenols, ethers, hydrocarbons and has wide fungicidal, herbicide and insecticide application, and in this study, its antineoplastic effects were evaluated. **Methods:** The present study evaluated the *in vitro* neoplastic activity of pyroligneous extracts against GBM. For this, a cytotoxicity assay was initially performed to evaluate the effects of the extracts on the viability of GBM02 after 48 hours of treatment. Then, the anti-migration effect was evaluated, after 24 hours of treatment, in GBM02 and, finally, the morphological analyzes (48h of treatment) of GBM02 by qualitative optical microscopy. All assays were performed in triplicate. Results were expressed as mean \pm SD. and statistically analyzed by one-way ANOVA followed by Dunnett's post-test, being considered significant when **** $p < 0.0001$ in relation to the DMEM-F12 culture medium. **Results:** All extracts inhibited GBM02 viability, the most effective were, respectively, Eucalyptus - EP - Eucalyptus (57.19% \pm 2.66 ****), Elephant grass - CE - Pennisetum purpureum (55.44% \pm 2.57****), Baru - BR - Dipteryx alata (53.93% \pm 2.77****), Garbage - LX (53.20% \pm 0.377****), Capim king - CK - Pennisetum purpureum schum (51.08% \pm 3.11****) and mesocarp coconut - CM - Cocos nucifera L.(35.54% \pm 10.89 ****) and, among them, the most potent was BR (IC50 0.022% [0.001 - 0.071 CI 95%]). Among these, BR (69.81%) and CK (68.41%) and LX (77.95%) inhibited GBM02 migration. The protoplasmic morphology, characteristic of GBM, was observed in the cells treated with DMEM-F12 and in the treatments with the extracts there was the appearance of cells with rounded cytoplasm, formation of cytoplasmic vacuoles and rupture of the nuclear membrane, typical of cells in apoptosis. **Conclusion:** Among all extracts, BR, CK and LX showed the most satisfactory antineoplastic activities. Thus, these extracts are promising to advance to the next stages of antineoplastic studies. **Financial Support:** CNPQ, INCT-INOVAR (573.564/2008-6), CAPES.

09.013 Enantiomers of Limonene – Influence of Stereoisomerism on Cell Migration and Viability. Affonso DD, Buglio KE, Machado Júnior RJ, Carvalho JE, Foglio MA, Ruiz ALTG FCF-Unicamp, Campinas, SP, Brazil

Introduction: The skin and its annexes constitute the largest organ of the human body. There are some skin pathologies characterized by hyperproliferation of keratinocytes, such as actinic keratosis. Several medicinal plants have been traditionally used in the treatment of dermal diseases. In many examples, these pharmacological effects were attributed to essential oils. These oils are mixtures of volatile chemicals, comprising short chain alcohols and esters, monoterpenes and sesquiterpenes among the major chemical classes. In this context and considering the possible interference of estereoisomerism on biological activity, this study aimed to evaluate the effects of *R*-(+)-limonene and *S*-(-)-limonene on viability and migration of HaCaT cells. **Methods:** *R*-(+)-limonene (97% purity, cat. no 183164) and *S*-(-)-limonene (96% purity, cat. no 218367) were purchased from Merck. Each sample were previously diluted in DMSO (1: 10 p/v) followed by serial dilution in medium to afford the final concentrations (0.15, 1.5, 15, 62.5, 125, 150, 250 and 500 µg/ml, in technical duplicate). Cell viability after 48h-exposure was accessed using monolayer (2D, 4×10^3 cell/well) and spheroids (3D, 1.2×10^4 cell/well) of HaCaT cells cultivated in RMPI 1640 supplemented with 5% fetal bovine serum (FBS, ideal growing conditions). Cell migration after 24h-exposure was evaluated by scratch assay (2×10^5 cell/well) in HaCaT cells cultivated in ideal growing condition or RMPI 1640 supplemented with 0.2% FBS (starving condition). Photomicrography register was done in time lapse inverted microscope (Zeiss LSM780) for 24 h, with regular image capture (1 capture/h, 3 microphotographs/well). Wound area was analyzed at 0, 9, 12, 18, and 24 h using ImageJ® software. Data were expressed as means \pm SD of at least two independent experiments. Statistical analyses were done (software GraphPad Prism 8®) using One-way ANOVA followed by Tukey's test (cell viability assay) or Two-way ANOVA followed by Bonferroni's test (scratch assay), considering as significant p-values \leq 0.05. **Results:** Under ideal growth condition, limonene did not affect the migration and viability of HaCaT cells, regardless concentration, exposure time and evaluated enantiomer. After 24 h, in starving condition, at highest concentration (500 µg/ml), both limonene enantiomers reduced significantly cell viability ($IC_{50} = 425,4 \pm 23,8$ and $220,7 \pm 23,8$ µg/ml for *R*- and *S*-limonene, respectively). This way, cell migration was considered in the concentration range 62.5 to 250 µg/ml Both enantiomers showed inhibitory activity been *S*-limonene more potent. In the spheroid model, both limonene enantiomers increased transversal area of spheroids along with a slight and significant reduction on keratinocyte viability. **Conclusion:** The inhibition of cell migration associated to cell viability reduction were suggestive to the potential use of limonene as an adjuvant in the treatment of actinic keratosis. Considering stereoisomerism, *S*-(-)-limonene seemed to be more potent than *R*-(+)-limonene. **Funding:** FAPESP (2011/01114-4), CNPq (429463/2018-9, 313440/2019-0), FAEPEX/UNICAMP (255/20, 2235/21, 2139/22), CAPES (Financing Code 001). **Acknowledgments:** to equipment and assistance provided by INFABIC at University of Campinas; INFABIC is co-funded by FAPESP (2014/50938-8) and CNPq (465699/2014-6).

09.014 **Acute Oral Toxicity of an Amazonian *Ludwigia* (onagraceae) Species.** Reis, LDS¹; Raiol-da-Silva, MC¹; Lobo, SKO¹; Conceição, BC¹; Silva, MN²; Silva, CYY²; Monteiro, MC³; Maia, CSF¹; Fontes-Júnior, EA¹ ¹UFPA, Lab. of Pharmacology of Inflammation and Behavior, Belém, PA, ²UFPA, Lab. of Liquid Chromatography, Belém, PA, ³UFPA, *in vitro* Assays, Immunology and Microbiology Lab., Belém, Pará

Introduction: The therapeutic use of plants has accompanied humanity since its origins, remaining strongly present among the Amazonian peoples. Despite the potential benefits they provide, their indiscriminate use can cause damage to biological systems, making it essential to develop research that elucidates their toxicity and establish safety criteria for application. Therefore, this work aims to investigate the toxicity of a methanolic extract of *Ludwigia sp.* (MELud), a plant native to the Amazon. **Methods:** Acute oral toxicity was evaluated in female rats ($n = 7/\text{group}$), through the oral administration of a limit dose (2000 mg/kg) of MELud and comparison with control animals administered with saline, in two clippings, evaluating the immediate and the late effects. In all groups, the manifestation of Hippocratic signs (HS) was evaluated in the first 4 h. The immediate effect groups were submitted to the open field (OF) test 2 h after administration and euthanized at the end of the HS evaluation, for the collection of vital organs (heart, liver, kidneys, and lungs), for macroscopic evaluation, and blood, for biochemical assessment of liver and kidney function. The late effect groups were submitted to OF 24 h after administration and followed up for 14 days, being evaluated daily for food and water consumption, weight gain, signs of toxicity, and occurrence of deaths. At the end of the period, they were euthanized, and samples were collected with the same pattern as the immediate effect groups. All procedures were approved by the Ethics Committee on Animal Use of the Federal University of Pará (CEUA 5251290922). Statistical analysis will be performed using the statistical program Sigma plot®. **Results:** No HS suggestive of toxicity or changes in feed and water intake patterns or weight gain were identified. In the OF, MELud increased the total distance walked ($p < 0.05$) and walking speed ($p < 0.05$) evaluated 4h after administration, but not 24h after. Walking in the center of the arena was increased at 4h ($p < 0.01$), but reduced at 24h ($p < 0.05$), in animals treated with MELud. In biochemical evaluation, serum levels of total proteins, albumin, ALT, AST, GGT, and creatinine of the animals treated with MELud remained like to control groups, both in immediate and late periods. In the immediate period, there was a reduction in cholesterol ($p < 0.05$), triglycerides ($p < 0.01$), and urea ($p < 0.001$) levels, but not in the late period. No macroscopic changes or changes in the relative weight of the organs were observed. **Conclusion:** The extract did not promote deaths or significative alterations that indicate toxicity and can be classified as a low-toxicity xenobiotic, with an estimated LD50 above 2000 mg/kg. Some effects, such as the increase in central ambulation in the OF and the reduction in cholesterol and triglyceride levels should be better evaluated, in order to verify their applicability in therapeutic contexts. **References:** Mendonça, L. A. B. Bra. Jou. of Bio., v. 80, p. 574-581, 2019. **Supported by:** Fapespa.

09.015 **Effects of *Alpinia zerumbet* Extract on Neurodegeneration and Locomotor Alterations Induced by 3, 3', 4, 4', 5-pentachlorobiphenyl (PCB 126).** Silva PHF¹, da Silva ACF¹, Alves CS¹, Falque WF¹, Lopes CFO¹, Filgueiras CC², Daleprane JB³, da Costa CA¹, Ognibene DT¹, Resende AC¹, de Bem GF¹. ¹UERJ, Dpt of Pharmacology and Psychobiology, Brazil; ²UERJ, Dpt of Physiological Sciences, Brazil; ³UERJ, Dpt of Basic and Experimental Nutrition, Brazil

Introduction: Polychlorinated biphenyls (PCBs) are synthetic compounds that can bioaccumulate and contaminate the global ecosystem. Studies identified the brain as a vulnerable target for these compounds. Substances with action on the Central Nervous System (CNS), such as polyphenols, have demonstrated a neuroprotective effect. Our group showed that the extract of fresh leaves of *Alpinia zerumbet* (AZE), rich in polyphenols, has antioxidant and anti-inflammatory effects in a hypertension model. **Objective:** Thus, the study aimed to evaluate the preventive effect of AZE on neurotoxicity and locomotor alterations induced by PCB126 in adult C57BL/6 mice. **Methods:** The experiments were accepted by the Protocol of Ethics Committee of the UERJ (CEUA/021/2021). Male C57BL/6 mice were divided into four groups: control (Control), Control+AZE (50 mg/kg/day in drinking water), PCB (2 mg/kg/once a week), PCB+AZE (2 mg/kg/once a week; 50 mg/kg/day), for four weeks. At the end of the experiment, the animals performed the elevated plus-maze test, being sacrificed. Oxidative stress was evaluated by spectrophotometry in the brainstem, cerebellum, midbrain, and left cortex homogenates. The data are presented as the means and standard error of the means. Differences among groups were analyzed by one-way and two-way analysis of variance (ANOVA) and followed by the post-hoc test of Tukey. **Results:** The decreased locomotor activity in the PCB group (59.39±2.96) compared to Control+AZE (75.99±2.81) was prevented by AZE in the PCB+AZE group (70.92±2.77). The time spent with open arms was not different among groups. In the brainstem, the PCB group (0.57±0.08) showed increased lipid peroxidation compared to the Control+AZE group (0.37±0.03), which was prevented by treatment with AZE in the PCB+AZE group (0.36±0.03). There was no statistical difference in the antioxidant enzyme activity of catalase (CAT) among groups. The decreased antioxidant enzyme activity of the superoxide dismutase (SOD) in the PCB group (32.38±3.59) compared to the Control (95.87±31.09) and Control+AZE (62.54±10.77) groups was prevented by treatment with AZE in PCB+AZE group (189.90±64.97). In the cerebellum, the oxidative damage was not different among groups. The AZE treatment prevented the reduction in CAT activity in the PCB+AZE group (0.92±0.27) compared to the Control+AZE (0.27±0.08) and PCB (0.29±0.05) groups. PCB group (18.37±1.43) showed decreased SOD activity compared to the Control+AZE group (77.72±9.54), which was prevented by treatment with AZE in the PCB+AZE group (60.67±12.95). In the midbrain, there was no statistical difference in lipid peroxidation and antioxidant SOD activity among groups. However, the PCB group (0.20±0.06) showed decreased CAT activity compared to the Control group (0.61±0.10), which was prevented by treatment with AZE in the PCB+AZE group (0.57±0.11). In the left cortex, lipid peroxidation was increased in the PCB group (0.64±0.12) compared to the Control+AZE group (0.36±0.03). Treatment with AZE prevented this increase in the PCB+AZE group (0.32±0.03). The CAT and SOD activities were not different among groups. **Conclusion:** Our preliminary results demonstrate that the extract prevented the development of PCB-induced locomotor deficits and did not cause anxiety-like behaviors. Furthermore, the extract also prevented oxidative damage and antioxidant activity reduction in different brain regions, suggesting a neuroprotective effect. **Funding:** FAPERJ e CAPES.

09.016 Polysaccharides from Guavira Waste: Biotechnological and Therapeutic Application in Inflammatory Bowel Disease. Mulinari-Turin de Oliveira N¹, Bueno LR¹, Schneider VS², Souza ML⁵, Barbosa da Luz B², da Costa Filho HB³, Sousa PSA⁴, Werner MFP², Rocha JF⁴, Gois MB⁵, Nicolau LAD⁴, Cordeiro LMC², Maria-Ferreira D¹. ¹IPPPP, FPP, PPG Biotecnologia Aplicada a Saúde da Criança e do Adolescente, Curitiba, Brazil; ²UFPR, Dpt de Bioquímica e de Farmacologia, Curitiba, Brazil; ⁴UFC, Fortaleza, Dpt de Fisiologia e Farmacologia, Brasil; ⁵UFDPPar Parnaíba, PPG em Biotecnologia, Brazil; ⁶UFR, Rondonópolis, Brazil

Introduction: Inflammatory bowel disease (IBD) is a recurrent and remitting disease of the gastrointestinal tract characterized by chronic inflammation with progressive structural and functional damage. Despite major advances on disease biology and clinical management, many IBD patients still do not respond to available drugs (Hazel & Connor, 2020). In this context, polysaccharides have gained attention due to their interesting biological activities (Li et al., 2021). Here, we investigated the antinociceptive, antidiarrheal and anti-colitis effects of polysaccharides from *Campomanesia adamantium* and *Campomanesia pubescens* waste (here referred to as CPW), and its possible mechanism of action. **Methods:** Female Swiss mice were used. Acetic acid, capsaicin, or mustard oil were used to assess visceral pain. Intestinal transit was assessed with a semi-solid marker. Antidiarrheal effect was assessed with the castor oil model. Acute colitis was induced by a single injection of acetic acid into the colon, and electrical resistance was determined. Acute and chronic colitis was induced by 5% DSS. Oxidative stress, inflammation, and histological analyzes were performed on colon samples. The viability of Caco-2 was determined, and the scratch assay was used to study wound closure. Pharmacokinetic and toxicological properties and molecular docking analyzes were performed using pkCSM and AutoDock, respectively. Kruskal-Wallis followed by Dunn's post-test, one- or two-way ANOVA followed by Bonferroni's multiple comparisons post-test were used to compare differences between groups. **Results:** CPW (10 mg/kg) reduced abdominal writhing, cell migration, capsaicin-induced visceral nociception, regulated intestinal motility, and castor oil-induced diarrhea. CPW reversed acetic acid-induced mucosal permeability, TEER and tissue weight. In DSS colitis, CPW reduced weight loss, disease score, colon shortening, oxidative stress, and inflammation. Colon architecture, collagen, and total number of mucus-secreting goblet cells were preserved by CPW. Treatment with CPW prevented weight loss and disease severity after the first cycle of the chronic DSS protocol and prevented colon shortening in both DSS cycles. CPW is not toxic to Caco-2 cells and accelerated wound closure. CPW showed optimal molecular affinity to interact with 3N8V, 5COX, 2J67, and 6RBF proteins, is not absorbed by the intestine, does not inhibit cytochrome P450 proteins, and does not exhibit AMES toxicity. **Conclusions:** The current study emphasizes CPW's biotechnological and therapeutic potential for the development of novel products for the treatment of inflammatory bowel diseases. This work was supported by Capes (Finance Code 001), the Instituto de Pesquisa Pelé Pequeno Príncipe, and CNPq (Grant numbers: 302195/2022-0 to DMF and 404717/2016-0, 310332/2015-0 and 307314/2018-9 to LMCC). Ethics Committee for the Use of Animals protocol number: 049-2019. **References:** Hazel, K. In Ther. Adv.Chronic Dis. V. 11, 2020. Li, C. Front. Pharmacol., V. 12, 2021.

09.017 Preliminary Analysis of Coagulotoxic Profile from Individual Venoms of Three Bothrops Species: A New Approach in Coagulotoxicity Studies. Galizio NC, Serino-Silva C, Silveira GPM, Sant'Anna S, Grego KF, Tanaka-Azevedo, AM, Morais-Zani K IBu, Lab. of Herpetology, São Paulo, SP, Brazil

Introduction: Snake envenomation is a neglected tropical disease responsible for approximately 2.5 million envenomation and 150,000 deaths per year. In Brazil, the Viperidae family includes the majority of species of highest medical importance, as they are responsible for most of snakebites accidents. Among the effects resulting from these accidents, haemostatic disorders are believed to play a central role in the pathophysiology of envenomation and prey capture. The intraspecific variability of snake venoms associated with their functional diversity is already known and it is particularly critical when considering their reactivity with antivenom. Considering the complexity of the envenomation caused by snake species from Viperidae family and the relevance of these species to public health, a multifaceted study comparing the coagulotoxic profile of these species and their neutralization by the antivenom produced is of extreme importance. In addition, studies focusing on specific coagulation factors could be of major importance for the bioprospecting of new drugs and bioproducts that help in the control of innate coagulopathies or those caused by other diseases. **Objective:** Thus, the present work proposes the characterization of the coagulotoxic profile of individual venoms of the *Bothrops atrox* (Bax), *B. jararaca* (Bj) and *B. jararacussu* (Bjs) snake species. **Results:** Preliminary results showed minor individual variation in all species studied. Bj presented the higher LAAO activity while Bjs presented the higher PLA₂ activity. Proteolytic activity on collagen showed slight individual variation among species. Coagulotoxic investigation demonstrated that DMC is highly variable among individuals in all species studied, even though, Bjs presented the most coagulant venom. Also, Bjs presented the higher activation of factor X. Fibrinogenolysis demonstrated individual variation and a high EDTA inhibition, indicating an important role of metalloproteinases (SVMP) in fibrinogen degradation. Surprisingly, SAB was not able to inhibit most of activities evaluated in recommended concentration. **Conclusion:** Interspecific and intraspecific venom variation is supported by our results, including in coagulotoxic assays. SVMPs play an important role in venom coagulotoxicity in genus *Bothrops*. The next steps will allow the evaluation of other species in genus *Bothrops* and *Lachesis*, and explore more coagulation factors, including activation of Factor XII and plasminogen; and, also, thromboelastography. This work is supported by FAPESP (2020/07268-2; 2021/07627-5) and CAPES (88887.639855/2021-00).

09.018 Gastroprotective Action of the Ethanolic Extract of the Fruit Peels of *Nephelium lappaceum* L. in Mice. Oliveira AS¹, Bianco LS¹, Palmeira DN¹, Oliveira e Silva AM², Albuquerque-Júnior RLC³, Correa CB⁴, Camargo EA¹. ¹UFS, Dpt of Physiology, Brazil; ²UFS, Dpt of Nutrition, Brazil; ³Unit, Research and Technology Institute, Brazil; ⁴UFS, Dpt of Morphology, Brazil

Introduction: Rambutan is the fruit of *Nephelium lappaceum* L. (Sapindaceae). It is consumed in many parts of the world and popularly used for various purposes, including stomach problems. The peels of rambutan contain a variety of phytochemicals, such as phenolic compounds, flavonoids and carotenoids, which add potential for biological activities. The present study evaluated the gastroprotective activities of the ethanolic extract of the fruit peels of *N. lappaceum* L. (EENL) in mice. **Methods:** EENL was characterized by chromatography coupled to mass spectrometry (RP-UHPLC-DAD). The experimental protocols were approved by the Animal Research Ethics Committee of Federal University of Sergipe (nº 1122270819). The ulcer model induced by acidified ethanol (60% ethanol/0.3 mol/L HCl) was used to evaluate the gastroprotective effect of EENL. In this model, the concentration of sulfhydryl compounds and lipid peroxidation in the gastric mucosa were also evaluated. The participation of non-protein sulfhydryl compounds (NP-SH), nitric oxide (NO), prostaglandins (PG), ATP-sensitive K⁺ channels (K_{ATP}) and hydrogen sulfide (H₂S) in the gastroprotective effect of EENL was investigated in this model of ulcer using pharmacological tools. The effect of EENL on gastric volume, acidity and pH was evaluated in the pylorus ligation model, as well as mucus on gastric contents. **Results:** Procyanidin B, epicatechin, ellagic acid and their derivatives (such as punicalin and pedunculagin) were identified in the EENL. Pretreatment with EENL (50, 100 and 200 mg/kg) reduced the area of gastric injury induced by acidified ethanol (p<0.01) and lipid peroxidation (p<0.001), and the doses of 100 and 200 mg/kg increased sulfhydryl content in the stomach (p<0.01 or 0.05, respectively) compared to the vehicle group. Pretreatment with N-ethylmaleimide (a non-protein sulfhydryl group blocker, 10 mg/kg, ip), indomethacin (inhibitor of prostaglandin synthesis, 10 mg/kg) or L-NAME (inhibitor of nitric oxide synthase, 70 mg/kg) inhibited the gastroprotective response caused by EENL (100 mg/kg; p<0.05 or 0.001), but there were no changes due to pretreatments with glibenclamide (a K_{ATP} channel blocker, 10 mg/kg, ip) or DL-propargylglycine (an inhibitor of hydrogen sulfide synthesis, 10 mg/kg). In addition, treatment with EENL (100 mg/kg) increased mucus production (p<0.001) and pH (p<0.01) and reduced the volume (p<0.001) and acidity (p<0.001) of the gastric secretion after pylorus ligation. **Conclusion:** The results demonstrate that EENL causes gastroprotective effect with the participation of sulfhydryl groups, prostaglandins, NO, and increased mucus production and modulation of parameters of gastric secretion. **Financial Support:** CAPES and CNPq.

09.019 The Beneficial Effects of *Euterpe oleracea* Mart. Seed Extract (ASE) and Exercise Training in Lipid Accumulation and Oxidative Stress in Liver and White Adipose Tissue in High-Fat-Fed Sprague-Dawley Rats. Silva DLB, Oliveira BC, Gouveia JF, Soares RA, Menezes MP, Cavaleira MA, Nogueira ACA, Silva EM, Ognibene DT, Costa CA, de Bem GF, Resende AC UERJ, Dept of Pharmacology

Silva DLB¹, Oliveira BC¹, Gouveia JF¹, Soares RA¹, Menezes MP¹, Cavaleira MA¹, Nogueira ACA¹, Silva EM¹, Ognibene, DT¹, Costa CA¹, de Bem GF¹, Resende AC¹ ¹ Department of Pharmacology. University of Rio de Janeiro State.

Introduction: The rising rates of obesity represent an urgent public health concern. Açai seed extract (ASE) promotes an anti-obesity effect, and physical exercise is a strategy for weight loss. **Objective:** This work aims to evaluate the impact of treatment with ASE and exercise training in lipid accumulation and oxidative stress in white adipose tissue (WAT) and liver in high-fat-fed Sprague-Dawley rats. **Methods:** All experimental procedures were approved by the Ethics Committee of IBRAG/UERJ (n^o 009/2022). Seventy-five male Sprague-Dawley rats were divided into five groups: CT (10% lipid diet), HF (55% lipid diet), HFA (HF + ASE 200 mg/kg/day), HFT (HF + training exercise) and HFTA (HF + physical training + ASE 200 mg/kg/day). The diets were offered for 16 weeks, and ASE or vehicle was administered by intragastric gavage from the tenth week along with the aerobic exercise training (training on a treadmill for 30 min/day, 5 days/week) for 6 weeks at the intensity of 60 to 70% of the maximum speed reached during the stress test maximum. Colorimetric assays kits were used for plasmatic analyses (n = 8-10). Slides of WAT and liver were used to determine the morphological alterations (n = 4-5). Oxidative damage was determined by the formation of malondialdehyde (MDA) (n = 7-11), while the antioxidant defense was evaluated through the activity of the enzymes superoxide dismutase (SOD) (n = 3-6), catalase (CAT) (n = 7-10) and glutathione peroxidase (GPx) (n = 5-7) in the homogenate of both tissues. **Results:** The HFA and HFTA groups showed a reduction in body mass gain (61.5% and 78.2%, respectively) compared to the HF group. Only the training associated with the ASE reduced plasma triglycerides (TG) levels when compared to the HF (35%) and HFT (35.5%), in addition to lowering hepatic levels of TG (58.5%) and cholesterol (42.6%) when compared to the HF group. All treatments reduced the plasma levels of hepatic transaminases TGO (A: 21%; T: 35.7%; TA: 36.4%) and TGP (A: 34.9%; T: 33.2%; TA: 43.5%) compared to the HF group. However, though ASE treatment reduced TGO levels compared to the HF group, TGO levels were improved in the HFA group (22.2%) compared to the CT group. All treatments reduced average adipocyte area in WAT (A: 53.2%; T: 56.4%; TA: 59.8%), as well as density of hepatic steatosis (A: 49.4%; T: 34.5%; TA: 33%) compared to the HF group. In WAT, all treatments reduced MDA levels compared to the HF group (A: 48.7%; T: 55.7%; TA: 53.5%). In the liver, ASE isolated and associated with exercise reduced MDA levels (A: 36.6%; TA: 51.1%) concerning the HF group. Regarding antioxidant enzymes activities in WAT, ASE alone or associated with exercise training promoted an increase of SOD (A: 670.8%; TA: 936.4%), CAT (A: 208.6%; TA: 185.4) and GPx (A: 60.3%; TA: 62.4%) compared to the HF group. In contrast, in the liver, ASE and exercise training alone increased the activity of antioxidant enzymes SOD (A: 221.5%; T: 173.4%), CAT (A: 105.2%; T: 70.6%), and GPx (A: 49.6%; T: 56.8%), and the association between treatments proved to be beneficial in increasing SOD activity (180%) and CAT (39.1%), but not GPx compared to the HF group. **Conclusion:** These findings demonstrate a beneficial effect of ASE and exercise alone in improving the plasma and hepatic lipid levels, reducing the average adipocyte area and hepatic steatosis, and improving oxidative stress. The association of both was also beneficial for reducing the gain in body mass and improving the hepatic lipid profile, suggesting that these are effective approaches to treating obesity.

09.020 *Gymnema sylvestre* Extract Inhibits the Intestinal Fat Absorption in Swiss Mice. Souza GH¹, Santos TFD², Silva BP¹, Bonetti CI³, Peralta RM¹, Bracht A¹, Sá-Nakanishi AB¹ ¹UEM, Dpt of Biochemistry, Maringá, Brazil; ²UEM, Dpt of Food Science; ³UEM, Dpt of Pharmaceutical Science.

Introduction: Obesity is a metabolic disorder caused by an excessive accumulation of fat in adipocytes, which may be related to a series of clinical complications. One way of treating obesity is through the inhibition of pancreatic lipase. However, these drugs cause several side effects. **Objectives:** Evaluate the effect of *Gymnema sylvestre* leaves extract on the fat absorption in enterocytes. **Materials and Methods:** *G. sylvestre* leaves extract was purchased from local pharmacy and was evaluated a dose-dependent effect of the extract on the olive oil tolerance test in mice. The animals received different doses (100, 250 and 500 mg/kg) of the extract previously the olive oil administration (5mL/Kg) via gavage. Plasma triglycerides were determined in fasting (zero time) and for 6 hours after administration of olive oil, through an AccuTrend® monitor device. **Results:** *G. sylvestre* extract prevented triglycerides increase induced by olive oil administration in a dose-dependent manner. The 100 mg/kg was able to inhibit the absorption of triglycerides by 61%, while there was an inhibition of 84% at the dose of 500 mg/kg. The IC₅₀ (the dose of the extract capable of inhibiting the intestinal absorption of fat by 50%), was of 68.36 mg/kg. The results were similar to the Orlistat (50 mg/kg), a drug reference that inhibits lipase enzyme. **Conclusion:** The extract of leaves of *G. sylvestre* is a potential formulation that can be used, at least as an adjuvant, in the treatment and management of fat absorption by gut cells in animals. **Financial Support:** Coordenação de Aperfeiçoamento de Pessoal de Nível Superior (CAPES) and Conselho Nacional de Desenvolvimento Científico e Tecnológico (CNPq).

09.021 The Antitumoral Effects of Melittin, a Peptide from *Apis mellifera* Venom, in Human Bladder Cancer Cells. Almeida TC¹, Poiato GEH¹, Boaventura de Oliveira AM¹, Marques-Porto R², da Silva GN³, Picolo G¹. ¹IBu, Lab. of Pain and Signaling, Brazil; ²IBu, Lab. of Development and Innovation, Brazil; ³UFOP, Toxicogenetic, Epidemiological and Clinical Study and Research Group, Brazil

Introduction: Bladder cancer is the 11th most common cancer in the world and is one of the tumors with the highest cost to health systems. The treatment of muscle-invasive bladder cancer involves surgery and systemic chemotherapy, however improvements in toxicity profile and aiming to reduce recurrence are needed. Thus, the identification of compounds with antineoplastic potential is necessary, and isolated molecules from natural products have received special attention. Melittin, the major compound found in the *Apis mellifera* venom (apitoxin), is a peptide containing 26 amino acids. Several pharmacological activities have been described for melittin, including antitumoral effects in different types of cancer. In this context, we aimed to investigate the antitumoral effects of melittin in bladder cancer cells.

Methods: UM-UC-3 human bladder cancer cells were treated with different concentrations of apitoxin or melittin (1.25 ? 10 µg/ml) for 24, 48, or 72 hours and the viability was measured by MTT assay. The action of melittin in the cell cycle progression was evaluated by flow cytometry and the interference with cell migration was analyzed by the wound healing assay. The long-term effect of melittin was assessed by clonogenic survival test. **Results:** The cytotoxic results demonstrated that apitoxin and melittin reduced cell viability in a time- and concentration-dependent manner. Since melittin was more potent than apitoxin, we followed the study investigating its mechanism of action. Melittin induced an increase in the sub-G1 content and reduced the percentage of cells at the G2/M phase. Cell migration was also decreased after melittin treatment. In addition, melittin reduced the clonogenic survival of bladder cancer cells.

Conclusion: These preliminary data indicate an interesting antitumoral effect of melittin in bladder cancer cells and support future studies to understand better its mechanism of action and develop approaches for its possible uses. **Financial Support:** FAPESP (processes numbers 2021/10344-5, 2019/17109-1, and 2013/07467-1)

09.022 Hepatoprotective and Nephroprotective Effects of the Methanolic Extract of *Sida rhombifolia* L. Aerial Parts in Mice. Heinichen OY, Arrúa WJ, Galeano AKC Universidad Nacional de Asunción, Facultad de Ciencias Químicas, Depto de Farmacología, Paraguay

Background: The liver and kidneys are the cornerstones for the maintenance of metabolism and homeostasis of the organism. Currently, both organs are involved in metabolic and inflammatory diseases considered a growing health problem in the world, which is why more accessible and safe treatment options are required for the general population. In such a context, *Sida rhombifolia* is a shrub with therapeutic potential that could be used to prevent/treat liver and kidney pathologies. **Objective:** Evaluation of the hepatoprotective and nephroprotective effects of the methanolic extract of aerial parts of *S. rhombifolia* L. against pharmacologically induced hepatotoxicity and nephrotoxicity in mice. **Methodology:** The aerial parts of the plant were collected and used to obtain the methanolic *S. rhombifolia* extract (rEMS). In vivo experiments were carried out with healthy adult Swiss albino male and female mice, weighing 25 to 35 g. All animal procedures were carried out in accordance with the ARRIVE and Animal Scientific Procedure UK guidelines and the current experiment was approved by the Bioethics Committee of the Faculty of Chemical Sciences (National University of Asunción) (CEI 545/2019). Acute oral toxicity of rEMS was performed in mice (female and male, n=5 groups) and overall performance was assessed with the subchronic toxicity assay (male, n=8). Gentamicin-induced acetaminophen-induced hepatotoxicity and nephrotoxicity assays were developed to assess the blood level of markers of liver and kidney damage (men and women, n=8). The doses of rEMS evaluated were 50, 100 and 200 mg/kg, and 150 mg/kg of silymarin was used as a control. **Results:** The results show that rEMS is safe up to 2000 mg/kg po and did not affect the general behavior of the mice. Regarding other biochemical parameters, all doses of rEMS significantly reduced GPT, ALP, and creatinine, compared to the acetaminophen and gentamicin groups, respectively. **Conclusion:** According to these results, the methanolic extract of the aerial parts of *Sida rhombifolia* L. did not present significant toxic effects in mice and, according to *in vivo* tests, it could have possible hepatoprotective and nephroprotective effects.

09.023 Effects of Chlorogenic and 3,5-Dicaffeoylquinic acids on the Proliferation and Differentiation of C2C12 Myoblasts. Quadros VA^{1,2,3}, da Silveira^{1,4}, Purgatto E^{2,3}, Moreira V¹. ¹Unifesp, Dept of Pharmacology, Brazil; ²FCF-USP Dept of Food and Experimental Nutrition; ³FoRC-USP, Food Research Center, São Paulo, Brazil; ⁴Associated Lab. for Sustainability and Technology in Mountain Region, Portugal.

The investigation of new compounds with pro-regenerative activity has raised clinical and scientific interest, since poor regeneration and/or remodeling following injuries to skeletal muscle tissue can lead to loss of tissue function, affecting the quality of life. Based on knowledge of the diversity of bioactive compounds obtained from vegetables and fruits and their benefits to human health, we particularly highlight phenolic acids such as chlorogenic acids (CA) compounds. Their well-known bioactivity, such as anti-inflammatory and antioxidant activity, suggest promising effects on skeletal muscle regeneration. In fact, some studies have demonstrated the potential activity of CA and its derivatives products in stimulating hypertrophy and inhibiting muscle tissue atrophy. This study aimed to investigate the direct effect of CA and 3,5-dicaffeoylquinic acid (3,5-DQA) on the proliferation and differentiation of C2C12 myoblasts *in vitro* model study. In the proliferation protocol, C2C12 myoblast cells were incubated for 24 h with CA (25 μ M) and 3,5-DQA (15 μ M), and for 72 h, to test the effects of these compounds on the differentiation stage. Proliferation by BrdU incorporation assay, Interleukin (IL)-6 quantification by ELISA and expression of myogenic transcription factors (MRF) such as MyoD, Myf-5, myogenin (Myog), Myf-6 and alpha-smooth muscle actin (α -SMA) by western blotting were performed. The data showed a significant increase ($p < 0.05$) in the proliferation of myoblasts stimulated by CA, in contrast to 3,5-DQA, which did not alter the number of cells, both in comparison with cells incubated only with DMEN (control). After 24 h, the incubation of C2C12 with CA and 3,5-DQA promoted a significant increase in the production of the main proliferative myokine IL-6 (60.3 \pm 16.3 and 54.8 \pm 12.0 pg/mL, respectively), when compared with control myoblasts (32.7 \pm 1.1 pg/mL). Furthermore, these compounds stimulated a significant increase ($p < 0.05$) in the expression of MRF proteins Myf-5 and MyoD in the proliferative phase of myoblasts. In the initiation of myogenic differentiation, cells incubated with CA and 3,5-DQA showed a significant increase ($p < 0.05$) in the Myog and Myf-6 expression, when compared to the respective control groups. The expression of specific myogenic markers α -SMA, was significantly ($p < 0.05$) up-regulated by incubating cells with CA, but not with 3,5-DQA, compared to the control group. Our data demonstrate for the first time that the phenolic compounds CA and 3,5-DQA have the ability to increase the proliferation of C2C12 myoblasts in culture by modulating key mediators such as IL-6 and MRFs involved in proliferation (Myf-5) and in the transition from proliferated to committed stage of myoblasts (MyoD). In addition, these compounds directly stimulate committed myocytes to differentiate into myotubes by upregulating Myog and Myf-6 MRFs, as well as α -SMA, which appears during myocyte elongation and myotube fusion. These data together indicate that the bioactive CA and 3,5-DQA can pharmacologically modulate initial myogenic processes involved in skeletal muscle regeneration after injury.

09.024 Hemodynamic and Vascular Effects of Perillyl Alcohol in Rats. Santos MRV¹; Rodrigues-Junior EO¹; Santana IR¹; Barreto AS²; Santos AM³; Santana-Júnior CC³; Oliveira AMS³; Serafini MR³; ¹UFS, Depto de Fisiologia; ²UFS, Depto de Educação em Saúde; ³UFS, Depto de Farmácia, Brazil

Introduction: Perillyl Alcohol (PA) is a cyclic alcohol monoterpene found in essential oils of various aromatic medicinal plants popularly used for hypertension treatment, such as lemongrass, mint and ginger. This study aimed to evaluate the hypotensive, bradycardic and vasorelaxant effects of PA in rats and to elucidate its possible mechanism of action. **Methods:** Male Normotensive Wistar rats (200 - 300 g) were used in all experiments. Hemodynamic effects were evaluated through catheters inserted in abdominal aorta and inferior vena cava. Mean Arterial Pressure (MAP) and Heart Rate (HR) were obtained before and after intravenous injection of PA (0.1; 0.3; 1; 3 and 10 mg/kg) in conscious animals in control or pre-treated with atropine conditions. The effect of PA (from 10^{-8} to 10^{-2} M) on vascular reactivity was assessed through concentration-response curves obtained in isolated rings from rat mesenteric artery intact or denuded of endothelium, both pre-contracted with Phenylephrine ($1 \mu\text{M}$) or KCl (80 mM). All procedures were approved by the Animal Research Ethics Committee of the Federal University of Sergipe (CEUA nº 2836060420; ID 000245). **Results:** In normotensive rats, PA induced hypotension (-3 ± 4 ; -5 ± 6 ; -7 ± 3 ; -31 ± 7 e $-39 \pm 6\%$, respectively, $n = 10$) and bradycardia (-11 ± 6 ; -6 ± 6 ; -18 ± 6 ; -35 ± 10 e $-60 \pm 7\%$, respectively, $n = 10$). In animals pre-treated with atropine, bradycardia was significantly attenuated (** $p < 0.01$), but hypotension was not changed. Furthermore, PA was able to induced vasodilation ($E_{\text{max}} = 113 \pm 7\%$, $n = 7$) that was not changed in endothelium-denuded rings, but significantly potentiated in preparations pre-contracted with KCl (80 mM). **Conclusion:** So far, the results demonstrate that PA induces hypotension and bradycardia in rats. Bradycardia appears to be caused by activation of cardiac muscarinic receptors. In addition, PA induces vasodilation, which are endothelium-independent and can involve voltage-gated Ca^{2+} channels. This vasodilation may be contributing to the hypotensive effect observed *in vivo*. **Financial Support:** CNPq (#305345/2019-2), FAPITEC/SE (#15 do EDITAL FAPITEC/SE/FUNTEC Nº 06/2021), and CAPES.

09.025 Assessment of the Potential Neuroprotective Effect of Aqueous Extract of *Eugenia dysenterica* DC in a Model of Cisplatin-Induced Peripheral Neuropathy *in vitro*.

Oliveira HR^{1,2}, Fehrenbacher JC², Guimarães PO³, Duarte, DB¹ ¹UnB, Dpt of Pharmacy, Lab. of Pharmacological Assays, Brazil; ²Indiana University School of Medicine, Dpt of Pharmacology and Toxicology, USA; ³UnB, Dpt of Pharmacy, Lab. of Natural Products, Brazil

Introduction: Chemotherapy-induced peripheral neuropathy (CIPN) is a clinical manifestation of the toxicity of several antitumoral drugs on the peripheral nervous system, such as platinum derivatives. Cisplatin, the class prototype, is an antitumor drug clinically used due to its ability to induce apoptosis in tumor cells. However, in neurons, cisplatin induces changes that will culminate in peripheral neuropathy (PN), a set of symptoms characterized by being predominantly sensory and dose-dependent. Among those symptoms, the patient develops paresthesia, sensory loss, and neuropathic pain. The referred effects occur because dorsal root ganglia (DRG) neurons are also targets of these drugs. Hence, there is an emerging need to protect the nervous system against CIPN treatment. Thus, we evaluated *in vitro* whether the aqueous extract of *Eugenia dysenterica* leaves (Cerrado plant known as Cagaita) has a neuroprotective role in the CIPN model, due to its antioxidant and anti-inflammatory activities and the already described neuroprotective effects. **Methods:** primary cultures of DRG cells from adult rats, A549 and neuron-like PC-12 cell cultures were established, which were treated with *E. dysenterica* extract in the presence or absence of cisplatin. The effects of these treatments on cisplatin neurotoxicity were analyzed using the cell viability evaluation by trypan blue exclusion, quantification of the release and total content of calcitonin gene-related peptide (CGRP) by radioimmunoassay, the synthesis of reactive oxygen species by fluorimetry, and measurement of neurite length by microscopy. **Results:** Were made concentration-effect curves using 0.3, 3, 30 and 100 ug/mL *E. dysenterica* and 1, 3, 10, 30 and 100 uM cisplatin and the chosen work concentration was 30 ug/mL and 30 uM, respectively. The treatment with 30 uM cisplatin for 24 hours did not induce cell death of DRG cells, but increased neuronal sensitization by 53.9% after capsaicin stimulus and 33.3% after KCl stimulus, and induced oxidative stress in PC-12 cells (increase of 57.1%), which were prevented by pretreatment with 30 ug/mL *E. dysenterica* extract. Also, we observed that cisplatin promotes inhibition of neurite outgrowth (18.0%), which was not prevented by the extract pretreatment. On the other hand, the treatment with 30 ug/mL *E. dysenterica* alone does not alter the DRG cell viability. Furthermore, we observed that the extract does not interfere with the antitumor activity (A549 cells) or the effect of cisplatin on neurites. **Conclusion:** The *E. dysenterica* extract is not toxic to the DRG cell culture and it does not interfere with the cisplatin's antitumoral activity. Also, it prevents the increase in neuronal sensitivity induced by cisplatin, as well as oxidative stress and cisplatin-altered neurite outgrowth. Finally, the *E. dysenterica* extract proved to be neuroprotective in the cisplatin-induced PN model. **Financial Support:** Grant numbers 407757/2013-9 (CNPq) and 193.000.668/2015 (FAPDF). This work was made in collaboration with the Laboratory of Natural Products of the UnB and we continued investigating the extract effects, once our aim was not evaluating the chemical composition of the aqueous extract of *E. dysenterica* leaves or identify the component with pharmacological activity, which it was already as can be seen bellow. - Souza, PM, *et. al* (2012) doi: 10.1371/journal.pone.0048589; - da Silva Prado LC, *et. al* (2014) doi: 10.1248/bpb.b13-00514; - Gasca CA, *et. al* (2017) doi: 10.1016/j.fct.2017.02.032; - Fidelis-de-Oliveira P, *et. al* (2020) doi: 10.1016/j.jep.2019.112520.

09.026 Ontogenetic Variation in Venom and Tail Coloration Relationship in *B. moojeni* and *B. atrox*. Garcia LNV, Galizio NC, Silveira GPM, Motta-Soares MV, Grego KF, Serino-Silva C, Tanaka-Azevedo A; Morais-Zani K. IBU, Dpt. of Herpatology, São Paulo, Brazil

According to the Brazilian Ministry of Health, approximately 70% of snakebite incidents in Brazil are caused by the genus *Bothrops*. The treatment for these accidents involves administering antivenom serum, which relies on understanding the overall composition of the venom in the entire genus to ensure efficacy. *Bothrops* snake bites can result in hemorrhage, coagulation disorders, edema, and myopathy, with coagulation being more pronounced in juveniles and edema being more prevalent in adult snakes. Juvenile snakes are born with varying intensities of tail coloration, categorized as I to V, with I being lighter and V indicating the absence of this distinct coloration. This coloration is used to lure the prey and changes over time, gradually losing its distinctive appearance. Due to the importance of understanding intraspecific venom variability, this research aimed to analyze the correlation between ontogenetic variation in venom and tail coloration in juvenile snakes. The study collected venom samples from juvenile *B. atrox* and *B. moojeni* (1 year old), analyzing them individually. Protein quantification was determined using the Bradford method, while venom composition was analyzed through SDS-page and HPLC protein profile. Proteolytic activity was assessed through collagenolytic and caseinolytic assays, with the latter conducted both with and without EDTA. Coagulation activity was also examined, and statistical tests (ANOVA) were performed on all **Results:** Both electrophoresis and HPLC showed protein profiles consistent with previous works. Regarding caseinolytic activity there was an overall trend of increased activity over time, both with and without EDTA, although the addition of EDTA resulted in a significant reduction compared to the samples without EDTA. However, when taking into consideration tail colorations, no significant correlation was detected. In terms of coagulation activity, there appeared to be an initial trend of increased coagulation capacity in human plasma associated with tail coloration, with individuals displaying tail coloration V (no coloration) displaying the highest overall procoagulant activity. The experiments conducted so far did not demonstrate a strong correlation between tail coloration and ontogenetic changes in venom. Furthermore, serine proteases play an important role in the coagulation disorders caused by *Bothrops* snake venom, and juveniles were expected to exhibit higher coagulation potency than adults. However, this was not clearly observed in the experiments as individuals with lower degrees of tail coloration showed longer coagulation times. Additionally, the caseinolytic activity with EDTA, which inhibits the action of metalloproteases, was very low suggesting the activity of serine proteases. This contradicted the expected high activity of serine proteases based on coagulation activity. This work is supported by FAPESP (2020/07268-2; 2021/07627-5), CNPq (309995/2022-1), Secretaria de Estado da Saúde de São Paulo and Fundação Butantan.

09.027 Methyl Cinnamate Suppresses TGF- β 1-Induced Epithelial-Mesenchymal Transition in Airway Epithelium Through Inhibition of NF- κ B p65 Translocation. Ferreira EGA, Barros ABB, Silva JP, Fidelix MSP, Carmo JOS, Santana JR, Barreto E UFAL, Lab. of Cell Biology, Brazil

Introduction: Epithelial-mesenchymal transition (EMT) is a critical pathological process involved in a variety of tissue fibroses. In this process, epithelial cells gradually acquire a mesenchymal (fibroblast-like) cell phenotype, that lead to the excessive accumulation of fibrous connective tissue in damaged tissue, which can lead to permanent scarring or organ malfunction. Therefore, drugs targeting EMT may be a promising therapy against fibrosis. Methyl cinnamate (MC), a phenylpropanoid derivative found in several medicinal plants, has been shown to have numerous bioactivities such as anti-inflammatory and antioxidant properties. However, to the best of our knowledge, the effects of methyl cinnamate on the process of EMT in human epithelial cells remain unknown. Therefore, the present study aimed to investigate the direct effects of methyl cinnamate on the TGF- β 1-induced EMT in A549 alveolar epithelial cells and explore the underlying molecular mechanisms. **Methods:** A549 cells were grown in DMEM medium supplemented with 2% fetal bovine serum, 1% penicillin/streptomycin, 2 mM L-glutamine and maintained in a humidified incubator at 37 °C with 5% CO₂. The cytotoxic effect of MC (1, 3, 10 and 30 μ M) was determined by MTT assay. A549 cells were stimulated with TGF- β 1 (10 ng/mL) with or without MC (10 μ M) co-treatment and the EMT phenotypic and functional features were evaluated 24h later. The morphological alterations were observed by light microscopy, while immunofluorescence staining was performed to confirm the expression of mesenchymal marker (vimentin), of signal transducer (phospho-Smad3), and of the nuclear translocation of NF- κ Bp65. Statistical differences were significant at $p < 0.05$ analysed by one-way ANOVA and Tukey's test. **Results:** The results revealed that MC no cytotoxic effects to any of concentrations tested after 24 h exposure. The stimulation with TGF- β 1 induced changes in cell morphology from epithelial-like to elongate fibroblast-like morphology, up-regulated the expression of vimentin, and increased cell migration. **Conclusion:** Our results demonstrate that methyl cinnamate can inhibit TGF- β 1-induced EMT, and suggests that suppression of nuclear translocation of NF- κ Bp65 may be responsible for this effect. **Financial Support:** CNPq, CAPES, BioproFar-BA and FAPEAL.

09.028 **Effects of β -Micrustoxin, Phospholipase A2 Isolated from *Micrurus lemniscatus* Snake Venom, on the Cytoskeleton of Astrocytes and Glioblastomas.** Tida-Oliveira CH, Sandoval MRL, Afeche SC. Ibu, Lab. of Pharmacology, São Paulo, SP, Brazil

Introduction: Phospholipases A2 are a set of enzymes that catalyze the hydrolysis of glycerophospholipids in the plasma membrane, converting them into fatty acids and lysophospholipids. When present in venom toxins from snakes of the Elapidae and Viperidae families, they act on the presynaptic neurons of the neuromuscular junction, depleting acetylcholine from the synaptic vesicles. Data from our laboratory demonstrated that β -micrustoxin, phospholipase A2 isolated from *Micrurus lemniscatus* snake venom, induced cell death in hippocampal neurons and reduced the astrocyte cell viability and proliferation, with an increase in the cell cycle regulatory proteins p53, p21 and p27 and a predominance of the G2/M phase of the cell cycle. One possibility to be considered is that β -micrustoxin may lead to a cell cycle arrest due to the activation of the transcription factor p53 as a result of damage to the centrosomes leading to disorganization of the mitotic spindle. This process may be a consequence of changes in the cellular cytoskeleton of astrocytes, since the composition of centrosomes depends on tubulin, a protein that makes up the cytoskeleton, or even changes in the actin cytoskeleton, resulting in disorganization of mitotic division. This work intended to study possible alterations induced by β -micrustoxin in the cytoskeleton of actin and tubulin in astrocytes and U138 glioblastomas. **Methods:** To obtain the astrocyte culture, pineal glands of Wistar rats were isolated and their cells dissociated with the papain enzyme. U138 glioblastomas were purchased from ATCC. Astrocytes and glioblastomas were cultured in Dulbecco's Modified Eagle's Medium (DMEM) at 37°C with 5% CO₂. Cells were plated for confocal microscopy (10⁴ cells/well), exposed to 20 nM β -micrustoxin for 24 h and labeled with SiR-actin, SiR-tubulin and Hoechst fluorophores. Images were acquired by confocal microscopy. MTT methodology was used to analyze glioblastomas cell viability for 96 h after β -micrustoxin incubation. **Results:** Exposure of glioblastomas to β -micrustoxin induced effects as the reduction of the cell size, narrowing of the actin cytoskeleton, but in the astrocytes evident alterations were not identified. U138 glioblastomas showed reduced cell viability over time induced by β -micrustoxin. **Conclusion:** β -micrustoxin seems to induce alterations in the actin cytoskeleton of U138 glioblastomas, but not in astrocytes. Viability reduction of glioblastomas over time could indicate an effect of β -micrustoxin on cell proliferation.

09.029 Evaluation of the Antitumor Activity of Gedunin in A-172 Human Glioblastoma Cells. Silva PRO^{1,3}, Correa AMC¹, Costa TEMM^{1,2}, Penido C^{1,2} ¹Fiocruz-Farmanguinhos, Lab. of Applied Pharmacology, Rio de Janeiro, Brazil ²Fiocruz, Center for Technological Development in Health, Rio de Janeiro, Brazil ³Institutional Program for Initiation Scholarships in Technological Development and Innovation.

Introduction: Glioblastoma is a highly aggressive tumor of the central nervous system. Its high mortality rate is due to the increased proliferative and angiogenic features and its resistance to the WHO-recommended treatment (surgical resection, radiotherapy, and chemotherapy with temozolomide). Treated patients have low survival rates (15 months), and only 5% survive 5 years after diagnosis. In this sense, searching for alternative treatments that increase survival and improve the quality of life of glioblastoma patients is extremely important. The heat shock protein (HSP) 90 is a molecular chaperone overexpressed under stress conditions, that participates in the regulation and stabilization of several client proteins involved in oncogenesis. Gedunin is a naturally occurring HSP90 inhibitor from Meliaceae species whose anti-inflammatory, analgesic, and antitumor activities have been described. In the present study, we sought to evaluate the effect of gedunin on the proliferation and migration of A-172 glioblastoma cells in *in vitro* models. **Methodology:** A-172 cells were seeded in 6 (1x10⁶/well), 24 (2x10⁵/well), or 96-well (2x10⁴/well) plates and treated with gedunin (6.25-100 μ M) or 17-AAG (a selective HSP90 inhibitor, used as reference inhibitor; 1 μ M) for 1, 24, or 48 hours. Transforming growth factor (TGF)- β 1 and interleukin (IL)-6 were evaluated in the cell supernatant by ELISA; metalloproteinase (MMP)-2 activity was evaluated in cell serum-free supernatant by zymography; glioblastoma cells migration was assessed by scratch assay, whereas cell viability by MTT reduction. **Results:** Gedunin significantly reduced the viability of A-172 cells after 48 h at concentrations of 50 and 100 μ M compared to the untreated group. TGF- β 1 and IL-6 levels (6.25 - 100 μ M), as well as MMP-2 activity (25 – 100 μ M) were reduced in the supernatant of A-172 cells after 1 h and 24 h of gedunin treatment. In addition, A-172 cell migration was impaired by gedunin treatment (6.25 and 12.5 μ M) after 24 and 48 h. **Conclusion:** Gedunin has *in vitro* antitumor activity against the human glioblastoma lineage A-172 by: *i*) reducing cell viability; *ii*) downmodulating invasiveness-related factors, and *iii*) impairing the migratory/invasive capacity of tumor cells. **Financial Support:** CNPq, Farmanguinhos, Fiocruz.

09.030 Soft Nanoparticles Containing Herbal Drugs for Treating Skin Pathologies: Scope Review. Almeida, IFR¹; Reolon, JB¹; Sari, MHM¹; Marchiori, C¹; Dallabrida, KG¹; Santos, JAR¹; Alves, FMS²; Bonini, JS¹; Ferreira, LM². ¹Unicentro, Dept of Pharmacy, Guarapuava-PR, Brazil. ²UFPR, Dept of Pharmacy, Curitiba - PR, Brazil

Introduction: The skin is a crucial organ, but skin disorders are often ignored. Topical drug administration has drawbacks, but plant extracts may offer a solution. Nanostructured topical formulations are gaining popularity due to their ability to enhance drug permeation and retention in the skin. Plant extracts can increase their effectiveness. This review focuses on the current status of soft-nanoparticles containing plant extracts for topical use in skin diseases. **Methods:** This study followed the Preferred Reporting Items for Systematic Reviews and Meta-Analyses (PRISMA) guidelines and the Joanna Briggs Institute manual. We conducted extensive research using various databases such as Scopus, Web of Science, and PubMed. To ensure accuracy, we implemented a specific search strategy that involved using relevant keywords related to herbal drugs in nano-based formulations for treating skin disorders. We used Boolean operators like "OR" and "AND" to refine our search. Our investigation included all studies written in the English language published until April 2023. **Results:** A total of 377 articles were found in the databases. After eliminating duplicates and using inclusion and exclusion criteria, 25 articles were selected. The most investigated pharmacogens were leaves (28%) and inflorescences (16%), with ethanolic extract (56%) being the most popular extractive solvent. Various nanosystems were used to load the extracts, including solid lipid nanoparticles (21.72%), nanoemulsions (17.85%), nanostructured lipid carriers (17.85%), liposomes, ethosomes, transfersomes (14.28%), and polymeric nanoparticles (28.57%). Some studies also created a final formulation suitable for topical application (60%), such as cream, hydrogel, polymeric film, and ointment, using the obtained nanocarriers. These studies examined the antioxidant, anti-inflammatory, UV protection, anti-aging, and wound-healing properties of various plant extracts incorporated into soft-nanoparticles based on *in vitro* and *in vivo* evaluations. Among the studies, a nanoemulsion using ethanolic extract of *Phyllanthus urinaria* was prepared, which showed antioxidant properties and controlled release when evaluated using a Franz cell and DPPH. A cream containing liposomes loaded with a *Curcuma longa* hydroalcoholic extract demonstrated photoprotective properties when tested *in vivo* for skin hydration and sebum content. A hydrogel containing *Phragmites communis* root extract-loaded solid lipid nanoparticles showed improved skin hydration. Methanolic extract of *Smilax china* and *Salix alba* was loaded into nanostructured lipid carriers and converted into a nanogel that effectively treated psoriasis *in vitro* and *in vivo*. Lastly, nanospheres were prepared using ethanolic extract of *Ilex paraguariensis* in nanospheres, which conferred additional protection to the phytochemical compounds and prolonged the antioxidant effect, suggesting promising potential for topical antioxidant therapy. **Conclusion:** To address concerns about herbal drugs, we need to standardize plant conditions, analyze the entire matrix, identify stable formulations, test toxicity, and conduct clinical trials. **Financial Support:** None.

09.032 **Beta Glucans obtained from *Pholiota nameko* does not Ameliorates DSS-Induced Ulcerative Colitis in Mice.** Silva RR¹, Zavadinack M², Baptista NZ¹, Amaral FKCW¹, Rosa-Filho SP¹, Iacomini M², Werner MFP¹. ¹UFPR, Pharmacology, ²UFPR, Biochemistry and Molecular Biology

Introduction: Ulcerative colitis (UC) is characterized by intense inflammation in the mucosa and submucosa of the intestine. Current treatment presents higher costs and great refractoriness rate with no precedent for cure, necessitating new therapeutic strategies. Numerous studies have addressed that consumption of polysaccharides isolated from fungi may play an immunomodulatory role in the gut microbiota. *Pholiota nameko* is a medicinal and edible mushroom, with proven antitumor, antioxidant and anti-inflammatory activities. This work aimed investigate an insoluble (1→3) (1→6)-β-D-glucan isolated from *P. nameko* (PNI) obtained from a residue subjected to autoclave extractions in aqueous and alkaline media in UC. **Methods:** UC were induced in female Swiss mice (30 g) with 5% Dextran Sulfate Sodium (DSS). Animals were treated orally (v.o.) with vehicle (water, 1 mL/kg) or PNI (1, 10 or 100 mg/kg) for 7 days. The clinical signs of the disease were monitored daily, such as weight loss, blood, and stool consistency for the disease activity index (DAI). Abdominal mechanical allodynia was evaluated by von Frey monofilaments in increasing order (0.008 - 0.6 g). From day 7 to 8, the nest building test was performed to assess the animal welfare. On the eighth day, the colon was collected and measured, one part was used for histology and the other part was homogenized for myeloperoxidase (MPO) assay. **Results:** DSS group displayed a colon length shortening of 18.10% when compared to the control group (10.44 ± 0.20 cm), and PNI treatment were not able to preserve colon size. Again, DSS group decreased in 4% the body weight from the 5th reaching 13.72% at the 8th day, whereas the PNI was unable to preserve the body weight and DAI. DSS increased mechanical allodynia in the day 8 in 1800%, 2050%, 650%, 600% e 715% for the monofilaments (0.008, 0.02, 0.07, 0.16 and 0.6 g) respectively, when comparated to control group (4 ± 2.67%; 4 ± 2.67; 12 ± 4.42; 14 ± 4.27; 12 ± 3.27). Additionally, evaluating animal welfare, DSS group presented a robust reduction of nesting activity of 59.46% in comparison to the control group (3.7 ± 0.26). Moreover, DSS increased MPO levels in colon in 135% when compared to control group (3.35 ± 0.68 D.O./mg of protein), which has not been modified by treatment with PNI. Finally, the histological evaluation of the acid or neutral mucin production was performed through Alcian Blue (AB) and periodic acid-Schiff (PAS) staining. The DSS group showed a decrease of 86% and 92% in PAS and AB, respectively, when compared to control group (42.60 ± 1.09 and 46.69 ± 2.63 pixels/field respectively), that was not restored with any dose of PNI treatment **Conclusion:** Though mushroom polysaccharides get a lot of attention, different isolation and purification procedures may result in distinct extracted molecules. In this regard, we found that the PNI was not provide any protection of colonic tissue in the DSS induced colitis in mice. We can hypothesize that the low solubility of (1→3) (1→6)-β-D-glucan could compromise the biological effect of this polysaccharide. **License Number of Ethics Committee:** CEUA/BIO - UFPR: approval number 1451. **Financial Support:** CAPES-Finance Code 001. UFPR.

09.033 Phytochemical Analyzes and Potential Effect Larvicidal and Repellent of Hydroalcoholic Extract from *Jacaranda puberula* Against *Aedes aegypti* (Linneus, 1762). Maccagnan JC, Monteiro M, Serpa PZ, Rezende RS, Busato MA, Roman-Junior WA Unochapeco

Introduction: the mosquito *Aedes aegypti* has been involved in epidemics worldwide due to the high vectorial competence for transmission of dengue virus, Zika, chikungunya, and yellow fever. Vector control strategies base their actions on mechanical, biological, and mainly chemical management, limited to substances with residual potential in the environment, and toxicity to non-target organisms. An alternative to synthetic agents is natural products. Thus, this work aimed to evaluate the larvicidal and repellent activity of the plant extract of *Jacaranda puberula*. **Methods:** the hydroalcoholic extract of *J. puberula* (HEJp) was obtained by maceration, subsequently submitted to UV/Vis spectrometric analysis (365 nm). The sample of HEJp was partitioned with solvents of increasing polarity. The ethyl acetate fraction was analyzed by high-performance chromatography (HPLC), and submitted a fractioning in chromatographic column. The subfractions obtained were analyzed, by ¹H and ¹³C NMR. For larvicidal evaluation, 3rd instar larvae were used. HEJp was tested at different concentrations (10, 50, 100, 250, and 500 µg/mL) (n=5), and evaluated every 12 h, totaling 72 h. Two positive controls were used: *Bacillus thuringiensis* var. Israeli-BTi, and Spinosad. For negative control, chlorine-free water (VEI). The repellent test was approved by the CEP (#5364. 434). In this trial, 30 female mosquitoes were used in each cage, with no access to blood feeds 24 h before testing. Mosquitoes were exposed to a hydroalcoholic solution containing 10% of *J. puberula* extract, for three minutes, totaling 4 h of exposure without reapplication of the spray, with verification of the repellent action every 30 min. The sting attempt was the parameter used to verify the repellent action. For the negative control, 70% alcohol was used, and for the positive control, a commercial formula containing N,N-Diethyl-3-methylbenzamide (DEET). Data treatment was performed using the Abbott formula, analysis of variance (Anova two-way), and Tukey's post hoc test (µg/mL corroborates the larvicidal efficacy for EHJp. As for the repellent effect, in the period between 0 and 30 min, the extract was able to repel 95.65% of the mosquitoes, showing intense effectiveness until 240 min, where there was 97.83% activity compared to the group VEI. **Conclusion:** The extract demonstrates a strong larvicidal and repellent effect, which may be related to the jacaranone present in the plant.

09.034 Fibrinogenolytic Activity of Venoms from Medically Important Snake Species in Brazil. Soares MVM, Serino-Silva C, Godoy TA, De Lima EO, Sant'Anna SS, Galizio NC, Grego KF, Silveira GPM, Tanaka Azevedo AM, Morais-Zani K. IBu, Brazil

Introduction: Accidents caused by venomous snakes are a major national and global public health problem. Due to the high fatality potential associated with these accidents, there is an increasing need for scientific research aimed at expanding our knowledge about the composition and activity of the venom from these animals. Studies show that the Viperidae family is one of the snake groups with the greatest variety of toxins that are related to the blood coagulation cascade, especially fibrinogen. Venoms can contain numerous types of these toxins, such as procoagulants and anticoagulants, which inhibit or rapidly degrade essential factors for blood homeostasis. Understanding the mechanism of action of these components is important not only to improve the manufacturing of antivenom used for the treatment of envenomation but also for the bioprospecting of new active principles with therapeutic purposes. For this project were included venoms of adult individuals of *Bothrops jararaca*, *Bothrops moojeni*, *Bothrops atrox*, *Bothrops leucurus*, *Bothrops erythromelas*, *Bothrops jararacussu*, *Bothrops alternatus*, *Bothrops neuwiedi*, *Crotalus durissus terrificus* e *Crotalus durissus collilineatus*. **Methods:** To carry out this work, the methodologies used were developed in three main steps: measurement of protein concentration in samples of snake venoms using the Bradford method, fibrinogenolysis assays under different conditions, including venom incubated with metalloprotease inhibitor (EDTA), antivenom, EDTA + antivenom, and saline for comparison at different incubation times (from 0 min to 2 hours) at 37 degrees Celsius. It was also necessary to perform polyacrylamide gel electrophoresis (SDS-PAGE) for visual and quantitative analysis of both the protein profile of the venoms and their different effects on fibrinogen. In these SDS-PAGE gels, degradation patterns of the alpha and beta chains of the human fibrinogen molecule were taken into account. The analyzed venoms showed interspecific differences between the studied genera (*Crotalus* and *Bothrops*). Additionally, differences were identified in the overall protein profiles of individual venoms between females and males of the same species. Regarding the fibrinolytic activity of these venoms, the alpha chain of fibrinogen was completely degraded in all samples, while the beta chain of most samples showed signs of degradation starting from the 30-minute mark. Lastly, we observed that the gamma chain, with lower molecular weight, did not show visual indications of degradation in any of the performed tests, even after additional incubations lasting 3 hours. **Results and Conclusion:** Incubations with EDTA were more successful in delaying fibrinogen degradation by the action of the venoms, while the antivenom was unable to neutralize the fibrinolytic activity of venoms from *Bothrops* species that were not included in the venom pool used for its preparation, but it proved to be more effective upon venoms from subspecies of *Crotalus*. This work was supported by FAPESP (2020/07268-2; 2021/07627-5), CNPq, Secretaria de Estado da Saúde de São Paulo and Fundação Butantan.

09.035 Evaluation of the Therapeutic Effect of Plant-Derived Dietary Fibers Rich in Polysaccharides in a Mouse Model of Polymicrobial Sepsis. Simão G^{1,2}, Braga LLVM^{1,2}, Rosa LB^{1,3}, Silva MLC^{1,3}, Ferreira DM^{1,2}, Cordeiro LMC⁴, Fenandes ES^{1,2} ¹IPPPP, Curitiba, PR, Brazil. ²FPP, PPG em Biotecnologia Aplicada à Saúde da Criança e do Adolescente, Curitiba, PR, Brazil. ³FPP, Graduação em Biomedicina, Curitiba, PR, Brazil. ⁴UFPR, Dept of Biochemistry and Molecular Biology, Curitiba, Brazil

Introduction: Sepsis is the main cause of death from infection, with high morbidity. Its mortality continues to rise, due to bacterial infections resistant to antibiotics (Algammal et al., 2023). In this context, an effective immunity is essential for good prognosis. Plants are a rich source of compounds with immunomodulatory actions. Plant-derived polysaccharides have gained attention as immune modulators and antioxidants (Liu et al, 2020; De Melo et al, 2022). Thus, the characterization of their biological activities is an interesting field for the development of novel therapies for sepsis. **Objective:** To investigate the effects of plant-derived soluble dietary fibres rich in polysaccharides (SDFRPs) in a mouse model of sepsis caused by cecal ligation and puncture (CLP). **Methods:** The effects of SDFRPs obtained from tamarillo (*Solanum betaceum*) and prum (*Prunus domestica*) were first assessed in a model of endotoxemia induced by lipopolysaccharide (LPS) in *Tenebrio molitor* larvae. Different doses (10-100 mg/kg) and treatment schemes were assessed. SDFRPs were also tested in male and female C57BL/6 mice with CLP-induced sepsis. Both the endotoxemic larvae and septic mice were compared with vehicle (saline)-treated animals. Endotoxemia in *T. molitor* and treatments: To assess the preventive effects of SDFRPs, the larvae (n= 20/group) received an intra-haemocoel (i.h) injection of tamarillo, plum or vehicle (10 µl/larvae). Then, after 2h, the animals received either i.h. LPS (10 µl; 106 EU/kg; *E. coli* serotype 0111: B4) or vehicle. In the curative scheme, the animals received either LPS or vehicle, and after 2h, different doses of SDFRPs. Different parameters were observed over 96h following endotoxemia induction: body weight, mobility, melanization and survival; in comparison to baseline measurements. CLP-induced sepsis in mice and preventive treatment: Mice (n= 20/group; 1 male: 1 female) received different doses of tamarillo SDFRPs (per os, daily, for 7 days) prior to sepsis induction. Sepsis was induced by CLP in mice previously anesthetized (intramuscular) with ketamine (75 mg/kg) + xylazine (1 mg/kg), under aseptic conditions. A laparotomy was performed, and the exposed cecum, connected to its base with silk suture 4.0, was perforated once with a 22G needle (Fernandes et al, 2012). Morbidity and mortality rates were registered prior to (baseline) and once a day, for 96h following CLP. Body weight and temperature, and disease severity (Mendes et al, 2016) were evaluated. **Results:** Whilst prum SDFRPs conferred no protection, those obtained from tamarillo reduced larvae mortality and morbidity (32-49% and 32-38%; respectively). Conversely, septic larvae treated with tamarillo gained weight. Of note, tamarillo-induced protection was irrespective of treatment scheme. No effects were seen for plum or tamarillo SDFRPs in vehicle-treated animals. When given to mice, tamarillo SDFRPs reduced mortality rates by 54% (males) and 100% (females). Similarly, morbidity was attenuated by 50%. Tamarillo had no effects on body weight. **Conclusion:** The results indicate that SDFRPs from tamarillo protect against sepsis. These are interesting findings indicating the need for studies on their mechanisms of action. **Funding:** CAPES, CNPq, INCT-INOVAMED and the Instituto de Pesquisa Pelé Pequeno Príncipe. References: ALGAMMAL, A. *Front. Microbiol.*, v.1, p.14, 2023. DE MELO, CML. *Braz. arch. biol. technol.* [INTERNET], 2022. FERNANDES, ES. *J. Immunol.*, v.1, p.188, 2012. LIU, S. *Evid Based Complement Alternat Med* [INTERNET], 2020. MENDES, SJF. *Int Immunopharmacol.*, v. 34, p. 60, 2016.

09.036 Phytochemical Analysis and *in silico* Evaluation of the Essential Oil of *Senecio brasiliensis*. Vida RL¹, Gindri AL², Pacheco PS², Machado MM³, Petreceli RR⁴, Brucker N^{1,4}
¹UFSM, Graduate Program in Pharmacology, Santa Maria, Brazil; ²URI, Dept of Health Sciences, Santiago, Brazil; ³Unipampa, Immunology and Applied Genetics Group, Uruguaiana, Brazil; ⁴UFSM, Graduate Program in Pharmaceutical Sciences, Santa Maria, Brazil

Introduction: Plant biodiversity constitutes an important source of substances that can be investigated as alternatives for application in several sectors, such as the pharmaceutical industry^{1,2}. The species *Senecio brasiliensis*, popularly known as maria-mole, is considered an invasive toxic plant, which is responsible for important economic losses in animal production due to its severe toxicity in cattle^{3,4}. In this sense, knowledge of its chemical components is required. Therefore, this study aimed to evaluate the chemical composition of the essential oil of *Senecio brasiliensis* and perform an *in silico* analysis. **Methods:** The plant was collected on November 3, 2022, in the municipality of Maçambará/RS, Brazil under geographic coordinates 29°10'17.6"S 55°23'31.6"W. After the identification of the plant material was carried out, the exsiccate was deposited in the herbarium of the Federal University of Santa Maria under number 22224 and its registration in SisGen under number AD8B684, and the essential oil was extracted from its leaves and flowers through hydrodistillation in a Clevenger apparatus. Subsequently, a phytochemical analysis was performed using gas chromatography coupled to mass spectrometry (GC-MS). To carry out the analysis of the molecular characteristics of the major compounds, the PubChem and Molinspiration platforms were used to describe the properties of the molecules, and to perform the compound probability property, based on Lipinski's Rule of Five. **Results:** Regarding the phytochemical analysis of the oil, characterization of 100% of the constituents was obtained, with greater emphasis on Bicyclogermacrene, Caryophyllene, Alpha-terpinolene, Germacrene-D, Limonene, Beta-Myrcene, among others. The major constituents were Bicyclogermacrene and Germacrene-D with 23.36 and 21.58%, respectively. The *in silico* analysis was performed for the major constituents, both with a molecular weight of 204.36 and with similar molecular patterns, the main result being that they present only one violation of Lipinski's Rule of Five (miLogP >5.0), thus showing that they have good oral bioavailability. **Conclusion:** These major components, due to their potential effects reported in other studies, may be promising for pharmacological use, providing relevant data for more advanced studies of the activity and the toxicity of these compounds. **Acknowledgment:** CAPES **References:** 1. MICHELETTI, SMF. *Rev. Bras. Paras. Vet.*, v.18, p. 44, 2009. 2. JYOTI. *Exp. Paras.*, v.201, p. 42, 2019. 3. SANDINI, TM. *Biotemas*, v.26, p.83, 2013. 4. STEGELMEIER, BL. *Vet. Clin. North Am. Food Anim. Pract.*, v. 27, 9. 419, 2011.

09.037 Topical Formulations Added *Schinus terebinthifolius* Extract: Evaluation of Quality and Antioxidant Activity. Ferrante LF, Nakano CT, Marinho JMR, Semeao LO, Pierotti SM, Casagrande R Georgetti SR UEL, Dept of Pharmaceutical Science, Health Sciences Center

Introduction: Ultraviolet radiation (UVR) increases the risk of various skin disorders, therefore leading to inflammation and oxidative stress. Several efforts have been made in the search for strategies to avoid oxidative stress generated by sun exposure. Given the background, antioxidants from vegetable origin may represent new options for manage and avoid oxidative stress-mediated disorders. In this sense, *Schinus terebinthifolius* is a plant rich in phenolic compounds, which have antioxidant properties and can provide new opportunities for treatment and prevention of diseases mediated by UVR like photoaging and skin cancer. Therefore, the objective of this work was to develop different semi-solid pharmaceutical forms varying lipid content, as well as the type of self-emulsifying bases and hydrophilic colloids added 5% of *S. terebinthifolius* leaves extract (SE) and to evaluate their physicochemical and antioxidant activity (aa) by DPPH and ABTS tests. **Methodology:** Eight semi-solid formulations (F1-F8) for topical use were developed using the phase inversion technique. Oil (O) and water (W) phase were heated separately at 70 °C. After the fusion of the solids, W phase was poured over O phase and mixed under constant agitation until the temperature reached 45 °C. After 24h, the SE (5.00%) was incorporated to the formulations at the room temperature. The formulations were stored sealed and protected from light and moisture for 24 hours at a controlled room temperature, before being submitted to subsequent tests. They were submitted to the centrifugation test, pH value, organoleptic evaluation (appearance, color and odor) and spreadability. In order to verify if F1-F8 were able to maintain the aa potential, the results were compared to ethanolic solution of SE in the same concentration in the reaction medium. **Results:** The chromatographic analysis confirmed the presence of secondary metabolites in the extract, validating the beneficial effects on the skin, potentially protecting and/or preventing oxidative damage caused by UVR exposure. All emulsions remained stable, showing no signs of physical instability even under centrifugation. Moreover, the pH values demonstrated compatibility with the pH of the skin. The spreadability of the formulations increased with the addition of weights, which suggests good spreadability and high yield. Regarding the aa, different responses were observed between the methods used, possibly due to their mechanism of action being different, as well as the possibility of interactions between the components of the extract and formulation. **Conclusion:** The developed semi-solid formulations containing *S. terebinthifolius* extract desmonstrated favorable properties and has the potential to serve as a topical antioxidant source for reducing oxidative damage in the skin.

09.039 Antioxidant Activity Evaluation, Prevention of Lipid Peroxidation and Voltammetric Analyzes of *Solanum lycocarpum* St. Hil. Gonçalves EER, Batista RAO, dos Santos CVE, Horta VQ, Braz HFG, Lemos AF, de Oliveira EJ, Rodrigues AP, Malagutti AR and Oliveira TS UFVJM, Dept of Pharmacy, Lab. of Experimental Pharmacology, FCBS, Diamantina, MG, Brazil

Introduction: Oxidative damage, often caused by reactive oxygen species (ROS), is known to contribute to neuronal damage and neurodegenerative disorders. Brain tissue is particularly susceptible to this type of damage, which can result in lipid peroxidation. This process can lead to the inhibition of neurotransmitter production, including acetylcholine, which plays a vital role in memory and learning [1, 2]. In this sense, this study aimed to evaluating voltammetric determination, antioxidant activity, and prevention of lipid peroxidation and a future level of experiments to analyze the anticholinesterase activities as well as neuroprotective effects of *S.lycocarpum* leaves hydroalcoholic extract (SLHE), in order to provide new information on the potential use of this plant against neurodegenerative disorders. **Methods:** *S.lycocarpum* leaves were collected in March 2023 in Diamantina, Minas Gerais, Brazil. Registration SisGen A88B22D. SLHE was prepared according to Thomaz DV (2018) [3]. The voltammetric experiments were performed in an electrochemical cell with the Ag/AgCl used as reference, a Pt foil as counter and the glassy carbon electrode (GCE) as working electrodes. The analysis was carried out in 0.1 mol L⁻¹ PBS (pH = 7.0) contained the SLHE and using a Autolab potentiostat/galvanostat. The electrochemical behaviour of the SLHE was investigated by cyclic voltammetry over the potential range from -0.1 to +1.0 V at scan rate (ν) of 100 mV s⁻¹. The cyclic voltammogram of 6.3 x 10⁻² mg/mL gallic acid solution in 0.1 mol L⁻¹ PBS (pH = 7.0) was also recorded at the same ν and potential range. The free radical scavenging activity was determined spectrophotometrically by reaction with 2,2-diphenyl-1-picrylhydrazyl (DPPH). TBARS levels were based on the reactivity of an end product of lipid peroxidation, malondialdehyde (MDA) with thiobarbituric acid (TBA) to produce a red adduct. The samples (homogenate of cerebral tissue) were incubated with SLHE (1, 3 and 10 mg/mL) or gallic acid 2 mg/mL for 1 hour, induced lipid peroxidation at 100°C for 15 min in acid medium and, thereafter, were centrifuged 30000 x for 10 min, and the reaction product was determined at 535nm. The level of lipid peroxides was expressed as nmoles of MDA released/mg protein. Gallic acid was used as standard. Experiments with animal tissue were conducted in accordance with the Conselho Nacional de Controle de Experimentação Animal (CONCEA) and were approved by the local Ethics in Research Committee (Protocol CEUA/UFVJM n^o 14/2020). Data are presented as mean \pm SEM of 7-9 experiments and analysed by Student's t-test or one-way ANOVA statistical tests when appropriate. P values less than 0.05 were considered significant. **Results and Discussion:** The cyclic voltammogram registered for the SLHE shows two anodic peaks with Epa1 = 0.22 V and Epa2 = 0.62 V, respectively. These anodic peaks are correlated to the oxidation of the species presents in the extract. Also, these oxidation peaks are indicative of the presence of polyphenolic compounds that possess antioxidant properties in the sample. The low Epa measured for the SLHE, when compared with the gallic acid ((Epa1 =0.36 V) indicate a higher antioxidant power of the species presents in the extract. As the concentration of SLHE is increased the levels of MDA decrease proportionally at concentrations of 1, 3 and 10 mg/mL (0.220 \pm 0.007, 0.121 \pm 0.003 and 0.105 \pm 0.004 TBA-RS per mg of protein, respectively) and the positive control at 2 mg/mL, showed 0.116 \pm 0.002 TBA-RS per mg of protein. Taken together, these results indicate that *S.lycocarpum* leaves may represent a prospective approach to neuroprotective assays and a possible candidate to reverse neuronal death. **Financial Support:** Coordenação de Aperfeiçoamento de Pessoal de Nível Superior (CAPES) and Conselho Nacional de Desenvolvimento Científico e Tecnológico (CNPq). **References:** [1] C. Cheignon *et al.* Oxidative stress and the amyloid beta peptide in Alzheimer's disease, *Redox biology* 14 (2018) 450-464. [2] F. Tang *et al.* The effects of melatonin and Ginkgo biloba extract on memory loss and choline acetyltransferase activities in the brain of rats infused intracerebroventricularly with beta-amyloid 1-40, *Life sciences* 71(22) (2002) 2625-31. [3] D.V. Thomaz *et al.*

Antioxidant and Neuroprotective Properties of *Eugenia dysenterica* Leaves, Oxidative medicine and cellular longevity 2018 (2018) 3250908.

09.040 Topical Preclinical Therapeutic Efficacy of a New Full-spectrum Cannabis Oil for Skin Diseases. Souza MHB¹, Ortega LYM¹, Maso JM¹, Kava J², Araújo FS², Stern CAJ¹, Otuki MF¹, Cabrini DA¹. ¹UFPR, PPG Pharmacology, Curitiba, Brazil. ²Lab. REAJA, Curitiba, Brazil

Introduction: A wide variety studies highlight the therapeutic potential of *C. sativa* products and its phytocannabinoids for a variety of skin conditions, including acne, atopic dermatitis, psoriasis, itching and pain. However, almost no studies have verified the topic effect of these products on the skin. The present study was carried out with the aim of evaluating the topic effect of a full-spectrum cannabis oil (OF) in mice. **Methods:** The tested OF was provided by Aura Pharma (Curitiba, Brazil, Lot #034), and prepared from dry leaves of *Cannabis sativa*. The effects of OF were evaluated in a model of skin inflammation with multiple applications of TPA (12-O-tetradecanoylphorbol-13-acetate), for 9 days, topically and intraperitoneally; and in a model of psoriasis induced by imiquimod (IMQ), topically (7 days), in C57BL/6 mice, with n between 3 and 8 animals (CEUA: #1479). In the TPA model, ear edema, histology and animal welfare were evaluated. In the IMQ model, psoriasis severity (PASI), spontaneous pruritus, animal welfare and histopathological analysis were analyzed. **Results:** Ear edema caused by multiple applications of TPA (2.5 µg/ear/20 µL) was reduced by topic OF 10% and 20%, and by intraperitoneal (IP) OF (10 mg/kg) from the 4th day onwards of application and lasted until the end of the experiment (9th day). Ear thickness and cellular infiltrate showed significant improvement in all treatments, while epidermal thickness significantly reduced for topic OF 10 and 20%. The evaluation of animal welfare showed a better nesting score with topic OF 20%. In the IMQ model, the OF cream 20% caused a reduction in the score in relation to the control, from the fourth day of the experimental protocol, in the evaluation of the PASI score (erythema, desquamation and scarification). Histological analyzes demonstrated more pronounced epidermal cellularity and thickness in IMQ and vehicle groups, while treatments with OF cream 20% and reference drug promoted less cellular infiltration and reduction of epidermal hyperplasia induced by IMQ. In the evaluation of animal welfare, there were no significant differences between treatments, while in the evaluation of spontaneous pruritus, there was an improvement for the group treated with OF cream 20%. **Conclusion:** Our study demonstrates that in OF used topically shows great potential for the treatment of various pathological skin conditions. **Financial Support:** INCT-INOVAMED, CAPES and CNPq

09.041 *Arrabidaea chica* (Humb. & Bonpl.) B. Verlot: Overview of the Ethnopharmacology, Phytochemistry and Biological Properties. Raiol da Silva MC, ReisLDS², Silva SCS, Luz DA, Maia CSF, Fontes-Júnior EA ICS-UFPA-UFPA, Belém, Pará, Brazil, Faculty of Pharmacy, Lab. of Pharmacology of Inflammation and Behavior, Belém, Pará, Brazil

Introduction: *Arrabidaea chica* (Humb. & Bonpl.), a erect tree popularly known as 'pariri' or 'crajiru', is commonly found in the Amazon and traditionally used to treat inflammation, wounds, ulcers, and fungal infections. The present study aimed to review the evidence available in the scientific literature on its traditional use, phytochemical constitution and pharmacological properties.

Methodology: Articles available in the PUBMED, SCIELO, SCOPUS and Google Scholar databases were selected based on the descriptors "Bignoniaceae or Bignoniaceae; *Arrabidaea chica* or Arrabidaea; Therapeutic Properties or Therapeutic Actions; Traditional Medicine or Traditional Therapeutics". **Results:** Phytochemical studies indicate the presence of flavonoids, especially anthocyanidins in *A. chica* extracts. Its toxicity (ethanolic extract) was evaluated in *Artemia salina*¹, in rats (oral; up to 3.5 g/kg) and mice (intraperitoneal; up to 2 g/kg)², showing no toxic effects. The study of its bioactive properties has shown its antioxidant activity, reducing the capacity to reduce the inflammation induced by snake venom suggesting a possible action of substances present in the aqueous extract from *A. chica* inhibiting toxins that induce these two pro-inflammatory processes and/or inhibiting endogenous factors that stimulate both pro-inflammatory processes³, the inflammation and nociception associated with osteoarthritis, possibly by COX inhibition⁴, and neuropathic nociception associated with sciatic nerve compression¹²; and its potential for wound treatment, showing *in vitro* and *in vivo* induction of fibroblast proliferation, increased collagen production and improved healing⁵⁻⁷. Activity has also been demonstrated against several types of infectious agents, including bacteria (*Salmonella typhimurium*, *Lactobacillus acidophilus*, *Escherichia coli*, and *Shigella sonnei*)⁸, fungi (*Candida albicans*)⁹ and protozoa (Leishmania and Trypanosoma)¹⁰. Additionally, antitumor¹¹ and antihypertensive¹ activity were evidenced. **Conclusion:** The knowledge accumulated in the scientific literature demonstrates that the medicinal species *Arrabidaea chica* has multiple activities, related to different mechanisms and, possibly, different phytoconstituents, presenting great potential for application in therapeutics for the treatment of infectious and non-communicable diseases, requiring additional studies, in order to better characterize its phytochemical and pharmacokinetic properties, elucidate its mechanisms of action, and validate its use in the future. **References:** ¹Cartagenes, MSS. Ciênc. Sau. v.16, n.2, p.98, 2014. ²Amaral RR. Lat. Am. Pharm., v.31, n.3, p.451, 2012. ³Oliveira, DPC. Braz. J. Pharm. v.19, n.2, p.1, 2009. ⁴Vasconcelos, CC. Int. J. Mol. Sci. v. 20, n.19, p.47, 2019. ⁵Salles, THC. Biomed. Mater. v.15, n. 16, p.1, 2020. ⁶Jorge, MP. Ethnopharm. v.118, n.1, p.361, 2008. ⁷Lima, LL. Mat. Sci. Eng. v.100, n.1, p.493, 2019. ⁸Ferreira, FAG. Ass. Bras. Inc. ciên. v.1, n.1, 2013. ⁹Brandão, CMM. Res. Soc. Dev. v.10, n.13, p.1, 2021. ¹⁰Silva-Silva, JV. Front. Pharm. v.12, n.1, p.1, 2021. ¹¹Ribeiro, AFC. Braz. J. Pharm. v.22, n.2, p.364, 2012. ¹²Lima, FCVM. Neur. Dis. Current. Res. v.2, n.2, p.1, 2022. **Financial Support:** FAPESPA.

09.042 Metabolic associated fatty liver disease: a challenge to the ethnopharmacological use of *Croton urucurana*. Silva GR¹, Albuquerque ER¹, Gasparotto-Junior A², Lívero F³. ¹Unipar Lab. of Pre-Clinical Research of Natural Products, Graduate Program in Animal Science with Emphasis on Bioactive Products, ²UFGD, Lab. of Cardiovascular Pharmacology, ³UFPR, Lab. of Cardiometabolic Pharmacology

Introduction: Metabolic associated fatty liver disease (MAFLD) results from the accumulation of fat in the liver, which can progress to serious complications, such as cirrhosis, liver failure and cellular hepatocellular carcinoma. It is estimated that MAFLD affects a quarter of the world's population and, despite studies for the development of new therapies, consistent drug treatments have not yet been established. In the search for new agents, *Croton urucurana* Baill., a plant widely used in traditional medicine and popularly known as 'sangra-d'água', stands out. Its leaves, bark and sap are used in the treatment of gastrointestinal, cardiovascular and endocrine diseases due to its anti-inflammatory, anti-ulcerogenic, anti-diarrheal, healing and hepatoprotective potential. However, the pharmacological efficacy of *C. urucurana* against MAFLD had not yet been investigated, justifying this study. **Methods:** To prepare the extract, leaves of *C. urucurana* were collected in the urban perimeter of Dourados, Mato Grosso do Sul, Brazil ("22°20.9299'South, 54°83.7713 West). An exemplary specimen (no. 5536) was deposited in the Herbarium of UFGD, and the study was registered in the National System of Genetic Heritage Management and Associated Traditional Knowledge (SisGen, no. A9CDAAE). Female Spontaneously Hypertensive Rats were divided into 5 groups ($n = 8$), received a 0.5% cholesterol-enriched diet and were exposed to cigarette smoke (9 cigarettes/day), for 10 weeks. During the last 5 weeks, the animals were orally treated daily with vehicle (filtered water; negative control group [C-]), ethanol-soluble fraction of *C. urucurana* (30, 100 and 300 mg/kg) or with enalapril and simvastatin (SIM+ENAL, two standard reference drugs that are commonly used to treat dyslipidemia and hypertension, respectively). One group of rats that were not exposed to these risk factors was also evaluated (basal group). Blood sample was collected for the analysis of cholesterol, triglyceride, alanine aminotransferase (ALT), and aspartate aminotransferase (AST) levels. The liver was collected for lipid quantification and was also processed for redox status and histopathological analysis. **Results:** Compared with the basal group, hypertension, dyslipidemia and smoking increased plasma and hepatic levels of total cholesterol and triglycerides (429% and 203%, respectively), as well as AST and ALT plasmatic levels in C- group. Regarding the tissue redox status, hepatic oxidative stress was observed, reflected by a decrease in reduced glutathione levels and an increase in lipoperoxidation and superoxide dismutase activity in C- group. Histopathological analysis indicated steatosis and massive lesions. Treatment with the *C. urucurana* extract (300 mg/kg) and SIM+ENAL decreased plasma and hepatic lipid levels. In contrast to SIM+ENAL, treatment with *C. urucurana* (300 mg/kg) reduced AST and ALT levels. Treatment with *C. urucurana* (300 mg/kg) completely reversed histopathological and oxidative changes, while the other doses of the extract and SIM+ENAL showed a partial effect. **Conclusion:** *Croton urucurana* extract exerted a promising lipid-lowering and hepatoprotective effect in an animal model of MAFLD. **Financial Support:** PROSUP-CAPES, CNPq and UNIPAR. **References:** Eslam, M. Gastroenterology, v. 158, p. 1999-2014, 2020. Tilg, H. Nat Rev Gastroenterol Hepatol, v. 17, p. 387-388, 2020. Coelho, F.C. J Relig Health, v. 58, p. 572-588, 2019. de Matos Cândido-Bacani, P. Toxicol Lett, v. 273, p.44-54, 2017.

09.043 Acute Pain and Edema Attenuation in Mice Treated with Essential Oil obtained from *Bulnesia sarmientoi* Lorentz Ex Griseb. Giesbrecht Toews, AC; Arrúa Báez, WJ; Hellión-Ibarrola, MC; Ibarrola Diaz, DA Universidad Nacional de Asunción, Depto de Farmacología. Facultad de Ciencias Químicas, San Lorenzo, Paraguay

Introduction: The use of opiate agonists, glucocorticoids, and non-steroidal anti-inflammatory drugs in the treatment of pain and inflammation has been associated with adverse reactions since its development. This fact has directed the search for agents with such properties toward medicinal plants. *Bulnesia sarmientoi* Lorentz ex. Griseb. (BS) is a tree native to the South American Gran Chaco and Native peoples have reported traditional uses of the hot infusion of wood sawdust as a blood purifier, sudorific, diuretic, and soothing for various conditions caused by pain and inflammation. The essential oil is mainly composed of sesquiterpene derivatives, such as the tertiary alcohols guaiol and bulnesol. Previous studies on various extracts indicate various pharmacological activities, including anti-inflammatory activity in vitro. This work proposes to determine the influence of the oral administration of the essential oil of *B. sarmientoi* on the nociceptive pain induced by thermal stimulation in the legs and tail, on the sub-plantar inflammation induced by carrageenan, and on the auricular inflammation induced by topical application of 13-acetate-12-O-tetradecanoylphorbol (TPA) in mice.

Materials and Methods: Induced nociception models employing thermal stimulation as the noxious agent (hot plate and tail flick by immersion in hot water) were used to study the potential antinociceptive activity in mice. For the study of the potential anti-inflammatory effect, models of induced edema in mice were used, via intra-plantar injection of carrageenan and topical auricular application of TPA. **Results:** The essential oil of the wood was shown to be safe and well tolerated orally and topically. A significant increase in the pain threshold was obtained in the thermally induced pain tests in the paws (98% compared to the negative control; $p < 0.001$) and tail (103%; $p < 0.01$) of animals treated with doses of 500, 750 and 1000 mg/kg of the essential oil, an effect compatible with a clear antinociceptive activity. In addition, a significant reduction of carrageenan-induced plantar edema (19%; $p < 0.01$) and edema by topical application of TPA in ears (38%; $p < 0.01$) of mice was observed, with effects consistent with an anti-inflammatory effect. **Conclusion:** The essential oil of BS was shown to be safe (up to 3000 mg/kg) and well tolerated orally and topically. It denotes the ability to increase the pain threshold consistent with the antinociceptive effect and the ability to reduce induced edema in harmony with anti-inflammatory activity. We do not know the molecular mechanisms responsible for effect observed, but we speculate that at least partially, an agonism on opioid receptors could be responsible for antinociception. In addition, inhibiting the synthesis of prostaglandins and other mediators catalyzed by the arachidonic acid pathway could possibly be responsible for the anti-edema action in mice. This research was primarily self-funded by the main author, with additional support provided by the resources available at the Facultad de Ciencias Químicas de la Universidad Nacional de Asunción

09.044 Comparative Venom Proteomes and Biochemical Profiles of Four South American Species of Rear-Fanged Snakes (Dipsadidae). Bonilla KAT¹, Bayona-Serrano JD², Hyslop S¹ ¹Unicamp Dept of Translational Medicine, Faculty of Medical Sciences, Campinas, SP, Brazil ²Ibu, Lab. of Applied Toxinology, São Paulo, SP, Brazil

Introduction: Compared to venoms of the families Elapidae (cobras, coral snakes, kraits, mambas and Australian elapids) and Viperidae (vipers and pitvipers), those of the Superfamily Colubroidea ('colubrids') remain poorly studied. However, compositional and functional studies of these venoms have shown a similar molecular diversity of toxins, lethal potencies and biological activities to elapid and viperid venoms, with several putative toxins being specific to this superfamily. Despite the diversity of South American colubrid species, few of these venoms have been studied in detail. In this work, we compared the proteomes and biochemical activities of venoms from four 'colubrid' species from Colombia: *Erythrolamprus bizona* (EB), *Erythrolamprus melanotus* (EM), *Leptodeira ornata* (LO) and *Pseudoboa neuwiedii* (PN). **Methods:** The biochemical characterization involved analyses by SDS-PAGE, gelatin zymography, reverse-phase and size exclusion high performance liquid chromatography and enzymatic assays in the absence and presence of selective inhibitors. Proteomic analyses involved shotgun/in gel digestion LC-MS/MS with data processing using the software PEAKS in conjunction with a database of snake sequences in Uniprot and unpublished specific transcriptomic databases. **Results:** The chromatographic and electrophoretic profiles of LO and EM were similar to each other, with >20 electrophoretic bands of 15-90 kDa, whereas those of PN and EB were simpler (~10 electrophoretic bands, 15-80 kDa). All the venoms showed gelatinolytic activity, with that of LO being the least potent. All venoms were highly proteolytic (azocasein) and fibrinogenolytic, with both activities being inhibited by EDTA (metalloproteinase inhibitor) but not by AEBSF (serine protease inhibitor). Only PN venom had PLA₂ activity, and all the venoms were devoid of esterase and L-amino acid oxidase. Proteomic analyses revealed different compositional patterns among the venoms: LO venom contained mainly P-III class snake venom metalloproteinases (SVMPs, 79%), C-type lectins (10%), cysteine-rich secretory proteins (CRISPs) (6%) and peptides (bradykinin-potentiating peptides and C-type natriuretic peptides) (5%). PN venom consisted mainly of P-III class SVMPs (57%), endogenous matrix metalloproteinases (10%), CRISPs (20%) and C-type lectins (13%). This venom was the only one with PLA₂ and PLA-B. EM and EB venoms had similar compositions that consisted mainly of P-III class SVMPs (50%), snake venom matrix metalloproteinases (svMMP, 40%) and CRISPs (10%). **Conclusion:** These results indicate that the main components of these venoms are metalloproteinases, with *Erythrolamprus* spp. containing mainly svMMPs found only in 'colubrids'. PN venom contained PLA₂, an uncommon component in 'colubrid' venoms. The role of most of these components in envenoming by these species is unknown. **Acknowledgment:** We thank the staff of the Life Sciences Core Facility (LaCTAD, UNICAMP) for the proteomic analyses and partial data analysis. **Financial Support:** This work was supported by CAPES (KATB; Finance code 001) and CNPq (SH; grant no. 313273/2018-9).

09.045 **Evaluation of the Hypoglycemic Effect of Curcumin and Micronized Curcumin in Diabetic Animals.** Schindler MSZ¹, Barufke M¹, Cort TD¹, Souza MA¹, Almeida MOP¹, Zanatta L², Magro, JD¹. ¹Unochapecó, Brazil, ²Udesc, Brazil

Introduction: *Diabetes mellitus* (DM) is a multifactorial metabolic disorder characterized by hyperglycemia. To increase the range of available treatments and considering the use of medicinal plants, curcumin (CURC), the major constituent of *Curcuma longa* L. has been studied due to its pharmacological properties. However, the main obstacle in its use is the low solubility, directly affecting the pharmacological effect. Micronization by supercritical CO₂ antisolvent (GAS) is a process with high potential for innovation, capable of increasing the solubility of CURC without harming the environment. The objective was to analyze the hypoglycemic potential of curcumin and micronized curcumin (MC) in diabetic animals.

Material and Methods: Micronization of CURC occurred employing the methodology of Aguiar (2016), with some modifications, using carbon dioxide as an antisolvent. Before the micronization process by GAS, CURC was dissolved in acetone (33.33 mg/mL) and the temperature and pressure parameters were set at 40 °C and 100 bar, respectively. The *in vivo* experimental protocol was approved by CEUA/UNOCHAPECÓ (015/2020) and male Wistar rats (45-60 days) were used. The induction of DM occurred by two intraperitoneal application of alloxan (120 mg/kg). On the seventh day, glycemia was checked to prove the diabetic state. The animals considered diabetic were distributed in the different experimental groups (n=6): diabetic control (DC) received tween 1%; diabetic treated with CURC at doses of 50, 100 and 250 mg/kg; diabetic treated with MC at 250 mg/kg; diabetic treated with insulin glargine (2-2.5 U/Kg). In the normal control animals the intraperitoneal applications and treatment was performed with saline. After the groups were divided, the animals received the first dose of the treatment and glycemia were checked 1, 2, and 3 hours after the first administration of the treatment using a glucometer. The treatments were applied until day 14. At day 14 blood glucose was checked, followed by euthanasia and collection of tissues (liver, muscle and intestine) for further analysis. Hepatic and muscle glycogen content was determined using the Krisman (1962) methodo with some modifications (Zanatta, 2008) and the activity of disaccharidases (maltase, saccharase and lactase) was determined according to Pereira (2011). Statistical analyses were performed using one-way or two-way ANOVA analysis followed by Bonferroni post-test. **Results:** The MC treated group showed a significant reduction in blood glucose and a significant increase in liver and muscle glycogen content when compared to the DC group at day 14. However, blood glucose and liver and muscle glycogen content were not affected at any of the tested doses of CURC. About the activity of disaccharidases, no inhibition was observed in any of the tested treatments. **Conclusions:** It was possible to observe hypoglycemic effect by the reduction of glycemia and increase of hepatic and muscle glycogen content only with MC. We emphasize that this is a preliminary study and further analysis is needed to investigate the effect of curcumin and MC on the metabolism of diabetic animals. **Acknowledgments:** UNOCHAPECÓ/UNIEDU, **References:** Aguiar, et al. *Ind. Crops Prod.*, v.89, 2016. Krisman, *Anal. Biochem.*, v. 4, 1962. Pereira, et al. *Nutrition*, v. 27, 2011. Zanatta, et al. *J. Nat. Prod.*, v.71, 2008.

09.046 **Ability of Doxycycline to Antagonize Bothrops Snake Venom Activities.** Cesar MO^{1,2}, Nogueira-Souza PD¹, Rocha-Junior JRS¹, Gomes-da-Costa PI¹, Granja-Santoro GPA¹, Monteiro-Machado M¹, Strauch MA¹, Melo PA¹ ¹ICB-CCS-UFRJ, Lab. de Farmacologia das Toxinas, Programa de Farmacologia e Química Medicinal, Rio de Janeiro, RJ, Brazil, ²IVB, Niterói, RJ-Brazil

Background: Crotalid snakebites induce local and systemic tissue damage which are associated with edema, the hemorrhage and myonecrosis that could result in permanent incapacitated sequels. Thus, could be prevent by the specific or polyvalent antivenoms, however, some tissue damage as the skin necrosis and myonecrosis are partially protected. Most of these viperid snake venoms are rich of active enzymes that can mainly, induce hemorrhage, edema and disturbed the blood coagulation. Many of these enzymes were isolated and characterized and there are a great number of metalloproteinases. It is relevant to investigate and develop new antivenoms that would help in the therapies of snakebite. Doxycycline is a tetracycline a antibiotic that have been described in the literature, not only as antibiotic, but also with various other uses such as being able to induce anti-inflammatory effect is also considered an inhibitor of Extracellular Matrix Metalloproteases (MMPs).

Methods: The effect of doxycycline on *in vitro* proteolytic activities was evaluated through the caseinolytic and collagenase activities of *Bothrops jararaca*, *Bothrops jararacussu* and *Bothrops atrox* venoms. These tests were performed with preincubation of 10 e 30 µg/mL of venom in the caseinolytic and collagenase assay, respectively, with different concentrations of doxycycline (10 and 30 µM) in both tests. The results of those enzymatic assays were obtained through the absorbance of different samples that was measured using a spectrophotometer. To investigate if doxycycline would be able to modulate the hemorrhage or the edematogenic activity of *Bothrops* venom, mice received intradermic injection of 1 mg/kg of each venom, as Melo et al., (1994). To estimate the edema, intramuscular injection on back of thigh muscle of venom (1 mg/kg) or venom preincubated with doxycycline (10 mg/kg). The thigh area (mm²) of the animals was measured with a caliper before the injection and 15, 30, 60, 90, 120 and 150 minutes after and by these areas were estimated the edema.

Results: The experiments showed that doxycycline was effective in reduce the proteolytic activity of *Bothrops* venom on substrates tested. The concentration of 10 µM of doxycycline was not able to decrease caseinolytic activity, but 30 µM inhibited 90% of this activity. On the collagenase assay, 10 µM of doxycycline neutralize 25 % and 30 µM inhibited 45 % of this activity indicating an ability to antagonize collagenase activity in a concentration dependent manner. In the experiment evaluating hemorrhage and edema activities doxycycline antagonized in all of tested mice, the hemorrhage and edema size in the dose of 10 mg/kg.

Conclusions: Our data show a relevant effects of doxycycline inhibition on venom proteolytic effects as well as on the hemorrhage and edema that is indicating this tetracycline as a potential agent on snakebite by crotalid snakes and help on regular therapy with the antivenoms. Further experiments are still needed to assess the neutralization of snake venom. Financial Support - FAPERJ; CAPES & CNPq

09.047 Anti-Inflammatory Properties of Alcoholic Fraction of *Agave sisalana* Residues.

Fracasso JAR¹, Costa LTS¹, Ferreira FY², Guarnier LP³, Ribeiro-Paes JT³, Bittencourt RAC⁴, Santos L. ¹FOA-Unesp-Araçatuba, PGG Biomaterials Sciences, Araçatuba, Brazil, ² Unesp-Assis, Dept of Biotechnology, São Paulo State University, Assis, Brazil, ³FMRP-USP, Dept of Genetics, Ribeirão Preto, Brazil ⁴ Unip-Assis, Dept of Biomedicine, Assis, SP, Brazil

Introduction: The uncontrolled inflammatory response, by promoting tissue death and injury, is known in clinical medicine as one of the main triggering factors of numerous diseases. Sapogenins, a plant secondary metabolite, have been shown to promote the reduction of this uncontrolled response and pain. A plant species with high concentrations of sapogenins in its phytochemical composition is the *Agave sisalana* (also known as sisal). From the leaf of this plant is obtained the hard fiber, it has great commercial value worldwide, but it represents only 5% of its weight, which means that the remaining 95% of the sisal leaf's weight is waste. In Brazil, the world's largest producer of sisal, thousands of tons regarding this plant's residue are generated and discarded at the planting site. Objective: This work evaluated the anti-inflammatory activity of the alcoholic fraction of sisal residue (AFS).

Methods: Initially, the presence of sapogenins in AFS was analyzed. Then, the cytotoxicity of AFS was determined *in vitro* by the MTT assay and the anti-inflammatory activity by the phagocytosis and stabilization of the red blood cell membrane. **Methods:** Finally, in the *in vivo* tests, carried out in Wistar rats, CEUA Process 002/2014, the carrageenan-induced paw edema method was used to evaluate the acute and chronic anti-inflammatory activity of the AFS and the formalin model for the analysis of its analgesic activity, both in the neurogenic and inflammatory phases. **Results:** The AFS phytochemical data confirmed the presence of sapogenins, hecogenin and tigogenin. *In vitro* tests revealed that AFS did not impair the viability of Peripheral Blood Mononuclear Cells (PBMC) ($p < 0.05$) and inhibited phagocytosis by macrophages (AFS 0.5 mg/mL ? $56.00 \pm 5.83\%$, AFS 1 mg/mL ? $64.00 \pm 1.58\%$ and the AFS 2 mg/mL ? $64.00 \pm 1.88\%$), as the positive dexamethasone control 0.05 mg/ml ($45.00 \pm 45.23\%$). Also, the AFS promoted stabilization of red blood cell membrane (AFS 0.5 mg/mL ? $97.53 \pm 0.07\%$, AFS 1 mg/mL ? $97.88 \pm 0.09\%$ and AFS 2 mg/mL ? $98.47 \pm 0.02\%$), such as dexamethasone 0.05 mg/ml ($99.07 \pm 0.18\%$). In *in vivo* studies, from the second hour onwards, the dose of 25 mg/kg of AFS was the only one capable of significantly decreasing paw edema ($p < 0.05$), at all evaluation times, both in acute inflammation and as chronic, confirming the anti-inflammatory activity of this fraction. Furthermore, in the formalin model, the analgesic activity of AFS 25 mg/kg was the closest to the positive control dexamethasone, in the two evaluated phases, neurogenic and inflammatory. **Conclusion:** It is likely that the anti-inflammatory and analgesic activities presented by AFS result from the presence of sapogenins in its phytochemical composition. Based on new phytochemical, pharmacological and toxicological tests, it is possible to predict the development of a new anti-inflammatory herbal medicine based on the thousands of tons of sisal waste that, until now, have been neglected in Brazil.

10. Cancer Pharmacology

10.001 Evaluation of the Effects of an M1 Macrophage Conditioned Medium and its Association with Cisplatin in Lung Cancer Cells. da Silva MM¹, Silva BO¹, Rego MBM¹, Pitta MGR¹, Pereira MC^{1,2} ¹NUPIT-SG-UFPE, ²UFPE, Depto de Fisiologia e Farmacologia

Introduction: Lung cancer is among the most numerous globally and responsible for the highest number of cancer deaths ⁽¹⁾. The tumor develops in an extremely complex microenvironment, where inflammation plays a fundamental role in tumorigenesis and tumor progression. The tumor microenvironment is mostly anti-inflammatory but can be polarized due to the macrophages' plasticity⁽²⁾. The conditioned media by macrophages can present different cytokines, chemokines, and growth factors, making it possible to study, *in vitro*, the effect of these molecules in different tumors. In recent years, immunotherapies aimed at tumor-associated macrophages have emerged; these treatments can act on macrophages' recruitment, survival, and repolarization⁽³⁾. This study evaluated *in vitro* the effects of the pro-inflammatory microenvironment in lung cancer alone or associated with cisplatin. **Methods:** U937 monocytes were differentiated into macrophages by exposure to 100nM PMA and 100ng/mL LPS for 48h. After differentiation, macrophages were seeded in serum-free medium for 24h, the supernatant was used as a conditioned medium (CM). Analysis of the cytokines expressed by the differentiated macrophages was performed previously, IL-1B, and IL-6 were greater expressed, and TNF-a was in a smaller proportion, confirming the pro-inflammatory phenotype. Cell viability of the NCI-H1299 (H1299), and A549 lung cancer cell lines, after being exposed to the CM alone or associated with different doses of cisplatin, were analyzed by MTT assay. Caspase 3, BAX, and caspase 1 gene expression in H1299 cells were analyzed after exposure to CM alone or in combination with cisplatin were analyzed using real-time PCR. Cell cycle of H1299 cells after exposure to CM and cisplatin was analyzed by staining with Annexin/PI by flow cytometry. **Results:** Exposure to CM for 72 hours reduced cell viability by 48,07% in the A549 cell line, and 35,71% in H1299, when compared to the control group. H1299 cells were exposed to cisplatin alone or in association with CM, at a dose of 10uM, it was observed that cisplatin reduced viability by 15,51%, and when the CM was also added, reduced the viability by 43,1% (p<0.001). Preliminary results showed that exposure to CM does not increase the expression of caspase 3 and BAX, genes related to apoptosis. However, there was an increase in the expression of caspase 1, a gene related to pyroptosis, more studies need to be carried out to confirm the results. The results also showed that there was an increase in H1299 cells arrested in the G0/G1 phase of the cell cycle when exposed to CM in association with cisplatin at a dose of 10uM, compared to the group exposed only to cisplatin. **Conclusion:** Exposure to a CM managed to reduce the cell viability of A549 and H1299 cells, in addition to potentiating the action of cisplatin at lower doses on viability and cell cycle. The death pathway related to the reduction in viability caused by the CM is not apoptosis. More studies need to be carried out to clarify whether the related death pathway is pyroptosis or another. **Financial Support:** This project was developed with the support of CNPq and FACEPE. **References:** Sung, H. *CA Cancer J Clin.* v.71, p.209, 2021. Anderson NM, *Curr Biol.* v.30, p.921, 2020. Roma-Rodriguez C, *Int J Mol Sci,* v.20, p.840, 2019.

10.002 Thiophene Derivatives Inhibited Cell Viability of Lung Cancer Cells. Nascimento ACM, Menezes EB, Carvalho VM, Silva BO, Pereira MC NUPIT-SG-UFPE

Introduction: Lung cancer is one of the most common causes of cancer-related deaths. It is also the leading cause of cancer death among men and the second leading cause of cancer death among women worldwide, with approximately 80% of which belongs to non-small cell lung cancer (NSCLC). In complex diseases like cancer, the resistance to chemotherapy in clinical reduces the efficiency of the available treatments, becoming urgent to search for novel molecules (1). Thiophene and its derivatives have surged as an influential scaffold, displaying several different pharmacological properties, including anticancer (2, 3). Therefore, the main goal of this study was to investigate the potential therapeutic effect of thiophene derivatives on lung cancer cells, which is representative of NSCLC. **Methods:** The MTT assay was utilized to evaluate the cellular viability of thiophene derivative compounds. H1299 cells (5×10^3 cells/well) were seeded onto 96-well plates in a final volume of 100 μ L. Soon after, thiophene was added to the medium at a series of different concentrations (10 μ M, 50 μ M, and 100 μ M) for 72 h incubation. Following incubation, 20 μ L MTT (0.5 mg/mL) was added to each well for 3 h reaction. Next, the supernatant was discarded, and the formazan product of MTT reduction was dissolved in 20% of sodium dodecyl sulfate. The optical density was detected at an absorbance wavelength of 570 nm. Solvent vehicle control received 0.1% of dimethyl sulfoxide (DMSO). **Results:** The results showed that thiophene derivative compounds, SB-44, SB-83, and SB-200, inhibited the viability of H1299 cells in a dose-dependent manner. After H1299 cells were exposed to thiophene derivatives for 72 h at a concentration, we observed a reduction in viability, especially for SB-200 and SB-44 (IC₅₀ 48.9 μ M and 57.3 μ M, respectively). SB-83 not showed a good cytotoxicity to lung tumor cancer cells (IC₅₀>100 μ M) wich contain a lateral indole ring. **Conclusion:** In conclusion, our study demonstrated that all thiophene derivative compounds suppressed NSCLC cells H1299 *in vitro*, and exhibited activities of viability inhibition. Furthermore, compound SB-200 showed promising results with 55% inhibition at a concentration of 50 μ M. However, further studies are needed to understand the mechanism by which thiophene derivatives act on lung cancer cells. **Financial Support:** This study is supported by Conselho Nacional de Desenvolvimento Científico e Tecnológico (CNPq), Coordenação de Aperfeiçoamento de Pessoal de Nível Superior (CAPES), Fundação do Amparo a Ciência e Tecnologia de Pernambuco, and Fundação de Desenvolvimento da Pesquisa of Brazil. **References:** 1. Zhong, L. Sig. Transduct Target Ther. v. 6, p. 201, 2021. 2. Zhao, M. ACS Omega, v. 4, p. 8874, 2019. 3. Gad, EM. Molecules, v. 25, p. 2523, 2020.

10.003 Effects of Proteolytic Fraction on Alt Levels and Hematological Profile in Two Murine Colorectal Cancer Models. Nascimento MCA^{1,3}; Batista CL^{2,3}; Cavalcante KDM^{1,3}; Paixão MS³; Melo AAS^{1,3}; Silva IS^{2,3}; Lopes MTP⁴, Ditz D^{2,3} ¹UFPI Biology Dept., ²UFPI, PPG Pharmacology; ³UFPI, Cancerology Lab., ⁴UFMG, Pharmacology Dept

Introduction: P1G10 is a cysteine protease fraction obtained from *V. cundinamarcensis*' latex that exhibits antimetastatic and anti-inflammatory effect in murine colorectal carcinoma (CCR) and in TNBS-induced colitis, respectively. Here, we investigated the ALT levels and hematological profile in two models of CCR treated with P1G10. **Methods:** Dimethylhydrazine (DMH) were administered twice a week (20 mg/kg, i. p.) for ten weeks in Balb/c mice. Then, animals were daily treated with P1G10 (0.3, 3.0 or 30 mg/kg, p.o.) for 21 days. A second CCR model was induced by dextran sulfate sodium (DSS) 2% in drinking water for 7 days followed by a single dose of azoxymethane (AOM) 10 mg/kg, i.p. Alanine aminotransferase levels (LabTest) and hematological parameters were assessed in DMH and DSS/AOM models. **Results:** DMH induction resulted in numerous polipoid lesions distributed along the colon mucosa while the DSS model induced a ponctual carcinomatoid lesion at the same region. DMH and P1G10 treatment did not show statistical difference in ALT levels compared to sham group. In addition, the hematological analysis showed a 62% increase ($p < 0.05$) in platelet count in P1G10 30 mg/kg treated animals compared with P1G10 0.3 mg/kg group. DMH and P1G10 30 mg/kg increased (60% and 75%, respectively; $p < 0.05$) the total leukocytes compared sham group. Although the statistical absence between negative control group and P1G10 30 mg/kg treated animals, the fraction increased the total leukocyte levels near to 9%. Moreover, between the DMH and DSS/AOM models, the last one reduced 57% ($p < 0.01$) total leukocytes compared to DMH group. **Conclusion:** P1G10 has the ability to promote leukocytosis and thrombocytosis, corresponding to immune and healing responses. Furthermore, the absence of hepatotoxic alterations shows the safety profile of the fraction. Regarding the induction models, it was observed that the DMH model has the higher inflammatory profile. **Support:** CAPES and CNPq

10.004 High PI3K-Alpha Expression is Associated with Rectal Cancer, Tumor Staging, and Treatment Modality. Silva RL¹, Conceição JVV¹, Camelo TS¹, Amorim JO¹, Ferreira LMM¹, Alves SG¹, Alcântara LG¹, Quispe CC¹, Freitas GL¹, Gurgel DC², Cunha MPSS³, Lima-Júnior RCP¹, Wong DVT¹. ¹UFC, ²IFCE ³ICC

Introduction: PI3Ks (phosphatidylinositol 3-kinase) enzymes are a group of kinases involved in cell growth, proliferation, and death. The involvement of the PI3K/AKT/mTOR pathway in cancer pathogenesis has been investigated. PI3K expression is a potential prognostic marker for colorectal cancer, but the importance of the specific isoform PI3K-alpha is unknown. This study aims to evaluate the association of PI3K-alpha expression with clinical-pathological variables in colorectal cancer patients. **Methods:** We conducted a cross-sectional observational study with 72 patients diagnosed with colorectal cancer between 2016 and 2018. Clinical data were collected, including gender, age at diagnosis, ICD (International Classification of Diseases), topography, differentiation grade, clinical staging, presence of metastasis and its location, chemotherapy regimen performed, family history of cancer, presence of comorbidities (hypertension and diabetes) and lifestyle habits (smoking and alcoholism). Additionally, we built a tissue microarray and used immunofluorescence to analyze primary tumor samples to determine the percentage of PI3K-alfa expression. Data were analyzed using the statistical software SPSS version 20. Ethics committee approval number: 4.515.891. **Result:** Among the subjects included, 52.8% were male individuals, 55.6% were diagnosed with cancer at age 60, and 58.5% had a family history of first-degree relative with cancer (n=38). According to the topography, 60% of tumors in the rectum presented with a high PI3K alfa expression, contrasting with the colon tumor samples, which mainly depicted a low PI3K-alpha expression (73%, $P < 0.05$). Patients with tumor staging I highly expressed PI3K-alpha, contrasting those with stage II-IV tumors, where low PI3K-alpha predominated ($P = 0.06$). Tumors from individuals (26.2%) that underwent a combination of neoadjuvant plus adjuvant chemotherapy showed high PI3K-alpha expression contrasting with a low marker expression in tumor samples from subjects treated with other chemotherapy modalities ($P < 0.01$). Additionally, PI3K-alpha high expression is positively associated with the absence of diabetes and tabagism ($P = 0.05$). No statistical significance was obtained with patient mortality and other parameters. **Conclusion:** High PI3K-alpha expression is mainly found in rectal cancer patients. The high levels of PI3K-alpha expression are associated with tumor staging and chemotherapy modality. Financial support: Ebserh, FUNCAP, CAPES, CNPq.

10.005 Effects of a 1:1 (CBD:THC) Extract of Cannabis in a Rectal Cancer Patient Undergoing Chemotherapy: A Case Report. Krefta E², Silva EG¹, Nascimento FP¹ ¹Unila, Lab. of Medical Cannabis and Psychedelic Science, Foz do Iguaçu, PR, Brazil; ²Descomplica UniAmérica, Foz do Iguaçu, PR, Brazil

Introduction: Colorectal cancer is an oncological condition that affects the large intestine, including the colon, rectum, and anus. Recommended treatment typically involves a combination of radiotherapy, chemotherapy and/or surgery when necessary. Chemotherapy is widely used in cancer treatment to destroy or inhibit the growth of malignant cells. However, improving the effectiveness and reducing the harmful side effects of chemotherapy remain challenges. Nausea, vomiting, insomnia, pain, and depressive symptoms are common adverse effects associated with this treatment. Recent studies have demonstrated the therapeutic potential of cannabis sativa in alleviating the adverse effects caused by chemotherapy. In this context, the case report investigated the effects of a cannabis sativa extract as an intervention to relieve such chemotherapy-related symptoms. **Methods:** A patient with colorectal cancer undergoing chemotherapy received a THC: CBD (1: 1) extract with a dosage of 5 mg per day as an intervention. Symptoms were assessed using the following scales: SF-36 quality of life questionnaire (SF-36), Morrow Assessment of Nausea and Emesis (MANE), Beck Depression Inventory-II (BDI-II), McGill Pain Questionnaire (MPQ), Pittsburgh Sleep Quality Index (PSQI), and Visual Analog Scale (VAS). Clinical assessments were conducted prior to the treatment (one evaluation) and subsequently evaluated one day after each chemotherapy session, which occurred every 15 days. The patient was evolved over the period of 157 days after the beginning of treatment. **Results:** Compared to the initial assessments, improvements were observed in the following aspects: functional capacity (36%), physical aspects (50%), pain (84%), general health status (25%), vitality (20%), social aspects (3%), emotional aspects (27%), and mental health (30%), as assessed by the SF-36 Quality of Life Questionnaire. The Beck Depression Inventory-II showed an improvement of 18%. Pain symptoms were improved 100% when evaluated by the McGill Pain Questionnaire. The Pittsburgh Sleep Quality index recorded a 38.8% improvement. The Visual Analog Scale for appetite showed a 90% improvement. **Conclusion:** This case report highlights the therapeutic potential of cannabis extract THC: CBD (1: 1) in improving adverse events of the chemotherapy. There was an improvement in quality of life, with decrease in nausea, vomiting, pain, depressive symptoms, and sleep disorder. These results underscore the importance of further research to understand the mechanisms of action and establish appropriate dosages. Therefore, future clinical studies are needed to meliorate our knowledge and explore cannabis as a therapeutic option in chemotherapy. **Protocolo caee** 68733923.3.0000.8527 do comitê de ética em pesquisa da Centro Universitário União Dinâmica Das Cataratas. **Financial Support:** CNPQ and UNILA

10.006 Effect of Aqueous Extract of *Moringa oleifera* Lam Leaves and Benzyl Isothiocyanate on Dimethylbenz[a]Anthracene-Induced Breast Cancer in Rats. Rojas-Armas JP¹, Arroyo-Acevedo JL¹, Palomino-Pacheco M², Ortiz-Sanchez JM³ ¹UNMSM, Section of Pharmacology, Faculty of Medicine, ²UNMSM, Section of Biochemistry, Faculty of Medicine, ³UNMSM Section of Physiology, Faculty of Medicine,

Rojas-Armas JP¹, Arroyo-Acevedo JL¹, Palomino-Pacheco M², Ortiz-Sanchez JM³. ¹Section of Pharmacology, Faculty of Medicine, UNMSM; ²Section of Biochemistry, Faculty of Medicine, UNMSM; ³Section of Physiology, Faculty of Medicine, UNMSM

Introduction: The most common cancer worldwide is breast cancer, which reached more than 2.2 million cases in 2020, with most cases and deaths occurring in low- and middle-income countries (WHO, 2023). *Moringa oleifera* is valued worldwide due to its multiple medicinal uses and is known as the miracle tree (Rode, 2022). The purpose of this study was to evaluate *in vivo* the activity of *Moringa oleifera* Lam aqueous leaf extract and benzyl isothiocyanate against induced breast cancer in rats. Isothiocyanate is the main component of *M. oleifera* and *in vitro* studies have demonstrated its effect against breast cancer cells (Bolanle, 2018; Xiao, 2012). **Methods:** Cancer was induced by administration of 7,12-dimethylbenz[a]anthracene (DMBA) at dose of 60 mg/kg, one-time, orally. A total of 48 rats were assigned to 8 groups (n = 6): Group I, received SSF (control); Group II, received DMBA; the following groups, in addition to DMBA received: Groups III, IV and V, aqueous extract of *Moringa oleifera* leaves at doses of 100, 250 and 500 mg/kg, respectively; and Groups VI, VII and VIII, benzyl isothiocyanate 5, 10 and 20 mg/kg body weight, respectively. Treatment was prolonged for 13 weeks. Data were expressed as mean \pm standard deviation and were analyzed with one-way ANOVA followed by Tukey's post hoc test. **Results:** With moringa extract at a dose of 500 mg/kg an average of 1.67 ± 1.03 tumors were observed, compared to 3.00 ± 1.26 tumors in the DMBA group ($p > 0.05$), producing a reduction of 44%; whereas, with benzylisothiocyanate at a dose of 20 mg/kg there were 2.00 ± 1.67 tumors and the reduction was 33%. The time to tumor appearance (latency) was longer with moringa extract at a dose of 500 mg/kg and with benzylisothiocyanate at 20 mg/kg, being 67.80 ± 9.86 days and 71.75 ± 5.38 days, respectively, compared to 59.83 ± 3.97 days in the DMBA group ($p > 0.05$). Likewise, a reduction in mean tumor weight was observed in each group in a dose-dependent manner; with moringa extract 500 mg/kg the value was 1.05 ± 0.08 g compared to 1.96 ± 1.26 g of the DMBA group ($p < 0.001$) with a reduction in cumulative tumor weight of 70.14%. With benzylisothiocyanate 20 mg/kg, the mean was 0.95 ± 0.03 g ($p < 0.001$ vs DMBA group) and the cumulative tumor weight reduction was 67.56%. In addition, improvement of histological grade evaluated on the basis of tubular differentiation, nuclear pleomorphism and number of mitoses was observed; thus, both moringa at doses of 250 and 500 mg/kg and benzylisothiocyanate 20 mg/kg were grade I compared to grade II of DMBA group. **Conclusions:** *Moringa oleifera* leaves aqueous extract and benzylisothiocyanate showed antitumor effect on induced breast cancer in rats, the effect could be partly related to the flavonoid and isothiocyanate content of the extract. **References:** Rode, SB. v. 14, p. 7, 2022; Sanganna, B. *Int J Curr Pharm Res.* v. 8, p. 54-56, 2016; Bolanle, J. PhD thesis, The State Univ. of N. Jersey, 2018; Xiao, D. *PLoS one* (2012)., v.7, p. e32597. **Financial Support:** Vicerrectorado de Investigación de la Universidad Nacional mayor de San Marcos. Ethics approval: 0154-20.

10.007 Characterization of the Antineoplastic Effects of Cephalochromin in Cellular Models of Acute Lymphoblastic Leucemia. Serra CSM¹, Vicari HP¹, Lima GC¹, Lima K², Nascimento MC², Rego EM², Ferreira MJP³, Costa-Lotufo LV¹, Machado-Neto JA¹. ¹ ICB-USP, Dpt of Pharmacology, Brazil; ²USP, Lab. of Medical Investigation in Pathogenesis and Targeted Therapy in Onco-Immuno-Hematology (LIM-31), Dpt of Internal Medicine, Hematology Division, FM, Brazil; ³ IB-USP, Dpt of Botany,, Brazil

Introduction: Acute lymphoblastic leukemia (ALL) is a malignant hematological neoplasm that originates from mutations in hematopoietic stem cells and affects the precursors of the lymphoid lineage. In adult patients, rates of refractoriness and relapse to current treatments are still high, so new therapeutic options are still needed. In pharmacological therapy, natural products are part of the backbone of ALL treatment, with consolidated examples being vinca alkaloids, doxorubicin, and cytarabine. Cephalochromin is a compound derived from the fermentation of the fungus *Cosmopora vilior* and has antiproliferative and cytotoxic activity through cell cycle arrest in A549 (human lung cancer) cells. Given the above, the present study aimed to investigate the antineoplastic potential of cephalochromin in a broad panel of ALL-derived cell lines. **Methods:** Cell lines derived from ALL Jurkat, MOLT-4, CEM, NALM6, Namalwa, Daudi, Raji, SUP-B15, and REH were exposed to vehicle or increasing doses of cephalochromin (0.001 to 20 μ M) for 72 hours. Jurkat, NALM6, and REH cells were used for time-dependent drug exposure experiments (24, 48, and 72h). The BCL2 inhibitor venetoclax was used as a reference drug. Cell viability was assessed by the methylthiazoletrazolium (MTT) assay. IC₅₀ was established by linear regression and statistical analyzes were performed by ANOVA and Bonferroni post-test and Spearman correlation test using GraphPad Prism software. A p-value < 0.05 was considered significant. **Results:** Cephalochromin treatment significantly reduces the viability of all ALL-derived cell lines in a concentration-dependent manner. IC₅₀ values for cephalochromin ranged from 1.3 to > 20 μ M at the 72 h treatment time. IC₅₀ values for venetoclax ranged from 0.003 to 18.8 μ M at the 72 h treatment time. In the correlation analysis, no association was observed between the IC₅₀ values for venetoclax and cephalochromin ($r = -0.13$, $p = 0.74$), indicating the absence of cross-resistance and suggesting different mechanisms of action between the drugs. Additionally, both cephalochromin and venetoclax showed time-dependent effects on cell viability ($p < 0.05$). **Conclusion:** Our results showed a potential cytotoxic profile of cephalochromin in ALL cellular models. Given the successful history of natural compounds in the therapy of acute leukemias, future studies on the mechanism of action of cephalochromin in this context are of interest. **Financial Support:** FAPESP, CNPq and CAPES.

10.008 Low Cytoplasmic Expression of High-Mobility Group B1 (HMGB1) is Associated with Ulceration, Breslow Index, and Adjuvant Treatment in the Primary Cutaneous Melanoma. Maia IFVC¹, Fonseca MRS², Choquenaira-Quispe C¹, Cajado AG¹, Florêncio KGD¹, Lima-Júnior RCP¹, Wong DVT¹. ¹UFC Fortaleza, Dpt. of Physiology and Pharmacology, Brazil; ²UFC Fortaleza, Walter Cantídio University Hospital, Brazil

Introduction: Primary melanoma is one of the most lethal primary skin neoplasms. Cell signaling disorders contribute to the pathogenesis of this cancer, and the gene expressions of such markers have been ostensibly studied. Therefore, investigating melanoma cell proliferation is critical to understanding tumor promotion and progression. In this sense, the HMGB1 protein is associated with cell proliferation and the development of metastases, mainly in the cell's nucleus. However, in situations of stress, that protein may be displaced to the cytoplasm and extracellular space, participating as a mediator of inflammation and being reported as damage-associated molecular patterns (DAMPs). To evaluate the nuclear and cytoplasmic expression of HMGB-1 in patients with melanoma and its association with clinical and pathological parameters. **Methods:** This is a retrospective and observational study. We included 73 individuals with primary melanoma from 2011 to 2016. Sociodemographic (age, sex, and origin), clinical (anatomical site [trunk and non-trunk], phototype [I - V]), pathological (ulceration, elastosis, Clark [I - V], and Breslow [≤ 2.00 to >2.00 mm]) data were obtained from the patient's electronic medical records. A Tissue Microarray (TMA) was built from paraffin-embedded primary tumor samples to evaluate the HMGB1 labeling by the indirect immunofluorescence technique. We quantified the fluorescence area and counted the HMGB1 cell location (nucleus and cytoplasm) using Fiji imaging software. The Chi-Square or Fisher's Exact tests were used for statistical analysis, with statistical significance set at $p < 0.05$. (Study approval number CEP-UFC nº 5.726.981). **Results:** We evaluated 82 cases of primary cutaneous melanomas in 73 patients. There was a predominance of 63.4% of women (53.25 ± 17.83 years) and 36.58% men (58.5 ± 13.64 years), with a median age of 56 years, mainly from the urban area (78.05%). Among the anatomical sites, the trunk was the most affected body site (63.4%). According to the skin phototype, types II (41.5%) and III (24.4%) were predominant. Regarding the criteria for skin layer invasion or Clark's scale, the most frequent levels of invasion were IV (36.6%) and V (19.5%). At histopathology, ulcerations were observed in 40.24% of the individuals. Additionally, the Clark's scale indicated significant skin invasion ($p=0.04$), which positively associated with HMGB1 expression. The Breslow index was higher in the >2.00 mm stratification, representing 52.4% of the cases. We also found that the low HMGB1 expression positively associates with ulceration, Breslow thickness, and the presence of adjuvant therapy ($p < 0.05$ vs high HMGB1 expressing tumors). Remarkably, no significance was found between nuclear labeling and any of the analyzed variables. **Conclusion:** Low HMGB1 cytoplasmic expression in melanoma is associated with pathological parameters mainly in patients undergoing adjuvant therapy. It suggests the HMGB1 release to the extracellular space to signal as a DAMP. The functional contribution of such finding and its correlation with therapeutic response is yet to be demonstrated. **Financial Support:** FUNCAP, CNPq, and CAPES.

10.009 Increased Resistin Serum Levels Associates with Neoadjuvant Chemotherapy Resistance in Breast Cancer Patients. Freitas GL¹, Quispe CC¹, Florêncio KGD¹, Silva LGF¹, Rodrigues MAP¹, Santos ABM¹, Sousa LSP¹, Silva RL¹, Gadelha EC¹, Cavalcante DIM¹, Silva PGB², Rocha-Filho DR³, Arruda LMA², Lima-Júnior RCP¹, Wong DVT¹. ¹NPDM-UFC, Lab. of Inflammation and Cancer Pharmacology, Center for Drug Research and Development, Brazil; ²Haroldo Juaçaba Hospital, Cancer Institute of Ceara, Brazil; ³Walter Cantídio University Hospital, Brazil

Introduction: Breast cancer (BC) is the type of malignant neoplasm that most affects women in the world. Among the numerous risk factors for the disease, excess adiposity is a behavioral factor directly associated with its development. This relationship may be associated with the chronic inflammatory state resulting from obesity and the imbalance of adipocytokines resulting from adipose tissue. Although there are mechanisms to explain this relationship, the information to understand this biological process is limited. Thus, this work aims to study the association between serum resistin levels and the development of resistance to neoadjuvant treatment in patients with BC. **Methods:** Approved by the Research Ethics Committee under protocol CAAE: 38654820.1.0000.5054. As a sample, we analyzed 81 female patients, aged between 18 and 80 years, with a primary diagnosis of BC, submitted to the doxorubicin/cyclophosphamide (AC) protocol. Patients were analyzed based on clinical and metabolic parameters. We stratified patients according to clinical response into two groups: complete response (CR) and no response (SR). Of these, two blood collections were performed in 67 patients, one before the first neoadjuvant chemotherapy (QN) session and the other after four QN sessions, for resistin dosages that were obtained by enzyme immunoassay (ELISA, R&D System). Data were tabulated in electronic spreadsheets and statistical analysis was performed using the Wilcoxon paired pairs signed rank test and the Mann-Whitney test using Prism® software, version 8.2.1 and SPSS®, version 17.0. **Results:** The mean age of the patients was 51.60 years (± 12.03). When performing the multivariate analysis of the group, we noticed that family history increases the chances of a complete clinical response by 2.45 times, regardless of other parameters, such as serum resistin concentration. Observing the data of the 67 patients included, it was possible to verify that after being treated with QN, the patients showed an increase in serum resistin levels (4565 ± 1136 ; $P < 0.05$) when compared with collections before QN (4376 ± 1207). Furthermore, when examining the data and comparing them with the clinical response, there was no significant difference between chemotherapy-responsive (4623 ± 813.6) and chemoresistant (4550 ± 1207) breast cancer patients. Furthermore, patients with non-QN-responsive breast cancer with serum resistin levels above the median cut-off have higher levels (5582 ± 380.9 ; $P < 0.05$) of the marker when compared to responsive patients (5175 ± 183.5). **Conclusion:** We found, therefore, that high levels of resistin are associated with resistance to QN in patients with BC. **Financial support:** Ebserh, FUNCAP, CAPES, CNPq.

10.010 Friedelin Induces Cancer Cell Death and Attenuates Tumor Angiogenesis in Animals with Ehrlich Ascitic Carcinoma. Silva ELES¹, Silva FA¹, Souza TPM¹, Almeida JH¹, Lucena LCP¹, Silva EC¹, Barreto E¹, Ferro JNS¹. ¹ICBS-UFAL, Maceió, AL, Brazil.

Introduction: Friedelin (FD) is a natural triterpene that shows important biological activities described, which includes the antitumoral potential *in vitro* (SUBASH-BABU. Exp Toxicol Pathol. v.8, p.630, 2017). Data presented in the 53rd SBFTE congress showed that FD reduces tumor progression parameters and the inflammatory infiltrate in the Ehrlich ascitic carcinoma model (EAC). **Aim:** Thus, we investigated FD effect in inducing death to neoplastic cells and modulating the tumor-associated angiogenesis. **Methods:** To achieve that, female swiss mice (10-14 weeks) were injected with EAC cells (5×10^6 ; i.p.) and randomly distributed in groups named: tumoral (TM), 5-fluorouracil (5-FU 200 $\mu\text{mol/kg}$), vehicle (EtoH 2%) and friedelin (FD50 $\mu\text{mol/kg}$). Animals were treated (i.p) from 6th to 10th day after tumoral induction, and 24h after the last treatment they were euthanized (thiopental 200 mg/kg, i.v.) to obtain the ascitic tumor content. Tumor cells were analyzed for cell viability, levels of tumor microenvironment (TME) mediators (tumor necrosis factor - TNF- α and vascular endothelial growth factor – VEGF) using ELISA method, cell death analyses through flux cytometry (kit PE apoptosis detection Annexin V/7AAD) and gene expression analysis of Bcl2 anti-apoptotic protein with RT-qPCR. The results were adopted as significant when $p < 0.05$. **Results:** Tumor cells from animals treated with FD showed membrane and nuclear alterations compatible with those observed in apoptotic cells (membrane bebbing, cromatin condensation and nuclear fragmentation), so we evaluated FD potential to induce cell death to EAC. FD reduced cell viability which was evaluated through trypan blue staining count and induced cell death through apoptosis, attenuating gene expression of the anti-apoptotic protein Bcl2. Cytokine modulation and growth factors in tumor region contribute to the formation of a favorable microenvironment for tumor cells, collaborating to its progression and induction of angiogenesis. Therefore, animals treated with FD demonstrated a 38% reduction in vessel area on the peritoneal region ($p < 0.05$ versus TM). Furthermore, due to TNF- α and VEGF on this context, it was verified that the animals treated with FD presented a 66% attenuation in the levels of the pro-angiogenic factor VEGF, as well as a 22% attenuation in the levels of TNF- α . The decrease in tumor progression due to the modulation of the inflammatory TME, induction of apoptosis and reduction of angiogenic factors led to an increase in the average survival of animals treated with FD, increasing life expectancy on 19.44% in relation to TM group animals. **Conclusion:** The results presented in this study show the pharmacological potential of FD on cancer, as evidenced in our preview studies *in vivo*, specially through the modulation of the TME on EAC model. However, further studies are needed to better elucidate the cellular, biochemical and molecular mechanisms involved in the response of this molecule on the EAC murine model.

10.011 Activity of the Cysteine Protease cms2ms3 and the VLA-4 Integrin Role in Stages of b16f10 Melanoma Metastasis. Leal BS¹, Ferreira LPF¹, Menezes DP¹, Lopes MTP², Sousa JMC³, Ferreira PMP¹, Dittz D¹ ¹UFPI PPG Pharmacology, Brazil; ²UFMG Pharmacology, Brazil; ³UFPI PPF Pharmaceutical Sciences

Introduction: Melanomas are malignant skin neoplasms originating from melanocytes cells. Once established, the primary tumor can invade the layers underlying the skin, initiating the process of metastasis. CMS2MS3 is a cysteine protease from *Vasconcellea cundinamarcensis*' latex that is cytotoxic and impaired adhesion and invasion of murine melanoma B16F10. This work evaluates the effect of CMS2MS3 and the involvement of VLA-4 integrin in B16F10 melanoma metastasis. **Methods:** B16F160 cells were treated for 48 h with 100 ug/mL of anti-VLA4 siRNA to obtain the B16F10-VLA-4-kd cell line. B16F10 and B16F10-VLA-4-kd viability was evaluated by 4% trypan blue exclusion after treatment with 10 µg/mL CMS2MS3 for 24 h. B16F10 or B16F10-VLA4-kd was treated with CMS2MS3 10 µg/mL for 24h. Then, resazurin (10 mg/mL) was added to cells that remained attached and the fluorescence intensity of viable cells was determined at 570/630 nm. After B16F10 or B16F10-VLA4-kd treatment with CMS2MS3 10 µg/mL for 24h, the cells were seeded in fibronectin coated wells and incubated for 2h. Then, adhered cells were stained with 0.5% crystal violet and solubilized with sodium dodecyl sulfate (SDS) 1% for quantification at 570 nm. B16F10 or B16F10-VLA-4-kd cells were seeded in 24-well plates and after 24 hours the cell monolayer was discontinued and exposed to 0.25% FBS, 10% FBS or CMS2MS3 at concentrations of 0.01, 0.1 or 1 µg/mL for 72 hours. Photomicrographs were obtained during the treatment period and the mean time of closing half of the monolayer was calculated using ImageJ. B16F10 or B16F10-VLA-4-kd cells labeled with Calcein-AM treated with CMS2MS3 10 ug/mL for 24h were seeded on plates containing a monolayer of SVEC4-10, after 2h the adhered cells were quantified at 495/515 nm. The B16F10 clonogenicity was assessed after a treatment with CMS2MS3 10 ug/mL for 12h, 24 and 48h. Then, after 10 days, cells were stained with crystal violet as previously described. **Results:** CMS2MS3 10 µg/mL for 24h did not alter significantly cell viability in melanoma that express (B16F10) or not (B16-F10-VLA-4-kd) VLA-4, although it promoted higher deadhesion (70% p<0.05) of B16F10 than B16F10-VLA4-kd. CMS2MS3 reduced in 60% (p<0.001) B16F10 adhesion on fibronectin when compared to untreated cells while this effect was near to 20% (p<0.0001) for B16F10-VLA-4-kd. Compared to B6F10, the adhesion of B16F10-VLA-4-kd on fibronectin was 11% (p<0.01) lower. B16F10-VLA-4-kd cells had an average migration time 54% shorter than B16F10 and the treatment with CMS2MS3 1 µg/mL was not able to change this behavior, indicating that VLA-4 integrin is important for the protease effect. Adhesion of B16F10 treated with CMS2MS3 to SVEC4-10 endothelial cells was reduced by approximately 30%. CMS2MS3 reduced the B16F10 clonogenicity after 12 h (93%), 24 h (86%) and 48 h (>99%) of treatment. **Conclusion:** The results show that CMS2MS3 acts in different stages of metastasis of B16F10 cells, in which the VLA-4 integrin is involved, also presenting itself as a possible target of protease action. **Support:** CAPES and CNPq.

10.012 Antioxidant and Cytotoxic Effect of Extracts of *Libidibia ferrea* on Breast Carcinoma Cells. Menezes DP^{1,2}; Ferreira LPF^{1,3}; Leal BS^{1,3}; Filho ESM⁴; Júnior GMV⁴; Dittz D^{1,2,3} ¹UFPI, Lab. of Experimental Cancerology, Brazil; ²UFPI, PPG Pharmaceutical Sciences; ³UFPI, PPG Pharmacology, Brazil; ⁴UFPI PPG Chemical.

Introduction: Breast cancer is the most prevalent tumor among women worldwide. Despite existing treatments, the effectiveness of cytotoxic chemotherapy is limited for some tumors, such as triple negative breast cancer (TNBC). *Libidibia ferrea*, a plant from Brazilian caatinga and cerrado, has anti-inflammatory, antimicrobial and antioxidant properties that indicate a potential antitumor activity. The aim of this study was to evaluate the antioxidant and cytotoxic effect of hydroalcoholic extracts of the leaves (EHFL) and fruits (EHFR) of *L. ferrea* on the TNBC cell line (MDA-MB-231). **Methods:** Extracts were obtained by exhaustive maceration of the leaves or fruits for 24 hours at room temperature, using 96% ethanol (v/v). Then, the samples were concentrated in a rotary evaporator and on a heating plate at 45°C. Total phenols (in equivalent of gallic acid, EAG) quantification was performed by reacting the extracts (25 to 250 mg/L) with Folin Ciocateu reagent for 30 min. The reduced reagent was quantified at 765 nm. Antioxidant activity was determined by scavenging of DPPH radical, using rutin (isolated flavonoid) and butylhydroxytoluene (BHT) at the same concentrations as positive controls. Cytotoxicity was determined by MTT assay after exposure of MDA cells (3×10^3 /100 μ L/well) to extracts (1.5 to 800 μ g/mL) for 72h. Then, formazan crystals generated by viable cells were solubilized in DMSO and the optical density determined at 570 nm. **Results:** EHFR has a total phenol content three folds higher (486 mg/g EAG) than in EHFL (159 mg/g EAG). The antioxidant effect of EHFR, at all concentrations, was significantly higher than EHFL, achieving three folds level at 150 mg/L. EHFR antioxidant activity was higher than BHT from 200 mg/L and, at 250 mg/L, higher than rutin. The 50% viability inhibitory concentration (IC-50) of MDA cells was 319 μ g/ml for EHFR and higher than 800 μ g/ml for EHFL. **Conclusion:** EHFR and EHFL have antioxidant activity and, probably due to total phenol content, this effect is higher for EHFR extract. The EHFR extract was more potent than EHFL in inhibiting TNBC cell viability.

10.013 Antioxidant Effect of Ascorbic Acid and its Cytotoxic Activity on Murine Breast Adenocarcinoma Cells. Ferreira LPF^{1,2}, Silva ACA^{2,3}, Santos BLB^{3,4}, LEAL BS^{1,2}, Cavalcante KDM¹, Nascimento MCA¹, Menezes DP^{1,3}, Silva MTBS^{2,3,4}, Dittz D^{1,2} ¹UFPI Lab. of Experimental Cancerology, Brazil; ²UFPI PPG Pharmacology, Brazil; ³UFPI PPG Pharmaceutical Sciences, Brazil; ⁴UFPI Lab. of Physiology, Brazil

Introduction: Doxorubicin (DOX) is one of the most effective anticancer drugs to treat different forms of cancer such as breast carcinoma, but its therapeutic usefulness is severely limited by its associated acute or chronic cardiotoxicity. Oxidative stress is related not only to the DOX-cardiotoxicity but also to the cancer etiology. This work aimed to analyze the antioxidant properties of ascorbic acid and its *in vitro* effect on murine breast adenocarcinoma cells as well as to induce the DOX-cardiotoxicity. **Methods:** Ascorbic acid (AA) at 2 - 14 ug/mL had its antioxidant property investigated through the DPPH and ABTS assays. Trolox at 2-14 ug/mL were used as positive control. The AA cytotoxicity was assessed by MTT assay. 4T1 breast carcinoma cells were exposed to AA (20- 0.04 ug/mL) or DOX (6 – 0.012 ug/mL) for 72h. Then, MTT 5 mg/mL was added and formazan crystals generated by viable cells were quantified at 560 nm. The cardiotoxicity was induced by intraperitoneally administration of DOX (3.75 mg/kg) three times a week for 14 days in Balb/c mice. Then animals were submitted to electrocardiogram **Results:** The 50% antioxidant effect (EC₅₀) of AA was 1500 ug/mL and 53.19 ug/mL in DPPH and ABTS assays, respectively. The 50% antioxidant effect (EC₅₀) of Trolox was 14.88 ug/mL and 12107 ug/mL in DPPH and ABTS assays, respectively. The 50% cytotoxicity concentration (CC₅₀) of AA in 4T1 cells was higher than 20 ug/mL. At the same cells, DOX CC₅₀ is 0.47 µg/mL. The animals treated with DOX followed changes compared to the normal control in the parameters: R-R interval (increased of 1.8 folds; p<0.05), heart rate (reduction of 40%; p<0.05), QT interval (increased of 50%; p<0.05), PR interval (reduction of 20%; p<0.05) and QRS interval (increased of 20%; p<0.05), indicating the establishment of cardiac damage through the administered dose. **Conclusion:** Ascorbic acid has antioxidant activity and lower cytotoxicity in breast carcinoma cells. Once the induction of DOX cardiotoxicity is standardized, the antioxidant role of AA could be investigated in this model in association or not with DOX. **Support:** CAPES and CNPq. **CEUA UFPI:** Protocol N^o 723/2022

10.014 Implication of Neuroinflammation Triggered by the Tumor Microenvironment in the Progression of Glioblastoma. Pimentel RS¹, Nóbrega AHL¹, De Sá Coutinho D¹, Santos, ARC2, Martins MA¹, Frozza RL², Bernardi A¹ ¹IOC-FIOCRUZ, Lab. of Inflammation, Rio de Janeiro, Brazil; ²IOC-FIOCRUZ Lab. on Thymus Research, Oswaldo Cruz Institute, FIOCRUZ, Rio de Janeiro, Brazil

Glioblastoma (GBM) represents the majority of glioma incidence, a highly aggressive and invasive grade IV astrocytic tumor. GBM has limited therapies and a high rate of recurrence [1]. The GBM tumor microenvironment (TME) is composed of tumor cells and non-tumor cells, such as tumor-associated macrophages (TAMs) and microglia, which are the most numerous non-neoplastic populations in the TME. The complex heterogeneous nature of GBM cells is facilitated by the local inflammatory TME, which mostly induces tumor aggressiveness and drug resistance [2, 3]. Thus, understanding the pathophysiology in the face of cellular communications present in the tumor microenvironment and neuroinflammation can determine ways to discover new therapeutic strategies. In this context, this study aims to evaluate the role of neuroinflammation in tumor progression in a preclinical model of GBM.

Methods: Intracerebral tumor was induced by injection of 2×10^5 of GL261 GBM cells into the right *striatum* of adult C57BL/6 male mice (8 weeks old, 200-230g) following a procedure adapted from Szatmári T., 2006. The negative control group (Sham) underwent the same procedure and was infused with 2 μ l of RPMI without GL261 cells. Mice were distributed into 4 groups as follows: (1) Sham (SH), (2) Tumor (TU), (3) Tumor + Minocycline (TU+MINO), (4) Tumor + Temozolomide (TU+TMZ). Animals from the TU+MINO group were pre-treated with Minocycline (30 mg/kg I.P. for 5 days before tumor induction), a pharmacological tool as an inhibitor of microglia/TAMs. Animals from the TU+TMZ group were treated with Temozolomide (10 mg/kg V.O. for 5 days after the 10th post-tumor induction) as a standard treatment for GBM. Animals were euthanized at 3, 5 or 15 days post-tumor induction. The brain hemispheres were separated and processed for *Western Blotting* and ELISA analysis. All procedures were approved by the Animal Ethics Commission of the Oswaldo Cruz Institution (CEUA IOC—License L-003/2019-A2 and L-006/2023). **Results:** No significant change in cytokine levels was observed within 15 days after tumor induction. A significant increase in the levels of the inflammatory mediators IL-6, IL-10, TGF- β , TNF- α , IL-1 β , and VEGF were found at 3 days post-tumor induction in brain tissue ($p < 0.0001$). Interestingly, pre-treatment with Minocycline reduced the levels of the cytokines 3 days post-tumor induction ($p < 0.0001$). Western blotting analyses showed an increase in GFAP ($p < 0.001$) and Iba-1 ($p < 0.05$) immunocontent in the ipsilateral hemisphere, indicating reactive astrogliosis and microglial activation, respectively, in the tumor group. Similar to the cytokines, the pre-treatment with minocycline significantly reduced GFAP ($p < 0.001$) and Iba-1 ($p < 0.05$) immunocontent. The results were expressed as the mean \pm SD. ($n = 5$) A two-way ANOVA was used with a Tukey's or followed by Newman-Keuls post test. **Conclusion:** Although more experiments are needed, our data suggest that through cytokines production astrocytes and microglia play a key role in the regulation of neuroinflammation in early stages of GBM development. Financing source: CNPq and FAPERJ (Grants #E-26/201.419/2021 and # E-26/202.807/2019).

11. Clinical Pharmacology, Pharmacokinetics, Pharmacogenomics and Toxicology

11.001 Evaluation of Exposure to Aluminum on Behavioral and Biochemical Parameters in Mice. Ferreira PYO, Uchenna N, Mota R, Okoh VI, Campos HM, Costa EA, Ghedini PC. UFG, Dpt of Pharmacology, Brazil

Introduction: Aluminum (Al) is the most environmentally available metal on the earth's surface and has numerous uses in the food, pharmaceutical, cosmetic and household product industries. However, Al is able to accumulate in tissues that make up the central nervous system (CNS) and its chronic accumulation in the brain induces neuronal death, resulting in deficits in cognition, memory, and behavior. Considering that there is an exponential growth of exposure to Al and its association with neurodegeneration, it is necessary to carry out studies with the aim to observe the effects and consequences of this contact, in order to contribute with information that can promote a better quality of health for the population.

Objective: Evaluate the effects of exposure to different concentrations of Al in mice, mimicking human exposure, at the concentrations to which people were (1 mg/day in 1950), are (30 mg/day) or will be exposed (100 mg/day in 2050), which corresponds to 0.1, 3.5 and 11 mg.kg⁻¹ in mice, respectively. **Methods:** Male Swiss mice (10 – 12 weeks old) were randomized into four groups (n = 10): Control (C); AlCl₃ 0.1 mg.kg⁻¹ (I); AlCl₃ 3.5 mg.kg⁻¹ (II); AlCl₃ 11 mg.kg⁻¹ (III). The C group received distilled water, while other groups received AlCl₃ in the respective doses, for 30 days, by gavage at a volume of 10 mL.kg⁻¹. At the 30th day, animals were submitted to behavioral tests (chimney, rotarod, open field and step-down tests) and twenty-four hours after the last behavioral evaluation, the mice were euthanized and cortex and hippocampus were dissected for biochemical analysis as malondialdehyde (MDA) levels, and catalase (CAT), superoxide dismutase (SOD), acetylcholinesterase (AChE) and butyrylcholinesterase (BuChE) activities. All protocols were approved by the Animal Research Ethical Committee of the Federal University of Goias (process n^o 074/2022). The statistical analysis was performed by one-way ANOVA followed by Dunnett's, considering significant when p < 0.05. **Results:** No differences were observed between groups in the behavioral tests (p > 0.05). However, when compared to the C group, Al promoted significant alterations in the biochemical tests. In the brain cortex, all groups treated with Al (I; II; and III) decreased the SOD (p = 0.0007; p = 0.007; and p = 0.001, respectively) and CAT (p < 0.0001 for all 3 doses) activities. The groups II (p = 0.0064) and III (p = 0.0002) showed an increased in MDA levels, and in AChE (p = 0.0009) and BuChE (p = 0.0171) activities in group III. In the hippocampus, CAT activity decreased in group I (p = 0.005), II (p = 0.01) and III (p = 0.0002), while SOD activity decreased in the group II (p = 0.0309) and III (p = 0.0057). In turn, the AChE and BuChE activities increased in group I (p = 0.0236 and p = 0.0337), II (p < 0.0001 and p = 0.0342), and III (p < 0.0001 and p = 0.0007), respectively. **Conclusion:** The results showed that the exposure to Al for 30 days led to alterations in the oxidative balance and in the cholinergic system, without affecting the behavior of the mice. The implications of these findings, as well as the alterations promoted by exposure to Al for a longer period of time, should be evaluated in further studies. **Financial Support:** CAPES.

11.002 Therapeutic Drug Monitoring of Voriconazole in Oncohematological Patients from Southern Brazil. Petreceli RR¹, Steffens NA¹, Linden R², Schwarzbald AV³, Zimmermann ES⁴, Brucker N^{1,5}. ¹UFSM, PPG Pharmaceutical Sciences, Brazil; ²Feevale, Lab. of Toxicology, Brazil; ³UFSM, Dpt of Clinical Medicine, Brazil; ⁴University of Florida, Center for Pharmacometrics & Systems Pharmacology, USA; ⁵UFSM, Dpt of Physiology and Pharmacology

Introduction: Voriconazole (VCZ) is a broad-spectrum triazole antifungal agent considered a first-line agent for the treatment and prophylaxis of invasive fungal infections (IFI). IFI's are important causes of morbidity in immunocompromised patients, such as oncohematological patients, resulting in longer hospitalization times and higher in-hospital mortality^{1,2,3}. Due to its narrow therapeutic range, therapeutic drug monitoring (TDM) has been recommended for VCZ to optimize clinical results while minimizing toxicity risks^{1,4}. This study aimed to evaluate VCZ trough concentrations in oncohematological patients treated at the University Hospital of Santa Maria (HUSM) as well as analyze possible influencing factors. **Methods:** Patients with hematological diseases in treatment or prophylaxis with VCZ were included. Steady-state trough plasmatic concentrations (C_{trough}) of VCZ were collected 30 min before the next dose and quantified with high-performance liquid chromatography coupled to a photodiode array detector (HPLC-DAD). The adopted therapeutic range was 1.0 to 5.5 mg/L. Clinical, demographic and laboratory data were collected from the patients' medical records. Statistical analysis was performed with IBM SPSS v.26.0 and GraphPad Prism v.8.4.3. This study was approved by the University's Research Ethics Committee (CAEE: 82281518.3.0000.5346). **Results:** In total, 45 patients were included, the median age was 38 years (range 2 to 71 years), and the most common diagnosis was Acute Myeloid Leukemia (42.5%) followed by Acute Lymphoid Leukemia (30%). Median daily dose was 400 mg/day (range 140 to 860), with oral administration being the most common route (57.6%). A wide interindividual C_{trough} variability was observed, with a median of 1.81 mg/L (range <0.02 to 11.31 mg/L). Median VCZ C_{trough} was slightly lower in pediatric patients (1.05 mg/L vs 1.84 mg/L), although not statistically significant. Subtherapeutic concentrations were observed in 35.59% of the samples, with 40% (n = 18) of the patients presenting at least one subtherapeutic C_{trough} . Meanwhile, suprathreshold concentrations corresponded to only 10.16% of the samples. Toxicity events related to VCZ were not found in the medical records. Correlations were observed between VCZ C_{trough} and daily dose ($r = 0.4340$, $p = 0.0007$), age ($r = 0.2708$, $p = 0.0398$) and BMI ($r = 0.4050$, $p = 0.0052$). **Conclusion:** TDM of hematological patients has shown a high occurrence of subtherapeutic levels over suprathreshold levels, implying an elevated risk of therapeutic failure. These results provided valuable data, highlighting the importance of plasmatic voriconazole quantification as a mean to increase therapeutic efficacy. **Financial Support:** CNPq, PIBIC/CNPq, CAPES, FAPERGS, and FIPE **References:** [1] Ashbee, HR. *J. Antimicrob. Chemother.*, v. 69, p. 1162, 2014. [2] Samanta, P. *J. Thorac. Dis.*, v. 13, p. 6695, 2021. [3] Pana, ZD. *J. Pediatric. Infect. Dis. Soc.*, v. 6(suppl_1), S3, 2017. [4] Shi, C. *Clin. Pharmacokinet.*, v. 58, p. 687, 2019.

11.003 Cytotoxicity and Oxidative Stress in Dermal Cel (HaCaT) Induced by Pesticides Glyphosate and Dicamba Isolated and Mixed. Silva JF, Nominato-Oliveira L, Julião RC, Guiloski IC IPPPP-FPP, Brazil

Introduction: Pesticides have been associated with the occurrence of cellular damage and interference of metabolic pathways, these damages are mostly observed in rural workers, due to occupational dermal exposure. Thus, this work aimed to evaluate the cytotoxicity and antioxidant system after exposure to the herbicides Glyphosate and Dicamba, isolated and in the mixture, in the keratinocytes (HaCaT cells). **Methods:** The HaCaT cells were exposed to 16, 160 and 1600 mg/L of Dicamba (DIC); 6, 60 and 600 mg/L of Glyphosate (GLY) and mixtures M1 (16 mg/L DIC + 6 mg/L GLY), M2 (160 mg/L DIC + 60 mg/L GLY) and M3 (1600 mg/L DIC + 600 mg/L GLY), for 24 and 72 h. For cytotoxicity assessment, cells were seeded in 96-well plates, at a concentration of 2.5×10^4 and analyzed by the PrestoBlue™ method. For the evaluation of the antioxidant system, cells were seeded in 6-well plates, at a concentration of 2×10^5 . Biomarkers analyzed were superoxide dismutase (SOD), glutathione peroxidase (GPx), glutathione S-transferase (GST) activities, and glutathione reduced (GSH) levels. Statistics were performed using the GraphPad Prism program, Data were analyzed by Kolmogorov-Smirnov normality test and one-way ANOVA, followed by Dunnett's post-test. **Results:** The highest concentration of pesticides was cytotoxic at 24 and 72 h. In 24 h, DIC decreased to 83.06% the number of viable cells, GLY decreased to 70.06%, and M3 to 47%. In 72h, DIC decreased to 69.01% in the number of viable cells, GLY decreased to 72.81% and M3 to 19.26%. In 24 h, the highest concentration of the mixture (M3) increased the SOD activity [F (9,81) = 3,554; p = 0,0013] and GPx activity [F (9,81) = 3,743; p = 0,0010]. An increase in the GST activity in the HaCaT cells was noted in the higher concentration of DIC (1600 mg/L) and M3 [F (9,81) = 3,476; p = 0,0017]. There was no significant change in biomarkers of the antioxidant system after 72 h of exposure to herbicides. These results indicate that GLY and DIC isolated or in the mixture are cytotoxic in acute exposure since the alterations started within 24 h. The mixture of these two pesticides caused damage to the antioxidant system since there were enzymatic changes at the highest mixture concentration. **Conclusion:** The pesticides glyphosate and Dicamba, alone or in combination, can cause cytotoxicity and activate the antioxidant system in keratinocytes of the HaCaT lineage, indicating that these pesticides may be capable of causing damage to the health of people exposed to these compounds. **Financial Support:** The authors would like to thank the Instituto de Pesquisa Pelé Pequeno Príncipe for the scholarship granted to Juliana Ferreira da Silva and the Fundação Araucária for the scholarship granted to Letícia Nominato-Oliveira. We would also like to thank the Instituto de Pesquisa Pelé Pequeno Príncipe for the equipment and materials used for the development of the experiment. **References:** Tudi, M. Int J Environ Res Public Health. v. 18, p. 1112, 2021. Curl, CL. Curr Environ Health Rep. v. 7, p.13, 2020.

11.004 Development and Validation of Physiologically-Based Pharmacokinetic Model (PBPK) of Cannabidiol in Health Volunteers. Herling A, Sakamoto GF, Caleffi-Marchesini ER, Lippa VNM, Piai JM, Macente J, Diniz A UEM, Pharmaceutical Sciences Post graduation Program; Dept of Pharmacy, Maringá, PR, Brazil

Introduction: In recent years, researchers have demonstrated the effectiveness of using cannabidiol (CBD) for the treatment of epilepsy. In December 2019, ANVISA published the Resolution of the collegiate board - RDC nº 327, which grants sanitary authorization for the manufacture and importation, as well as establishes requirements for the commercialization, prescription, dispensation, monitoring and inspection of cannabis products for medicinal purposes (WEBER et al., 2022). Currently, there are technologies capable of assisting in conducting safer and more effective therapies for patients. Pharmacometry can help in the pharmacokinetic investigation of cannabidiol. One approach to pharmacokinetic analysis is physiologically based pharmacokinetic modeling (PBPK) (FUHR et al., 2021). The aim of the present study was to present a PBPK model of CBD in healthy adults aged 18 to 55 years. **Methods:** Three data sets of CBD plasma concentrations after IV and oral administration were used to guide model development and six clinical studies for model validation. PBPK modeling was performed using the Gastroplus® software. The validation criterion assumed was the mean value of the error doubled between 0.5 and 2.0 for maximum plasma concentration (C_{max}) and area under the curve (AUC). The value of the volume of distribution (V_d) guides the viability of the model. Sensitivity analysis was applied to explore the significance of the parameters assumed in the model. **Results:** Full-PBPK models for IV and oral administration assuming predicted information on metabolic clearance and permeability. The Poulin & Theil delivery model was assumed for IV administration and the Lukacova delivery model for oral. Acceptance criteria for both models were met. The sensitivity evaluation showed that the solubility and permeability impact parameters have a significant impact on C_{max} and AUC and were considered critical for the oral model, being compared with the observed data values, which ranged from 1683.3 to 2713 h.ng/ml for AUC and 336.2 to 524.5 ng/ml for C_{max} (OHLSSON et al., 1986; SCHOEDEL et al., 2020; TAYLOR et al., 2018). Therefore, experimental solubility data were adopted, with a value of 0.003 mg/mL at pH 7. Cannabidiol has a high apparent volume of distribution (250-450 L/kg) in healthy adults and the simulated V_d was between this range, confirming that the drug is widely distributed throughout the body. **Conclusion:** The *in vitro* solubility data and predicted permeability parameters were able to simulate all clinical conditions tested, demonstrating that the PBPK model developed and validated for the drug cannabidiol can be used for clinical and biopharmaceutical applications.

11.005 Development and Verification of PBPK Model for Ketamine. Piai JMB¹, Goes PRN¹, Lippa VNM¹, Martins F¹, Taffarel MO², Diniz A¹ ¹UEM, Dept of Pharmacy, Pharmaceutical Sciences Post graduation Program, Maringá, PR, Brazil, ²UEM, Dept of Veterinary Medicine,, Umuarama-PR, Brazil

Introduction: Ketamine (KET) is a derivative of phencyclidine, distributed as a racemic mixture that has recently gained off-label use for the management of acute and chronic pain in both adult and pediatric patients. This is primarily attributed to its potential applications in pain therapy, neurology, and psychiatry [1]. Physiologically-based pharmacokinetic modeling (PBPK) is a mathematical and computational modeling approach that enables the representation of an actual organism, depicting the human body as a collection of compartments, which can physiologically correspond to tissues, organs, and other physiological spaces. It facilitates the simulation of physiological conditions governing the interaction between the drug and the organism [2]. The development of a PBPK model for KET serves as the initial stride towards conducting diverse investigations, encompassing dose prediction and adjustment, studies in ontogenic populations, potential drug interactions, and other areas [1]. **Aim:** The objective of this study was to establish and validate a PBPK model for KET and its active metabolite norketamine (norKET) for both enantiomers (R-S) in order to facilitate subsequent investigations. **Methods:** Full-PBPK models for KET and norKET were developed using Simcyp Simulator®. All pharmacokinetic (PK), physicochemical, and biopharmaceutical parameters were acquired from the literature. The simulated PK profiles and parameters were compared against observed data to evaluate the predictive capability of the model. PBPK models for intravenous (IV) and oral administration were constructed for healthy volunteers to assess the PK parameters of the compounds. The adequacy of the model was determined by calculating the mean error (MFE), where MFE values ranging from 0.5 to 2.0 are deemed acceptable. The PK parameters employed for assessing the model were the area under the curve (AUC), maximum plasma concentration (C_{max}), and time to reach maximum concentration (T_{max}). **Results:** The PBPK models were developed to cover both IV and oral administration of KET/norKET, considering their R and S enantiomeric forms. Separate models were created for each molecule. The selection criteria for the S-KET model included ranges of 0.63 to 1.71 for AUC, 0.67 to 1.82 for C_{max}, and 0.96 to 1.05 for T_{max}. For S-norKET, MFE values for AUC ranged from 1.12 to 1.54, for C_{max} from 0.92 to 1.85, and for T_{max} from 0.5 to 1.5. In the case of R-KET, the MFE values varied from 0.71 to 1.7 for AUC, from 0.7 to 1.7 for C_{max}, and from 0.96 to 1.05 for T_{max}. Regarding its metabolite, R-norKET, the AUC values ranged from 0.87 to 1.35, for C_{max} from 0.62 to 1.61, and for T_{max} from 0.51 to 1.5. All tested models demonstrated acceptability. **Conclusion:** The generated model was validated according to the obtained predicted/observed ratios. From this it is possible to apply the developed model to other studies involving KET and norKET.

11.006 Microdoses of Cannabinoids Reverse Memory Impairments in Alzheimer's Patients: A Clinical Trial, Double-Blind, Randomized, and Placebo-Controlled. Cury RM¹, Silva T¹, Le-Quesne AHM¹, Florentino I¹, Krefta E^{1,2}, Silva EG¹, Pamplona FA¹, Bicca MA³, Nascimento FP¹. ¹Unila, Lab. of Medical Cannabis and Psychedelic Science, Foz do Iguaçu, PR, Brazil. ²Uniamérica University Center, Foz do Iguaçu, PR, Brazil, ³Johns Hopkins University, Faculty of Medicine

Introduction: Alzheimer's disease (AD) is characterized by the accumulation of neurotoxins derived from beta-amyloid fractions and hyperphosphorylation of tau protein, leading to neurodegeneration and cognitive impairment. Despite extensive research on new therapies for AD, recent advancements have been limited, and there is no consensus or promising new treatment on the horizon. The relationship between dementia, inflammation, beta-amyloid fractions, and alterations in the endocannabinoid system in experimental models of AD has been reported. However, there are currently only a few published studies investigating the effects of cannabinoids on AD pathology. Cannabinoid-based therapy has emerged as a potentially crucial approach for treating incurable neurodegenerative diseases. This study hypothesizes that the dysregulation of the endocannabinoid system is associated with AD and that microdoses of cannabinoids can restore brain function without inducing significant side effects. **Methods:** The effects of microdoses of cannabinoids on patients with AD were evaluated through a randomized, double-blind, placebo-controlled clinical trial. Patients were selected based on the criteria set by the National Institute of Neurological and Communicative Disorders and Stroke and the Alzheimer's Disease and Related Disorders Association. The participants were divided into two groups, with one group receiving 500 µg of tetrahydrocannabinol and 350 µg of cannabidiol, and the other group receiving a placebo. The researchers involved in the study remained blinded until the end. The study spanned a duration of 6 months, with monthly clinical assessments utilizing the Mini Mental State Examination (MMSE), AD Rating Scale (ADAS-cog), and DSRS tools. Additionally, cerebrospinal fluid (CSF) samples were collected at baseline (T0) and at the end of the study (T6) to quantify brain-derived neurotrophic factor (BDNF) and total tau. **Results:** A total of 141 participants were evaluated, with 113 being excluded based on the criteria, leaving 28 participants. Of these, 24 completed the study. Randomization resulted in homogeneity between the groups in terms of epidemiological, sociodemographic, and clinical characteristics. The treatment with Cannabis increased the memory score of patients in the MMSE test compared to patients who received placebo. Through the analysis using ANCOVA test, there was a statistical difference between the Cannabis group and the placebo group with $p=0.028$ at the sixth month of treatment. However, no statistically significant differences were found in ADAS-cog ($p=0.854$) and DSRS ($p=0.725$) scores. Repeated measures ANOVA did not yield any significant differences in BDNF and total tau levels between the groups or at T0 and T6. **Conclusion:** This study is unprecedented in world literature and demonstrates for the first time that Cannabis is capable of effectively treating the mnemonic symptoms of Alzheimer's disease, reversing cognitive damage caused by the disease and/or stabilizing patients in their stages for at least 6 months. Further studies with a larger number of patients should be conducted to extend these findings. However, the results presented here are exceptional and point us towards a new treatment for Alzheimer's disease in the near future. **Financial Support:** UNILA, CNPq and Fundação Araucária

11.007 Evaluation of AOPP Levels in the Diagnosis and Prognosis of Endometriosis: Systematic Review and Meta-Analysis. Pereira LG¹, Campara KMR¹, Rech CT¹, Rodrigues P¹, Viero FT¹, Trevisan GS¹ ¹UFSM, Santa Maria, Dpt of Physiology and Pharmacology, Brazil

Endometriosis is defined by the presence of endometrial-like tissue outside the uterus, usually on the pelvic peritoneum and ovaries. This pathology affects 6 to 10% of women and is associated with debilitating pelvic pain and infertility. Furthermore, it is a pro-inflammatory condition characterized by elevated concentrations of cytokines, growth factors, and alteration in oxidative balance. The diagnosis and prognosis of endometriosis are still a challenge, with laparoscopy as the gold standard (Giudice, LC. N. Engl. J. Med. v. 362, p. 2389, 2010). Thus, the importance of studying possible serum markers for the disease is highlighted, since none has yet been validated that can determine the establishment of the pathology. In this sense, it has been described that advanced oxidation protein products (AOPPs) are involved in the oxidative stress response *in vivo*, circulating in the blood of patients for a long period until their degradation, making them a promising target as a serum marker of disease (Kokot, I. Antioxi., v. 10, p. 1097, 2021). However, the literature has not yet described the possible use of these compounds as markers or indicators of this pathology. Therefore, the objective of this project is to compile data from studies through a systematic review and meta-analysis to seek evidence on increased levels of AOPP in patients with endometriosis. The review was conducted based on the PRISMA guidelines and registered in the International Prospective Register of Systematic Reviews (PROSPERO). The search was carried out in the Embase, Pubmed, and Scopus databases considering the descriptors: advanced oxidation protein products (AOPP), endometriosis, as well as their terms according to the Medical Subject Heading. Screening for inclusion or exclusion of articles was performed by two independent reviewers. Clinical trials investigating AOPP levels in patients with endometriosis compared to the control group published in the last 30 years were included. A total of 499 articles were found, of which only 11 were considered eligible for the systematic review and meta-analysis. Higher levels of AOPP in serum and peritoneal fluid have been observed in patients with endometriosis compared to healthy patients. In addition, patients with severity III/IV endometriosis also had higher levels of AOPP compared to controls. The results are valid in 95% of cases ($p < 0.05$). Therefore, we can conclude that increased levels of AOPP in serum, peritoneal fluid may be related to the presence of endometriosis. In this sense, there is a need for further studies aimed at assessing AOPP levels as a potential serum marker of endometriosis, as well as its relationship with the stages of the disease. Work supported by CNPq [process #303531/2020-7].

11.008 Teratogenic Effects of the Dicamba Herbicide in Zebrafish (*Danio rerio*) Embryos.
Felisbino K, Kirsten N, Milhorini SS, Marçal IS, Schiessl R, Bernet K, Nominato-Oliveira L, Guiloski IC ¹IPPPP-FPP, Brazil

Dicamba has been used around the world for 60 years, but few studies have been conducted on its environmental safety and health effects, particularly on teratogenic effects. Therefore, this study evaluated the acute toxicity, teratogenic effects, oxidative stress, and neurotoxicity of Dicamba in zebrafish embryos. The project was approved by the Committee on Ethics in the Use of Animals (CEUA), of the Instituto de Pesquisa Pelé Pequeno Príncipe, under number 059-2020. The study was based on the OECD Test Guideline Fish Embryo Acute Toxicity (FET) Test 236. The embryos were exposed to concentrations of 4.5, 18, 72, and 288 mg/L of Dicamba for 96 h. Teratogenicity, parameters of zebrafish embryo development, and oxidative stress biomarkers were assessed. The LC₅₀ found was 217 mg/L, indicating that the embryos are resistant to the herbicide. Among the teratogenic effects, yolk sac edema predominated, with a significant increase at 288 mg/L of Dicamba. In addition to malabsorption of nutrients (grey yolk sac) with a significant increase at 72 mg/L. Other effects such as hemorrhage, spinal and eye malformations, and dwarfism have also been observed. The hatching rate was reduced at the highest concentration, and at the other concentrations, a decrease was noticeable within 48 h of exposure, indicating a delay in development. Neurotoxic effects were observed at 288 mg/L of Dicamba. In the higher concentration, Dicamba caused an increase in GPx activity and GSH and LPO levels. SOD activity was inhibited at all concentrations of the herbicide. This study shows that the Dicamba had teratogenic effects on zebrafish embryos even at low concentrations, including the concentration of 18 mg/L, which according to the USEPA (2018) is allowed in drinking water, leading to developmental delays, malformations, edema, and malabsorption of nutrients. Exposure also increased the production of free radicals, causing oxidative cell damage and reduced activity of antioxidant enzymes, which can lead to deleterious changes in biomolecules and cell membranes. In addition, it highlights the need for more studies on the effects of the herbicide and a reassessment of toxicity categorization.

11.009 Development of PBPK Model for Leishmanicidal Candidate in Rats: First Step Before Translation Interspecies. Teixeira FEG, Bitencourt IC, Oliveira MT, Haas SE INCT-Inofar-Unipampa, Lab. de Farmacologia e Farmacomètria, Uruguaiiana, RS, Brazil

Introduction: Leishmaniasis is still a common disease in endemic areas, the dogs are considered disease reservoirs in urban areas. In Rio Grande do Sul, Brazil, the vector of this disease was found in urban areas, so the dogs may be exposed and continue transmitting this disease. Due to the extremely limited therapeutic arsenal for the treatment of Leishmaniasis, new options should be explored. LASSBio-1736 was developed to be a drug candidate for the treatment of Leishmaniasis and have been demonstrated efficacy against the promastigote forms of *L. major* [1]. Its pharmacokinetic (PK) in rats was described in a previous study in our group and demonstrated the terminal half-life ($t_{1/2}$), clearance (CL), and tissue distribution, showing characteristics PK agree to other leishmanicidal drugs [2]. Physiologically Based Pharmacokinetics (PBPK) Modeling is an *in silico* tool that integrates data about pharmacokinetic and physiological information of humans and animals. In face of that, having PK data in rats, for example, it's possible to extrapolate data for other specie [3]. **Objective:** This study aims to development a PBPK model for LASSBio-1736 in rats using published data, with to perspective to translation for dogs. **Methods:** Computer simulations were performed with GastroPlus V.9.8.3. software (Simulations Plus Inc., Lancaster, USA). Information on logD, pKa, and molecular weight was obtained from ADMET Predictor V.10.4. (Simulations Plus Inc., Lancaster, USA). Pharmacokinetic data of LASSBio-1736 intravenous (3.2 mg/kg) administration in rats was extracted from Moraes et al, 2017, to perform PBPK model development. Firstly, through the PKPlus™ module, models with one, two, and three compartments were obtained. After that, the PBPK model was obtained through the PBPKPlus™ module. To evaluate of plasmatic curves observed versus simulated calculated predict error parameter for concentration maximum (Cmax), area under the curve (AUC), and coefficient of determination (Rsq). **Results:** The compartmental analysis demonstrated adequate results for all parameters, corroborating with results found in Moraes et al., 2017 [2]. Predicted and observed PK profiles were similar and calculated error ranged from 0.5-2. Then, it was possible to build a PBPK model for rats with adequate characteristics. **Conclusion:** The proposed PBPK model was able to describe the observations in rats. Then, it will be used and scaled from rat to dog. **Acknowledgments:** Financial support master scholarship from CAPES/Brazil and from CNPq/Brazil and INCT-Inofar. **References:** 1. ALVES, MA. RSC Adv., v. 10, p. 12384, 2020. 2. MORAES, BS. Xenobiotica, v. 48, p. 1, 2017. 3. MOULD, DR. CPT: Pharmacometrics Syst Pharmacol., v. 1, p. 1, 2013.

11.010 Are Age and Sex Relevant Factors for the Pharmacokinetics of Benznidazole in Patients with Chronic Chagas Disease in the Indeterminate Form? Silveira GPE^{1,4}, Portela LF², Pinto DP¹, Maciel EA², Silva DMD¹, Silva JA³, Saavedra LB², Costa AR², Carneiro FM², Silva GMS², Hasslocher-Moreno AM², Vannier-Santos MA³, Saraiva RM², Estrela R^{2,4,5}
¹FIOCRUZ Rio de Janeiro, Pharmacokinetics Lab., Brazil; ²FIOCRUZ Rio de Janeiro, Evandro Chagas National Institute of Infectious Diseases, Brazil; ³FIOCRUZ Rio de Janeiro, Innovations in Therapies, Education and Bioproducts Lab., Brazil; ⁴ENSP-FIOCRUZ Rio de Janeiro, PPG in Public Health and Environment, Brazil; ⁵UFRJ Rio de Janeiro, Faculty of Pharmacy, Brazil;

Introduction: Chagas disease (CD) is caused by the protozoan *Trypanosoma cruzi*. It is estimated that 70 million people are at risk of infection in 21 countries in the Americas. Benznidazole (BDZ) is the main drug used in CD chemotherapy and its toxicity can lead to discontinuation of treatment with a frequency close to 30%. The incidence of adverse events is higher among women. Very few and incomplete studies have focused on the pharmacokinetics of BDZ in patients. The aim of this study was to characterize the pharmacokinetic profile of BDZ in patients with chronic indeterminate CD, identifying possible factors of population variability. **Methods:** The research protocol was approved by research ethics committee (CAAE 47219021.5.0000.5262; opinion number 4.777.595) and conducted in Rio de Janeiro – Brazil. This is a single-center, non-blinding study. Adult patients of both sexes aged 18 to 70 years old with chronic indeterminate CD form were included in this study. The patients received 300 mg/day of BDZ for 60 days. BDZ plasma concentrations were monitored in blood plasma in the first, seventh, fourteenth, thirtieth and sixtieth days of treatment. HPLC-MS/MS was used to determine BDZ concentrations. Pharmacokinetic parameters of absorption, distribution and elimination were determined for each age group and sex. **Results:** BDZ exposure was higher in women compared to men after receiving a single dose (1st day). C_{max} was 33% higher ($P = 0.00013$) and AUC_{last} was 37% higher ($P = 0.000901$) among women. These differences, however, were no significant after normalizing the pharmacokinetic parameter for the administered dose by weight (mg/kg) (C_{max}/D and AUC_{last}/D). After multiple doses (14th day) no sex difference was observed ($P < 0.05$), although $T_{1/2}$ was higher in men. The $T_{1/2}$ calculated after chronic use of BDZ was higher for patients older than 50 years. Greater C_{max} and AUC were observed at steady state for these patients compared to younger patients ($P < 0.05$). Patients with a body mass index (BMI) greater than 30 kg/m² had lower C_{max} and AUC compared to those with a lower BMI ($p < 0.05$), after a single dose. $T_{1/2}$ was 70% higher in patients with BMI greater than 30 kg/m² after multiple doses. **Conclusion:** Differences in BDZ pharmacokinetics observed between sexes appear to be related to the greater body mass of men compared to women. **Financial Support:** CNPq; FAPERJ

11.011 Population pharmacokinetic modeling of vildagliptin in a preclinical model of type 2 diabetes. Dias BB, Olivo LB, Andrade C, Menin RH, Araújo BV UFRGS, Pharmacokinetic and PK/PD Modeling Lab., Porto Alegre, RS, Brazil

Introduction: Diabetes is a metabolic disease originated from different mechanisms that result in hyperglycemia (1). Reducing the direct and indirect damage related to this hyperglycemia is the main objective of diabetes treatment, which can be done with hypoglycemic agents such as vildagliptin (2,3). To improve pharmacological treatment, the use of modeling and simulation (M&S) can be applied to reduce costs and improve treatment of drugs already on the market, ensuring better pharmacological treatment for patients (4). Our research group has previously investigated the impact of diabetes on free plasma and free liver concentrations of vildagliptin using microdialysis technique in diabetic rats (5). The aim of this study was to apply popPK modeling to describe vildagliptin plasma concentrations in diabetic animals to further correlate tissue free concentrations with their hypoglycemic effect. **Methods:** Plasma and free tissue concentrations of vildagliptin (n= 5 and 6, respectively) have already been evaluated by previous studies, at a dose of 50 mg/kg intravenously. Diabetes was induced in the animals by administration of alloxan 2 % intravenously(6). The data were used for the popPK model using the non-linear mixed effects models. For the model building plasma free concentrations were estimating considering the plasma protein binding of 9%. Free concentrations obtained by microdialysis were described by the integral over each collection interval. Model selection was guided by significantly change in the value of the objective function (OFV), visual exploration of goodness-of-fit (GOF) plots and precision of model parameters reflected as the relative standard error (%RSE). **Results:** A two compartment model with linear elimination was applied to describe plasma concentrations in diabetic rats. Population parameters were CL: 2.91 L/h/kg (0.5 %RSE), V1: 1.52 L/kg (0.6 %RSE), Q1: 2.25 L/h/kg (1.7 %RSE), V2: 1.91 L/kg (0.8 %RSE). The model was expanded to 3 compartments to include free liver concentrations, with a bi-directional transport between plasma and liver with Q_{in} : 0.313 L/h/kg (0.8 %RSE), Q_{out} : 1520 L/h/kg (1 %RSE), and V3: 346 L/h/kg (1.7 %RSE). Residual error modeled as log-additive was divided for plasma (0.197 μ g/L) and microdialysis data (0.16 μ g/L). Interindividual variability was included exponentially in CL (16 %), Q1 (91 %), V3 (246 %) and Q_{out} (88 %). **Conclusion:** From the developed population model, it was possible to describe the population pharmacokinetic parameters of vildagliptin in diabetic animals, which will be used for simulations and for establishing a relationship with the pharmacodynamics of the drug. With the use of modeling and simulation, it will be possible to predict different pharmacological therapeutic scenarios and improve the treatment of type 2 diabetics. **Financial Support:** Coordination for the Improvement of Higher Education Personnel (CAPES, Brazil). **References:** 1. Tinajero, MG, Malik VS. *Endocrinol Metab Clin North Am.* v. 50(3), p. 337, 2021. 2. Bahia LR et al. *Diabetol Metab Syndr.* v. 11(54), p. 1, 2019. 3. Wu Y et al. *Int J Med Sci.* v. 11(11), p. 1185, 2014. 4. Mould DR, Upton RN. *CPT Pharmacometrics Syst Pharmacol.* v. 2(4), p. 1, 2013. 5. de Andrade C et al. *Biomed Chromatogr.* v. 28(e38), p. 1, 2014. 6. Lerco M et al. *Acta Cir Bras.* v. 18(2), p. 132, 2003.

11.012 Pharmacodynamic Analysis of 2% Lidocaine with or without 1:100.000 Epinephrine Pilot Study. Oliveira GM¹, Dionísio TJ², Faria FAC², Calvo AM², Santos CF^{1,2}
¹HRAC-USP, Brazil; ²Bauru School of Dentistry, University of São Paulo, Brazil

Introduction: Lidocaine is the most used local anesthetic in dentistry worldwide, being one of the oldest sodium channel blockers on the market and considered the safest amide local anesthetic. Even so, it can cause some side effects on the cardiovascular system and the central nervous system, especially when accidental administration occurs directly into a blood vessel, and the association with vasoconstrictors, especially epinephrine, is a strategy to minimize these effects. This study evaluated the pharmacodynamic parameters (PD) of lidocaine, associated or not with epinephrine, and their effects on hemodynamic parameters in Brazilian patients. The pharmacodynamic effects of lidocaine were evaluated in healthy patients who received infiltrative injection of a 2% lidocaine with (LA) or without (L) 1: 100,000 epinephrine. **Methods:** In this pilot study, a PD evaluation was performed in 14 patients (with some degree of periodontal disease) who received infiltrating sulcular injection in the upper molar region of 2% lidocaine with or without 1: 100.000 epinephrine for scaling and root planing. Before and during the procedure, data of systolic (SBP), diastolic (DBP) and mean arterial pressure (MAP), blood oxygen saturation (BOS) and heart rate (HR) were monitored by the equipment Dixtal® (DX2021 model, Dixtal Biomédica Ind and Com Ltda). **Results:** Before the procedure, at the 1st infiltration, 5 minutes after the procedure beginning and in the end of the process, among these, the five parameters were recorded. There was no difference between the local anesthetic used, lidocaine associated with 1: 100.000 epinephrine (LA) or not (L), especially after injection (SBP 105.42 ± 10.26 (LA) and 101.85 ± 8.2mmHg (L); DBP 63.14 ± 3.7 (LA) and 61.25 ± 6.70mmHg (L); MAP 77.14 ± 4.91 (LA) and 74.71 ± 6.55mmHg (L); BOS 97.42 ± 1.71 (LA) and 98.14 ± 1.42 SpO2 (L); HR 74.42 ± 13.17 (LA) and 68.28 ± 10.6BPM (L)) and five minutes after the start of the procedure (SBP 107.57 ± 6.92 (LA) and 105.85 ± 9.9mmHg (L); DBP 63.28 ± 4.78 (LA) and 69.5 ± 6.72mmHg (L); MAP 78.14 ± 4.77 (LA) and 79.57 ± 7.32mmHg (L); BOS 97.85 ± 2.34 (LA) and 98.57 ± 1.11SpO2 (L); HR 74.85 ± 11.18 (LA) and 66 ± 11.69BPM (L)). **Conclusion:** There are few studies that evaluate pharmacodynamic parameters (PD) of local anesthetics in the literature, therefore the study of lidocaine and its effects on cardiovascular and central nervous system of patients is fundamental. In this pilot study it was found that the association of epinephrine with lidocaine did not interfere with intraoperative hemodynamic parameters. **Financial Support:** FAPESP 2017/12725-0; 2022/11140-7 and CAPES 001. **References:** SANTOS, CF. *Journal of Oral and Maxillofacial Surgery*, v. 65, n. 12, p. 2445, 2007. SENES, A. M. *Journal of Dental Research*, v. 94, n. 9_suppl, p. 166S, 2015.

11.013 Pharmacokinetics and Pulmonary Delivery of JME-209, A Novel Mexiletine Analogue with Limited Action in Na⁺ channels and Activity against Bronchoconstriction and Airway Inflammation in Mice. Santos, GCM¹, Gomes, HS¹, Coutinho, DS¹², Pinto, DP², Fonseca, LB², Nascimento, VA¹², Costa, JCS³, Cotias, AC¹, Silva, PMR¹, Martins, MA¹
¹Fiocruz, Lab. of Inflammation, ²Fiocruz, Equivalence and Pharmacokinetics Service, ³Fiocruz, Vice Presidency of Production and Innovation in Health

Introduction: Prior studies have demonstrated the capacity of local anaesthetics, such as mexiletine and lidocaine, to control bronchoconstriction and airway inflammation, but the disruptive effect on bronchodilator neurogenic reflexes caused by Na⁺ channels blockade significantly impairs their application in clinical settings. We have been interested in discovering local anaesthetic analogues with attenuated activity in Na⁺ channels to treat chronic obstructive lung disorders. We report here the pharmacodynamic and pharmacokinetic properties of the compound 1-([1,1'-Biphenyl]-4-aryloxy)-2-propanamine (JME-209), a novel mexiletine analogue screened for reduced activity in Na⁺ channels.

Methods: Changes in Na⁺ current, trachea ring contraction and mast cell degranulation were assessed *in vitro*. Lung function and inflammatory changes were studied in methacholine-induced bronchoconstriction and steroid-resistant lung inflammation murine models. JME-209 pharmacokinetics was evaluated in plasma and lung tissue samples of A/J mice using the HPLC-MS/MS technique. All procedures involving the use of experimental animals were previously approved by FIOCRUZ's ethics committee CEUA - L002/20. **Results:** The potency of inhibition by JME-209 of carbachol-induced trachea constriction and allergen-induced mast cell degranulation was superior to mexiletine, regardless of the 80-fold reduction on its potency in inhibiting Na⁺ current as compared to mexiletine. JME-209 (30 mg/kg, oral) inhibited methacholine-induced mouse airway obstruction within 3 h, 6 h and 24 h post-treatment [mean, 46% ($P = 0.04$) $n=6$, 66% ($P = 0.003$) $n=7$ and 62%, ($P = 0.007$) $n=7$, respectively], having formoterol (10 mg/kg) inhibitory values of 49%, 54% and 0%, respectively. JME-209 also inhibited LPS-induced airway hyper-reactivity (62%), neutrophilic infiltration (42%) and KC generation (67%), whereas dexamethasone (1 mg/kg, oral) was inactive in this model. Pharmacokinetic experiments of JME-209 showed rapid absorption, reaching a mean maximal concentration (C_{max}) of 235.80 ng/mL in 0.69 h maximum time (T_{max}) after a dose of 30 mg/kg with terminal plasma half-life (T_{1/2}) of 5.71 h. The area under the curve from time zero to the last sampling time (AUC_{0-t}) and under the zero to infinity (AUC_{0-∞}), 3265.4 and 3266.3 ng/mL*h, respectively, indicate good absorption following oral exposure to the mouse organism. In lung tissue, we observed values of C_{max} of 13.07 µg/g in 0.75 h with T_{1/2} of 3.85 h, AUC_{0-t} and AUC_{0-∞} of 246.83 and 247.59 µg/g*h, respectively, which also indicate good biodistribution. **Conclusion:** These findings show that JME-209 is a mexiletine analogue with reduced potency towards Na⁺ channels and marked activity against bronchoconstriction and glucocorticoid-insensitive airway inflammation following oral administration. This study also provides pharmacokinetic data developed for the JME-209 assessment in plasma and lung tissue samples, indicating that JME-209 is rapidly absorbed and presents a profile of elimination half-life of about 6 h after oral treatment. **Financial Support:** CNPq, FAPERJ

11.014 Pharmacokinetic/Pharmacodynamic (PK/PD) Model on the Influence of CYP2C9 for Meloxicam and its Major Metabolite from Saliva Samples by LC MS/MS. Calvo AM, Oliveira GM, Ferreira NR, Smera CSS, Dionísio TJ, Santos CF FOB-USP, Dpt of Biological Sciences, Brazil

Introduction: The pharmacokinetics (PK) and pharmacodynamics (PD) of non-steroidal anti-inflammatory drugs can be significantly altered by the influence of polymorphisms such as *CYP2C9*. The present study evaluated the PK/PD parameters in saliva after consumption of a meloxicam tablet, in healthy subjects. A rapid and sensitive Liquid Chromatography-Tandem Mass Spectrometry (LC-MS/MS) method was developed and validated for the determination of meloxicam, its main metabolite, 5?-carboximeloxicam, and PGE₂ in saliva. **Methods:** Sixteen individuals (12 non-mutated and 4 mutated for *CYP2C9*) had unstimulated total saliva collected in a falcon tube (4 mL) sequentially before and after taking a meloxicam tablet (15 mg) at the following times: 0.25, 0.5, 0.75, 1, 1.5, 2, 3, 4, 5, 6, 8, 11, 24, 48, 72 and 96 h. **Results:** With the data obtained, it was possible to observe that all PK analyzes were performed and when we compared mutated and non-mutated individuals, there was no statistically significant difference, but when analyzing the mean concentrations obtained throughout the entire collection period of the samples, there were differences between the groups, mainly in the fastest collections, of 0.5; 1 and 1.5 hours after ingestion of a 15 mg meloxicam tablet (p₂ inhibition, despite showing a trend, no statistically significant differences were observed when comparing the groups of mutated and non-mutated individuals. All validation data, such as accuracy, precision, and repeatability intra- and inter-assay, were less than 15%. **Conclusion:** Results showed statistically significant differences in the mean concentrations obtained in samples with shorter times after ingestion of a 15 mg meloxicam tablet, but in relation to PK parameters and their relationship with PGE₂ inhibition, when divided into mutated and non-mutated groups, was not significant, most likely due to the reduced number of mutated individuals that we were able to group at the end of the experiment. Bauru School of Dentistry/University of São Paulo Ethics Committee approval: CAAE 92312318.4.0000.5417 **Financial Support:** FAPESP 2017/12725-0 **References:** Oliveira, GM. *Metabolites*, v.13; p.1106, 2022. Oliveira, GM. *Prostaglandins Other Lipid Mediat.*, v. 163, p.106672, 2022.

11.015 5-Fluorouracil Therapeutic Drug Monitoring in Patients with Gastrointestinal Cancer in Treatment at the University Hospital of Santa Maria. Somavilla B¹, Baco LS¹, Petreceli RR¹, Linden R², Silva LC², Antunes LCM³, Brucker N¹ ¹UFMS, Dpt. of Physiology and Pharmacology, PPG Pharmaceutical Sciences, Brazil; ²FEEVALE, Lab. of Toxicology, Brazil; ³UFMS, Dpt. Hematology and Oncology, Brazil

Introduction: 5-fluorouracil (5-FU) is a pyrimidine analog chemotherapeutic widely used in the treatment of gastrointestinal cancers. According to current clinical protocols, 5-FU prescriptions are calculated using body surface area (BSA) as a parameter. However, this dosage form leads to a wide range in exposure and toxicity, since it has no potential relationship with plasma clearance^{1,2}. Studies have demonstrated that BSA based doses results in underdosage for most patients³. Therapeutic drug monitoring (TDM) can be a useful tool in reducing toxicity and achieving of better therapeutic rates^{4,5}. Although in Brazil there is no official recommendation, in many countries TDM is recommended to all patients receiving 5-FU through continuous infusion (CI), in association with other drugs or not^{6,7,8}. In this context, in association with other relevant clinical parameters, the area under the curve (AUC) for 5-FU is considered an adequate option to evaluate and adjust for exposure and toxicity⁴. The aim of this study was to quantify 5-FU plasmatic levels and calculate the attained AUC in BSA based doses. **Methods:** In total, 15 patients (n=15) undergoing treatment for gastrointestinal tract cancer at the University Hospital of Santa Maria were included. Steady-state blood samples were collected in EDTA tubes, between 18 and 20 h after infusion start. An AUC of 20-30 mg.h/L was considered therapeutic. Plasmatic levels of 5-FU were measured with ultra performance liquid chromatography (UPLC-MS) and the respective AUC calculated. This study was approved by the Federal University of Santa Maria's Research Ethics Committee (CAEE: 44256821.5.0000.5346). Clinical data was collected from patients' medical records. **Results:** BSA based doses of 5-FU were administered through CI over 24 or 46 h. Mean AUC was 20.70 ± 7.85 mg.h/L during the first chemotherapy cycle, 2 patients (13.33%) presented suprathereapeutic AUC (>30 mg.h/L), 3 patients (20%) presented therapeutic levels (20-30 mg.h/L) and 10 patients (66.66%) presented subtherapeutic levels (<20 mg.h/L). Mean age was 63.07±10.15 years. The most prevalent tumor was Colon (26.66%), followed by Esophagus (20%), Pancreas and Rectum (13.33%) and Cholangiocarcinoma, Stomach, Liver and Gallbladder (1%). The protocols used were FOLFOX (73.33%), FOLFIRINOX (20%) and FLOT (6.66%). **Conclusion:** The results obtained in this preliminary study provide relevant information about the AUC achieved in patients undergoing 5-FU treatments with doses based on BSA. Routine TDM would be a useful tool to maintain adequate pharmacokinetic parameters in these patients. There are numerous variables to be studied to elucidate intra and interindividual variability. Thus, TDM can contribute to the elucidation of these issues and potentially reduce risks and improve treatment efficacy, providing more favorable clinical outcomes to the patient. **Financial Support:** PIBIC/CNPq, CNPq and FAPERGS. **References:** [1] GAMELIN, E. J Clin Oncol Off J Am Soc Clin Oncol., v. 17, p. 1105, 1999. [2] LEE, JJ. Cancer Chemother Pharmacol., v. 78, p. 447, 2016. [3] SAAM, J. Clin Colorectal Cancer., v 10, p. 203, 2011. [4] BEUMER, JH. Clin Pharmacol Ther., v. 105, p. 598, 2019. [5] HASHIMOTO, Y. Anticancer Research., v. 40, p. 465, 2020. [6] DOLAT, M. Pharmaceuticals, v. 13, p. 416, 2020. [7] MACAIRE, P. Eur J Cancer., v. 111, p. 116, 2019. [8] MORAWSKA, K. Oncotarget, v. 9, p. 11559, 2018.

11.016 Antidepressants and Ejaculation Time: A Peripheral Mechanism. Campitelli RS¹, Afonso PPL¹, De Nucci G^{1,2,3} ¹UNICAMP, Dpt. of Pharmacology, Campinas, Brazil; ²USP, Dpt. of Pharmacology, São Paulo, Brazil, ³Universidade Brazil, Fernandópolis, Brazil

Introduction: Ejaculation is a physiological process which consists in semen expulsion. From the many types of ejaculatory dysfunction, premature ejaculation is one of the biggest complaints of men, with a worldwide prevalence estimated at 30% 1. The clinical use of tricyclic antidepressants such as clomipramine has been associated with delayed ejaculation and is a treatment of premature ejaculation 2, as well as the selective serotonin reuptake inhibitor (SSRI) paroxetine 3. In vitro, clomipramine antagonizes the human vas deferens contractions induced by 6-nitrodopamine (the major catecholamine released by this tissue), revealing a peripheral action of this drug on a structure related to ejaculation 4. Thus, the aim of this study is to determine the time to ejaculate from healthy men and evaluate the interference of a single administration of antidepressants. **Methods:** This is an open, randomized, double-blinded, three periods pilot clinical trial. 18 healthy men from 20 to 41 years old, with no alcohol excessive consumption (<35g/day), current drug treatment or history of sexual/erectile dysfunction were selected, and 2 of them were excluded from the results because of abandonment. In each period, they went to a clinic and randomly took placebo (PLA), clomipramine 25mg (CLO), or paroxetine 20mg (PAR), one capsule in the morning and another in the afternoon. The next day, they returned to the clinic and in a private room masturbated themselves, while they were given a timer to turn on and off when initiating and finishing the activity. This happened three times spaced within a week, and all the volunteers took the three capsules, one each time, in a random order. The semen was collected and given to the researchers. We are performing experiments with higher washout period to discard carryover effects. The data was evaluated by confidential interval and t test, FDA does not recommend testing normality, parametric statistics are more robust. This study was approved by the Ethics Committee for Research with Human Beings of the Biomedical Science Institute of University of São Paulo. All the volunteers were paid and signed a consent term. **Results:** The CI 80% in seconds for each group was: PLA 498,4-687,9; PAR 764,2-1561,5 and CLO 1176-2457,3. Both PAR and CLO had higher average values compared to placebo group (PLA 593,1; PAR 1162,9; CLO 1816,6), and this difference was statistically significant in unilateral unpaired t test in the comparison between PLA and PAR (p=0,048), PLA and CLO (p=0,015), but not in the comparison between PAR and CLO (0,143). **DISCUSSION** The central effects of antidepressants occur just weeks after the beginning of the therapy⁵. In this study, these drugs were sufficient to delay ejaculation in healthy men with the oral use of CLO and PAR just a day before, which is theoretically not enough to have central repercussions. Development of tricyclic compounds that do not cross the blood-brain barrier may be a potential interesting and safer therapeutic approach for the treatment of premature ejaculation. The authors thanks FAPESP. **References** 1. Carson, C. *Int. J. Imp. Res.* 18.1 (2006): S5-S13. 2. Wu, P-C. *Sex. Med.* 9.1 (2021): 100283-100283. 3. Zhang, D. *BMC Uro.* 19.1 (2019): 1-12. 4. Britto-Jr, J. *Andr.* 10.8 (2022): 1540-1547. 5. Rayner, L. *Palliat. Med.* 25.1 (2011): 36-51.

11.017 Therapeutic Drug Monitoring and Population Pharmacokinetic Analysis of Meropenem in Hospitalized Patients: A Preliminary Study. Corrêa GL¹, Petreceli RR², Somavilla B¹, Steffens NA², Zimmermann ES³, Brucker N^{1,2} ¹UFSM, Dpt. of Physiology and Pharmacology; ²UFSM, PPG Pharmaceutical Sciences, Brazil; ³University of Florida, Center for Pharmacometrics & Systems Pharmacology, USA

Introduction: Meropenem (MP) is a broad-spectrum carbapenem antibiotic¹. It presents antimicrobial activity against many gram-negative, gram-positive, and anaerobic bacteria and a relatively low toxicity^{1,2}. MP is used primarily to treat moderate to severe polymicrobial or nosocomial infections³. In this sense, therapeutic drug monitoring (TDM) is emphasized as a strategy to optimize doses to reduce possible adverse effects and promote maximum therapeutic efficacy, especially considering the increased antimicrobial resistance. Association of TDM with population pharmacokinetics (popPK) is essential to determine variability sources, allowing model-based TDM-guided dose individualization⁴. In this context, the aim of this study was to quantify plasmatic levels of MP and estimate the popPK parameters in patients treated at the University Hospital of Santa Maria (HUSM). **Methods:** Steady-state blood samples were collected at 3 different times: peak (C_{max} , 30 minutes after the last dose), trough (C_{min} , 30 minutes before the next dose) and an intermediate sample timed between doses (C_{int}). Quantification of plasmatic MP was performed by high-performance liquid chromatography coupled to a photodiode array detector (HPLC-DAD). Statistical analysis was performed with GraphPad Prism v.8.4.3. PopPK analysis was performed using MONOLIX™ v.2023R1. This study was approved by the University's Research Ethics Committee (CAEE: 28559520.6.0000.5346). **Results:** In total, 63 samples were collected from 28 patients, The results of C_{max} were $23.76 \pm 16.54 \mu\text{g/mL}$, C_{min} $2.92 \pm 3.03 \mu\text{g/mL}$ and C_{int} $9.6 \pm 10.52 \mu\text{g/mL}$. A group of 13 patients (29 samples) was selected for preliminary popPK analysis. A one-compartment linear elimination model provided the best results regarding goodness of fit plot, parameter estimation accuracy and model stability. The following parameters were estimated: volume of the central compartment ($V = 31.16 \text{ L}$; RSE% 24.6); total body clearance ($CL = 12.58 \text{ L/h}$; RSE% 14.31); standard deviation of the random effects $\omega_V = 44\%$, $\omega_{CL} = 26\%$; a proportional error model was adopted, with $b = 0.28$. **Conclusion:** These preliminary results provide important information about the plasmatic concentration of MP in hospitalized patients. However, analysis of clinical, laboratory and pharmacokinetic data is necessary to determine which groups of patients can benefit most from TDM, improving therapy efficacy and safety. In addition, further model development and covariate effect analysis would also provide useful information for dosing optimization and individualization in patients. **Financial Support:** CNPq, PIBIC/CNPq, FAPERGS, CAPES and FIPE. **References:** [1] Steffens, NA. *J. Clin. Pharm. Ther.* v. 46, p. 610, 2021. [2] Linden, P. *Drug Saf.* v. 30, p. 657, 2007. [3] Baldwin, CM. *Drugs.* v.68, p. 803, 2008. [4] Guidi, M. *J. Clin. Pharmacol.* v. 62, p. 125, 2022.

11.018 A Phase-4 Cohort Study in Healthcare Workers Following COVID-19 Vaccination at the University of Brasília Hospital: Population Profile and Longitudinal Humoral Response. Silva VEG¹, Oliveira HR¹, Silva DLM^{2,3}, Duarte, DB^{1,4}. ¹UnB Brasília, Lab. of Pharmacological Assays, Dpt. of Pharmacy, Brazil; ²HUB-UnB, Brazil; ³UnB Brasília, PPG in Public Health, Brazil ⁴UnB, PPG in Tropical Medicine, Brasília, Brazil

Abstract: The coronavirus disease-19 (COVID-19) caused a severe impact worldwide, and in Brazil, until now we have had more than seven hundred thousand deaths. As a novel disease without a treatment, different strategies were used to counteract its impact, including vaccination. COVID-19 vaccines demonstrated to be safe and effective in phase III studies, however, real-world data are necessary to better understand their effectiveness and the duration of the immunological response. In this perspective, we investigated the sociodemographic variables and immunological response in vaccinated healthcare workers at the University of Brasília Hospital (HUB) that participate in the “Safety and Effectiveness of Vaccines Distributed by the National Vaccination Program, in Health Workers (SEVACOV-PRO)” study. **Methods:** This is a cohort study that included participants 18 years of age or older who are healthcare workers at HUB, vaccinated and oligosymptomatic during at least one episode of COVID-19 confirmed by PCR or antigen test. The sociodemographic data and the blood samples were obtained during the visits to the clinical center that were designated V1 (first visit), V5 (12 months after first dose), V6 (18 months after first dose), and V7 (24 months after first dose). The anti-Receptor Binding Domain (RBD) antibody titers to COVID-19 were measured through the chemiluminescence microparticle immunoassay. All data of this study was collected from September 2021 to January 2023. **Results:** We observed that 80.56% of our sample were female, the age 31-40- and 41-50-years old age range constitutes the biggest group (34% each) and the self-declared race/color most prevalent was white (47.40%). Also, undergraduate technician was the predominant worker category (37.04%), followed by physicians (23,83%) and nurses (16,58%). In addition, the income of the majority of our sample was between 5 and 10 thousand Brazilian currency (26.16%). In relation to humoral response, at V1 participants who never reported COVID-19 and had a booster dose presented higher titers of anti-RBD antibody (124X) compared to those with only 2 doses. In participants that had a prior positive COVID-19 test anti-RBD antibody titers were 9X higher. During the omicron wave, levels of anti-RBD antibodies were not different between participants with 2 or 3 doses that had COVID-19, however, in participants that never reported COVID-19 levels of antibodies were only comparable when they had a booster. At V7, a second booster increased 1,4X the anti-RBD antibody titers when compared to only three doses, regardless of the vaccinal scheme. **Conclusion:** Our data demonstrated that booster doses can increase antibody titers regardless of prior infection with SARS-CoV-2

Funding: Ministry of health.

11.019 Pharmacokinetics of Intravenous and Intramuscular Nalbuphine in Domestic Chickens (*Gallus gallus domesticus*) Anesthetized with Isoflurane. Menin RH¹, Olivo LB¹, Santos EAR², Dias BB¹, Queiroga LB², Cardozo HC², Picoli R², Oliveira TF², Monteiro ER², Araújo BV¹ ¹UFRGS, Pharmaceutical Sciences Graduate Program, Porto Alegre, Brazil ²UFRGS, Veterinary Sciences Graduate Program, Porto Alegre, Brazil

Introduction: Nalbuphine is a synthetic κ -agonist and μ -antagonist opioid used as an analgesic¹. The pharmacokinetics of nalbuphine varies according to the animal species in which it's administered, and the pharmacokinetic parameters in chickens of the *Gallus gallus domesticus* species anesthetized with isoflurane are unknown^{2,3,4}. Therefore, this work aimed to determine the pharmacokinetics of nalbuphine administered intravenously (IV) and intramuscularly (IM) in chickens anesthetized with isoflurane. **Methods:** A randomized crossover study was conducted with IV and IM administration at a dose of 12.5 mg/kg in six chickens anesthetized by inhalation with isoflurane 5%. The washout period was one week between experiments. Blood samples were collected at pre-set times within 8 hours of dosing and plasma concentrations were determined by a in-house validated liquid chromatography-mass spectrometry. For both routes of administration, a population analysis was performed using NONMEM software (version 7.4, ICON Development Solutions, Ellicott City, MD, USA). **Results:** Plasma concentrations of nalbuphine was described using a 3-compartment model with linear elimination. The parameters obtained by the population analysis were CL of 7.59 L/h/kg, the bioavailability of 98% IM, Ka equivalent to 1.5h⁻¹, V1 of 1.4 L/kg, V2 of 0.57 L/kg, V3 of 2.5 L/kg, Q1 of 0.25 L/h/kg and Q2 of 11 L/h/kg. The interindividual variability (IIV) was included in CL, with the value of 3.3 (CV%, residual standard error, RSE: 25). **Conclusion:** After intravenous and intramuscular administration in chickens anesthetized with isoflurane, nalbuphine showed high volume of distribution and clearance, in addition to presenting excellent bioavailability when administered intramuscularly (98%). **Financial Support:** Coordination for the Improvement of Higher Education Personnel (CAPES, Brazil). **References:** [1] KUKANICH, B.; et al. Veterinary Anesthesia and Analgesia, v. 5, p. 207-226, 2015. [2] HO, S. T.; et al. Biopharm Drug Dispos, v. 16, p. 695-703, 1995. [3] LO, M. W.; et al. Eur J Clin Pharmacol, v. 33, p. 297-301, 1987. [4] KELLER, D. L.; et al. Am J Vet Res, v. 72, n. 6, p. 741-745, 2011.

11.020 Randomized Controlled Clinical Trial in Patients with Alzheimer's Disease: Analysis of The Effects of THC and CBD on Biochemical Markers and Inflammatory Cytokines. Florentino INA, Le Quesne AM, Krefta E, Cury RM, Silva T, Cezar-dos-Santos F, Silva EG, Nascimento FP Unila Laboratory of Medicinal Cannabis and Psychedelic Science (LCP), Foz do Iguaçu, PR, Brazil

Introduction: Alzheimer's Disease (AD) is the most common form of dementia, characterized by progressive and irreversible neurodegeneration. Pathological features include the buildup of amyloid β -containing extracellular plaques, phosphorylated tau protein-containing neurofibrillary tangles, and chronic neuroinflammation. Currently, approximately 55 to 60 million individuals worldwide are affected by dementia, with estimates predicting a tripling of this number by 2050 (Sabbagh, MN. *Nat. Rev. Neurol.*, v. 19, p. 71, 2023). While current treatments for AD do not halt or reverse disease progression, recent studies have shown the potential anti-inflammatory effects of Cannabis sativa (*C. sativa*) as a therapeutic option (Aso, E. *Farmacol. Frontal.*, v. 5, p. 37, 2014). This study aims to investigate the effects of a 12-month treatment with *C. sativa* by analyzing biomarkers in cerebrospinal fluid (CSF), including amyloid- β (A β), total Tau (tTau), Brain-Derived Neurotrophic Factor (BDNF), Lipoxin A4 (LA4), and cytokines TNF- α , IL-1 β , IL-6, and IL-10. **Methods:** A randomized, double-blind, placebo-controlled clinical trial was conducted involving 26 AD patients over a 12-month period. The participants were divided into two groups: the treated group, which received a daily oral administration of an extract containing 0.5mg THC/0.35mg CBD, and the placebo group. After an initial 6-month period, the placebo group was switched to a dosage of 1mg THC/1mg CBD per day, while the treated group maintained their dosages. CSF samples were collected from the patients at baseline, 6 months, and 12 months after treatment initiation. The enzyme-linked immunosorbent assay (ELISA) method was used to measure the specific biomarkers in the CSF samples. Statistical analysis was performed using a mixed effects model followed by Bonferroni post-hoc test. **Results:** After 1 year of treatment, changes in markers were observed when compared with baseline measurements. The main biomarkers, A β and tTau, showed mean increases of 8.33% and 1.43%, respectively. Furthermore, also increased BDNF levels by 200% and LA4 by 8.33%. The pro-inflammatory cytokines IL-6 and TNF- α reduced their values by 67.57% and 100%, respectively. Nevertheless, there was an increase in the pro-inflammatory cytokine IL-1 β by 25%. On the other hand, the anti-inflammatory cytokine IL-10 increased by 8.57%. However, no statistical differences were observed in CSF samples between groups after 1 year of treatment ($p > 0.05$). **Conclusion:** Although no statistical differences were found between the patient groups in CSF samples, the observed variations suggest the need for further quantification over a longer duration of treatment. It is possible that long-term cannabinoid treatment could significantly alter the levels of these biomarkers. **Financial Support:** Coordenação de Aperfeiçoamento de Pessoal de Nível Superior (CAPES), LCP and UNILA.

11.021 Beta-Caryophyllene Mitigates Short-Term Memory Impairment in Aflatoxin-B1-Intoxicated Rats. Dallabrida KG¹, Silveira AR², Rosa EVF², Sampaio TB^{1,2}, Santos JT², Oliveira MS², Furian AF², Sari MHM^{1,2} ¹Unicentro, Dpt. o de Farmácia, Guarapuava, PR; ²UFSM, PPG em Farmacologia, Santa Maria, RS.

Introduction: Aflatoxin B1 (AFB₁) is a mycotoxin produced primarily by the fungi *Aspergillus flavus* and *A. parasiticus*, that has a high toxic and carcinogenic potential due to its ability to induce oxidative stress. Human exposure occurs through ingesting contaminated food, such as improperly stored grains (1). Additionally, AFB₁ seems to have a neurotoxic effect that leads to memory impairment (2). Beta-caryophyllene (BCP) is a sesquiterpene found in the essential oil of some plants, such as black pepper and oregano, that has extensive bioactivity. Recently, BCP was approved as a food additive in several countries, recognized as a safe component that can be consumed with foods contaminated with AFB₁, for example (3). Therefore, this study investigated whether BCP plays a role in attenuating memory impairment caused by AFB₁ intoxication. **Methods:** Male Wistar rats were divided into four groups (n = 8-9 animals/group): control (C), treated with 2% dimethyl sulfoxide (DMSO) intragastrically (i.g.) + 0.9% NaCl and 0.05% Tween 80 intraperitoneally (i.p.); AFB₁ (250 µg/kg, i.g. + 0.9% NaCl and 0.05% Tween 80, i.p.); BCP (100 mg/kg, i.p. + 2% DMSO, i.g), and AFB₁ + BCP (AFB₁ 250 µg/kg, i.g. + BCP 100 mg/kg, i.p). Animals were treated for 14 days and then subjected to the open field test (OFT) and the object recognition task (ORT), to evaluate cognitive functions. Animals were trained, and after 1 h of training, short-term memory (STM) was assessed. The long-term memory (LTM) was evaluated 24 h after training. The recognition memory measurement (recognition index; RI) was the percentage of total exploration time the animal spent examining the novel object. The data were evaluated by the Two-way ANOVA followed by Neuman-Keuls' test. **Results:** OFT results reveal that all the treatments showed no significant difference between groups above crossing and elevation numbers (p>0.05), suggesting that the protocol administration did not induce motor or exploratory dysfunction and discarding possible artifacts in behavioral memory assessments. ORT results show that all groups presented the same time of exploration for the two objects in the training section (p>0.05). However, in the STM test, animals that received only AFB₁ demonstrated lower performance in object recognition (p<0.05), as demonstrated by the recognition index ± standard deviation (C = 0.7180 ± 0,08842; AFB₁ = 0.6040 ± 0,1037; BCP = 0.7339 ± 0,07920; AFB₁ + BCP = 0.7282 ± 0,08635, respectively). Interestingly, animals treated with AFB₁ + BCP showed a high performance (RI = 0.7282 ± 0,08635), suggesting that BCP administration prevents cognitive damage induced by AFB₁ exposure (p<0.05). No significant differences between groups (p>0.05) were observed in the LTM test. Thus, these data suggest that AFB₁ exposure induces STM impairment, without affecting LTM, and BCP treatment can minimize this damage. **Conclusion:** AFB₁ can alter brain functions prejudicing STM formation, and BCP, which can be consumed together with food contaminated, may counteract these effects. **Financial Support:** FAPERGS, CNPq, and CAPES. **References:** (1) Silveira, AR, et al. Chem. Bio. Interac., v. 348, p. 109635, 2021. (2) Gugliandolo, E, et al. Animals, v. 10(5), p. 898, 2020. (3) Sharma, C, et al. Current Pharmac. Design, v. 22, p. 3237, 2016.

11.022 A Longitudinal Immunogenicity Analysis in Healthcare Workers Following COVID-19 Vaccination: A Cohort Study. Aroucha DF¹, Duarte DB^{1,2}, Silva DLM^{2,3,4} ¹UnB Brasília, PPG in Tropical Medicine, Brazil. ²UnB Brasília, Dpt. of Pharmacy, Brazil. ³HUB Brasília, University of Brasília Hospital, Brazil. ⁴UnB Brasília, PPG in Public Health, Brazil

Introduction: The Coronavirus disease 19 (COVID-19) vaccines were developed and approved in a record time and the phase III studies demonstrated that they are effective and safe. However, population-based follow-up studies are important to assess immunogenicity, safety, and effectiveness in the real world. In fact, healthcare workers on the front lines of medical care are highly exposed to the virus and were classified as one of the priority groups for vaccination. Therefore, the aim of our study which is still ongoing, is to evaluate immunogenicity of COVID-19 vaccines 24 months after the first dose in healthcare workers.

Methods: This is a prospective observational cohort study, involving participants working in hospitals and basic health units across the Federal District of Brazil. We collected sociodemographic data, vaccination history, and blood samples to evaluate antibody anti-receptor binding domain (RBD) titers, using SARS-CoV-2 IgG II Quant, a chemiluminescence assay from Abbott. The primary COVID-19 vaccination regimen had 2 doses and subsequently doses received were considered boosters. **Results:** From 837 participants recruited, 831 (99%) are vaccinated and 6 (1%) are unvaccinated. The age of the majority of our population (34%) is between 40 - 49 years old and 685 (82%) participants are female. As May 2023, 828 participants completed the primary scheme, 778 (93.6%) received 1 booster, and 582 (70%) received 2 boosters. As the primary scheme, 691 (83%) had 2 doses of CoronaVac and among those with 1 booster, the Pfizer vaccine was the most prevalent 184 (22%). For the second booster, 233 (28%) received Pfizer, 190 (23%) received Janssen, and 138 (16.6%) AstraZeneca. There is no statistical difference in anti-RBD titers in vaccinated groups, comparing the first visit and the last visit which occurred until March of 2022 and 2023, respectively. However, participants with 1 or 2 boosters had higher anti-RBD titers than those with only 2 doses in the first visit (24x and 28x, respectively). When we compared the immunological response in the last visit, we observed that participants with 2 boosters had higher anti-RBD titers than those with only 2 doses (2,5x). Furthermore, 589 (71%) of our cohort had COVID-19, however, of vaccinated participants, only 1 (0.12%) was hospitalized after diagnosis of COVID-19. **Conclusion:** The majority of participants that are vaccinated with 2 boosters presented mild cases of COVID-19. Booster doses are important to maintain immunogenicity and higher antibody anti-RBD titers.

11.023 PBPK Modeling Application as Guidance for Oral Ketamine Prescription for Analgesia in Different Populations. Lippa VNM¹, Goes PRN¹, Martins F¹, Taffarel MO², Piai JMB¹, Diniz A¹ ¹UEM, PPG Pharmaceutical Sciences; Dept of Pharmacy, Maringá, PR, Brazil ²UEM, Dept of Veterinary Medicine, Umuarama-PR, Brazil

Introduction: Ketamine (KET) is an anesthetic drug firstly synthesized in 1962 that has been used more often for its potential use for pain therapy, neurology and psychiatry. Commercially available as a racemic mixture, KET is commonly administrated by intravenous injection, though it has been used in oral form for chronic and acute pain therapy as well [1]. Physiologically-based pharmacokinetic modelling (PBPK) is a pharmacometric tool used to evaluate the movement of a drug through the body, by using differential equations, aiming to achieve a physiologically realistic model, capable of predicting with a certain accuracy how a drug in a specific formulation will interact with our organism [2]. **Aim:** The objective of this study was to evaluate the impact of population and aging over the pharmacokinetic parameters of KET and its most active metabolite norketamine (norKET). **Methods:** WebPlotDigitizer 4.4 and PKAnalix® 2019R2 were used to organize 27 clinical datasets available in the literature for the different administration route IV (n=16) and oral (n=11), ethnics Caucasian (n=24), Japanese (n=1) and Chinese(n=2) and age adult (n=18) and children (n=9) populations. Simcyp Simulator® version 20 was used to develop and validate the PBPK models for KET and norKET. Simulations of children stratified ages of Caucasian, Japanese and Chinese were performed to predict possible differences in plasma exposition of KET. **Results:** The most important enzyme involved in the metabolic biotransformation of KET into norKET, contributing with about 80%, is the CYP2B6. The ethnic population showed that Japanese and Chinese presented plasma KET exposition 60% higher compared to Caucasian. The ontogeny did not prove differences in plasma exposition for Japanese and Chinese children when compared to adults. For Caucasian, only children between 0 to 2 years old presented an increasing up to 40% the plasma exposition compared to adults. **Conclusion:** The PBPK model was able to predict differences in plasma KET exposition and point out risks related to the dose administrated of KET in different populations. This data could be used to prevent anesthetic effects, and to propose more adequate posology regimens for the KET prescription for analgesia. **Financial Support and Acknowledgments:** The authors would like to thank CAPES, CNPq, FINEP, FAPESP and Araucária Foundation for the financial support and Certara for the software license. **References:** [1] Dulin, Palliat. Med., J. 32, p.2, 2020. [2] Jamei, Curr. Pharmacol. Rep., v.2(3), p.161, 2016. [3] Pearce, Drug Metab. Dispos., v.44, p.948, 2016.

11.024 Model-Informed Precision Dosing for Tacrolimus to Improve Graft-Host-Disease Prevention in Brazilian Patients. Olivo LB¹, Pinhatti AV², Wermann S¹, Porto GO¹, Dias BB¹, Zuckermann J², Daudt LE³, Araújo BV¹ ¹UFRGS, Pharmaceutical Sciences Graduate Program; Porto Alegre; Brazil ²HCPA-UFRGS, Pharmacy Service, Porto Alegre, Brazil ³HCPA-UFRGS, Hematology Service, Porto Alegre, Brazil

Introduction: Tacrolimus (TAC) is an immunosuppressive drug used to prevent graft-versus-host disease (GVHD) after hematopoietic stem cell transplantation (HSCT)¹. Despite being widely used in clinical practice, TAC present high variability in its pharmacokinetic (PK) parameters, making it difficult to reach the target window². The aim of this work was to develop a population pharmacokinetic (popPK) model of TAC for Brazilian patients at Hospital de Clínicas de Porto Alegre. **Methods:** Starting dose of 0.3 mg/kg by continuous infusion were administered to patients submitted to HSCT. Therapeutic drug monitoring (TDM) was performed to guarantee plasma TAC concentration at a therapeutic window of 10-20 ng/mL. Doses were adjusted using empiric HCPA protocols. TDM retrospective data was used to model building. The model was developed using NONMEM® (Icon). Interindividual variability (IIV) was analyzed between subjects. Several demographic and biochemical covariates were tested to explain IIV. External validation was calculated by absolute prediction error (APE%) for population and individual predictions using extra patients' plasma samples. **Results:** A one-compartment model was built from samples of 50 patients (5 – 60 y.o.) treated with TAC. IIV was explained by adding patients' age and hematocrit (HCT) as covariates in clearance (CL). The typical value of CL and Vd were estimated to be 9.37 L/hr and 155 L, respectively. The IIV of CL and Vd were 30 and 101%, respectively. Model internal validation was performed through a visual predictive check and a non-parametric bootstrap. Individual and population APE% were 22.96 and 17.19, respectively. The algorithm for individualized TAC therapy was $\text{Dose (mg)} = \text{Cpss_target} * 9.37 * (\text{AGE}/26.84)^{0.353} * (-0.0072 * \text{HCT}) * e^{(0.09)}$. **Conclusion:** A popPK model for TAC was successfully built for Brazilian patients. The equation can be used to personalize doses and ensure a successful post-transplant outcome. This is the first popPK model for TAC built in Brazil. A specific model for our population provides more secure and precise information regarding target attainment. **Acknowledgments:** Hospital de Clínicas de Porto Alegre – Porto Alegre – Brazil [1] Sharma N, et al. *Cancers (Basel)*. v.13(4), p.613, 2021. [2] Cheung J, et al. *Can J Hosp Pharm*. v.73(1), p.37-44, 2020.

11.025 Pharmacokinetics and Biotransformation of JMXiBn, a Bupivacaine Analogue with Limited Action in Sodium Channels and Improved Activity Against Asthma Changes. Nascimento VA¹³, Cotias AC¹, Coutinho DS¹³, Santos GCM¹, Costa JCS², Silveira GPE³, Pinto DP³, Fonseca LB³, Silva PMR¹, Martins MA¹ - ¹IOC-Fiocruz, Lab. of Inflammation, ²Fiocruz, Vice Presidency of Production and Innovation in Health, ³Fiocruz, Equivalence and Pharmacokinetics Service, Brazil

Introduction: Prior studies show that nebulised lidocaine might be an applicable asthma treatment, but adverse effects associated with anaesthesia of the airways limit clinical use. In a parallel investigation, we demonstrated the therapeutic potential of a bupivacaine analogue, JMXiBn [(RS)-1-benzyl-N-(2,6-dimethylphenyl) piperidin-2-carboxamid], synthesised and screened for reduced local anaesthetic activity. This study investigated the pharmacokinetics of JMXiBn, as well as the contribution of the putative metabolite, pypecolil-xylydide (PPX), to the protective pharmacological effect of JMXiBn on asthma changes. **Methods:** A/J Mice (n=7) sensitised to a mixture of Al(OH)₃ and ovalbumin (OVA) were challenged intranasally with 25 µg OVA for four days. Treatments with PPX (1%, aerosol) or dexamethasone (3 mg/kg, oral) were given immediately after the ovalbumin challenge. Lung function, inflammatory changes and mucus production were evaluated. To assess the pharmacokinetic parameters, we administered JMXiBn (5 mg/kg, intravenously) to healthy mice. Plasma samples were collected before and at different time points post-treatment. JMXiBn and PPX concentrations were determined using an HPLC-MS/MS method and calculated as per the time of plasm collection in samples from distinct animals in groups of 6 animals. Pharmacokinetic parameters were determined using the PKSolver 2.0 program and analysed using the non-compartmental model of intravenous administration. All experimental procedures involving animals were approved by the Committee on Use of Laboratory Animals of Oswaldo Cruz Foundation, license L002/2020-A3. **Results:** The *in vivo* pharmacokinetics results showed that HPLC-MS/MS conveniently measured concentrations of JMXiBn and PPX in mouse plasma samples. The methods were validated for linear concentration-response curves of 1 to 1000 ng/mL and 1 to 500 ng/mL concerning JMXiBn and PPX, respectively. Following intravenous administration, JMXiBn reached a maximum mean concentration (C_{max}) of 2390 ng/mL in a maximum time (T_{max}) of 1 min. PPX reached a peak plasma concentration (C_{max}) of 174 ng/mL in these samples within 5 min. The values for terminal plasma half-life (T_{1/2}) of JMXiBn and PPX were 92 min and 110 min, respectively. The area under the curve from time zero to the last sampling time (AUC_{0-t}) of JMXiBn and PPX were 26773 and 12968 ng*min/ml, respectively. We also found that the mice responded with severe airway hyperreactivity, leukocyte infiltration, mucus exacerbation, and increased levels of IL-4, IL-13, KC, and eotaxin-1, all of which were sensitive to PPX but not dexamethasone. **Conclusion:** This work provides fundamental insights into the pharmacokinetics parameters of JMXiBn, pointing out its rapid biotransformation into PPX following intravenous administration into mice. In addition, it is demonstrated that aerosolised PPX can inhibit pivotal inflammatory and functional asthma changes in a murine model of glucocorticoid-resistant asthma, suggesting that PPX could contribute, at least in part, to the pharmacological effect presented by JMXiBn in this system. **Financial Support:** FAPERJ and CNPq.

12. Drug Discovery and Development

12.001 Nose-to-brain Delivery of A Cationic Nanoemulsion Containing the Phytocannabinoid β -Caryophyllene for Anticonvulsant Therapy. Lopes DS¹, Pacentchuk CN¹, Chade ES¹, Oliveira MS², Bernardi LS¹, Oliveira PR¹ ¹Unicentro, Dpt of Pharmacy, Guarapuava, Brazil; ²UFMS, PPG Pharmacology, Santa Maria, Brazil

Introduction: Intranasal delivery systems have been proposed as alternative routes for drug delivery to the brain, primarily for treating diseases that affect the central nervous system such as Epilepsy.¹ That pathology is characterized by a predisposition to spontaneous seizures, and affects more than 50 million people worldwide.² The β -caryophyllene is a phytocannabinoid with anticonvulsant potential, and has shown pharmacological interesting studies, as a naturally occurring selective agonist of the subtype 2 cannabinoid receptor (CB2), and antagonist to cannabinoid receptor (CB1), thus avoiding the undesirable psychoactive effects linked to modulation CB1 receptor.^{3,4} But the BCP has limited oral bioavailability, caused by its low aqueous solubility, therefore, one of the strategies to overcome this problem is the use of nanoemulsions (NE). NE are promising to overcome the inherent properties of oils, including high volatility, low solubility and stability, in addition, they have the ability to deliver drugs to the brain, enhancing their therapeutic effect and minimizing possible side effects.⁵ **Objective:** Thus, considering that developing a cationic nano emulsion containing BCP (BCP-NE) may be useful in nose-to-brain delivery, this study aimed to develop and characterize BCP-NE and its putative anticonvulsant effect via the nose-to-brain route in rats using the pentylenetetrazole (PTZ)-induced seizure model. **Methods:** BCP-NE was prepared by spontaneous emulsification. The oil phase consisted of BCP (40 mg mL⁻¹), lecithin (20 mg), oleylamine (0.5 mM) and an aqueous phase of water and glycerin. Physicochemical and morphological characterization and the content and encapsulation efficiency of BCP were determined in the BCP-NE. Physical stability was evaluated at room temperature, refrigeration and oven. The anticonvulsant potential of BCP-NE was evaluated *in vivo*. **Results:** The BCP-NE showed a droplet size of 244.03 ± 15.67 nm with a polydispersity index of 0.18 ± 0.04 and a zeta potential of 41.1 ± 1.57 mV. The BCP trapping efficiency was 98% at a BCP content of 40 mg mL⁻¹. The NE-BCP conditions were evaluated in one month. During the study, NE-BCP did not show visible separation, remaining stable and within the limits of the criteria, of droplet size, zeta potential and PDI, which indicates stability. To evaluate the putative anticonvulsant effect of BCP-NE administered intranasally, behavioral and EEG changes were monitored against PTZ-induced seizures in rats. In this way, it was observed that the latency for tonic-clonic seizures was delayed in the animals to which BCP-NE was administered intranasally when compared to the EEG from animals that received the vehicle. However, based on the *in vivo* test and the use of EEG, as it is the gold standard test to assess the time of seizure onset, we believe that NE-BCP reached the brain intranasally. Herein, we demonstrated for the first time that BCP-NE administered via the intranasal route, protects against PTZ-induced seizures in rats. **Conclusion:** Altogether, these results demonstrate that BCP-NE administered via the intranasal pathway has anticonvulsant potential, indicating that the developed system nose-to-brain drug delivery offers favorable delivery of BCP. **References:** 1 Misra, SKKP. Colloids Interfaces 1(3): 27. 2023. 2 World health organization. 2023. 3 Oliveira, CC. et al. Epilepsy Behav 56: 26-31. 2016. 4 Tchekalarova, J. et al. Seizure 57: 22-26. 2018. 5 Sarpietro, MG., et al. Thermochim. Acta 600: 28-34. 2015.

12.002 New Thiophene Derivative with Anti-inflammatory Activity. Costa ABA¹, França PRC¹, Paiva JPB¹, Freitas RHCN², Guidinele MCB², Rocha DR², Fernandes PD¹ ¹ICB-UFRJ, Institute of Biomedical Science, Drug Discovery Research Program, Lab. of Pharmacology of Pain and Inflammation, Rio de Janeiro, Brazil. ² UFF, Lab. for the Synthesis of Molecules of Biological Interest, Institute of Chemistry, Rio de Janeiro, Brazil

Introduction: Inflammation is a complex and necessary component to response a biological, chemical, or physical stimulus. Cellular and molecular events that initiate and regulate the interactions between inflammatory process remain a source of ongoing investigation [1]. Most common drugs indicated are the non-steroidal anti-inflammatory drugs (NSAID). However, due to the diversity of their side effects the continue search for new substances is still a goal for researchers. Thiophene-based analogues have been fascinated a lot of scientists as a potential class of biologically active compounds due to many pharmacological properties such as anti-cancer, anti-inflammatory, antimicrobial, anti-hypertensive, and anti-atherosclerotic properties. Thus, the aim of the work was evaluating the anti-inflammatory and antinociceptive effects of thiophene derivative in models of acute inflammation [2]. **Methods:** Female Swiss Webster mice (28-32g, n=6-8) were used in carrageenan-induced cell migration into the subcutaneous air pouch (SAP) model. Mice were orally treated with 45-A (1, 3 or 10 $\mu\text{mol/kg}$). After 1 hour, mice received carrageenan (0.5%, 1 mL) or saline injection into SAP and 24 hours later mice are euthanized, and exudate collected for further measurements. Results are presented as media \pm S.D. Statistical analysis were performed by ANOVA followed by Tukey test (* $p < 0.05$). The protocol for use of animals was approved by CEUA/UFRJ and received the number 35/19. **Results:** Animals treated with carrageenan showed an increased number of leukocytes that migrated to SAP ($84.4 \pm 25^* \times 10^6$ cells/mL) when compared to vehicle-treated group ($0.86 \pm 0.62 \times 10^6$ cells/mL). All doses tested inhibited leukocyte migration when compared to carrageenan group: 1 $\mu\text{mol/kg}$: $42.6 \pm 22.0^* \times 10^6$ cells/mL; 3 $\mu\text{mol/kg}$: $31.6 \pm 19.6^* \times 10^6$ cells/mL and 10 $\mu\text{mol/kg}$: $16.2 \pm 6.6^* \times 10^6$ cells/mL. Furthermore, 3 and 10 $\mu\text{mol/kg}$ reduced cell migration even when comparing with the positive group (dexamethasone, 9 $\mu\text{mol/kg}$; $27.3 \pm 13.1 \times 10^6$ cells/mL). The production of TNF- α in the SAP supernatant increased in carrageenan group ($211.3 \pm 125.8^*$ pg/mL) when compared to vehicle group (45.2 ± 30.1 pg/mL). Pre-treatment with dexamethasone significantly reduced TNF levels ($65.1 \pm 37.0^*$ pg/mL). Pre-treatment 45-A also significantly reduced TNF- α production in their higher doses: 1 $\mu\text{mol/kg}$: 121.0 ± 19.3 pg/mL; 3 $\mu\text{mol/kg}$: 53.0 ± 17.5 pg/mL*; 10 $\mu\text{mol/kg}$ $34.7 \pm 19.5^*$ pg/mL. **Conclusion:** These results suggest that 45-A, a new thiophene derivative, have anti-inflammatory effects demonstrated through the reduction of leucocyte migration and cytokine production. **Financial Support:** CAPES, CNPq and FAPERJ. **Technical assistance:** Alan Minhó **Animal donation:** Instituto Vital Brazil **References:** [1] Germolec, D. R. *Methods Mol. Biol.*, v. 1803, p. 57, 2018. [2] Abedinifar, F. *Mol. Divers.*, v. 25, p. 2571, 2021.

12.003 Anti-inflammatory Effects of New Molecules Based on Cannabidiol. Campos RM¹, Paiva JPB¹, Lontra ACP¹, Invencio CGG¹, Silva IMF², Franco GRR², Gontijo VS², Viegas-Junior. C², Fernandes PD¹ ¹ICB-UFRJ, Program of Reserch and Drug Discovery, Lab. of Pharmacology of Pain and Inflammation, Rio de Janeiro, RJ, Brazil, ²PeQuiM-Unifal, Lab. of Research in Medicinal Chemistry, Alfenas, MG, Brazil

Introduction: the resolution of inflammation has emerged as a critical endogenous process that protects host tissues from prolonged or excessive inflammation that can become chronic. Failure of the resolution of inflammation is a key pathological mechanism that drives the progression of numerous inflammation-driven diseases. (1). The treatment for some pathologies using NSAIDs or SAIDs during a long time can have a lot of side effects so the aim of the chemistries is found new molecules with great effects and fewer side effects. As we know the canabidiol has been a target for treatment of many disorders, exerting anti-inflammatory, immunomodulatory and analgesic effects [2]. Here we show some datas from two new canabidiol analogs in an inflammatory pre-clinical model. **Methods:** female Swiss Webster mice (28-32 g, n = 6-8) were injected with carrageenan for evaluate the anti-inflammatory effects and treated orally with the analogues (PQM290 e PQM-291) at doses of 1, 3 and 10 $\mu\text{mol/kg}$ and 1h later they received an injection of carrageenan (0.5%, 1 mL) or saline (NaCl 0.9%) in the SAP. After 24h, the animals were euthanized and the SAP exudate was collected for leukocyte counts and cytokine measurement. Results are presented as mean \pm SD. Statistical analysis was performed by ANOVA followed by Tukey's test (* $p < 0.05$). The protocol for the use of animals was approved by CEUA/UFRJ and received number 35/19. **Results:** carrageenan injected in SAP leads to an increase in cellularity ($129 \pm 19.5 \times 10^3 \text{cells}/\mu\text{L}$) when compared to the saline-injected group ($3.12 \pm 1.6 \times 10^3 \text{cells}/\mu\text{L}$). The group of animals treated with PQMs significantly reduced leukocyte migration, as follows: PQM290 1 $\mu\text{mol/kg}$: $83.6 \pm 15.0 \times 10^3 \text{cells}/\mu\text{L}$; 3 $\mu\text{mol/kg}$: $129.9 \pm 40.8 \times 10^3 \text{cells}/\mu\text{L}$; 10 $\mu\text{mol/kg}$: $98.8 \pm 14.4 \times 10^3 \text{cells}/\mu\text{L}$. PQM-291 1 $\mu\text{mol/kg}$: $92 \pm 16.4 \times 10^3 \text{cells}/\mu\text{L}$; 3 $\mu\text{mol/kg}$: $83.9 \pm 7.4 \times 10^3 \text{cells}/\mu\text{L}$; 10 $\mu\text{mol/kg}$: $85.5 \pm 33.7 \times 10^3 \text{cells}/\mu\text{L}$. The group dexamethasone shown also a reduction when compared to the group carrageenan, dexamethasone 9 $\mu\text{mol/kg}$: $53.5 \pm 18.8 \times 10^3 \text{cells}/\mu\text{L}$. The production of cytokine IL-6 was measured and shown an increase in the group carrageenan ($965.40 \pm 233.0 \text{ pg/mL}$) compared to the group saline ($53 \pm 21.5 \text{ pg/mL}$). The pre-treatment shown an effect reducing the production of this marker. PQM-290: 1 $\mu\text{mol/kg}$: $425.1 \pm 105.2 \text{ pg/mL}$; 3 $\mu\text{mol/kg}$: $185.5 \pm 117.1 \text{ pg/mL}$; 10 $\mu\text{mol/kg}$: $33.5 \pm 21.0 \text{ pg/mL}$. PQM-291 1 $\mu\text{mol/kg}$: $1097.5 \pm 135.4 \text{ pg/mL}$; 3 $\mu\text{mol/kg}$: $1037.4 \pm 130.2 \text{ pg/mL}$; 10 $\mu\text{mol/kg}$: $849.1 \pm 193.1 \text{ pg/mL}$. The group dexamethasone (9 $\mu\text{mol/kg}$) also show a reduction ($344.45 \pm 203.0 \text{ pg/mL}$). **Conclusion:** initial results suggest that cannabidiol-based molecules (PQM-290 and PQM-291) caused a significant reduction in leukocyte migration. **Financial Support:** CAPES, CNPq and FAPERJ **Acknowledgments:** Alan Minho for technical assistance, Instituto Vital Brazil for animal donation **References:** (1) Panigrahy D., Pharmacol Ther. Nov;227: 107879. 2021 (2) Burstein S., Bioorg. Med. Chem. Apr 1;23(7): 1377-85. 2015

12.004 Ketoconazole Cocrystal as an Alternative to Improve the Solubility and Antifungal Activity. Chade ES², Goes AKS¹, Brancalione RC², Bernardi LS², Zela SJ¹, Murakami FS³, Oliveira PR^{1,2} ¹Unicentro, PPG Pharmaceutical Sciences, Guarapuava, Brazil; ²Unicentro, Dpt of Pharmacy, Guarapuava, Brazil; ³UFPR, PPG Pharmaceutical Sciences, Curitiba, Brazil

Introduction: Solubility is a decisive factor for therapeutic efficacy¹. Ketoconazole (KET) is an antifungal agent with high permeability and low solubility². The use of cocrystal has been a critical approach to increasing the solubility of poorly water drugs. Recent research found the bioavailability enhancement 6-7 times with ketoconazole cocrystal^{3,4}. Thus, this work was to evaluate the MIC of ketoconazole cocrystal. **Methods:** The cocrystals of KET with succinic acid (SAC) were prepared by reaction crystallization method at room temperature by mixing reagents to create supersaturated solutions with precipitation and subsequently, characterized by FT-IR, DRX, MEV, and DSC-TG methods⁵. The minimum inhibitory concentration (MIC) was determined using a colorimetric method capable of correlating absorbance with viable microorganisms' concentration (CFU mL⁻¹)⁶. Ketoconazole (KET), and cocrystal of KET-SAC, were evaluated, and strains of the yeast *Candida albicans* (ATCC 10231) were used. Samples of KET, KET-SAC, and SAC (control) were prepared at 500 µg/mL concentrations using sterile purified water. For the positive control, the antimicrobial ketoconazole was used at a concentration of 500 µg/mL, also was determined the Inhibitory Concentration (IC) 50 % and IC 90 %. **Results:** The MICs were determined by visual readings, considered the last concentrations where there was no development of pink coloration, resulting from the reduction of TTC by microbial metabolism. The MIC of KET and the physical mixture was 62.5µg/ml. Meanwhile, the KET-SAC cocrystal's MIC was 31.2µg/ml; the cocrystal also showed lower IC50% and IC90% results than KET. **Conclusion:** These results can prove that the cocrystallization technique enhanced the solubility and also has an advantageous antifungal activity, requiring more *in vivo* studies with cocrystals. **Financial Support:** This research was funded by Coordenação de Aperfeiçoamento de Pessoal de Nível Superior—Brasil (CAPES) - Finance Code 001; Fundação Araucária de Apoio ao Desenvolvimento Científico e Tecnológico do Estado do Paraná (FA) and Conselho Nacional de Desenvolvimento Científico e Tecnológico (CNPq). **References:** 1. SILVA, F. Euro. J. of Pharm. and Biopharm, v. 187, p. 156, 2023.; 2. CHOI, F. D. J. of Derm. Tre., v. 30, p. 760, 2019.; 3. SHI, K. Pharm. Res., 2023.; 4. MARTIN F. Mol Pharm., v. 17, p. 919, 2020.; 5. GUO, M. Act. Pharm. Sin., v. 11, p. 2537, 2021.; 6. VEIGA. J. of Micro. Met., v. 162, p. 50, 2019.

12.005 Development of a Preclinical Model for the Screening of New Drugs for the Treatment of Osteoporosis in Diabetics. Cartman L, Cotias AS, Chaves AS, Silva PMR, Martins MA, Carvalho VF IOC-Fiocruz, Lab. of Inflammation, Rio de Janeiro, Brazil

Introduction: Diabetes mellitus is a chronic metabolic disease characterized by chronic hyperglycemia accompanied by insufficient insulin secretion and impaired action. Diabetes can induce damage in the skeletal system, causing bone loss and even osteoporosis. Osteoporosis is a systemic bone disease characterized by low bone mass and bone microarchitecture destruction, resulting in increased bone fragility and susceptibility to fractures. Currently, more than 35% of diabetic patients exhibited bone loss, of which approximately 20% met the diagnostic criteria for osteoporosis. Although control of hyperglycemia is the basic treatment for diabetic bone disease, the improper use of hypoglycemic agents is also considered to be associated with an increased risk of fracture in patients with diabetes. Thus, our objective was to investigate if alloxan-induced diabetes is a useful preclinical model for the screening of new drugs for the treatment of osteoporosis in diabetics. **Methods:** Male Swiss-Webster mice (5-6 weeks old with 20 to 25g) were obtained from Oswaldo Cruz Foundation breeding colony and used in accordance with the guidelines of the Committee on Use of Laboratory Animals of Oswaldo Cruz Institute (CEUAIOC/Fiocruz, license L-027/2016). Diabetes was induced by a single intravenous injection of alloxan (65 mg/kg) in male Swiss-Webster mice, and all the analysis were performed 21 days after diabetes induction. The femurs of the mice were scanned with a microcomputed tomography (PerkinElmer GX2 microCT), and the analysis of the bone microarchitecture was performed using the Analyze 14.0 software. **Results:** We showed that diabetes-induced a decrease in the both cortex ($36 \pm 0.75 \text{ mm}^3$ and $26 \pm 0.8 \text{ mm}^3$ to non-diabetic and diabetic mice, respectively, mean \pm SEM, $n = 6$, $p < 0.05$) and trabecular bone mineral density (BMD) ($4.2 \pm 0.19 \text{ mm}^3$ and $3.3 \pm 0.16 \text{ mm}^3$ to non-diabetic and diabetic mice, mean \pm SEM, respectively, $n = 6$, $p < 0.05$), bone volume fraction (BV/TV) ($74 \pm 0.55 \%$ and $66 \pm 0.85 \%$ to non-diabetic and diabetic mice, respectively, mean \pm SEM, $n = 6$, $p < 0.05$), and trabecular thickness (Tb.Th) ($0.21 \pm 0.014 \text{ mm}$ and $0.17 \pm 0.008 \text{ mm}$ to non-diabetic and diabetic mice, respectively, mean \pm SEM, $n = 6$, $p < 0.05$) compared with non-diabetic mice, in parallel to an increase in the specific bone surface (Bs.Bv) ($7.6 \pm 0.3 \text{ mm}^{-1}$ and $9.6 \pm 0.16 \text{ mm}^{-1}$ to non-diabetic and diabetic mice, respectively, mean \pm SEM, $n = 6$, $p < 0.05$). Furthermore, we did not showed alteration in the cortical porosity (Ct.Po), number of pores (Po.N), pore volume (Po.V), and trabecular separation (Tb.Sp) between non-diabetic and diabetic mice. **Conclusion:** Our findings showed that diabetes-induced changes in bone microarchitecture compatible with osteoporosis. Therefore, this model can be used to screen innovative compounds for the treatment of osteoporosis in diabetics. **Financial Support:** IOC, INCT-NIM, CAPES, FAPERJ, JICA, and Ministério da Saúde.

12.006 Emerging Perspectives in the Applications of Artificial Intelligence in Drug Development: A Systematic Review. Maciel ACM¹, Leandro IMC¹, Sato MDO¹, Sato RMS¹.
¹FEMPAR, Dpt of Medicine

Introduction: The popularization of Artificial Intelligence (AI) techniques in the health sciences has yielded applications in pharmacology, such as predictive models for drug development based on biological and clinical data. However, given the incipient nature of these applications, a comprehensive synthesis and a critical review of the literature remains necessary to identify future directions for advancement in this field. This study aims to address novel perspectives for innovation and drug development aided by AI tools. **Methods:** A systematic review was conducted following Preferred Reporting Items for Systematic Reviews and Meta-Analyses (PRISMA) guidelines and evaluated using A MeaSurement Tool to Assess systematic Reviews (AMSTAR) criteria. Searches were conducted in PubMed (N= 22) and LILACS (N= 149) databases using the terms: pharmacology, clinical pharmacology, and artificial intelligence. Articles published from 2018 to 2023 in English, Portuguese, or Spanish were included. Duplicate items and those not meeting eligibility criteria were excluded. **Results:** Out of 171 articles, 27 were selected, which encompass cross-sectional and longitudinal studies. These studies focus on mathematical representations for understanding drug interactions and temporal dynamics, with emphasis on pharmacokinetics and pharmacodynamics. AI algorithms exhibit notable progress in predicting functional peptides, thus optimizing the identification of therapeutic candidates. The efficacy of these algorithms is evidenced through the coherence of the generated predictions with the analysis and interpretation of clinical and laboratory data. The assimilation of these advances leads to the conception and acceleration of clinical trials, therefore facilitating the identification of inappropriate candidates and generating substantial cost savings. The integration of machine learning (ML) and deep learning (DL) refines model calibration, healthcare personalization, and dosage precision. Thus, the application of AI shows to be an effective tool in biomedical research by expediting studies and discoveries. Nevertheless, challenges such as algorithm standardization, ethical foundations for data use and privacy, and algorithmic biases remain obstacles to the widespread adoption. **Conclusion:** The novel AI tools, such as ML and DL, in conjunction with biological databases, offer an innovative perspective in active ingredient discovery and pharmacological clinical trials. Despite the relatively limited availability of validated algorithms and the still incipient use of technology in clinical practice, there is a clear potential for a revolution in data processing and computational science in pharmacology. **Financial Support:** Self-funded.

12.007 Encapsulation of Seriniquinone into PLGA Nanoparticles Improves its Solubility and Prolongs its Release. Miguel RA¹, Hirata AS¹, Martins TS², Lopes LB¹, Costa-Lotufo LV¹. ¹ICB-USP, Dpt of Pharmacology, Brazil; ²Unifesp-Diadema, Dpt of Chemistry, Brazil

Introduction: Seriniquinone (SQ) is a cytotoxic substance with selectivity to melanoma cell lines. SQ mechanism of action involves dermcidin targeting, and autophagy and apoptosis activation. Despite being a promising drug candidate, *in vivo* studies with SQ have been precluded by its poor aqueous solubility (0.06 μM). To overcome this limitation, SQ was encapsulated into biocompatible and biodegradable poly (D,L-lactide-co-glycolide) nanoparticles (PLGA-NPs). In this work, nanoparticle characterization, evaluation of SQ release kinetics and of the antimelanoma activity of this new nanocarrier (PLGA-SQ-NPs) were conducted. **Methods:** NP size and morphology were characterized by scanning electron microscopy (SEM). Thermogravimetric analysis (TGA) and differential scanning calorimetry (DSC) were used to investigate the solubilization process of SQ in PLGA-SQ-NPs. SQ release was evaluated by placing the PLGA-SQ-NPs in dialysis bags (14 kDa pores), which were immersed in PBS containing 6% tween 80 (w/v) as receptor fluid at 37°C under continuous stirring. SQ quantification was performed using high performance liquid chromatography (HPLC). SQ antineoplastic activity was assessed in SK-MEL-28 (BRAV600E) and SK-MEL-147 (NRASQ61R) cell lines. 48h-treatments were carried out with SQ solution (in DMSO), unloaded PLGA-NPs or PLGA-SQ-NPs (0.00032-5 μM), with dacarbazine (0.00064-125 μM) and doxorubicin (0.00064-10 μM) as positive controls. Then, proliferation and viability were evaluated with sulforodamine B (SRB) and confirmed by Trypan blue exclusion assays. To verify whether shorter exposure times of melanoma cells to SQ and PLGA-SQ-NPs, cells were treated for 6h and seeded in another plate with SQ- or NP-free medium to assess the clonogenic capacity after this acute exposure. **Results:** NPs displayed spherical shape and size ranging from 200 to 400 nm, with no SQ precipitates. TGA and DSC data corroborate these findings with the absence of SQ endothermic peak at 279 °C after encapsulation, as well as with an increase of 10°C in the degradation onset temperature of PLGA-SQ-NPs when compared with blank NPs. After 96h, 16.5% of SQ content was released from the nanoparticles, while SQ diffusion from a control solution reached 89.9% after only 6h. SRB and Trypan blue assays demonstrated that SQ had similar activity as DOX and inhibits 50% of cell growth in both cell lines with concentrations ~625-fold more toxic than dacarbazine. PLGA-SQ-NPs displayed a similar concentration-response curve as SQ in solution. Blank NPs stimulated cell proliferation in low to moderate concentrations (equivalent to 0.00032-1 μM) and inhibited ~20% of cell growth in the highest dose tested (5 μM). Treatment with SQ solution or PLGA-SQ-NPs in the range of 0.7-1.6 μM for 6h resulted in a reduction of 35.1-56.9% in the number and of 17.2-25.5% in the size of colonies after 6-8 days. **Conclusion:** PLGA-NPs enabled SQ dispersion in aqueous-based vehicles. No reduction of SQ activity on melanoma models was reported upon its encapsulation in the NPs despite its prolonged release. **Financial Support:** São Paulo State Research Support Foundation (FAPESP) (2020/09270-4; 2015/17177-6; 2022/15832-0, 2018/13877-1, 2020/06613-8, 2022/05133-8, 19/08582-5, 17/17844-8) and The National Council for Scientific and Technological Development (CNPq) (306866/2020-0; 380363/2023-2; 130248/2023-1). **Acknowledgements:** We acknowledge Moacir Francisco de Brito, Sonia Rodrigues Leite, Helori Vanny Domingos and Dr Simone Aparecida Teixeira for technical support. **Reference:** Hirata, AS. *Mar. Drugs*. v. 20(5). p. 301. 2022.

12.008 Potential New Compounds for the Treatment of Inflammatory Diseases: New Synthetic Structural Analogues of Cannabidiol. Lontra ACP¹, Paiva JPB¹, Invencio CGG¹, Gontijo VS², Franco GRR², Viegas-Junior C², Fernandes PD¹ ¹ICB-UFRJ, Program of Research and Drug Discovery, Lab. of Pharmacology of Pain and Inflammation, Rio de Janeiro, RJ, Brazil, ²PeQuiM-Unifal, Lab. of Research in Medicinal Chemistry, Alfenas, MG, Brazil

Introduction: Inflammation is involved in the pathophysiological process of several diseases such as inflammatory bowel diseases, COVID-19 and certain types of cancer. This occurs because this process, which previously acted as a defense mechanism against the aggression promoted by physical, chemical, or biological agents and in favor of tissue repair, becomes exacerbated and detrimental to the organism [1,2]. As cannabidiol (CBD) has already known anti-inflammatory properties [3], synthetic structural analogues of CBD were synthesized to explore its effects in preclinical models of acute inflammation and nociception. **Methods:**

Female Swiss Webster mice (n=6-8) were used in model of carrageenan-induced cell migration into the subcutaneous air pouch (SAP). Treatment was realized orally with PQM-275 or PQM-276 (1, 3 or 10 $\mu\text{mol/kg}$) 24h before the carrageenan (0.5%, 1 ml) injection into the SAP. Exsudate were used to leukocyte count and cytokine measurement. The capsaicin-induced licking response was used to evaluate antinociceptive potential of the substances. Results are presented as media \pm sd. Statistical analysis was calculated by ANOVA followed by Bonferroni's test (*p<0.05). **Results:** PQMs reduced leukocyte migration at 3 doses tested. Saline-Vehicle: $3.4 \pm 3.7 \times 10^3 \text{ cel}/\mu\text{L}$; Dexamethasone (9 $\mu\text{mol/kg}$): $53.5 \pm 17.5 \times 10^3 \text{ cel}/\mu\text{L}$; Carrageenan-Vehicle: $157.3 \pm 71.4 \times 10^3 \text{ cel}/\mu\text{L}$; PQM-275: 1, 3 and 10 $\mu\text{mol/kg}$: $84.6 \pm 45.8 \times 10^3 \text{ cel}/\mu\text{L}$; $71.6 \pm 44 \times 10^3 \text{ cel}/\mu\text{L}$; $52.4 \pm 36.5 \times 10^3 \text{ cel}/\mu\text{L}$ respectively; PQM-276: 1, 3 and 10 $\mu\text{mol/kg}$: $76.3 \pm 28.7 \times 10^3 \text{ cel}/\mu\text{L}$; $59.0 \pm 32.4 \times 10^3 \text{ cel}/\mu\text{L}$; $71.6 \pm 24.6 \times 10^3 \text{ cel}/\mu\text{L}$ respectively. PQMs also reduced TNF- α levels. Saline-Vehicle: $70.7 \pm 17.8 \text{ pg/mL}$; Dexamethasone: $104 \pm 37.5 \text{ pg/mL}$; Carrageenan-Vehicle: $330.3 \pm 97.4 \text{ pg/mL}$; PQM-275: 1 $\mu\text{mol/kg}$: $225.8 \pm 58.8^* \text{ pg/mL}$; 3 $\mu\text{mol/kg}$: $229.7 \pm 82.4^* \text{ pg/mL}$; 10 $\mu\text{mol/kg}$: $128 \pm 33.4^* \text{ pg/mL}$; PQM-276: 1 $\mu\text{mol/kg}$: $153.8 \pm 80.9^* \text{ pg/mL}$; 3 $\mu\text{mol/kg}$: $143.7 \pm 39.7^* \text{ pg/mL}$; 10 $\mu\text{mol/kg}$: $143.2 \pm 44.4^* \text{ pg/mL}$. Significant activity was also observed in the capsaicin-induced licking test. PQM-275: 1, 3 and 10 $\mu\text{mol/kg}$: $44.2 \pm 15.4^* \text{ sec}$ (35% reduction); $28.6 \pm 7.5^* \text{ sec}$ (58% reduction); $31.4 \pm 4^* \text{ sec}$ (53.9% reduction), respectively; PQM-276: 1, 3 and 10 $\mu\text{mol/kg}$: $58.4 \pm 9.7 \text{ sec}$ (14.3% reduction), $48.4 \pm 10.5^* \text{ sec}$ (29% reduction) and $23 \pm 5.1^* \text{ sec}$ (66.2% reduction), respectively, comparing with vehicle-treated group: $68.2 \pm 11.4 \text{ sec}$. **Conclusion:** Both substances showed significant effects at preclinical models of acute inflammation and nociception, suggesting its anti-inflammatory and antinociceptive potential. **Financial Support:** CAPES, CNPq and FAPERJ **Animal Research Ethical Committee:** CEUA/UFRJ 31, 35/19. **Acknowledgments:** Alan Minho for technical assistance, Instituto Vital Brazil for animal donation **References:** 1. Feehan KT. *Trends. Mol. Med.*, v. 25, p198-214, 2019. 2. Hirano T. *Int. Immunol.*, v. 33, p127-148, 2021 3. Atalay S. *Antioxidants.*, v. 9, p. 21, 2019.

12.009 New Cinamoyl-N-acyldrazone Analogues of Cannabidiol Produce Analgesic Effects in Acute and Chronic Nociception Models in Mice. Oliveira EA¹, Silva IMF², Franco GRR², Gontijo VS², Viegas-Junior C², Fernandes PD¹, Giorno TBS¹ ¹ICB-UFRJ, Drug Discovery Research Program, Pain and Inflammation Pharmacology Lab., Brazil. ²PeQuiM-UNIFAL, Research Lab. in Medicinal Chemistry, Brazil

Introduction: Cannabidiol (CBD), the second largest pharmacologically active component in *C. sativa*, has analgesic, anti-inflammatory, antioxidant, anxiolytic, antitumoral and antiemetic effects [1]. Furthermore, CBD and some of its analogues also have effects in models of acute and chronic pain [2] such as fibromyalgia [3]. The aim of this study was to evaluate the analgesic effects of new CBD analogues (PQMs -292, -293, -300 and -301) in models of acute and chronic nociception. **Methods:** PQMs -292, -293, -300 and -301 were orally administered to female Swiss Webster mice (20-30g, 8-10 weeks, n=8-10) at the doses of 1, 3 or 10 $\mu\text{mol/kg}$ and evaluated for peripheral nociception using the capsaicin-induced paw licking model and central nociception using the hot plate test. For the evaluation of a possible activity of PQMs in chronic nociception were used reserpine-induced fibromyalgia model. Statistical analysis was performed by ANOVA and Bonferroni's post-test (* $p < 0.05$). Results are expressed as mean \pm SD of time in seconds (latency) and mean \pm SD of AUC. **Results:** PQMs -292, -293, -300 ou -301 showed significant activity in the peripheral nociception model as observed by the results obtained in capsaicin-induced paw lincking at doses of 3 and 10 $\mu\text{mol/kg}$ significantly compared to the vehicle (PQM-292: 3 $\mu\text{mol/kg}$ =23.4 \pm 6.4*sec. (55.3%); 10 $\mu\text{mol/kg}$ =25.2 \pm 4.2*sec. (51.9%);PQM-293: 3 $\mu\text{mol/kg}$ =26.2 \pm 4.2*sec. (49.8%); 10 $\mu\text{mol/kg}$ =21.8 \pm 3.6*sec. (60.5%);PQM-300: 3 $\mu\text{mol/kg}$ =20.7 \pm 3.8*sec. (60.5%); 10 $\mu\text{mol/kg}$ =20.6 \pm 6.7*sec. (60.5%);PQM301: 3 $\mu\text{mol/kg}$ =2.6 \pm 4.0*sec. (47.2%); 10 $\mu\text{mol/kg}$ =22.7 \pm 11.8*sec. (56.6%) *versus* 52.3 \pm 15.9 sec. of vehicle-treated group. In the hot plate test, PQMs significant increased the AUC when compared with the vehicle group and in some cases was similar or higher than that value of morphine group or CBD group (PQM-292, PQM-293, PQM-300 and PQM-301: 10 $\mu\text{mol/kg}$ = 7,134.5 \pm 1,203.9*; 4,104.0 \pm 1,306.7*; 4,728.0 \pm 2,708.6* and 2,942.0 \pm 2,026.1*; 3 $\mu\text{mol/kg}$ =5,224.0 \pm 2,861.3*; 2,85.0 \pm 1,445.8* ; 1,077.4 \pm 1,136.7* and 1,458.6 \pm 2,274.4*; 1 $\mu\text{mol/kg}$ = (5,167.5 \pm 4,609.6; 10,359.5 \pm 2,774.0* ; 5,586.0 \pm 3,680.3*; and 1,741.0 \pm 1,401.4*, respectively, *versus* vehicle-treated group (443.7 \pm 44.9), morphine-treated group (2,619.5* \pm 937.8) and CBD-treated group (2,339.5* \pm 1,615.8). In reserpine-induced fibromyalgia model, PQMs -292, -293,-300,-301 increased the AUC at a dose of 10 $\mu\text{mol/kg}$ when compared to the reserpine-induced group (13.9 \pm 1.5*, 13, 1 \pm 1.5*11.1 \pm 0.8*, 13.1 \pm 1.0* respectively, *versus* reserpine group=8.2 \pm 1.4), indicating that the treatment increased the latency of the animals. **Conclusion:** In this way, PQMs -292,-293,-300 and -301 have an antinociceptive effect in acute and chronic pain models, but the investigation of their mechanisms of action is still in progress. **Financial Support:** CNPq and FAPERJ **Acknowledgments:** Alan Minho for technical assistance, Instituto Vital Brazil for animal donation. **References:** [1]Amin, MR. *Adv. Exp. Med. Biol.*, v. 1162, p. 151, 2019.[2]Silva-Cardoso, GK. *Neuropharmacology*, v. 19, p. 108712, 2021. [3]Berger, AA., *Best Pract. Res. Clin. Anaesthesiol.*, v. 34(3), p. 617, 2020.

12.010 Development and Pharmacological Evaluation of a Novel H₂S-Triamcinolone Hybrid-Releasing Nanoemulsion in Wound Resolution. Souza ALC¹, Gois GA¹, Cerqueira ARA¹, Teixeira SA¹, Muscará MN¹, Caliendo G², Lopes LB¹, Costa SKP¹ ¹Depto de Farmacologia, Instituto de Ciências Biomédicas, Universidade de São Paulo. ²Università degli Studi di Napoli Federico II, Italy.

Introduction: Skin injuries, including burns, accounts for significant cost to the healthcare systems due to the lack of satisfactory treatments¹. Studies show that the endogenous gasotransmitter hydrogen sulfide (H₂S) plays an important role in the normal skin, and newly developed H₂S donors possess therapeutic potential to treat skin injuries and diseases². Various delivery systems including nanoparticles have been suggested as effective delivery of anti-inflammatory drugs. This project was carried out to evaluate and characterize the compatibility of the H₂S-steroid hybrid molecule aryl thiamides (TBZ)-triamcinolone with a delivery (nanoemulsion) system, as well as to determine the pharmacological profile of this molecule on fibroblast wound-healing capabilities *in vitro*. **Methods:** A nanostructured delivery system was developed to incorporate the H₂S hybrid molecule, consisting of aqueous (90%; poloxamer 127 1%) and oily phases (10%; acid oleic: monolein; 8: 2) prepared separately. The H₂S hybrid molecule was added to the aqueous phase, and further homogenized with the oily phase, and kept in a sonicator (4 min, 30s on-off) immediately before the experiments. The evaluation of the formulation stability with the H₂S hybrid was carried out at temperatures ranging from -20°C to 5 - 22°C. Cytotoxicity and the pharmacological profile of the test molecule was performed via 3-(4,5-dimethylthiazol-2-yl)-2,5-diphenyltetrazolium bromide (MTT) reduction method (570 nm), and the wound healing test on 3T3 fibroblast cells treated with DMEM or delivery system containing the hybrid molecule, respectively. **Results:** The formulation development tests revealed by the technique of Dynamic Light Scattering (DLS) no difference in particle size (Z-average) between the empty system and system containing the H₂S hybrid (344.1 ± 7.108 and 419 ± 7.8, respectively). The stability of the formulation was altered at -20°C, but no significant differences were observed in the range of 22°C and 5°C after 48h evaluation period, indicating that the formulation *per se* can be kept in various temperature range. There was no significant change in the Polydispersity index (Pdl) of the formulation after 48h evaluation. In the wound healing *in vitro* test (3T3 fibroblast cells), the treatment with H₂S hybrid molecule at a concentration of 1.95 to 7.81 µM, into the delivery system did not show cytotoxicity, resulting in IC₅₀ (18 µM). After 24h of the superficial lesion in the cell culture, treatment with the formulation containing the test molecule (0.02, 0.2, 2 and 20 µM) did not significantly differ from the untreated wound-healing. In the analyzed period of 24 h, the closure of the wound-healing was almost completed. **Conclusion:** Using the nanoemulsion to control the delivery of H₂S (TBZ)-triamcinolone hybrid introduced the opportunity to fine tune the pharmacological concentration of H₂S *in vitro*; however, the potential benefit of the delivery system containing the H₂S hybrid molecule could not be revealed. **Financial Support:** CAPES (001), CNPq (312514/2019-0), Fapesp. **References:** 1. Int. J. Environ. Res. Public. Health., v. 19, p. 1338., 2. Br. J. Pharmacol., v. 177, p. 857, 2020.

12.011 The Promising Treatment of Acute Inflammation with New Hybrids Capsaicin-Curcumin. Paiva JPB¹; Lontra,ACP¹; Invencio CGG¹; Ribeiro LV²; Campos TG²; Viegas-Junior C², Fernandes PD¹ ¹ICB-UFRJ, Program of Research and Drug Discovery, Lab. of Pharmacology of Pain and Inflammation, Rio de Janeiro, RJ, Brazil, ²PeQuiM-Unifal, Lab. of Research in Medicinal Chemistry, Alfenas, MG, Brazil

Introduction: Inflammation is a complex pathological condition associated with exaggerated human immune system involving various activated immune cells and biomolecules. Current therapy for inflammatory diseases is limited to the steroidal and non-steroidal anti-inflammatory agents. The chronic use of these drugs is reported to cause severe adverse effects like gastrointestinal, cardiovascular, and renal abnormalities. There is a massive need to explore new anti-inflammatory agents with selective action and lesser toxicity. Plants and isolated phytoconstituents are promising and interesting sources of new anti-inflammatories. [1]. In this respect, it was made a hybridization between the structure of curcumin and capsaicin, result in the substances PQM-310 and PQM-311. The aim of the work was evaluating the anti-inflammatory activity, using pre-clinical model of acute inflammation.

Methods: Female Swiss Webster mice (28-32g, n=6) were used carrageenan-induced cell migration into the subcutaneous air pouch (SAP) model. Mice were orally treated with PQM-310 or PQM-311 (1, 3 or 10 mg/kg). After 1 hour, mice received carrageenan (0,5%, 1 mL) or saline injection into SAP and 24 hours later mice are euthanized, and exudate collected for further measurements. Results are presented as media \pm sd. Statistical analysis were performed by ANOVA followed by Tukey's test (* p <0.05). **Results:** Both substances significantly reduced cell migration when comparing to the carrageenan group ($79.0 \pm 20.3 \times 10^3$ cells/ μ L) compared to the group saline ($21.0 \pm 6.9 \times 10^3$ cells/ μ L), the standard drug used were dexamethasone 2,5 mg/kg: $16.8 \pm 2.1 \times 10^3$ cells/ μ L, show a reduction in the cell migration. The pre-treatment with the molecules, also shown a reduction PQM-310: 1 mg/kg: $39.6 \pm 4.3 \times 10^3$ cells/ μ L; 3 mg/kg: $32.0 \pm 11.9 \times 10^3$ cells/ μ L and 10 mg/kg: $19.3 \pm 7.2 \times 10^3$ cells/ μ L. PQM-311, 1 mg/kg: $37.9 \pm 6.5 \times 10^3$ cells/ μ L; 3 mg/kg: $41.9 \pm 13.7 \times 10^3$ cells/ μ L and 10 mg/kg: $30.7 \pm 13.2 \times 10^3$ cells/ μ L. The cytokine IL-1 β production was also reduced when compared with the group carrageenan (774.14 ± 249.9 pg/mL) this group was compared to the group saline (93.7 ± 22.9 pg/mL), showing and increase of the production of this cytokine. PQM-310: 1 mg/kg: 130.8 ± 73.9 pg/mL; 3 mg/kg: 119.1 ± 49.8 pg/mL; 10 mg/kg: 380.2 ± 131.8 pg/mL and PQM-311: 1 mg/kg: 180.1 ± 82.4 pg/mL; 3 mg/kg: 244.6 ± 36.1 pg/mL; 10 mg/kg: 164.6 ± 97.7 pg/mL, **Conclusion:** The results suggest that both substances (PQM-310 and PQM-311) present anti-inflammatory activity since both reduced cell migration induced by carrageenan and reduced the production of cytokine IL-1 β . **Financial Support:** CAPES, CNPq and FAPERJ **Acknowledgments:** Alan Minho for technical assistance, Institute Vital Brazil for animal donation **References:** Patil KR, Mahajan U.B., Int. J. Mol. Sci. 20(18): 4367. 2019. [1]

12.012 Lipid Nanocarriers for Chemoprevention of Breast Cancer: Co-encapsulation of Fenretinide and Perillyl Alcohol, *in vitro* Cytotoxicity and *in vivo* Localization. Malagó ID, Salata GC, Machado-Neto JA, Lopes LB. ICB-USP, Dpt of Pharmacology, Brazil

Introduction: Chemoprevention is an important strategy to prevent and/or reduce the recurrence of breast cancer in high-risk women. However, the available options have severe adverse effects and low patient adherence [1]. Fenretinide and perillyl alcohol (POH) are promising compounds for breast cancer preventive therapy; nevertheless, adverse effects upon systemic administration could limit their use [2, 3]. The aim of this work was to develop nanostructured lipid carriers (NLC) for coencapsulation and sustained release of fenretinide and POH directly in the mammary tissue, thus increasing local concentration of the drugs and reducing adverse effects. **Methods:** Firstly, the effect of combining fenretinide and POH at various ratios (1: 0-1: 4 w/w) on the viability of MCF-7 and MDA-MB-231 breast cancer cells was assessed using MTT. Subsequently, nanocarriers were prepared, and the effect of drug incorporation (0.5-2%) on the size, polydispersity index (Pdl), zeta potential and rheological behavior was assessed. *In vitro* release studies were conducted for POH (1%) and fenretinide (0.5%) over 24 h using Franz diffusion cells. The influence of fenretinide and POH co-encapsulation in the selected NLC on the viability of MCF-7 and MDA-MB-231 cells was assessed using MTT and compared to drug solutions. An *in vivo* localization study in the mammary tissue of rats was performed using the NLC loaded with a fluorescent marker (Alexa Fluor 647). **Results:** The combination between fenretinide and POH had an enhanced cytotoxic effect compared to fenretinide alone, but there were no pronounced differences comparing the 1: 1 and 1: 4 (w/w) ratios; therefore, the 1: 1 and 1: 2 ratios were selected for encapsulation in the NLCs. The NLC displayed a mean size of 291.8 ± 13.8 , Pdl of 0.204 ± 0.034 and zeta potential of -20.9 ± 2.7 . The NLC presented Newtonian rheological behavior, which was not altered by POH at 1%; higher concentrations increased viscosity (4-fold). After 24 h, 46.8% of POH and 2.5% of fenretinide were released. The NLC containing only fenretinide (0.5%) presented a higher IC_{50} compared to the solution (2.5-fold). Co-encapsulation with POH (1%) reduced cell viability, leading to similar IC_{50} values as a fenretinide solution, despite the prolonged drug release. The NLC enabled local retention of Alexa Fluor for 30 days, suggesting prolonged release, and did not cause irritation according to a histological analysis and the HET-CAM assay. **Conclusion:** The developed NLC presented adequate physicochemical characteristics and was able to promote sustained drug release. It provided promising results regarding cytotoxicity in breast cancer cells, *in vivo* localization and irritation potential. **Financial Support:** Financial support was received from CAPES (001), CNPq, INCT Nanofarma and FAPESP (2022/00997-4, 2018/13877-1). **References:** 1. Cazzaniga, M. J Biomed Biotechnol, v. 2012, p. 985620, 2012. 2. Veronesi, U. Annals of oncology, v. 17, p.1065, 2006. 3. Chen, TC. Am J Cancer Res, v. 5, p. 1580, 2015.

12.013 Development and Characterization of a Nanostructured Lipid Carrier for Doxycycline Encapsulation. Conceição M¹, Di Filippo LD¹, Duarte JL¹, Pedrazzi JFC², Nascimento GC^{2,3}, Del-Bel E^{2,3}, Chorilli M¹, Gremião MPD¹ ¹FCF-Unesp, Araraquara, SP, Brazil, ²FMRP-USP, Neuroscience Graduate Program, Ribeirão Preto, SP, Brazil, ³FORP-USP, Dept of Basic and Oral Biology, Ribeirão Preto, SP, Brazil

Introduction: Doxycycline (DOX) is a broad-spectrum antibiotic used for the treatment of skin, respiratory, urinary and sexually transmitted infections such as chlamydia and gonorrhea. Recently, anti-inflammatory and neuroprotective actions of DOX towards Alzheimer's and Parkinson's diseases have brought insights for its repurposed use. Thus, the present work presents a nanobased drug delivery system that might be useful both for general and repurposed use of DOX. **Methods:** Doxycycline hyclate from Sigma-Aldrich® underwent solubility test by UV spectrophotometry with 4 different liquid lipids namely: caprylic triglyceride, castor oil, grape seed oil and isopropyl myristate. Excess DOX was mixed with each oil and stirred for 24 hours. The material was then centrifuged and analyzed by UV spectrophotometry at 360 nm [1-3]. The nanostructured lipid carriers (NLCs) were obtained by fusion-emulsification and ultrasonication method, as follows: the aqueous phase comprised of ultra-purified water and the oil phase made by Compritol, DOX (8 mg), Tween 20, and isopropyl myristate were heated to 65-70 °C. The aqueous phase was slowly added to the oil phase under continuous magnetic stirring. The pre-formulation was sonicated in a QSonica Q700 instrument for 5 min [1]. After being stored for 24 hours at room temperature, an aliquot of the formulations was dissolved in methanol for particle size and polydispersity index (PDI) analysis by Dynamic Light Scattering (DLS) and zeta potential (ZP) by electrophoretic mobility in a Zetasizer NanoZS90 instrument. Encapsulation efficiency (EE%) analysis was performed by UV spectrophotometry at 360 nm [3]. **Results:** The liquid lipid of choice for DOX was isopropyl myristate, with higher concentrations of DOX (929.38 ug/mL) as revealed by solubility test. As second place was grape seed oil (328.09 ug/mL) followed by caprylic triglyceride (318.29 ug/mL) and castor oil (245.61 ug/mL). As for particle size, ZP, and PDI, DOX NLCs presented averages of 65.57 nm, -3.48 mV and, 0.237, respectively. These values are interpreted as a stable formulation with minimum particle size that favors drug delivery. As for EE%, the resulting percentage of 91.36% once more reveals that DOX NLCs were efficient in encapsulating the drug with a significant value when considering drug delivery systems. **Conclusion:** The experiment demonstrated that DOX can be encapsulated in NLC composed of the aforementioned materials, with isopropyl myristate being a suitable liquid lipid for the formulation. Thus, doxycycline encapsulation by using nanostructured lipid carriers is a feasible strategy with promising results. **Financial Support:** Coordenação de Aperfeiçoamento de Pessoal de Nível Superior ? Brasil (CAPES) ? Finance Code 88887.801886/2023-00. São Paulo Research Foundation (FAPESP), grant #2023/04282-2. **References:** Di Filippo LD. Int J Pharm. 25; 618: 121682. 2022 Humayoon, R. J Pharm Drug Deliv Res, 3(2). 2014 Kogawa, AC. Int. J. Pharm. Sci. 2250-0480. 2012

12.014 Copaifera Oilresin in the Treatment of Pulmonary Inflammation Caused by Sars-Cov-2. Almeida PG¹, Vanzan DF², Clarindo FA³, Coelho-dos-Reis JGA³, Cabral LM², Fernandes PD¹ ¹ICB-UFRJ, Drug Discovery Research Program, Lab. of Pharmacology of Pain and Inflammation ²UFRJ, Pharmacy College, Dept of drugs and Medicines. Brazil. ³ICB-UFGM, Dept of Microbiology, Lab. of Basic and Applied Virology, Minas Gerais, Brazil

Introduction: COVID-19 (Coronavirus Disease-19), caused by the SARS-Cov-2 virus (Severe acute respiratory syndrome coronavirus 2), is responsible for a pandemic in which more than 21 million cases and almost 600,000 deaths occurred in Brazil (1). Although most people with COVID-19 recover within two weeks, some patients have debilitating conditions called “Post-COVID-19 Syndrome” or long-term COVID. Patients with COVID-19 who progress to acute respiratory distress syndrome have an intense cytokine release syndrome, described as a “cytokine storm”, which appears to be associated with most of the deleterious effects of the disease (2). In Pará state (Amazon region, Brazil), people of all ages and social classes consider Copaiba oilresin one of the most important natural drugs from the Amazon region. This oilresin is mainly composed of sesquiterpenes (93.5-99.7%), where its major component is β -caryophyllene (36-85%). In addition, other sesquiterpenes such as trans-Cadine-1(6),4-diene (0.6-24.6%), β -elemene (0.7-2.9%), α -copaene (0.6 -18.1%) and α -humulene (4.2-11.3%) can be found in *Copaifera multijuga* oilresin (3). Several parts and preparations of the plant are used in folk medicine (4). Copaiba oleoresin exhibits a variety of biological actions, including anti-inflammatory (5), antibacterial and antifungal activities. The aim of the work was evaluating the effects of a lipidic nanoformulation prepared with *Copaifera* against pulmonary inflammation induced by attenuated SARS-CoV-2. **Methods:** Female Swiss Webster mice (28-32g, n=6) were used in the intranasal instillation model with inactivated virus (1000 PFU/50 μ L). After 7 days, the animals were euthanized and bronchoalveolar lavage (BAL) was collected to quantify the leukocyte infiltrate and inflammatory mediators. Lung tissue was removed and prepared for histological sections for immunocytochemical analysis. In this protocol, the animals also received treatment with a *Copaifera multijuga* nanoemulsion (at doses of 30, 100 or 150 mg/kg), 1 hour before instillation. Results are presented as media \pm sd. Statistical analysis were performed by ANOVA followed by Tukey test (*p<0.05). **Results:** All doses of *Copaifera multijuga* nanocomposite significantly reduced leukocyte migration 7 days after virus instillation. Vehicle-treated group: $4,695 \pm 2,390 \times 10^6$ cells/mL; Copaiba: 30 mg/kg: $1,350 \pm 725.4 \times 10^6$ cells/mL; 100 mg/kg: $1,638 \pm 617.5 \times 10^6$ cells/mL and 150 mg/kg: $1,029 \pm 682.2 \times 10^6$ cells/mL. The nanocomposite also significantly reduced production of TNF- α into the BAL: 30 mg/kg: $514.9 \pm 298.8 \text{ pg/mL}$; 100 mg/kg: $250.5 \pm 251.3 \text{ pg/mL}$; 150 mg/kg: $229.7 \pm 200.3 \text{ pg/mL}$ when comparing with vehicle-treated group ($3,845 \pm 2,140 \text{ pg/mL}$). **Conclusion:** The results suggest that the lipidic nanocomposite of *Copaifera multijuga* drastically reduced the inflammatory response caused by instillation of SARS-CoV-2 attenuated virus activity. Taken together these data could indicate that a new nanocomposite could be a useful tool for inflammatory events caused by the virus.

12.015 Evaluation of antinociceptive and anti-inflammatory activity of *Pseudotrimezia juncifolia* (Klatt) Lovo & Gil. Minho AS¹, Almeida GP¹, Vieira RF², Rezende CM³, Fernandes PD¹. ¹ICB-UFRJ Rio de Janeiro, Brazil; ²EMBRAPA, Genetic Resources and Biotechnology, Brasilia, Brazil; ³UFRJ Rio de Janeiro, Chemistry Institute, Brazil

Introduction: Plant species represent a great resource of substances with biological activity. The Iridaceae family consists mainly of herbs, which are present in tropical and subtropical areas and represents 67 genera and 1,870 species. In Brazil, there are 14 genera [1]. *Pseudotrimezia juncifolia* is popularly used as a blood purifying agent, anti-inflammatory, healing of intermittent wounds and in the treatment of psoriasis and skin ulcers [2,3]. **Method:** The plant was collected at the Botanical Garden of Brasilia (voucher specimen # 120227). The material was subjected to decoction and to lyophilization. Lyophilized material was orally administered to mice (10, 30 or 100 mg/kg) 60 minutes before the assay. Nociception and inflammation have been assessed by the hot plate test (HP), formalin (FL)- or capsaicin (CL)-induced licking response or carrageenan-induced cell migration into subcutaneous air pouch (SAP). Acetylsalicylic acid (ASA, 200 mg/kg), morphine (2.5 mg/kg) and dexamethasone (2.5 mg/kg) were used as controls. Female Swiss webster mice (22-30 g, n = 6-8) were used for the assays. Results are compared with vehicle-treated group and expressed as mean \pm SD and statistical analysis were done by ANOVA followed by Newman-Keuls multiple comparison test (* $p < 0.05$). **Results:** Our data demonstrate that the treatment significantly reduced chemical-induced nociceptive response in both formalin- and capsaicin-induced licking response. FL/neurogenic (10 mg/kg = $24.8 \pm 5^*$ sec; 30 mg/kg = $25.2 \pm 6.8^*$ sec; 100 mg/kg = $35.7 \pm 8.1^*$ sec) and FL/inflammatory (10 mg/kg = $109.6 \pm 38.5^*$ sec; 30 mg/kg = $13.2 \pm 11.6^*$ sec; 100 mg/kg = $138.4 \pm 63.6^*$ sec) phases when comparing with vehicle-treated group (67.2 ± 12.8 and 398.1 ± 81.5 sec), ASA ($47.1 \pm 10.9/213.1 \pm 92.9$ sec) morphine ($28.8 \pm 10.9/278.7 \pm 88.3$ sec). Tea also significantly reduced capsaicin-induced licking response (10 mg/kg = $16.5 \pm 4.4^*$ sec; 30 mg/kg = $29.9 \pm 10.6^*$ sec; 100 mg/kg = $26.7 \pm 8.7^*$ sec) after comparison with vehicle-treated group (56.6 ± 10.3 sec). In the thermal model of nociception (HP) the area under the curve was increased after treating mice with all 3 doses of *P. juncifolia* (10 mg/kg = $7,186 \pm 1,460^*$; 30 mg/kg = $11,374 \pm 2,075^*$; 100 mg/kg = $10,240 \pm 2,075^*$ when comparing with vehicle-treated group = $2,639 \pm 1,420$). The anti-inflammatory effect was observed since it inhibited carrageenan-induced leukocyte migration (10 mg/kg = $38 \pm 26.5^* \times 10^3$ cells/mL; 30 mg/kg = $35.3 \pm 23^* \times 10^3$ cells/mL; 100 mg/kg = $45 \pm 25.3^* \times 10^3$ cells/mL versus $145.9 \pm 54.3 \times 10^3$ cells/mL in vehicle-treated group that received only carrageenan in SAP or $34.4 \pm 15.1 \times 10^3$ cells/mL in mice receiving saline in SAP and pretreated with vehicle). Cytokines (TNF α and IL1- β) production were also reduced: TNF α : IL1- β : 10 mg/kg = 245.6 ± 52.3 pg/mL; 30 mg/kg = 203.5 ± 49.3 pg/mL; 100 mg/kg = 358.8 ± 99.6 pg/mL, when comparing with vehicle-treated group receiving only carrageenan in SAP (TNF α 137.5 ± 54.7 pg/mL; IL1- β : 78.7 ± 31.78 pg/mL) or vehicle-treated group receiving only saline in SAP (TNF α 70.2 ± 66.2 pg/mL; IL1- β : 570.1 ± 152.6 pg/mL). Some flavonoids (luteolin, taxifolin, isoorientin, catechin) were identified by HPLC/ESI-MS/MS. **Conclusion:** *Pseudotrimezia juncifolia* presented antinociceptive and anti-inflammatory effects confirming that the tea can be used in popular medicine for treating inflammatory and pain processes. **References:** [1] CHUKR, N. et al. Iridaceae Flora Fanerogâmica do Estado de São Paulo. 2003. [2] VAN DEN BERG, ME VI Simpósio de Plantas Mediciniais do Brasil, p. 163, 1980. [3] GODINHO, CC Universidade Estadual Paulista "Júlio de Mesquita Filho", 2012.

12.016 R-954 Improve Inflammation and Infertility Parameters in Experimental Mouse Endometriotic Model. França PRC¹, Paiva JPB¹, Sirois P², Fernandes, PD¹ ¹ICB-UFRJ, Drug Discovery Research Program, Lab. of Pharmacology of Pain and Inflammation, Rio de Janeiro, Brazil, ²Laval University, CHUL Research Center. Quebec, Canada

Introduction: Endometriosis is a challenging condition of reproductive-aged women, causing problems ranging from chronic pain to infertility. It is characterized by an estrogen-dependent stroma and endometrial glands found predominantly, but not exclusively, in the pelvic compartment [1]. Currently available drugs are only efficacious in treating endometriosis-related pain, however it's not a targeted treatment. The R-954, a BK receptor antagonist, demonstrated improve neuropathic pain, inflammatory edema, hyperglycemia and contributed to the ameliorate the acute lung injury [2]. Thus, the aim of this work is available anti-inflammatory properties of R-954 and evaluate pregnancy loss in pregnant female mice with endometriosis. **Methods:** Female Swiss Webster mice (25-30g, n=7) were anesthetized with intraperitoneal injection of ketamine/xylazine. The abdomen was opened to expose the uterus. One uterine horn was ligated at both the uterotubal junction and the cervical end, and the intermediate segment was removed and split longitudinally. Pieces with 5-mm were sectioned. These explants were then anchored onto the peritoneum. After 35 days, the abdomen was opened to assess the viability of the endometrial explants. With confirmation of the ectopic cysts, the animals were divided and treated with: R-954 (2 and 5 mg/kg, s.c), progesterone (1 mg/kg, p.o) or vehicle, for 15 consecutive days. At the last day the animals were euthanized, and the ectopic cyst were collected for. Infertility parameters were evaluated in pregnant females with endometriosis. The number of implantations, resorptions and fetal weights were evaluated through cesarean section. The results are presented as mean±SD and statistical analysis were performed by ANOVA followed by Tukey's post-test (*p<0.05). Protocols for animal use received number 33/19 (COBEA/UFRJ/Brazil). **Results:** Immunohistochemical analysis showed that R-954 group reduced the immunodistribution of VEGF in endometriotic cyst: 2 mg: 2073.6±1041.6* O.D and 5 mg/kg: 1023.3±544.0* O.D, when compared to vehicle (8101.3±2434.5 O.D) and progesterone (10114.3±3849.9 O.D) groups. VEGFR2 immunodistribution was also reduced in animals were pre-treated with R-954: 2 mg/kg: 3305.0±944.6* O.D and 5 mg/kg: 3319.2±689.5*, when compared to vehicle (7222.7±864.9 O.D) and progesterone (13406.3±2640.0 O.D) groups. Pregnant females were treated in the first seven days of pregnancy with R-954. Only 5 mg/kg reduced the number of resorptions/females: 2 mg/kg: 2.0±1.8 and 5 mg/kg: 0.4±0.5*, when compared to vehicle group: 2.6±0.8. The highest dose of R-954 also improve the number of total fetus/females: 2 mg/kg: 5.8±2.4 and 5 mg/kg: 6.5±1.6, when compared to vehicle group: 4.1±1.0.

Conclusion: The treatment with R-954 in female or pregnant female with endometriosis showed a reduced in angiogenic factor that its important for the growth of endometriotic cyst and prevent the pregnant loss. **Financial support:** CAPES, CNPq and FAPERJ. **Technical assistance:** Alan Minhó **Animal donation:** Instituto Vital Brazil **Reference:** [1] Filip L, Medicina (Kaunas). V.56, p.1, 2020. [2] Gobeil F Jr., Peptides., v.52, p.82. 2014

12.017 *Acrocomia aculeata* (Bocaiuva) Pulp Oil in the Prevention and Treatment of Acute Liver Injury in Mice. Gonçalves AR¹, Nunes AA¹, Tadokoro MM¹, da Silva TC², Santos RN¹, Cogliati B², Moreno SE¹. ¹ UCDB, Graduate Program in Biotechnology, ² USP, Graduate Program in Pathology

Introduction: Vegetable oils, such as Bocaiuva Pulp Oil (BPO), contain abundant antioxidant compounds and beneficial fatty acids. Studies suggest that this oil may have positive impacts on the prevention and treatment of cardiovascular, metabolic, inflammatory, oxidative, and liver diseases. Furthermore, previous studies have shown that BPO possesses anti-inflammatory, antimutagenic, and chemoprotective properties due to its phytochemical constitution, including oleic acid and carotenoids. It is also suggested that BPO may be a promising in prevention and treatment of liver damage, which is associated with oxidative stress, inflammatory responses, and impaired metabolic homeostasis. Therefore, the objective of this study was to investigate the potential effect of BPO on the prevention and treatment of acute non-alcoholic liver injury induced by acetaminophen in mice. **Methodology:** *Acrocomia aculeata* fruits were collected in Mato Grosso do Sul State. The pulp was dried in a forced air circulation oven at 60 °C until the moisture content reached approximately 10%. BPO was obtained using a Soxhlet apparatus with hexane as the organic solvent, which was subsequently removed in a rotary evaporator at 40 °C. Mice (C57-B16) were treated with BPO (2.5 mL/kg) for seven days prior to induction of hepatic damage by acetaminophen (ACT). The project was approved by the Ethics in the Use of Animals Committee (CEUA 003/2022). **Results:** The organoleptic profile of BPO indicated its suitability for consumption, and the composition analysis revealed the presence of unsaturated fatty acids, with oleic acid being the most abundant. The BPO-treated group exhibited significantly decreased levels of alanine aminotransferase (50%) and a reduction in hepatic necrotic area compared to the ACT group. **Conclusion:** In summary, BPO attenuated the ACT-induced alterations in serum and hepatic tissue in mice, likely due to its antioxidant and anti-inflammatory properties. **Acknowledgements:** CNPq, FUNDATEC and UCDB, for the financial support and scholarships COIMBRA, M. C.; JORGE, N.. **Foo Res. Int.**, v. 44, n. 7, p. 2139–2142, 2011. NUNES, Â. A. et al.; **Pla. Foo. for Hum. Nut.**, v. 73, n. 1, p. 61–67, 2018. COSTA, G.A.; BUCCINI, D.F.; ARRUDA, A.L.A.; FAVARO, S.P.; MORENO, S.E. **Ciên. e Tec. de Ali. (online)**, v. X, p. 1-9, 2020.

12.018 Imatinib Analogues Containing Indole Derivatives as Potential Antineoplastic

Agents. Silva TAN¹, Almeida PG¹, Oliveira AP^{2,3}, Bastos MM^{2,3}, Boechat N^{2,3}, Fernandes PD^{1,3}
¹ICB-UFRJ, Program of Research in Drug Discovery, Lab. of Pharmacology of Pain and Inflammation, Rio de Janeiro, Brazil. ²Fiocruz-Farmanguinhos, Lab. of Drug Synthesis, Rio de Janeiro, Brazil. ³ICB-UFRJ, Graduate Program in Pharmacology and Medicinal Chemistry, Rio de Janeiro, Brazil.

Introduction: Cancer is a generic term used to classify a group of malignant diseases characterized by the disorderly growth of cells that can invade other organs and tissues, a process known as metastasis (1,2). Cancer is the second leading cause of death in the world, accounting for nearly 10 million deaths. In 2020, 19.3 million new cases of cancer were reported worldwide. The most incidents were breast (2.26 million); lung (2.21); colon and rectum (1.93 million); prostate (1.41 million); non-melanoma skin (1.20 million) and stomach (1.09 million). In this project, new molecules were synthesized by hybridization containing the phenylaminopyrimidinepyridine group as a pharmacophoric group. **Methods:** Cell lines used were H1299 (ATCC® CRL-5803, lung adenocarcinoma) and HT29 (ATCC® HTB-38, colorectal adenocarcinoma). All cells were growth in DMEM medium (with 10% fetal bovine serum). Each cell line was incubated with crescent concentrations of each substance (1a-1e; 2a-2e; 3e) and after 24 hours cell viability was evaluated using violet crystal method (3). Inhibitory concentration that reduced cell viability in 50% (IC₅₀) was calculated using GraphPad Prism 8.02 software. **Results:** Our data indicates that IC₅₀ for 1a-1e; 2a-2e; 3e against H1299 (lung adenocarcinoma) was 7.77 μM; 12.54 μM; 19.54 μM; 14.33 μM; 11.02 μM; 26.32 μM; 21.07; 17.05 μM; 15.64 μM; 18.44 μM and 14.33 μM. The cytotoxic effect of these substances against HT29 cell line (colorectal adenocarcinoma) demonstrated that the IC₅₀ values were 9.01 μM; 10.65 μM; 7.68 μM; 23.68 μM; 20.04 μM; 27.33 μM; 18.24 μM; 19.25 μM. **Conclusions:** Taken together our data are suggestive that series 1 analogues seem to be most effective than series 2 analogues. The effects against lung or colorectal adenocarcinoma were similar and did not indicate specific effect of series 1 analogues. these preliminary results indicate that it is worth continuing the studies to identify the most promising molecules and their possible mechanisms of action. **Financial Support:** CAPES, CNPq and FAPERJ **Acknowledgments:** Alan Minho for technical assistance. **References:** 1) Inca 2022-<https://www.gov.br/inca/pt-br/assuntos/cancer/o-que-e-cancer> 2) Choi, H. G.; Sim, T.; Gray, N.; Zhou, W.; Chang, J. W.; Zhang, J.; Weisberg, E. Fused heterocyclic compounds and their uses. WO2010144909 (2010). 3) Costa, RSA; Assreuy, JA. Nitric oxide inhibits irreversibly P815 cell proliferation: involvement of potassium channels. Cell Prolif. 2002, 35, 321-332.

12.019 Possible New Therapies in the Field of Inflammation: Evaluation of the Antinociceptive and Anti-Inflammatory Profile of New Structural Analogues of Cannabidiol. Invencio CGG¹, Paiva JPB¹, Lontra ACP¹, Franco GRR², Fernandes IM², Gontijo VS², Viegas-Junior C², Fernandes PD¹ ¹ICB-UFRJ, Drug Discovery Research Program, Pain and Inflammation Pharmacology Lab., Rio de Janeiro, Brazil. ²Unifal-PeQuiM, Medicinal Chemistry Research Lab., Alfenas-MG, Brazil

Introduction: Inflammation is a normal response of the body to tissue injury, which triggers an immune defense cascade[1]. Medicinal Cannabis is becoming promising in research for pain and inflammation due to its antinociceptive and anti-inflammatory characteristics and could be an alternative to current drugs. This work intends to analyze 4 new cannabidiol analogues (named PQM-242, PQM-243, PQM-244 and PQM-245) in acute preclinical models of nociception and inflammation. **Methods:** Swiss Wester mice (25-30g) were pretreated orally with 1, 3 or 10 $\mu\text{mol/kg}$ of each analog 1h before injection of formalin (2.5%) into one of the paws or carrageenan (1%) into the subcutaneous air pouch (SAP). The response in the formalin model (FPL) was assessed in the 1st phase (0-5min) and 2nd phase (15-30min) after formalin injection as paw licking time (seconds). At SAP, 24h after carrageenan injection the animals were euthanized and the exudate collected for various measurements. Results are presented as mean \pm SD and statistical analysis was done by ANOVA/Bonferroni post-test (* $p < 0.05$). **Results:** In FPL, the group that received vehicle treatment presented 57.1 \pm 20.6s and 189.1 \pm 57.6s response for 1st and 2nd phases, respectively. The data obtained in the 1st phase show: PQM-242: 1 $\mu\text{mol/kg}$: 13.6 \pm 7.2*s; 3 $\mu\text{mol/kg}$: 33.7 \pm 5.3*s; 10 $\mu\text{mol/kg}$: 38.9 \pm 10.9s. PQM-243: 1 $\mu\text{mol/kg}$: 38.8 \pm 8.3s; 3 $\mu\text{mol/kg}$: 16.2 \pm 2.5*s; 10 $\mu\text{mol/kg}$: 29.2 \pm 4.8*s. PQM-244: 1 $\mu\text{mol/kg}$: 29.5 \pm 12.1s; 3 $\mu\text{mol/kg}$: 33.5 \pm 4.5s; 10 $\mu\text{mol/kg}$: 17.9 \pm 6.5*s. PQM-245: 1 $\mu\text{mol/kg}$: 30.9 \pm 8.1s; 3 $\mu\text{mol/kg}$: 46.6 \pm 13.2s; 10 $\mu\text{mol/kg}$: 27.8 \pm 4.1*s. None of the substances presented significant effect in the 2nd phase of the model. In SAP, a significant reduction in leukocyte migration is observed in all doses used. Saline group: 8.1 \pm 6.9celsx10³/ μL . Carrageenan group and pre-treated with vehicle: 238.4 \pm 88.8celsx10³/ μL . PQM-242: 1 $\mu\text{mol/kg}$: 112.9 \pm 17.9*célsx10³/ μL ; 3 $\mu\text{mol/kg}$: 136.8 \pm 45.4*célsx10³/ μL ; 10 $\mu\text{mol/kg}$: 101.1 \pm 6.7*célsx10³/ μL . PQM-243: 1 $\mu\text{mol/kg}$: 243.3 \pm 62.8célx10³/ μL ; 3 $\mu\text{mol/kg}$: 277.1 \pm 48.8célx10³/ μL ; 10 $\mu\text{mol/kg}$: 114.3 \pm 46.7* célsx10³/ μL . PQM-244: 1 $\mu\text{mol/kg}$: 136.2 \pm 38.8*célsx10³/ μL ; 3 $\mu\text{mol/kg}$: 129.3 \pm 68.9* célsx10³/ μL ; 10 $\mu\text{mol/kg}$: 147.5 \pm 66.7*célsx10³/ μL . PQM-245: 1 $\mu\text{mol/kg}$: 165.8 \pm 84.2 célsx10³/ μL ; 3 $\mu\text{mol/kg}$: 75.4 \pm 66.5*célsx10³/ μL ; 10 $\mu\text{mol/kg}$: 157.6 \pm 74.5*célsx10³/ μL . **Conclusion:** The data indicate that the 4 novel molecules evaluated present an antinociceptive and anti-inflammatory profile, which justifies the continuity of the trials to prove the mechanism of action and identify the most potent molecules. **Financial Support:** CNPq and FAPERJ **Acknowledgments:** Alan Minho for technical assistance, Instituto Vital Brazil for animal donation. **References:** [1] Godson, Catherine, et al. *Annu. Rev. Pharmacol. Toxicol.* 63:429–48, vol. 63, 2023.

12.020 Oblongifolin A and Gutiferone E Isolated from Brazilian Red Propolis Show Antimicrobial Activity Against Methicillin-Resistant *Staphylococcus aureus* (MRSA).

Almeida JFS, Ripari N, Sforcin JM. IBB-Unesp-Botucatu, Dept of Chemical and Biological Sciences, Brasil.

Introduction: Red propolis is a resinous product made by bees in northeast Brazil, showing several biological activities such as the antimicrobial one. Infections caused by methicillin-resistant *Staphylococcus aureus* (MRSA) have been a problem due to the resistance to most β -lactam antibiotics. Thus, it is necessary to discover new compounds that display an inhibitory action on MRSA strains, such as red propolis compounds, which already exerts an antibacterial action (Ripari et al., 2023). **Objectives:** to analyze the antimicrobial activity of oblongifolin A and Gutiferone E isolated from red propolis against MRSA strains. **Methodology:** The antimicrobial action of Oblongifolin A and Gutiferone E was evaluated by the broth microdilution assay (CLSI, 2019), where the minimum inhibitory (MIC) and minimum bactericidal (MBC) concentrations were obtained for a strain of MRSA from the Hospital das Clínicas da Faculdade de Medicina de Botucatu/UNESP (H55), a community strain for skin infections USA300 and a standard strain MRSA ATCC 33591. **Results:** oblongifolin A showed MICs for strain H55 from 7.81 to 31.25 $\mu\text{g}/\text{mL}$; for USA300 from 31.25 to 62.5 $\mu\text{g}/\text{mL}$ and for ATCC 33591 from 62.5 $\mu\text{g}/\text{mL}$, while the MBCs were 31.25 - 62.5, 125 - 250 and 125 - 250, respectively. Gutiferone E showed MICs (H55 = 40 $\mu\text{g}/\text{mL}$; USA300 = 40 $\mu\text{g}/\text{mL}$; ATCC = 10 $\mu\text{g}/\text{mL}$) and MBCs (H55 = > 80 $\mu\text{g}/\text{mL}$; USA300 = 80 $\mu\text{g}/\text{mL}$ and ATCC 33591 = 20 $\mu\text{g}/\text{mL}$) with approximate concentrations for strains USA300 and ATCC. Ceftaroline positive control (MIC: H55 = 7.81; USA300 = 31.25; ATCC 33591 = > 62.5 $\mu\text{g}/\text{mL}$) and Cefoxitin negative (MIC: H55 = 3.125; USA300 = 12.5 a 25; ATCC 33591 = > 50 $\mu\text{g}/\text{mL}$) were carried out. **Conclusion:** Oblongifolin A and Gutiferone E, isolated from red propolis, presented a strong inhibitory and bactericidal action, which may be a possible explanation for the anti-MRSA action exhibited by this propolis sample, in addition to indicate its potential inclusion in new therapies to contain MRSA infections. **References:** Clinical and Laboratory Standards Institute. CLSI Document 2019: M100-S29. Ripari, N., Pereira, A. F. M., Júnior, A. F., Rall, V. L. M., Aldana-Mejía, J. A., Bastos, J. K., & Sforcin, J. M. (2023). *Journal of Applied Microbiology*, v. 134. p.1, 2023. Financial support: FAPESP (2017/04138-8 and 2023/01282-1)

12.021 Anti-inflammatory and Antinociceptive Activity of the New Cannabidiol Analogues. Gonçalves MICM¹, Almeida PG¹, Gontijo VS², Franco GRR², Viegas CJ², Fernandes PD¹. ¹ICB-UFRJ, Program of Research in Drug Discovery, Lab. of Pharmacology of Pain and Inflammation, Rio de Janeiro. Brazil. ²Unifal-PeQuiM, Lab. of Research in Medicinal Chemistry, Alfenas, MG, Brazil

Introduction: Inflammation is a defense response that occurs after cellular damage. The inflammatory reaction can be characterized by a series of events, such as increased blood flow and vascular permeability in the affected region. Anti-inflammatory drugs are differentiated into steroidal and non-steroidal anti-inflammatory drugs. Regular ingestion of large doses over a long period can cause kidney, gastrointestinal and cardiovascular damage. Therefore, it is necessary to develop drugs that act on other inflammatory mediators, such as interleukins, TNF- α and proteins related to apoptosis, with different mechanisms of action, and may also act on multiple targets in inflammation. Thus, two new carvone-derived cannabidiol analogues (PQM-304 and PQM-305) were synthesized in order to evaluate a possible effect in preclinical models. The structure of these analogues cannot be disclosed, as well as their chemical names, because they are confidential for patent application. [1] **Methods:** Female Swiss Webster mice (22-30 g, n = 6-8) were used in carrageenan-induced cell migration into the subcutaneous air pouch (SAP) and formalin-induced paw licking (FPL) models. Mice were orally treated with PQM-304 or PQM-305 (1, 3 or 10 $\mu\text{mol/kg}$). After 1 hour, mice received carrageenan (0,5%, 1 mL) or saline injection into SAP and 24 hours later mice are euthanized, and exudate collected for further measurements. [3] FPL has two phases. 1st (neurogenic phase) of 0-5 min and 2nd (inflammatory phase) of 15-30 min after injection of formalin. The time (seconds, s) that the animal remains licking the paw injected with formalin (2.5%, 20 μL) was counted with a stopwatch [2]. Results are presented as media \pm sd. Statistical analysis were performed by ANOVA followed by Bonferroni test (* $p < 0.05$). **Results:** PQM-304 at doses 1, 3 and 10 $\mu\text{mol/kg}$, inhibited leukocyte migration in a dose- dependent manner, vehicle-treated group: $159.4 \pm 44.4 \times 10^6 \text{cells/mL}$; PQM-304 1 $\mu\text{mol/kg}$: $83.8 \pm 31.1 \times 10^6 \text{cells/mL}$ (47.4%); 3 $\mu\text{mol/kg}$: $76.1 \pm 22.4 \times 10^6 \text{cells/mL}$ (52.5%); 10 $\mu\text{mol/kg}$: $65.2 \pm 21.3 \times 10^6 \text{cells/mL}$ (29%). PQM-305 1 $\mu\text{mol/kg}$: $34 \pm 21 \times 10^6 \text{cells/mL}$ (83%); 3 $\mu\text{mol/kg}$: $30.5 \pm 17.1 \times 10^6 \text{cells/mL}$ (84.7%); 10 $\mu\text{mol/kg}$: $46.9 \pm 36.6 \times 10^6 \text{cells/mL}$ (76.5%). Treatments with PQMs (at 10 $\mu\text{mol/kg}$) did not significantly reduce licking time in the neurogenic and inflammatory phase of the paw licking model. 1st phase: Vehicle= $55 \pm 21 \text{s}$; PQM-304: $40.1 \pm 15.2 \text{ sec}$; PQM-305: $39.5 \pm 16.4 \text{ sec}$; 2nd phase: Vehicle= $171.2 \pm 36.1 \text{ s}$; PQM-304: $275.2 \pm 153.5 \text{ sec}$; PQM-305: $189.5 \pm 56.2 \text{ sec}$. **Conclusion** The results suggest that both substances (PQM-304 and PQM-305) present anti-inflammatory activity and justify the continuity of experiments in the search of new prototypes. **Financial Support:** CAPES, CNPq and FAPERJ **Acknowledgments:** Alan Minho for technical assistance, Institute Vital Brazil for animal donation. **References:** [1] Lessa, M.A.; Cavalcanti, I.L.; Figueiredo, N.V.; Cannabinoid derivatives and the pharmacological management of pain, 2016. [2] Hunskaar, S e Hole, K., Pain, v. 30, p. 3, 1987. [3] Raymundo, L.J.R.P.; Guilhaon C.C.; Alviano, D. S; et al., Jethnopharmacol, v. 134, p. 3, 2011.

12.022 Investigation on the Anti-Inflammatory Effect of *Aloysia gratissima* Essential Oil.

Kuhn KZ¹, Souza MA², Sanaiotto O¹, Provinelli AC¹, Barufke M¹, Schindler MSZ², Mazon SC², Brusco I², Scapinello J³, Dal Magro J², Müller LG² ¹Unochapecó, School Sciences, Chapecó; ²Unochapecó, PPG in Environmental Sciences, Chapecó; ³UDESC Graduate Program in Food Science and Technology, Pinhalzinho, Brazil

Introduction: Among the cultivated and/or native plants in Brazil, the genus *Aloysia* stands out, containing 34 cataloged species, among them *Aloysia gratissima* (Gillies & Hook.) Tronc. It is a plant with applications in folk medicine for bronchial infections, lung disorders, nervous system disorders (depression, anxiety), inflammatory processes, etc. Some evidence, already characterized by our research group, points to the anti-inflammatory potential of the *A. gratissima* leaf extract obtained by supercritical fluid (CO₂). Thus, in order to improve these results, it is important to investigate the anti-inflammatory effect and the mechanisms of action of the essential oil of *A. gratissima* leaves obtained by hydrodistillation in animal models.

Materials and methods: Leaves of *A. gratissima* were manually separated from the branches and dried without exposure to sunlight at room temperature. Afterwards, they were crushed and subjected to extraction in a Clevenger-type apparatus for 2 h. The oil obtained from *A. gratissima* (OAG) was analyzed using high-resolution gas chromatography coupled to mass spectrometry (GC-MS) to identify the chemical profile. The in vivo experimental protocol was approved by CEUA/UNOCHAPECÓ (022/2020) and performed in male Swiss mice (25g - 35g). The anti-inflammatory effect of OAG was investigated in the carrageenan-induced peritonitis test (1% 0.25 mL, ip), and the mechanism of action was evaluated through the analysis of myeloperoxidase (MPO) and prostaglandin E₂ levels in the peritoneal lavage of the animals. Mice were treated orally 1 hour before injection and divided into 3 experimental groups 1: Vehicle – NaCl 0.9% - v.o. -10ml/kg; 2: Positive control - dexamethasone 10 mg/kg po; 3: OAG 1 mg/kg, v.o. After 4h, they were euthanized and 3 ml of heparinized PBS were added intraperitoneally. After collection of peritoneal lavage, leukocytes were counted in the Neubauer chamber, and MPO activity and PGE₂ levels were analyzed. Trials were conducted in a randomized, double-blind fashion. Results were analyzed by one-way analysis of variance (ANOVA) followed by the Bonferroni test. The significance level was set at $p < 0.05$. **Results and conclusion:** The major compounds present in the essential oil were pinocanphone (17.4%), β -pinene (15.84%) and guaiol (11.82%), in addition to the presence of other compounds such as (-) - acetate of trans-pinocarvil, isopinocanphone, γ – elementene, β – cubebene, caryophyllene oxide, caryophyllene, bunesol, trans - pinocarveol, elixene, (-) – spatulenol, (-) – myrtenol, β – terpineol acetate in smaller amounts respectively. In the peritonitis assay, it was found that the animals treated with OAG and dexamethasone had a decrease in the number of leukocytes/mm³ in the peritoneal lavage when compared to the vehicle group ($P < 0.05$), and there was no difference between the animals treated with OAG and dexamethasone. MPO activity in peritoneal lavage showed a significant difference between dexamethasone and OAG and vehicle ($P < 0.05$). There was a downward trend ($P = 0.058$) in PGE₂ levels in the peritoneal lavage of the OAG-treated group. **Conclusion:** OAG had an anti-inflammatory effect, this effect may be related to the chemical constitution of the oil and is consistent with other findings of the research group for the plant species. Financial Support: UNOCHAPECÓ/UNIEDU, CAPES, FAPESC TO 2020TR735.

12.023 New Serotonin Amide Analogs with Promising Anti-Inflammatory and Anti-Nociceptive Potential. ¹Menezes JAF; ¹Almeida PG; ¹Giorno TBS; ²Rezende CM; ²Lima FA; ¹Dias PF ¹ICB-UFRJ, Program of Research and Drug Discovery, Lab. of Pharmacology of Pain and Inflammation, Rio de Janeiro. Brazil ²IQ-UFRJ, Lab. Aroma Analysis, Rio de Janeiro. Brazil

Inflammation is the body's response to tissue injury and the invasion of organisms by pathogens [1]. NSAIDs are the most commonly prescribed drugs in the world [2]. However, these drugs cause several adverse effects (i.e. gastrointestinal discomfort, bleeding, renal alterations) [3]. Therefore, research is still needed to identify new molecules with anti-inflammatory and analgesic potential and fewer adverse effects. In this regard, new molecules derivatives of serotonin amides (C10:5-HT, C12:5HT and C16:5HT), were synthesized with the objective to evaluate the new compounds using preclinical models of inflammation and/or pain.

Methods: Nociception and inflammation were evaluated by the formalin-induced licking (FIL) response and by the carrageenan-induced cell migration (SAP) models, respectively. Female Swiss Webster mice (22-30g, n = 6-8) were used. In the FIL mice received oral treatment 1h before the formalin injection. In SAP, mice received oral treatment 1h before carrageenan or saline injection into the SAP. After 24h mice were euthanized, and the exudates were collected for further measurements. Serotonin amides were tested at doses of 0.1, 1 or 10 mg/kg. Results are expressed as mean±SD. Statistical analysis was performed by ANOVA followed by Tukey's test (*p < 0.05). **Results:** The treatment with serotonin amides significantly reduced the licking time in both phases of FIL: 1st phase: Vehicle = 42.6±12.6sec; C10:5-HT/0.1 mg/kg = 35.8±10sec; C10:5-HT/1 mg/kg = 32.5±7.8sec; C10:5-HT/10 mg/kg = 30.9±11.2*sec; C12:5-HT/0.1 mg/kg = 34.1±11sec; C12:5-HT/1 mg/kg = 29.5±5.5*sec; C12:5-HT/10 mg/kg = 26.4±4.5*sec; C16:5-HT/0.1 mg/kg= 37.8±10.8sec; C16:5-HT/1 mg/kg= 32.9±7.8sec; C16:5-HT/10 mg/kg= 22.5±3.3*sec; 2nd phase: Vehicle= 173.8±43.8sec; C10:5-HT/0.1 mg/kg= 149.8±16.7sec; C10:5-HT/1 mg/kg= 145.2±15.1sec; C10:5-HT/10 mg/kg= 100.6±23.7*sec; C12:5-HT/0.1 mg/kg= 95.2±17.8*sec; C12:5-HT/1 mg/kg= 97.5±18.7*sec; C12:5-HT/10 mg/kg= 119.2±38.2*sec; C16:5-HT/0.1 mg/kg = 132.5±11.8*sec; C16:5-HT/1 mg/kg = 144.8±29*sec; C16:5-HT/10 mg/kg = 98.2±29*sec. In SAP it was observed a significant reduction in cell migration induced by carrageenan when mice were pretreated with all 3 doses of the 3 serotonin amides. Saline in SAP: 0.84±0.34x10⁶ cells/μL; carrageenan in SAP: 74.8±3.5x10⁶ cells/μL; pretreatment with dexamethasone (2.5 mg/kg): 10.8±4.7x10⁶ cells/μL; C10:5-HT: 0.1 mg/kg: 22.2±9.5*x10⁶ cells/μL; 1 mg/kg: 34.2±9.2*x10⁶ cells/μL and 10 mg/kg: 77.8±8.9x10⁶ cells/μL. C12:5-HT:0.1 mg/kg: 24.7±5.9*x10⁶ cells/μL; 1 mg/kg: 20.5±9.8*x10⁶ cells/μL and 10 mg/kg: 27.3±9.2*x10⁶ cells/μL; C16:5-HT: 0.1 mg/kg:22.7±7.8*x10⁶ cells/μL; 1 mg/kg: 33.1±8.9*x10⁶ cells/μL; 10 mg/kg: 27.3±7.2*x10⁶ cells/μL. **Conclusion:** The results suggest that all three serotonin amides present anti-inflammatory and antinociceptive activities. Although data are preliminary results are suggestive of a promising effect. Financial Support: CAPES, CNPq and FAPERJ Acknowledgments: Alan Minho for technical assistance, Institute Vital Brazil for animal donation **References:** [1] Sugimoto, M. A. et al. *Frontiers in Immunology*, v. 7 p. 1, 2016. [2] Ruiz-Irastorza, G.; Danza, A.; Khamashta, M., *Rheumatology*. 51(7):1145–1153. 2012. [3] Brunton, L.L. *Goodman & Gilman: As Bases Farmacológicas da Terapêutica*. 12^a ed. Rio de Janeiro: McGraw-Hill, p. 973. 2012.

13. Pharmacology Education and Technology

13.001 The Educational Game DiscoverRx as a Tool for Scientific Divulcation on the Drug Discovery and Development Process. Noël F¹, Xexéo G², Marques P², Mangeli E², Parreiras MV², Baptista JPH², Blanchard F^{1,2}, Böhme GA^{1,2}, Paiva BD², Maluf MBV^{1,2}, Ribeiro JASB^{1,2}, Duran J², Olaso MF², Mothé A^{1,2}, Costa IMS². ¹UFRJ, Lab of Molecular and Biochemical Pharmacology, Rio de Janeiro, Brazil; ²UFRJ, Lab of Ludology, Engineering and Simulation, COPPE, Rio de Janeiro, Brazil

Introduction: The use of serious games is becoming increasingly popular for teaching scientific concepts as they are considered important tools for an active learning. We previously described the SCREENER, an original educational board-cards game with online resources, that was created for teaching the Drug Discovery and Development (DDD) process in graduate programs of pharmacology (Noël, F. Braz. J. Med. Biol. Res., v. 54, p. e11786, 2021). To target a younger and lay audience, we have to consider that the so called "digital natives" are brought up in media where everything is vivid, graphic, fast and intense and are active participants rather than passive observers (Prensky, M. In: Digital Game-Based Learning, ch.2, 2001). Considering the new needs and preferences of adolescents who generally have little patience for lecture and step-by-step logic, we decided to create the digital game DiscoverRx for playing on smartphones. **Methods:** We idealized seven sequential mini-games, each corresponding to one of the seven stages of the DDD process described in the SCREENER. To illustrate each stage, we choosed a task based on its representability and possibility to allow different mechanics. DiscoverRx was developed in the Unity game engine according to the LUDES-GD methodology based on five stages: conception, design, production, evaluation and packaging (Mangeli E., In: Anais Trilha de Artes & Design-Simpósio Brasileiro de Games e Entretenimento Digital (SBGames), v. 20, p. 143, 2021). The art direction aimed a playful communication with inclusive characters and avoidance of emotional triggers and stereotypes. We used a combination of "Line art" and "Flat art" styles, with very vivid and saturated colors. Four options of language are available (Portuguese, English, Spanish and French). **Results:** The first beta version of this app containing the first three mini-games was launched during the SBFTE and SBGames events in October 2022 and is freely available at the google play store. The first mini-game illustrates the screening of active compounds (in vitro test for all-of-none response). The second game illustrates the hit-to-lead stage (in vivo test of potency). The third mini-game illustrates the lead optimization (alteration of the chemical structure to enhance a pharmacokinetic property). The game will be successively updated, with the following four mini-games, like new chapters in a series. A "final" version (1.0) was launched in April 2023 after corrections, including some bugs, made in accordance with the tests performed both by adolescents from eight different classrooms and by three senior scientists with experience in Pharmacology and/or Pharmacy and in games. **Conclusion:** DiscoverRx is a digital game under development that appears to be well-accepted by the target audience, at least in Brazil, and could be an interesting tool for divulgating the complex and harmful process of DDD to adolescents and the general population. **Financial support:** CNPq; FAPERJ.

13.002 Prevention of Drug Abuse Through an Academic Experience and Scientific Methodology: An Experience Through a Short-Duration Summer Course. Cunha JM, de Lima Silva AHB, De-Oliveira BR; Grieshaber LE; Waltrick APF, Visnheski BRC; Liebl B, Manuitt P; Da-Silva ACF, Ribeiro LA; Lívero FAR, Andre E, Zanoveli JM UFPR Depto de Farmacologia, Setor de Ciências Biológicas

Introduction: Adolescence is a critical risk period for the onset of substance use and can lead to public health problems, burdening the healthcare system, as these young individuals will experience substance-related health issues very early. The fact that young people tend to underestimate the negative effects of drugs, especially alcohol, exposes them to risky situations and overall health impairments. Given the challenge of treating addiction, programs aimed at preventing drug misuse are considered the most important intervention, with youth being the primary target audience. **Objectives:** To clarify the mechanism of action of abused drugs and their harmful effects to high school students from schools located in socially vulnerable areas through academic experiences and the scientific method by offering a short-duration summer course (5 days duration). **Methods:** The summer course followed the model proposed by the National Network for Education and Science: New Talents in the Public Network, conceived by Prof. Leopoldo de Meis from UFRJ. The course's curriculum was determined based on questions asked by participating students about the topic of substance abuse, grounded in their reality. Leading up to the summer course, the scholarship recipients and other collaborators constructed models and educational materials, anticipating the targeted curriculum related to students' questions, as well as the minimum necessary content for understanding the mechanism of action of abused drugs and their harms. The questions were not directly answered but were instead addressed through hypotheses formulated by the students themselves, which were tested through the design of experiments (application of the scientific method). All procedures were supervised by graduate students and collaborating professors. **Results:** On the first day, the students (15 in total) formulated questions regarding the course theme. The monitors were instructed to organize the course's daily layout by theme, and all questions were answered using the scientific method (through activities, experiments, enactments, always in a playful manner). Experiments were conducted to illustrate the effects of different alcohol concentrations (mimicking different alcohol levels) on the coloration and integrity of samples of bovine liver. Furthermore, a model of a human head was constructed, where neurotransmitters responsible for different addiction phases were represented by LED lights (such as dopamine, glutamate, and noradrenaline; varying in intensity), and a mock trial theater was staged with cigarettes as the defendant, among other activities. At the end of the course, the students participated in a science fair showcasing their week-long learnings and experiments that validated their hypotheses about the mechanism of abused drugs and their consequences on the body. **Conclusion:** The immersion in the academic environment through the summer course not only raised awareness among students about the harms of drug abuse but also led to 85% of them participating in the Annual Meeting of the Brazilian Society for the Advancement of Science. **Financial Support:** PROEC-UFPR, INOVAMED.

14. Pharmacology: Other

14.001 Effects of Lithium Microdose Treatment on Strength and Muscle Mass Loss Associated with Sarcopenia in a Murine Model with Accelerated Aging. Castellano M¹, Malerba HN², Maia J¹, Marques ICS¹, Barrence FAC¹, Viel TA^{1,2} ¹EACH-USP, Lab. of Neurofarmacology of Aging, PPG Gerontology, Brazil ² ICB-USP, PPG Pharmacology, Brazil

Introduction: Sarcopenia is a multifactorial, progressive and generalized disease of the skeletal muscle system. It leads to the involuntary loss of quality and quantity of muscle mass and to a reduction in strength and physical function¹. Common to aging and influenced by environmental, genetic and risk factors throughout life, it leads to decline in mobility, increase in falls and fractures resulting in loss of independence^{1,2}. The amount of muscle mass is regulated by the dynamic balance of anabolic and catabolic stimuli. In old age, physiological changes seem to disturb this homeostasis leading to anabolic resistance³. Glycogen Synthase Kinase-3-beta (GSK3 β) is an enzyme that influences several cellular processes due to its role as a modulator of the response to hormonal, nutritional and cellular stress stimuli⁴. Furthermore, GSK3 β acts as a negative regulator in important pathways such as global protein synthesis, ribogenesis and muscle atrophy^{4,5} and is upregulated in age-related diseases⁶. Thus, the objective of this work was to investigate the effects of long-term treatment with lithium in microdose, a known GSK3 β inhibitor, on the loss of strength in a murine model of accelerated aging. **Methods:** Male senescence-accelerated mice prone (SAMP-8) were treated or not with low-dose lithium carbonate (Li) until they reached 7 and 10 months of age. Li was added to drinking water and offered ad libitum at a final dose of 0.25 mg/kg/day starting when the animals were 21 days old. Upon reaching the ages of 7 and 10 months old, the animals underwent a hanging time test consisted of hanging the animal under a wire mesh until it could not hold anymore. The time was registered and divided by the animal weight, generating a score named holding impulse (HI). In each time point the HI was compared between untreated (Control) and Li-treated (Intervention) SAMP-8. After that, animals were anesthetized and killed by decapitation. The anterior tibial and extensor digitorum longus muscles were extracted and immediately frozen for future analysis. CEUA EACH/USP: 008/2021. **Results:** Data from the literature show that SAMP-8 have maximum muscle strength at 7 months old. After this age, a decrease in muscle mass and strength is observed. At 7 months of age, treatment with lithium significantly increased HI in Intervention group by 1.4 fold (430.2 ± 125.5 s/g, n=6) when compared to the Control group (297.7 ± 77.6 s/g, n=10, p=0.020). In the same way, at 10 months of age, the chronic treatment with low-dose lithium maintained a significant increase in HI of the Intervention group (417.6 ± 75.2 s/g, n=7) by 1.3 fold when compared to the Control group (312.4 ± 97.2 s/g, n=9, p=0.022). **Conclusion:** It was already shown by our group and others that chronic low-dose Li treatment promotes neuroprotection preventing the memory loss and degeneration associated to Alzheimer's disease in both clinical and animal models of the pathology. In SAMP-8, chronic treatment with the same low-dose since weaning promoted an increase in animals' strength in both adult and old ages. The effects in infant and the molecular mechanisms that supports this observed behavior are being studied in our laboratory. **Financial Support:** Fapesp (2020/14133-6). **References:** 1. Cruz-Jentoft AJ, Age Ageing, Vol. 48, p. 16, 2019. 2. Dawson-Hughes B, Osteoporos Int., Vol. 27, p. 3139, 2016. 3. Cruz-Jentoft AJ, Lancet, Vol. 393, p. 2636, 2019. 4. Aweida D, J. Cell Biol., Vol. 217, p. 3698, 2018. 5. Mirzoev TM, Int. J. of Mol. Sci., Vol. 22, p. 5081, 2021. 6. Souder DC, GeroScience, Vol 41, p. 369, 2019.

14.002 Bystander effects of Mesenchymal Stem Cells on Aspects Relating to Cell Migration Control. Almeida B, Amon RLR, Pedro AN, Makiyama EN, Fock RA. FCF-USP, PPG Pharmacy, São Paulo, Brazil

Introduction: The biological effects of radiation depend on a variety of factors, such as dose, environmental conditions, and the sensitivity of the biological system. Moreover, radiation damages not only the cells of interest, but also healthy cells. In both therapeutic strategies and accidental radiation exposures, the literature has devoted efforts to understanding the ByStander effect. The ByStander effect translates the cellular responses received by non-irradiated cells adjacent to the cells that received the radiation. In several malignant hematological diseases, ionizing radiation is used as a therapeutic tool to destroy the focus of malignant cells present in the bone marrow. However, the ByStander effect, especially on the effects on the mesenchymal stem cells (MSCs) and hematopoietic, are still little explored. MSCs are a group of important cells for the formation of the hematopoietic microenvironment, acting by several mechanisms, and the release of soluble factors are of high importance for the control of hematopoiesis and cell migration. From this, this work aims to evaluate the ByStander effect on MSCs and possible changes in migration control. Having as partials results the action of irradiation indirectly, characterizing factors that could, through the ByStander effect, influence the hematopoietic cells in relation to cell migration. **Methods:** The C₃H₁₀T_{1/2} (ATCC®) lineage consists of Mesenchymal Stem Cells. They were cultured in flasks with DMEM (Dulbecco's Modified Eagle Medium) and irradiated in a 60Co telecobalt device in the Experimental Radiotherapy Sector of UNIFESP-EPM in different doses. Therefore, experimental analyses were performed in relation to gene expression, by rtPCR. Cell cycle, DNA damage, by flow cytometry, and cell senescence. Besides the production of cytokines, by ELISA method. The supernatant of the irradiated MSCs at doses of 0 and 6Gy was filtered to plates with hematopoietic cells (C1498, ATCC®) of leukemic lineage, which were not irradiated. The gene expression, by rtPCR, and the migratory mechanism of these cells was analyzed in a Trans-Well filter. **Results:** The evaluation of the ByStander effect on cell migration was initially done by rtPCR, of genes related to cell migration. The group of C1498 cells were submitted to non-irradiated and irradiated supernatants. However, the results found showed no statistically significant difference. The data extracted from the migration of C1498 strain cells on the effect of irradiated MSC conditioned medium, demonstrated that 6Gy conditioned medium increased the cell migration rate. **Conclusion:** From the results obtained so far, it is possible to conclude that the production of soluble factors by irradiated MSCs is affected as from a dose of 6Gy. In relation to the ByStander effect, it is possible to observe the influence on the migration of hematopoietic cells, however without alterations in genes involved in the control of cell migration. **Financial support:** CAPES (888876887842022-00) and FAPESP (202V08658-1). **References:** NAJAFI, Journal Biomedical Physics & Engineering, v. 4, n. 4, p. 163, 2014. YAHYAPOUR, R. Current Radiopharmaceuticals. v. 11, n. 1, p. 34, 2018. ZHANG C. Front Oncol. v. 11, p. 670464, 2021.

14.003 Irradiated Mesenchymal Stem Cells: Influence of the Bystander Effect on Hematopoiesis Controls. Amon RLR, Almeida B, Pedro AN, Makiyama EN, Fock RA FCF-USP, PPG Pharmacy, São Paulo, Brazil

Introduction: Ionizing radiation has long been used as a diagnostic and therapeutic tool, especially in the treatment of cancer. In therapy, the goal of radiation is to cause irreversible damage to the DNA leading the tumor cell to die by apoptosis. In this context, there is a great challenge for radiobiology, since it has been observed that genetic and biochemical changes also apply to cells adjacent to the target cells, called bystander effect. With radiation being used for the treatment of hematological diseases it is necessary to understand the involvement of cells that form the hematopoietic niche, such as mesenchymal stem cells (MSCs). These cells have the function of modulating hematopoiesis, and, when affected by radiation, they can alter the process of hematopoiesis reconstruction, by the action of the bystander effect. This work aimed to characterize MSCs radiobiologically and to evaluate the bystander effect in relation to the cell cycle, proliferation and differentiation of hematopoietic cells. **Methods:** The lineage C3H10T1/2 (ATCC®), these being Mesenchymal Stem Cells (MSC), were cultured in flasks with DMEM (Dulbecco's Modified Eagle Medium) and irradiated in a 60Co telecobalt equipment in the Experimental Radiotherapy Sector of UNIFESP-EPM at different doses. In these cells, experiments were performed to evaluate viability and cell cycle by flow cytometry; cell senescence by beta-galactosidase; production of soluble factors by ELISA. The supernatant of the cells irradiated with 6Gy dose was filtered and used in the system and conditioned culture with C1498 hematopoietic lineage cells (ATCC®) to evaluate the bystander effect. Evaluation of gene expression by rtPCR as well as culture in methylcellulose were used to evaluate this bystander effect in relation to cycle controllers and proliferation. **Results:** Regarding the influence of the bystander effect towards gene modulation in C1498, differences were observed in the CCND1 and GATA3 genes. And, related to culture on methylcellulose, the C1498 colonies formed showed different morphologies. The colonies in the control group were denser in shape compared to the irradiated group. **Conclusion:** MSCs are radiobiologically resistant up to a dose of 4Gy, presenting significant alterations only above doses of 6Gy. With this, irradiated MSCs, nevertheless viable, can promote modulation of hematopoietic cells, in an indirect way, called the bystander effect. This effect on hematopoietic lineage cells has been shown to promote alterations in CCND1 and GATA3, as well as modulate clonogenic capacity. **Financial Support:** CAPES (888876887912022-00) and FAPESP (202V08658-1). **References:** NOGUEIRA-PEDRO, International Journal Of Radiation Biology, v. 98, n. 11, p. 1619, 2022.NAJAFI, Journal Biomedical Physics & Engineering, v. 4, n. 4, p. 163, 2014.MATELLÁN, Genes, v. 11, n. 2, p. 195, 2020.

14.004 Use of Konjac Glucomannan-Enriched Gummy Candy on Biochemical, Oxidative Parameters, Appetite Reduction, and Anthropometric Measurements in Overweight Women. Sandri G¹, Fernandes ACS¹, Muxfeld L², Motta NG¹, Skonieski C³, Fagundes KR¹, Chaves DB¹, Suthovski G¹, Gallina AL⁴, Borstmann SMA¹, Martini MC¹, Wagner TCL¹, Benvegnú DM¹ ¹UFFS - Campus Realeza/PR - PPG em Saúde, Bem-Estar e Produção Animal Sustentável na Fronteira Sul ²Unioeste, UEM. PPG em Ciência de Alimentos ³UFSM, ⁴Unioeste-Campus Guarapuava

Introduction: Obesity is a chronic disease, considered a global public health problem. *Konjac glucomannan* (KGM) is a dietary fiber polysaccharide that has demonstrated its effects on appetite. Thus, the aim of this study was to evaluate the effect of KGM-enriched gummy candies on some parameters in overweight women. **Methods:** study participants were recruited through social networks and signed a consent form to participate in the study. This work was carried out after approval by the Research Ethics Committee of the Federal University of Fronteira Sul under number 88518618.1.0000.5564. Participants were randomly divided into two groups: KGM Group (candy enriched with KGM) and PG Group (placebo) (candy enriched with golden flaxseed flour). The candies were produced by the researchers with funding from the company Gum's Diet. Participants were instructed to consume 2 candies/day for 14 days. Each individual answered three types of questionnaires about their health status and the regular intensity of hunger before, during and after consuming the candy. To measure anthropometric measurements of weight and height, a digital scale and a portable stadiometer were used. To measure waist circumference (WC) a tape measure was used. To measure the biochemical and oxidative parameters, blood samples were collected from the participants. The dosage of glycemia, total cholesterol, triglycerides, high-density lipoprotein, low-density lipoprotein and very low-density lipoprotein were measured using commercial kits. The levels of lipid peroxidation, glutathione, protein thiol and vitamin C were quantified according to methods already used in the literature. **Results:** 42 overweight women, between 18 and 45 years old, without pathologists, participated in the study. When evaluating the questionnaires, it was identified that the KGM group reported a reduction in the intensity of hunger, when compared to the PG group. Regarding body classification, there were no differences between groups. Regarding the WC measurement, the KGM group showed a significant reduction in these measurements. Finally, regarding biochemical and oxidative parameters, no significant differences were found between and within groups. **Conclusion:** after consuming gummy candy enriched with KGM, there was a significant reduction in the participants' WC, as well as a reduction in the intensity of hunger, in addition to being considered an innovative proposal.

14.005 Development and Evaluation of Nanostructured Lipid Carriers for co-delivery of Simvastatin and Adenosine for the treatment of Difficult-to-Heal Cutaneous Ulcers Daré RG¹, Lopes LB¹. ¹ USP São Paulo, Dpt of Pharmacology, Brazil

Introduction: It is well known that certain conditions hinder the wound healing process, including *diabetes mellitus* (Reinke, 2012), and originate complex/chronic wounds. These types of wounds require agents that stimulate angiogenesis and cell proliferation. In the field of dermatology, lipid nanoparticles have gained attention as carriers for effective topical treatments due to their advantages over conventional formulations (Pardeike, 2009). The present study aims to develop, characterize, and evaluate nanostructured lipid carriers co-encapsulating simvastatin and adenosine (NLC-S/A) for improvement of the wound healing process. **Methods:** The nanoparticles were prepared by hot homogenization technique followed by sonication. Various solid and liquid lipids, along with hydrophilic surfactants were tested to optimize the formulation. The nanoparticles were characterized for size, polydispersity, zeta potential, morphology, and association efficiency (AE). Physicochemical stability was evaluated under three storage conditions (4°C, 25°C and 40°C). *In vitro* activity was assessed in NIH-3T3 and HaCat cell lines: cell viability, proliferation and wound closure (using the scratch-wound assay). Skin permeation and retention profile were evaluated in pig ear skin. **Results:** The optimized formulation contained two different drug ratios: NLC-S/A 2%/2% (simvastatin and adenosine at 2% relative to total lipid content) and NLC-S/A 0.6%/2% (0.6% simvastatin and 2% adenosine). Formulations showed an average size of ≈ 200 nm, polydispersity index ≈ 0.150 , zeta potential ≈ -20.0 mV, and spherical morphology. The AE for simvastatin and adenosine were $\approx 99\%$ and $\approx 13\%$, respectively, independently on the drug content added. The nanoparticles displayed excellent physicochemical stability during a 60-day storage period. NLC-S/A 2%/2% significantly decreased cell viability starting from $0.8 \mu\text{g/mL}_{\text{simvastatin}}/0.8 \mu\text{g/mL}_{\text{adenosine}}$ for NIH-3T3 and $3.1 \mu\text{g/mL}_{\text{simvastatin}}/3.1 \mu\text{g/mL}_{\text{adenosine}}$ for HaCat. NLC-S/A 0.6%/2% showed a decrease in cell viability starting from $2 \mu\text{g/mL}_{\text{simvastatin}}/6.2 \mu\text{g/mL}_{\text{adenosine}}$ for NIH-3T3 and $8 \mu\text{g/mL}_{\text{simvastatin}}/25 \mu\text{g/mL}_{\text{adenosine}}$ for HaCat. Regarding cell proliferation, for NIH-3T3, NLC-S/A 0.6%/2% showed activity at concentrations of $0.25\text{-}0.5 \mu\text{g/mL}_{\text{simvastatin}}/0.8\text{-}1.6 \mu\text{g/mL}_{\text{adenosine}}$ ($\approx 50\%$ proliferation). This activity was not observed for NLC-S/A 2%/2%. For HaCat, NLC-S/A 0.6%/2% showed activity at concentrations of $0.25\text{-}6.2 \mu\text{g/mL}_{\text{simvastatin}}/0.8\text{-}2 \mu\text{g/mL}_{\text{adenosine}}$ (145-107% proliferation), while NLC-S/A 2%/2% showed a lower proliferative effect. In scratch-wound assay, for NIH-3T3, NLC-S/A 0.6%/2% exhibited 52% wound closure, while NLC-S/A 2%/2% exhibited 25%. For HaCat, NLC-S/A 0.6%/2% exhibited 86% closure, while NLC-S/A 2%/2% exhibited 50% closure. There was an increase in the cutaneous permeation of the drugs when associated with NLC-S/A 0.6%/2%, but cutaneous retention was more pronouncedly increased (4.6 and 3 time for simvastatin and adenosine, respectively) compared to drug solutions. **Conclusion:** The NLC-S/A 0.6%/2% exhibited superior biocompatibility, enhanced cell proliferation, improved wound closure and promoted tissue localization of simvastatin and adenosine, highlighting its potential application in promoting tissue repair. Reinke, JM. *Eur. Surg. Res.*, v. 49, p. 35, 2012. Pardeike, J. *Int. J. Pharm.*, v. 366, p. 170, 2009. **Acknowledgements:** Coordenação de Aperfeiçoamento de Pessoal de Nível Tecnológico (CAPES), Conselho Nacional de Desenvolvimento Científico e Tecnológico (CNPq) and FAPESP (001, 150937/2022-9, 2018/13877-1, 2022/12876-7).

14.006 Norfloxacin Cocrystal as an Alternative to Improve Biopharmaceutical and Antimicrobial Properties. Brancalione RC¹, Gomes SN¹, Biscaia IFB¹, Murakami FS², Lopes DS¹, Bernardi LS¹, Oliveira PR¹. ¹Unicentro, Dpt. of Pharmacy, PPG of Pharmaceutical Sciences, Guarapuava, Brazil; ²UFPR, Dpt. of Pharmacy, PPG of Pharmaceutical Sciences, Curitiba, Brazil

Cocrystals are structurally homogeneous crystalline materials formed by at least two neutral compounds that are found in defined stoichiometric quantities and are solid at ambient temperature [1]. [2]. Norfloxacin (NFX) is a broad-spectrum antibacterial drug, used for the treatment of urinary tract infections, which has low solubility and low permeability, presenting low bioavailability [3,4,5]. In the present study, we reproduced the development of an NFX cocrystal using isonicotinamide (INA) as a coformer, already described in the literature [6] in order to evaluate its biopharmaceutical properties, such as dissolution and solubility, in addition to its antimicrobial properties that had not been evaluated until then. **Methods:** The cocrystals were obtained using a 1:1 ratio of drug and coformer (31,9 mg of NFX and 11,2 mg of INA) diluted in 8 mL of chloroform [6], and the chloroform was left to evaporate in a water bath with a controlled temperature of 30 °C. The dissolution was evaluated under supersaturated conditions and the solubility at the eutectic point of cocrystal and NFX in both water and fasted state simulated intestinal fluid (FaSSIF). The antimicrobial activity was evaluation using the colorimetric microdilution assay [7]. NFX, cocrystal (COC), and the physical mixture of NFX with INA (PM) were evaluated, and standard strains of *Escherichia coli*, *Pseudomonas aeruginosa*, and *Staphylococcus aureus* were used. Using the microdilution technique, it was possible to determine the minimum inhibitory concentration (MIC) of antimicrobial compounds and inhibitory concentration of 50% (IC50%) and 90% (IC90%) of the microorganisms. Results: In the kinetic study the cocrystal showed 1.8 times higher dissolution than NFX in water at 60 min and 1.3 times higher in FaSSIF at 180 min. The cocrystal also had an increase in solubility of 8.38 times in water and 6.41 times in FaSSIF when evaluating the eutectic point. The improvements in the biopharmaceutical properties of NFX with cocrystallization were reflected in improved antimicrobial action for the three microorganisms analyzed when compared to NFX and the physical mixture of NFX and INA, as shown in the results of minimum inhibitory concentration (MIC) and inhibitory concentration of 50% (IC50%) and 90% (IC90%). **Conclusion:** These results show that the NFX cocrystal has biopharmaceutical and microbiological advantages when compared to the NFX drug, and for this reason it is necessary to continue the in vivo studies of this cocrystal. **Financial Support:** This research was funded by Coordenação de Aperfeiçoamento de Pessoal de Nível Superior, Brasil (CAPES) [Coordination for the Improvement of Higher Education Personnel]?Finance Code 001 and Fundação Araucária. **References:** 1. Aakeröy, CB. Cryst Eng Comm, v. 7, p. 439, 2005. 2. Sekhon, BS. Ars Pharm, v. 50, p. 99, 2009. 3. Al-Tamtah, S. Pharm Res., v. 12, p. 413, 2015. 4. Kamble, R. Integr Med Res., v. 11, p. 512, 2017. 5. Gadebusch, HH. Int J Antimicrob Agen., v. 1, p. 3, 1991. 6. Basavoju, S. Cryst Growth Des., v. 6, p. 2699, 2006. 7. Veiga, A. J Microbiol Methods, v. 162, p. 50, 2019.

14.007 Prophylactic Effect of *Ilex paraguariensis* Hydroalcoholic Extract and Ibuprofen on LPS-induced Acute Liver Injury. Marchiori C¹, Santos JAR¹, Bezerra RLA¹, Schwab EDP¹, Medeiros IS¹, Somensi LB³, Bahr AC³, Bonini JS¹, Gregório E^{2,3}, Silva WCFN¹. ¹Unicentro, Depto de Farmácia, Guarapuava, Brasil, ²UFRGS, Depto de Fisiologia, Porto Alegre, Brasil, ³Uniarp, Depto de Medicina, Caçador, Brasil

Introduction: Lipopolysaccharide (LPS) administered to induce by different metabolic pathways, an inflammatory process. Considering anti-inflammatory and antioxidant properties found in some plants, *Ilex paraguariensis* (Aquifoliaceae) is composed of polyphenols, xanthines, alkaloids, flavonoids, and saponins that confer such properties. Ibuprofen, a non-steroidal anti-inflammatory drug (NSAID), is an inhibitor of production of pro-inflammatory mediators. However, there are reports of hepatotoxicity induced by ibuprofen. In this study, we evaluated the influence of *Ilex paraguariensis* and ibuprofen by doses already established in the literature, on markers of liver injury after intraperitoneal (IP) injection of LPS in rats.

Methods: For execution of this study, 65 male Wistar rats were utilized, divided into 7 groups: naive, saline (sal), *Ilex paraguariensis* (30 mg/mL), ibuprofen (50 mg/mL), sal+LPS, *Ilex*+LPS, ibuprofen+LPS. The animals were prophylactically treated with *Ilex* or ibuprofen for 7 days orally. After 7 days, the animals in the sal+LPS, *Ilex*+LPS, and ibuprofen+LPS groups received an IP injection of LPS at a dose of (200 µg/kg). Passed two weeks, the animals were euthanized, and the liver was removed, cleaned, and weighed. The homogenate was made with a portion of the liver for ALT, AST, and calcium tests. For the determination of the biochemical parameters ELISA kits were employed through kinetic and colorimetric methods. Every experiment followed the "Principles of laboratory animal care" (NIH publication N° 85-23, revised 1996), approved by the CEUA/UNICENTRO animal use ethics committee under n° 022/2022. **Results:** Meaningful growth in AST enzymes was found in the *Ilex*+LPS group when compared to the ibuprofen+LPS, sal+LPS, and ibuprofen groups ($p < 0.05$) and the naive and sal groups ($p < 0.005$). Regarding the ALT enzyme, no significant differences were found. The ibuprofen+LPS group demonstrated meaningful growth in liver tissue calcium concentrations compared to the sal and *Ilex* groups. Finally, it was not verified significant morphometric differences in the liver between the groups. **Conclusion:** This study shows that administration of *Ilex paraguariensis* at a dose of 30 mg/mL and ibuprofen at a dose of 50 mg/mL, prophylactically administered for seven days, followed by systemic inflammatory induction via LPS, influences markers of liver injury. Financial Support: Conselho Nacional de Desenvolvimento Científico e Tecnológico (CNPq), Fundação de Amparo à Pesquisa e Inovação de Santa Catarina (FAPESC) e Associação de Estudos, Pesquisa e Auxílio às Pessoas com Alzheimer (AEPAPA).

14.008 Influence of *Ilex paraguariensis* Hydroalcoholic Extract and Ibuprofen on Biochemical Parameters of Rats submitted to Intraperitoneal LPS Injection. Santos, JAR1, Marchiori, C1, Bezerra, RLA1, Schwab, EDP1, Medeiros, IS1, Somensi LB3, Bahr AC3, Bonini JS1, Gregório E2,3, Silva WCFN¹. 1Unicentro, Depto de Farmácia, Guarapuava, Brasil. 2UFRGS, Depto de Fisiologia, Porto Alegre, Brasil. 3Uniarp, Depto de Medicina, Caçador, Brasil.

Introduction: Inflammation is an immune and protective response of the body. Agents such as Lipopolysaccharide (LPS) present in the membrane of gram-negative bacteria can cause inflammation by activating different pathways. Carbohydrate, protein, and lipid metabolism can be influenced by inflammation and LPS administration. In this context, some plants are being studied because they have a potential regulatory effect on the inflammatory response. *Ilex paraguariensis* (Aquifoliaceae), popularly known as mate herb, has been used in liver protection and anti-inflammatory. Such pharmacological properties are related to methylxanthines, saponins, and phenolic compounds. In this study, the influence of the hydroalcoholic extract of *Ilex paraguariensis* on the biochemical parameters of rats that were exposed to LPS was verified. **Methods:** To carry out this study, 65 male Wistar rats were divided into seven groups: naive, salt (saline), *Ilex* (30mg/mL), ibuprofen (50mg/mL), salt+LPS, *Ilex*+LPS, ibuprofen+LPS. The animals were prophylactically treated for seven days by oral administration. After seven days, the animals in the sal+LPS, *Ilex*+LPS, and ibuprofen+LPS groups received an intraperitoneal (IP) injection of LPS at a dose of (200 µg/kg). Two weeks after the IP injection of LPS, the animals were euthanized, and blood was collected via cardiac puncture. Finally, biochemical analyzes were performed (glucose, cholesterol, triglycerides, and albumin). To determine the biochemical parameters, ELISA kits were used through the kinetic and colourimetric methodology. All experiments were by the "Principles of laboratory animal care" (NIH publication N° 85-23, revised 1996), approved by the CEUA/UNICENTRO animal use ethics committee under opinion 022/2022. **Results:** A significant increase in triglycerides was found in the ibuprofen+LPS group ($p < 0.05$) when compared to the group that received only salt (saline). No significant differences were found in the analysis of glucose, albumin, and cholesterol. **Conclusion:** It was demonstrated that administering LPS at a 200 µg/kg dose does not influence the biochemical parameters (glucose, albumin, and cholesterol). However, ibuprofen increased triglyceride concentrations at a dose of 50mg/mL, prophylactically administered for seven days, followed by systemic inflammatory induction via LPS. **Financial Support:** This study was funded by the National Council for Scientific and Technological Development (CNPq), Fundação de Amparo à Pesquisa e Inovação de Santa Catarina (FAPESC), Associação de Estudos, Pesquisa e Auxílio às Pessoas com Alzheimer (AEPAPA).

14.009 Ayahuasca and Grief: Investigating the Determinants of Therapeutic Potential.

Souza AA, Gonçalves JRP, Pontieri GC, Rodrigues GC, Hirata F, Donato MF, Nascimento, FP, Fermino FA Unila, Lab. of Medical Cannabis and Psychedelic Science, Foz do Iguacu, PR, Brazil

Introduction: The Ayahuasca drink (AYA), composed mainly of dimethyltryptamine (DMT) and β -carbolines, has been used for medicinal purposes due to its therapeutic potential in situations of psychic suffering. However, there are still gaps in knowledge about the factors that can influence its effects. Therefore, the aim of this study is to investigate some of these factors that may contribute to the therapeutic potential of AYA in the grief reframing process.

Methods: From August 23, 2021, to July 12, 2022, two online questionnaires were administered. The first questionnaire comprised open and closed questions that corresponded to variables of interest, while the second consisted of 20 closed questions, which provided a score indicating the intensity of grief symptoms before and after the drink of AYA. The inclusion criteria for the study included individuals over 18 years old who had experienced a significant loss and used AYA. Data analysis was conducted using SPSS software. Paired comparison tests, such as the Wilcoxon test or Student's t-test, were employed for within-group comparisons, whereas the Mann-Whitney comparison test and the Kruskal-Wallis test with Dunn's post-hoc analysis were used for between-group comparisons. A significance level of $p < 0.05$ was adopted. **Results:** A total of 171 individuals participated in the study, with a majority being female (66.7%). Comparisons were made among groups that utilized AYA in different types of rituals. The sample was stratified as follows: Shamanic ritual (54.39%), Non-Shamanic (12.28%), Santo Daime (12.28%), Neo shamanic (11.11%), and others (9.94%). No significant differences were found between the groups. However, individually, all groups exhibited a reduction in scores before and after the intervention ($p < 0.01$). Additionally, we analyzed whether the intention to use AYA to alleviate feelings related to the loss would be a determining factor by comparing groups with and without this intention. It was found that the group with the intention had higher initial scores compared to the group without it ($p < 0.0001$). However, the final scores showed no significant difference ($p > 0.94$), and both groups experienced a reduction in scores before and after the loss ($p < 0.0001$). Finally, we examined whether seeking any form of help prior to using AYA had an impact. The analysis revealed that those who had sought help before using AYA had better scores compared to those who hadn't ($p < 0.0001$). However, this finding did not persist after using the substance ($p > 0.97$). Furthermore, both groups experienced reduced scores before and after the intervention ($p < 0.0001$). **Conclusion:** Our findings suggest that the type of ritual performed with AYA does not significantly influence the process of reframing the experience of loss. Similarly, we observed that the intention to seek a new meaning of grief through the use of AYA is not a decisive factor in the outcomes achieved. Finally, we conclude that seeking alternative forms of help to cope with loss before using AYA does not determine its effects in this process.

14.010 Ayahuasca and Grief: Exploring Evidences of a New Therapeutic Perspective in Reframing Losses. Pontieri GC, Gonçalves JRP, Rodrigues GC, Souza AA, Hirata F, Donato MF, Nascimento, FP Fermino FA Unila, Lab. of Medical Cannabis and Psychedelic Science, Foz do Iguaçu, PR, Brazil

Introduction: From an ethnopharmacological perspective, the components of ayahuasca (AYA), a psychoactive drink traditionally used in ritualistic contexts by indigenous peoples of Latin America, have been studied for their medicinal potential, in particular the dimethyltryptamine (DMT) and β -carbolines. Among its subjective effects, the redefinition of beliefs, memories and traumas stands out, offering therapeutic potential in situations of psychic suffering, including grief. This study aims to investigate the effects of AYA ingestion in the process of reframing losses. **Methods:** This is a descriptive and retrospective study with a quantitative approach, conducted with individuals over 18 years old who have experienced significant losses and have used ayahuasca afterwards, regardless of the context and frequency. For evaluation, two semi-structured questionnaires were made available through social networks and institutional emails, with an online application from August 23, 2021 to July 12, 2022. The first questionnaire contained open-ended questions that identified the participants' profiles, while the second consisted of 20 closed questions aimed at investigating the effects of the AYA experience on the phenomenon of grief. The answers were scored and transformed into a score that establishes a direct relationship, in which the higher its value, the greater the impact of the loss. Data analysis was performed using SPSS software. Paired comparison tests (Wilcoxon test or Student's t-test) were used to assess differences in the grief scale. A significance level of $p < 0.05$ was adopted. **Results:** The study included 171 individuals, with a predominance of female participants (66.7%) and the most frequent age group being 25-34 years (28.1%). Comparing the group that had already consumed AYA before the grieving process with the group that had not yet consumed it, a reduction in scores related to the redefinition of loss was observed for all participants after using AYA ($p < 0.05$), with a reduction of 39.75% and 51.89%, respectively. Further, those who had previously consumed AYA before grieving showed better acceptance of the loss process compared to those who only used it after the loss. Furthermore, a relationship was observed between the number of times an individual ingested the drink and their score. Participants who used the drink once had a smaller reduction in the final score (39.13%) compared to individuals who used it two to five times (50.65%), six to ten times (64.63%), and more than ten times (60.38%). However, there was verified a significant reduction in the scores in all groups regardless. After the AYA experience, participants reported improvement in personal relationships (69.01%), and sleep (69.59%). Additionally, when asked about having successfully overcome his loss, it was observed that the use of AYA was able to head the sample toward the partial or total overcoming of grief after the beverage's use (66.67%). **Conclusion:** There is a direct relationship between reframing losses through AYA. Individuals who used the drink demonstrated the ability to promote improvement in the symptoms of grief, which can serve as a therapeutic alternative for this condition.

14.011 *Ilex Paraguariensis* Hydroalcoholic Extract and Ibuprofen Alter Organ Morphometry in Wistar Rats. Medeiros IS¹, Bezerra R¹, Schwab E¹, Somensi LB³, Bahr AC³, Bonini JS¹, Gregório E^{2,3}, Silva WCFN¹ ¹Unicentro, Depto de Farmácia, Guarapuava, Brasil. ²UFRGS, Depto de Fisiologia, Porto Alegre, Brasil. ³Uniarp, Depto de Medicina, Caçador, Brasil

Introduction: *Ilex paraguariensis* is a plant of the *Aquifoliaceae* family, has a rich chemical composition, with phenolic substances, saponins and methylxanthine. Phenolic compounds are known for their extensive antioxidant capacity as well as anti-inflammatory properties. However, little is known if its effects cause morphometric changes in organs such as kidneys, stomach and heart. This study aimed to verify the anti-inflammatory potential of the crude hydroalcoholic extract of *Ilex paraguariensis* in the morphometric alterations of the organs of male Wistar rats, compared to Ibuprofen at a concentration of 50mg/mL, given its analgesic and anti-inflammatory actions. The leaves of *Ilex paraguariensis* were collected at EMBRAP's land in the city of Caçador-SC in February 2023. The crude extract was extracted from the dried leaves by maceration with EtOH:H₂O (30:70,v/v) at room temperature. Then the extract was concentrated under reduced pressure at 45 °C, followed by lyophilization. **Methods:** 24 male rats weighing 250g±30g were divided into four groups (n=6): naive, saline, Ibuprofen (50mg/mL), and Ilex (30mg/mL). The animals were submitted to standard conditions with natural cycles of 12h light/dark and temperature between 20±2°C. The groups received saline, ibuprofen and Ilex via gavage for seven days. After administration, the animals were sacrificed, and the heart, kidneys and stomach were removed, cleaned, dried and weighed. Statistical analysis was performed using the ANOVA test and p<0.05 was considered significant. Correlations between the data obtained were calculated using the statistical option of the MS Excel software. All experiments followed the "Principles of care for laboratory animals" (NIH publication n°85-23, revised 1996), and were approved by the CEUA/UNICENTRO animal ethics committee under opinion 022/2022. **Results:** There was a significant increase (p<0.05) in the total heart weight of the animals that received the Ilex extract when compared to the Ibuprofen, naive and saline group. This result was confirmed when evaluating the total weight of the ventricles and atrium. Regarding the weight of the kidneys, we verified a significant decrease (p<0.05) in the weight of the Ilex and ibuprofen groups when compared to the saline and naïve groups. As for stomach weight, no significant differences were found. **Conclusion:** We demonstrated the administration of Ilex at a dose of 30mg/mL for seven days influences the wet weight of the heart and kidneys of Wistar rats. In contrast, ibuprofen at a dose of 50mg/mL causes a decrease in organ weight in an anti-inflammatory condition. Therefore, the results obtained prove the need for a greater number of studies involving the morphological aspects of the organs most susceptible to the actions of *Ilex paraguariensis* as well as its toxic effects. **Financial Support:** This study was financially supported by the National Council for Scientific and Technological Development (CNPq), Research and Innovation Foundation of Santa Catarina (FAPESC), Association for Studies, Research and Assistance to People with Alzheimer's (AEPAPA).

14.012 Aging and Protein Malnutrition Impair Hematopoiesis and Favors Malignant Cells Through Bone Marrow Mesenchymal Stem Cells. Gonçalves CES¹, da Silva RO¹, Hastreiter AA¹, Vivian GK¹, Makiyama EN¹, de Freitas S¹, Borelli P¹, Fock RA¹. ¹FCF-USP, Dpt. of Clinical and Toxicological Analyses, PPG Pharmacy: Physiopathology and Toxicology, Brazil

Introduction: Protein malnutrition (PM) is a common finding among elderly individuals [1], but the relationship between aging and PM and its relationship with the bone marrow (BM) microenvironment remains poorly understood. Inside this microenvironment, BM Mesenchymal Stem Cells (MSCs) act as regulators of hematopoiesis by interacting with both hematopoietic and non-hematopoietic cell populations directly and indirectly [2,3]. With that in consideration, the aim of this study was to evaluate how PM when associated with aging influences the hematopoietic regulatory capacity of BM MSCs. **Methods:** Young and aged mice were fed with a normoproteic or hypoproteic (12 or 2% of protein, respectively) diet and had their nutritional, biochemical and hematological parameters evaluated. BM MSCs were characterized following the recommendations of the International Society for Cellular Therapy [4] and had their secretome, gene expression, autophagy, reactive oxygen species production (ROS) and double-stranded breaks were evaluated. Additionally, regulatory potential of MSCs over hematopoiesis was evaluated using *in vitro* and *in vivo* models in association with the C1498 murine acute myeloid leukemia cell lineage (TIB-49TM, ATCC[®]). Lastly, mice from all groups were challenged with the C1498 cell lineage (TIB-49TM, ATCC[®]) to measure BM invasiveness and to estimate mice survival during a 12-day period. This study was performed following its approval by the institutional animal care committee (CEUA-FCF Protocol #544). **Results:** Aging and PM altered the biochemical parameters of mice while also changing the peripheral blood and BM cell populations. In regards to the MSCs, their autophagy was affected by aging both in the presence or absence of PM. The production of ROS and frequency of double-stranded breaks were most heavily affected in aged MSCs. The MSCs' secretome and gene expression were also affected by aging as well as by PM. Aging and PM directly influenced the hematopoietic regulatory characteristics of MSCs by affecting hematopoietic genes related to pluripotency, while aging also impaired the differentiation of C1498 cells. Both young and aged malnourished groups displayed a higher frequency of malignant cells in the BM following their injection in the peripheral blood, therefore showing a higher invasiveness. Lastly, malnourished aged mice had the lowest percentage of survival when compared with all other groups, while young normally-fed mice maintained a 100% survival rate. **Conclusion:** Aging and PM can lead to changes in the BM microenvironment that favors the development of malignant cells, and these can be at least partially induced by an impaired function of BM MSCs. **References:** [1] Deer, RR. *Curr. Opin. Clin. Nutr. Metab. Care.*, v. 18, p. 248-53, 2015. [2] Comazzetto, S. *Dev. Cell.*, v. 56, p. 1848-60, 2021. [3] Morrison, SJ. *Nature.*, v. 505, p. 327-34, 2014. [4] Dominici, M. *Cytotherapy.*, v. 8, n. 4, 2006. **Financial Support:** CNPq and FAPESP.

14.013 The Pioglitazone Treatment Combined with Cold Exposure Increase the Thermogenic Capacity of Brown and White Adipose Tissue in Mice without Affecting the Energy Expenditure.

Valdivia LFG¹, Sousa E², Jardim GFR², Festuccia WTL³, Reckziegel P^{1,2} ¹InFar-Unifesp, PPG em Farmacologia, Depto de Farmacologia, Centro de Farmacologia e Biologia Molecular, São Paulo, Brazil; ²FCF-USP, Depto de Análises Clínicas e Toxicológicas, São Paulo, Brazil; ³ICB-USP, Depto de Fisiologia e Biofísica, São Paulo, Brazil

Introduction. Cold exposure and the use of PPAR γ agonists, such as rosiglitazone, have been reported to stimulate brown adipose tissue (BAT) and beige adipocytes to generate heat during non-shivering thermogenesis. However, their combined effects during chronic cold exposure are not fully understood. This study aimed to investigate the effects of chronic cold exposure combined with pioglitazone, a PPAR γ agonist, on thermogenesis in BAT and white adipose tissue (WAT) of mice, as well as their impact on energy expenditure. **Methods.** Male C57BL/6 mice (CEUA-ICB/USP, #8874310719) were treated or not with pioglitazone (30 mg/kg/day) and exposed to 21°C or 7°C (cold) during 15 days. The interscapular BAT (iBAT) and inguinal WAT (iWAT) were used for evaluation of mass, histology, UCP1 content and gene expression. Mice were evaluated by indirect calorimetry, and core body temperature during the β 3-agonist CL316,243 test. Statistical analyses were performed by two-way ANOVA and Tukey's test ($P < 0.05$). **Financial support:** São Paulo Research Foundation (FAPESP processes #2019/25943-1, 2021/03717-0 and 2023/02579-8). **Results.** The combined therapy of pioglitazone and cold exposure led to increased BAT mass and decreased WAT mass. Histological analyses revealed increased unilocularity in iBAT and multilocularity of adipocytes in iWAT. Furthermore, the combined therapy increased UCP1 levels and the expression of genes related to thermogenesis (UCP1, DIO2, PGC1 α , CIDEA, and CPT1 α), adipogenesis (FABP4), lipid metabolism (PPAR α , GYK, LPL, ATG, CD36, GPAT1, and DGAT1), and glucose uptake (GLUT1 in iBAT and GLUT4 in iWAT) in the analyzed adipose tissues. Regarding energy expenditure (O_2 consumption and CO_2 production) of the animals, no significant differences were observed between the Cold and Pio+Cold groups, but cold exposure increased these parameters compared to the Control group. The impact of the observed increased thermogenic machinery resulting from the combined therapy was only evident in the body temperature of animals during the CL316,243 test conducted under thermoneutral conditions. **Conclusion.** This study provides an animal model demonstrating significant modulation of adipose tissue markers related to thermogenesis. However, it is evident that an increase in total UCP1 alone is insufficient to enhance energy expenditure, implying that increased UCP1 content alone cannot be expected to ameliorate obesity.

14.014 Modulation of *in vivo* Adiposity and *in vitro* Adipogenesis Via Nrf2/Keap1 Pharmacological Signaling. Valença HM, Moraes JA, Valença SS ICB-UFRJ, Rio de Janeiro, Brazil

Introduction: Obesity is characterized by an imbalance between energy intake and energy expenditure that triggers abnormal growth of adipose tissue, resulting in an increase in size (hypertrophy) and in the number of adipocytes (hyperplasia). This dysfunction culminates in an increased profile of inflammatory adipokine release and increased production of reactive oxygen species (ROS) to the detriment of antioxidant defenses, establishing the condition of oxidative stress. Furthermore, the transcription factor Nrf2 is primarily responsible for activating the transcription of genes linked to the antioxidant response. Dimethylfumarate (DMF) as well as its metabolite monomethylfumarate (MMF) are Nrf2 activators and therefore strategic antioxidants from a molecular point of view. Therefore, the objective of this work was to characterize and identify the mechanisms of action of the Nrf2 activator, DMF, applied to metabolic disorders associated with obesity through *in vivo* and *in vitro* studies. **Methods:** Murine 3T3-L1 preadipocytes were cultured in DMEM supplemented with 10% bovine serum and induced to differentiate using medium supplemented with insulin (10 µg/ml), dexamethasone (0.25 µM) and IBMX (0.5 mM) for 7 days. To determine the effect of MMF on adipogenesis, groups of cells were incubated with 10, 30 and 100 µM of MMF and Oil Red O staining assay assessed intracellular lipid accumulation. Preadipocytes were assigned to control (CTR) or CTR+MMF, cells grown in DMEM+MMF (100 µM); MIX, cells cultured with differentiation mix; and MIX+MMF. The inflammatory profile of these cells was observed, as well as the production of ROS. Male mice of the C57BL/6 strain were divided into CTR groups (fed a standard diet); CTR+DMF (standard diet and DMF treatment); HFHSD (fed with a diet rich in lipid and sucrose); HFHSD+DMF (diet rich in lipids and sucrose and treatment with DMF). The weight of the animals was monitored weekly, DMF was administered from the 12th week onwards by gavage at a dose of 120 mg/kg, and glucose and insulin were measured. After euthanasia, the adipose tissue was homogenized and analyzed. **Results:** Western blot analysis showed increased PPAR γ expression in the MIX group compared to the CTR, while the MIX+MMF group maintained levels equal to the CTR. Triacylglycerol levels remained low in the MIX+MMF group, and increased in the MIX group. There was an increase in ROS in the LPS and MIX groups, but not in the LPS+MMF and MIX+MMF groups. Furthermore, there was a reduction in the activation of the NF κ B pathway in the LPS+MMF and MIX+MMF groups. Finally, the MIX group induced an increase in the secretion of the adipokines adiponectin and resistin, while the MIX+MMF group remained the same as the CTR. Mice from the CTR and CTR+DMF groups gained less weight when compared to the HFHSD group. The HFHSD and HFHSD+DMF groups maintained similar weights until the 12th week, when the group that received DMF began to lose weight, reaching a weight similar to the CTR and CTR+DMF groups. DMF reduced the visceral and subcutaneous fat weight of animals in the HFHSD+DMF group. DMF also reduced blood glucose, improved glucose tolerance, reduced insulin resistance and the secretion of pro-inflammatory molecules in the treated group. Finally, DMF was able to decrease leptin levels and increase adiponectin levels in the HFSD+DMF group. **Conclusion:** Therefore, these data demonstrate that DMF can be a negative regulator of adipogenesis, serving as a basis for future pharmacological strategies to control obesity.

14.015 Study of Tissue Impregnation by Ibuprofen as an Emerging Pollutant found in the Waters of the Bengala River (NF-RJ). Fujimaki CMO¹, Soares, MA², Miranda ALP¹. ¹UFRJ, PPG Pharmaceutical Sciences, Brazil; ²UFRJ, PPG Endocrinology, Faculty of Medicine, Brazil

Introduction: The growing use of pharmaceuticals around the world has given rise to a new class of environmental pollutants called emerging pollutants (EP). EP are potentially toxic substances found in the environment in low concentrations, whose long-term risks for several living organisms and for human health are not known yet. These substances are introduced into aquatic environments through excreta or discharges and when organisms are exposed they can cause the same health consequences as persistent organic pollutants due to their continuous entry into the environment. The objective of this work was to determine and quantify the presence of ibuprofen and its metabolites in springs of the Bengala River (Nova Friburgo, RJ), and to evaluate the impact of this contamination on health through tissue impregnation tests. **Method:** The experimental groups, n= 3/group, male and female mice, 21 days old, were divided into: 1- drinking water (control); 2- spring water; 3- drinking water with ibuprofen and kept under treatment for 120 days. At the end of this period, they formed couples who continued the chronic exposure treatment to obtain the F1 generation. LC/MS-MS was used for transgenerational tissue impregnation analyses. **Result:** The mass spectrometry analysis of the animals in the intervention group - spring water and in the intervention group - drinking water containing a known concentration of ibuprofen, showed the presence of ibuprofen, as well as its metabolites, through the m/z fragments 161, 175, 177, 205, 207 and 221 in adipose, hepatic, pancreatic, cerebral and gonadal tissues, in addition to blood, where the impregnation content varies between animals. The m/z 175, 177 and 221 are ionic fragments from the metabolites 2-hydroxyibuprofen, 3-hydroxyibuprofen from phase I metabolism and the taurine conjugate, phase II. Macroscopically, we can observe changes in the uterine structure of animals in groups 2 and 3, treated with water from the source and with drinking water containing known concentration of ibuprofen, respectively. The LC/MS-MS analysis of the control group - drinking water, did not demonstrate the presence of ibuprofen or its metabolites. During the experiment weight, glycemia and allodynia were evaluated. **Conclusion:** Tissue impregnation was successfully achieved. Medications that act as nonsteroidal anti-inflammatory drugs, such as ibuprofen, can act as emerging pollutants with potential endocrine-disrupting activity.

Authors Index

A			
Abboud KY	09.006	Alves Junior EB	08.001, 08.011, 08.015
Abreu FVG	04.003, 04.015, 04.023, 04.051	Alves LP	02.029
Abreu VHP	04.016	Alves MCO	01.007
Acevedo JLA	10.006	Alves MG	04.042
Afeche SC	09.028	Alves RR	08.015
Afonso DD	09.013	Alves SG	10.004
Afonso PPL	11.016	Alves VF	04.014, 04.045, 04.049
Agnes JP	05.016	Alves VP	08.001, 08.002, 08.010, 08.011
Aguiar GPS	02.033	Amanda J	04.055, 09.047
Aguiar SCR	02.038	Amantnecks JA	04.010
Akamine EH	06.030	Amaral CF	04.012, 04.013, 04.021
Albernaz L	06.035	Amaral FKCW	05.006, 09.010, 09.032
Albuquerque AO	02.030	Amatnecks JA	04.005
Albuquerque CFG	02.026, 02.029, 02.042, 04.004, 04.006	Amon RLR	14.002, 14.003
Albuquerque ER	09.042	Amorim JDO	10.004
Albuquerque-Junior R	09.018	Andrade CD	11.011
Alcantara LG	10.004	Andrade GM	02.030
Alencar NMND	04.018	Andrade LGD	03.004
Alexopoulos I	01.008	Andrade LM	02.030
Almada OYH	09.022	Andre E	13.002
Almeida ARB	01.007	Andrighetto N	05.007
Almeida B	14.002, 14.003	Andriolo IRL	08.004
Almeida CJLR	04.041	Anibal C	05.009
Almeida Filho OP	03.025, 05.022	Ansolin LD	03.008, 08.013
Almeida FRC	04.028, 05.001, 05.002, 05.012, 05.014	Antonio W	08.012, 08.013
Almeida IDFR	09.030	Antunes E	06.014, 06.017, 07.006, 07.007
Almeida JFSD	12.020	Antunes LCM	11.015
Almeida JH	10.010	Aparecida M	04.014, 04.049
Almeida JOCS	07.005	Aquino ACQ	03.022
Almeida MAP	02.026, 02.042, 04.004, 04.016, 04.026, 04.047	Aquino CC	04.019
Almeida MD	04.037	Aquino PEA	02.011
Almeida MM	06.034	Aragon D	02.036
Almeida PG	12.014, 12.015, 12.018, 12.021, 12.023	Arantes ACS	04.023, 04.037, 04.050, 04.051
Almeida RT	01.001, 01.012	Araruna MEC	08.001, 08.011
Almeida SST	01.001, 01.012	Araujo BV	11.011, 11.019, 11.024
Almeida TC	09.021	Araujo FS	09.040
Almeida VEF	02.016, 02.017, 02.018, 02.022, 02.023, 02.029, 04.016, 04.026, 07.008	Araujo LDS	01.014
Alsou'b DFB	05.015	Araujo RB	01.010
Alves ADS	06.030	Arboit F	03.004
Alves AF	08.015	Arcanjo DDR	04.028, 07.005
Alves APNN	04.018	Armas JPR	10.006
Alves CDS	09.015	Aroucha DF	11.022
Alves FMS	09.030	Arruda LM	10.009
Alves GF	06.022	Assis DSA	02.004
Alves J	06.004	Assis VO	06.013
		Assis-Mendonca GRA	07.007
		Assolini JP	09.004
		Assreuy J	06.008
		Augusto IDL	04.024, 04.027, 04.032, 04.036, 04.055
		Avellar MCW	07.004

Ayres TA	03.027	Bem GFD	06.012, 09.015, 09.019
Azeredo EL	04.022	Benatti MN	06.033
Azevedo CTD	04.031	Benvegna DM	14.004
Azevedo GAD	04.044, 04.048	Benvenuti L	05.016
B		Bernardi A	01.011, 04.031, 10.014
Baco LSD	11.015	Bernardi LS	12.001, 12.004, 14.006
Baez WJA	03.012, 06.020, 09.022, 09.043	Bernet K	11.008
Bagri K	01.014	Bertoglio LJ	02.014, 02.020, 03.006, 03.013, 03.020
Bahr A	14.007, 14.008, 14.011	Bertollo AG	03.002, 03.008
Bandeira SMA	02.011	Bertozzi M	04.017
Baptista G	07.009	Betti AH	03.027
Baptista JP	13.001	Bezerra MM	08.001, 08.002, 08.011
Baptista NZ	09.032	Bezerra RLA	14.007, 14.008, 14.011
Barbosa BLSS	04.003	Biano LS	09.018
Barbosa E	03.027	Biavatti MW	03.018
Barbosa GF	05.022	Bicca MA	11.006
Barbosa I	08.022	Biscaia IFB	14.006
Barbosa JM	06.024	Bispo MDB	09.012
Barbosa LA	02.027	Bitencourt IC	11.009
Barcelos RB	02.015	Bittencourt RADC	09.047
Barichello A	08.013	Blanchard F	13.001
Barilli LA	02.006	Bochi GV	02.013, 03.004, 05.011
Bariviera JL	02.021	Boechat N	12.018
Baroni MC	02.016, 02.017, 02.018, 02.022, 02.023	Bohme G	13.001
Barrence FAC	02.044, 14.001	Bohnen LC	03.002, 03.008
Barreto A	09.024	Bohrer GP	04.014
Barreto E	01.013, 04.054, 09.005, 09.027, 10.010	Bolzan JA	03.009
Barreto LSH	02.034	Bonancea AM	06.001, 06.023, 06.028
Barros ABB	01.013, 04.054, 09.005, 09.027	Bonato JM	02.002
Barros BC	08.015	Bonato VLD	06.006
Barros GMDO	01.014	Bonetti CI	01.004, 09.020
Barros PRD	06.006	Bonfa IS	04.038
Bartkuhn M	01.008	Bonfim JPC	05.003, 05.017
Basilio MI	02.009	Bonini JS	09.030, 14.007, 14.008, 14.011
Bastiani CDS	02.019	Borelli P	04.008, 14.012
Bastos FGT	07.005	Borges J	04.020
Bastos JK	02.009, 04.029, 08.003, 08.004, 08.014	Borges VDF	04.046
Bastos MM	12.018	Borstmann SMA	14.004
Batista CL	10.003	Bortoluzzi A	02.025
Batista LM	08.001, 08.002, 08.010, 08.011, 08.015	Bozza PT	02.026, 02.042, 04.004, 04.016, 04.026, 04.047
Batista LP	02.020	Bracht A	09.020
Batista RADO	06.026, 09.039	Bracht L	01.004
Batistela VR	04.021	Braga F	04.032, 04.036
Bauer ER	02.009	Braga LLVDM	09.006, 09.035
Bayona-serrano JD	09.044	Brait DRH	04.020
Becari C	06.002, 06.003, 06.004, 06.015, 06.019, 06.024, 06.027	Brancalione RC	12.004, 14.006
Beghini ACG	07.006, 07.007	Brandao BDJ	07.003
Behrens MDDD	04.006	Brasiel PGDA	04.025
Bel EAD	03.015	Braz HFG	09.039
Beltrami VA	04.034	Bressan AFM	06.025
		Brigido MC	06.036
		Brito AKS	07.005

Brito EDS	06.035	Carlos AS	07.008
Brito MASM	04.006, 04.047	Carmo JDODS	09.005, 09.027
Brito MSC	09.010	Carneiro F	06.025
Britto-Júnior J	06.009, 06.014, 06.017, 06.037	Carneiro FM	11.010
Brucker N	04.002, 09.036, 11.002, 11.015, 11.017	Carneiro FS	04.024, 04.027, 04.036, 04.040
Brum EDS	05.011	Carraro E	02.032
Brum GFD	02.013	Carttman L	04.003, 12.005
Brunch P	06.002	Carvalho AFS	04.024, 04.027, 04.032, 04.036, 04.040, 04.055
Bruschi ML	02.001	Carvalho JE	09.013
Brusco I	12.022	Carvalho MAJ	02.011
Bruscoli S	04.024	Carvalho VF	04.003, 04.025, 04.030, 04.031, 04.037, 04.050, 04.052, 12.005
Buccini DF	03.025, 05.022	Carvalho VM	10.002
Bueno LR	09.016	Casagrande R	04.017, 04.042, 09.037
Bueno MO	09.004	Cassol JV	03.002
Bufalo MC	05.008, 05.013	Castellano M	02.044, 03.026, 14.001
Buglio KE	09.013	Castro HA	04.051
Buregon JS	04.002	Castro RS	05.009
Burger ME	02.003, 02.015, 02.024, 02.028	Castro-Faria-Neto HC	02.016, 02.017, 02.018, 02.022, 02.023, 02.026, 02.029, 02.042, 04.004, 04.016, 04.025, 04.026, 04.047, 04.051, 07.008
Busato MA	09.033	Cavalcante CMB	09.012
Buzatto MV	03.008, 08.012, 08.013, 08.018, 08.019	Cavalcante DIM	10.009
C		Cavalcante KDM	05.001, 10.003, 10.013
Cabral LM	12.014	Cavalcante MLS	05.002, 05.012, 05.014
Cabrini D	09.040	Cavalheira MA	06.012, 09.019
Caixeta RS	04.024, 04.027, 04.032, 04.036, 04.040, 04.055	Cazarin CA	02.009, 03.001, 08.021
Cajado AG	04.018, 04.019, 10.008	Cebinelli GCM	06.032
Cajado VJ	02.038	Centa A	09.004
Calazans M	05.021	Cerqueira ARA	12.010
Caletti G	02.010	Cervini R	09.004
Caliendo G	04.049, 12.010	Cesar ESL	07.005
Calmasini FB	07.002	Cesar MDO	09.046
Calvo AM	11.012, 11.014	Cezar-dos-santos F	11.020
Camargo EA	09.018	Chade ES	12.001, 12.004
Camarini R	04.014	Chagas MDSDS	04.006
Camelo TDS	10.004	Charao MF	03.027
Camilo L	04.055	Chateaubriand PHP	02.016, 02.017, 02.018, 02.022, 02.023, 07.008
Campitelli RR	11.016	Chaves ADS	04.003, 04.025, 04.030, 04.052, 12.005
Campo RDM	02.036	Chaves DBD	14.004
Campos AJR	07.005	Chaves JO	06.035
Campos HM	01.005, 02.027, 02.035, 02.037, 11.001	Chiavegatto S	06.017
Campos LB	06.003	Chinen LY	02.002
Campos R	06.009	Chorilli M	12.013
Campos RDM	06.016, 06.037	Chudzinski-tavassi AM	05.013
Campos RM	12.003		
Campos TG	12.011		
Candido CS	04.044, 04.048		
Candido G	02.001		
Capibaribe VCC	02.011		
Capoani GT	03.008		
Cardoso C	04.024, 04.027, 04.032, 04.036, 04.040, 04.055		
Cardoso NC	03.011		
Cardozo HG	11.019		

Cimarosti H	06.010	Coutinho DDS	04.030, 04.037,
Clarindo FA	12.014		04.050, 10.014,
Claudino BFDO	08.015		11.013, 11.025
Coelho AA	02.040, 03.005	Coutinho-silva R	01.003
Coelho DMN	02.011	Couto AESD	06.003, 06.019,
Coelho LDDS	02.007, 11.026		06.024, 06.027
Coelho-dos-reis JGA	12.014	Couto CER	02.041
Cogliati B	12.017	Crippa JA	03.015
Cohen M	01.008	Cruz EKM	02.034
Comar FMDSS	04.013, 04.021	Cruz JGDS	06.020
Comar FMSS	04.012	Cuman RKN	04.012, 04.013,
Comar JF	01.004		04.021
Conceicao BC	09.014	Cunha CMCD	04.016
Conceicao JVVD	10.004	Cunha FQ	04.015, 04.041,
Conceicao M	12.013		04.046, 06.032
Cooper D	04.040	Cunha JCLD	02.007, 11.026
Cordeiro LMC	09.006, 09.016,	Cunha JMD	05.003, 05.017,
	09.035		13.002
Cordeiro RSB	04.031	Cunha LDD	06.006
Cornelio ML	04.028	Cunha MBD	09.045, 12.022
Correa AMC	04.009, 09.029	Cunha MDPSSD	10.004
Correa CB	09.018	Cunha T	05.009
Correa GDL	04.002, 11.017	Curty MDS	02.016, 02.017,
Correa JC	01.002		02.018, 02.022,
Correa LB	04.022		02.023
Correia BL	01.004	Cury BJ	02.009, 08.003,
Correia-de-Sá PJDS	05.014		08.004, 08.021
Corsi C	06.003, 06.015,	Cury R	11.006
	06.019, 06.027	Cury RDM	11.020
Cort TD	09.045	D	
Costa ABA	12.002	D'Ávila JC	07.008
Costa AR	11.010	da Costa Filho HB	09.016
Costa BG	03.018	da Silva Filho FA	06.026
Costa CAD	06.012, 09.015,	Dalben MB	02.006
	09.019	Dalenogare DP	05.011
Costa EA	11.001	Daleprane JB	09.015
Costa FF	07.002	Dallabrida KG	09.030, 11.021
Costa I	13.001	Dallagnol P	03.002
Costa JCSD	04.031, 11.013,	Dallazen JL	04.049, 05.015
	11.025	Dallegrave E	03.027
Costa JEM	03.009, 03.010	Daniel CF	02.025, 02.033
Costa LTS	04.001, 09.047	Dantas PB	06.024, 06.027
Costa M	02.016, 02.017,	Dare RG	14.005
	02.018, 02.023	Daudt LE	11.024
Costa MF	02.042, 04.004,	Del-Bel E	03.014, 12.013
	04.047	Delfrate G	06.008, 06.022
Costa Neto CM	04.046	Demico PDJ	09.002
Costa PIG	06.034, 09.046	Denadai-souza A	08.017
Costa RA	04.005, 04.010	De-souza LSP	10.009
Costa RMD	06.004, 06.006,	Dias BB	11.011, 11.019,
	06.027, 06.033		11.024
Costa SKP	01.007, 04.049,	Dias JL	02.033
	05.015, 06.031,	Dias Júnior BC	03.017
	08.017, 12.010	Dias Junior QM	03.019
Costa TEMM	09.029	Dias KT	08.005
Costa TJ	06.033	Dias L	09.011
Costa V	04.027, 04.032,	Diaz AKGR	06.020, 09.022
	04.033, 04.055	Diaz DAI	03.012, 06.020,
Costa VF	04.041		09.043
Costa VRM	04.033	Diniz A	11.004, 11.005,
Costa-Lotufo LV	10.007, 12.007		11.023
Couceiro FYGM	09.008	Diniz AFA	08.015
		Dionisio TJ	11.012, 11.014

Dittz D	05.001, 05.002, 05.012, 05.014, 10.003, 10.011, 10.012, 10.013	Ferrari SSAR	01.001, 01.012
Donato Júnior J	04.045	Ferrarini SRF	04.026, 04.047
Donato M	02.036, 03.024, 14.009, 14.010	Ferraz CR	04.017
Donato MF	02.045	Ferraz CV	08.018, 08.019
Dong BE	08.007	Ferraz GB	03.025
Dornelles FN	04.043	Ferraz SLNES	05.012
Dourado TDMH	06.005	Ferreira BF	03.023
Dragunas G	04.045	Ferreira DM	09.006, 09.016, 09.035
Duarte CDM	01.001, 01.012	Ferreira EGA	01.013, 04.054, 09.005, 09.027
Duarte DA	04.046, 06.025	Ferreira FY	04.001, 09.047
Duarte DB	09.025, 11.018, 11.022	Ferreira GDC	04.015
Duarte IDG	05.021	Ferreira GG	04.023
Duarte JL	12.013	Ferreira J	05.011, 05.016
Dugaich VF	06.002, 06.003, 06.015, 06.019, 06.024, 06.027	Ferreira JCB	05.019
Duque EA	02.047, 04.045	Ferreira JGDJ	03.027
Duran J	13.001	Ferreira JV	04.038
Dutkevicz N	08.009	Ferreira LM	09.030
E		Ferreira LMM	10.004
Eckert FB	03.009, 03.010	Ferreira LPF	10.011, 10.012, 10.013
Eller S	02.010	Ferreira MJP	10.007
Engevik AC	04.019	Ferreira MV	05.003, 05.017
Evora P	06.024	Ferreira NR	11.014
F		Ferreira PB	08.015
Fagundes A	06.024	Ferreira PMP	05.001, 05.002, 05.012, 10.011
Fagundes KR	14.004	Ferreira PYO	01.005, 02.027, 11.001
Fagundes C	01.008	Ferreira RGL	02.023
Falque WF	09.015	Ferreira SCDAF	09.012
Faria FACD	11.012	Ferreira TPT	04.011, 04.037, 04.051
Faria R	05.010	Ferreirinha MDFO	05.014
Faria RX	05.020	Ferrero M	04.030
Farias ERA	02.007, 02.027, 02.035, 02.037, 11.026	Ferrero R	01.008
Farias JC	06.032	Ferro JNS	10.010
Fazan-Júnior R	06.032	Festuccia WTL	14.013
Fehrenbacher J	09.025	Fidelix MDSP	01.013, 09.005, 09.027
Felipe JL	04.038	Figueiredo V	02.016, 02.017, 02.018, 02.022, 02.023, 07.008
Felisbino K	11.008	Filgueiras CC	09.015
Felix FB	04.034, 04.036	Filippo LDD	12.013
Fermino F	03.024, 14.009, 14.010	Florencio KGD	10.008, 10.009
Fernandes ACS	14.004	Florentino I	11.006
Fernandes AJM	04.023	Florentino INA	11.020
Fernandes D	06.008	Floriano RS	09.002, 09.008
Fernandes ES	09.035	Fock RA	04.008, 04.056, 14.002, 14.003, 14.012
Fernandes HB	08.008	Foglio MA	09.013
Fernandes MML	04.038	Foguel D	04.015
Fernandes PACM	04.053, 07.003	Fonseca LBD	11.013, 11.025
Fernandes PD	12.002, 12.003, 12.008, 12.009, 12.011, 12.014, 12.015, 12.016, 12.018, 12.019, 12.021, 12.023	Fonseca MFR	02.007, 02.027, 02.035, 02.037, 11.026
Ferrante LF	04.017, 04.042, 09.037	Fonseca MRSD	10.008
		Fontana T	02.013
		Fontes-junior EDA	09.014, 09.041
		Fontoura MB	02.003
		Formagio ASN	04.007, 04.020

Fracasso JAR	04.001, 09.003	Goldoni FC	05.016
Frajblat M	04.049	Gomes APLN	02.034, 02.038
Franca PRDCD	12.002, 12.016	Gomes BQ	06.013
Franca TCS	02.009, 08.004, 08.014, 08.021	Gomes BRB	02.004, 02.034
Francelino DMC	08.015	Gomes DB	08.012
Franciosi A	04.017	Gomes DS	06.035, 06.036
Francisco DF	06.003, 06.019	Gomes EDT	07.006
Francisco K	04.047	Gomes FV	03.014
Franco A	08.022	Gomes GMO	01.001, 01.012
Franco D	06.015, 06.027	Gomes HDS	04.037, 04.050, 11.013
Franco GDRR	12.003, 12.008, 12.009, 12.019, 12.021	Gomes LDS	05.012
Frare JM	05.007, 05.011	Gomes SN	14.006
Freitas AKMSDOF	03.022	Gomez R	02.010, 02.019
Freitas GBLD	05.012	Goncalves ADR	12.017
Freitas GDL	04.018, 10.004, 10.009	Goncalves CEDS	04.008, 14.012
Freitas R	08.022	Goncalves D	06.025
Freitas RHCND	12.002	Goncalves EER	09.039
Freitas SD	04.008, 04.056, 14.012	Goncalves JRP	14.009, 14.010
Freitas-Filho EG	06.006	Goncalves MICM	12.021
Freitas-Júnior RAF	03.025, 05.022	Goncalves MR	04.033
Freitas-Junior RAO	03.022	Goncalves R	02.032
Fronza MG	03.023	Goncalves TT	01.010, 06.025
Frozza RL	01.011, 10.014	Goncalves WA	04.040
Fujimaki CMDO	14.015	Goncalves-de-Albuquerque CFG	04.016, 04.026, 04.047
Furian AFF	11.021	Gonsalez SR	06.035
G		Gontijo VS	12.003, 12.008, 12.009, 12.019, 12.021
Gadelha EC	10.009	Gordon EM	08.007
Gadelha KKL	04.019	Gouveia JF	06.012, 09.019
Galant LS	04.041, 04.046	Granja MG	02.029
Galizio NDC	09.001, 09.009, 09.017, 09.026	Granja-Santoro GPAP	09.046
Galizio NDCG	09.034	Grego KF	09.001, 09.009, 09.017, 09.026, 09.034
Gallina AL	14.004	Gregorio E	14.007, 14.008, 14.011
Galvao GM	02.035	Gregorio T	07.009
Galvao R	05.010	Grieshaber LE	13.002
Galvao RMDS	05.020	Grossi L	04.027, 04.036
Gao E	06.018	Guerrero TN	06.036
Garcia LNV	09.026	Guidinele MCB	12.002
Gasparetto RL	02.041	Guilherme GO	05.003, 05.017
Gasparini MV	06.025	Guiloski IC	11.003, 11.008
Gasparotto-Junior A	09.042	Guimaraes FS	03.013, 03.014, 03.015
Gazarini L	02.014	Guimaraes NC	02.004
Gehlen G	03.027	Guimaraes PO	09.025
Georgetti SR	09.037	Gurgel DC	10.004
Gepetti P	05.018	Gutierrez MV	03.008, 08.013, 08.018, 08.019
Gerhard GM	02.041	H	
Ghedini PC	01.005, 02.027, 02.035, 02.037, 11.001	Haas SE	11.009
Giesbrecht A	09.043	Hahmeyer MLDS	06.029
Gindri AL	09.036	Hajna Z	05.015
Giorno TBS	12.009, 12.023	Hallak JE	03.015
Glaser RD	01.008	Harms C	06.010
Godinho RO	01.006, 01.009	Hastreiter AA	14.012
Godoy TADG	09.034	Heiner M	01.008
Goes AKS	12.004	Hellion-ibarrola MDC	09.043
Goes PRND	11.005, 11.023	Helyes Z	05.015
Gois GA	12.010	Henrique	06.002
Gois MB	04.019, 09.016		

Henriques GDM	03.017	Lanza M	02.025
Henriques MDGMO	04.009	Lara ES	04.024, 04.027, 04.032, 04.036, 04.040, 04.055
Herling AA	11.004		
Hermes ME	02.041		
Herold S	01.008	Lara LDS	06.034, 06.035, 06.036
Hirata AS	12.007		
Hirata F	03.024, 14.009, 14.010	Lattig G	06.010
		Leal BDS	10.011, 10.012, 10.013
Hirsch E	04.018	Leal MB	02.019
Hollas VG	02.031	Leandro IMDC	12.006
Honorio MDS	04.029	Leandro MDO	04.041
Horta VQ	09.039	Leiria LO	01.010
Horvath AI	05.015	Leite JA	02.007, 02.027, 02.035, 02.037, 11.026
Hosh N	05.019		
Hosomi N	06.004, 06.006		
Hyslop S	09.002, 09.008, 09.011, 09.044	Lemos AF	09.039
I		Lencina JDS	04.038
Iacomini M	09.032	Le-quesne A	11.006
Iglesias L	03.007	Liebl B	05.017, 13.002
Ignacio ZM	03.002, 03.008	Lima A	04.019
Insuela DBR	04.025, 04.030	Lima AAD	05.005
Invencio CGGD	12.003, 12.008, 12.011, 12.019	Lima AJDO	03.017
		Lima AP	11.026
Izolan LDR	02.010, 02.019	Lima APD	02.007
J		Lima AT	06.014
Jardim GFR	14.013	Lima ATS	06.009
Jeronimo DT	08.003, 08.004	Lima EBDS	04.024, 04.032, 04.033, 04.055
Jesus CDPS	07.001		
Jesus CHA	05.017	Lima EOVDLD	09.034
Joca S	03.014	Lima FA	12.023
Jociany	06.019	Lima FB	07.009
Jordani MC	06.003, 06.015	Lima GC	10.007
Juca PM	02.047	Lima GDM	04.045
Juliao RC	11.003	Lima K	10.007
Juvencio BA	02.011	Lima LDS	04.014
K		Lima LMTR	05.004
Kanashiro A	04.046	Lima SDA	04.033
Kava J	09.040	Lima VFD	06.014
Kerppers II	02.032	Lima-Junior RCP	04.018, 04.019, 10.004, 10.008, 10.009
Kettelhut I	06.025		
Kiataki LGS	04.014, 04.049	Lindemann H	03.008
Kirsten N	11.008	Linden R	11.002, 11.015
Klein Junior L	02.041	Linder AE	06.011
Klugh K	06.037	Lippa VNM	11.004, 11.005, 11.023
Knust FM	03.008		
Koch WJ	06.018	Lippi BK	04.044, 04.048
Kohara NAN	02.002	Lisboa SFDS	02.040, 03.005, 03.023
Kohara NN	02.001		
Kovacs HZ	06.027	Livero FADR	09.042, 13.002
Krefta E	10.005, 11.006, 11.020	Lobo MDGB	05.014
		Lobo SKDO	09.014
Kreuz K	03.002	Locateli G	08.018
Kuhn KZ	02.025, 02.033, 12.022	Locatelli C	09.004
		Logu FD	05.006
Kumagai CM	04.042	Lomonte B	09.008
Kunst FM	08.013, 08.019	Longo B	02.009, 03.001, 08.021
L		Lontra ACP	12.003, 12.008, 12.011, 12.019
Lacerda-Júnior FF	08.015		
Lagente V	04.011	Lopes ALF	08.022
Landgraf MDAV	04.044, 04.048	Lopes CFO	09.015
Landgraf RG	04.044, 04.048	Lopes DS	12.001, 14.006

Lopes MCB	03.008	Marques ICDS	02.044, 03.026, 14.001
Lopes MTP	10.003, 10.011	Marques LADC	06.031
Lopes RDR	04.037, 04.050	Marques P	13.001
Lorenzon F	07.009	Marques-porto R	09.007, 09.021
Lossavaro PKDMB	04.038	Martinez PEY	03.012
Lucena LCP	10.010	Martini MC	14.004
Lustosa R	02.016, 02.017, 02.018, 02.022	Martins ACR	02.031
Luz BB	08.020, 09.016	Martins BB	05.019
Luz DA	09.041	Martins DG	04.034
Luz K	09.004	Martins F	11.005, 11.023
M		Martins MA	01.011, 04.003, 04.011, 04.015, 04.023, 04.025, 04.030, 04.031, 04.037, 04.050, 04.051, 04.052, 10.014, 11.013, 11.025, 12.005
Maccagnan JC	09.033	Martins MCCE	07.005
Macedo JL	07.005	Martins NS	06.006
Macente J	11.004	Martins PMRES	04.003, 04.011, 04.015, 04.023, 04.025, 04.030, 04.031, 04.037, 04.050, 04.051, 04.052, 11.013, 11.025, 12.005
Machado AK	02.013, 02.013		
Machado Júnior RJ	09.013		
Machado MM	09.036		
Machado MR	06.006, 06.025, 06.032, 06.033		
Machado MS	02.009		
Machado MV	02.027		
Machado-neto JA	10.007, 12.012		
Maciel ACM	12.006		
Maciel ER	11.010		
Maciel JB	09.002		
Magalhães LRDF	02.011		
Magalhães NDS	04.030, 04.052		
Magalhães PJC	04.019	Martins RB	06.033
Magro JD	09.045, 12.022	Martins T	03.009
Maia CDSF	09.014, 09.041	Martins TDS	12.007
Maia IDFVC	04.018, 10.008	Maso JM	09.040
Maia J	02.044, 03.026	Mathias-Netto FC	06.016
Mainieri NDS	01.003	Matias DO	05.004
Makiyama EN	04.008, 04.056, 14.002, 14.003, 14.012	Matos JHB	03.016
		Mattos CBD	03.027
		Mazon S	12.022
		Mazzaron M	06.013, 06.021, 06.027
Makowieski LP	08.003		
Malago ID	12.012	Medeiros ISS	14.007, 14.008, 14.011
Malagutti AR	09.039		
Malainou C	01.008	Medeiros JD	03.002, 03.008
Malerba HN	02.044, 03.026	Medeiros JVR	04.019, 08.022
Mallmann ASV	02.011	Medina C	04.047
Mallmann MP	02.021	Melhado IVS	04.014, 04.045, 04.049
Maluf M	13.001		
Mangeli E	13.001	Mello CF	03.017
Manuitt P	13.002	Mello GCD	07.007
Marangoni JA	04.007, 04.020	Mello MMB	06.013
Marcas IS	11.008	Mello MMBD	06.021, 06.027
Marchesini ERC	11.004	Melo AADS	10.003
Marchetti BM	06.005	Melo ALDS	08.009
Marchiori C	09.030, 14.007, 14.008	Melo CDPBD	04.042
		Melo PDA	06.034, 06.035, 09.046
Marianno P	04.014		
Marinho EAV	03.017	Melo SRD	02.006
Marinho JMR	09.037	Mendes AVDS	07.005
Marino-neto J	03.010	Menegatti R	01.005, 02.035
Marins RDCEE	11.010	Menezes D	10.013
Mariot LN	06.022	Menezes DPD	10.011, 10.012
Markus RP	01.002, 04.053, 07.003	Menezes EBD	10.002
		Menezes JAF	12.023
Marques APA	03.023	Menezes MPD	06.012, 09.019
Marques BVD	06.030	Menin RH	11.011, 11.019

Mermelstein C	01.014	Moura-Neto V	09.012
Meschick CG	09.003	Muller LG	02.025, 02.033, 02.041, 12.022
Mestriner F	06.002, 06.003, 06.004, 06.015, 06.019, 06.024, 06.027	Munhoz CD	02.047, 03.025, 04.045, 05.022
Metz VG	02.024, 02.028	Murakami FS	12.004, 14.006
Meyer E	02.002	Muscara MN	01.007, 04.014, 04.049, 06.031, 08.017, 12.010
Mezzomo G	02.005, 03.021	Muxfeld L	14.004
Miguel MVO	06.001, 06.023, 06.028	N	
Miguel RDA	12.007	Naidek AF	08.020
Milanesi LH	02.003	Nakagi VS	06.002, 06.027
Milani H	02.001, 02.002, 02.012	Nakanishi ABDS	01.004, 09.020
Milhorini SDS	11.008	Nakanoo CT	09.037
Mingoti MED	03.002	Narcizo LL	04.007, 04.020
Minho AS	12.015	Nardi GM	06.022
Miorando D	08.012, 08.013, 08.018, 08.019	Narzetti RA	03.002
Miranda AL	05.010	Nascimento ACM	10.002
Miranda ALP	14.015	Nascimento FP	02.031, 02.036, 02.045, 03.024, 10.005, 11.006, 11.020, 14.009, 14.010
Miranda ALPD	05.004, 05.020	Nascimento GC	12.013
Monção Filho ES	10.012	Nascimento LMM	03.006, 03.020
Mondes PHDL	07.003	Nascimento MC	10.007
Monica FZ	06.017, 07.006, 07.007	Nascimento MCA	10.003, 10.013
Montagner TRS	02.013	Nascimento MDLS	06.036
Monteiro AHA	04.024, 04.032, 04.055	Nascimento RRD	04.019
Monteiro ER	11.019	Nascimento VDA	11.013, 11.025
Monteiro M	09.033	Nash C	06.016
Monteiro MC	09.014	Nassini R	05.006, 05.018
Monteiro WM	09.002	Navegantes L	06.025
Monteiro-machado M	09.046	Negreiros NGS	04.044, 04.048
Montuori-andrade ACM	04.024, 04.027, 04.032, 04.036	Nekrasius LB	01.002
Moraes BPTD	02.026, 02.042, 04.004, 04.016, 04.026, 04.047	Neves BRO	04.008
Moraes FMD	02.029	Neves EDPFI	02.007, 02.027, 02.035, 02.037, 11.026
Moraes JAD	14.014	Neves JA	08.008
Moraes MEAD	06.016	Neves KN	04.043
Moraes MOD	06.016	Neves VGO	06.013
Moraes-de-Souza IMDS	04.026	Nguyen TAV	06.004
Morais-zani KD	09.001, 09.009, 09.017, 09.026, 09.034	Nicolas	04.029
Moreira F	03.007	Nicolau LAD	04.019, 08.022, 09.016
Moreira FADS	04.028, 08.008	Nin MSN	02.010
Moreira MSAM	09.012	Nobrega AH	10.014
Moreira V	09.023	Nobrega AHL	01.011
Moreno AM	07.008	Nobrega MEDCG	04.037, 04.050
Moreno AMH	11.010	Noel F	13.001
Moreno SE	03.025, 05.022, 12.017	Nogueira ACA	09.019
Moresco R	05.011	Nogueira LS	07.004
Morriso FDP	03.027	Noletto TG	03.019
Moriya HT	04.014, 04.045, 04.049	Nominato-Oliveira L	11.003, 11.008
Mota R	11.001	Nucci GD	06.009, 06.014, 06.016, 06.017, 06.037, 11.016
Mothe A	13.001	Nunes AA	12.017
Motta NG	14.004	Nunes PCG	04.022
Moura-da-silva AM	09.002	Nunes RKS	02.009, 03.001, 08.021
		Nyamkondiwa K	06.037

O

Obadia N	02.016, 02.017, 02.018, 02.022, 02.023
Ognibene D	06.012, 09.015, 09.019
Okada LY	06.006
Okoh VI	11.001
Olaso M	13.001
Oliveira ALD	07.007
Oliveira AM	09.024
Oliveira AMBD	09.007, 09.021
Oliveira APD	08.022, 12.018
Oliveira AS	09.018
Oliveira ASDSS	07.005
Oliveira BCD	06.012, 09.019
Oliveira BMMD	08.013
Oliveira BRD	13.002
Oliveira BSD	02.041
Oliveira CLD	03.003, 03.009, 03.010
Oliveira CVD	06.032
Oliveira EAD	12.009
Oliveira EJD	09.039
Oliveira FDA	04.028
Oliveira FRMBD	06.010
Oliveira GDM	11.012, 11.014
Oliveira GRD	06.001, 06.023, 06.028
Oliveira HRD	09.025, 11.018
Oliveira IN	09.002
Oliveira JPD	04.049, 08.017
Oliveira Junior PC	04.007, 04.020
Oliveira JVD	02.025, 02.033
Oliveira JVS	02.011
Oliveira LCD	02.007, 11.026
Oliveira LFGD	06.009
Oliveira LLRD	02.007, 11.026
Oliveira LMD	03.019
Oliveira MA	04.045, 08.006
Oliveira MGD	06.017, 07.007
Oliveira MS	02.021, 12.001
Oliveira MSO	11.021
Oliveira MTD	11.009
Oliveira NFD	01.003
Oliveira NMTD	09.006, 09.016
Oliveira PR	12.001, 12.004, 14.006
Oliveira PVD	02.025, 02.033
Oliveira RDCM	08.008
Oliveira RMWD	02.001, 02.002, 02.012
Oliveira SMD	05.011
Oliveira TALD	04.022
Oliveira TD	08.005, 08.006
Oliveira TFD	02.010, 11.019
Oliveira TSD	06.026, 09.039
Oliveira-Neto JT	06.006, 06.032
Olivo LB	11.011, 11.019, 11.024
Oly CM	04.053
Ortega LYM	09.040
Ortiz-sanchez JM	10.006
Otuki M	09.040

P

Pacagnelli FL	09.008
Pacentchuk CN	12.001
Pacheco FDS	04.025
Pacheco G	08.022
Pacheco PDS	09.036
Pacini ESA	01.006, 01.009
Padua TA	04.009
Paes JTR	04.001
Pagliarani B	01.005
Paglioichi ACDS	03.001
Paiva B	13.001
Paiva JPB	12.002, 12.003, 12.008, 12.011, 12.016, 12.019
Paiva RVN	07.003
Paixao MDS	05.002, 10.003
Palmeira DN	09.018
Palomino-pacheco M	10.006
Pamplona FA	11.006
Panzenhagen AC	02.020
Pappis L	02.013
Parreiras M	13.001
Pase CS	02.024, 02.028
Passos ASCD	01.010
Passos BP	04.007, 04.020
Passos GR	07.006, 07.007
Passos TG	03.019
Pauli KB	02.031, 02.045
Pedersoli CA	06.025
Pedrazzi JFC	03.015, 12.013
Pedro AN	14.002, 14.003
Peixe CDMS	07.009
Pelosi GG	06.001, 06.023, 06.028
Penido C	09.029
Peralta RM	09.020
Pereira AAR	03.026
Pereira BB	09.011
Pereira DA	07.002, 07.002
Pereira GC	03.004
Pereira GH	02.006
Pereira LG	11.007
Pereira LM	04.022
Pereira MC	10.001, 10.002
Pereira RM	02.027
Pereira SAP	05.012, 05.014
Pereira VG	03.024
Pereria RM	02.037
Peres DS	05.007, 05.011
Perobelli JE	07.004
Perretti M	04.033, 04.040
Pervizaj-Oruqaj L	01.008
Pessoa MLDS	08.001, 08.002, 08.010, 08.011
Pessoa MMB	08.010
Peterson L	06.037
Petreceli RR	04.002, 09.036, 11.002, 11.015, 11.017
Piai JM	11.004, 11.005, 11.023
Picoli R	11.019

Picolo G	05.013, 09.007, 09.021	Ramos HP	06.010
Pierotti SM	04.017, 04.042, 09.037	Ramos KCM	11.007
Pigatto G	05.009	Ramos LVR	06.021
Pilati S	03.001	Rampelotto PH	02.005, 03.021
Pilati SFM	08.014	Rangel GDFP	04.018
Pillat MM	05.011	Raymundi AM	03.011, 03.013
Pimenta GF	06.005, 07.001	Razera A	02.032
Pimentel RS	01.011, 10.014	Reboucas MDO	02.011
Pimentel VD	05.001	Rech CT	11.007
Pinhatti AV	11.024	Reckziegel P	14.013
Pinheiro CDS	04.028	Rego EM	10.007
Pinheiro MO	09.045	Rego MBDM	10.001
Pinheiro-Neto FR	05.012	Reis LDDS	09.014, 09.041
Pinter E	05.015	Reolon JB	09.030
Pinto DP	11.010, 11.013, 11.025	Resende ADC	06.012, 09.015, 09.019
Pinto HMC	06.035	Rez TDG	03.027
Pinto IC	04.042	Rezende CMD	12.015, 12.023
Pires ALA	04.023	Rezende RDS	09.033
Pires JCB	03.025	Rhoden SDL	04.007, 04.020
Pires LG	09.047	Ribeiro FDOS	08.022
Pires TRC	04.015	Ribeiro J	13.001
Piton E	02.013, 03.004	Ribeiro LDA	13.002
Pitta MGDR	10.001	Ribeiro LV	12.011
Poblete LS	05.004	Ribeiro MR	04.014, 04.045, 04.049
Poiato G	09.021	Ribeiro MS	06.002, 06.003, 06.015, 06.019, 06.024, 06.027
Pollo LAE	03.018	Ribeiro PC	04.051
Pont GCD	09.004	Ribeiro-paes JT	09.047
Pontieri GC	14.009, 14.010	Ripari N	12.020
Porfiro LMDO	06.026	Rita JCS	02.016, 02.017
Portela Junior VVM	03.004	Ritta JCS	02.018, 02.022, 02.023
Portela LFPF	11.010	Ritter P	04.017
Portilla MIC	02.036	Rocha AM	09.002
Porto GO	11.024	Rocha DRD	12.002
Potje SR	06.033	Rocha EMTD	04.012, 04.013, 04.021
Prado APSD	01.011	Rocha EV	06.013
Premont RT	06.018	Rocha IR	06.026
Prickaerts J	03.011	Rocha JA	04.019, 09.016
Prospero DFA	05.012, 05.014	Rocha M	04.032
Provinelli AC	02.025, 02.033, 02.041, 12.022	Rocha VN	03.017
Pucca M	09.002	Rocha-filho DRD	10.009
Pulcinelli RR	02.010, 02.019	Rocha-junior JR	09.046
Pupo AS	04.046	Rodrigues AP	09.039
Purgatto E	09.023	Rodrigues CCA	04.042
Q		Rodrigues D	06.006, 06.032
Quadros VA	09.023	Rodrigues FC	04.041, 04.046
Queiroga LB	11.019	Rodrigues GDC	14.009, 14.010
Queiroz ACQ	09.012	Rodrigues GZP	03.027
Queiroz CRT	07.005	Rodrigues MAF	09.001
Queiroz LY	06.022	Rodrigues MAP	10.009
Queiroz-junior CM	04.024, 04.027, 04.033, 04.036	Rodrigues P	05.007, 05.011, 05.018, 11.007
Quesne AHML	11.020	Rodrigues SDOR	04.026
Quintao NLM	05.016	Rodrigues SF	08.005, 08.006
Quintas LEM	01.014, 02.037	Rodrigues-junior E	09.024
Quispe CC	04.018, 10.004, 10.008, 10.009	Roman Junior WA	03.002, 03.008, 08.018, 08.019, 09.033
R		Rosa AR	02.005, 03.021
Radoski RE	04.042		
Ramos ADS	04.041		

Rosa EVFR	11.021	Santos ARC	01.011, 10.014
Rosa Filho SP	05.006, 09.010, 09.032	Santos BLBD	04.028, 08.008, 10.013
Rosa HZR	02.015	Santos CF	11.012, 11.014
Rosa JLOD	02.003, 02.015, 02.024, 02.028	Santos CVED	09.039
Rosa LBD	09.035	Santos EARD	11.019
Rosa PH	02.005, 03.021	Santos EDSRS	09.012
Rosales T	06.018	Santos F	02.036
Rosas EC	04.022	Santos FDSD	04.047
Rossato DR	02.003, 02.015, 02.028	Santos FM	04.033
Rossini BC	06.007	Santos GCM	11.013, 11.025
Roversi KR	02.015	Santos GJ	07.009
Roy R	06.018	Santos GP	06.012
Rubin M	03.017	Santos GT	05.011, 05.018
Ruiz ALTG	09.013	Santos HBDS	04.037
Russo RC	04.024, 04.027	Santos JAR	09.030, 14.007, 14.008
S		Santos JD	06.032
Sa YAPJD	04.023	Santos JEDS	06.029
Saavedra LB	11.010	Santos JMD	04.007, 04.020
Safraid GF	04.002	Santos JR	02.032
Saito P	04.042	Santos JTDS	11.021
Sakamoto GF	11.004	Santos Júnior GQ	06.037
Salata GC	12.012	Santos KMMD	04.042
Salerno G	01.010	Santos LC	07.003, 07.009
Sales A	03.014	Santos LD	04.001, 09.003, 09.047
Sales ISL	02.011	Santos LDD	06.007
Salles JP	05.010, 05.020	Santos MARFD	06.034, 06.035, 06.036
Sampaio AMKV	04.002	Santos MEFD	07.003
Sampaio TB	02.032, 11.021	Santos MFC	08.003, 08.004
Sanaiotto O	02.025, 02.033, 12.022	Santos MRVD	09.024
Sandoval MRL	09.028	Santos MVDDR	07.005
Sandri G	14.004	Santos RDN	12.017
Sandrim V	06.007	Santos RSD	02.001
Sant'anna JN	07.003	Santos SDODS	04.009
Santana ADCC	04.003, 04.031, 04.037, 04.050, 11.013, 11.025, 12.005	Santos SMD	04.007, 04.020
Sant'ana BH	02.010, 02.019	Santos TFD	09.020
Santana GCDS	05.005	Santos TMD	06.011
Santana I	09.024	Santos TS	04.017
Santana JDS	05.022	Santos UJ	01.002
Santana JR	01.013, 04.054, 09.005, 09.027	Santos WPD	04.043
Santana JVDS	03.025	Saraiva RM	11.010
Santana-Junior C	09.024	Sari MHM	09.030
Santangelo E	07.009	Sari MHMS	11.021
Sant'anna MBM	09.007	Sartim MA	09.002
Sant'anna SS	09.017, 09.034	Sartori AA	04.029
Santiago MSA	07.004	Sato MDO	12.006
Santin JR	05.016	Sato RMS	12.006
Santos AAD	07.005, 08.005, 08.006	Sato Y	03.023
Santos ABMD	10.009	Satori NA	01.006, 01.009
Santos ACD	02.009, 03.001, 08.004, 08.014, 08.021	Savio LEB	01.003
Santos ADA	03.017	Sayao PGF	04.016
Santos ADC	03.007	Scapinello J	12.022
Santos AM	09.024	Scavone C	02.037, 04.014
Santos APAD	02.029	Schiebel CS	09.006
		Schiess MC	05.008
		Schiessl R	11.008
		Schindler MSZ	09.045, 12.022
		Schio ACZ	02.025, 02.033
		Schlemmer F	01.001, 01.012
		Schlemper SRDM	08.009
		Schlemper V	08.009

Schneider AH	04.015, 04.041	Silva FDMD	04.018
Schneider VS	09.016	Silva FHD	07.002
Schons T	02.005, 03.021	Silva FVD	08.008
Schran RG	05.016	Silva GD	09.021
Schwab EDP	14.007, 14.008, 14.011	Silva GHO	04.012, 04.013, 04.021
Schwarzbald AV	11.002	Silva GMSD	11.010
Seeger W	01.008	Silva GRD	09.042
Segat HJS	02.015	Silva GSDA	05.008, 05.013
Seito LN	04.009	Silva HDFTD	08.003
Selvakumar B	01.008	Silva IDS	07.008
Semeao LDO	04.017, 04.042, 09.037	Silva ILCD	07.005
Senna EL	04.043	Silva IMF	12.003, 12.009, 12.019
Serafini M	09.024	Silva IP	02.040
Serino-silva C	09.001, 09.009, 09.017, 09.026, 09.034	Silva IS	10.003
		Silva IVM	04.021
		Silva JAD	11.010
Serpa PZ	08.018, 09.033	Silva JF	06.004, 06.025, 07.003, 11.003
Serra CSM	10.007		
Serra MF	04.031	Silva JHM	02.030
Severino B	04.049	Silva JKSDS	09.012
Sforcin JM	04.029, 12.020	Silva JP	01.013, 04.054, 09.005, 09.027
Siebel AM	02.025, 02.033		
Sievers J	03.001	Silva JRTD	09.007
Signori L	08.009	Silva JSD	06.032
Silva A	10.013	Silva KCD	08.022
Silva AA	03.017	Silva KGN	06.001, 06.023
Silva ACA	04.028	Silva KPDS	04.026, 04.047
Silva ACAE	01.014	Silva KSD	09.006
Silva ACD	03.019	Silva LC	11.015
Silva ACDAF	09.015	Silva LDDS	01.001, 01.012
Silva ACF	13.002	Silva LGFD	10.009
Silva AHBDL	02.046, 03.016, 13.002	Silva LMD	02.009, 03.001, 03.001, 08.003, 08.003, 08.004, 08.004, 08.012, 08.013, 08.014, 08.018, 08.019, 08.021, 08.021
Silva AMD	05.011		
Silva AMOE	09.018		
Silva AR	02.026, 02.029, 02.042, 04.004, 04.006, 04.016, 04.026, 04.030, 04.047	Silva M	10.013
		Silva MC	02.022
Silva AXDS	09.012	Silva MCD	05.004, 06.032
Silva BAD	08.015	Silva MCRD	09.014, 09.041
Silva BDO	10.001, 10.002	Silva MED	04.007, 04.020
Silva BP	09.020	Silva MLC	09.035
Silva CAA	06.032	Silva MLD	08.001, 08.002, 08.011
Silva CLM	01.003		
Silva CMDSD	06.026	Silva MMD	10.001
Silva CYYE	09.014	Silva MND	09.014
Silva D	08.022	Silva MSD	05.005
Silva DF	09.007	Silva N	06.025
Silva DLB	06.012, 09.019	Silva PGDB	10.009
Silva DLMD	11.018, 11.022	Silva PHFD	09.015
Silva DMAD	02.011	Silva PRDO	04.009, 09.029
Silva DMDD	11.010	Silva RL	04.018, 10.004, 10.009
Silva EC	10.010		
Silva EGD	02.031, 02.036, 10.005, 11.006, 11.020	Silva ROD	14.012
		Silva RRD	05.006, 09.010, 09.032
Silva ELEDs	10.010	Silva SCSD	09.041
Silva EMD	06.012, 09.019	Silva SS	02.007, 02.027, 02.035, 02.037, 11.026
Silva ES	04.043		
Silva FAD	10.010		

Silva T	02.031, 11.006, 11.020	Sousa PCVD	02.030
Silva TAND	12.018	Souto HDA	04.016
Silva TCD	12.017	Souza AAD	14.009, 14.010
Silva TFDQE	02.009, 03.001, 08.003, 08.004, 08.021	Souza ALCD	12.010
Silva VEGD	11.018	Souza BLD	02.031, 02.045
Silva VPD	04.034, 04.040	Souza CCP	06.007
Silva WCFND	14.007, 14.008, 14.011	Souza FHV	02.004, 02.034, 02.038
Silva Z	01.002	Souza FLD	03.018
Silva-Filho SE	04.038	Souza FMD	06.032
Silva-Neto JA	06.025, 06.027	Souza GHD	01.004, 09.020
Silveira ARD	11.021	Souza IMD	02.026, 02.042, 04.016, 04.047
Silveira GDO	03.024	Souza J	04.032
Silveira GPED	11.010, 11.025	Souza LEMD	02.024
Silveira GPMD	09.017, 09.026, 09.034	Souza LMD	04.011, 04.025
Silveira TD	09.023	Souza MAD	09.045, 12.022
Silveira THRE	07.002	Souza MFD	04.007, 04.020
Simao G	09.035	Souza MHBD	09.040
Simomura VL	08.013, 08.019	Souza ML	09.016
Siqueira BH	06.034	Souza MM	05.013
Siqueira MFRD	02.029	Souza MMD	02.009, 03.001, 03.018
Siqueira RA	07.008	Souza PDN	06.034, 06.035, 09.046
Sirois P	12.016	Souza PEN	02.004, 02.038
Skonieski C	14.004	Souza PSDA	09.016
Smera CSS	11.014	Souza RRLDS	02.037
Soares AW	04.044, 04.048	Souza TAD	05.005
Soares ES	06.010	Souza TPM	10.010
Soares GMV	04.016	Souza-Junior FJC	03.005
Soares HADS	06.032	Spicigo CC	03.024
Soares LA	02.014, 02.020, 03.020	Splendor MC	02.002, 02.012
Soares MA	14.015	Stamler JS	06.018
Soares MBP	05.005	Steffens NA	11.002, 11.017
Soares MVM	09.026, 09.034	Steffler AM	08.013, 08.019
Soares RDA	06.012, 09.019	Stein C	05.011
Sohn JMB	03.011, 03.013	Stern CAJ	03.011, 03.013, 05.006, 08.020, 09.040
Soletti JIS	09.012	Strauch M	09.046
Somavilla B	11.015, 11.017	Strelow RD	03.018
Somens LB	08.012, 08.013, 08.018, 08.019, 14.007, 14.008, 14.011	Suaiden AS	04.045
Sordi RD	06.010, 06.022	Sugimoto MA	04.040
Sousa CM	06.026	Suman PR	03.010
Sousa DPD	05.001, 05.002	Sun RC	08.007
Sousa ED	14.013	Suthovski G	14.004
Sousa EPD	09.001, 09.009	Tadokoro MM	12.017
Sousa FCFD	02.011	Taffarel MO	11.005, 11.023
Sousa G	08.022	T	
Sousa GLS	02.004, 02.034, 02.038	Tamura AS	01.003
Sousa JKD	04.019	Tamura EK	07.003
Sousa JMDCE	10.011	Tanaka-Azevedo AM	09.001, 09.009, 09.017, 09.026, 09.034
Sousa KDS	01.002	Tarozzi A	01.005
Sousa LPD	04.024, 04.027, 04.032, 04.034, 04.036, 04.040, 04.055	Tavares J	02.030
Sousa MCD	04.028, 08.008	Tavares LP	04.027, 04.036
Sousa Neto BP	04.028	Tavares VB	02.025, 02.033
		Tavares-de-lima W	04.014, 04.045, 04.049, 08.005, 08.006
		Teixeira DMT	02.004
		Teixeira FEG	11.009

Teixeira LFLS	08.022	Viegas-Junior. C	12.003, 12.008,
Teixeira MM	04.024, 04.027,		12.009, 12.011,
	04.032, 04.033,		12.019, 12.021
	04.034, 04.036,	Vieira Junior GM	10.012
	04.055	Vieira RF	12.015
Teixeira NC	03.018	Viel TA	02.044, 03.026,
Teixeira SA	01.007, 04.014,		14.001
	04.049, 06.031,	Viero FT	03.004, 05.011,
	12.010		05.018, 11.007
Tekus V	05.015	Villar JAFP	02.027
Tellis CMJ	04.006	Villarreal CF	05.005
Tida-Oliveira CH	09.028	Visnhesk BRC	13.002
Timah B	05.001, 05.002,	Vivian GK	14.012
	05.012, 05.014	W	
Tirapelli CR	06.005, 06.013,	Wagner TCL	14.004
	07.001	Wallace JL	08.017
Toffoli-kadri MC	04.038	Waltrick APF	13.002
Toni DCD	03.010	Wanderley CWDS	04.041
Tonussi CR	04.043	Waters CM	08.007
Torres-Bonilla KA	09.002, 09.008,	Weiss A	01.008
	09.011, 09.044	Werle I	03.006
Tostes RDCAP	06.004, 06.006,	Wermann S	11.024
	06.025, 06.027,	Werner MFDP	05.006, 08.020,
	06.032, 06.033		09.010, 09.016,
Trambaioli BM	04.042		09.032
Trevisan G	05.007, 11.007	Wilhelm J	01.008
Triches F	03.003, 03.003,	Wong DVT	04.018, 04.019,
	03.009, 03.010		10.004, 10.008,
Trichez VDK	04.020		10.009
Trindade P	02.042, 04.004	X	
Uchenna N	11.001	Xavier ME	01.001, 01.012
V		Xexeo G	13.001
Valachinski AW	02.009, 03.018	Ximenes V	09.003
Valadares MC	02.007, 11.026	Ximenes VF	04.001
Valdivia LFG	14.013	Y	
Vale DLD	04.042	Yanagisawa H	06.004
Vale ML	04.019	Yanomine M	03.024
Valenca HDM	14.014	Z	
Valenca SDS	08.007, 14.014	Zaidan I	04.024, 04.027,
Valentim JT	02.011		04.032, 04.036,
Valerio RR	01.011		04.040, 04.055
Vannier-santos MA	11.010	Zambelli VO	05.008, 05.013,
Vanzan DF	12.014		05.019
Varela B	03.002	Zampronio AR	04.005, 04.010
Vargas P	06.006	Zanatta L	09.045
Varjao MTDSV	09.012	Zaninelli T	04.017
Varon JCG	09.011	Zanotto-Filho A	05.016
Vasconcelos J	06.003, 06.015	Zanoveli JM	02.046, 03.016,
Vasquez YR	04.045		05.003, 05.017,
Vazquez-armendariz AI	01.008		13.002
Vecchia CAD	08.018	Zatz R	06.017
Veloso JJ	08.013, 08.019	Zavadinack M	09.032
Ventura TJTV	05.014	Zela SJ	12.004
Venzon L	02.009, 03.001,	Ziani P	02.005, 03.021
	08.003, 08.021	Zilli GAL	02.019
Verri Junior WA	05.003, 05.017,	Zimmermann ES	11.002, 11.017
	09.003	Zingali RB	06.036
Versa SG	03.027	Zuardi A	03.015
Viana AFSC	08.008	Zuckermann J	11.024
Viana MDM	05.005		
Viana RDS	04.054		
Vicari HP	10.007		
Vida RLD	04.002, 09.036		
Vidueiros J	09.009		

